

National Transportation Safety Board

Office of Research and Engineering

Washington, DC 20594



HWY22MH003

MATERIALS LABORATORY

Factual Report 23-036

March 29, 2023

(This page intentionally left blank)

A. ACCIDENT INFORMATION

Location: Pittsburgh, Pennsylvania
Date: January 28, 2022
Vehicle: Fern Hollow Bridge
Investigator: Dennis Collins (HS-22)

B. COMPONENTS EXAMINED

Summary of "Forbes Avenue Over Fern Hollow Bridge Collapse Investigation: Steel Mechanical and Materials Testing Factual Report" and "Forbes Avenue Over Fern Hollow Bridge Collapse Investigation: Weld Microstructure Factual Report".

C. EXAMINATION PARTICIPANTS

Group Chair Adrienne Lamm
National Transportation Safety Board
Washington, DC

Party Coordinator Justin Ocel
Federal Highway Administration
Baltimore, MD

Group Member Ryan Slein
Federal Highway Administration
McLean, VA

D. DETAILS OF THE EXAMINATION

On Friday, January 28, 2022, about 6:37 a.m. eastern standard time, the Fern Hollow bridge, which carried Forbes Avenue over the north side of Frick Park, in Pittsburgh, Allegheny County, Pennsylvania, experienced a structural failure. As a result, the 447-foot-long bridge fell approximately 100 feet into the park below.

1.0 Structure Description

The bridge superstructure was a frame-floorbeam-stringer system with two parallel lines of rigid "K" frames. Each frame was comprised of three-span, continuous welded I-shaped steel girders, and two inclined, welded steel I-shaped legs. The structure was unique in that the legs were bolted to I-girders. The entire superstructure was made from weld-fabricated uncoated weathering steel plates. The ends of the girders rested on reinforced concrete caps on stone masonry abutments, and each leg rested atop reinforced concrete thrust blocks. The bents of the bridge

referred to the legs and thrust blocks, taken together with their associated cross bracing.

Figure 1 shows a plan view composite photo of the collapsed structure with the locations of the legs underneath the structure outlined and labeled. The bridge legs were individually labeled according to bent number and bridge side. The first index of the naming convention is "B" for bent. The second index is the numeric "1" or "2", meant to indicate the first and second bent away from the near abutment. The final index is the letter "L" or "R", representing left or right when looking east from the near abutment. Thus, B1R refers to the leg in bent 1 on the right side of the bridge.

In Figure 1, the plan view composite photo is compared to schematics in plan view and elevation view orientations, with the components of the bridge labeled consistent with the latest bridge inspection report.¹ Figure 2 shows the plan view composite photo of the collapsed structure relative to the elevation view schematic, with each leg identified.

The bridge legs were a built-up I-shape cross-section configuration of web plate bracketed by flanges. The width of bridges legs tapered slightly from the top down, with a second, sharper taper resulting in a trapezoidal-shaped shoe at the bottom of the leg. The width of the flanges was oriented perpendicular to the direction of the girders, with the web plate perpendicular to the width of the flanges. A schematic showing the outward facing side of a leg mating with a girder with all structural elements labeled is shown in Figure 3. A schematic showing a detailed view of the labeled structural elements in the bottom of a leg is shown in Figure 4.

2.0 Specimen Location and Extraction

The details of the accident scene post-collapse are given in NTSB reports Structural Factors Group Chair's Factual Report and NTSB Materials Laboratory Factual Report 23-009. While on-scene, NTSB investigators, along with engineers from Federal Highway Administration (FHWA), identified and retained material from all four bridge legs and the girders attached directly there above to capture each steel plate thickness that comprised the structure. This was done to ensure every steel plate used in the structure could be tested to ensure it met specifications. FHWA agreed to complete mechanical and materials testing of the retained material, which is documented in a report being reviewed here titled "Forbes Avenue Over Fern Hollow Bridge Collapse Investigation: Steel Mechanical and Materials Testing Factual Report", hereafter referred to as the FHWA Mechanical report, which is attached in Appendix A.

¹ "2021 Routine Bridge Safety Inspection Report, City of Pittsburgh, Allegheny County, Forbes Avenue over Fern Hollow and Nine Mile Run" by Gannett Fleming, Inc.

After the evidence had been collected and during examination of records from the construction of the bridge, specifically while reviewing numerous mill testing reports (MTRs), steel plates of the same thickness and heat code were noted as used in multiple locations in the bridge. In total, there were 20 unique heat and plate thickness combinations. To avoid duplicative efforts by testing all the material extracted, only the number of specimens needed to capture the mechanical and material properties from each unique steel plate were machined and tested. The exact location of each specimen tested is described in sections 1.1 and 3 of the FHWA Mechanical report.

3.0 Material Tested

Per the MTRs, bridge construction utilized two types of plates produced by different manufacturers. United States Steel Corporation (Pittsburgh, PA) produced plates specified to meet ASTM A588-71 Grade B. Bethlehem Steel Corporation (Bethlehem, PA) produced plates specified to meet ASTM A588 Grade A, without specifying the year of the standard. Changes were made to the ASTM A588 standard over the years the plates were produced (1972-1974). Comparisons of Grade A and Grade B material and changes to the standard are discussed extensively in section 4.3 of the FHWA Mechanical report.

Within the MTRs, 2 plates were listed as Grade A, 7 plates were listed as Grade B, and 16 plates could not be definitively tied to either Grade A or Grade B. Thus, while there were ostensibly 20 unique heat and plate thickness combinations, specimens representing 25 separate plates of material were tested.

While reviewing design plans post-collapse, investigators noted the top transverse stiffener in the legs (indicated in Figure 5) was specified to be constructed from plate with 0.75 inch thickness, while the remainder of the transverse stiffeners were specified to be constructed from plate with 0.4375 inch thickness.² However, examination of the collected evidence revealed the top transverse stiffeners were constructed of plate with 0.8125 inch measured thickness. During review of the MTRs for the plate material, investigators were unable to locate the parent heat from which the 0.8125-inch plates nested. Thus, no specifications to which tested mechanical and material properties could be compared were available. As a result, and coupled with the information that the collapse initiated at the bottom of a leg and not the top, the plate material from which the top transverse stiffeners were constructed was not tested.

² "Reconstruction of Forbes Avenue Bridge Over Fern Hollow & Approaches" by City of Pittsburgh Department of Public Works Bureau of Engineering, sheet no. 14.

The retained material was transported to and stored at FHWA Turner-Fairbank Highway Research Center (TFHRC) in McLean, VA for future testing.

4.0 Mechanical and Materials Testing

The mechanical and materials testing of all the bridge steel evidence was performed by FHWA personnel at TFHRC. The methodology and results of the testing are presented by FHWA in the report attached in Appendix A. A summary of the testing performed is provided below. All testing was performed per ASTM standards as required in City of Pittsburgh material specifications.³

4.1 Tensile Testing

The design plans called for the steel to be used for construction of the bridge was ASTM A588⁴. For plates of thickness 4 inches or less, ASTM A588 specifies nominal yield strength of 50 ksi and ultimate tensile strength of 70 ksi, with elongation at fracture specified as 18% in 8 inches or 21% in 2 inches. The MTRs for each heat of material reported the yield strength, ultimate tensile strength, and percent elongation at fracture determined via testing prior to shipment of the material; MTR values for each heat are listed in section 4.1 the FHWA Mechanical report.

Tensile specimens were prepared in duplicate per the method described in the FHWA report, following the ASTM A370 specification⁵. 21 of the 25 specimens met the specification; 4 specimens did not meet the minimums outlined in ASTM A588. One specimen was 4% below the yield strength and 1% below the ultimate tensile strength, two specimens met the yield strength but were 1% below the ultimate strength, and one specimen met both the yield and ultimate tensile strength but was 11% below the specified percent elongation at fracture.

The tensile testing results are listed in summary in section 5.1 and in full in Appendix D of the FHWA Mechanical report.

³ "Specifications for Materials and Construction, 1938 Specifications and 1962 Addendums" by City of Pittsburgh, page 9.

⁴ ASTM A588 "Standard Specification for High-Strength Low-Alloy Structural Steel, up to 50 ksi [345 MPa] Minimum Yield Point, with Atmospheric Corrosion Resistance", ASTM International, West Conshohocken PA.

⁵ ASTM A370 "Standard Test Methods and Definitions for Mechanical Testing of Steel Products", ASTM International, West Conshohocken PA.

4.2 CVN Impact Testing

The MTRs specified the plates were to pass a Charpy v-notch (CVN) impact test at 15 foot-pounds at positive 40 degrees Fahrenheit; MTR values are listed in section 4.2 of the FHWA Mechanical report.

CVN specimens were prepared in triplicate per the method described in the FHWA report, following the ASTM A370 specification. All tested specimens met the requirement for impact testing listed on the MTRs.

The CVN impact testing results are listed in summary in section 5.2 and in full in Appendix E of the FHWA Mechanical report.

4.3 Compositional Analysis

The ASTM A588 specification lists a chemical composition that was compared to specimens measured using glow discharge spectroscopy (also called spark atomic emission spectrometry). The glow discharge spectroscopy was performed twice per specimen and averaged, per ASTM E415 specification⁶.

The 2 plates listed as Grade A met the specifications for Grade A per ASTM A588. Of the 7 plates listed as Grade B, 6 plates met the specifications for Grade B per ASTM A588 and 1 plate was non-conformant. For the remaining 16 plates, 2 plates were non-conformant regardless of if they were Grade A or Grade B. An additional 6 plates would have been non-conformant if Grade B but conformant if Grade A. 10 plates were conformant for both Grade A and Grade B specifications.

The composition results are listed in summary in section 5.3 and in full in Appendix F of the FHWA Mechanical report.

4.4 Metallographic Examination

After fractures were discovered at the end plates on the tops of two legs while on scene (evaluated in NTSB Materials Laboratory Factual Report 23-011), assessment of the welds at the tops of the legs was desired. Consequently, the welds between the top of each leg and the base plate at both the acute and obtuse angles were cross-sectioned and examined.

The design plans called for a U-groove weld at the leg flange-to-endplate interface, with a far side reinforcing fillet weld.⁷ No details about partial versus

⁶ ASTM E415 "Standard Test Method for Analysis of Carbon and Low-Alloy Steel by Spark Atomic Emission Spectrometry", ASTM International, West Conshohocken PA.

⁷ "Reconstruction of Forbes Avenue Bridge Over Fern Hollow & Approaches" by City of Pittsburgh Department of Public Works Bureau of Engineering, sheet no. 14.

complete joint penetration were given. Examination of the cross-sections showed they were partial joint penetration welds with double-bevel groove geometry. The bevel preparation varied, with the two legs of Bent 1 having similar preparation and the two legs of Bent 2 having similar preparation.

Most of the welds showed a lack of fusion with either sidewall, with some welds displaying no fusion. Cracks were observed in welds on Leg B1R and B2L; the cracks either had pack rust consistent with occurring some time ago or else appeared fresh and consistent with occurring during the collapse. None of the cracks displayed characteristics consistent with fatigue cracking. The welds in Leg B1L and Leg B2R did not have cracks observed.

Detailed observations from the metallographic examinations are given in section 5.4 and macroetched images are shown in Appendix G of the FHWA Mechanical report.

4.5 Weld Microstructure Examination

Due to the non-conformance to specification for the composition of some plates, along with the lack of fusion of the examined flange-to-endplate welds, investigators desired further analysis of the weld quality on the bridge. FHWA agreed to complete additional hardness and microstructure work to examine the welds, which is documented in a report being reviewed here titled "Forbes Avenue Over Fern Hollow Bridge Collapse Investigation: Weld Microstructure Factual Report", hereafter referred to as the FHWA Weld report, which is attached in Appendix B.

The flange-to-endplates welds of the Span 1 and Span 2 flanges for Leg B1R were further examined by performing hardness tracts traversing the base metal, heat affected zone (HAZ), and weld metal, as well as analyzing the microstructure at each hardness test indentation.

The hardness of the specimens in the HAZ were higher than either the base metal or the weld metal, and the weld metal had slightly higher hardness than the base metal. Several hardness readings in the HAZ were above the threshold value likely to predict a microstructural change. The hardness results are summarized in section 3.1 of the FHWA Weld report.

The microstructure of the base metal consisted of pearlite and ferrite, while the weld metal microstructure was comprised of several forms of ferrite. The microstructure in the HAZ had smaller pearlite colonies and ferrite grains compared to the base metal, as well as areas of martensite. The microstructure of the hardness tracts traversing the Span 1 flange and the Span 2 flange are shown in section 3.2 and section 3.3, respectively, of the FHWA Weld report.

Submitted by:

Adrienne V. Lamm
Materials Engineer

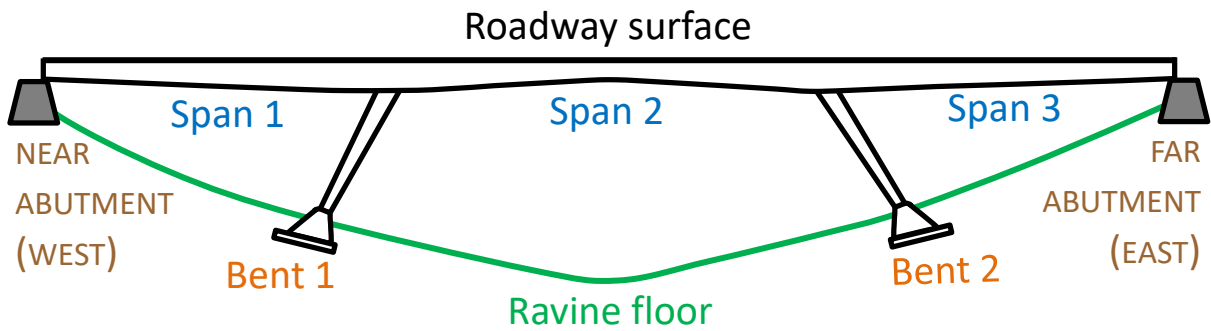
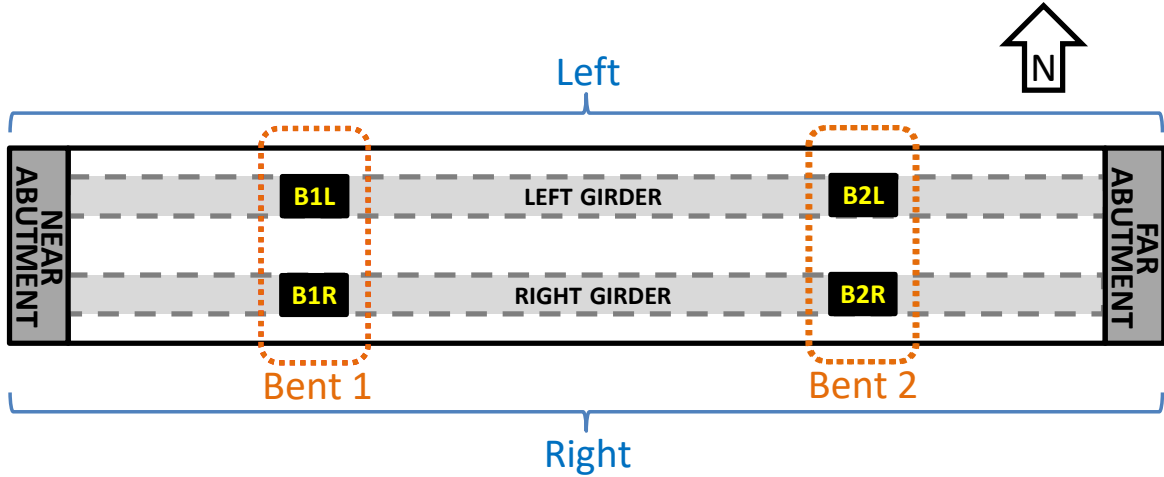


Figure 1. Plan view composite photo (top) compared to schematics in plan view and elevation view orientations (middle and bottom, respectively).

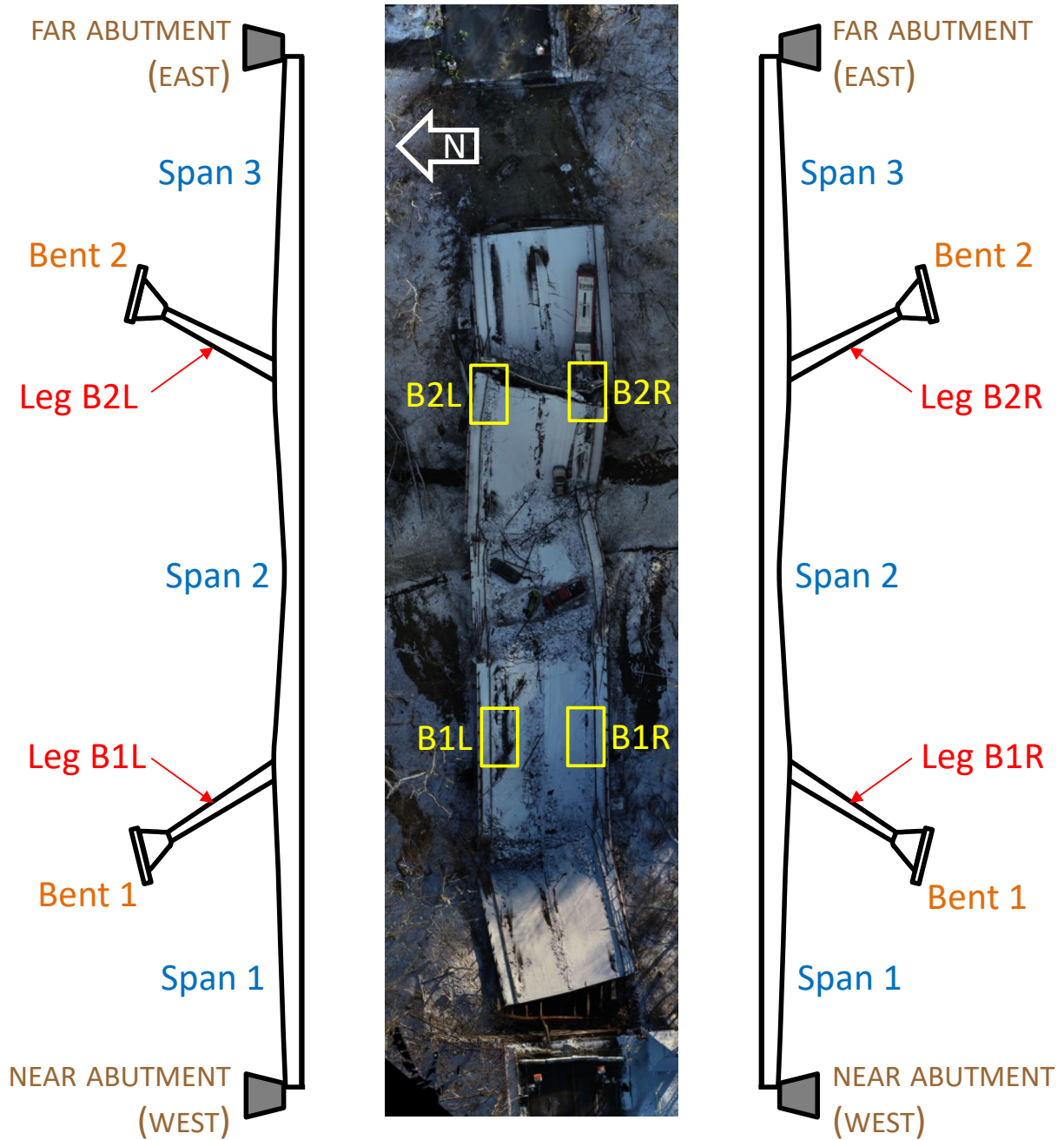


Figure 2. Plan view composite photo of the collapsed structure relative to the elevation view schematic.

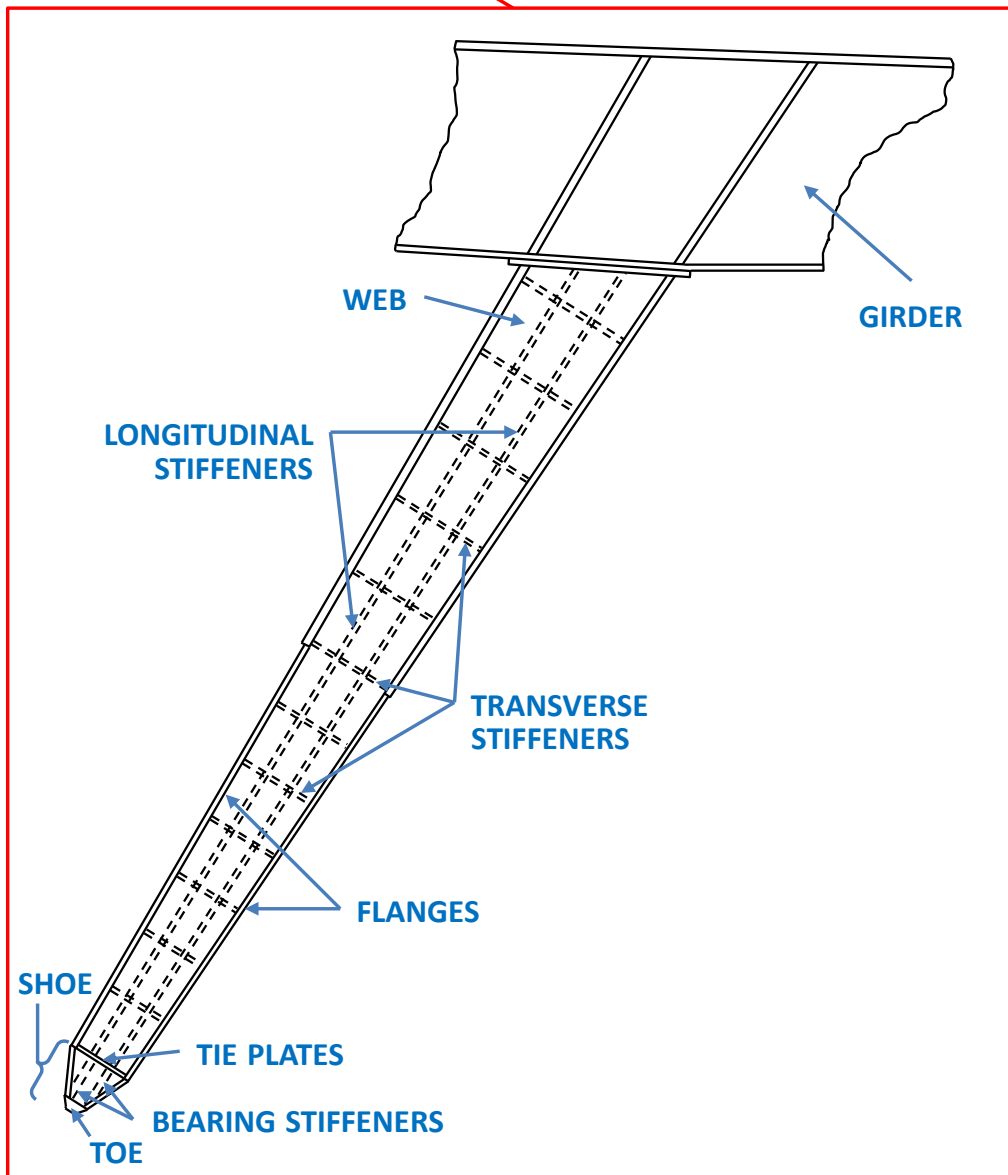
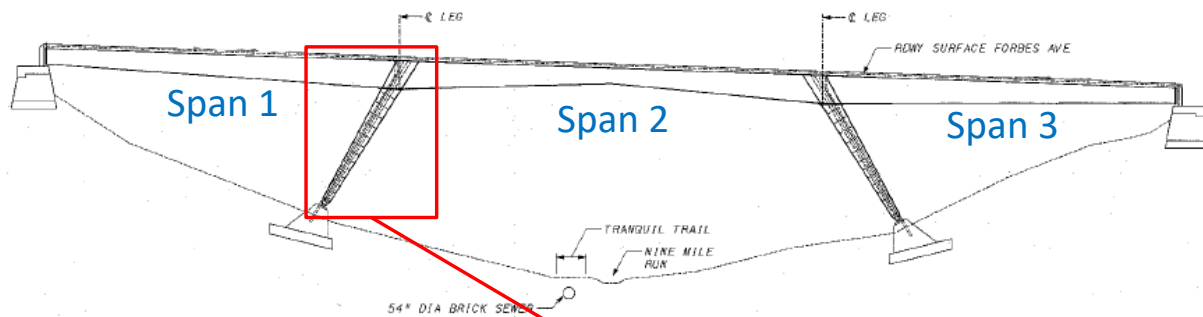


Figure 3. Schematic showing the outward facing side of a leg mating with a girder with all structural elements labeled. (Schematic not to scale)

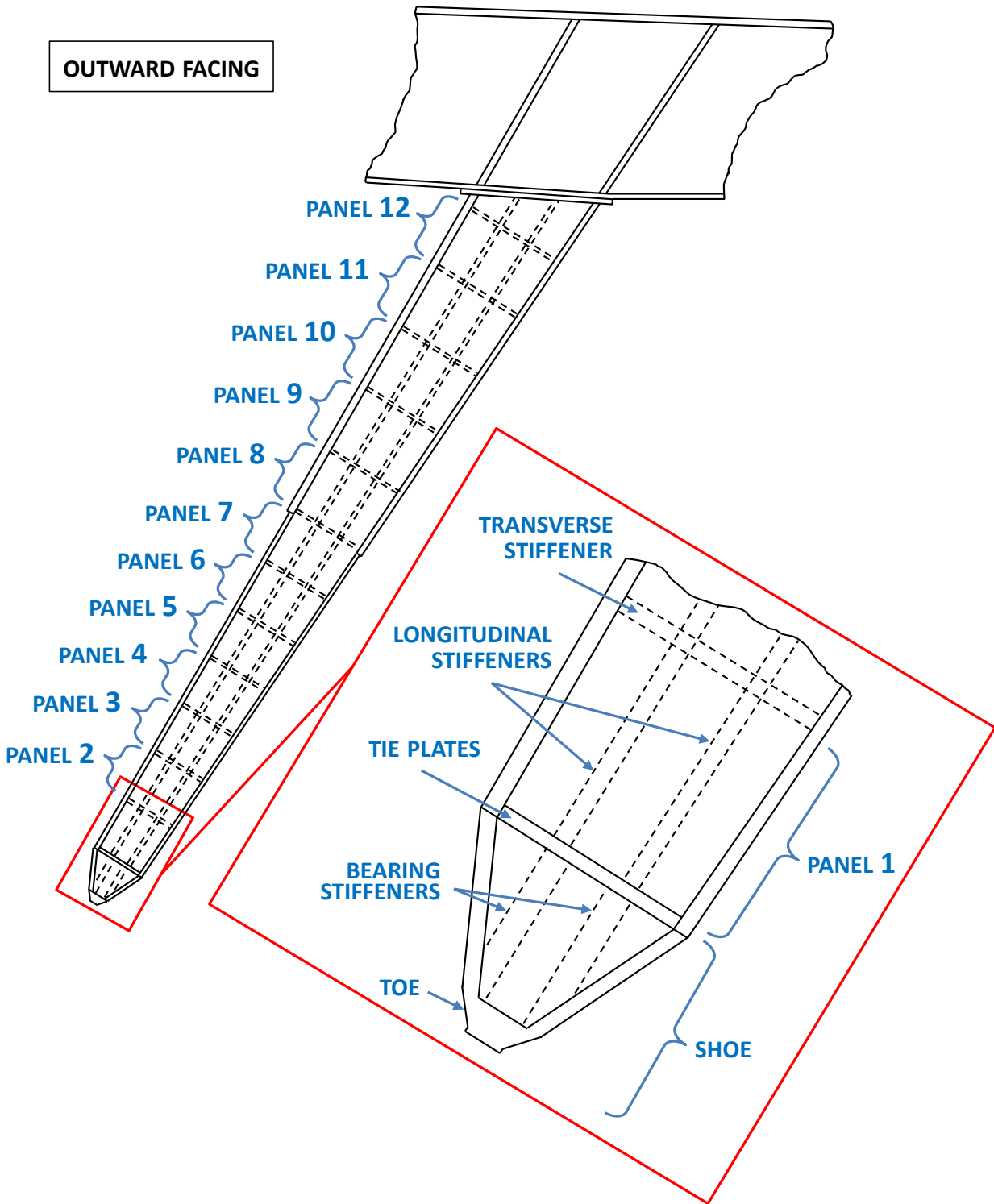


Figure 4. Schematic showing a detailed view of the labeled structural elements in the bottom of a leg. (Schematic not to scale)

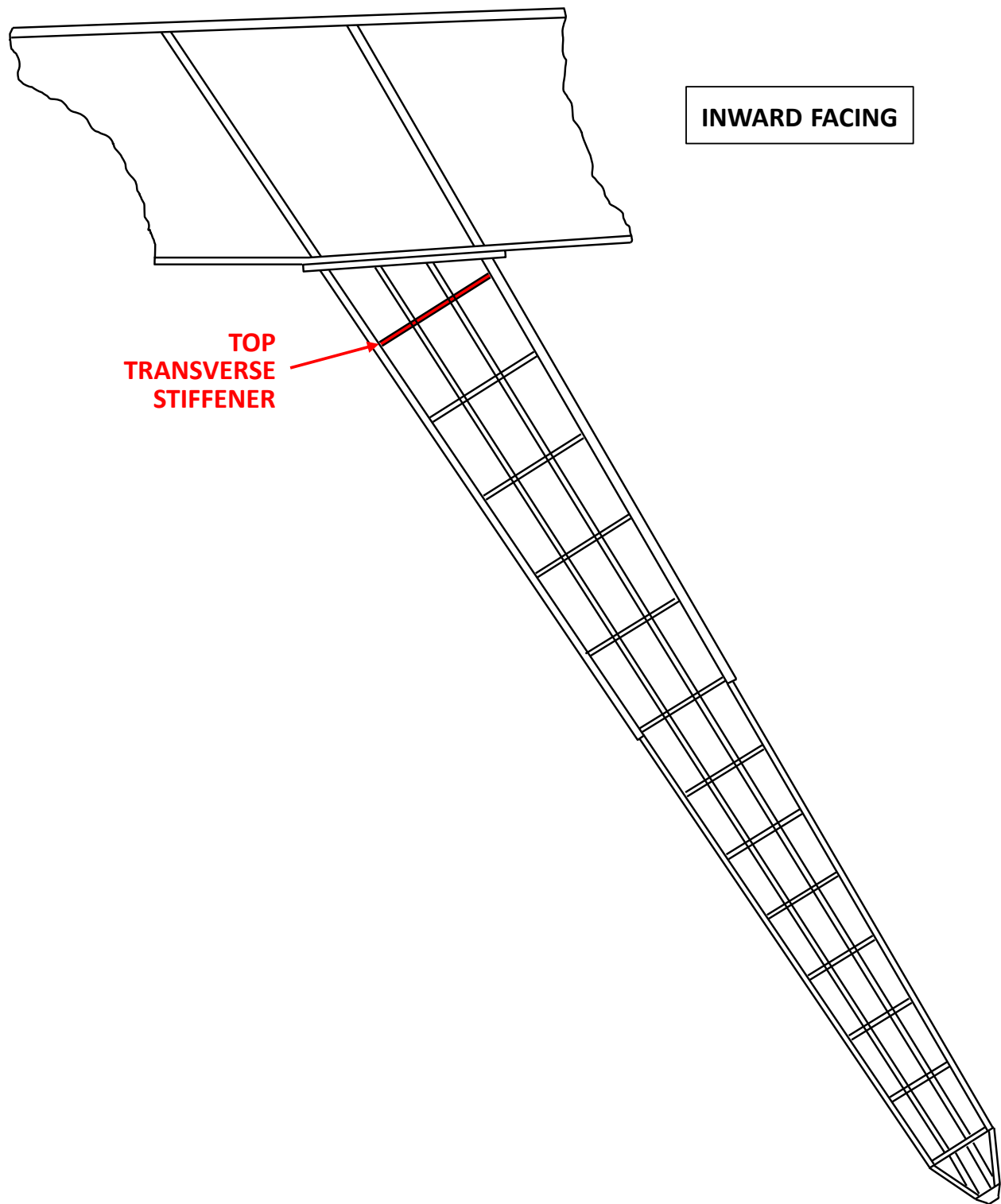


Figure 5. Schematic showing the inward facing side of a leg with the top transverse stiffener highlighted in red. (Schematic not to scale)

APPENDIX A - "Forbes Avenue Over Fern Hollow Bridge Collapse Investigation: Steel Mechanical and Materials Testing Factual Report", prepared by Federal Highway Administration (FHWA)

Forbes Avenue Over Fern Hollow Bridge Collapse Investigation: Steel Mechanical and Materials Testing Factual Report

Prepared For:
National Transportation Safety Board
NTSB Accident ID: HWY22MH003

Prepared by:

Ryan Slein, Ph.D.
Federal Highway Administration
Turner-Fairbank Highway Research Center
6300 Georgetown Pike, McLean, VA 22101

Justin Ocel, Ph.D., P.E.
Federal Highway Administration
Resource Center Structures Team
31 Hopkins Plaza, Suite 840
Baltimore, MD 21201

Benjamin Graybeal, Ph.D., P.E.
Federal Highway Administration
Turner-Fairbank Highway Research Center
6300 Georgetown Pike, McLean, VA 22101

March 28, 2023

Table of Contents

List of Figures iii

List of Tables xi

List of Abbreviations xii

1 Introduction..... 1

 1.1 Description of structural components retained after the collapse 1

 1.2 Report scope..... 8

2 Testing plan..... 8

 2.1 Work completed at the bridge collapse site 9

 2.2 Work conducted outside of TFHRC 9

 2.3 Work conducted by NTSB at TFHRC 9

 2.4 Description of evidence storage at FHWA 9

 2.5 Testing Completed by FHWA at TFHRC..... 9

 2.5.1 Tensile testing 10

 2.5.2 CVN testing 11

 2.5.3 Chemistry assessment 12

 2.5.4 Metallographic assessment 14

3 Cut plan..... 15

4 MTR Assessment 18

 4.1 MTR tensile comparison..... 18

 4.2 MTR CVN comparison..... 19

 4.3 MTR chemistry comparison..... 20

5 Test Results..... 25

 5.1 Tensile test results..... 25

 5.2 CVN results..... 28

 5.3 Chemistry results 30

 5.4 Metallographic results..... 33

 5.4.1 General Observations..... 33

 5.4.2 Leg 1 (B1R) 34

 5.4.3 Leg 2 (B1L)..... 35

 5.4.4 Leg 3 (B2L)..... 36

 5.4.5 Leg 4 (B2R) 36

Acknowledgements..... 37

References.....	37
Appendix A: Record of Evidence prior to Cutting	39
Appendix B: Cutting Plan.....	56
Appendix C: Specimen Extraction Shop Drawings	71
Appendix D: Tensile Test Results	95
Appendix E: CVN Test Results	130
Appendix F: GDS Results.....	179
Appendix G: Macroetches	184
Appendix H: Supporting Calibration, Service, and SRM Documentation	205

List of Figures

Figure 1. Orthomosaic Plan View (from NTSB).	1
Figure 2. Elevation View, looking north (modified from NTSB provided figure).	1
Figure 3. B1R – South-West Leg.	4
Figure 4. B1L – North-West Leg.	5
Figure 5. B2L – North-East Leg.	6
Figure 6. B2R – South-East Leg.	7
Figure 7. Tensile coupon dimensions.	10
Figure 8. Design weld profile versus the observed profile for B1R.	35
Figure 9. Design weld profile versus the observed profile for B1L.	35
Figure 10. Design weld profile versus the observed profile for B2R.	37
Figure A.1. B1R – NTSB-STR-001.	40
Figure A.2. B1R – NTSB-STR-002 & NTSB-STR-003.	40
Figure A.3. B1R – NTSB-STR-004.	41
Figure A.4. B1R – NTSB-STR-005.	41
Figure A.5. B1R – NTSB-STR-006.	42
Figure A.6. B1R – NTSB-STR-007.	42
Figure A.7. B1R – NTSB-STR-008.	43
Figure A.8. B1R – NTSB-STR-009.	43
Figure A.9. B1R – NTSB-STR-010.	44
Figure A.10. B1R – NTSB-STR-011.	45
Figure A.11. B1L – NTSB-STR-012.	45
Figure A.12. B1L – NTSB-STR-013.	46
Figure A.13. B1L – NTSB-STR-014.	46
Figure A.14. B1L – NTSB-STR-015.	47
Figure A.15. B1L – NTSB-STR-016.	47
Figure A.16. B1L – NTSB-STR-017.	48
Figure A.17. B2L – NTSB-STR-018.	48
Figure A.18. B2L – NTSB-STR-019 & NTSB-STR-020.	49
Figure A.19. B2L – NTSB-STR-021.	49
Figure A.20. B2L – NTSB-STR-022.	50
Figure A.21. B2L – NTSB-STR-023.	50
Figure A.22. B2L – NTSB-STR-024.	51
Figure A.23. B2L – NTSB-STR-025.	51
Figure A.24. B2R – NTSB-STR-026.	52
Figure A.25. B2R – NTSB-STR-027.	52
Figure A.26. B2R – NTSB-STR-028A (Taken at TFHRC).	53
Figure A.27. B2R – NTSB-STR-028B (Taken at TFHRC).	53
Figure A.28. B2R – NTSB-STR-029.	54
Figure A.29. B2R – NTSB-STR-030.	54
Figure A.30. B2R – NTSB-STR-031.	55
Figure A.31. B2R – NTSB-STR-032.	55
Figure B.1. B1R – NTSB-STR-001.	57
Figure B.2. B1R – NTSB-STR-002.	58
Figure B.3. B1R – NTSB-STR-006.	58
Figure B.4. B1R – NTSB-STR-007.	59

Figure B.5. B1R – NTSB-STR-008.....	59
Figure B.6. B1R – NTSB-STR-009.....	60
Figure B.7. B1L – NTSB-STR-012.....	61
Figure B.8. B1L – NTSB-STR-014.....	62
Figure B.9. B1L – NTSB-STR-016.....	63
Figure B.10. B2L – NTSB-STR-018.....	64
Figure B.11. B2L – NTSB-STR-022.....	65
Figure B.12. B2L – NTSB-STR-024.....	66
Figure B.13. B2R – NTSB-STR-026.....	67
Figure B.14. B2R – NTSB-STR-028B.....	68
Figure B.15. B2R – NTSB-STR-029.....	69
Figure B.16. B2R – NTSB-STR-031.....	70
Figure C.1. 1A – NTSB-STR-001.....	72
Figure C.2. 1B – NTSB-STR-001.....	72
Figure C.3. 1C – NTSB-STR-002.....	73
Figure C.4. 1C – NTSB-STR-002.....	73
Figure C.5. 1D – NTSB-STR-004.....	74
Figure C.6. 1E – NTSB-STR-003.....	75
Figure C.7. 1Q – NTSB-STR-006.....	76
Figure C.8. 1H – NTSB-STR-007.....	76
Figure C.9. 1U – NTSB-STR-007.....	77
Figure C.10. 1N – NTSB-STR-008.....	77
Figure C.11. 1T – NTSB-STR-009.....	78
Figure C.12. 1V – NTSB-STR-011.....	79
Figure C.13. 2A – NTSB-STR-012.....	80
Figure C.14. 2B – NTSB-STR-012.....	80
Figure C.15. 2D – NTSB-STR-014.....	81
Figure C.16. 2E – NTSB-STR-014.....	82
Figure C.17. 2Q – NTSB-STR-014.....	83
Figure C.18. 2T – NTSB-STR-016.....	83
Figure C.19. 2U – NTSB-STR-016.....	84
Figure C.20. 3A – NTSB-STR-018.....	84
Figure C.21. 3B – NTSB-STR-018.....	85
Figure C.22. 3E – NTSB-STR-020.....	86
Figure C.23. 3F – NTSB-STR-020.....	87
Figure C.24. 3Q – NTSB-STR-022.....	88
Figure C.25. 3T – NTSB-STR-024.....	88
Figure C.26. 3U – NTSB-STR-024.....	89
Figure C.27. 4A – NTSB-STR-026.....	89
Figure C.28. 4B – NTSB-STR-026.....	90
Figure C.29. 4E – NTSB-STR-028A.....	91
Figure C.30. 4F – NTSB-STR-028A.....	92
Figure C.31. 4Q – NTSB-STR-028B.....	93
Figure C.32. 4R – NTSB-STR-029.....	93
Figure C.33. 4U – NTSB-STR-029.....	94
Figure C.34. 4T – NTSB-STR-031.....	94
Figure D.1. Stress-strain curve for specimen 1A1.....	96

Figure D.2. Stress-strain curve for specimen 1A2.....	96
Figure D.3. Stress-strain curve for specimen 1B1.....	97
Figure D.4. Stress-strain curve for specimen 1B2.....	97
Figure D.5. Stress-strain curve for specimen 1C1.....	98
Figure D.6. Stress-strain curve for specimen 1C2.....	98
Figure D.7. Stress-strain curve for specimen 1H1.....	99
Figure D.8. Stress-strain curve for specimen 1H2.....	99
Figure D.9. Stress-strain curve for specimen 1N1.....	100
Figure D.10. Stress-strain curve for specimen 1N2.....	100
Figure D.11. Stress-strain curve for specimen 1Q1.....	101
Figure D.12. Stress-strain curve for specimen 1Q2.....	101
Figure D.13. Stress-strain curve for specimen 1T1.....	102
Figure D.14. Stress-strain curve for specimen 1T2.....	102
Figure D.15. Stress-strain curve for specimen 1V1.....	103
Figure D.16. Stress-strain curve for specimen 1V2.....	103
Figure D.17. Stress-strain curve for specimen 2A1.....	104
Figure D.18. Stress-strain curve for specimen 2A2.....	104
Figure D.19. Stress-strain curve for specimen 2B1.....	105
Figure D.20. Stress-strain curve for specimen 2B2.....	105
Figure D.21. Stress-strain curve for specimen 2Q1.....	106
Figure D.22. Stress-strain curve for specimen 2Q2.....	106
Figure D.23. Stress-strain curve for specimen 2T1.....	107
Figure D.24. Stress-strain curve for specimen 2T2.....	107
Figure D.25. Stress-strain curve for specimen 3A1.....	108
Figure D.26. Stress-strain curve for specimen 3A2.....	108
Figure D.27. Stress-strain curve for specimen 3B1.....	109
Figure D.28. Stress-strain curve for specimen 3B2.....	109
Figure D.29. Stress-strain curve for specimen 3Q1.....	110
Figure D.30. Stress-strain curve for specimen 3Q2.....	110
Figure D.31. Stress-strain curve for specimen 3T1.....	111
Figure D.32. Stress-strain curve for specimen 3T2.....	111
Figure D.33. Stress-strain curve for specimen 4A1.....	112
Figure D.34. Stress-strain curve for specimen 4A2, where the DIC camera unexpectedly shutoff.....	112
Figure D.35. Stress-strain curve for specimen 4A2 duplicate (machined from 4A3).....	113
Figure D.36. Stress-strain curve for specimen 4B1.....	113
Figure D.37. Stress-strain curve for specimen 4B2.....	114
Figure D.38. Stress-strain curve for specimen 4Q1.....	114
Figure D.39. Stress-strain curve for specimen 4Q2.....	115
Figure D.40. Stress-strain curve for specimen 4R1.....	115
Figure D.41. Stress-strain curve for specimen 4R2.....	116
Figure D.42. Stress-strain curve for specimen 4T1.....	116
Figure D.43. Stress-strain curve for specimen 4T2.....	117
Figure D.44. Stress-strain curve for specimen 1U1.....	117
Figure D.45. Stress-strain curve for specimen 2U1.....	118
Figure D.46. Stress-strain curve for specimen 3U1.....	118
Figure D.47. Stress-strain curve for specimen 4U1.....	119
Figure D.48. Completed tensile and chemical specimens for plate 1A (1A1, 1A2, 1A4).....	119

Figure D.49. Completed tensile and chemical specimens for plate 1B (1B1, 1B2, 1B4).....	120
Figure D.50. Completed tensile and chemical specimens for plate 1C (1C1, 1C2, 1C4).....	120
Figure D.51. Completed tensile and chemical specimens for plate 1H (1H1, 1H2, 1H4).....	121
Figure D.52. Completed tensile and chemical specimens for plate 1N (1N1, 1N2, 1N4).....	121
Figure D.53. Completed tensile and chemical specimens for plate 1Q (1Q1, 1Q2, 1Q4).....	122
Figure D.54. Completed tensile and chemical specimens for plate 1T (1T1, 1T2, 1T4).....	122
Figure D.55. Completed tensile and chemical specimens for plate 1V (1V1, 1V2, 1V4).....	122
Figure D.56. Completed tensile and chemical specimens for plate 2A (2A1, 2A2, 2A4).....	123
Figure D.57. Completed tensile and chemical specimens for plate 2B (2B1, 2B2, 2B4).....	123
Figure D.58. Completed tensile and chemical specimens for plate 2Q (2Q1, 2Q2, 2Q4).....	123
Figure D.59. Completed tensile and chemical specimens for plate 2T (2T1, 2T2, 2T4).....	124
Figure D.60. Completed tensile and chemical specimens for plate 3A (3A1, 3A2, 3A4).....	124
Figure D.61. Completed tensile and chemical specimens for plate 3B (3B1, 3B2, 3B4).....	124
Figure D.62. Completed tensile and chemical specimens for plate 3Q (3Q1, 3Q2, 3Q4).....	125
Figure D.63. Completed tensile and chemical specimens for plate 3T (3T1, 3T2, 3T4).....	125
Figure D.64. Completed tensile and chemical specimens for plate 4A (4A1, 4A2, 4A3 (4A2 duplicate), 4A4).....	126
Figure D.65. Completed tensile and chemical specimens for plate 4B (4B1, 4B2, 4B4).....	126
Figure D.66. Completed tensile and chemical specimens for plate 4Q (4Q1, 4Q2, 4Q4).....	127
Figure D.67. Completed tensile and chemical specimens for plate 4R (4R1, 4R2, 4R4).....	127
Figure D.68. Completed tensile and chemical specimens for plate 4T (4T1, 4T2, 4T4).....	127
Figure D.69. Completed tensile and chemical specimens for longitudinal stiffener plate (1U1, 2U1, 3U1, 4U1, 1U4, 2U4, 3U4, 4U4).....	128
Figure E.1. Shear fracture surfaces for plate 1A.....	132
Figure E.2. Shear fracture surfaces for plate 1B.....	132
Figure E.3. Shear fracture surfaces for plate 1C.....	133
Figure E.4. Shear fracture surfaces for plate 1H.....	133
Figure E.5. Shear fracture surfaces for plate 1N.....	134
Figure E.6. Shear fracture surfaces for plate 1Q.....	134
Figure E.7. Shear fracture surfaces for plate 1T.....	135
Figure E.8. Shear fracture surfaces for plate 1V.....	135
Figure E.9. Shear fracture surfaces for plate 2A.....	136
Figure E.10. Shear fracture surfaces for plate 2B.....	136
Figure E.11. Shear fracture surfaces for plate 2Q.....	137
Figure E.12. Shear fracture surfaces for plate 2T.....	137
Figure E.13. Shear fracture surfaces for plate 3A.....	138
Figure E.14. Shear fracture surfaces for plate 3B.....	138
Figure E.15. Shear fracture surfaces for plate 3Q.....	139
Figure E.16. Shear fracture surfaces for plate 3T.....	139
Figure E.17. Shear fracture surfaces for plate 4A.....	140
Figure E.18. Shear fracture surfaces for plate 4B.....	140
Figure E.19. Shear fracture surfaces for plate 4Q.....	141
Figure E.20. Shear fracture surfaces for plate 4R.....	141
Figure E.21. Shear fracture surfaces for plate 4T.....	142
Figure E.22. Shear fracture areas for specimen 1AX using a Mask Area Method (left) and a Pixel Intensity Method (right).....	144

Figure E.23. Shear fracture areas for specimen 1AY using a Mask Area Method (left) and a Pixel Intensity Method (right).....	144
Figure E.24. Shear fracture areas for specimen 1AZ using a Mask Area Method (left) and a Pixel Intensity Method (right).....	145
Figure E.25. Shear fracture areas for specimen 1BX using a Mask Area Method (left) and a Pixel Intensity Method (right).....	145
Figure E.26. Shear fracture areas for specimen 1BY using a Mask Area Method (left) and a Pixel Intensity Method (right).....	146
Figure E.27. Shear fracture areas for specimen 1BZ using a Mask Area Method (left) and a Pixel Intensity Method (right).....	146
Figure E.28. Shear fracture areas for specimen 1CX using a Mask Area Method (left) and a Pixel Intensity Method (right).....	147
Figure E.29. Shear fracture areas for specimen 1CY using a Mask Area Method (left) and a Pixel Intensity Method (right).....	147
Figure E.30. Shear fracture areas for specimen 1CZ using a Mask Area Method (left) and a Pixel Intensity Method (right).....	148
Figure E.31. Shear fracture areas for specimen 1HX using a Mask Area Method (left) and a Pixel Intensity Method (right).....	148
Figure E.32. Shear fracture areas for specimen 1HY using a Mask Area Method (left) and a Pixel Intensity Method (right).....	149
Figure E.33. Shear fracture areas for specimen 1HZ using a Mask Area Method (left) and a Pixel Intensity Method (right).....	149
Figure E.34. Shear fracture areas for specimen 1NX using a Mask Area Method (left) and a Pixel Intensity Method (right).....	150
Figure E.35. Shear fracture areas for specimen 1NY using a Mask Area Method (left) and a Pixel Intensity Method (right).....	150
Figure E.36. Shear fracture areas for specimen 1NZ using a Mask Area Method (left) and a Pixel Intensity Method (right).....	151
Figure E.37. Shear fracture areas for specimen 1QX using a Mask Area Method (left) and a Pixel Intensity Method (right).....	151
Figure E.38. Shear fracture areas for specimen 1QY using a Mask Area Method (left) and a Pixel Intensity Method (right).....	152
Figure E.39. Shear fracture areas for specimen 1QZ using a Mask Area Method (left) and a Pixel Intensity Method (right).....	152
Figure E.40. Shear fracture areas for specimen 1TX using a Mask Area Method (left) and a Pixel Intensity Method (right).....	153
Figure E.41. Shear fracture areas for specimen 1TY using a Mask Area Method (left) and a Pixel Intensity Method (right).....	153
Figure E.42. Shear fracture areas for specimen 1TZ using a Mask Area Method (left) and a Pixel Intensity Method (right).....	154
Figure E.43. Shear fracture areas for specimen 1VX using a Mask Area Method (left) and a Pixel Intensity Method (right).....	154
Figure E.44. Shear fracture areas for specimen 1VY using a Mask Area Method (left) and a Pixel Intensity Method (right).....	155
Figure E.45. Shear fracture areas for specimen 1VZ using a Mask Area Method (left) and a Pixel Intensity Method (right).....	155

Figure E.46. Shear fracture areas for specimen 2AX using a Mask Area Method (left) and a Pixel Intensity Method (right).....	156
Figure E.47. Shear fracture areas for specimen 2AY using a Mask Area Method (left) and a Pixel Intensity Method (right).....	156
Figure E.48. Shear fracture areas for specimen 2AZ using a Mask Area Method (left) and a Pixel Intensity Method (right).....	157
Figure E.49. Shear fracture areas for specimen 2BX using a Mask Area Method (left) and a Pixel Intensity Method (right).....	157
Figure E.50. Shear fracture areas for specimen 2BY using a Mask Area Method (left) and a Pixel Intensity Method (right).....	158
Figure E.51. Shear fracture areas for specimen 2BZ using a Mask Area Method (left) and a Pixel Intensity Method (right).....	158
Figure E.52. Shear fracture areas for specimen 2QX using a Mask Area Method (left) and a Pixel Intensity Method (right).....	159
Figure E.53. Shear fracture areas for specimen 2QY using a Mask Area Method (left) and a Pixel Intensity Method (right).....	159
Figure E.54. Shear fracture areas for specimen 2QZ using a Mask Area Method (left) and a Pixel Intensity Method (right).....	160
Figure E.55. Shear fracture areas for specimen 2TX using a Mask Area Method (left) and a Pixel Intensity Method (right).....	160
Figure E.56. Shear fracture areas for specimen 2TY using a Mask Area Method (left) and a Pixel Intensity Method (right).....	161
Figure E.57. Shear fracture areas for specimen 2TZ using a Mask Area Method (left) and a Pixel Intensity Method (right).....	161
Figure E.58. Shear fracture areas for specimen 3AX using a Mask Area Method (left) and a Pixel Intensity Method (right).....	162
Figure E.59. Shear fracture areas for specimen 3AY using a Mask Area Method (left) and a Pixel Intensity Method (right).....	162
Figure E.60. Shear fracture areas for specimen 3AZ using a Mask Area Method (left) and a Pixel Intensity Method (right).....	163
Figure E.61. Shear fracture areas for specimen 3BX using a Mask Area Method (left) and a Pixel Intensity Method (right).....	163
Figure E.62. Shear fracture areas for specimen 3BY using a Mask Area Method (left) and a Pixel Intensity Method (right). Note this specimen did not separate in two pieces.	164
Figure E.63. Shear fracture areas for specimen 3BZ using a Mask Area Method (left) and a Pixel Intensity Method (right).....	164
Figure E.64. Shear fracture areas for specimen 3QX using a Mask Area Method (left) and a Pixel Intensity Method (right).....	165
Figure E.65. Shear fracture areas for specimen 3QY using a Mask Area Method (left) and a Pixel Intensity Method (right).....	165
Figure E.66. Shear fracture areas for specimen 3QZ using a Mask Area Method (left) and a Pixel Intensity Method (right).....	166
Figure E.67. Shear fracture areas for specimen 3TX using a Mask Area Method (left) and a Pixel Intensity Method (right).....	166
Figure E.68. Shear fracture areas for specimen 3TY using a Mask Area Method (left) and a Pixel Intensity Method (right).....	167

Figure E.69. Shear fracture areas for specimen 3TZ using a Mask Area Method (left) and a Pixel Intensity Method (right).....	167
Figure E.70. Shear fracture areas for specimen 4AX using a Mask Area Method (left) and a Pixel Intensity Method (right).....	168
Figure E.71. Shear fracture areas for specimen 4AY using a Mask Area Method (left) and a Pixel Intensity Method (right).....	168
Figure E.72. Shear fracture areas for specimen 4AZ using a Mask Area Method (left) and a Pixel Intensity Method (right).....	169
Figure E.73. Shear fracture areas for specimen 4BX using a Mask Area Method (left) and a Pixel Intensity Method (right).....	169
Figure E.74. Shear fracture areas for specimen 4BY using a Mask Area Method (left) and a Pixel Intensity Method (right).....	170
Figure E.75. Shear fracture areas for specimen 4BZ using a Mask Area Method (left) and a Pixel Intensity Method (right).....	170
Figure E.76. Shear fracture areas for specimen 4QX using a Mask Area Method (left) and a Pixel Intensity Method (right).....	171
Figure E.77. Shear fracture areas for specimen 4QY using a Mask Area Method (left) and a Pixel Intensity Method (right).....	171
Figure E.78. Shear fracture areas for specimen 4QZ using a Mask Area Method (left) and a Pixel Intensity Method (right).....	172
Figure E.79. Shear fracture areas for specimen 4RX using a Mask Area Method (left) and a Pixel Intensity Method (right).....	172
Figure E.80. Shear fracture areas for specimen 4RY using a Mask Area Method (left) and a Pixel Intensity Method (right).....	173
Figure E.81. Shear fracture areas for specimen 4RZ using a Mask Area Method (left) and a Pixel Intensity Method (right).....	174
Figure E.82. Shear fracture areas for specimen 4TX using a Mask Area Method (left) and a Pixel Intensity Method (right).....	175
Figure E.83. Shear fracture areas for specimen 4TY using a Mask Area Method (left) and a Pixel Intensity Method (right).....	175
Figure E.84. Shear fracture areas for specimen 4TZ using a Mask Area Method (left) and a Pixel Intensity Method (right).....	176
Figure G.1. Macroetch of 1D5 with planar reference scales.....	185
Figure G.2. Macroetch of 1D6 with planar reference scales.....	185
Figure G.3. Macroetch of 1D7 with planar reference scales.....	186
Figure G.4. Macroetch of 1D8 with planar reference scales.....	186
Figure G.5. Macroetch of 1D9 with planar reference scales.....	187
Figure G.6. Macroetch of 1E5 with planar reference scales.....	187
Figure G.7. Macroetch of 1E6 with planar reference scales.....	188
Figure G.8. Macroetch of 1E7 with planar reference scales.....	188
Figure G.9. Macroetch of 1E8 with planar reference scales.....	189
Figure G.10. Macroetch of 1E9 with planar reference scales.....	189
Figure G.11. Macroetch of 2D5 with planar reference scales.....	190
Figure G.12. Macroetch of 2D6 with planar reference scales.....	190
Figure G.13. Macroetch of 2D7 with planar reference scales.....	191
Figure G.14. Macroetch of 2D8 with planar reference scales.....	191
Figure G.15. Macroetch of 2D9 with planar reference scales.....	192

Figure G.16. Macroetch of 2E5 with planar reference scales.....	192
Figure G.17. Macroetch of 2E6 with planar reference scales.....	193
Figure G.18. Macroetch of 2E7 with planar reference scales.....	193
Figure G.19. Macroetch of 2E8 with planar reference scales.....	194
Figure G.20. Macroetch of 2E9 with planar reference scales.....	194
Figure G.31. Macroetch of 3E5 with planar reference scales.....	195
Figure G.32. Macroetch of 3E6 with planar reference scales, taken in the vertical position (90-degree planar rotation) for improved camera focus.....	195
Figure G.33. Macroetch of 3E7 with planar reference scales, taken in the vertical position (90-degree planar rotation) for improved camera focus.....	196
Figure G.34. Macroetch of 3E8 with planar reference scales. The right half of the specimen separated during preparation and is supported by a machined 1-2-3 block.....	196
Figure G.35. Macroetch of 3E9 with planar reference scales.....	197
Figure G.36. Macroetch of 3F5 with planar reference scales.....	197
Figure G.37. Macroetch of 3F6 with planar reference scales.....	198
Figure G.38. Macroetch of 3F7 with planar reference scales.....	198
Figure G.39. Macroetch of 3F8 with planar reference scales.....	199
Figure G.40. Macroetch of 3F9 with planar reference scales.....	199
Figure G.41. Macroetch of 4E5 with planar reference scales.....	200
Figure G.42. Macroetch of 4E6 with planar reference scales.....	200
Figure G.43. Macroetch of 4E7 with planar reference scales.....	201
Figure G.44. Macroetch of 4E8 with planar reference scales.....	201
Figure G.45. Macroetch of 4E9 with planar reference scales.....	202
Figure G.46. Macroetch of 4F5 with planar reference scales.....	202
Figure G.47. Macroetch of 4F6 with planar reference scales.....	203
Figure G.48. Macroetch of 4F7 with planar reference scales.....	203
Figure G.49. Macroetch of 4F8 with planar reference scales.....	204
Figure G.50. Macroetch of 4F9 with planar reference scales.....	204

List of Tables

Table 1: Description of the structural steel.	3
Table 2: Mill testing report heats.	8
Table 3: Ultra-violet wavelength calibration for glow discharge spectrography using the NIST 1269 SRM.	13
Table 4: SRM measurement confirmation.	14
Table 5: SRM drift throughout the duration of testing.	14
Table 6: Designation for the first three alphanumeric characters of the specimen identifier.	15
Table 7: Cut plan summary.	17
Table 8: Reported yield strength, ultimate strength, and elongation from the relevant MTRs.	19
Table 9: Impact energy results from the provided MTRs.	20
Table 10: Percent weight element composition requirements for ASTM A 588 Grade A & Grade B per the 1971 specification with ASTM A 6-70 tolerances.	22
Table 11: MTR percent weight element composition.	22
Table 12: MTR conformance to ASTM A 588-71 Grade A & Grade B.	23
Table 13: MTR carbon equivalency and corrosion indices from ASTM G101-20.	25
Table 14: Summary of tensile testing results.	26
Table 15: Summary of CVN results.	29
Table 16: Conformance to ASTM A 588-71 Grade A with and without ASTM A 6-70 tolerances for heats specified as Grade A in the MTR.	30
Table 17: Conformance to ASTM A 588-71 Grade B with ASTM A 6-70 tolerances for heats specified as Grade B in the MTR.	30
Table 18: Percent weight element composition requirements for ASTM A 588-71 Grade A & Grade B with ASTM A 6-70 tolerances (as presented in Table 5) and the composition range restrictive to both grades.	31
Table 19: Conformance of plate that could not be tied to a specific heat to the restrictive requirements of both Grade A & B, as presented in Table 18.	31
Table 20: GDS measured carbon equivalency and corrosion indices from ASTM G101-20.	32
Table D-1: Tensile test results for all specimens.	128
Table D-1 (cont.): Tensile test results for all specimens.	129
Table E-1: CVN impact results in the L-T direction.	131
Table E-2: Percent shear fracture areas of CVN specimens.	143
Table E-3: Lateral expansion of CVN specimens.	177
Table E-3 (cont.): Lateral expansion of CVN specimens.	178
Table F-1: Raw GDS measurements.	180
Table F-1 (cont.): Raw GDS measurements.	181
Table F-2: Averaged GDS measurements per specimen.	182
Table F-3: NIST SRM 1269 checks.	183
Table F-4: Drift check with condition block.	183

List of Abbreviations

AASHO	American Association of State Highway Officials
AASHTO	American Association of State and Highway Transportation Officials
ASTM	American Society for Testing and Materials
AWS	American Welding Society
FHWA	Federal Highway Administration
NIST	National Institute of Standards and Technology
NTSB	National Transportation Safety Board
TFHRC	Turner-Fairbank Highway Research Center
<i>CE</i>	carbon equivalency
<i>CI</i>	corrosion index
CNC	computerized numerical control
CVN	Charpy vee notch
DIC	digital image correlation
F_y	yield strength (ksi)
F_u	ultimate strength (ksi)
GDS	glow discharge spectrography
MP	mega-pixel
MTR	mill test report
SRM	standard reference material
STR	structural (a component of the evidence identifier to signify mechanical/material testing)
UTM	universal testing machine
<i>Fe</i>	Iron
<i>C</i>	Carbon
<i>Cb</i>	former name for Niobium (<i>Nb</i>)
<i>Mn</i>	Manganese
<i>P</i>	Phosphorous
<i>S</i>	Sulfur
<i>Si</i>	Silicon
<i>Ni</i>	Nickle
<i>Cr</i>	Chromium
<i>Mo</i>	Molybdenum
<i>Cu</i>	Copper
<i>V</i>	Vanadium
<i>Nb</i>	Niobium (formerly known as Columbium (<i>Cb</i>))
<i>Zr</i>	Zirconium
<i>Ti</i>	Titanium

1 INTRODUCTION

The Fern Hollow Bridge carried Forbes Avenue over Fern Hollow and 9 Mile Run through Frick Park within the City of Pittsburgh, Pennsylvania. The bridge used a rigid, K-frame superstructure type built-up with ASTM A 588 uncoated weathering steel. On January 28th, 2022, the bridge collapsed. Investigators from the National Transportation Safety Board (NTSB) were dispatched to the scene. Engineers from the Federal Highway Administration (FHWA) were also dispatched to the scene to assist NTSB with the investigation. During the on-site investigation, evidence was collected which was to be later used to assist in determining the cause of the bridge failure.

The extracted evidence was transported to the FHWA’s Turner-Fairbank Highway Research Center (TFHRC) in McLean, Virginia for testing and assessment.

1.1 Description of structural components retained after the collapse

To assist in orientation of the evidence being tested, Figs. 1 and 2 provide a plan view orthomosaic photograph and elevation view line drawing of bridge. The plan view includes cardinal coordinates and a naming convention for the legs and abutments, consistent with the latest bridge inspection report. The first index of the naming convention is “B” for bent. The second index is the numeric “1” or “2”, meant to indicate the first and second bent away from the near (west) abutment. The final index is the letter “L” or “R”, representing left or right when looking east from the near abutment.



Figure 1. Orthomosaic Plan View (from NTSB).

Figure 2 provides labels for each span and similar detail about the supports as was shown in Fig. 1. Note that the obtuse angle at the top of each leg corresponds to Span 2, while the acute angle corresponds to Span 1 for the legs in Bent 1 and Span 3 for the legs in Bent 2.

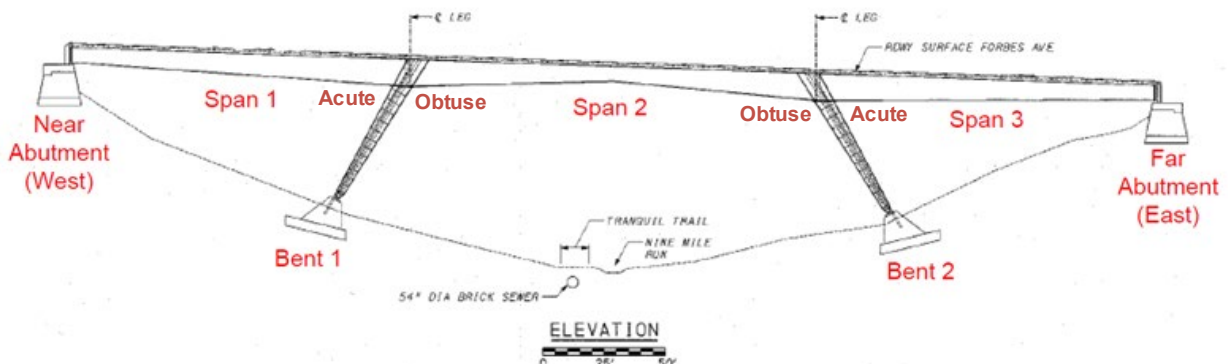


Figure 2. Elevation View, looking north (modified from NTSB provided figure).

Note that the mill testing reports (MTRs) were not located until the end of May 2022. Therefore, at the time of the extraction of components to be retained (in early February 2022), each unique plate thickness making up each leg, and the girder plate directly above each leg, had been assumed to come from a unique heat and given a unique evidence number by NTSB. Table 1 summarizes the location, provides a description, and gives approximate dimensions (measured prior to being flame cut from the recovered steel pieces on the collapse site; photos provided in Appendix A) for each recorded piece of evidence. Note that evidence numbers and a description of the wire cable from the lateral bracing retrofit are excluded from this document for brevity. Figures 3 through 6 supplement Table 1 by providing marked-up design drawings overlaid with each piece of evidence.

The legs are I-sections with three web plate thicknesses ($\frac{1}{2}$ -inch, $\frac{11}{16}$ -inch, and $\frac{13}{16}$ -inch), two flange thicknesses ($2\frac{1}{4}$ -inch and $2\frac{1}{2}$ -inch), one transverse stiffener plate thickness to stiffen the leg web ($\frac{7}{16}$ -inch), one longitudinal stiffener plate thickness to stiffen the leg web ($\frac{1}{2}$ -inch), and one “tie plate” anchoring the change in flange taper at the top of the shoe ($\frac{3}{4}$ -inch). Note that the term “shoe” corresponds to the base of each leg, circled in Figs. 3 through 6. The girder I-sections above the legs have a web plate of $\frac{13}{16}$ -inch thickness and flange plates of $3\frac{1}{8}$ -inch thickness. Table 2 summarizes the mill testing certificate heat numbers for each aforementioned thickness.

Table 1: Description of the structural steel.

Leg	Item Description	Evidence Number	Approximate Dimensions
B1R	Top Flange Girder & Web Girder	NTSB-STR-001	24"x96"x39"
	Bot Flange Girder	NTSB-STR-002	24"x129"x17"
	Span 2 (Obtuse) End Plate Weld	NTSB-STR-003	24"x129"x33"
	Span 1 (Acute) End Plate Weld	NTSB-STR-004	24"x12"x8"
	Span 2 Fracture Face	NTSB-STR-005	12"x6"x5"
	Panel 11, Web	NTSB-STR-006	8"x54"x8"
	Panel 10, Web & Flanges	NTSB-STR-007	69"x55"x24"
	Panel 7, Span 2 Flange	NTSB-STR-008	24"x3"x45"
	Panel 4, Web	NTSB-STR-009	27"x32"x7"
	Separated Span 2 Flange from Shoe	NTSB-STR-010	31"x80"x67"
	Shoe & Span 1 Flange	NTSB-STR-011	132"x62"x41"
B1L	Top Flange Girder & Web Girder	NTSB-STR-012	24"x40"x116"
	Bot Flange Girder	NTSB-STR-013	138"x24"x19"
	End Plate Web, Flanges, & Welds	NTSB-STR-014 [†]	114"x24"x40"
	Panel 5, Web	NTSB-STR-015	42"x21"x7"
	Panel 3, Web & Flanges	NTSB-STR-016	44"x47"x24"
	Shoe	NTSB-STR-017	83"x44"x24"
B2L	Top Flange Girder & Web Girder	NTSB-STR-018	70"x40"x24"
	Bot Flange Girder	NTSB-STR-019	125"x25"x24"
	End Plate Welds	NTSB-STR-020	114"x24"x5"
	Span 3 Fracture Face	NTSB-STR-021	12"x6"x7"
	Panel 11, Web, Flanges & Long. Stiff	NTSB-STR-022	56"x74"x24"
	Panel 8, Web	NTSB-STR-023	25"x54"x8"
	Panel 3, Web & Flanges	NTSB-STR-024	44"x49"x24"
	Shoe	NTSB-STR-025	24"x44"x84"
B2R	Top Flange Girder & Web Girder	NTSB-STR-026	70"x24"x20"
	Bot Flange Girder	NTSB-STR-027	125"x24"x20"
	End Plate Welds	NTSB-STR-028A	118"x94"x41"
	Panel 12, Web & Flanges	NTSB-STR-028B	118"x94"x41"
	Panel 9, Web	NTSB-STR-029	54"x32"x8"
	Panel 6, Span 3 Flange	NTSB-STR-030	45"x24"x3"
	Panel 3, Web	NTSB-STR-031	36"x44"x10"
	Shoe & Span 2 Flange	NTSB-STR-032	48"x120"x48"

[†]NTSB-STR-014 has weld assessment as well as mechanical and material testing. The corresponding label font in Fig. 4 is colored accordingly.

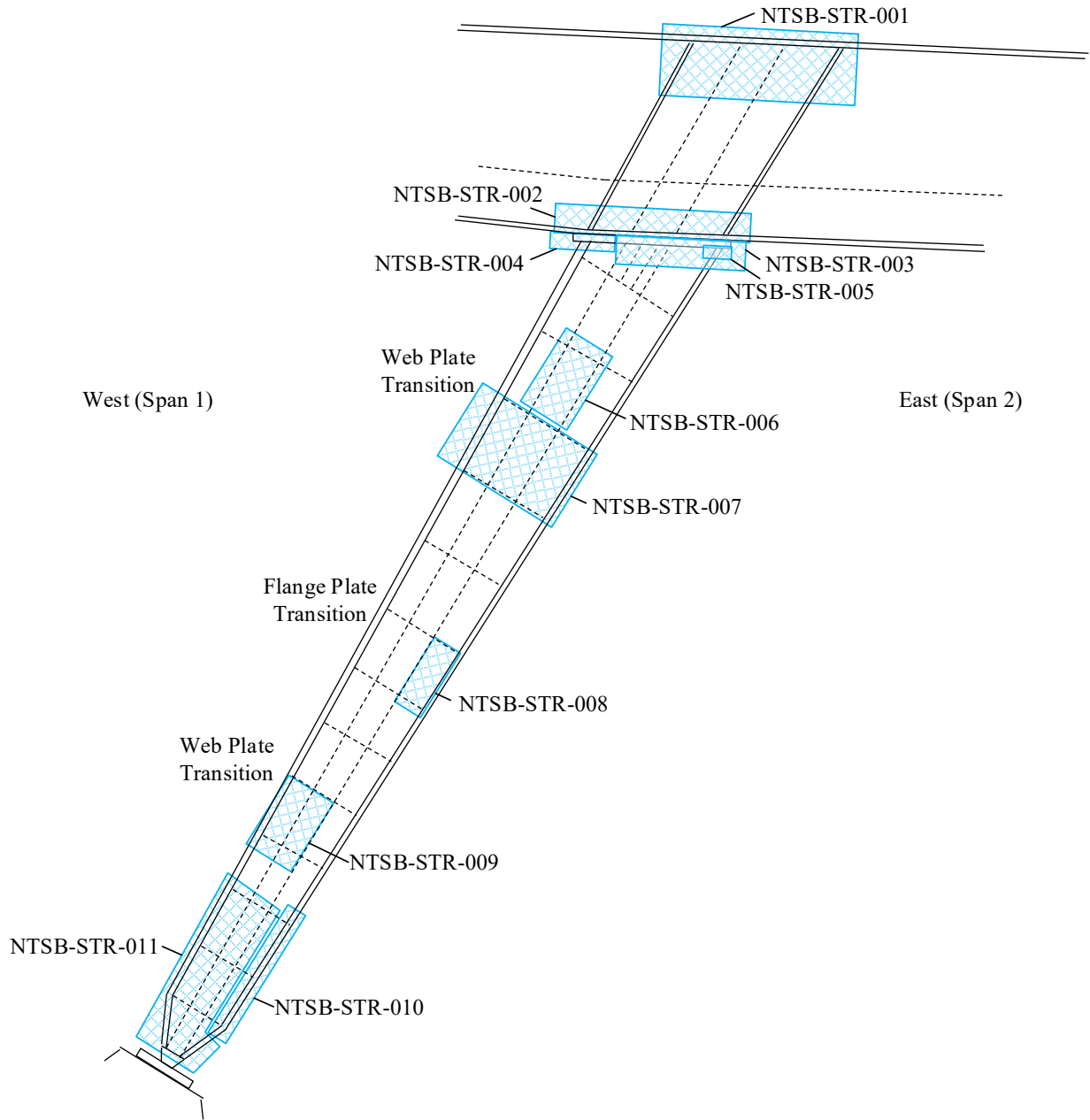


Figure 3. B1R – South-West Leg.

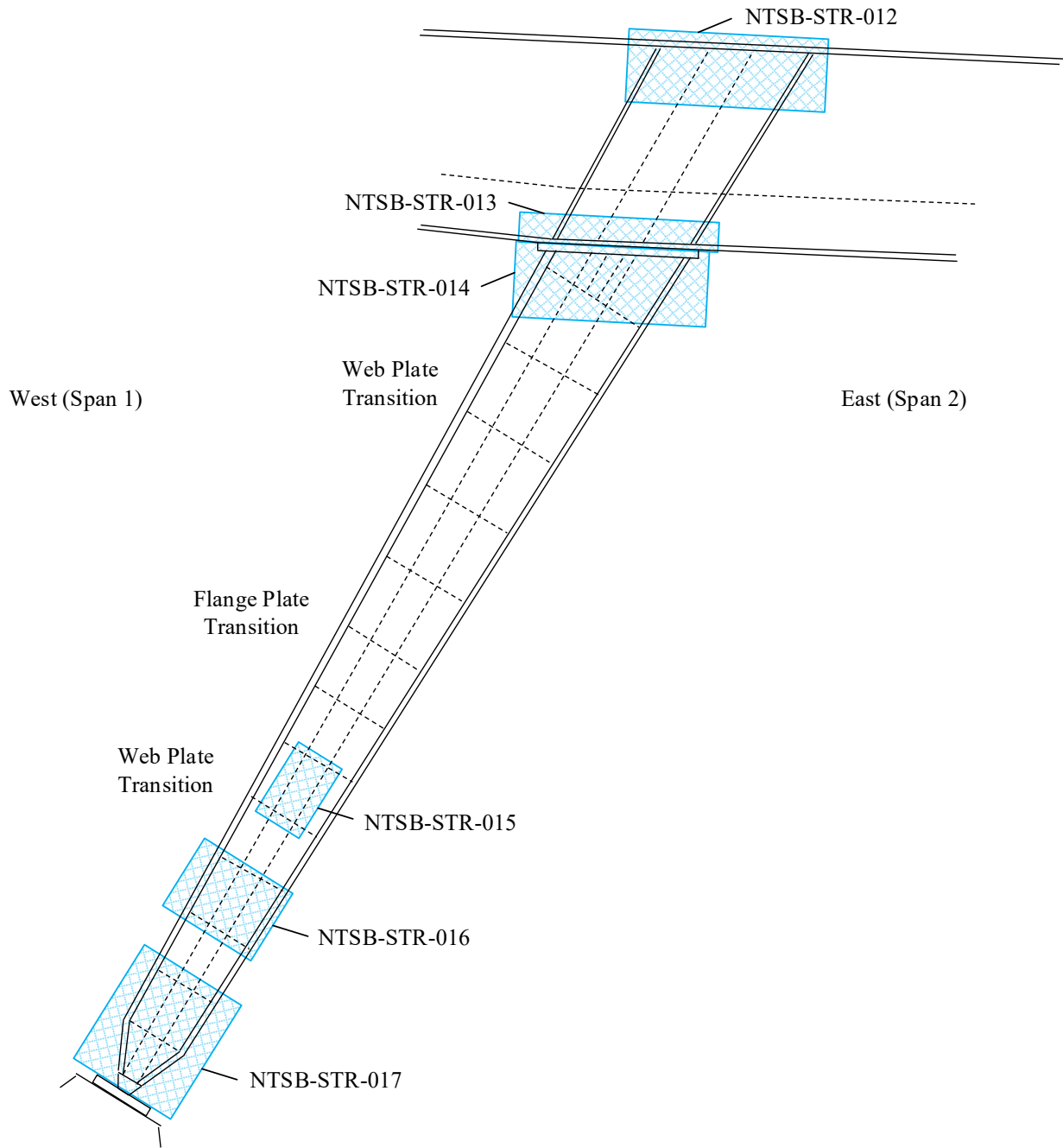


Figure 4. B1L – North-West Leg.

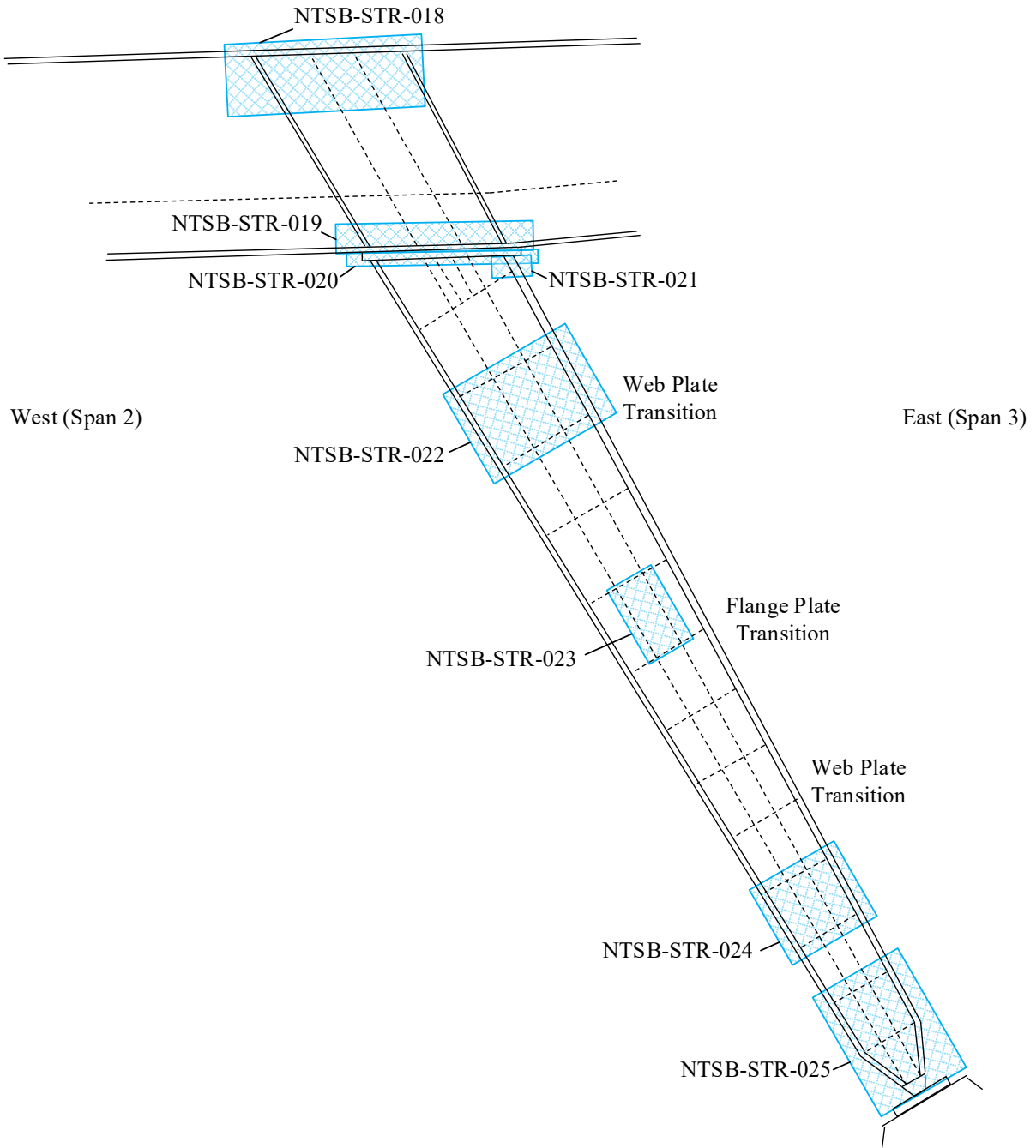


Figure 5. B2L – North-East Leg.

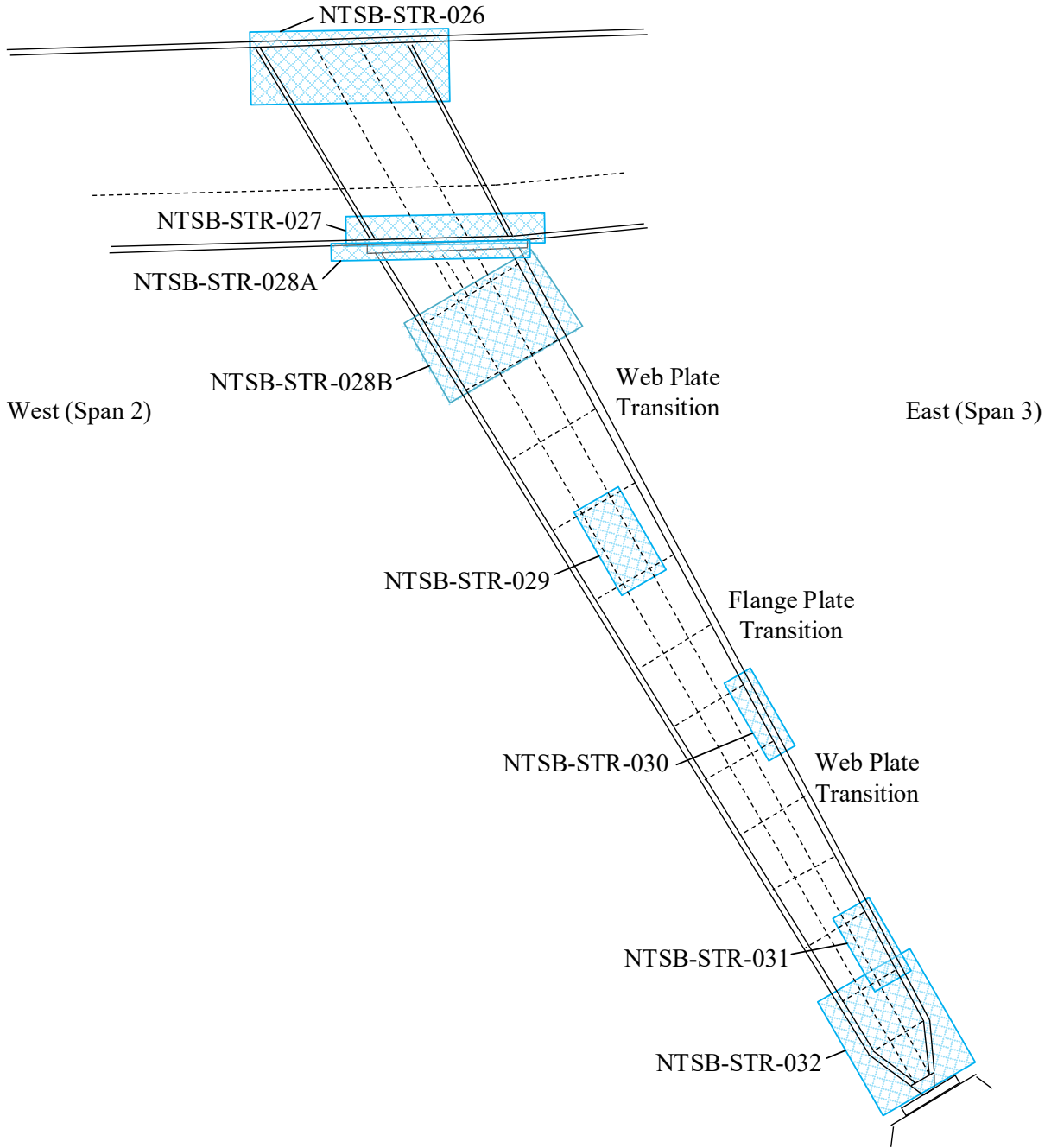


Figure 6. B2R – South-East Leg.

Table 2: Mill testing report heats.

Plate Thickness (inches)	Heat Number(s)	Notes
1/2	422H2271, 74C184, 661H632, 661H352, 662H868, 645H218, 645H090, 650J220	It was not possible to strictly associate plates with Heat Numbers based on plate dimensions. Therefore, it was assumed that every 1/2-inch thick plate was unique.
1/16	74C184, 662H404	Delivered plate dimension indicate leg webs could only have come from Heat 74C184.
3/4	658J291	Single heat number for the “tie plate”.
13/16	801H11600, 801H12930, 801H15770, 802E00400, 74C184	It was not possible to strictly associate plates with Heat Numbers based on plate dimensions. Therefore, it was assumed that every 13/16-inch thick plate was unique.
2 1/4	649H558	Single heat number for leg flanges.
2 1/2	67C262, 659H518	Delivered plate dimensions indicate leg flange could only have come from Heat 67C262.
3 1/8	422H3271, 421H1431, 649H558	Plate dimensions of delivered plate indicate all girder bottom flanges came from Heat 649H558. Girder top flanges came from Heats 422H3271 and 421H1431, thus each top flange sample was considered unique.

1.2 Report scope

This factual report documents the evidence received by TFHRC and describes the assessments and testing completed on the evidence. The cumulative testing plan encompasses work done within and exterior to TFHRC; presentation herein of test results is limited to mechanical and material testing performed by TFHRC personnel.

2 TESTING PLAN

All relevant structural steel within the legs and girders was specified to be ASTM A 588 with nominal 50 ksi yield and 70 ksi tensile strength. Tensile coupons were pulled in duplicate for each unique heat in each leg and in the portion of the girder above each leg. Charpy vee notch (CVN) specimens were tested in triplicate for each unique heat and thickness.

Metallographic assessment of the welds between the top of each leg and its end plate, at both the obtuse (Span 2) and acute (Span 1; Span 3) angles, investigated weld quality and the possibility of fatigue cracking. Assessment was done by conducting five, equally spaced macro etches across the width of intact welds that had not fractured open during the collapse.

Assessment of the chemical composition of the steel was conducted on each unique heat using glow discharge spectrography.

NTSB conducted fractography on exposed fracture surfaces of interest within each leg.

NTSB contracted an external vendor to conduct corrosion mapping on the base of each leg (generally from the base of the shoe through the first web panel) using a structured light metrology technique.

2.1 Work completed at the bridge collapse site

FHWA assisted NTSB in identifying and marking evidence to be cut from larger portions of the legs and girders for retention and testing.

NTSB conducted laser scanning at the bridge collapse site to document the global geometry of key parts of the structure. The leg pieces were scanned in the upright (standing on a flange face) condition prior to cutting out evidence specimens for further testing. Similarly, the girder pieces were scanned; however, these pieces were generally scanned with the plane of the web parallel to the ground. Specimens were pressure washed when large amounts of dirt and debris were present. Exclusive of the corrosion mapping of the components near the shoe (conducted at TFHRC), the resolution of the laser scan is expected to be sufficient for analytical modeling and other assessments requiring measured geometry.

2.2 Work conducted outside of TFHRC

The shoe of each leg (NTSB-STR-010 & NTSB-STR-011, NTSB-STR-017, NTSB-STR-025, and NTSB-STR-032) was cleaned by dipping each piece of evidence in a caustic bath, a process generally used as a precursor step for hot-dip galvanizing, by V&S Galvanizing in Columbus, OH. The caustic bath was used in lieu of other options (e.g., a low pressure (<80 psi) abrasive cleaning) that may damage very thin plate.

After cleaning, the pieces were received at TFHRC in late March 2022.

NTSB conducted fractography on exposed fracture surfaces of interest within each leg at their laboratory.

2.3 Work conducted by NTSB at TFHRC

NTSB contracted an external vendor to conduct corrosion mapping on the base of each leg using a structured light metrology technique. Scans were conducted at TFHRC in September 2022 by CreaForm using their proprietary MetraSCAN 3D and HandyScan 3D devices. These higher fidelity metrology scans supplemented the laser scanning discussed in Section 2.1 of this report.

2.4 Description of evidence storage at FHWA

Upon receipt at TFHRC, the cleaned shoes were stored inside the TFHRC Structural Testing Lab until the completion of corrosion mapping in September 2022. After completion of the corrosion mapping the specimens were stored in a secure external location within the gated property of TFHRC. Fracture faces (NTSB-STR-005 and NTSB-STR-021) were temporarily stored inside locked federal office space, then transferred to NTSB's laboratory in April 2022.

All other structural steel pieces, steel in build-up wooden boxes, and cables were stored at a secure location within the gated property of TFHRC.

2.5 Testing Completed by FHWA at TFHRC

Each unique heat for the legs, and for the girder portion above the legs, had two tensile coupons pulled to rupture per ASTM A370, triplicate standard CVNs tested per ASTM A370, and chemical assessment completed per ASTM E415. Additionally, metallographic assessment of the welds between the flanges and base plate at the tops of each leg was completed. Original fabrication shop drawings were not found by any of the associated parties, and no splices between plates of the same size were observed, so it is assumed that within each leg, steel of the same continuous plate thickness is from the same heat. One coupon blank was also extracted per unique heat; this blank has been retained but will only be machined and tested if justified. Note that CVNs and the coupon blank were not extracted for the longitudinal stiffeners.

2.5.1 Tensile testing

Tensile coupons were tested with their longitudinal direction aligned with the speculated direction of roll in the steel plate. Due to length and width of most plates, the direction of roll for flanges, webs, and longitudinal stiffeners had to be aligned with the long direction of the member. The direction of roll for transverse stiffeners and the “tie plate” was not specifically known, but tensile specimens were oriented in a direction of their greatest direction. This detail is noted because in the modern era, hot-rolled plate is tensile tested in the transverse direction, but per ASTM A 6 up through 1974, testing was performed in the longitudinal direction. (Note that up through the mid-1990s, ASTM included a space between the letter and number of specification titles; the space was later removed.)

2.5.1.1 Tensile testing protocol

Eight-inch and two-inch gauge length plate-type specimens were fabricated according to the geometric requirements described in in ASTM A370-21 Figure 4. All specimens have eight-inch gauge lengths except for specimens from the plate in evidence number NTSB-STR-009 (denoted as 1T in the cut plan) and the “tie plate” (denoted as 1V in the cut plan). A two-inch gauge length was needed for NTSB-STR-009 to satisfy thickness requirements caused by excessive plate distortion, pitting corrosion, and general section loss. A two-inch gauge length was needed for the “tie plate” since the clear distance between stiffeners welded to the plate was only 10-inches. Both plate type coupons included an optional taper of width resulting in no more than a 0.015-inch difference between the ends of the reduced section and the center per ASTM A370-21 Figure 4 Note 3. The specimens were machined flat to remove distortion and nonuniform corrosion per ASTM A370-21 Section 5.3. Figure 7 of this report shows dimensions for both plate-type tensile coupons.

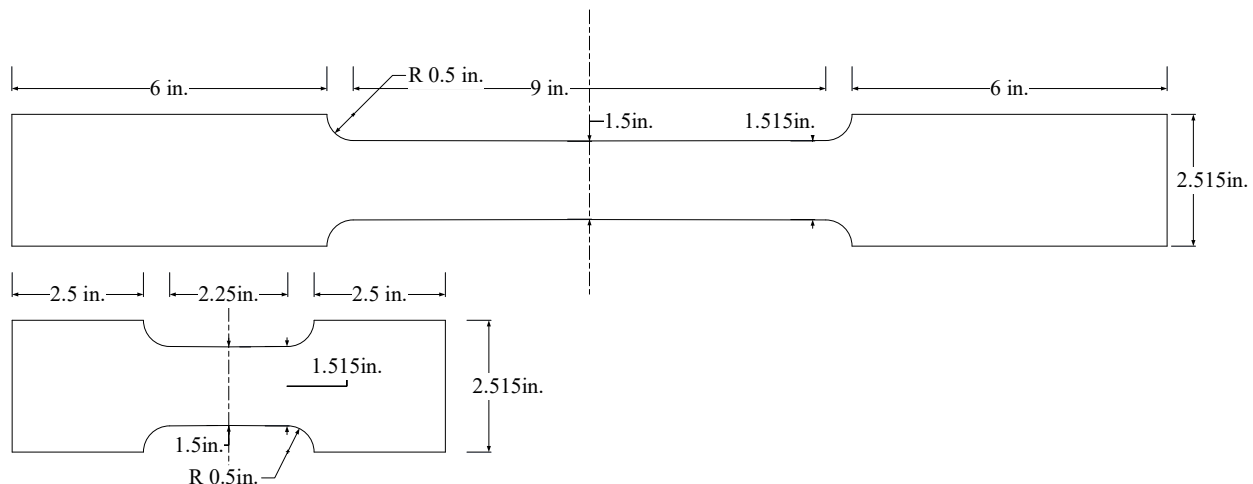


Figure 7. Tensile coupon dimensions.

The tension testing was conducted in a MTS 244.51 220-kip capacity and a MTS 311.41 550-kip capacity servovalve controlled hydraulic test frame. Machine conformance and testing procedure follow ASTM A370-21. The 220-kip frame was used for tensile specimens with a thickness less than or equal to $1 \frac{5}{8}$ -inch, The 550-kip frame had the required capacity to test the remaining thicker specimens. Each frame was fitted with side-loading hydraulic wedge grips for gripping onto specimens. Each frame was controlled by a dedicated controller and computer that also collected data throughout the execution of each test. Machine

calibration certificates are provided in Appendix H; note that on the calibration certificate a blank highlighted box indicates that the machine was within tolerance.

The same loading program was used for both machines. The program requires the user to enter the specimen “reduced length” as it is used to determine the crosshead displacement rate. A succinct description of the loading program is as follows:

1. The user enters the reduced length of the specimen.
2. The initial displacement rate is set at 0.015 in./min. per inch of reduced length.
3. At an axial strain of 0.015, the displacement rate increases to 0.016 in./min. per inch of reduced length.
4. At an axial strain of 0.020, the displacement rate increases to 0.021 in./min. per inch of reduced length.
5. At an axial strain of 0.025, the displacement rate increases to 0.032 in./min. per inch of reduced length.
6. At an axial strain of 0.030, the displacement rate increases to 0.055 in./min. per inch of reduced length.
7. At an axial strain of 0.035, the displacement rate increases to 0.109 in./min. per inch of reduced length. This loading rate does not change for the remainder of the test.

For determining yield strength, ASTM A370-21 requires the displacement rate to be between $1/160$ and $1/16$ in./min. per inch of reduced length in the specimen. For determining tensile strength, ASTM A370-21 requires the displacement rate to be between $1/20$ and $1/2$ in./min. per inch of reduced length in the specimen. Therefore, the loading program fits within and is on the slower end of the ASTM A370-21 displacement rate ranges.

A video extensometer was used to monitor strain and capture elongation at fracture. This device operates on the principle of digital image correlation (DIC). The video camera is able to track the motion of image pixels, and through calibration, pixels are converted to specimen displacements. Uniaxial strain was determined by analyzing the captured video extensometer data over the gauge length of the specimen. DIC camera calibration certificates are provided at the end of the report.

2.5.2 CVN testing

The construction plans for the bridge stated that design was in accordance with the AASHTO Standard Specifications for Highway Bridges – 10th Edition (1969) and welding was in accordance with the AWS D2.0 Specifications for Welded Highway and Railway Bridges – 8th Edition (1969). Between these two specifications, weldments from ASTM A 588 had mandatory CVN energy requirements for the base metal and weld metal.

2.5.2.1 CVN testing protocol

Standard sized CVN specimens were fabricated in the L-T orientation for all plates. That is, the long dimension of the CVN specimen was aligned with the assumed direction of roll for the tension specimens, and the notch was cut such that the fracture during testing would propagate transverse to the roll direction. Samples were taken from the $1/4$ thickness for all plates to match the practice used in the early 1970’s, unless the plate is less than $7/8$ -inch thick wherein the sample was taken from the center of the plate. Machine

conformance, fabrication dimensions and tolerance requirements for standard size specimens, and testing procedure all followed ASTM A370 (supplemented by ASTM E23). The impact requirements were 15 ft-lbf @ 40°F for the base metal; weld metal was not tested for conformance. A 300 ft-lbf Tinius Olsen impact testing machine was used to conduct the testing. Machine calibration certificates are provided in Appendix H.

2.5.3 Chemistry assessment

Provided mill test reports show that the two plate manufacturers, United States Steel Corporation and Bethlehem Steel Corporation, explicitly specified Grade A and B of ASTM A 588. Grades A and B specify composition limits for iron, carbon, manganese, phosphorus, sulfur, silicon, chromium, copper, and vanadium. Grade B further specifies composition limits for nickel.

2.5.3.1 Chemistry testing protocol

Verification of chemical conformance to ASTM A 588-71 (see Section 4.3 for discussion of the binding year) was checked through the use of glow discharge spectrography (analogous with spark atomic emission spectrometry). This testing process follows ASTM E415-21 in which element mass fractions are measured through the concentration of photons emitted at various ultra-violet wavelengths of a plasma discharge from the sample.

Chemistry was conducted using a LECO GDS500A for each unique heat, as identified in Table 2. Per Section 13.2 and 14.1 of ASTM E415-21, each sample was measured twice and averaged for the calculation of the element mass fractions. The GDS500A service report is included in Appendix H.

Care was taken to ensure contamination of the chemistry did not occur during specimen preparation by excluding the use of silicon carbide and aluminum oxide sanding paper, and instead using 120 grit zirconium sanding paper (LECO GDS Sample Preparation Guide 12.17, see Appendix H). Note ASTM A 588-71 Grade A & Grade B does not specify a required zirconium content.

Prior to testing, all manufacturer recommended practices were followed including a 48-hour minimum warm-up cycle of the testing machine. Following ASTM E415-21 Section 12.1, multiple conditioning (i.e., drift correction) samples were run until machine stabilization occurred; thereafter calibration and testing were completed. Verification of calibration against the standard reference material (SRM) was checked prior to, twice during, and after completion of the testing. Conditioning and calibration results are provided in Appendix F.

NIST Check Standard 1269 (Line Pipe Steel) was used as the verifier; Table 3 provides the corresponding calibrated ultra-violet wavelengths.

Table 3: Ultra-violet wavelength calibration for glow discharge spectrography using the NIST 1269 SRM.

Element	Discharge wavelength (nm)
Iron	249
Carbon	165
Manganese	403
Phosphorus	177
Sulfur	180
Silicon	Calculated
Nickel	341
Chromium	Calculated
Molybdenum	386
Copper	327
Vanadium	411
Columbium	405
Zirconium	360
Titanium	334

Note that “Calculated” defers to the equipment manufacturer’s method for measuring mass fraction calibration for the accumulated photons.

LECO (the equipment manufacturer) recommends that the acceptance of the measured results be assessed using a total uncertainty budget, following a sum of errors procedure using the error propagation law (see Appendix H), as shown in Equation 1.

$$\text{Test Result} = \text{Certified Value} \pm (s * t) \quad (1)$$

The SRM was measured four times; resulting in a t value of 2.776 for a two tail 95% confidence interval. The certified value is explicitly stated in the SRM NIST Certificate. The uncertainty, s , is the square root of the sum of the squares (NIST 2012), where the considered uncertainties are those reported in the NIST certificate, a known machine mass fraction measurement tolerance of 0.008, and the standard deviation of the magnitudes of the verification checks (intra-laboratory precision and bias). It is noted that additional uncertainty, such as interlaboratory precision and bias, will likely increase the bounds of the confidence interval. A summary of the SRM values, the verification checks, and calculated bounds of a 95% confidence interval is provided in Table 4.

Table 4: SRM measurement confirmation.

Element	NIST 1269 SRM		GDS 1269 SRM Checks				Statistics		
	Certified Value (% weight)	Estimated Uncertainty	Start	During (First)	During (Second)	Finish	Standard Deviation	Upper Limit	Lower Limit
Carbon	0.298	0.004	0.300	0.293	0.300	0.300	0.003	0.324	0.272
Manganese	1.35	0.02	1.376	1.373	1.401	1.389	0.011	1.417	1.283
Phosphorus	0.012	0.002	0.010	0.011	0.011	0.011	0.000	0.035	0.000
Sulfur	0.0061	0.0004	0.003	0.004	0.003	0.002	0.001	0.028	0.000
Silicon	0.189	0.008	0.190	0.190	0.184	0.182	0.004	0.222	0.156
Copper	0.095	0.005	0.090	0.091	0.085	0.084	0.003	0.123	0.067
Nickel	0.108	0.005	0.104	0.104	0.106	0.107	0.001	0.134	0.082
Chromium	0.201	0.009	0.190	0.192	0.200	0.198	0.004	0.236	0.166
Vanadium	0.004	0.001	0.011	0.011	0.011	0.011	0.000	0.026	0.000
Molybdenum	0.036	0.003	0.034	0.034	0.038	0.039	0.002	0.061	0.011
Lead	0.005	0.001	—	—	—	—	—	—	—
Aluminum	0.016	0.003	—	—	—	—	—	—	—

Note: “—” indicates that the element mass fraction is not specified in ASTM A 588 and therefore not presented here.

From Table 4, all the elements have all checks fall within the expected confidence interval. Note that lead and aluminum are certified in the NIST 1269 SRM but are not a specified in the ASTM A 588 composition, therefore the statistics are excluded.

Drift of the verification samples throughout the duration of the testing are summarized in Table 5.

Table 5: SRM drift throughout the duration of testing.

Element	Initial 1269 SRM Check (% weight)	Difference from initial (% weight)		
		During (First)	During (Second)	Final
Carbon	0.30	0.01	0.00	0.00
Manganese	1.38	0.00	-0.03	-0.01
Phosphorus	0.01	0.00	0.00	0.00
Sulfur	0.00	0.00	0.00	0.00
Silicon	0.19	0.00	0.01	0.01
Copper	0.09	0.00	0.00	0.01
Nickel	0.10	0.00	0.00	0.00
Chromium	0.19	0.00	-0.01	-0.01
Vanadium	0.01	0.00	0.00	0.00
Molybdenum	0.03	0.00	0.00	-0.01

2.5.4 Metallographic assessment

Metallographic assessment of the welds between the top of each leg and the base plate, at both the obtuse (Span 2) and acute (Span 1; Span 3) angles, was assessed for fatigue cracking and quality of the weld. Assessment was done by sectioning through the weld at five equally spaced points across the width of intact welds. Sections were ground, polished, and etched with a 5-percent solution of nitric acid in ethyl alcohol (Nital) to expose the weld macrostructures and any discontinuities within them.

Images were captured in a light box using a 20.2 MP camera with a dynamic optical lens set to roughly 20 mm at an approximately 16 in. standoff.

3 CUT PLAN

The labeling scheme for specimens cut from evidence follows a three-character alphanumeric identifier. The first character is a number assigned to an individual leg as shown in Table 6. The second character represents the location from which the plate was cut in the leg or girder. Leg and location designators are provided in Table 6. The third character represents a replicate designator. For coupons, the replicate number follows increasing coupon numbers representing north to south for flange plate and uphill to downhill for web and stiffener plate. The coupon blank is always given the replicate number “3”. A sample for chemistry was taken from the grip portion of each coupon labeled with the replicate number “1”; this sample was captured after mechanical testing was complete and was given a replicate number “4”. Replicate numbers between five and nine were used for weld macro-etches across the width of an intact weld, increasing from north to south. CVN designators use sequential letters “X”, “Y”, and “Z”. Replicant designators are also summarized in Table 6. As an example, the northern coupon extracted from the Span 2 Leg Flange (2 1/4-inch thickness) in Panel 7 of B1R corresponds to the identifier “1N1”.

Table 6: Designation for the first three alphanumeric characters of the specimen identifier.

Leg Designator	Leg	Location Designator	Plate Location	Replicate Designator	Description
1	B1R	A	Girder Top Flange	1	North/Uphill
2	B1L	B	Girder Web	2	South/Downhill
3	B2L	C	Girder Bottom Flange	3	Blank
4	B2R	D	Span 1 End Plate	4	Chemistry
		E	Span 2 End Plate	5 to 9	Weld Etches
		F	Span 3 End Plate	0	North to South Additional Weld Section
		G	Span 1 Leg Flange – 2 1/2-inch Thickness	X, Y, Z	CVN
		H	Span 2 Leg Flange – 2 1/2-inch Thickness		
		J	Span 3 Leg Flange – 2 1/2-inch Thickness		
		K	Span 1 Leg Flange – 2 1/4-inch Thickness		
		N	Span 2 Leg Flange – 2 1/4-inch Thickness		
		P	Span 3 Leg Flange – 2 1/4-inch Thickness		
		Q	Leg Web – 13/16-inch Thickness		
		R	Leg Web – 11/16-inch Thickness		
		T	Leg Web – 1/2-inch Thickness		
		U	Longitudinal Stiffener		
		V	Transverse Stiffener in the Shoe – Referred to as the “tie plate”		

Table 7 summarizes the cut plan for conducting mechanical testing, weld assessment, and chemistry. The cut plan reflects the exclusion of multiple specimen replicates when plates were identified to come from the same heat (see details provided in Table 2). Bolts and loose components were tracked by evidence number but not given unique identifiers.

Appendix B provides line drawings of nested specimens for mechanical testing and for weld assessment on the steel received at TFHRC. A minimum of 1 1/2-inch clear space was provided around the test specimens as a barrier for flame cut heat affected zones and for vertical bandsaw blade kerf. Final specimens were cut to shape using a computerized numerical control (CNC) mill. The nesting patterns were marked up with soap stone on the evidence (not shown) to ensure sufficient clear plate was available for each cut. The web in each leg has a tapered depth, where the leg is deep towards the girder and shallow at the shoe. Conservatively, the line drawings represent the web depth as constant using the depth of 42-inches, the measured depth in Panel 3. Note that the distance between the longitudinal stiffeners is more than sufficient to nest three 8-inch gauge length coupons with the 1 1/2-inch clear space.

After rough cutting, further cuts were made on a vertical band saw to make the pieces workable for machining. Detailed shop drawings are provided in Appendix C.

Line drawings for weld assessment are drawn as nominal. Many of the welds have partial or substantial fractures. In these cases, if a sufficient length of weld remained intact, five macro etches were taken across a uniform spacing of the remaining weld. All weld line drawings are provided in Appendix C.

Table 7: Cut plan summary.

Leg	Evidence Number	Evidence Sub-Labeling and Testing Protocol								
		Tensile Testing			Weld Assessment	Fractography	Corrosion Mapping	CVN	Chemistry	Cut Plate
		220 kip	550 kip	Blank						
B1R	NTSB-STR-001	1B1, 1B2	1A1, 1A2	1A3, 1B3				1AX, 1AY, 1AZ, 1BX, 1BY, 1BZ	1A4, 1B4	1A, 1B
	NTSB-STR-002		1C1, 1C2	1C3				1CX, 1CY, 1CZ	1C4	1C, 1C
	NTSB-STR-003				1E5, 1E6, 1E7, 1E8, 1E9, 1E0					1D, 1E
	NTSB-STR-004				1D5, 1D6, 1D7, 1D8, 1D9, 1D0					
	NTSB-STR-005					1				
	NTSB-STR-006	1Q1, 1Q2		1Q3				1QX, 1QY, 1QZ	1Q4	1Q
	NTSB-STR-007	1U1	1H1, 1H2	1H3				1HX, 1HY, 1HZ	1H4, 1U4	1H, 1U
	NTSB-STR-008		1N1, 1N2	1N3				1NX, 1NY, 1NZ	1N4	1N
	NTSB-STR-009	1T1, 1T2		1T3				1TX, 1TY, 1TZ	1T4	1T
	NTSB-STR-010					1	1			
	NTSB-STR-011	1V1, 1V2		1V3			1	1VX, 1VY, 1VZ	1V4	1V
B1L	NTSB-STR-012	2B1, 2B2	2A1, 2A2	2A3, 2B3				2AX, 2AY, 2AZ, 2BX, 2BY, 2BZ	2A4, 2B4	2A, 2B
	NTSB-STR-013									
	NTSB-STR-014	2Q1, 2Q2		2Q3	2D5, 2D6, 2D7, 2D8, 2D9, 2D0, 2E5, 2E6, 2E7, 2E8, 2E9, 2E0			2QX, 2QY, 2QZ	2Q4	2D, 2E, 2Q
	NTSB-STR-015									
	NTSB-STR-016	2T1, 2T2, 2U1		2T3				2TX, 2TY, 2TZ	2T4, 2U4	2T, 2U
	NTSB-STR-017						1			
B2L	NTSB-STR-018	3B1, 3B2	3A1, 3A2	3A3, 3B3				3AX, 3AY, 3AZ, 3BX, 3BY, 3BZ	3A4, 3B4	3A, 3B
	NTSB-STR-019									
	NTSB-STR-020				3E5, 3E6, 3E7, 3E8, 3E9, 3E0, 3F5, 3F6, 3F7, 3F8, 3F9, 3F0					3E, 3F
	NTSB-STR-021					1				
	NTSB-STR-022	3Q1, 3Q2		3Q3				3QX, 3QY, 3QZ	3Q4	3Q
	NTSB-STR-023									
	NTSB-STR-024	3T1, 3T2, 3U1		3T3				3TX, 3TY, 3TZ	3T4, 3U4	3T, 3U
	NTSB-STR-025						1			
B2R	NTSB-STR-026	4B1, 4B2	4A1, 4A2	4A3, 4B3				4AX, 4AY, 4AZ, 4BX, 4BY, 4BZ	4A4, 4B4	4A, 4B
	NTSB-STR-027									
	NTSB-STR-028A				4E5, 4E6, 4E7, 4E8, 4E9, 4E0, 4F5, 4F6, 4F7, 4F8, 4F9, 4F0					4E, 4F
	NTSB-STR-028B	4Q1, 4Q2		4Q3				4QX, 4QY, 4QZ	4Q4	4Q
	NTSB-STR-029	4R1, 4R2, 4U1		4R3				4RX, 4RY, 4RZ	4R4, 4U4	4R, 4U
	NTSB-STR-030									
	NTSB-STR-031	4T1, 4T2		4T3				4TX, 4TY, 4TZ	4T4	4T
	NTSB-STR-032						1			
Testing Count		32	14	21	48	3	5	63	25	-

¹ Testing of evidence is nondestructive.

4 MTR ASSESSMENT

The MTR for each heat of steel used in the bridge were compiled by NTSB and provided to TFHRC in late May 2022. The steel heats are described in Table 2. These MTRs allow for comparison between the reported mechanical and chemical properties of the steel and the specified requirements that were in effect at the time of the steel production.

4.1 MTR tensile comparison

All available MTRs reported the yield strength, ultimate strength, and elongation for each heat. Results are summarized in Table 8. A result is shown as conformant if all mechanical metrics exceed the specified minimums which are delineated in ASTM A 588-71 and reproduced at the bottom of the table. For heats with more than one MTR, the lowest value for each measurement across all heats of the respective thickness is presented in the table. Values are reported to the relevant significant digits per ASTM A370-21 Annex 8 and ASTM E29 Section 7.4.

Table 8: Reported yield strength, ultimate strength, and elongation from the relevant MTRs.

Plate Thickness (inches)	Heat Number	F_y (ksi)	F_u (ksi)	Elongation (%)	Pass or Fail A 588-71?
1/2	422H2271	61.0	81.5	19 (in 8")	Pass
	74C184	61.0	87.0	21 (in 8")	Pass
	661H632	58.0	85.0	24 (in 8")	Pass
	661H352	64.5	91.0	20 (in 8")	Pass
	662H868	67.0	85.5	23 (in 8")	Pass
	645H218	70.5	91.0	21 (in 8")	Pass
	645H090	67.0	92.5	21 (in 8")	Pass
	650J220	56.0	81.0	26 (in 8")	Pass
11/16	74C184	58.5	82.5	23 (in 8")	Pass
3/4	658J291	60.0	81.0	25 (in 8")	Pass
13/16	801H11600	64.0	82.5	19 (in 8")	Pass
	801H12930	52.0	71.0	26 (in 8")	Pass
	801H15770	55.0	74.0	25 (in 8")	Pass
	802E00400	54.0	74.0	21 (in 8")	Pass
	74C184	58.5	82.5	23 (in 8")	Pass
2 1/4	649H558	58.0	85.5	24 (in 8")	Pass
2 1/2	67C262	64.0	95.0	26 (in 2")	Pass
3 1/8	649H558	63.0	88.0	22 (in 8")	Pass
	422H3271	57.0	82.0	30 (in 2")	Pass
	421H1431	54.0	77.0	29 (in 2")	Pass
A588-71 Limits		50.0	70.0	18 (in 8") 21 (in 2")	

4.2 MTR CVN comparison

The majority of the MTRs included CVN data, however several heats did not. Where MTR data was reported, testing was conducted at 40°F and all impact strengths surpassed the 15 ft-lbf requirement for base metal. Results are summarized in Table 9. For heats with more than one MTR, the lowest average value across all heats of the respective thickness is reported. Values are reported to the nearest ft-lb per ASTM A370-21 Annex 8 and ASTM E29 Section 7.4.

Table 9: Impact energy results from the provided MTRs.

Plate Thickness (inches)	Heat Number	Average Impact Energy (ft-lbf)	Pass or Fail 15 ft-lbf?
1/2	422H2271	45	Pass
	74C184	74	Pass
	661H632	44	Pass
	661H352	51	Pass
	662H868	Missing	–
	645H218	Missing	–
	645H090	Missing	–
	650J220	35	Pass
11/16	74C184	37	Pass
3/4	658J291	Missing	–
13/16	801H11600	26	Pass
	801H12930	131	Pass
	801H15770	114	Pass
	802E00400	75	Pass
	74C184	60	Pass
2 1/4	649H558	38	Pass
2 1/2	67C262	61	Pass
3 1/8	649H558	36	Pass
3 1/8	422H3271	25	Pass
	421H1431	Missing	–

Note: “–” indicates that the MTR value is missing and thus the impact energy conformance of the material is unknown.

4.3 MTR chemistry comparison

The provided MTRs show that the two plate manufacturers, United States Steel Corporation and Bethlehem Steel Corporation, explicitly specified Grade A and B. All plate provided from Pittsburgh, PA (US Steel) was specified to meet ASTM A 588-71 Grade B. All plate provided from Bethlehem, PA (Bethlehem) was specified to meet ASTM A 588 Grade A requirements but did not include the standard’s year. Dates on the MTRs ranged from 1972 to 1974; it is relevant to identify the binding specification since there were changes to the grades of interest over the fabrication years.

The following are excerpts from ASTM year-on-year proceedings regarding changes to the A 588 standards between 1969 and 1975,

- “A 588 - 69 (formerly A 588 - 68), Specification for High-Strength Low-Alloy Structural Steel with 50,000 psi Minimum Yield Point to 4 in. Thick (Subcommittee II) (effective July 18, 1969)
 - A new grade, Grade H (Kaisaloy 50 CR) was added.”

- “A 588 - 70 (formerly A 588 - 69), Specification for High-Strength Low-Alloy Structural Steel with 50,000 psi Minimum Yield Point to 4 in. Thick (Subcommittee II) (effective April 13, 1970)
 - This revision eliminated modifications and made requirements more consistent, added a new grade as requested by Jones & Laughlin Steel Corp., and revised carbon requirement of Grade B as requested by Bethlehem Steel Corp.”
- “A 588 - 70a (formerly A 588 70), Specification for High-Strength Low-Alloy Structural Steel with 50,000 psi Minimum Yield Point to 4 in. Thick (Subcommittee A01.02) (effective Oct. 2, 1970)”
 - The analysis terms were revised and the former check analysis requirements were deleted.”
- “A 588 - 74 (formerly A 588 - 71), Specification for High-Strength Low-Alloy Structural Steel with 50,000 psi Minimum Yield Point to 4 in. Thick (Subcommittee A01.02) (approved July 29, 1974)”
 - The specification was reapproved with no revisions.

However, after reviewing physical copies of the ASTM A 588 standards over the relevant years there seems to be an error in the synoptic proceedings. The revised requirement for the carbon content of Grade B, changing from setting a range of 0.10-0.20 percent to setting a maximum value of 0.20 percent, did not change until the ASTM A 588-74 edition. It also appears that ASTM A 588-70a and ASTM A 588-71 are synonymous documents. Therefore, ASTM A 588-71 (ASTM A 588-70a) is taken as the governing specification of the fabrication years for steel from both US Steel and Bethlehem.

ASTM A 588 was first listed as a steel composition under the purview of ASTM A 6 in the 1968a edition. In the 1970 edition of ASTM A 6, a product analysis tolerance was introduced to all steels within the scope of ASTM A 6, with specified chemistry tolerances in Section 4.1¹ and Tables B through E. Applicability of the ASTM A 6-70 tolerances is directly stated in Section 2.1 of ASTM A 588-71. Therefore, all assessments of chemistry herein include the tolerances specified in ASTM A 6-70, summarized in Table 10. Note ASTM A 6-70 chemical analysis tolerances of elements specified for Grades A and B did not change through ASTM A 6-74 and are taken as representative over the time of fabrication.

The chemical compositions, performed by ladle analysis (explicitly stated for the Grade A steels and assumed for the Grade B steel based on the fabrication year), from the MTRs are summarized in Table 11. Table 12 compares the stated MTR chemistries in Table 11 to the chemistry limits required for conformance presented in Table 10. Mass fraction values are reported to parallel the significant digits provided in the MTRs.

¹Section 4.1 states that “*rimmed or capped steel is characterized by a lack of homogeneity in its composition, especially for the elements carbon, phosphorous, and sulphur; therefore, the limitation for these elements shall not be applicable unless misapplication is clearly indicated.*” Rimming and capping are steel production processes where the casting has modified exposure to the atmosphere, minimizing the formation of gas voids in the ingot. The MTRs do not report this production information and it is therefore unclear as to whether the clause in Section 4.1 is applicable.

Table 10: Percent weight element composition requirements for ASTM A 588 Grade A & Grade B per the 1971 specification with ASTM A 6-70 tolerances.

Element	Chemical Requirements by Heat Analysis including ASTM A 6-70 tolerances — Composition (%)	
	Grade A	Grade B
Carbon	0.07-0.23	0.07-0.24
Manganese	0.85-1.30	0.70-1.30
Phosphorus	≤ 0.05	≤ 0.05
Sulfur	≤ 0.06	≤ 0.06
Silicon	0.13-0.33	0.13-0.33
Nickel	...	0.22-0.53
Chromium	0.36-0.69	0.36-0.74
Copper	0.22-0.43	0.17-0.43
Vanadium	0.01-0.11	0.005-0.10

Note: “...” indicates that no upper or lower limits are specified for the respective element.

Table 11: MTR percent weight element composition.

Plate Thickness (inches)	Heat Number	Element (% weight composition)								
		<i>C</i>	<i>Mn</i>	<i>P</i>	<i>S</i>	<i>Si</i>	<i>Ni</i>	<i>Cr</i>	<i>Cu</i>	<i>V</i>
1/2	422H2271	0.13	0.98	0.009	0.019	0.24	0.28	0.51	0.28	0.026
	74C184	0.15	1.15	0.010	0.026	0.23	0.09	0.56	0.29	0.030
	661H632	0.10	1.09	0.010	0.021	0.26	0.33	0.57	0.26	0.050
	661H352	0.10	1.19	0.011	0.029	0.29	0.33	0.57	0.25	0.050
	662H868	0.08	1.12	0.013	0.035	0.26	0.32	0.57	0.27	0.050
	645H218	0.08	1.20	0.013	0.024	0.29	0.32	0.58	0.24	0.060
	645H090	0.10	1.14	0.010	0.019	0.36	0.33	0.58	0.25	0.050
	650J220	0.08	1.06	0.010	0.022	0.28	0.30	0.59	0.26	0.050
11/16	74C184	0.15	1.15	0.010	0.026	0.23	0.09	0.56	0.29	0.030
3/4	658J291	0.08	1.02	0.010	0.019	0.26	0.29	0.57	0.24	0.050
13/16	801H11600	0.12	0.92	0.005	0.020	0.22	0.34	0.50	0.24	0.030
	801H12930	0.11	0.85	0.006	0.017	0.24	0.29	0.55	0.26	0.030
	801H15770	0.11	0.89	0.008	0.019	0.21	0.29	0.54	0.25	0.020
	802E00400	0.11	0.89	0.008	0.028	0.23	0.36	0.50	0.28	0.030
	74C184	0.15	1.15	0.010	0.026	0.23	0.09	0.56	0.29	0.030
2 1/4	649H558	0.10	1.21	0.013	0.030	0.29	0.33	0.60	0.30	0.070
2 1/2	67C262	0.17	1.18	0.010	0.020	0.24	0.17	0.56	0.34	0.060
3 1/8	649H558	0.10	1.18	0.016	0.030	0.25	0.31	0.58	0.27	0.060
	422H3271	0.13	1.04	0.019	0.028	0.25	0.35	0.54	0.27	0.026
	421H1431	0.13	1.09	0.018	0.029	0.28	0.33	0.56	0.28	0.026

Table 12: MTR conformance to ASTM A 588-71 Grade A & Grade B.

Plate Thickness (inches)	Heat Number	Specified Grade	Compliant to ASTM A 588-71 with ASTM A 6-70 tolerances (Y/N) ^{a?}								
			<i>C</i>	<i>Mn</i>	<i>P</i>	<i>S</i>	<i>Si</i>	<i>Ni</i>	<i>Cr</i>	<i>Cu</i>	<i>V</i>
1/2	422H2271	B	Y	Y	Y	Y	Y	Y	Y	Y	Y
	74C184	A	Y	Y	Y	Y	Y	Y	Y	Y	Y
	661H632	B	Y	Y	Y	Y	Y	Y	Y	Y	Y
	661H352	B	Y	Y	Y	Y	Y	Y	Y	Y	Y
	662H868	B	Y ^b	Y	Y	Y	Y	Y	Y	Y	Y
	645H218	B	Y ^b	Y	Y	Y	Y	Y	Y	Y	Y
	645H090	B	Y	Y	Y	Y	N	Y	Y	Y	Y
	650J220	B	Y ^b	Y	Y	Y	Y	Y	Y	Y	Y
11/16	74C184	A	Y	Y	Y	Y	Y	Y	Y	Y	Y
3/4	658J291	B	Y ^b	Y	Y	Y	Y	Y	Y	Y	Y
13/16	801H11600	B	Y	Y	Y	Y	Y	Y	Y	Y	Y
	801H12930	B	Y	Y	Y	Y	Y	Y	Y	Y	Y
	801H15770	B	Y	Y	Y	Y	Y	Y	Y	Y	Y
	802E00400	B	Y	Y	Y	Y	Y	Y	Y	Y	Y
	74C184	A	Y	Y	Y	Y	Y	Y	Y	Y	Y
2 1/4	649H558	B	Y	Y	Y	Y	Y	Y	Y	Y	Y
2 1/2	67C262	A	Y	Y	Y	Y	Y	Y	Y	Y	Y
3 1/8	649H558	B	Y	Y	Y	Y	Y	Y	Y	Y	Y
	422H3271	B	Y	Y	Y	Y	Y	Y	Y	Y	Y
	421H1431	B	Y	Y	Y	Y	Y	Y	Y	Y	Y

^aY – Denotes compliance to the specified grade, N – Denotes that the heat does not conform to the specified grade.

^bIf the clause defined in footnote¹ is applicable then these heats will not be within conformance for carbon content.

Table 12 shows a single heat, heat 645H090, falls outside of conformance defined in Table 10.

Two performance characteristics that are dependent on conformance with weathering steel chemistry requirements are: 1) the hardenability of the steel and how this can affect the weldability, and 2) the effect that the chemistry would have on atmospheric corrosion resistance.

Hardenability can be assessed by various means. One common procedure is to calculate the carbon equivalency (*CE*) since carbon is the primary hardenability element in the steel. This is done via equation where the proportional hardenability effect of other elements is added to carbon. American Welding Society codes utilize the following equation.

$$CE = C + \frac{Mn+Si}{6} + \frac{Cr+Mo+V}{5} + \frac{Ni+Cu}{15} \quad (\text{AWS D1.5 G6.1.1}^2)$$

The calculated carbon equivalency provides a metric for the likelihood of potential hydrogen-induced cracking in the weld heat affected zone. Lower carbon equivalencies indicate less potential for these defects to form with the threshold of concern usually beginning with *CE* values greater than 0.45. Table 13 summarizes the *CE* values for the relevant MTRs and for a “typical” A588 composition as listed in ASTM G101-20.

Similar to hardenability, the atmospheric corrosion resistance of a weathering steel can be quantified by various means, with one common procedure in the US being to use one of the methods delineated in ASTM G101-20. G101 calculates a corrosion loss rate relative to reference data sets at multiple domestic and international exposure sites for steels of known makeup. Two methods, 1) the Predictive Method Based on the Data of Townsend (G101 Section 6.3.2), and 2) the Predictive Method Based on the Data of Larabee and Coburn (G101 Section 6.3.1), correlate that loss to a respective corrosion index (*CI*). The calculated *CI* ranges from 0 to 10, where 0 represents the corrosion index for pure iron and 10 represents a very corrosion resistant alloy. While (with the exception of heat 645H090), the MTRs indicated conformance with ASTM A588 at the time of construction, modern UWS metallurgical practice (ASTM A588-19 Section 5.3; introduced in ASTM A588-97 and revised to use the Predictive Method Based on the Data of Larabee and Coburn for the calculated *CI* value in ASTM A588-01), weathering steel shall have a *CI* of at least 6.0. Table 13 summarizes the Townsend *CI* and the Larabee and Coburn *CI* values for the relevant MTRs and for a “typical” A588 composition as listed in ASTM G101-20.

² This equation replicates the equation from Clause F6.1.1 in the 2020 Edition of the AASHTO/AWS D1.5M/D1.5 *Bridge Welding Code*. The AWS *CE* equation builds upon the Dearden-O’Neill (Dearden and O’Neill 1940) equation with the addition of a term for silicon because the work performed by Dearden and O’Neill only used low-silicon steel. Subsequent to their research, steel producers commonly began engaging silicon-killing, a process that increases steel homogeneity and decreases porosity, leading to products that had appreciable silicon compositions which had to be accounted for in weldability.

Table 13: MTR carbon equivalency and corrosion indices from ASTM G101-20.

Plate Thickness (inches)	Heat Number	<i>CE</i>	<i>CI</i> (G101 6.3.2)	<i>CI</i> (G101 6.3.1)
1/2	422H2271	0.48	5.31	6.28
	74C184	0.52	5.16	6.07
	661H632	0.49	5.60	6.37
	661H352	0.51	5.55	6.37
	662H868	0.47	5.25	6.46
	645H218	0.49	5.70	6.32
	645H090	0.51	5.95	6.47
	650J220	0.47	5.58	6.37
11/16	74C184	0.52	5.16	6.07
3/4	658J291	0.45	5.48	6.15
13/16	801H11600	0.45	5.09	6.04
	801H12930	0.44	5.26	6.19
	801H15770	0.44	5.13	6.09
	802E00400	0.45	4.98	6.38
	74C184	0.52	5.16	6.07
2 1/4	649H558	0.53	5.73	6.69
2 1/2	67C262	0.56	5.63	6.41
3 1/8	649H558	0.51	5.50	6.48
	422H3271	0.50	5.43	6.55
	421H1431	0.52	5.55	6.62
Reference – G101 Typical A588		–	6.14	6.67

Note: “–” indicates that the *CE* can be calculated using the reference chemistry in ASTM G101, but it would not necessarily be representative of the product specification.

5 TEST RESULTS

This section presents the results of the testing regiment summarized in Table 7 following the methods described in Section 2.5. Testing was conducted from early November 2022 through January 2023, including a technical exhibition day open to all parties in the investigation, held on November 16 at TFHRC to demonstrate conformance of the testing protocol.

5.1 Tensile test results

Testing of specimens 3Q2 and 1N2 was conducted on November 16, 2022, as a part of the technical demonstration for the parties involved in the investigation. The remainder of the specimens were tested between November 10, 2022 and December 9, 2022.

Table 14 provides the average yield stress and ultimate stress results of the duplicate tensile specimens per unique heat, reported to the nearest tenth of a ksi. The stress-strain curves, documented in Appendix D, did not always have a clearly defined yield plateau. Therefore, the reported yield stress was determined for all specimens using the Total Extension Under Load Method, per ASTM A370-21 Section 14.1.3, at a specified

strain of 5000×10^{-6} in./in. The reported ultimate stress is the maximum observed load over the original cross-sectional area at the middle of the tapered width coupon, per ASTM A370-21 Section 14.3. Table 14 also includes the elongation at fracture, per ASTM A370-21 Section 14.4.4.1. Calibration for the noncontact extensometer, calibrated following ASTM E83-16, is included in Appendix H. Values are reported to the relevant significant digits per ASTM A370-21 Annex 8 and ASTM E29 Section 7.4. For reference, mechanical requirements for ASTM A 588-71 are provided at the bottom of Table 14.

Table 14: Summary of tensile testing results.

Plate	F_y (ksi)	F_u (ksi)	Elongation at Fracture (%)	Pass or Fail A 588-71?
1A ¹	53.5	81.5	27 (in 8")	Pass
1B	54.0	77.5	22 (in 8")	Pass
1C	53.0	77.5	28 (in 8")	Pass
1H	66.0	96.0	21 (in 8")	Pass
1N ¹	55.0	79.5	27 (in 8")	Pass
1Q	59.0	87.0	20 (in 8")	Pass
1T	52.0	77.5	35 (in 2")	Pass
1U	56.5	79.5	18 (in 8")	Pass
1V	56.0	81.0	25 (in 2")	Pass
2A	55.0	82.5	26 (in 8")	Pass
2B	47.9	69.0	28 (in 8")	Fail
2Q	60.5	88.5	18 (in 8")	Pass
2T	53.5	76.5	22 (in 8")	Pass
2U	57.5	79.0	20 (in 8")	Pass
3A	53.0	81.0	26 (in 8")	Pass
3B	49.3	72.5	22 (in 8")	Fail
3Q	59.0	88.5	18 (in 8")	Pass
3T	54.5	79.0	21 (in 8")	Pass
3U	56.0	80.5	16 (in 8")	Fail
4A ²	55.0	83.0	26 (in 8")	Pass
4B	49.6	72.5	23 (in 8")	Fail
4Q	58.0	86.0	19 (in 8")	Pass
4R	56.0	74.5	23 (in 8")	Pass
4T	52.0	75.5	22 (in 8")	Pass
4U	57.5	80.5	18 (in 8")	Pass
A 588-71 Limits	50.0	70.0	18 (in 8") 21 (in 2")	

Note: Shaded cells indicate that at least one measured mechanical value is outside of the specified limits in ASTM A 588-71.

¹Specimens 1A1 and 1N1 had an interlock trip near the conclusion of the test, resulting in a loss of loading in the servo-hydraulic system. The reported elongation at fracture represents the sum of the accumulation of strain prior to the interlock being tripped and the additional straining from the reloading until fracture.

²Reported values for 4A represent the sum of measured values from specimen 4A1 and a duplicate test of specimen 4A2. During the testing of the original specimen 4A2, the DIC camera unexpectedly ceased recording data and was therefore excluded from Table 14 but is reported in Appendix D.

Table 14 shows that 4 of the 25 unique heats fall outside of mechanical conformance with ASTM A 588-71. The measured yield and ultimate strength for plate 2B are both less than the requirement. Plates 3B and 4B also have measured yield strengths less than the requirement but had conformant measured ultimate strengths. Plate 3U has a measured yield and ultimate strength within conformance but does not meet the specified elongation requirement.

It is important to note that the tensile specimens were not extracted from virgin steel. As the bridge was in service for half a century, and experienced large deformations during the collapse, there is the potential that plastic strain was accumulated at any time between plate fabrication and specimen testing. If prior yielding did exist in a tested plate, the observed stress-strain curves might exhibit an artificially larger measured yield strength due to strain hardening. The ultimate stress would likely be unaffected unless the accumulation of plastic strain was very large. The measured elongation would directly decrease with the accumulation of plastic strain. However, recognize that when selecting the locations for specimen extraction, care was taken to locate plate with minimal distortion to attempt to minimize the influence of plastic strain accumulation on the captured mechanical properties.

Given their location in the bridge, it is highly unlikely that the measured strengths for plates 2B, 3B, and 4B were out of conformance due to damage history. These plates are $13/16$ -in. web plate located in the girder. The MTRs, from Table 2, showed that a few of the $13/16$ -in. heats that could make up the girder web plate were close to the ASTM A 588-71 mechanical limits. It is possible that a slower testing strain rate could account for a slight reduction in the measured yield strength; however, the testing protocol of the MTRs is not explicitly known and thus potential differences in procedure between the tests conducted herein and the MTRs are speculative.

Plate 3U, a $1/2$ -in. longitudinal stiffener plate, is out of conformance due to an insufficient elongation capacity. The reduction in measured elongation capacity versus the reported MTR elongations is possibly due to the aforementioned accumulation of plastic strain. Additionally of note is the location of fracture in the tensile specimen which may have affected the overall result. ASTM A370-21 Section 14.4.2 states that the measured elongation may not be representative of the material if any part of the fracture takes place outside of the middle half of the gauge length, unless the measured elongation meets the minimum requirements specified. Appendix D documents the necking location along the length of each specimen. For plate 3U, the specimen had the fracture initiate just outside of the middle half of the gauge length and therefore the reported elongation for this specimen may not be representative of the material. Additional tests of 3U were not conducted as the material is not virgin and therefore it is unknown if or where internal flaws exist, potentially driving the initiation of fracture to a different location within the length of the reduced section.

It is important to note three instances during the testing of the tensile specimens wherein the standard testing protocol was not followed. During the testing of specimens 1A1 and 1N1, an interlock tripped near the conclusion of the test, resulting in a loss of loading in the servo-hydraulic system. An interlock is a safety protocol implemented into the software to ensure control of the testing system. The testing protocol had several displacement and load interlocks in place where if a user specified load, displacement, or stain limit was surpassed then the program would cause the servo-hydraulic system to immediately, rapidly decrease the applied load. After relaxing the interlock limits, both tests were resumed and continued through to rupture. The reported elongations in Table 14 represent the sum of the accumulation of strain prior to the interlock being tripped and the additional straining from the reloading until fracture. Recognize, however, that this reloading was not necessary as both specimens had already satisfied the required ASTM A 588-71

tensile strength and elongation limits prior to the interlock tripping. NTSB was consulted regarding the decision not to machine and test duplicate specimens.

Finally, during the testing of specimen 4A2 the DIC camera unexpectedly ceased recording data after the test was well into the strain hardening region (approximately an axial strain of 0.09). The test continued, ending with a load-deflection curve and measured strengths similar to specimen 4A1. After consulting with NTSB, it was decided to machine the coupon blank 4A3 and repeat the test so as to obtain an accurate elongation measurement. Results in Table 14 represent the average of 4A1 and the replicate cut from the coupon blank. Results for all three specimens are presented in Appendix D. There were no other instances of issues with the DIC camera.

5.2 CVN results

Specimens 1BZ, 1VX, 1AX, 2AX, 4AX were tested on November 16, 2022 as a part of the technical demonstration for the parties involved in the investigation. The remainder of the specimens were tested on December 9, 2022. On both days the zero and windage loss were checked. The zero was consistently accurate to a 0 ft-lbf indication per ASTM E23-18 Section 9.1.1.2. The windage loss was consistently indicating 10 ft-lbf over the 11 half swings, i.e., the reading was within 1 ft-lbf, per ASTM E23-18 Section 9.1.1.3.

Table 15 provides the averaged results of the three replicate CVN specimens per unique heat, reported to the nearest ft-lbf per ASTM A370-21 Annex 8 and ASTM E29 Section 7.4. Note that the specimen 3BY test was run successfully and resulted in an unbroken specimen that did not stop the hammer; thus per ASTM E23-18 Section 9.3.3.1 the result from 3BY was excluded from the average for the 3B plate. All measured heats passed the required 15 ft-lbf requirement of the time (AASHO 1969), following interpretation of the test results per ASTM A370-21 Section 27.1.1.1. The measured impact energy for each specimen is provided in Appendix E.

Table 15: Summary of CVN results.

Specimen	Averaged Recording (ft-lbf)	Pass or Fail 15 ft-lbf at 40 °F?
1A	54	Pass
1B	36	Pass
1C	97	Pass
1H	25	Pass
1N	132	Pass
1Q	25	Pass
1T	59	Pass
1V	23	Pass
2A	35	Pass
2B	100	Pass
2Q	29	Pass
2T	86	Pass
3A	65	Pass
3B ¹	141	Pass
3Q	22	Pass
3T	65	Pass
4A	43	Pass
4B	101	Pass
4Q	66	Pass
4R	90	Pass
4T	76	Pass

¹Note that specimen 3BY was unbroken and excluded from the average for 3B plate per ASTM E23-18 Section 9.3.3.1.

The temperature of each test specimen was measured with a calibrated thermometer and recorded to the nearest tenth of a degree Fahrenheit. The results are presented in Appendix E Table E-1. The specimens were soaked for at least 5 minutes in a chilled denatured alcohol thermal bath per ASTM A370-21 Section 26.1.1. The test temperatures for all specimens were within the required 40 ± 2 °F per ASTM A370-21 Section 25.1. Note that zero and windage losses were remeasured with no change in either value between the different test days.

A stopwatch was used to ensure that the time between the specimen removal from the thermal bath and the release of the hammer was less than 5.0 seconds per ASTM A370-21 Section 26.2.2. There was one instance on the technical demonstration day where the time exceeded the 5.0 seconds for specimen 1VX; the test was halted prior to releasing the hammer and the specimen was resubmerged in the thermal bath. After the 5-minute minimum soak time had elapsed the test was conducted.

The estimated percent shear fracture area (to the nearest 5%) and respective images are provided in Appendix E Table E-2 per ASTM A370-21 Section 26.4.2.1(4). Images were captured in a light box using a 20.2 MP camera with a dynamic optical lens set to roughly 120 mm at approximately a 12 in. standoff. Measured shear fracture areas are calculated through both a Mask Area Method and a Pixel Intensity Method. The Mask Area Method utilizes a user defined superimposed trace of the total fracture area (the red outline in Appendix E) and a trace of the non-shear fracture area (the yellow outline in Appendix E).

The difference represents the shear fracture area. The Pixel Intensity Method calculates the shear fracture area based on color intensity of each pixel in grayscale images of the samples. The method uses a constant intensity threshold of 85 or greater to denote the shear fracture areas. Note that the simpler Mask Area Method seemed to be more consistent with visual shear fracture areas shown in ASTM A370-21 Figure 14.

Measured lateral expansion results are reported in Appendix E Table E-3 per ASTM A370-21 Section 26.4.3 and ASTM E23-18 Figure 6.

5.3 Chemistry results

All GDS measurements were captured on December 16, 2022. Tables 16 and 17 show whether the specimens are conformant with respective grades of ASTM A 588-71 including ASTM A 6-70 tolerances in cases where plate could be tied to a specific heat, shown in Table 2. Note that only elements included in Table 10 are applied for verifying conformance, herein, excluding GDS output presented in Appendix F.

Table 16: Conformance to ASTM A 588-71 Grade A with and without ASTM A 6-70 tolerances for heats specified as Grade A in the MTR.

Sample	Element Conformant (Y/N)?								
	<i>C</i>	<i>Mn</i>	<i>P</i>	<i>S</i>	<i>Si</i>	<i>Ni</i>	<i>Cr</i>	<i>Cu</i>	<i>V</i>
1H4	Y	Y	Y	Y	Y	Y	Y	Y	Y
4R4	Y	Y	Y	Y	Y	Y	Y	Y	Y

Table 17: Conformance to ASTM A 588-71 Grade B with ASTM A 6-70 tolerances for heats specified as Grade B in the MTR.

Sample	Element Conformant (Y/N)?								
	<i>C^a</i>	<i>Mn</i>	<i>P^a</i>	<i>S^a</i>	<i>Si</i>	<i>Ni</i>	<i>Cr</i>	<i>Cu</i>	<i>V</i>
1A4	Y	Y	Y	Y	Y	Y	Y	Y	Y
1C4	Y	Y	Y	Y	Y	Y	Y	Y	Y
1N4	Y	N	Y	Y	N	N	N	N	Y
1V4	Y	Y	Y	Y	Y	Y	Y	Y	Y
2A4	Y	Y	Y	Y	Y	Y	Y	Y	Y
3A4	Y	Y	Y	Y	Y	Y	Y	Y	Y
4A4	Y	Y	Y	Y	Y	Y	Y	Y	Y

^aIf the steel is rimmed or capped then the ASTM A 6-70 tolerances do not apply for select elements. This situation necessitates reevaluation for conformance.

Note: Shaded cells indicate the reported value is outside of the specified limits for Grade B in ASTM A 588-71.

From the GDS measurements with ASTM A 6-70 tolerances, Table 16 shows that all analyzed plate able to be identified as Grade A are conformant. Table 17 shows that specimen 1N4 is out of conformance for manganese, silicon, nickel, chromium, and copper; all other analyzed plate able to be identified as Grade B are conformant.

In cases where plate that could not be tied to a specific heat, the specimen conformance was checked against both Grade A and Grade B (the two listed grades throughout the MTRs encompassing the relevant plates that were tested). The percent element weight composition ranges restrictive to both grades, including respective tolerances per ASTM A 6-70, are provided in Table 18. Tables 19 shows whether the specimens are conformant with this range.

Table 18: Percent weight element composition requirements for ASTM A 588-71 Grade A & Grade B with ASTM A 6-70 tolerances (as presented in Table 5) and the composition range restrictive to both grades.

Element	Chemical Requirements by Heat Analysis including ASTM A 6-70 tolerances — Composition (%)		Restrictive to Requirements of both Grade A & B
	Grade A	Grade B	
Carbon	0.07-0.23	0.07-0.24	0.07-0.23
Manganese	0.85-1.30	0.70-1.30	0.85-1.30
Phosphorus	≤ 0.05	≤ 0.05	≤ 0.05
Sulfur	≤ 0.06	≤ 0.06	≤ 0.06
Silicon	0.13-0.33	0.13-0.33	0.13-0.33
Nickel	...	0.22-0.53	0.22-0.53
Chromium	0.36-0.69	0.36-0.74	0.36-0.69
Copper	0.22-0.43	0.17-0.43	0.22-0.43
Vanadium	0.01-0.11	0.005-0.10	0.01-0.10

Note: “...” indicates that no upper or lower limits are specified for the respective element.

Table 19: Conformance of plate that could not be tied to a specific heat to the restrictive requirements of both Grade A & B, as presented in Table 18.

Sample	Element Conformant (Y/N)?								
	<i>C</i> ^a	<i>Mn</i>	<i>P</i> ^a	<i>S</i> ^a	<i>Si</i>	<i>Ni</i> ^b	<i>Cr</i>	<i>Cu</i>	<i>V</i>
1B4	Y	Y	Y	Y	Y	Y	Y	Y	Y
1Q4	Y	Y	Y	Y	Y	N	Y	Y	Y
1U4	Y	Y	Y	Y	Y	Y	Y	Y	Y
1T4	Y	Y	Y	Y	Y	N	Y	Y	Y
2B4	Y	Y	Y	Y	Y	Y	Y	Y	Y
2Q4	Y	Y	Y	Y	Y	N	Y	Y	Y
2T4	Y	Y	Y	Y	Y	N	Y	Y	Y
2U4	Y	Y	Y	Y	Y	Y	Y	Y	Y
3B4	Y	Y	Y	Y	Y	Y	Y	Y	Y
3Q4	Y	N	Y	Y	Y	N	Y	Y	Y
3T4	Y	N	Y	Y	Y	N	Y	Y	Y
3U4	Y	Y	Y	Y	Y	Y	Y	Y	Y
4B4	Y	Y	Y	Y	Y	Y	Y	Y	Y
4Q4	Y	Y	Y	Y	Y	N	Y	Y	Y
4U4	Y	Y	Y	Y	Y	Y	Y	Y	Y
4T4	Y	Y	Y	Y	Y	N	Y	Y	Y

^aIf the steel is rimmed or capped then the ASTM A 6-70 tolerances do not apply for select elements. This situation necessitates reevaluation for conformance.

^bSpecimens 1Q4, 1T4, 2Q4, 2T4, 3Q4, 3T4, 4Q4, and 4T4 all have measured nickel contents lower than what is specified in Grade B; however, these specimens may be conformant if in fact the plate was specified as Grade A.

Note: Shaded cells indicate the reported value is outside of the specified limits in ASTM A 588-71.

Table 19 shows that specimens 1Q4, 1T4, 2Q4, 2T4, 3Q4, 3T4, 4Q4, and 4T4 fall outside of the mass fraction range limited by the overlap of Grades A & B; all other analyzed plates not able to be identified

specifically as Grade A or B are conformant. Specimens 1Q4, 1T4, 2Q4, 2T4, 3Q4, 3T4, 4Q4, and 4T4 all have measured nickel contents lower than what is specified in Grade B; however, these specimens may be conformant if in fact the plate was specified as Grade A. Specimens 3Q4 and 3T4 both surpass the manganese upper ASTM A 588-71 limit (with ASTM A 6-70 tolerances) for both grades and are therefore out of conformance regardless of specified MTR grade. However, it is important to note that the magnitude that manganese surpasses the upper limit is within the measurement uncertainty, s , in Equation 1.

As discussed in Section 4.3, two potential concerns with the chemistry requirements of a weathering steel being out of conformance are: 1) the hardenability of the steel and how this can affect the weldability, and 2) the effect that the chemistry would have on atmospheric corrosion resistance. Table 20 summarizes the CE , Townsend CI , and the Larabee and Coburn CI values for the GDS measurements and for a “typical” A588 composition as listed in ASTM G101-20.

Table 20: GDS measured carbon equivalency and corrosion indices from ASTM G101-20.

Plate Thickness (inches)	Specimen	CE	CI (G101 6.3.2)	CI (G101 6.3.1)
1/2	1T4	0.55	5.28	6.12
	1U4	0.48	5.67	6.17
	2T4	0.50	5.34	5.92
	2U4	0.49	5.68	6.12
	3T4	0.57	5.47	6.26
	3U4	0.49	5.84	6.09
	4T4	0.52	5.47	5.92
	4U4	0.48	5.58	6.16
11/16	4R4	0.54	5.20	5.94
3/4	1V4	0.49	5.22	6.02
13/16	1B4	0.48	5.40	5.97
	1Q4	0.55	5.41	6.14
	2B4	0.44	5.30	5.94
	2Q4	0.56	5.49	6.06
	3B4	0.49	5.42	6.32
	3Q4	0.58	5.59	6.06
	4B4	0.49	5.50	6.06
	4Q4	0.56	5.29	6.05
2 1/4	1N4	0.43	4.86	3.79
2 1/2	1H4	0.60	5.95	6.52
3 1/8	1A4	0.56	5.71	6.50
	1C4	0.53	6.01	6.68
	2A4	0.55	5.74	6.51
	3A4	0.54	5.69	6.51
	4A4	0.54	5.72	6.44
Reference – G101 Typical A588		–	6.14	6.67

Note: “–” indicates that the CE can be calculated using the reference chemistry in ASTM G101, but it would not necessarily be representative of the product specification.

The calculated carbon equivalency provides a metric for the hardenability of the steel resulting from activities like welding. Low *CE* values (<0.28) indicate that the steel should be easily weldable, tolerant of little to no preheat, and is insensitive to low hydrogen practice. High *CE* values (>0.50) indicate steel which requires more care using a combination of low hydrogen practice, preheat, and perhaps post-heat treatment. Table 20 indicates that the majority of the measured specimens have *CE* values greater than 0.50 which, if proper welding procedures were not used, could have created embrittled heat-affected zones in the base metal from welding.

The calculated corrosion index provides a metric for corrosion resistance ranging from 0 to 10, where 0 represents the *CI* for pure iron and 10 represents a very corrosion resistant alloy. Table 19 indicates that nearly all of the measured specimens have a Townsend *CI* and a Larabee and Coburn *CI* below that of typical A588 steel.

Element mass fractions for each GDS burn per specimen are documented in Appendix F.

5.4 Metallographic results

Macroetching of the sectioned leg flange-to-endplate welds was conducted on December 16, 2022. Photographic documentation of all etches are provided in Appendix G. Each image includes two planar scales to measure weld size and crack properties. The first planar scale is a graded ruler placed directly on top of the specimen. The second scale is a protractor, with various additional calibration references, elevated to be at a plane common with the macroetch.

The sections below highlight general observations from all macros and then specific observations for the two welds per leg.

5.4.1 General Observations

The design plans for the bridge specified the leg flange-to-endplate weld as a single-sided U-groove with a far side reinforcing fillet. There was no information in the weld symbol tail indicating it was required to be a complete joint penetration weld.

- Each macroetch demonstrates these welds were fabricated as partial joint penetration welds using a double-bevel groove geometry.

The design plans for the bridge specified the leg web-to-endplate weld as a double bevel groove. There was no information in the weld symbol tail indicating it was required to be a complete joint penetration weld.

- Macroetches of the web-to-endplate weld were not specifically produced; however, in the extent seen in some of the macros complete joint penetration of the web to the endplate in the vicinity of the leg flanges was not observed.

In review of the 1969 Edition of AWS D2.0 “Specifications for Welded Highway and Railway Bridges,” there were no prequalified T-joint partial-joint penetration welds. Thus, the fabricator would have had to specifically qualify this type of weld; however, with no preserved documentation of approved shop drawings, approved welding joint design, or approved welding procedures, it is unclear whether the weld type was qualified.

Based on macroetches taken over the leg webs (Figure G.3, Figure G.8, Figure G.13, Figure G.18, Figure G.43, Figure G.48), it appears that the leg I-shape (leg flanges and leg web) was welded first, then the leg

end was cut to the correct angle to mate against the endplate, then the endplate was welded. This sequence is evidenced through the leg flange welds which were not continuous through the leg web.

- The bevel preparation for the flange to the inside of the I-shape appears to have been cut with a drop bandsaw. The bandsaw cut through the flange, but also into the leg web for some distance that varied with each leg. The sawcut in the leg web was welded over to seal the cut.

The bevel preparation on the flange was not consistent between the four legs. Preparation was similar for the two Bent 1 legs, and also similar for the two Bent 2 legs, indicating each pair of bent legs was likely fabricated at different points in time.

None of the welds seemed to achieve significant fusion to either sidewall of the weld preparation. Sometimes there appeared to be no fusion. This indicated either poor access with the small bevel angles, particularly in the two Bent 1 legs, or inadequate welding procedure with either low heat input and/or poor angle of the electrode while welding.

5.4.2 Leg 1 (B1R)

Welds 1D# (where “#” is a number from 5 to 9, see Figure C.5) were flange welds where the web had the obtuse angle. 1D5 was on the north side of the leg (interior of bridge) while 1D9 was on the south side of the leg (exterior of bridge).

- All 1D# welds were cracked on the exterior acute angle and into the endplate base metal. It appears the crack may have originated at the toe of the weld at the center of the weld length (over the leg web) and fractured out a divot of endplate base metal from under the exterior acute angle weld. The divot was exacerbated towards the interior of the bridge where the crack even propagated into the obtuse weld from its root.
- The shape of the divots is not perpendicular to an expected stress field in the endplate; therefore, these are suspected to be fractures, not fatigue cracks.
- The divot crack in 1D5 was full of pack rust, indicating that its occurrence predated the collapse by some length of time. The remaining four macros did not have pack rust indicating those fractures were likely the result of the collapse.

Welds 1E# (where “#” is a number from 5 to 9, see Figure C.6) were flange welds where the web had the acute angle. 1E5 was on the north side of the leg (interior of bridge), 1E9 was on the south side of the leg (exterior of bridge).

- The 1E8 and 1E9 welds completely removed a divot of endplate base metal over half of the weld length to the exterior of the bridge. The divot went from the toe-to-toe of the two welds from each side of the joint.
- The 1E7 macro over the web shows two cracks extending into the endplate base metal. One crack originated from the exterior obtuse weld toe; the second crack originated from the root of the interior acute weld.
- The 1E5 and 1E6 welds on the interior side of the bridge had no observable cracks.

Figure 8 shows the weld profile for the design drawings and compares them against observed groove type, bevel pitch, and bevel depth.

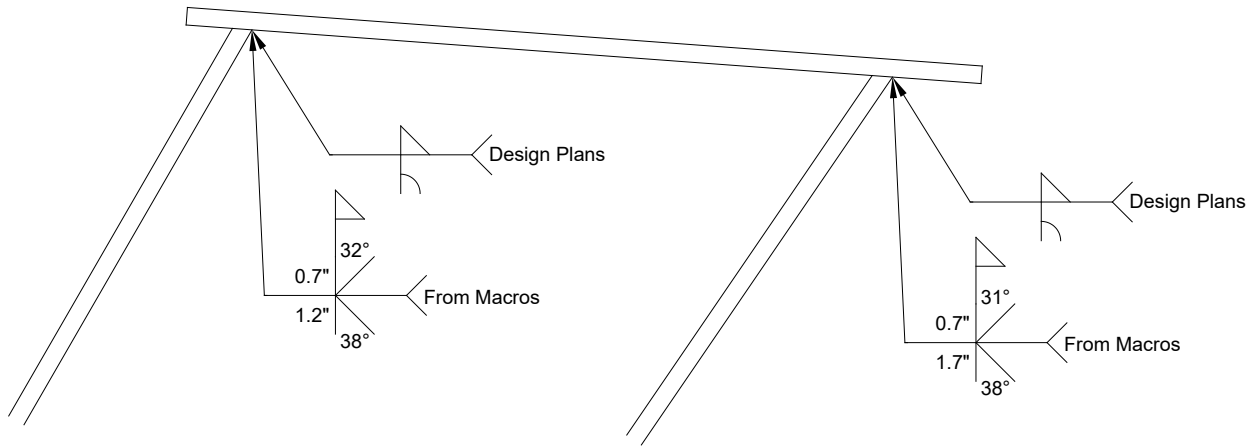


Figure 8. Design weld profile versus the observed profile for B1R.

5.4.3 Leg 2 (B1L)

Welds 2D# (where “#” is a number from 5 to 9, see Figure C.15) were flange welds where the web had the obtuse angle. 2D5 was on the north side of the leg (exterior of bridge) while 2D9 was on the south side of the leg (interior of bridge).

- None of these welds were observed to have cracks.

Welds 2E# (where “#” is a number from 5 to 9, see Figure C.16) were welds where the web had the acute angle. 2E5 was on the north side of the leg (exterior of bridge) while 2E9 was on the south side of the leg (interior of bridge).

- None of these welds were observed to have cracks.

Figure 9 shows the weld profile for the design drawings and compares them against observed groove type, bevel pitch, and bevel depth.

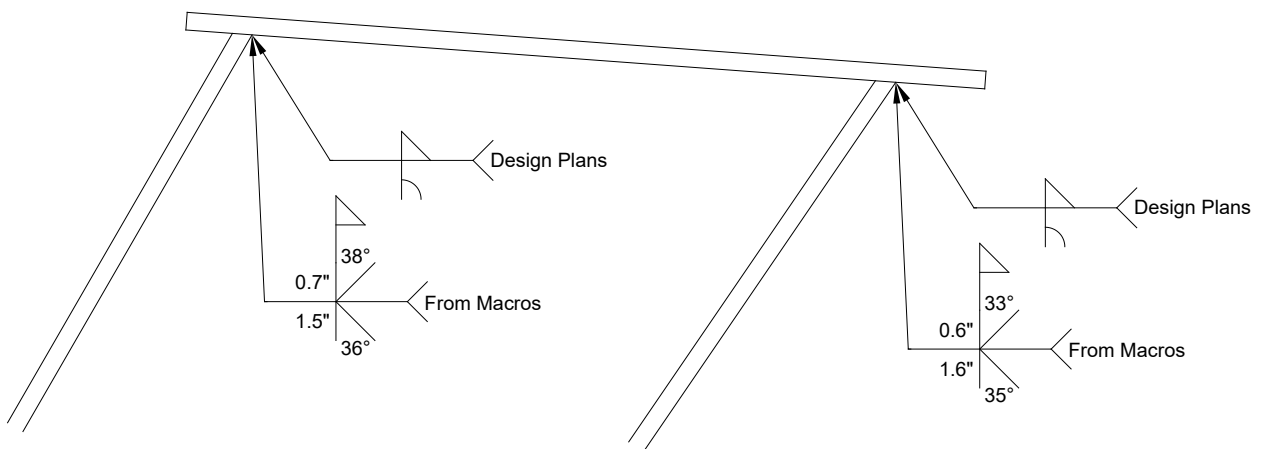


Figure 9. Design weld profile versus the observed profile for B1L.

5.4.4 Leg 3 (B2L)

Welds 3E# (where “#” is a number from 5 to 9, see Figure C.22) were welds where the web had the acute angle. 3E5 was on the north side of the leg (exterior of bridge) while 3F9 was on the south side of the leg (interior of bridge).

- The leg flange, leg webs, and weld nuggets are missing from these macroetches because the fracture surface was retained by NTSB for a fractographic analysis.
- A portion of the endplate divoted out along with the weld, and even fractured the endplate through its thickness. Without the other side of the macro, more description cannot be made at this time.

Welds 3F# (where “#” is a number from 5 to 9, see Figure C.23) were welds where the web had the obtuse angle. 3F5 was on the north side of the leg (exterior of bridge) while 3F9 was on the south side of the leg (interior of bridge).

- 3F5 and 3F6 appear to have fractured along the fusion zone of the leg flange.
- 3F7 (over the centerline of the web) has no visible leg’s web-to-endplate weld or leg’s flange-to-endplate acute weld, this is due to very poor fusion near the flange-web-end plate junction. There was a fracture through the fusion zone of the obtuse weld joining the flange to the endplate.
- 3F8 and 3F9 fractured in the base metal of the leg flange; the welds appear sound.

No information on the weld profile is provided for B2L due to insufficient information regarding the profile of the fractured weld nugget.

5.4.5 Leg 4 (B2R)

Welds 4E# (where “#” is a number from 5 to 9, see Figure C.29) were welds where the web had the acute angle. 4E5 was on the north side of the leg (interior of bridge) while 4E9 was on the south side of the leg (exterior of bridge).

- No cracks were observed in the welds; they all appeared sound.
- 4E7 (over the web), 4E8, and 4E9 show a fracture in the endplate base metal through its thickness originating at the toe of the outer weld nugget. 4E5 and 4E6 show that the fracture through the thickness of the base metal propagated beyond the weld toe, indicating that there was likely little to no fusion into the endplate over the exposed weld toe.

Welds 4F# (where “#” is a number from 5 to 9, see Figure C.30) were welds where the web had the obtuse angle. 4F5 was on the north side of the leg (interior of bridge), 4F9 was on the south side of the leg (exterior of bridge).

- No cracks we observed in the welds; they all appeared sound.

Figure 10 shows the weld profile for the design drawings and compares them against observed groove type, bevel pitch, and bevel depth.

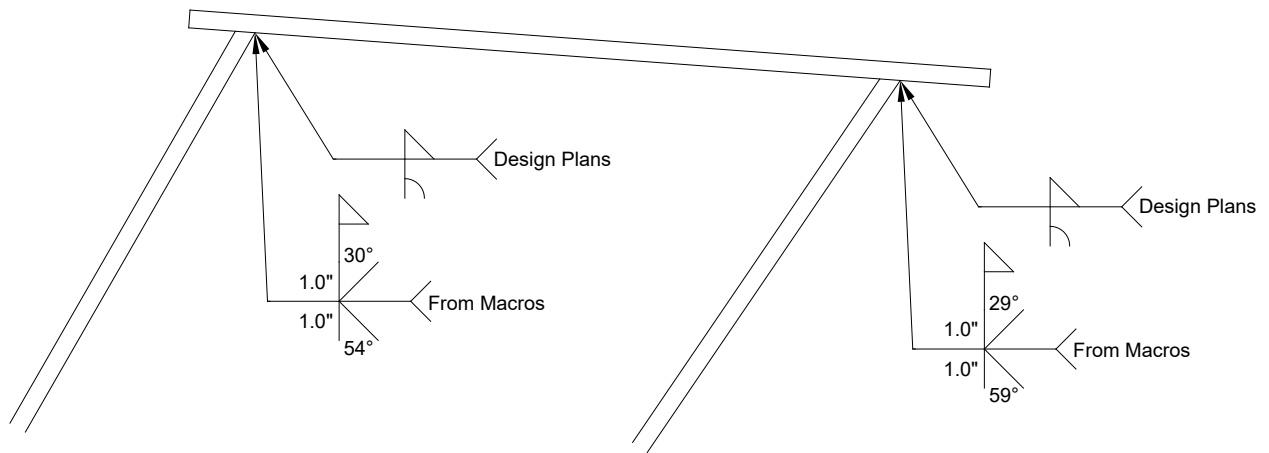


Figure 10. Design weld profile versus the observed profile for B2R.

ACKNOWLEDGEMENTS

The authors would like to thank Federal and Contractor personnel from the TFHRC Structures Laboratory, Machine Shop, and Chemistry Laboratory for their many contributions from assisting in specimen extraction and testing to providing technical guidance. The authors would also like to acknowledge and thank personnel across FHWA's Headquarters, Resource Center, and Division Offices for providing technical guidance related to the investigation.

REFERENCES

- AASHTO (1969). "Standard Specifications for Highway Bridges.", 10th Edition, American Association of State Highway Officials, Washington, D. C.
- ASTM A 6. (1968a). "Standard Specification for General Requirements for Delivery of Rolled Structural Steel Plates, Shapes, Sheet Piling, and Bars for Structural Use." ASTM Annual Book of Standards, Part 4. ASTM International. West Conshohocken, PA.
- ASTM A 6. (1970). "Standard Specification for General Requirements for Delivery of Rolled Structural Steel Plates, Shapes, Sheet Piling, and Bars for Structural Use." ASTM Annual Book of Standards, Part 4. ASTM International. West Conshohocken, PA.
- ASTM A 6. (1974). "Standard Specification for General Requirements for Delivery of Rolled Structural Steel Plates, Shapes, Sheet Piling, and Bars for Structural Use." ASTM Annual Book of Standards, Part 4. ASTM International. West Conshohocken, PA.
- ASTM A 588. (1969). "Standard Specification for High-Strength Low-Alloy Structural Steel with 50,000 psi Minimum Yield Point to 4 in. Thick." ASTM Annual Book of Standards, Part 4. ASTM International. West Conshohocken, PA.
- ASTM A 588. (1970). "Standard Specification for High-Strength Low-Alloy Structural Steel with 50,000 psi Minimum Yield Point to 4 in. Thick." ASTM Annual Book of Standards, Part 4. ASTM International. West Conshohocken, PA.

ASTM A 588. (1971). “Standard Specification for High-Strength Low-Alloy Structural Steel with 50,000 psi Minimum Yield Point to 4 in. Thick.” ASTM Annual Book of Standards, Part 4. ASTM International. West Conshohocken, PA.

ASTM A 588. (1974). “Standard Specification for High-Strength Low-Alloy Structural Steel with 50,000 psi Minimum Yield Point to 4 in. Thick.” ASTM Annual Book of Standards, Part 4. ASTM International. West Conshohocken, PA.

ASTM A 588. (1997). “Standard Specification for High-Strength Low-Alloy Structural Steel with 50 ksi Minimum Yield Point to 4 in. Thick.” ASTM Annual Book of Standards, Part 4. ASTM International. West Conshohocken, PA.

ASTM A 588. (2001). “Standard Specification for High-Strength Low-Alloy Structural Steel with 50 ksi [345 MPa] Minimum Yield Point to 4 in. [100-mm] Thick.” ASTM Annual Book of Standards. ASTM International. West Conshohocken, PA.

ASTM A 588. (2019). “Standard Specification for High-Strength Low-Alloy Structural Steel with 50 ksi [345 MPa] Minimum Yield Point, with Atmospheric Corrosion Resistance.” ASTM Annual Book of Standards. ASTM International. West Conshohocken, PA. ASTM A370. (2021). “Standard Test Methods and Definitions for Mechanical Testing of Steel Products.” ASTM Annual Book of Standards. ASTM International. West Conshohocken, PA.

ASTM E23. (2018). “Standard Test Methods for Notched Bar Impact Testing of Metallic Materials.” ASTM Annual Book of Standards. ASTM International. West Conshohocken, PA.

ASTM E29. (2022). “Standard Practice for Using Significant Digits in Test Data to Determine Conformance with Specifications.” ASTM Annual Book of Standards. ASTM International. West Conshohocken, PA.

ASTM E83. (2016). “Standard Practice for Verification and Classification of Extensometer Systems.” ASTM Annual Book of Standards. ASTM International. West Conshohocken, PA.

ASTM E415. (2021). “Standard Test Method for Analysis of Carbon and Low-Alloy Steel by Spark Atomic Emission Spectrometry.” ASTM Annual Book of Standards. ASTM International. West Conshohocken, PA.

ASTM G101. (2020). “Standard Guide for Estimating the Atmospheric Corrosion Resistance of Low-Alloy Steels.” ASTM Annual Book of Standards. ASTM International. West Conshohocken, PA.

ASTM Proceedings (1971). “Committee Reports.” Vol. 71. ASTM International. West Conshohocken, PA.

AWS D1.5 (2020). “Bridge Welding Code.” 8th Edition, American Welding Society. Miami, FL.

AWS D2.0. (1969). “Specifications for Welded Highway and Railway Bridges.” 8th Edition, American Welding Society. Miami, FL.

Dearden, J., and O'Neill, H. (1940). *A guide to the selection and welding of low alloy structural steels*. Trans. Inst. Weld. 3: 203-214.

NIST (2012). “SEMATECH e-Handbook of Statistical Methods.” Accessed January 17, 2023. <https://doi.org/10.18434/M32189>

Appendix A: Record of Evidence prior to Cutting



Figure A.1. B1R – NTSB-STR-001.



Figure A.2. B1R – NTSB-STR-002 & NTSB-STR-003.



Figure A.3. B1R – NTSB-STR-004.



Figure A.4. B1R – NTSB-STR-005.



Figure A.5. B1R – NTSB-STR-006.



Figure A.6. B1R – NTSB-STR-007.



Figure A.7. B1R – NTSB-STR-008.



Figure A.8. B1R – NTSB-STR-009.



Figure A.9. B1R – NTSB-STR-010.



Figure A.10. B1R – NTSB-STR-011.



Figure A.11. B1L – NTSB-STR-012.



Figure A.12. B1L – NTSB-STR-013.



Figure A.13. B1L – NTSB-STR-014.



Figure A.14. B1L – NTSB-STR-015.



Figure A.15. B1L – NTSB-STR-016.



Figure A.16. B1L – NTSB-STR-017.



Figure A.17. B2L – NTSB-STR-018.



Figure A.18. B2L – NTSB-STR-019 & NTSB-STR-020.



Figure A.19. B2L – NTSB-STR-021.



Figure A.20. B2L – NTSB-STR-022.



Figure A.21. B2L – NTSB-STR-023.



Figure A.22. B2L – NTSB-STR-024.



Figure A.23. B2L – NTSB-STR-025.



Figure A.24. B2R – NTSB-STR-026.



Figure A.25. B2R – NTSB-STR-027.



Figure A.26. B2R – NTSB-STR-028A (Taken at TFHRC).



Figure A.27. B2R – NTSB-STR-028B (Taken at TFHRC).



Figure A.28. B2R – NTSB-STR-029.



Figure A.29. B2R – NTSB-STR-030.



Figure A.30. B2R – NTSB-STR-031.



Figure A.31. B2R – NTSB-STR-032.

Appendix B: Cutting Plan

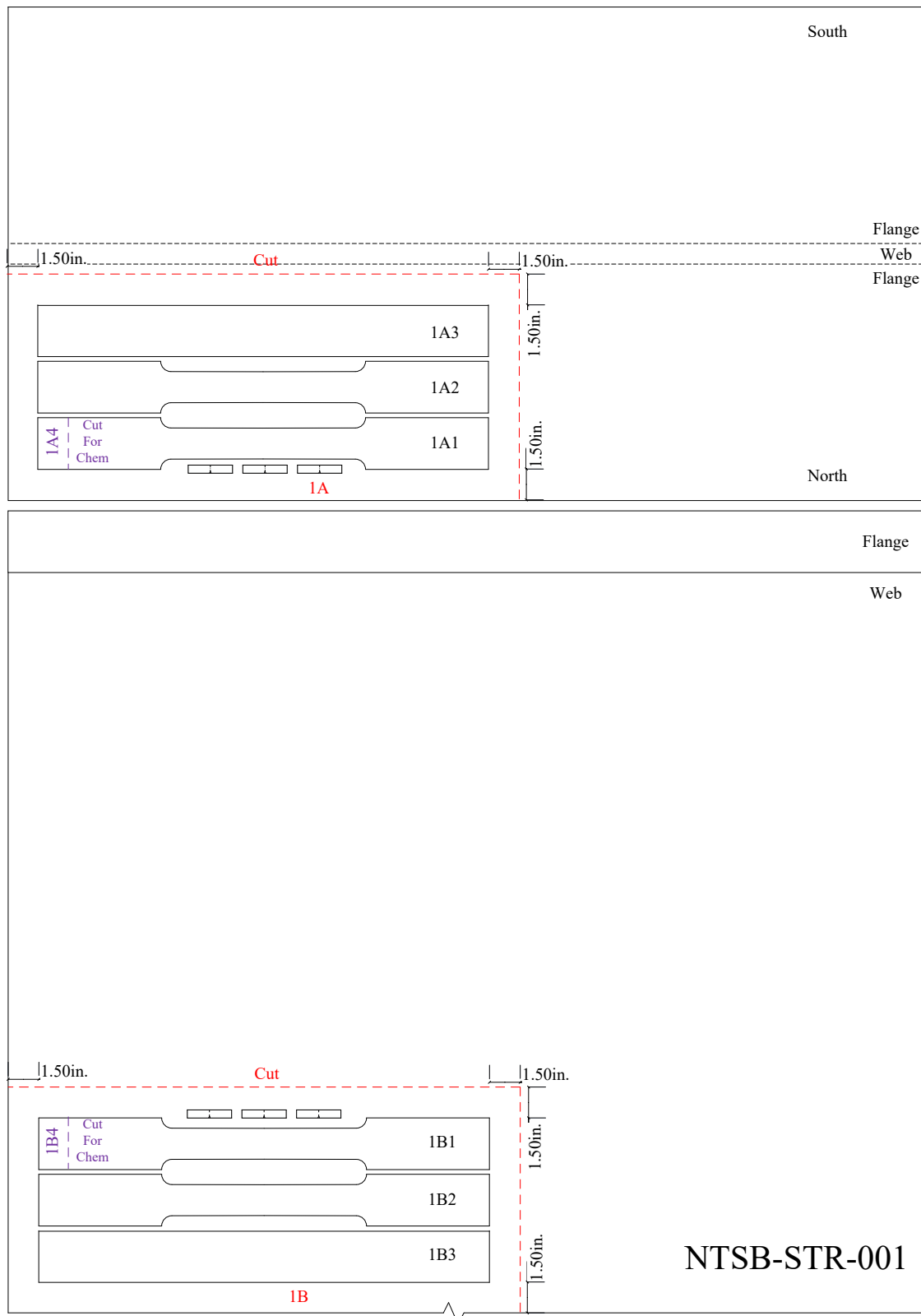


Figure B.1. B1R – NTSB-STR-001.

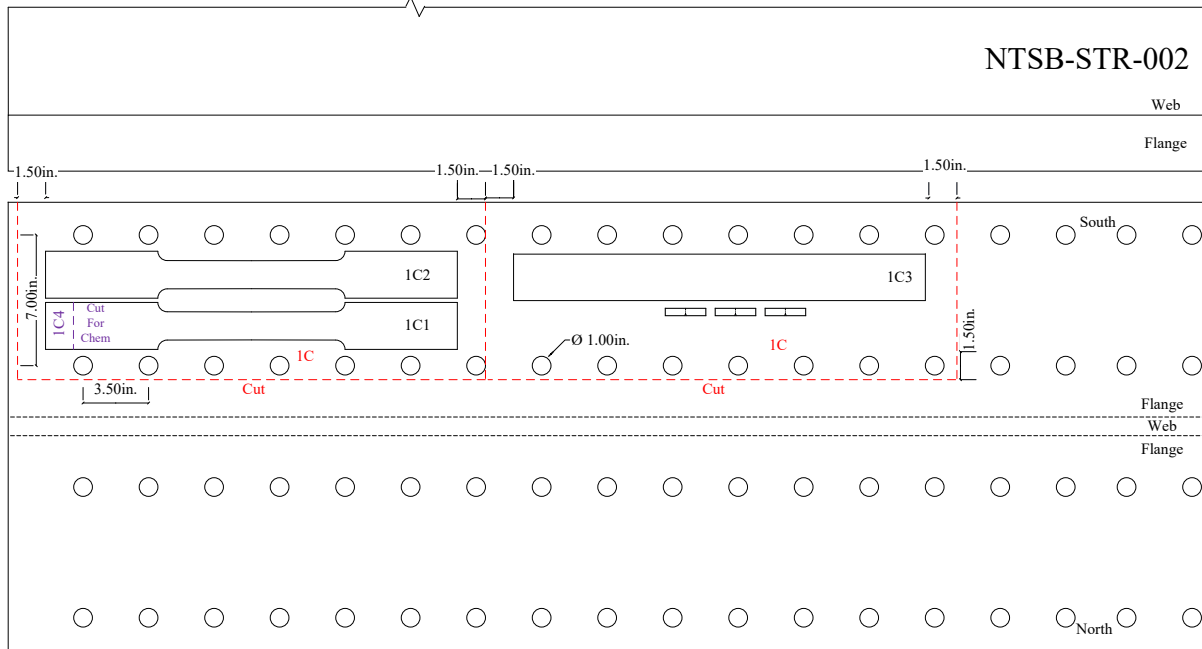


Figure B.2. B1R – NTSB-STR-002.

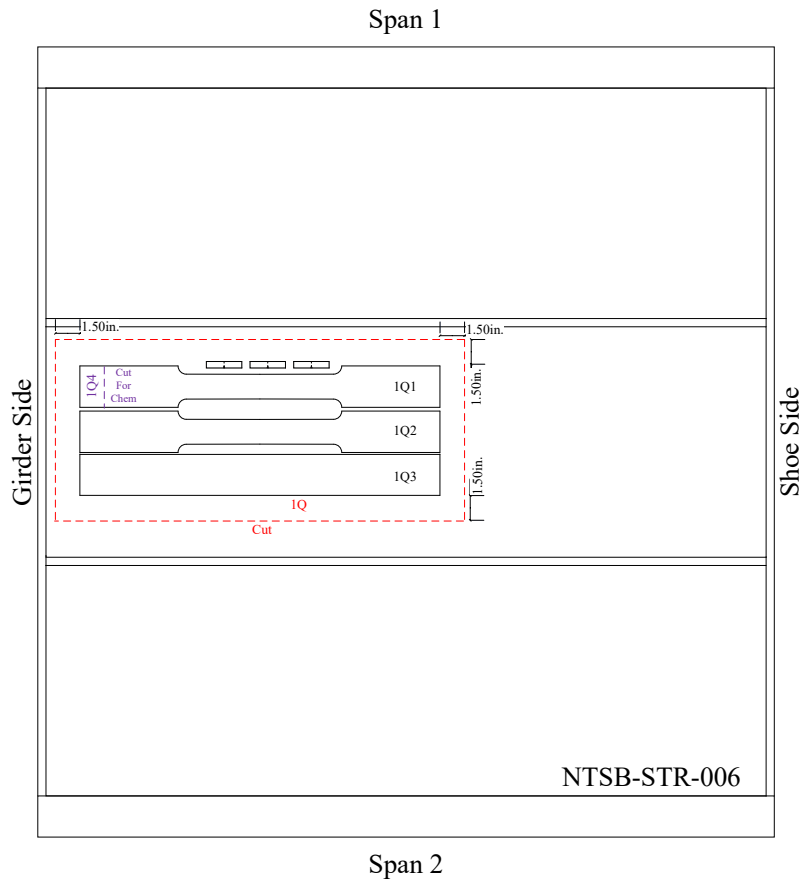
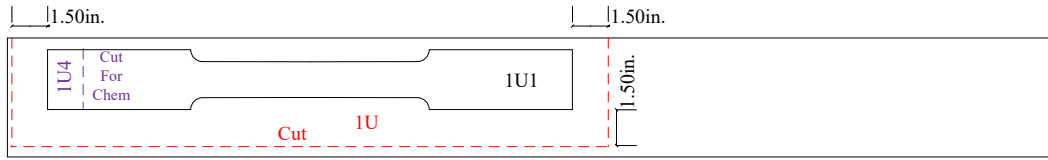


Figure B.3. B1R – NTSB-STR-006.



Span 1 Longitudinal Stiffener

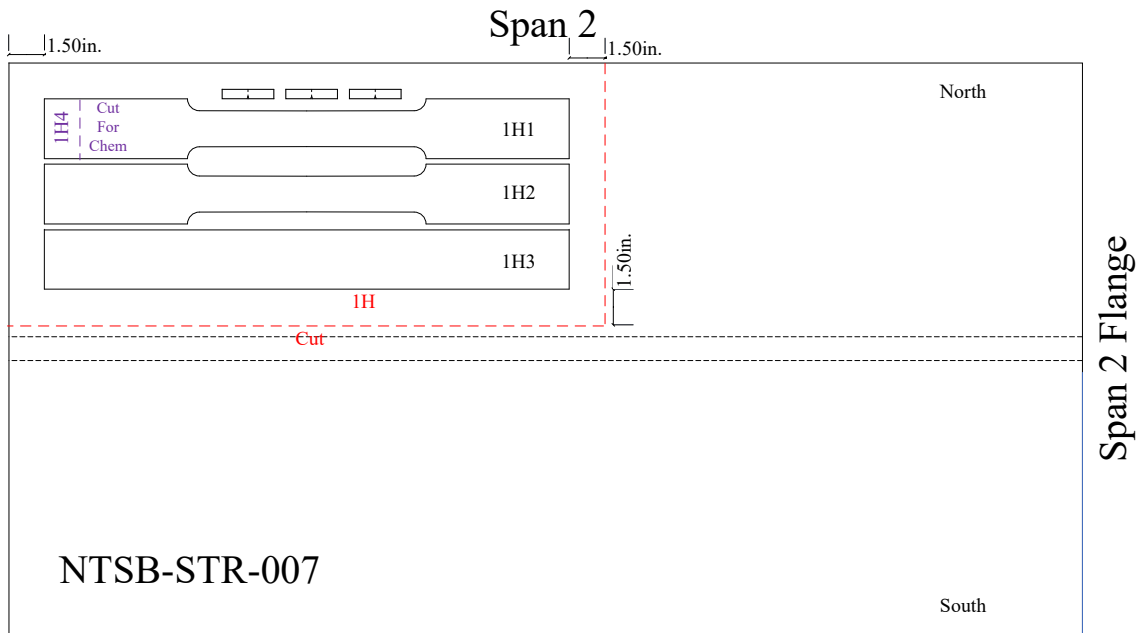


Figure B.4. B1R – NTSB-STR-007.

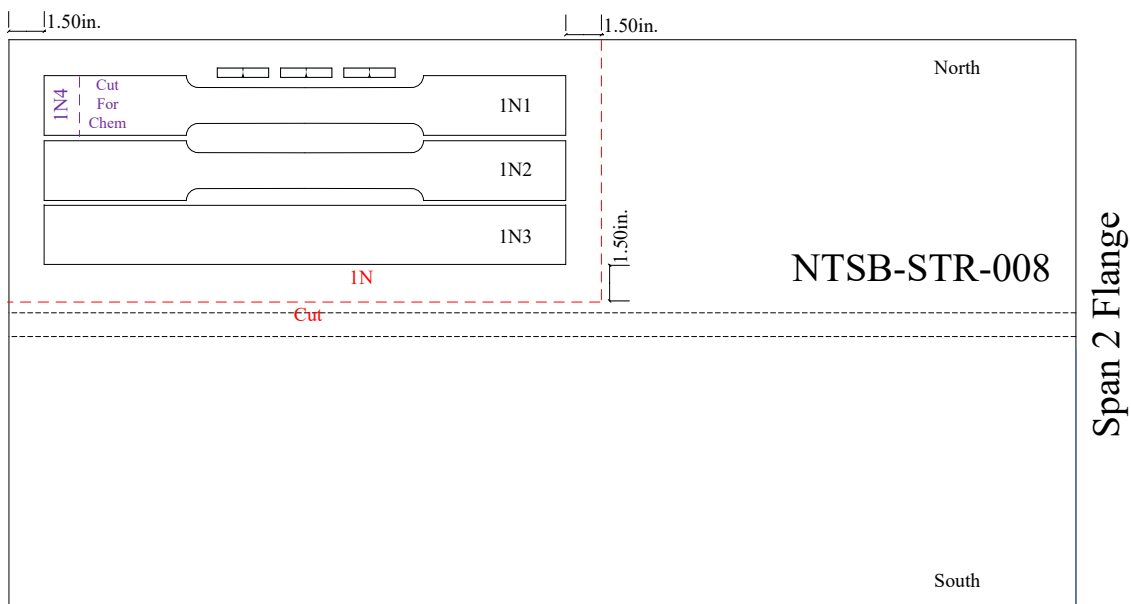


Figure B.5. B1R – NTSB-STR-008.

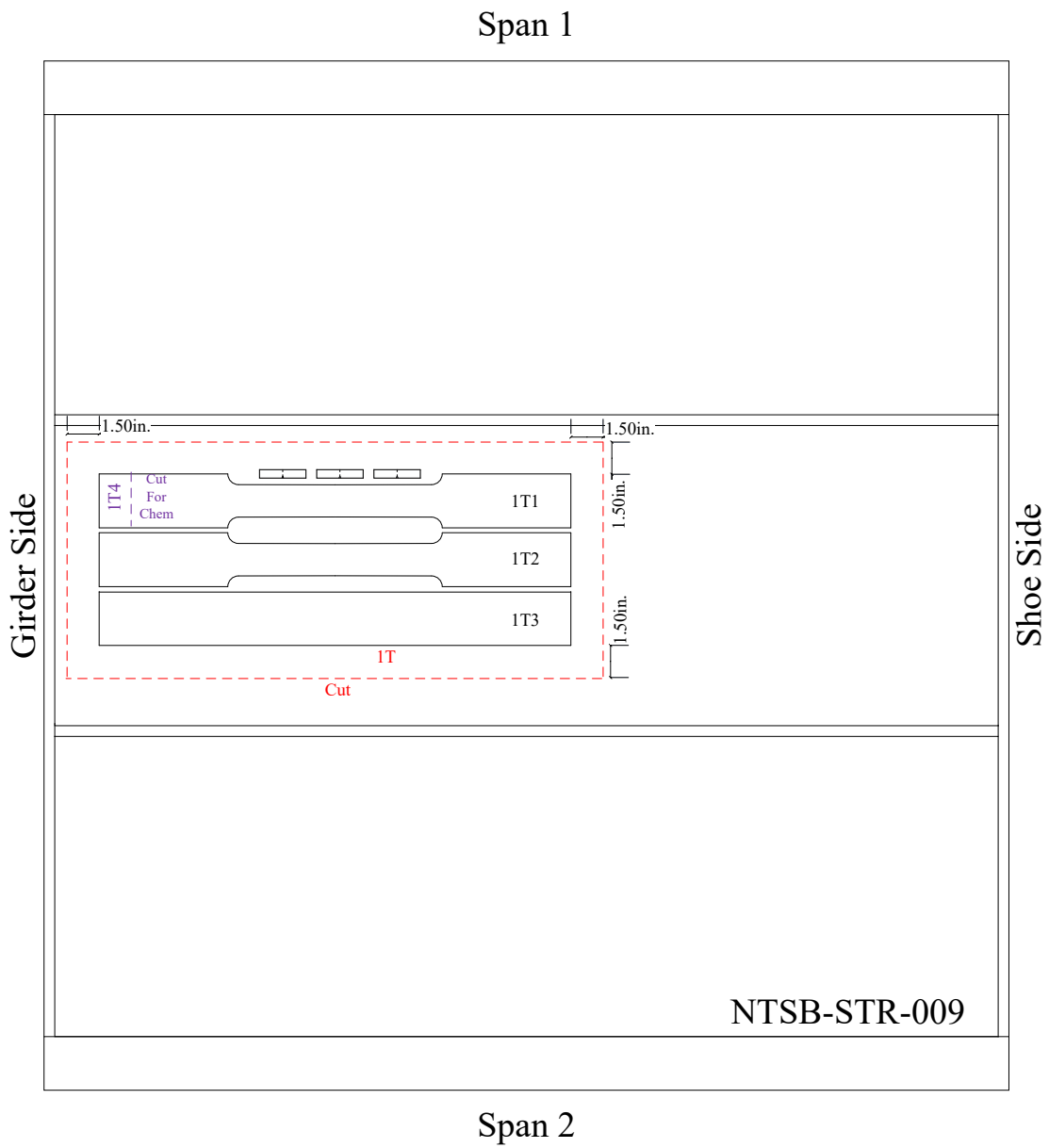


Figure B.6. B1R – NTSB-STR-009.

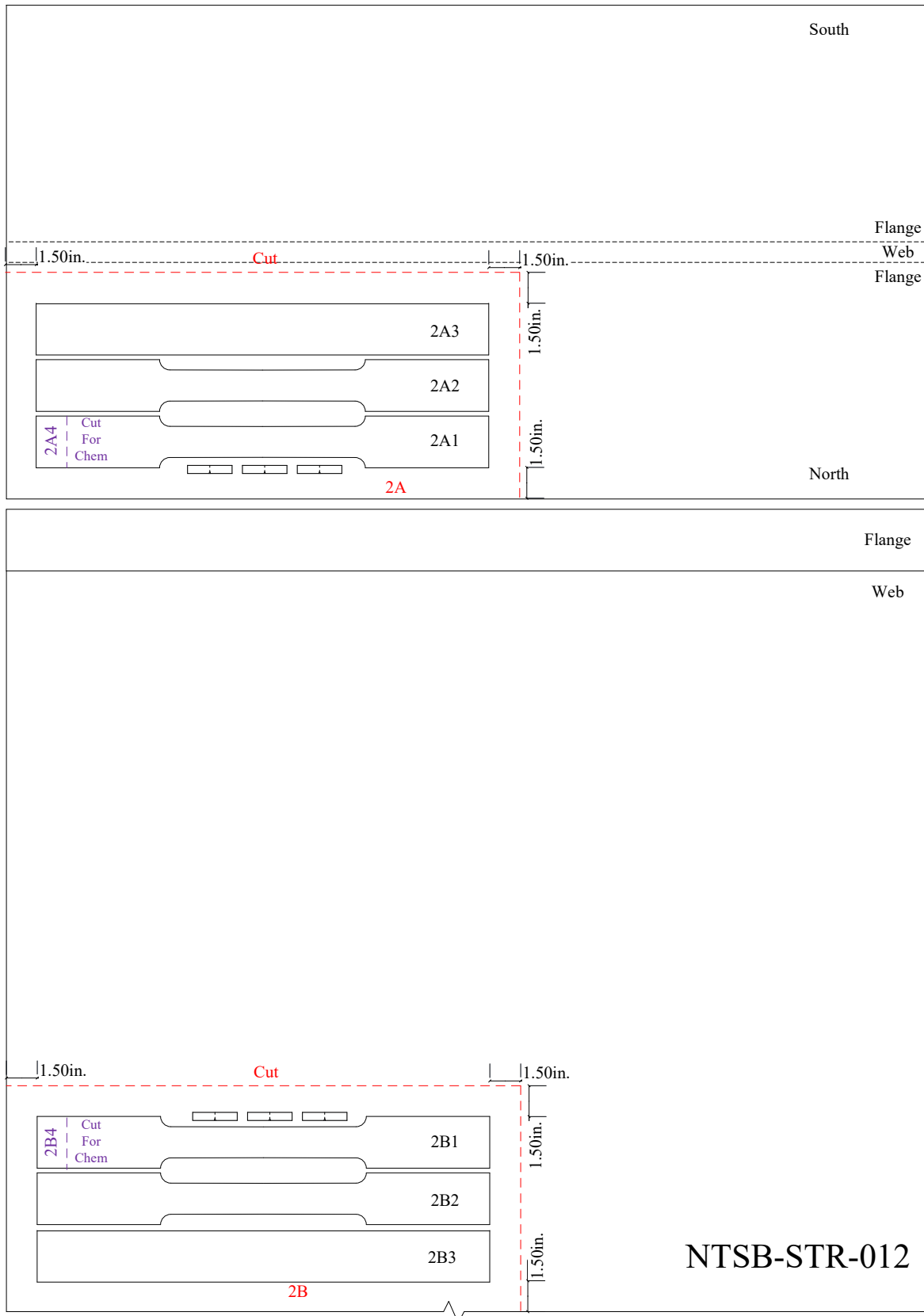


Figure B.7. B1L – NTSB-STR-012.

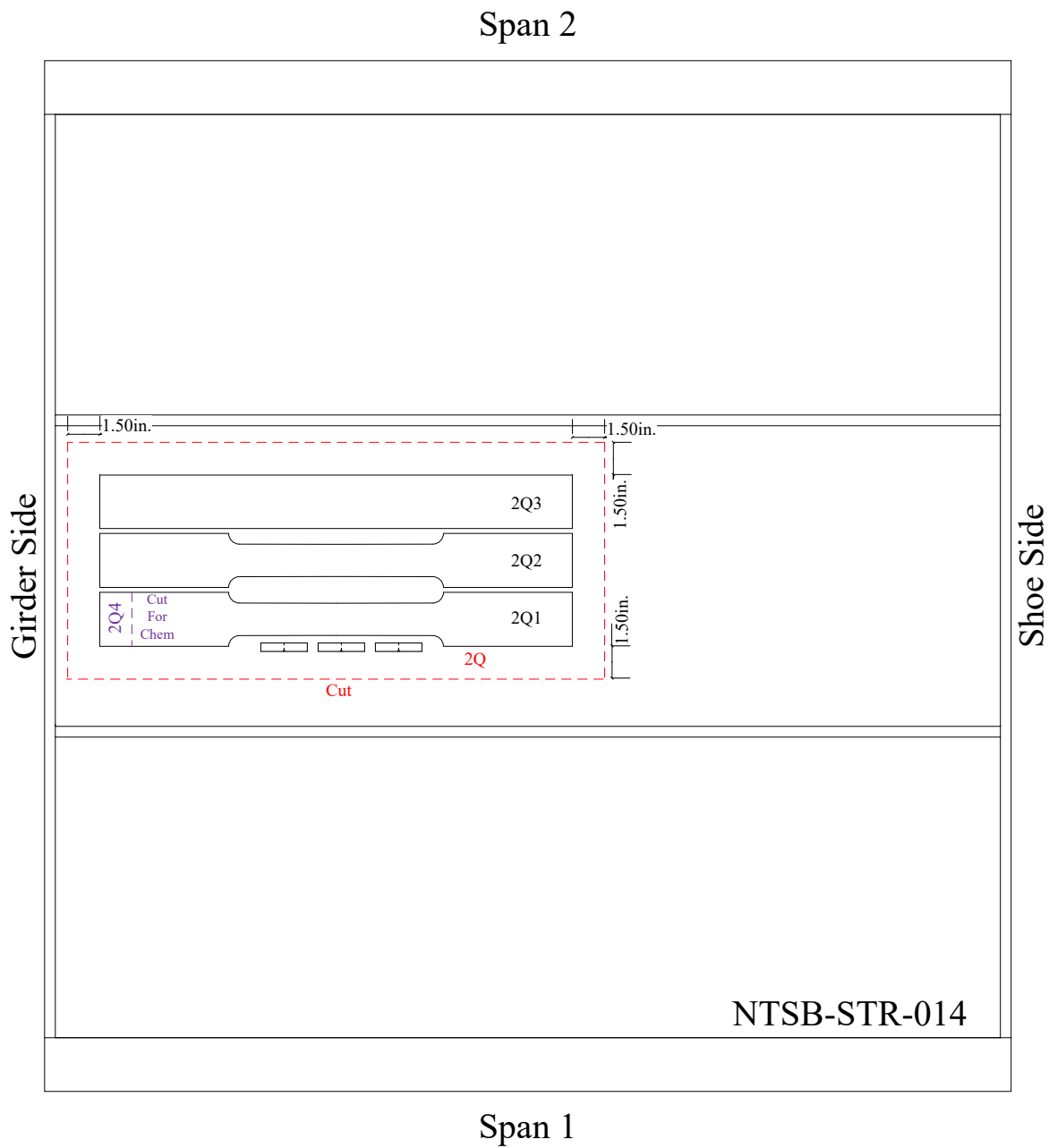
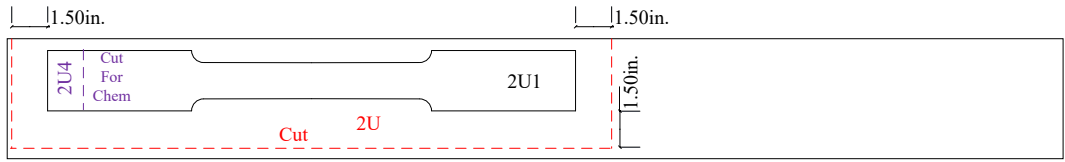
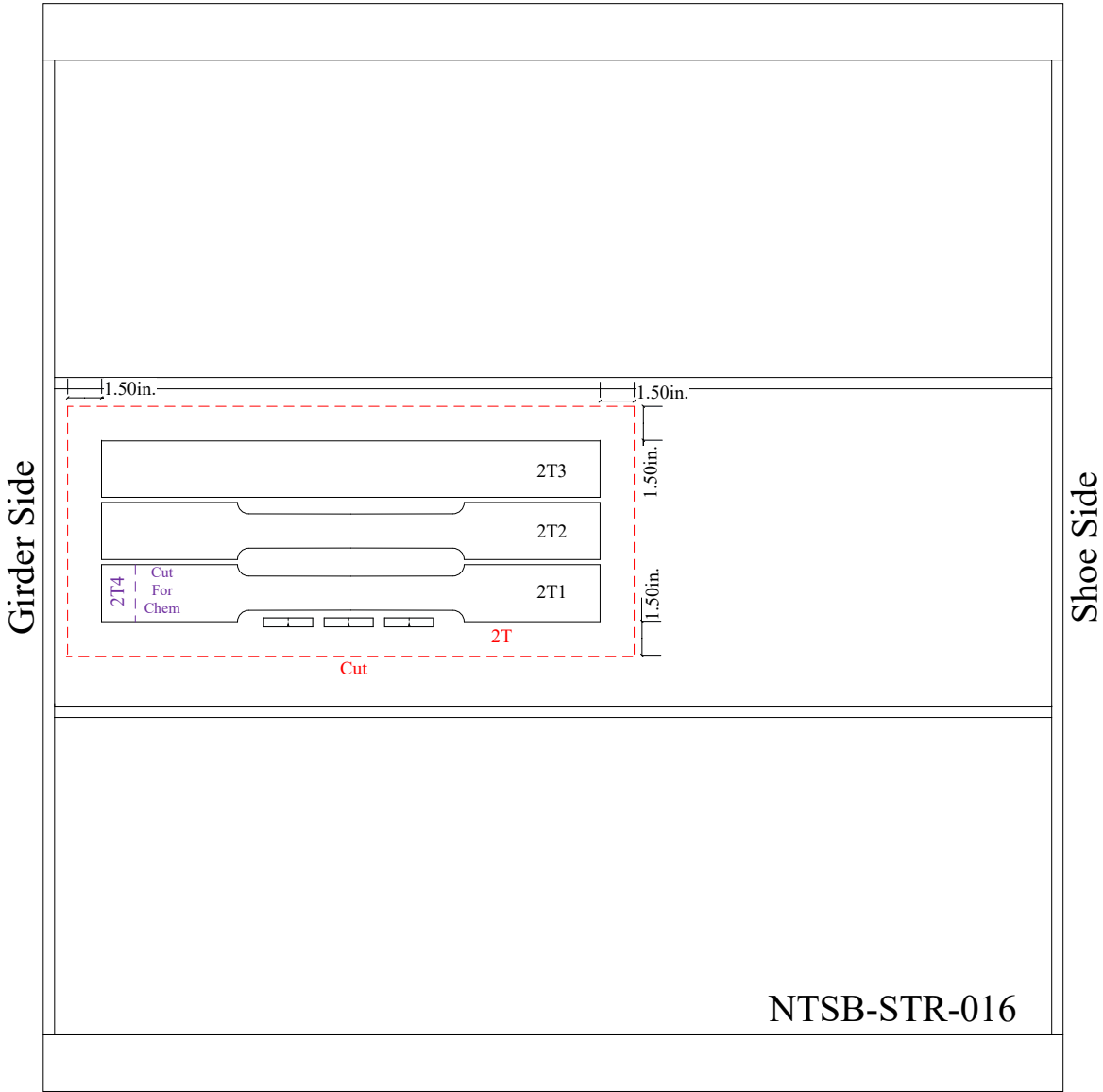


Figure B.8. B1L – NTSB-STR-014.



Span 2 Longitudinal Stiffener

Span 2



Span 1

Figure B.9. B1L – NTSB-STR-016.

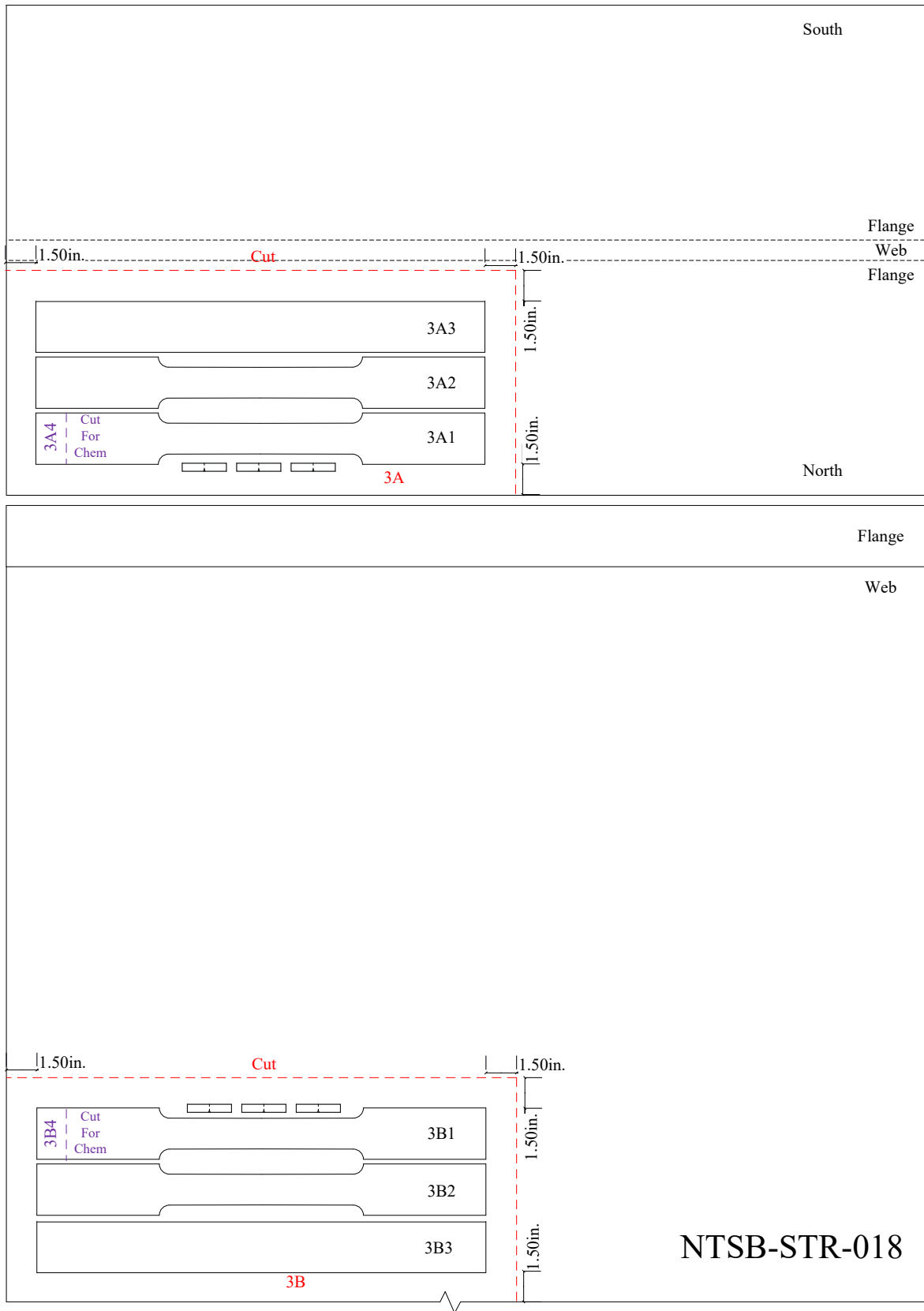


Figure B.10. B2L – NTSB-STR-018.

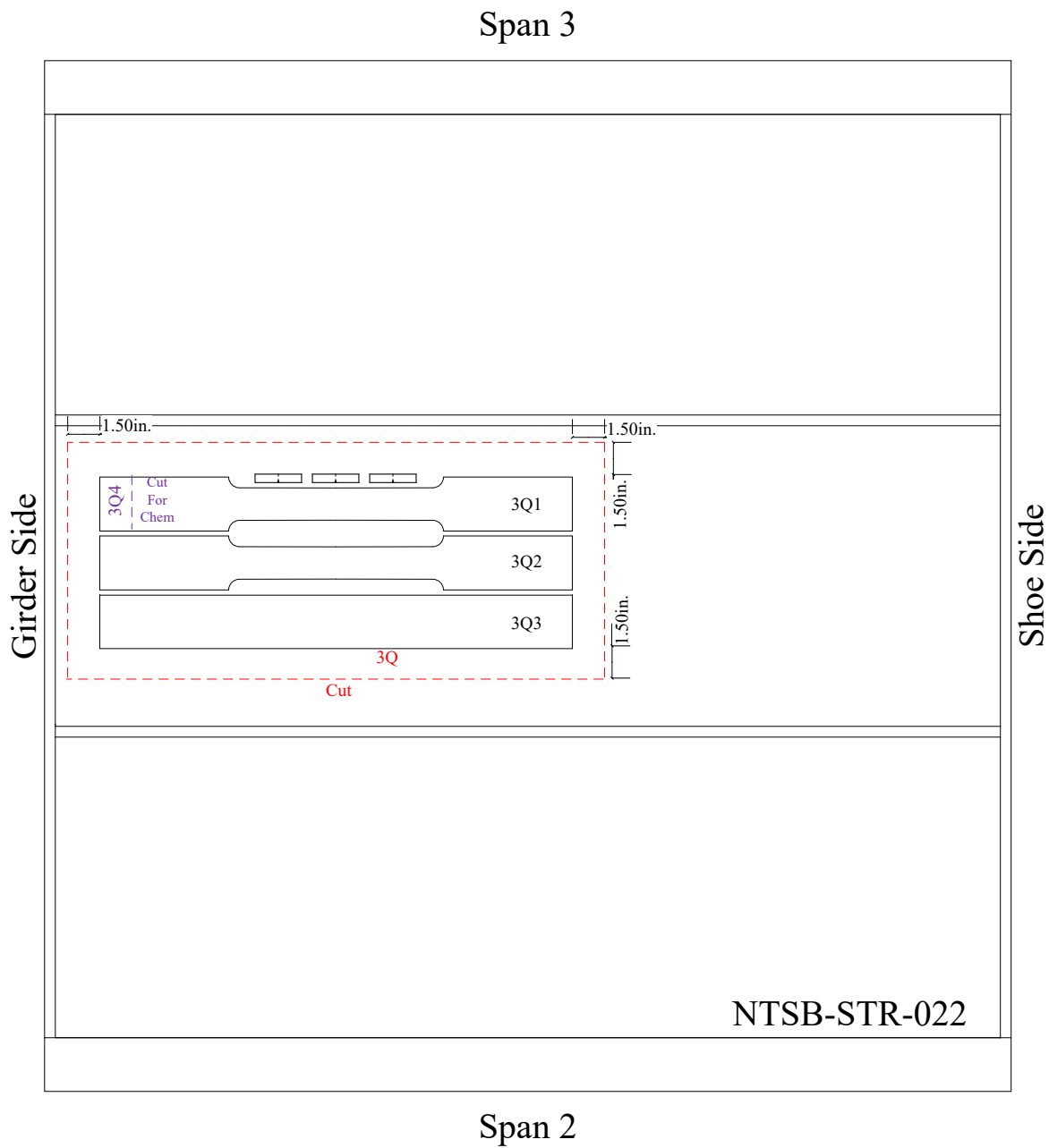
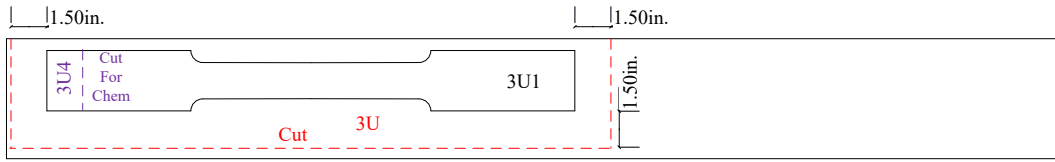
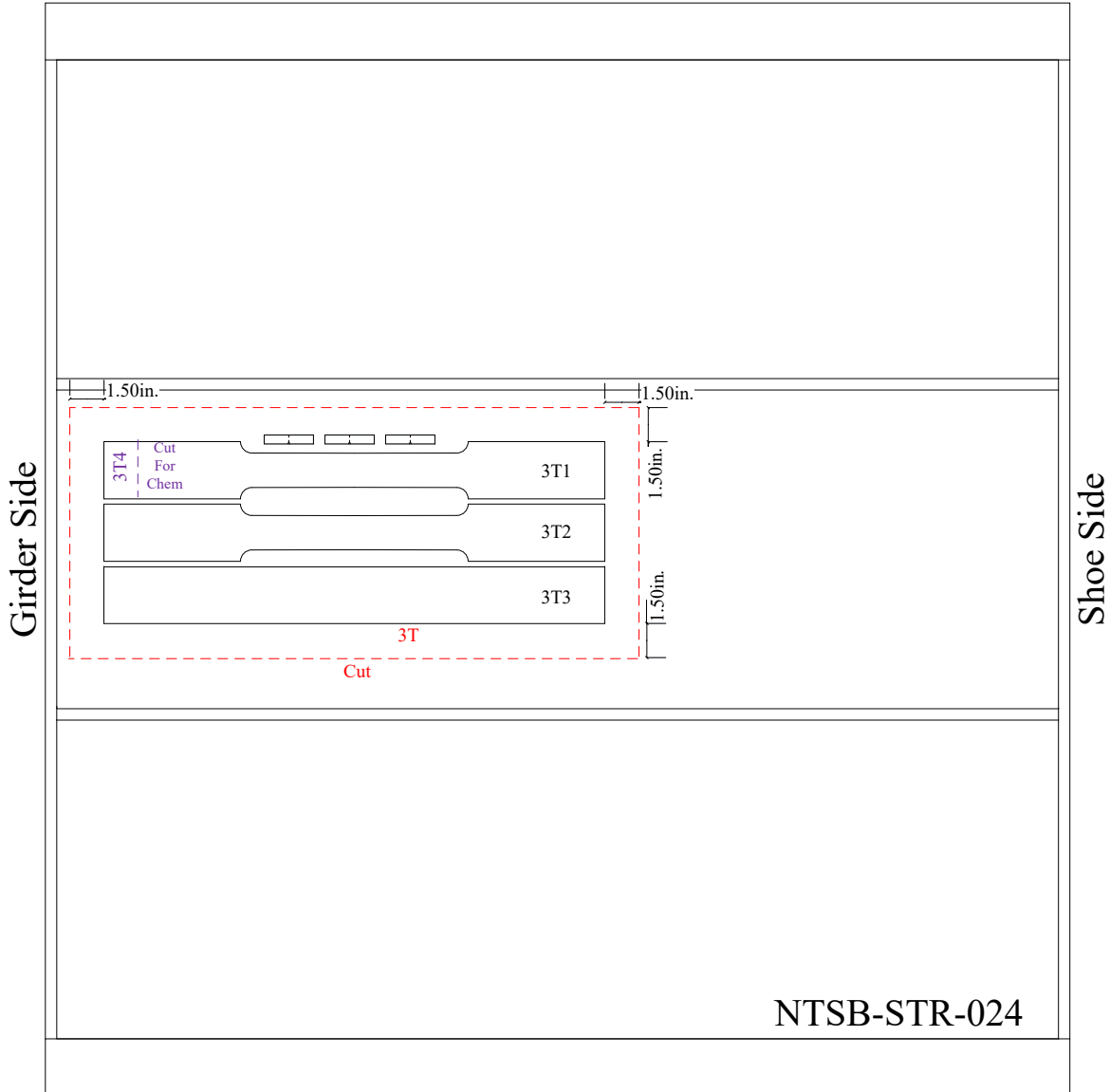


Figure B.11. B2L – NTSB-STR-022.



Span 3 Longitudinal Stiffener

Span 3



Span 2

Figure B.12. B2L – NTSB-STR-024.

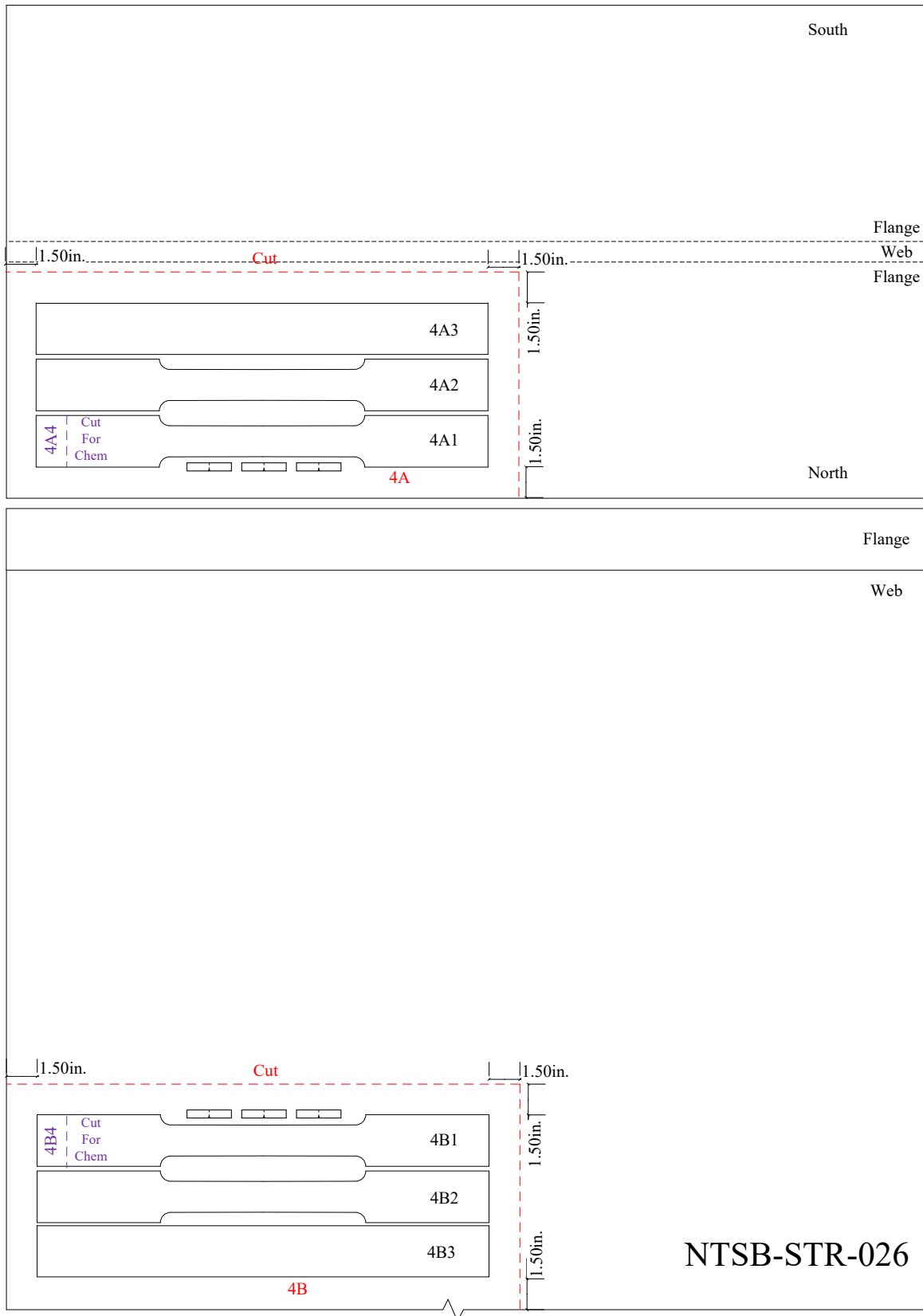


Figure B.13. B2R – NTSB-STR-026.

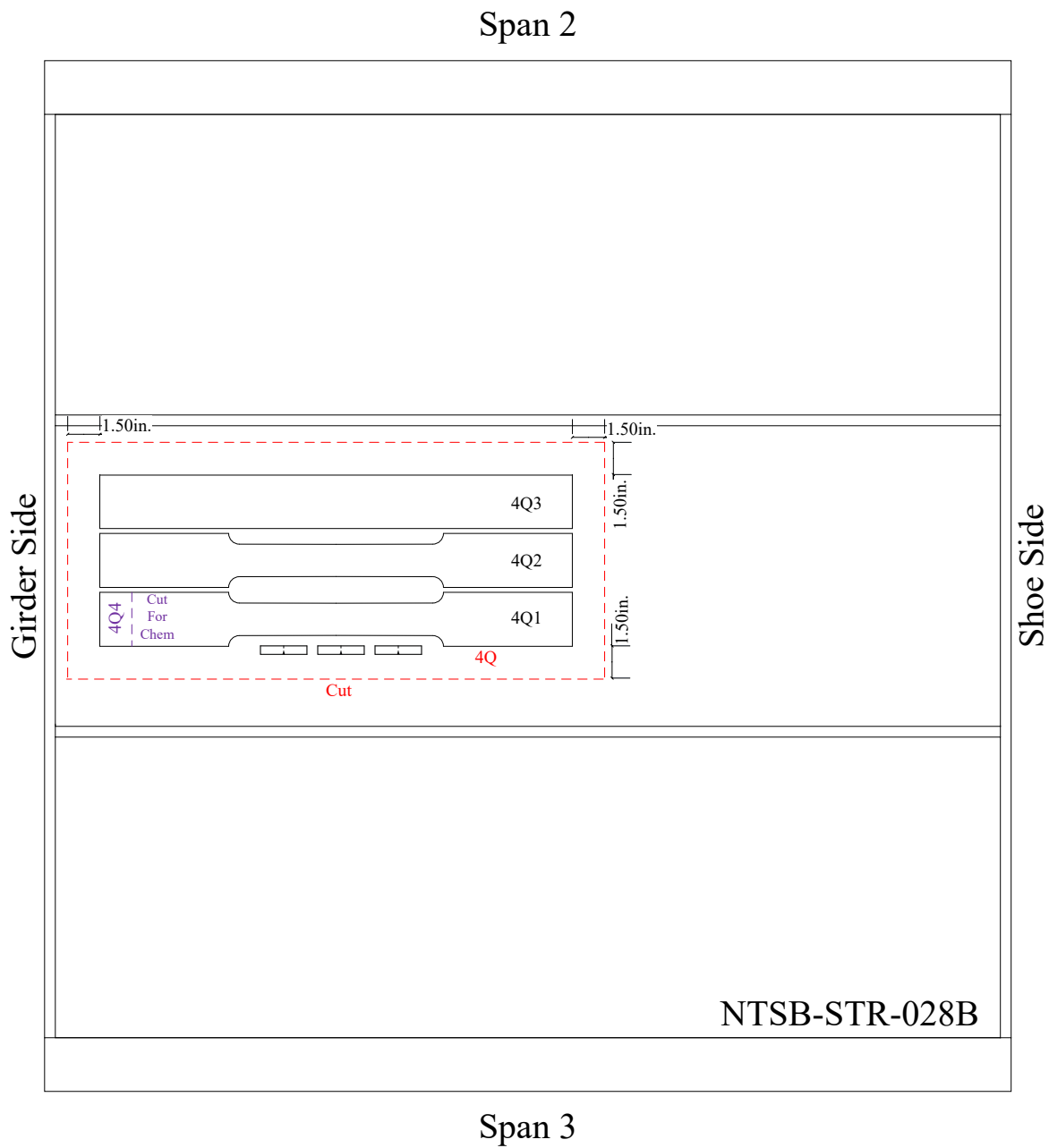


Figure B.14. B2R – NTSB-STR-028B.

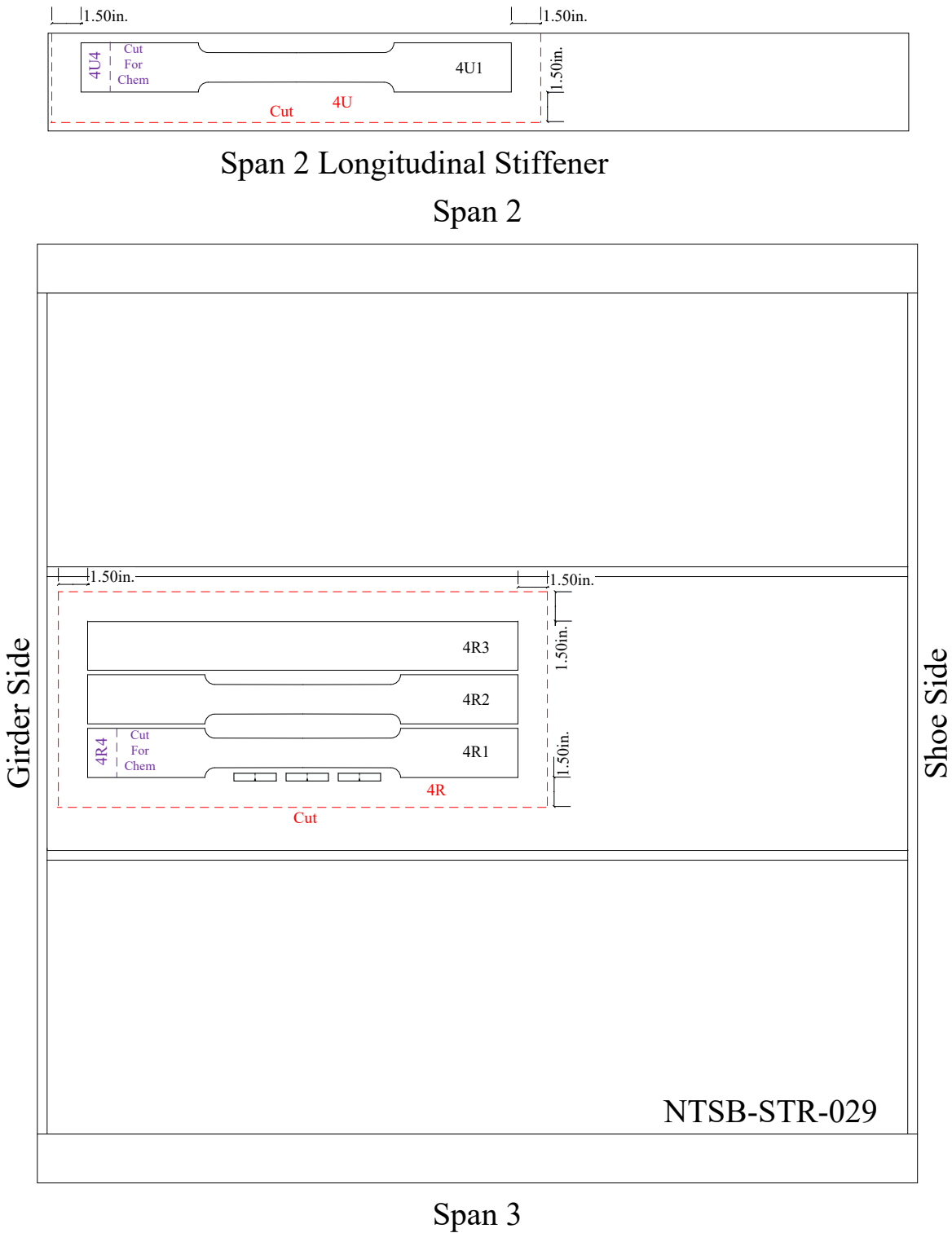


Figure B.15. B2R – NTSB-STR-029.

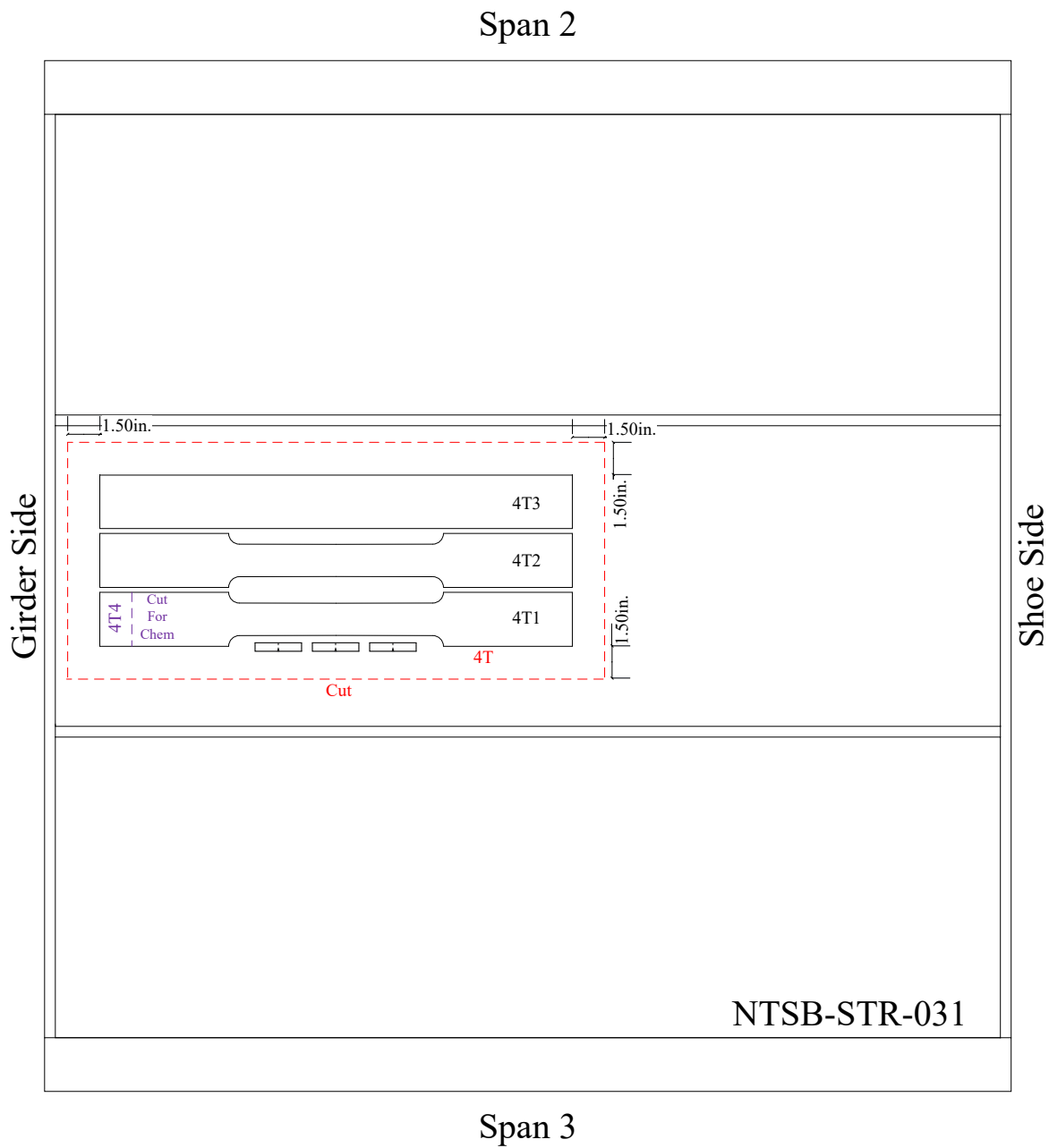
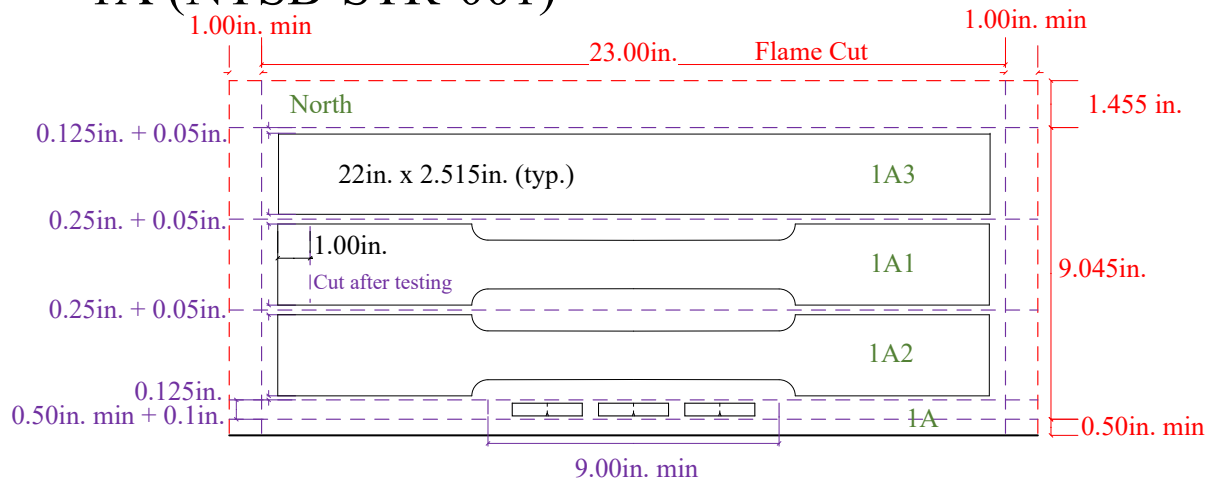


Figure B.16. B2R – NTSB-STR-031.

Appendix C: Specimen Extraction Shop Drawings

1A (NTSB-STR-001)



¹CVNs are nested in the L-T orientation, rough cut into a 9.00in. x 0.5in. min strip including kerf for 0.035in. blade (i.e. at least 0.5in material remaining across the width)

²Mill scale/patina layer from the CVN strip is not faced.

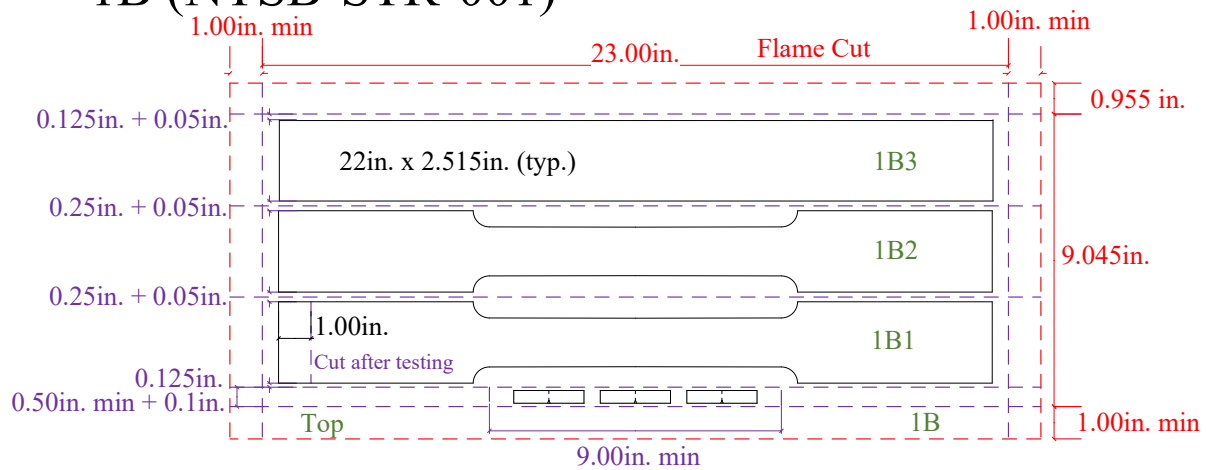
³Component names are punched on both ends of the coupons, blank, and CVN strip.

⁴All scrap is labeled 1A with a paint pen.

⁵Coupons and blanks have a 2.515in. grip width to allow taper in the gage length.

Figure C.1. 1A – NTSB-STR-001.

1B (NTSB-STR-001)



¹CVNs are nested in the L-T orientation, rough cut into a 9.00in. x 0.5in. min strip including kerf for 0.035in. blade (i.e. at least 0.5in material remaining across the width)

²Mill scale/patina layer from the CVN strip is not faced.

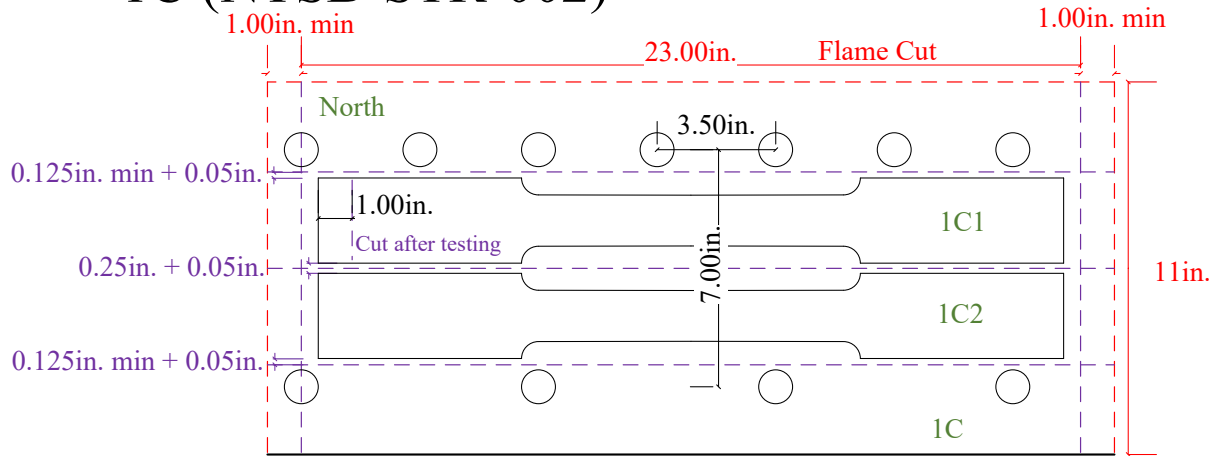
³Component names are punched on both ends of the coupons, blank, and CVN strip.

⁴All scrap is labeled 1B with a paint pen.

⁵Coupons and blanks have a 2.515in. grip width to allow taper in the gage length.

Figure C.2. 1B – NTSB-STR-001.

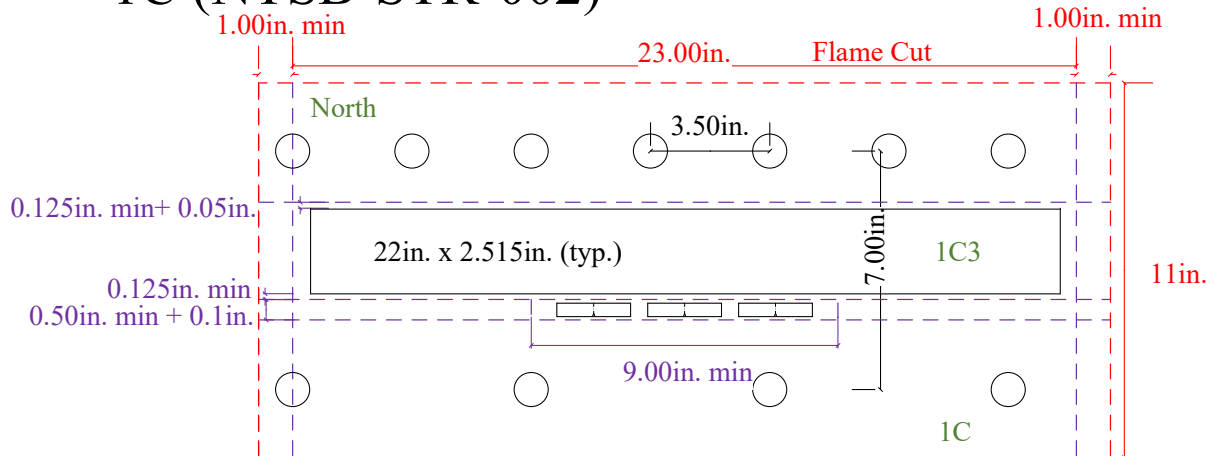
1C (NTSB-STR-002)



- ¹Component names are punched on both ends of the coupons.
- ²All scrap is labeled 1C with a paint pen.
- ³Coupons have a 2.515in. grip width to allow taper in the gage length.

Figure C.3. 1C – NTSB-STR-002.

1C (NTSB-STR-002)



- ¹CVNs are nested in the L-T orientation, rough cut into a 9.00in. x 0.5in. min strip including kerf for 0.035in. blade (i.e. at least 0.5in material remaining across the width)
- ²Mill scale/patina layer from the CVN strip is not faced.
- ³Component names are punched on both ends of the blank and CVN strip.
- ⁴All scrap is labeled 1C with a paint pen.
- ⁵Blank has a 2.515in. grip width.

Figure C.4. 1C – NTSB-STR-002.

1D (NTSB-STR-004)

- ¹ Cut lines are spaced 1 in. from the weld toes
- ² Punch component names on both the east and west ends
- ³ All scrap can be labeled 1D with a paint pen, spray paint, or punch

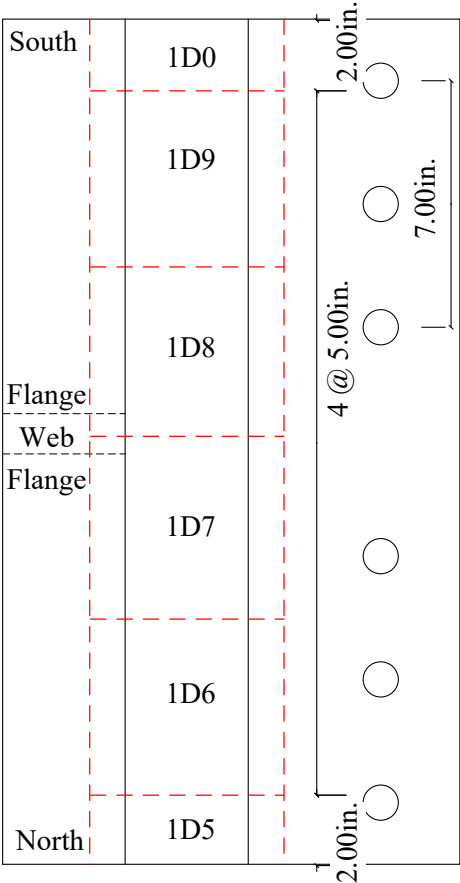
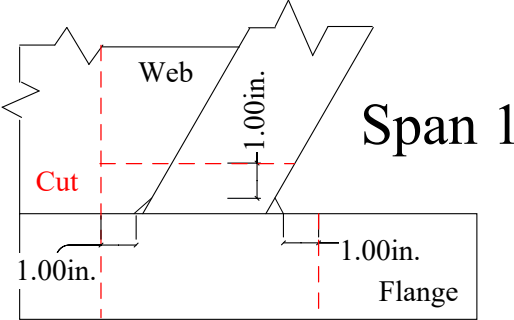
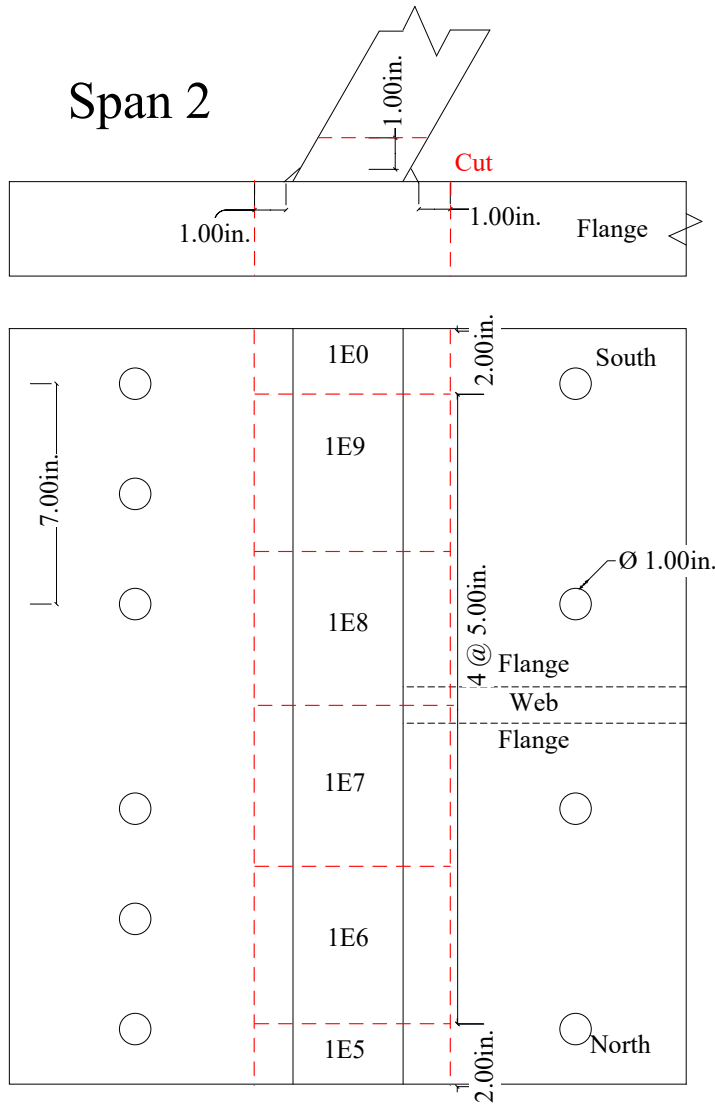


Figure C.5. 1D – NTSB-STR-004.



1E (NTSB-STR-003)

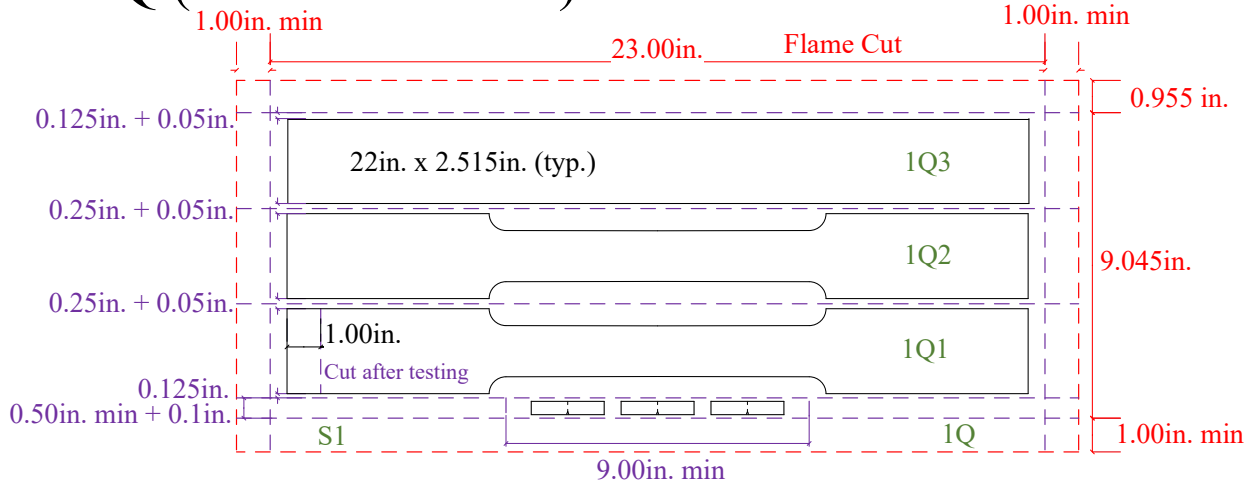
¹Cut lines are spaced 1 in. from the weld toes

²Punch component names on both the east and west ends

³All scrap can be labeled 1E with a paint pen, spray paint, or punch

Figure C.6. 1E – NTSB-STR-003.

1Q (NTSB-STR-006)



¹CVNs are nested in the L-T orientation, rough cut into a 9.00in. x 0.5in. min strip including kerf for 0.035in. blade (i.e. at least 0.5in material remaining across the width)

²Mill scale/patina layer from the CVN strip is not faced.

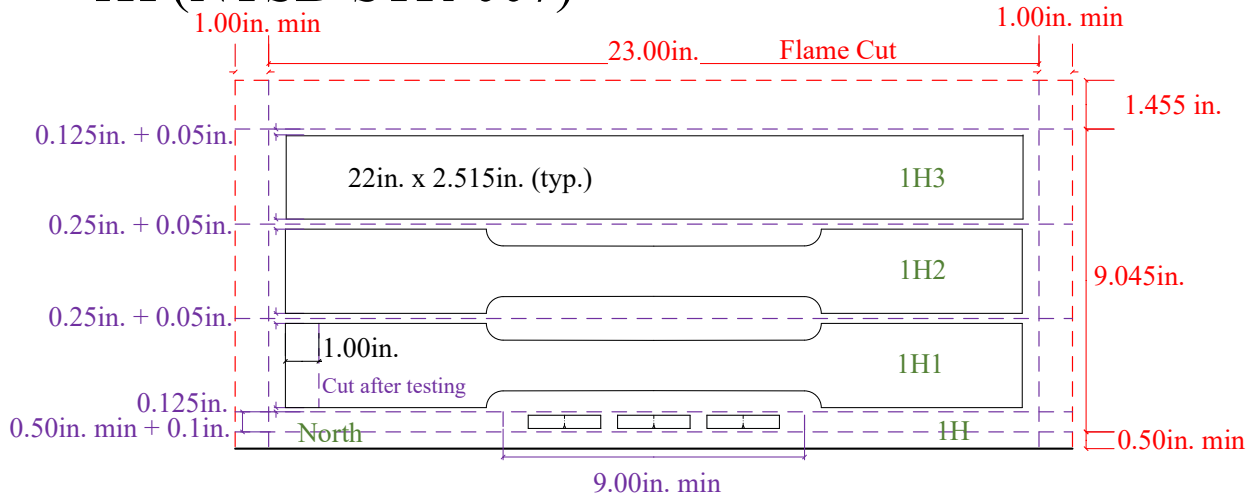
³Component names are punched on both ends of the coupons, blank, and CVN strip.

⁴All scrap is labeled 1Q with a paint pen.

⁵Coupons and blanks have a 2.515in. grip width to allow taper in the gage length.

Figure C.7. 1Q – NTSB-STR-006.

1H (NTSB-STR-007)



¹CVNs are nested in the L-T orientation, rough cut into a 9.00in. x 0.5in. min strip including kerf for 0.035in. blade (i.e. at least 0.5in material remaining across the width)

²Mill scale/patina layer from the CVN strip is not faced.

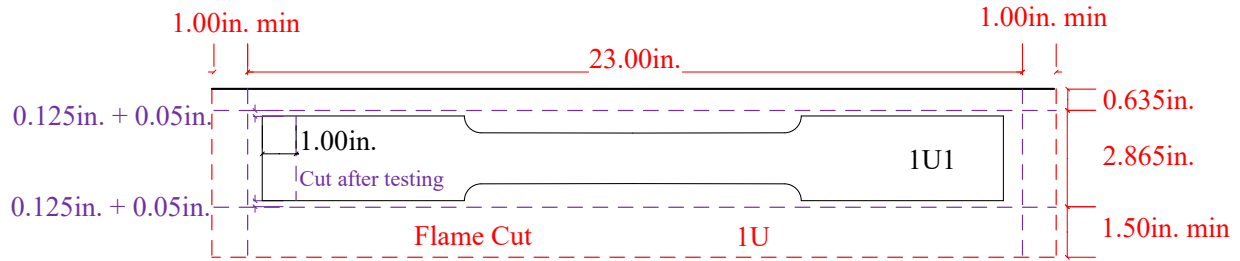
³Component names are punched on both ends of the coupons, blank, and CVN strip.

⁴All scrap is labeled 1H with a paint pen.

⁵Coupons and blanks have a 2.515in. grip width to allow taper in the gage length.

Figure C.8. 1H – NTSB-STR-007.

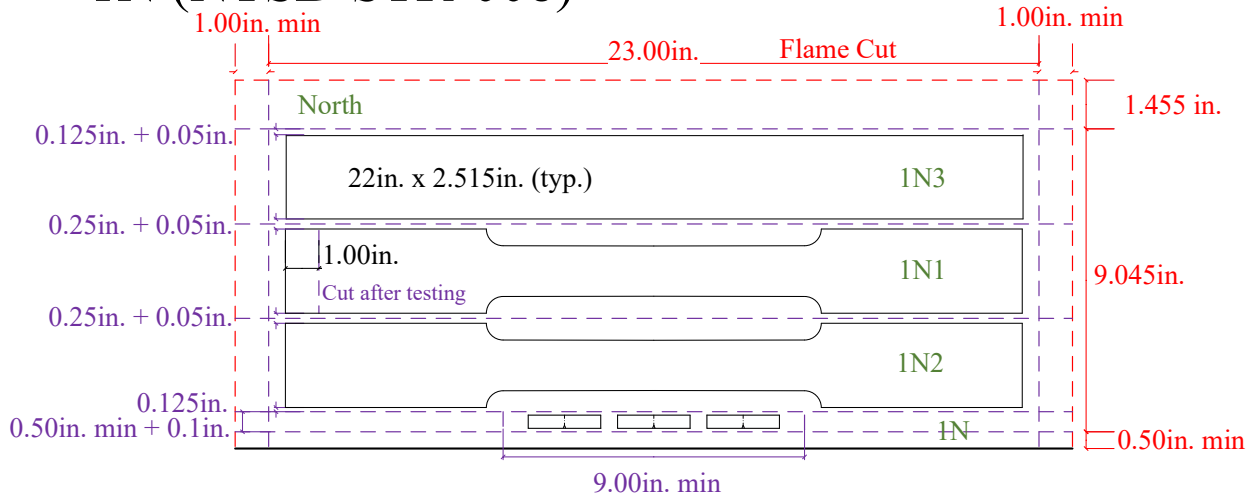
1U (NTSB-STR-007)



- ¹Component names are punched on both ends of the coupons.
- ²All scrap is labeled 1U with a paint pen.
- ³Coupons have a 2.515in. grip width to allow taper in the gage length.

Figure C.9. 1U – NTSB-STR-007.

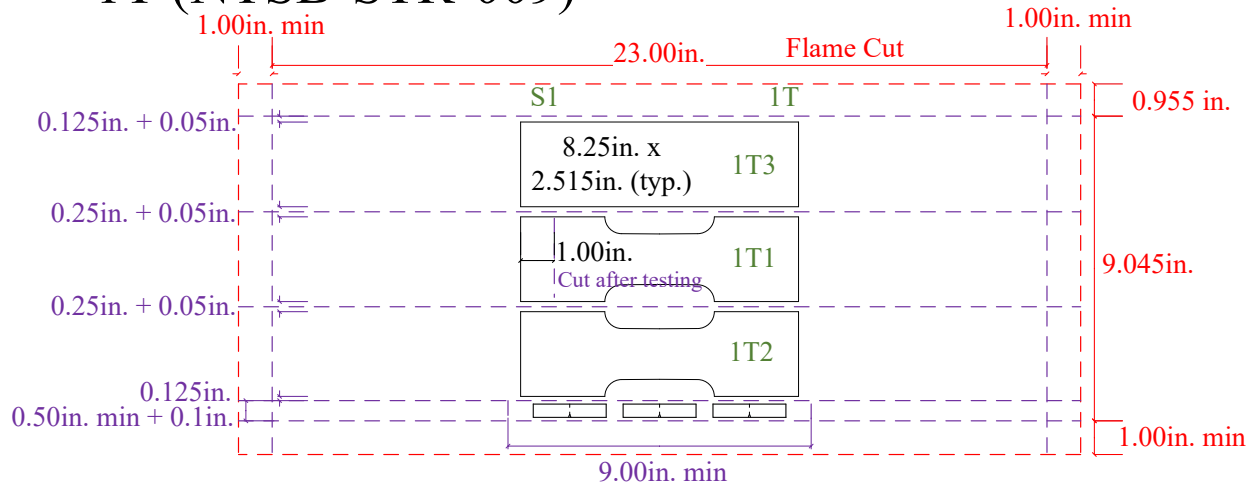
1N (NTSB-STR-008)



- ¹CVNs are nested in the L-T orientation, rough cut into a 9.00in. x 0.5in. min strip including kerf for 0.035in. blade (i.e. at least 0.5in material remaining across the width)
- ²Mill scale/patina layer from the CVN strip is not faced.
- ³Component names are punched on both ends of the coupons, blank, and CVN strip.
- ⁴All scrap is labeled 1N with a paint pen.
- ⁵Coupons and blanks have a 2.515in. grip width to allow taper in the gage length.

Figure C.10. 1N – NTSB-STR-008.

1T (NTSB-STR-009)



¹CVNs are nested in the L-T orientation, rough cut into a 9.00in. x 0.5in. min strip including kerf for 0.035in. blade (i.e. at least 0.5in material remaining across the width).

²Min CVN thickness of 0.394in. Take CVNs from S1 if the plate thickness is greater on that end, and/or shift the CVN/coupon grouping left/right.

³Mill scale/patina layer from the CVN strip is not faced.

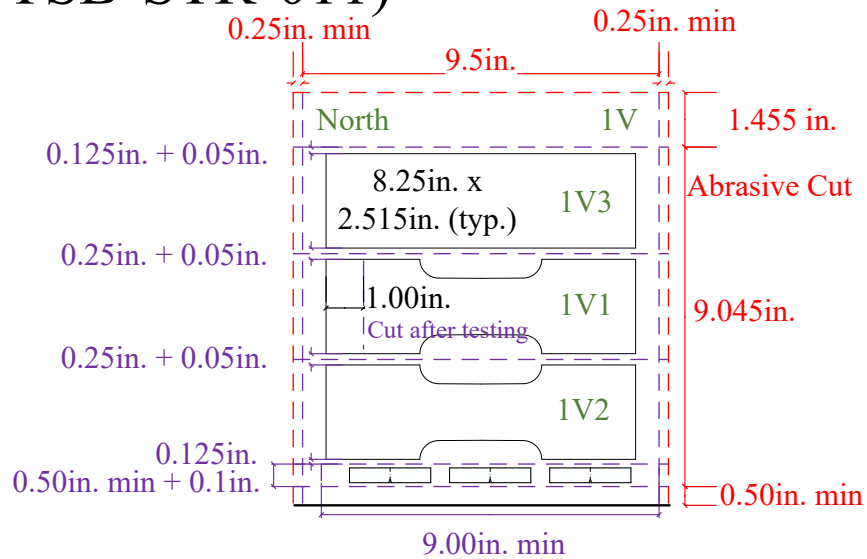
⁴Component names are punched on both ends of the coupons, blank, and CVN strip.

⁵All scrap is labeled 1T with a paint pen.

⁶Coupons and blanks have a 2.515in. grip width to allow taper in the gage length.

Figure C.11. 1T – NTSB-STR-009.

1V (NTSB-STR-011)



¹CVNs are nested in the L-T orientation, rough cut into a 9.00in. x 0.5in. min strip including kerf for 0.035in. blade (i.e. at least 0.5in material remaining across the width)

²CNV strip is offset to the right 5/16in. such that the 9in. strip starts on the edge of the bandsaw line to minimize the HAZ influence.

³Mill scale/patina layer from the CVN strip is not faced.

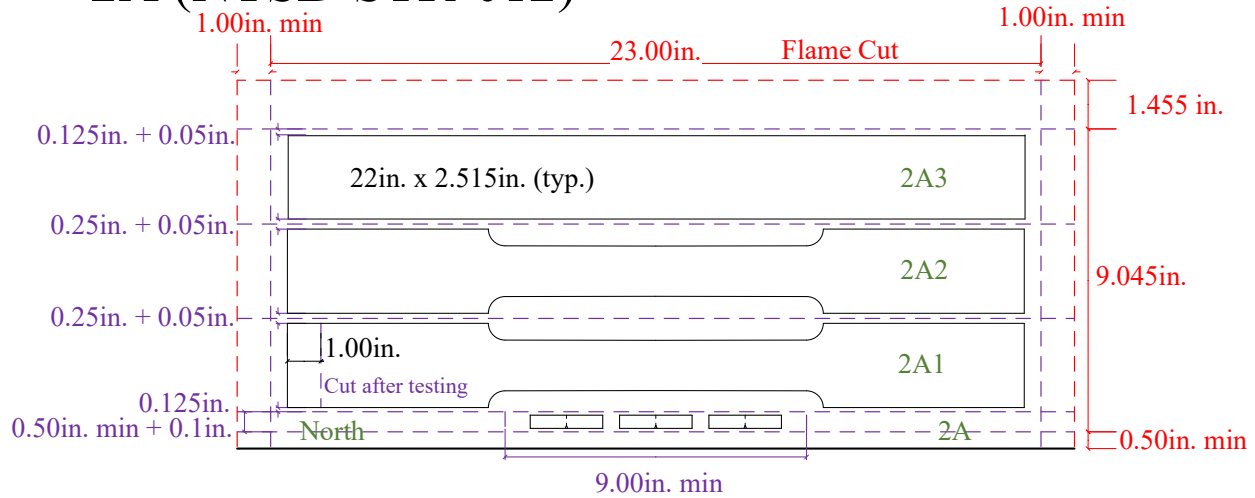
⁴Component names are punched on both ends of the coupons, blank, and CVN strip.

⁵All scrap is labeled 1V with a paint pen.

⁶Coupons and blanks have a 2.515in. grip width to allow taper in the gage length.

Figure C.12. 1V – NTSB-STR-011.

2A (NTSB-STR-012)



¹CVNs are nested in the L-T orientation, rough cut into a 9.00in. x 0.5in. min strip including kerf for 0.035in. blade (i.e. at least 0.5in material remaining across the width)

²Mill scale/patina layer from the CVN strip is not faced.

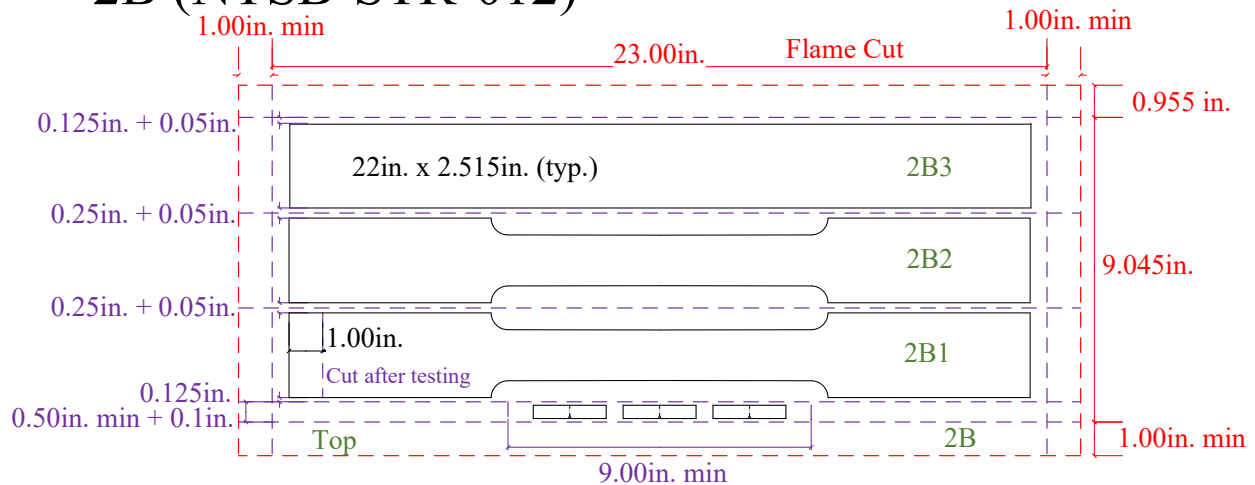
³Component names are punched on both ends of the coupons, blank, and CVN strip.

⁴All scrap is labeled 2A with a paint pen.

⁵Coupons and blanks have a 2.515in. grip width to allow taper in the gage length.

Figure C.13. 2A – NTSB-STR-012.

2B (NTSB-STR-012)



¹CVNs are nested in the L-T orientation, rough cut into a 9.00in. x 0.5in. min strip including kerf for 0.035in. blade (i.e. at least 0.5in material remaining across the width)

²Mill scale/patina layer from the CVN strip is not faced.

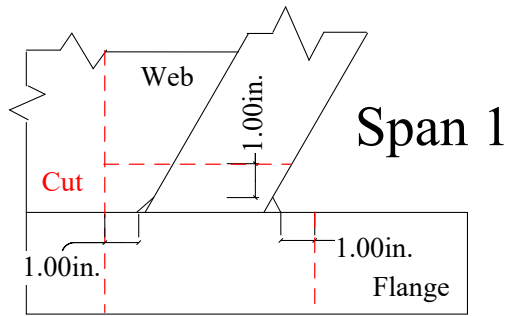
³Component names are punched on both ends of the coupons, blank, and CVN strip.

⁴All scrap is labeled 2B with a paint pen.

⁵Coupons and blanks have a 2.515in. grip width to allow taper in the gage length.

Figure C.14. 2B – NTSB-STR-012.

2D (NTSB-STR-014)



¹Cut lines are spaced 1in. from the weld toes

²Punch component names on both the east and west ends

³All scrap can be labeled 2D with a paint pen, spray paint, or punch

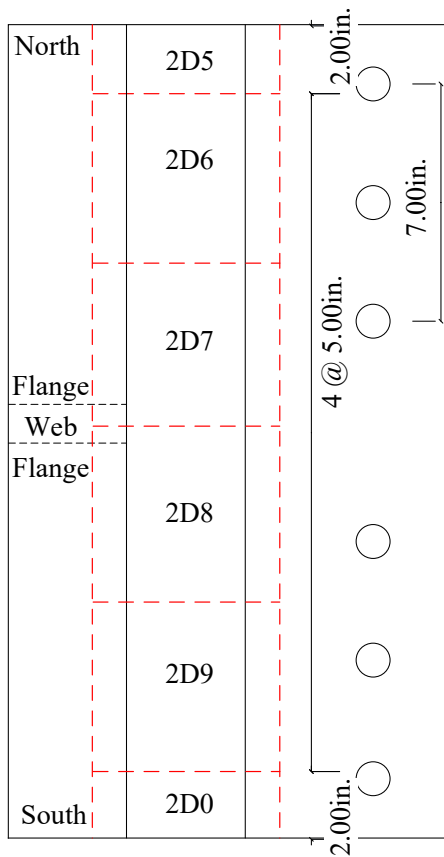
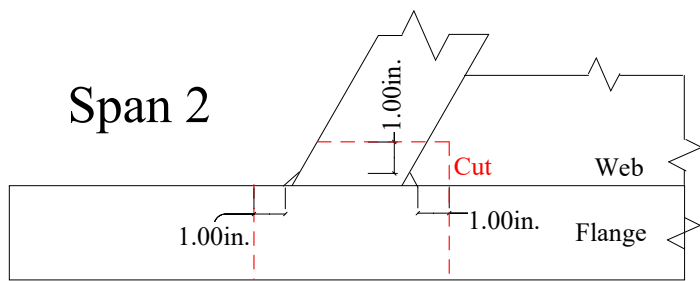


Figure C.15. 2D – NTSB-STR-014.



2E (NTSB-STR-014)

¹Cut lines are spaced 1in. from the weld toes

²Punch component names on both the east and west ends

³All scrap can be labeled 2E with a paint pen, spray paint, or punch

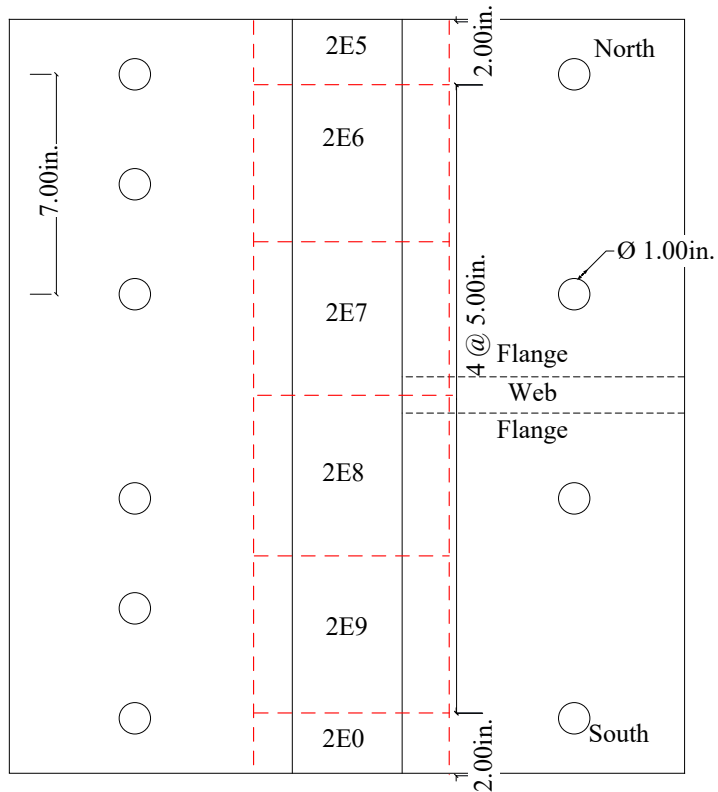
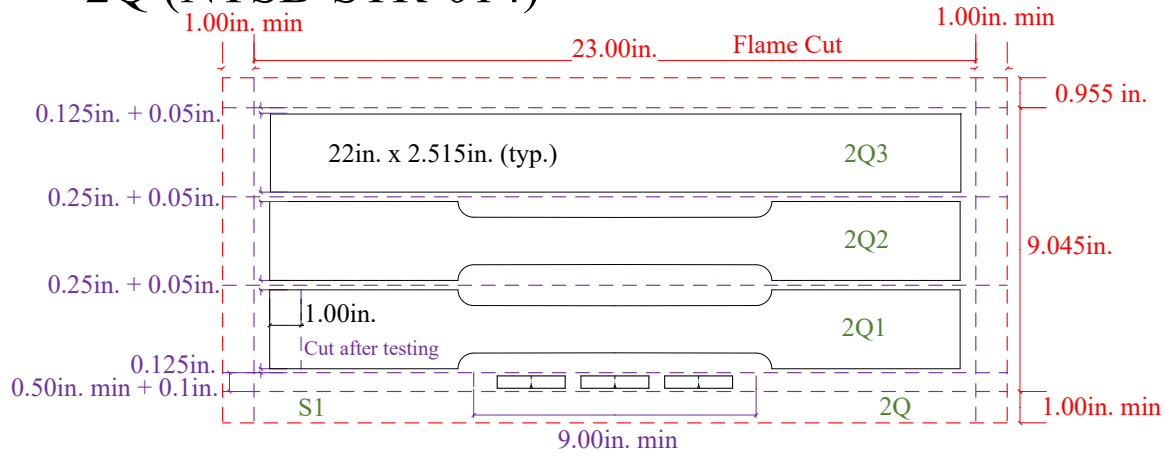


Figure C.16. 2E – NTSB-STR-014.

2Q (NTSB-STR-014)



¹CVNs are nested in the L-T orientation, rough cut into a 9.00in. x 0.5in. min strip including kerf for 0.035in. blade (i.e. at least 0.5in material remaining across the width)

²Mill scale/patina layer from the CVN strip is not faced.

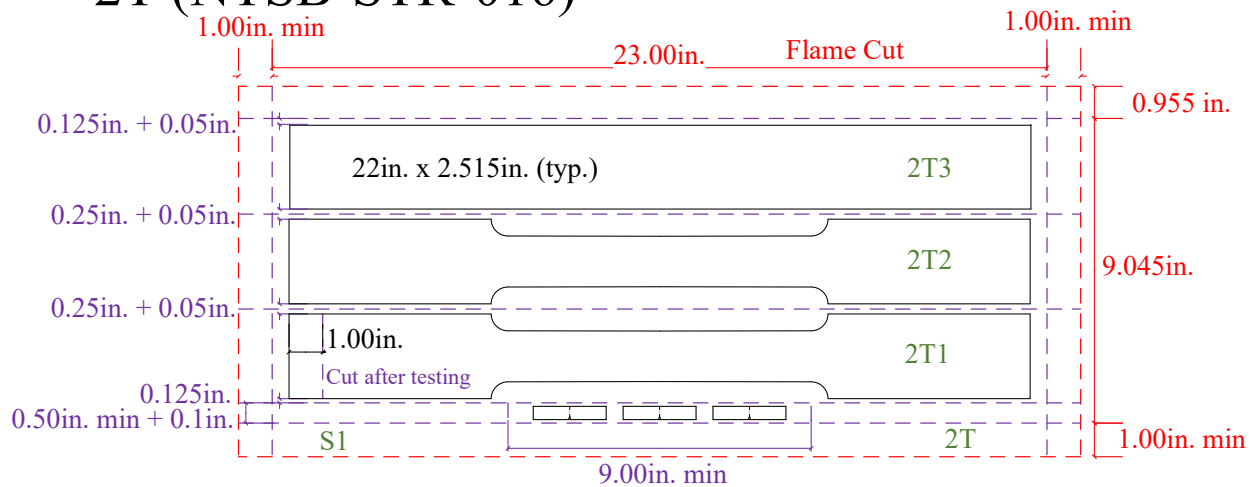
³Component names are punched on both ends of the coupons, blank, and CVN strip.

⁴All scrap is labeled 2Q with a paint pen.

⁵Coupons and blanks have a 2.515in. grip width to allow taper in the gage length.

Figure C.17. 2Q – NTSB-STR-014.

2T (NTSB-STR-016)



¹CVNs are nested in the L-T orientation, rough cut into a 9.00in. x 0.5in. min strip including kerf for 0.035in. blade (i.e. at least 0.5in material remaining across the width)

²Mill scale/patina layer from the CVN strip is not faced.

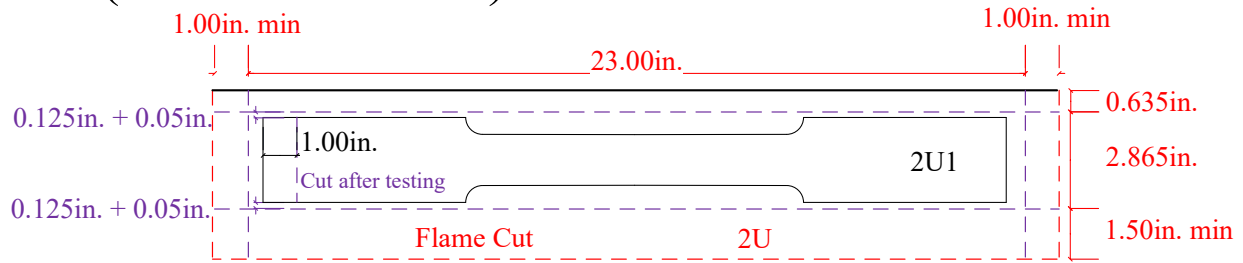
³Component names are punched on both ends of the coupons, blank, and CVN strip.

⁴All scrap is labeled 2T with a paint pen.

⁵Coupons and blanks have a 2.515in. grip width to allow taper in the gage length.

Figure C.18. 2T – NTSB-STR-016.

2U (NTSB-STR-016)



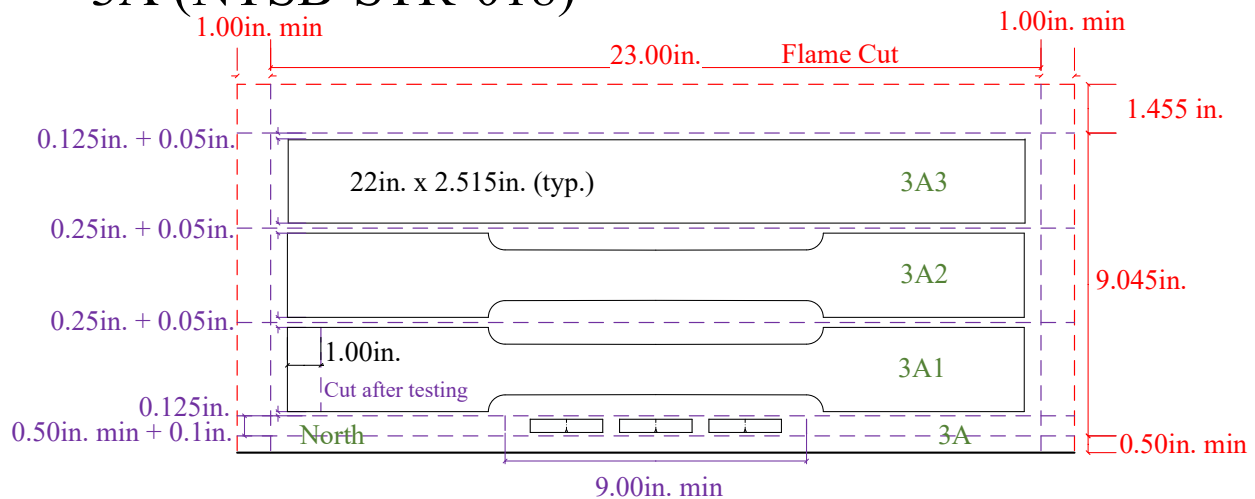
¹Component names are punched on both ends of the coupons.

²All scrap is labeled 2U with a paint pen.

³Coupons have a 2.515in. grip width to allow taper in the gage length.

Figure C.19. 2U – NTSB-STR-016.

3A (NTSB-STR-018)



¹CVNs are nested in the L-T orientation, rough cut into a 9.00in. x 0.5in. min strip including kerf for 0.035in. blade (i.e. at least 0.5in material remaining across the width)

²Mill scale/patina layer from the CVN strip is not faced.

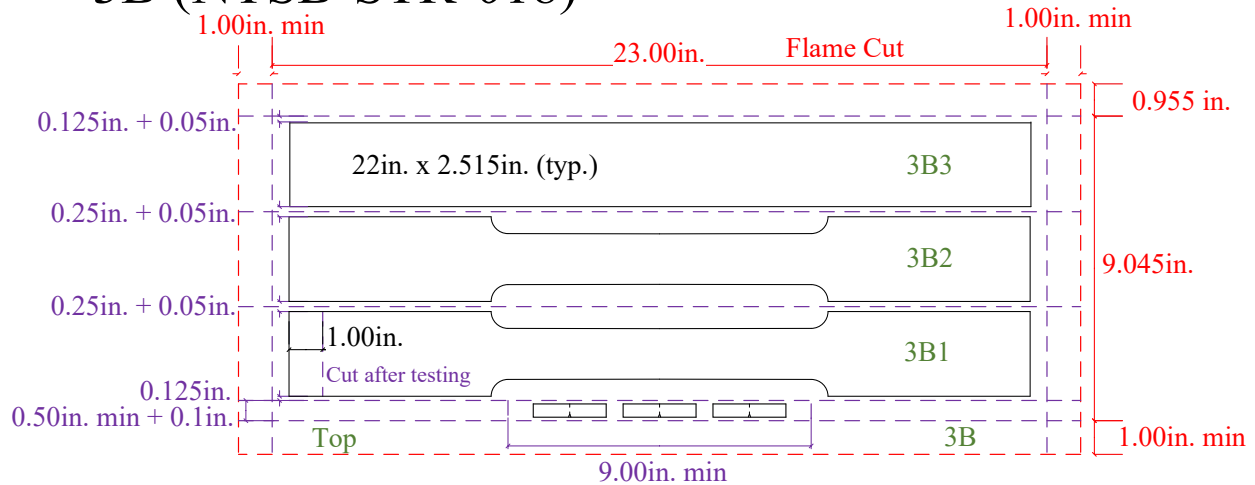
³Component names are punched on both ends of the coupons, blank, and CVN strip.

⁴All scrap is labeled 3A with a paint pen.

⁵Coupons and blanks have a 2.515in. grip width to allow taper in the gage length.

Figure C.20. 3A – NTSB-STR-018.

3B (NTSB-STR-018)



¹CVNs are nested in the L-T orientation, rough cut into a 9.00in. x 0.5in. min strip including kerf for 0.035in. blade (i.e. at least 0.5in material remaining across the width)

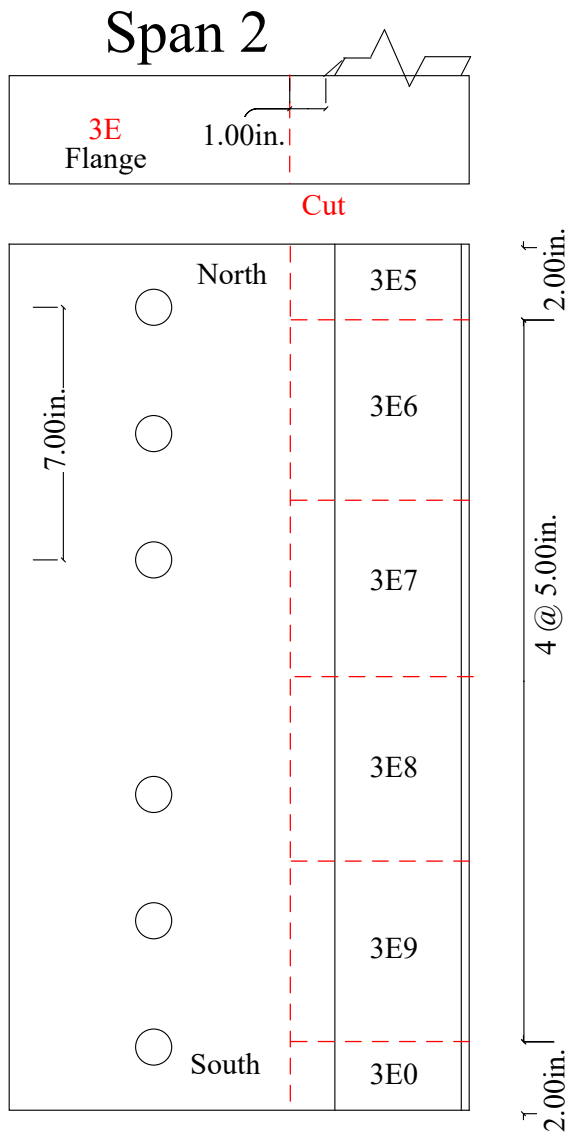
²Mill scale/patina layer from the CVN strip is not faced.

³Component names are punched on both ends of the coupons, blank, and CVN strip.

⁴All scrap is labeled 3B with a paint pen.

⁵Coupons and blanks have a 2.515in. grip width to allow taper in the gage length.

Figure C.21. 3B – NTSB-STR-018.



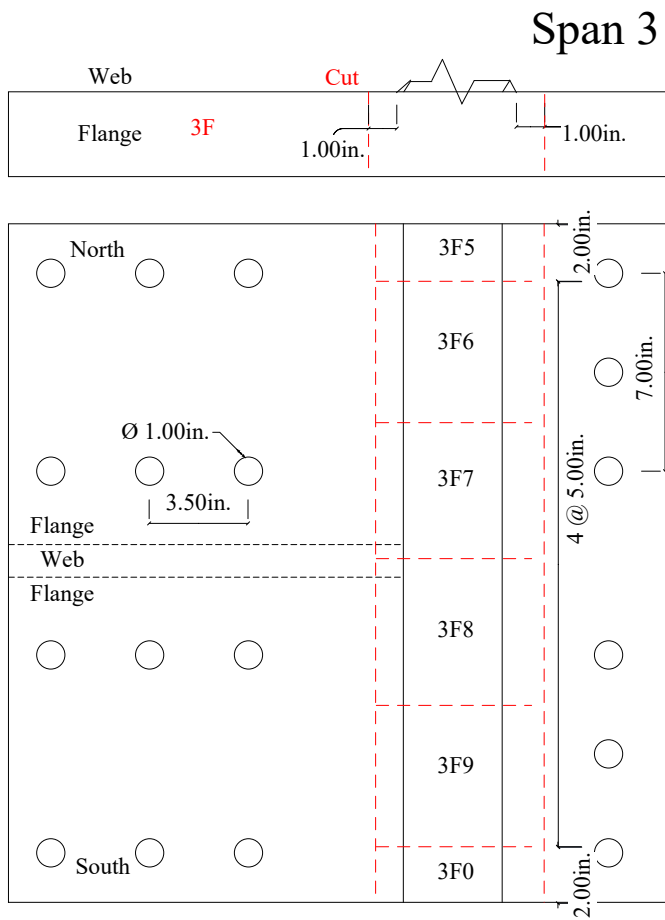
3E (NTSB-STR-020)

¹Cut lines are spaced 1in. from the weld toes

²Punch component names on both the east and west ends

³All scrap can be labeled 3E with a paint pen, spray paint, or punch

Figure C.22. 3E – NTSB-STR-020.



3F (NTSB-STR-020)

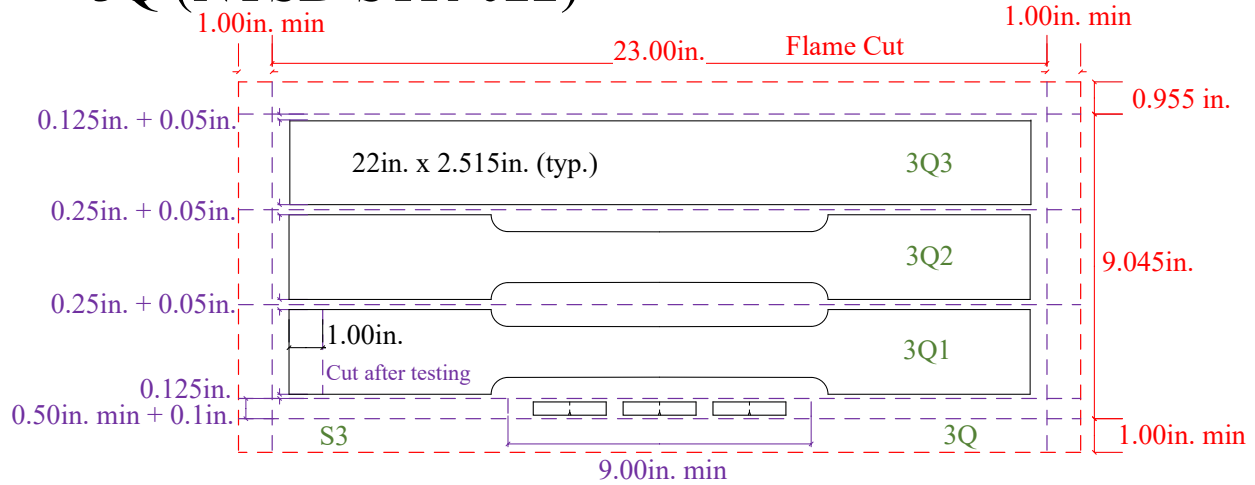
¹Cut lines are spaced 1in. from the weld toes

²Punch component names on both the east and west ends

³All scrap can be labeled 3F with a paint pen, spray paint, or punch

Figure C.23. 3F – NTSB-STR-020.

3Q (NTSB-STR-022)



¹CVNs are nested in the L-T orientation, rough cut into a 9.00in. x 0.5in. min strip including kerf for 0.035in. blade (i.e. at least 0.5in material remaining across the width)

²Mill scale/patina layer from the CVN strip is not faced.

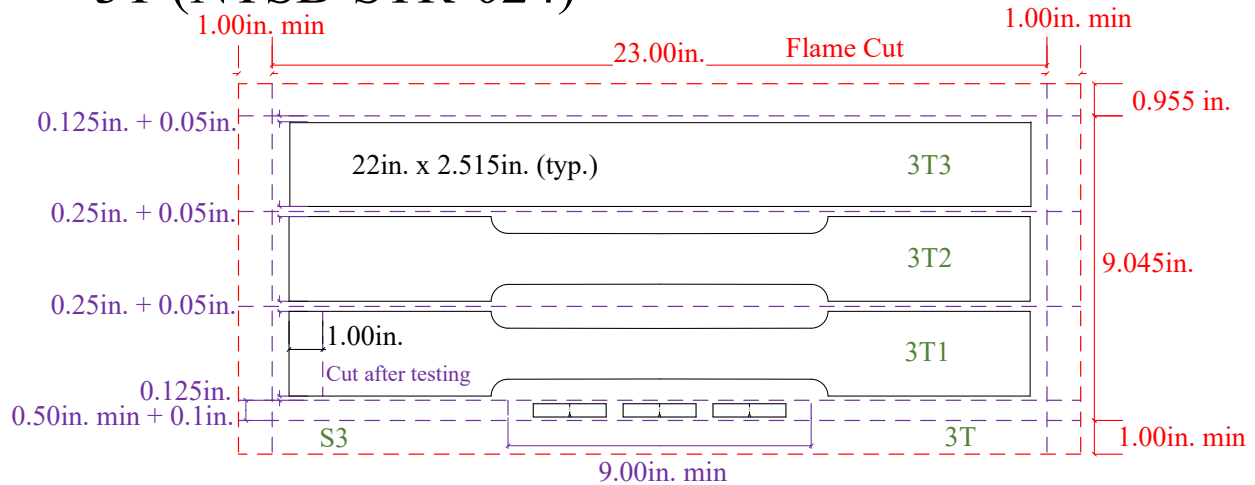
³Component names are punched on both ends of the coupons, blank, and CVN strip.

⁴All scrap is labeled 3Q with a paint pen.

⁵Coupons and blanks have a 2.515in. grip width to allow taper in the gage length.

Figure C.24. 3Q – NTSB-STR-022.

3T (NTSB-STR-024)



¹CVNs are nested in the L-T orientation, rough cut into a 9.00in. x 0.5in. min strip including kerf for 0.035in. blade (i.e. at least 0.5in material remaining across the width)

²Mill scale/patina layer from the CVN strip is not faced.

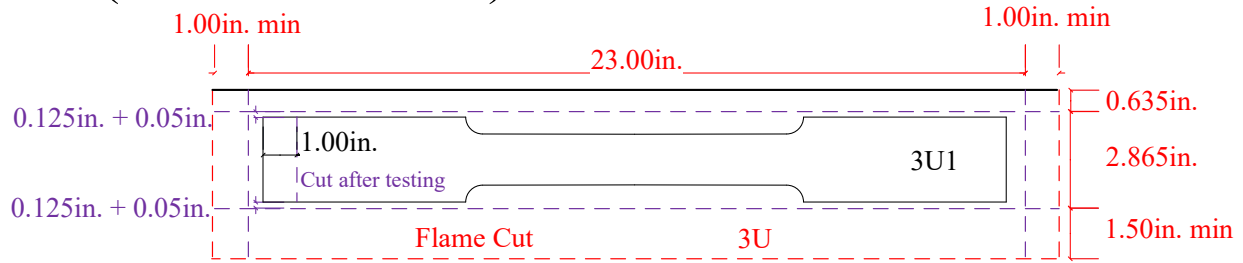
³Component names are punched on both ends of the coupons, blank, and CVN strip.

⁴All scrap is labeled 3T with a paint pen.

⁵Coupons and blanks have a 2.515in. grip width to allow taper in the gage length.

Figure C.25. 3T – NTSB-STR-024.

3U (NTSB-STR-024)



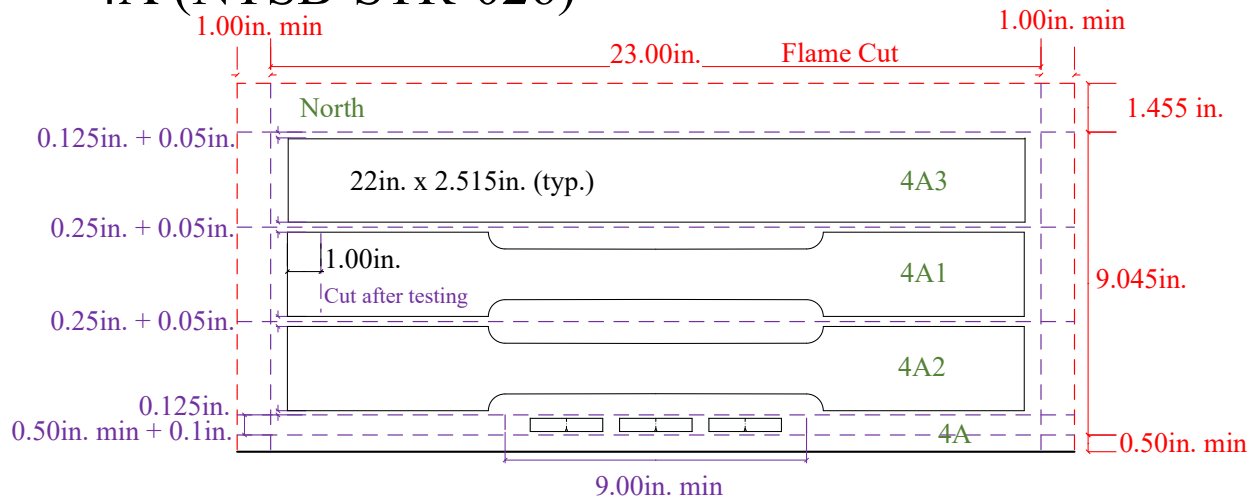
¹Component names are punched on both ends of the coupons.

²All scrap is labeled 3U with a paint pen.

³Coupons have a 2.515in. grip width to allow taper in the gage length.

Figure C.26. 3U – NTSB-STR-024.

4A (NTSB-STR-026)



¹CVNs are nested in the L-T orientation, rough cut into a 9.00in. x 0.5in. min strip including kerf for 0.035in. blade (i.e. at least 0.5in material remaining across the width)

²Mill scale/patina layer from the CVN strip is not faced.

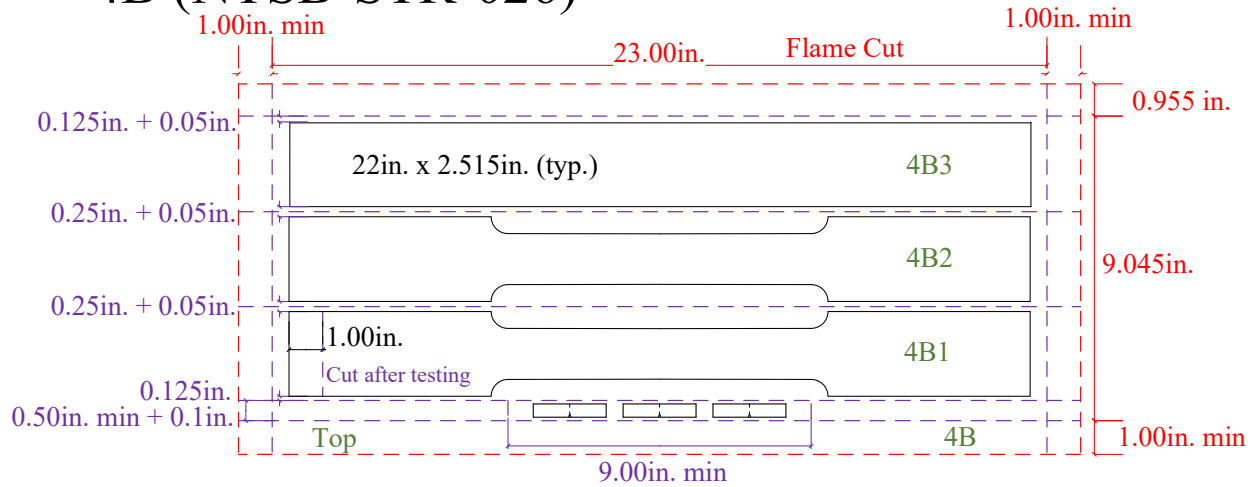
³Component names are punched on both ends of the coupons, blank, and CVN strip.

⁴All scrap is labeled 4A with a paint pen.

⁵Coupons and blanks have a 2.515in. grip width to allow taper in the gage length.

Figure C.27. 4A – NTSB-STR-026.

4B (NTSB-STR-026)



¹CVNs are nested in the L-T orientation, rough cut into a 9.00in. x 0.5in. min strip including kerf for 0.035in. blade (i.e. at least 0.5in material remaining across the width)

²Mill scale/patina layer from the CVN strip is not faced.

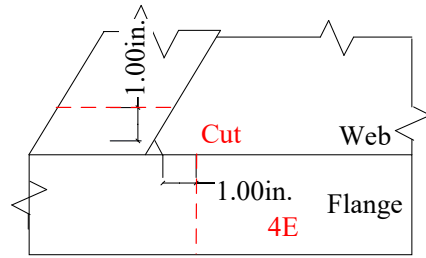
³Component names are punched on both ends of the coupons, blank, and CVN strip.

⁴All scrap is labeled 4B with a paint pen.

⁵Coupons and blanks have a 2.515in. grip width to allow taper in the gage length.

Figure C.28. 4B – NTSB-STR-026.

Span 2



4E (NTSB-STR-028A)

¹Cut lines are spaced 1in. from the weld toes

²Punch component names on both the east and west ends

³All scrap can be labeled 4E with a paint pen, spray paint, or punch

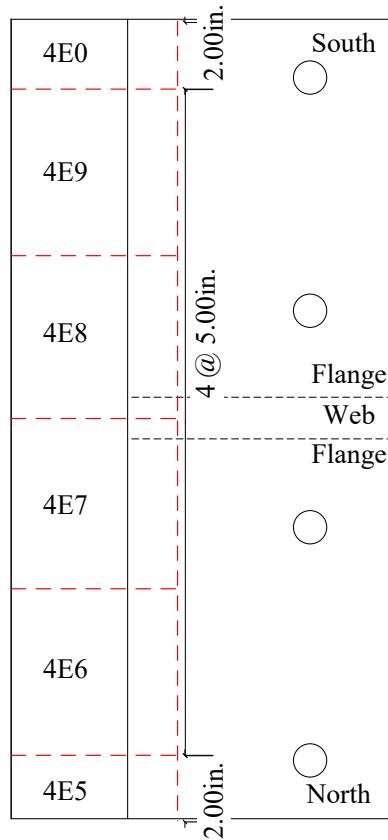
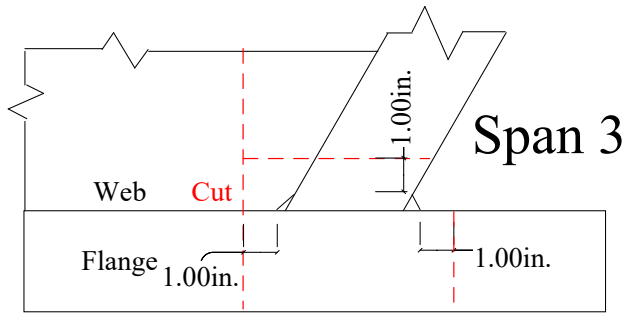


Figure C.29. 4E – NTSB-STR-028A.



4F (NTSB-STR-028A)

¹Cut lines are spaced 1 in. from the weld toes

²Punch component names on both the east and west ends

³All scrap can be labeled 4F with a paint pen, spray paint, or punch

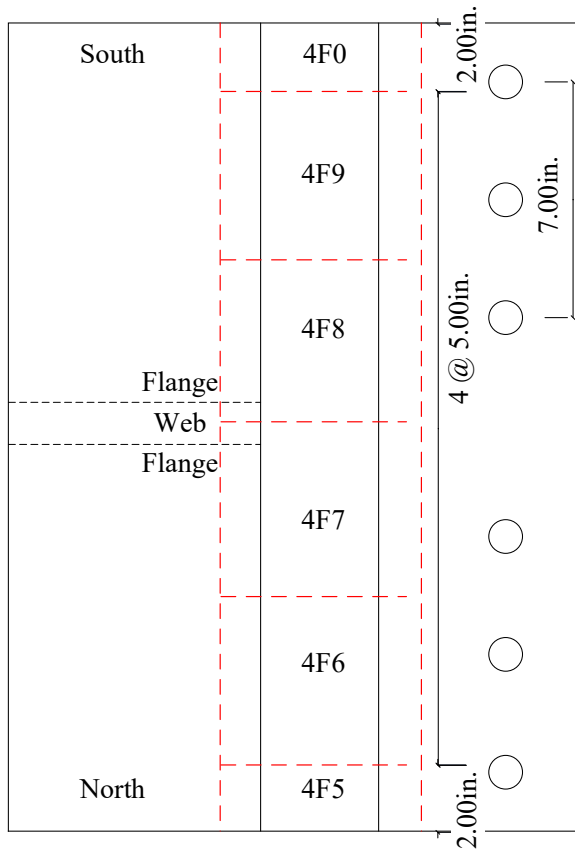
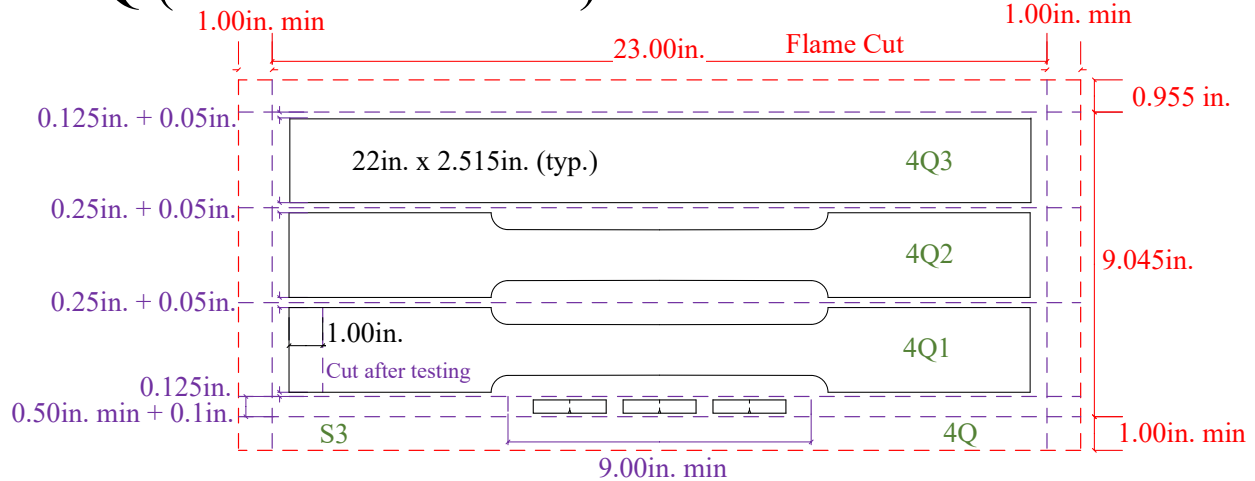


Figure C.30. 4F – NTSB-STR-028A.

4Q (NTSB-STR-028B)



¹CVNs are nested in the L-T orientation, rough cut into a 9.00in. x 0.5in. min strip including kerf for 0.035in. blade (i.e. at least 0.5in material remaining across the width)

²Mill scale/patina layer from the CVN strip is not faced.

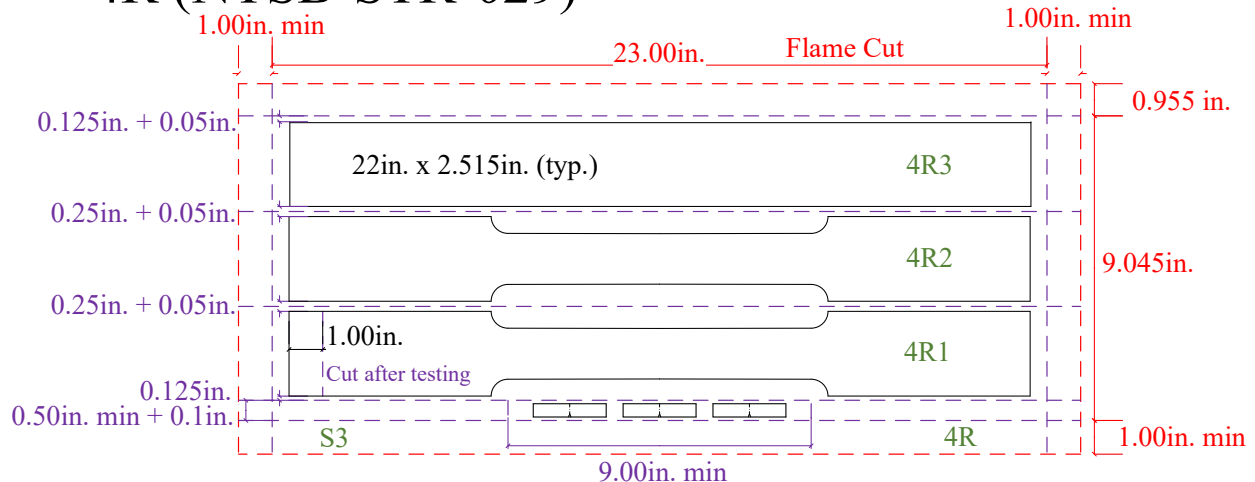
³Component names are punched on both ends of the coupons, blank, and CVN strip.

⁴All scrap is labeled 4Q with a paint pen.

⁵Coupons and blanks have a 2.515in. grip width to allow taper in the gage length.

Figure C.31. 4Q – NTSB-STR-028B.

4R (NTSB-STR-029)



¹CVNs are nested in the L-T orientation, rough cut into a 9.00in. x 0.5in. min strip including kerf for 0.035in. blade (i.e. at least 0.5in material remaining across the width)

²Mill scale/patina layer from the CVN strip is not faced.

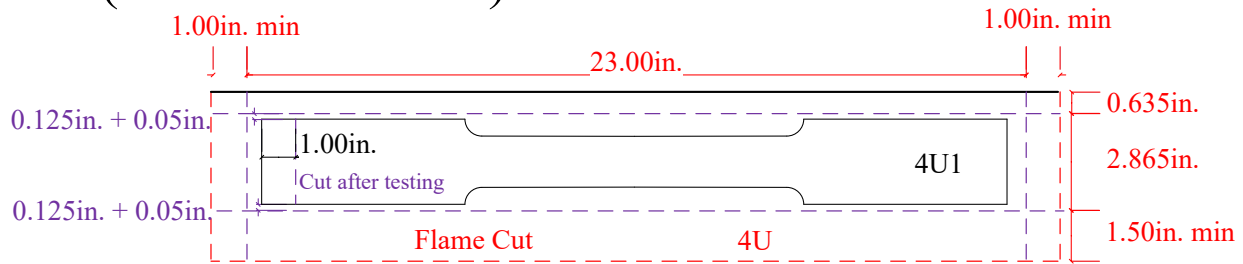
³Component names are punched on both ends of the coupons, blank, and CVN strip.

⁴All scrap is labeled 4R with a paint pen.

⁵Coupons and blanks have a 2.515in. grip width to allow taper in the gage length.

Figure C.32. 4R – NTSB-STR-029.

4U (NTSB-STR-029)



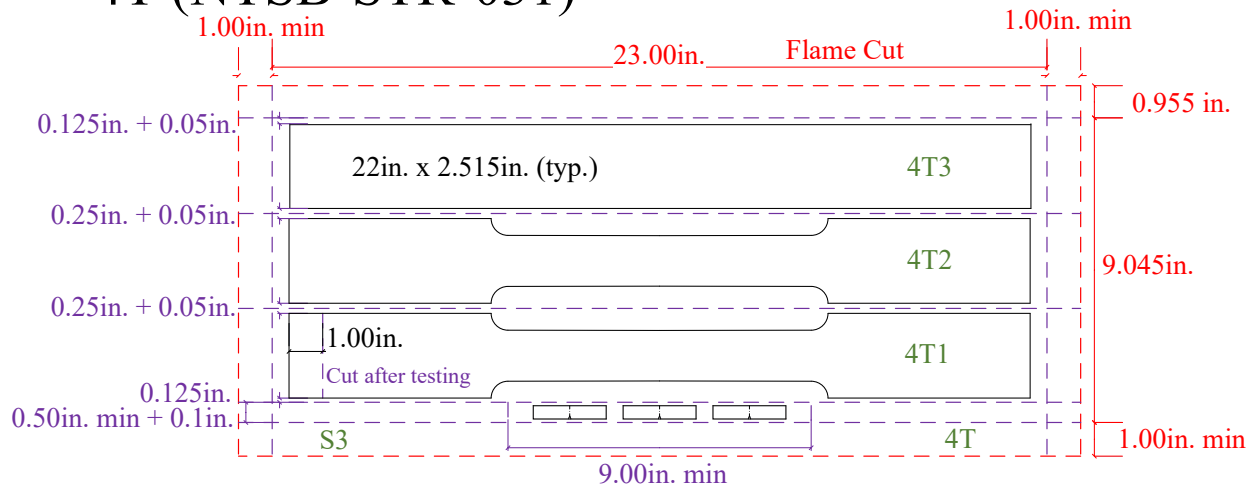
¹Component names are punched on both ends of the coupons.

²All scrap is labeled 4U with a paint pen.

³Coupons have a 2.515in. grip width to allow taper in the gage length.

Figure C.33. 4U – NTSB-STR-029.

4T (NTSB-STR-031)



¹CVNs are nested in the L-T orientation, rough cut into a 9.00in. x 0.5in. min strip including kerf for 0.035in. blade (i.e. at least 0.5in material remaining across the width)

²Mill scale/patina layer from the CVN strip is not faced.

³Component names are punched on both ends of the coupons, blank, and CVN strip.

⁴All scrap is labeled 4T with a paint pen.

⁵Coupons and blanks have a 2.515in. grip width to allow taper in the gage length.

Figure C.34. 4T – NTSB-STR-031.

Appendix D: Tensile Test Results

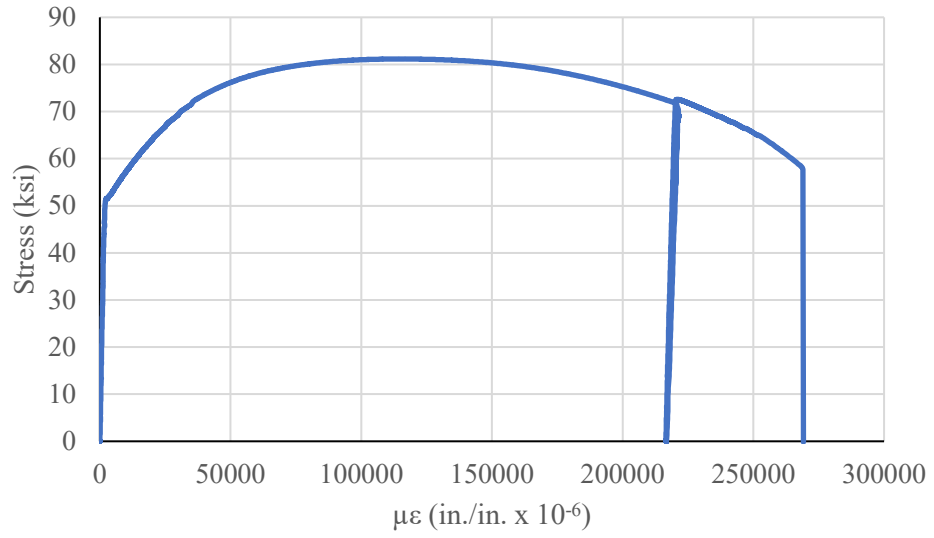


Figure D.1. Stress-strain curve for specimen 1A1.

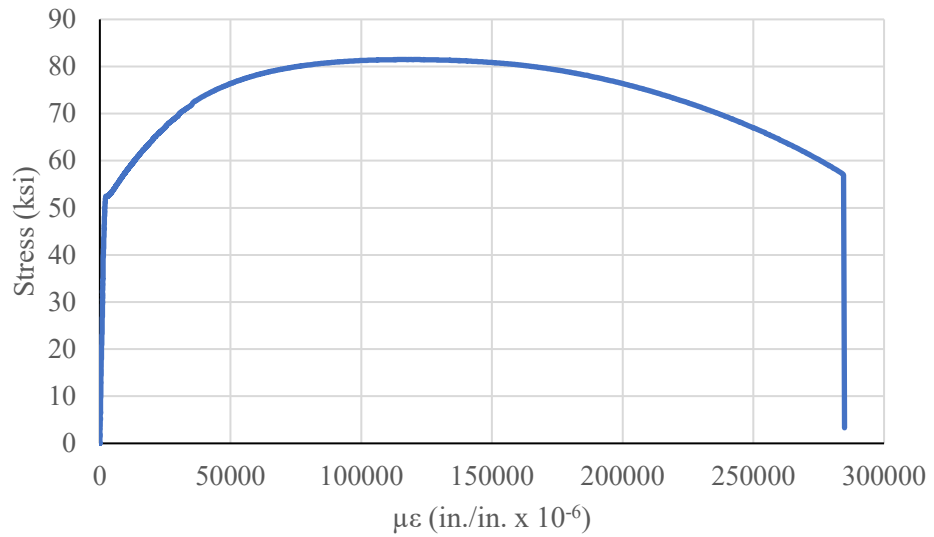


Figure D.2. Stress-strain curve for specimen 1A2.

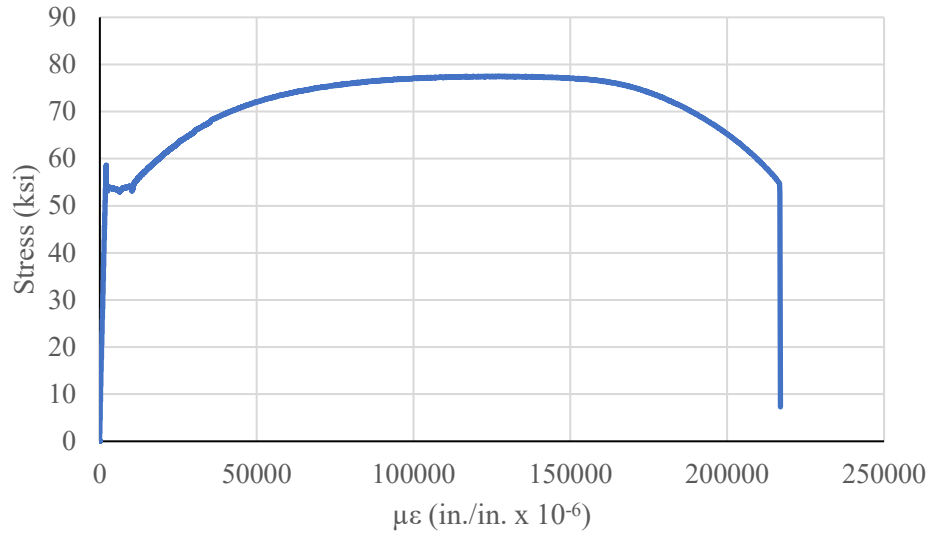


Figure D.3. Stress-strain curve for specimen 1B1.

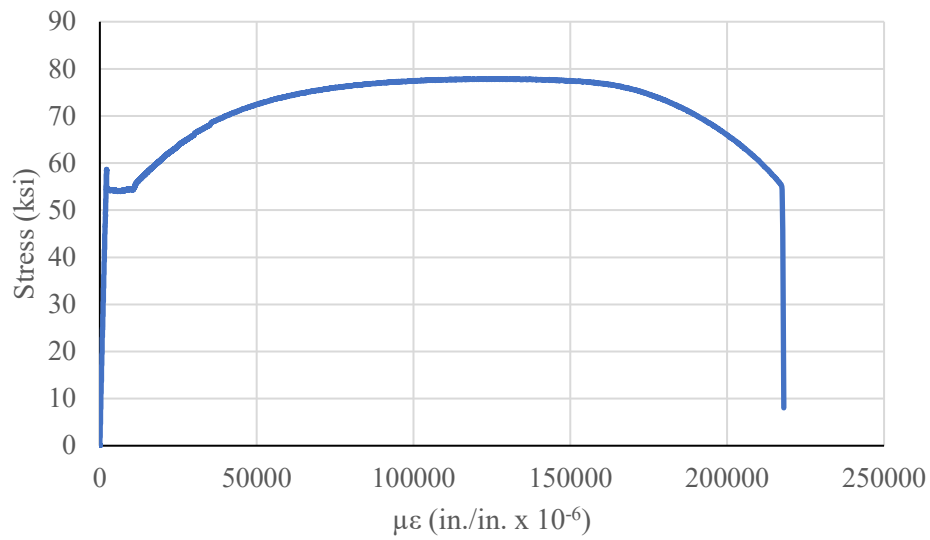


Figure D.4. Stress-strain curve for specimen 1B2.

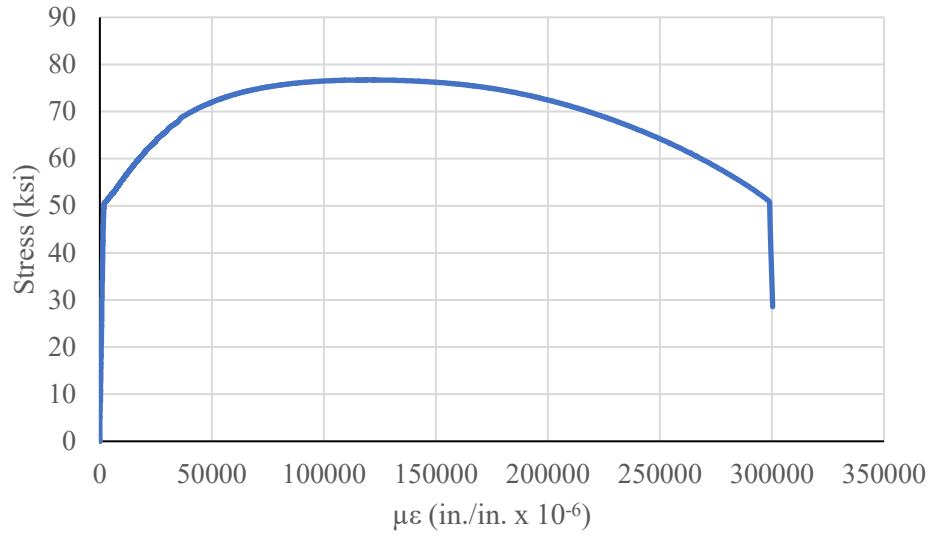


Figure D.5. Stress-strain curve for specimen 1C1.

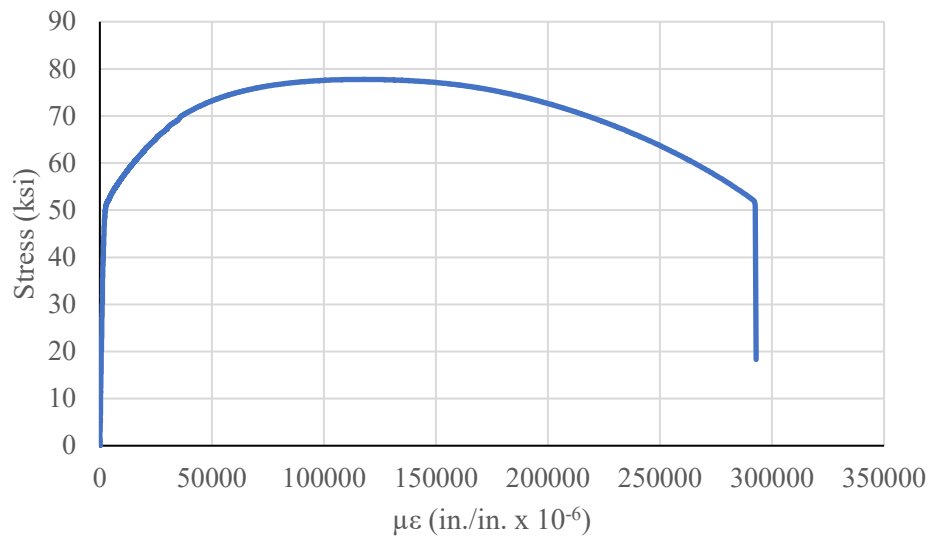


Figure D.6. Stress-strain curve for specimen 1C2.

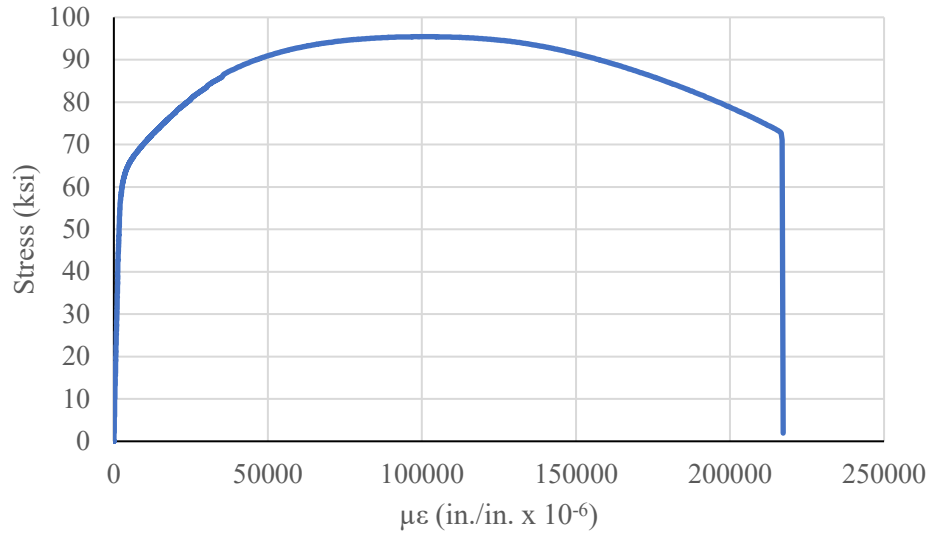


Figure D.7. Stress-strain curve for specimen 1H1.

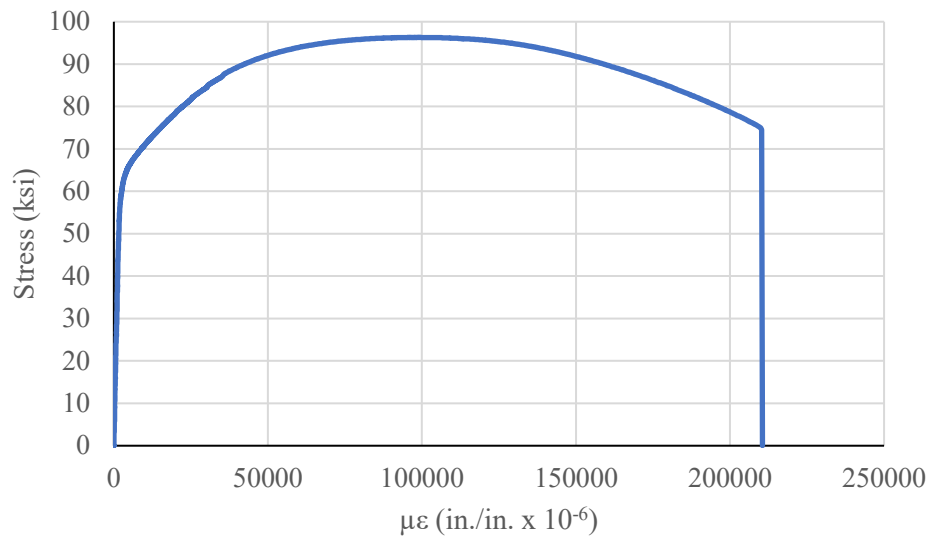


Figure D.8. Stress-strain curve for specimen 1H2.

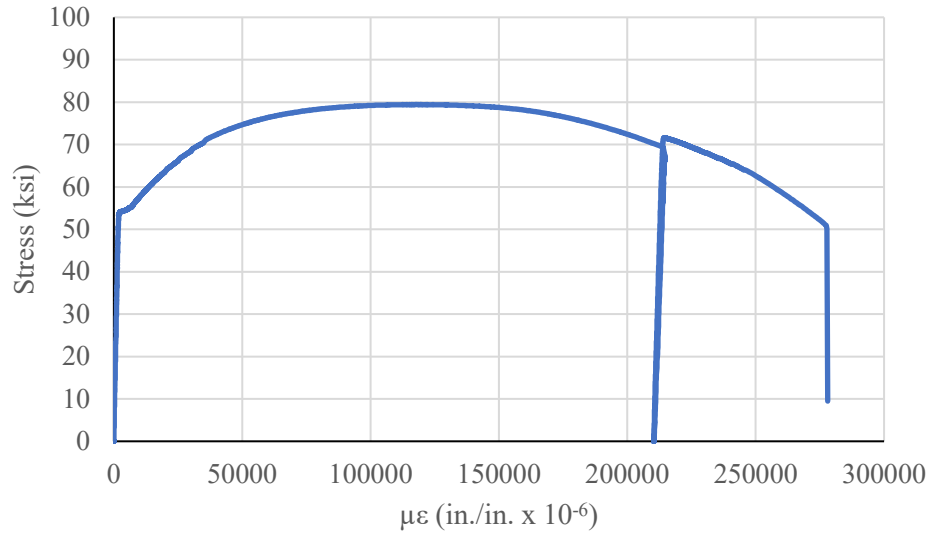


Figure D.9. Stress-strain curve for specimen 1N1.

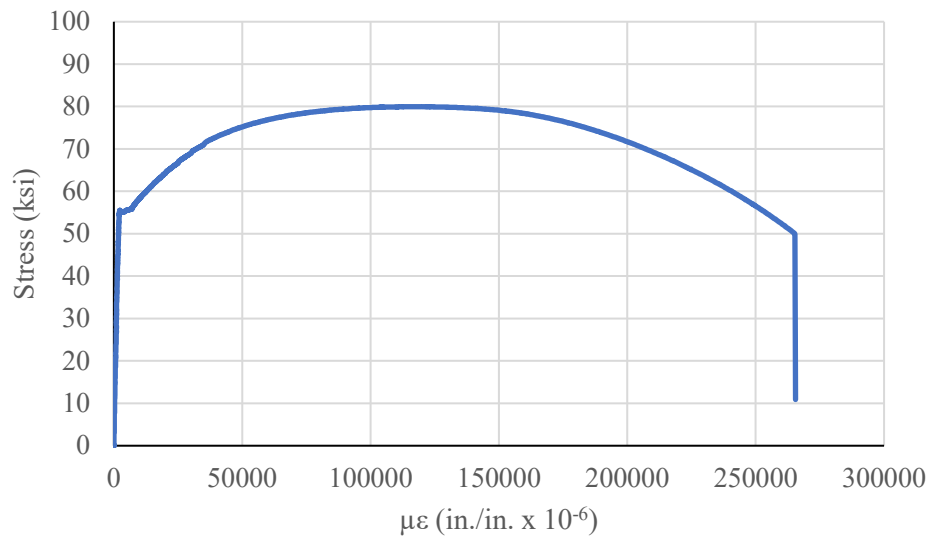


Figure D.10. Stress-strain curve for specimen 1N2.

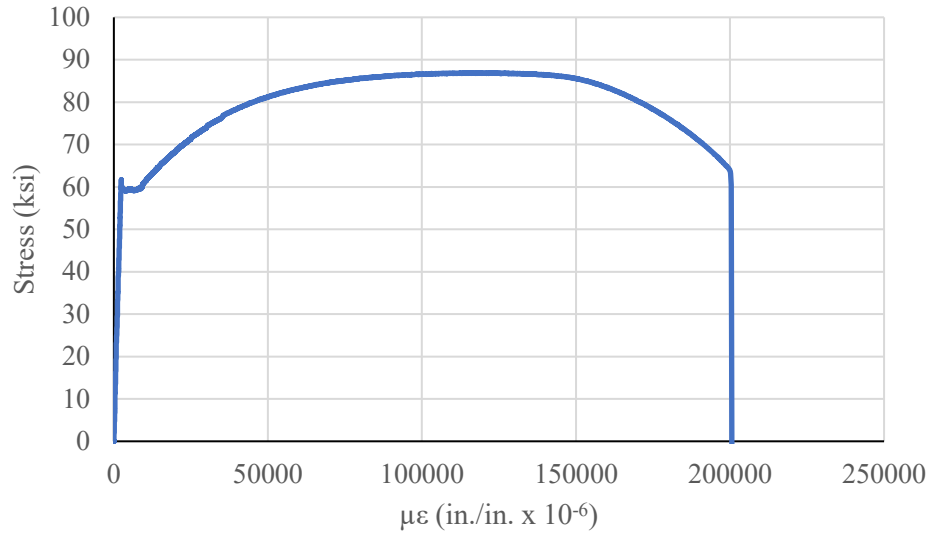


Figure D.11. Stress-strain curve for specimen 1Q1.

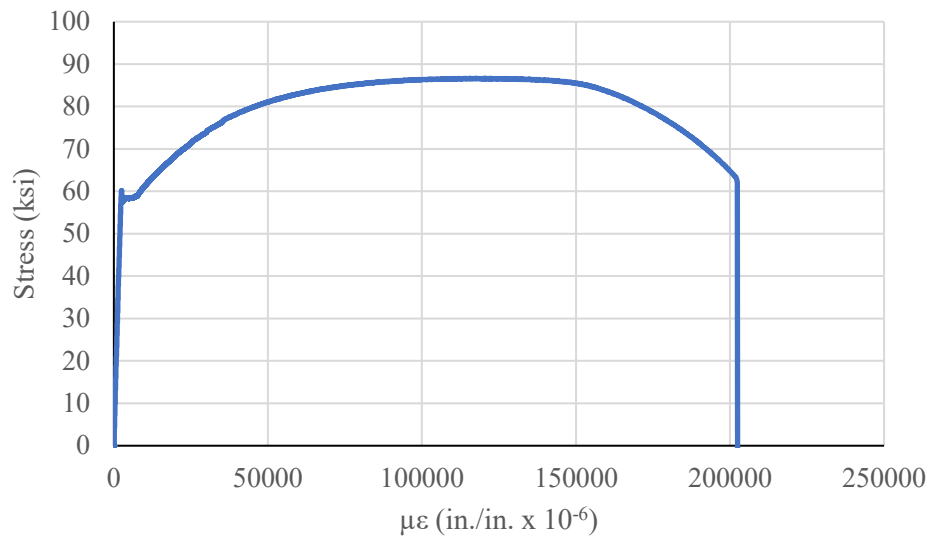


Figure D.12. Stress-strain curve for specimen 1Q2.

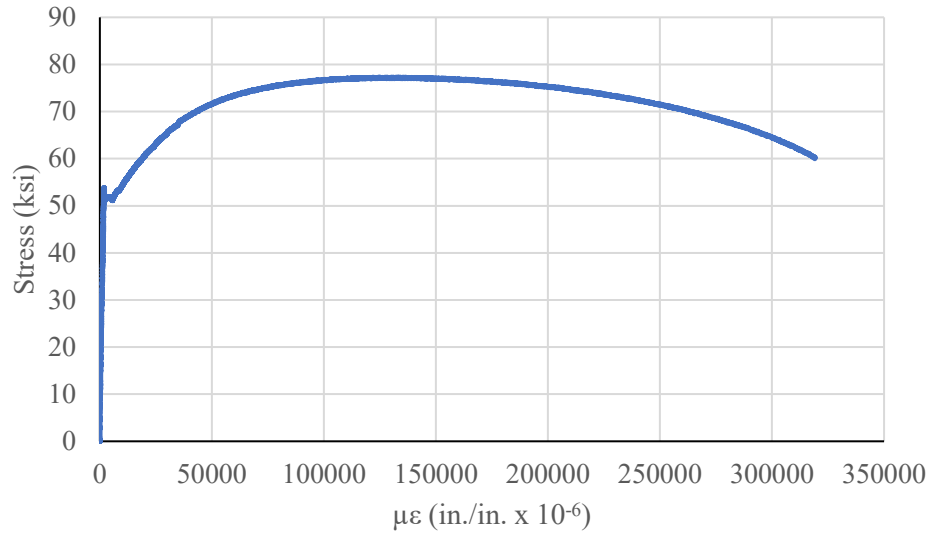


Figure D.13. Stress-strain curve for specimen 1T1.

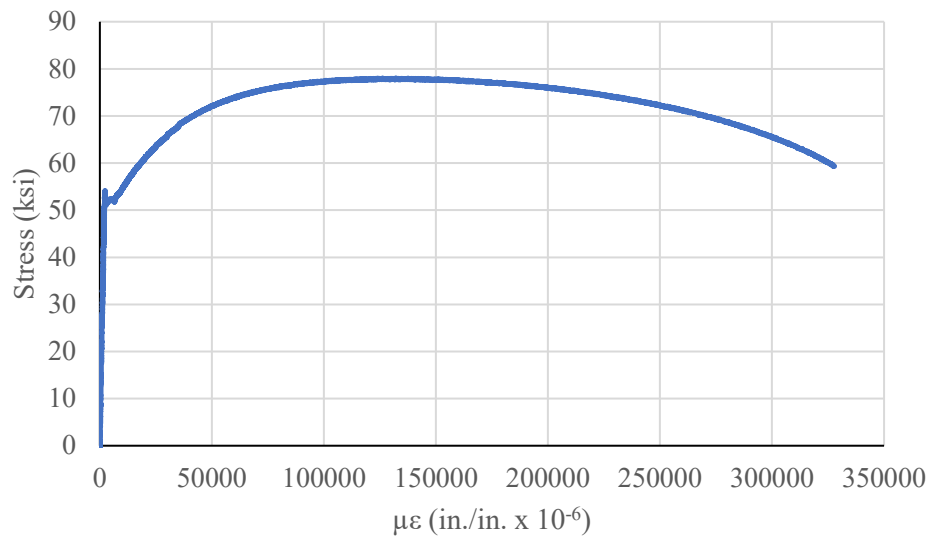


Figure D.14. Stress-strain curve for specimen 1T2.

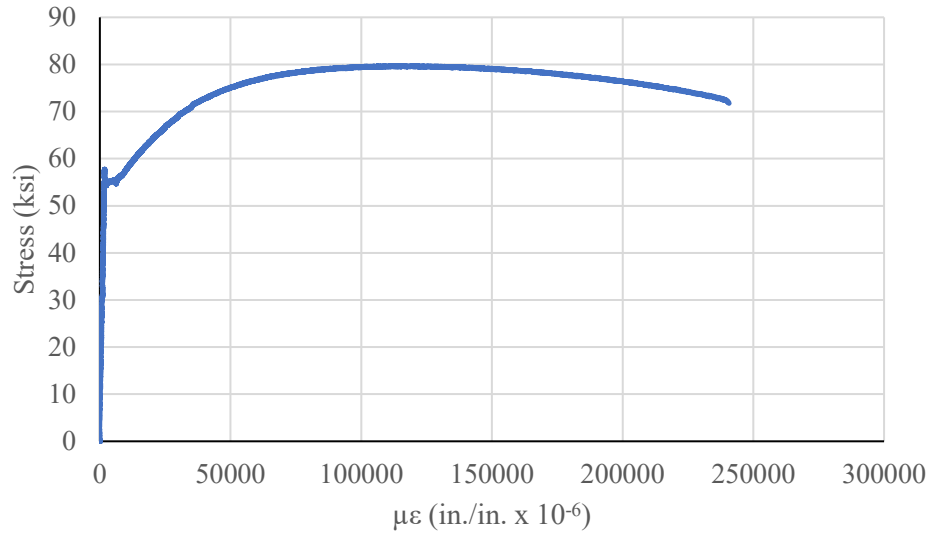


Figure D.15. Stress-strain curve for specimen 1V1.

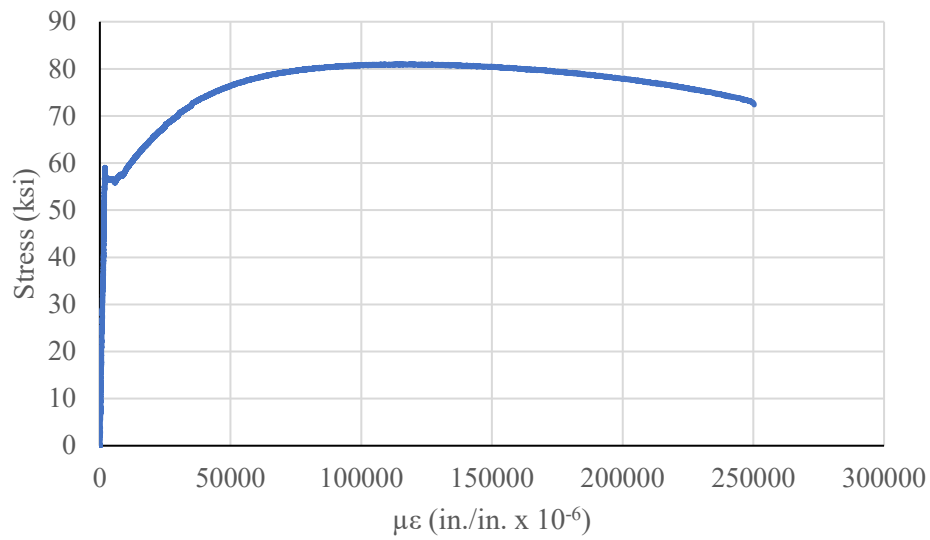


Figure D.16. Stress-strain curve for specimen 1V2.

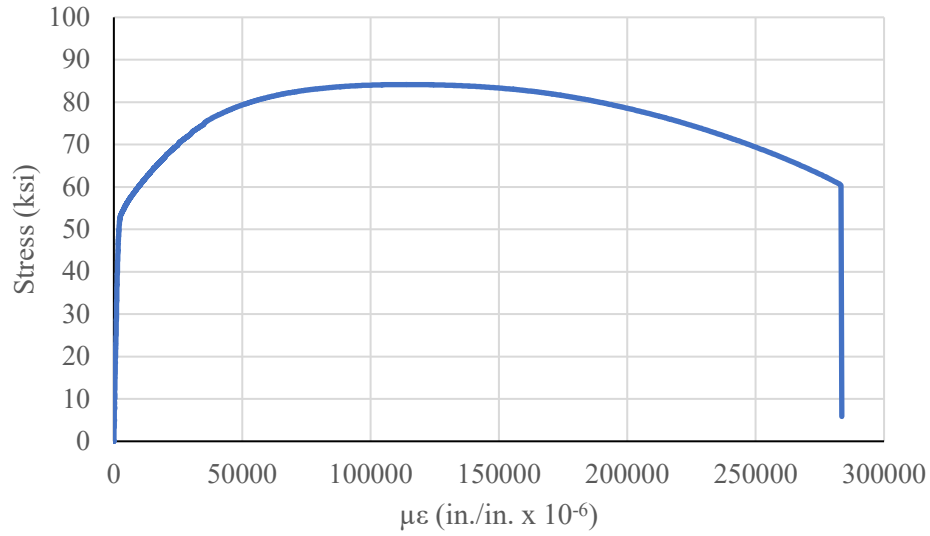


Figure D.17. Stress-strain curve for specimen 2A1.

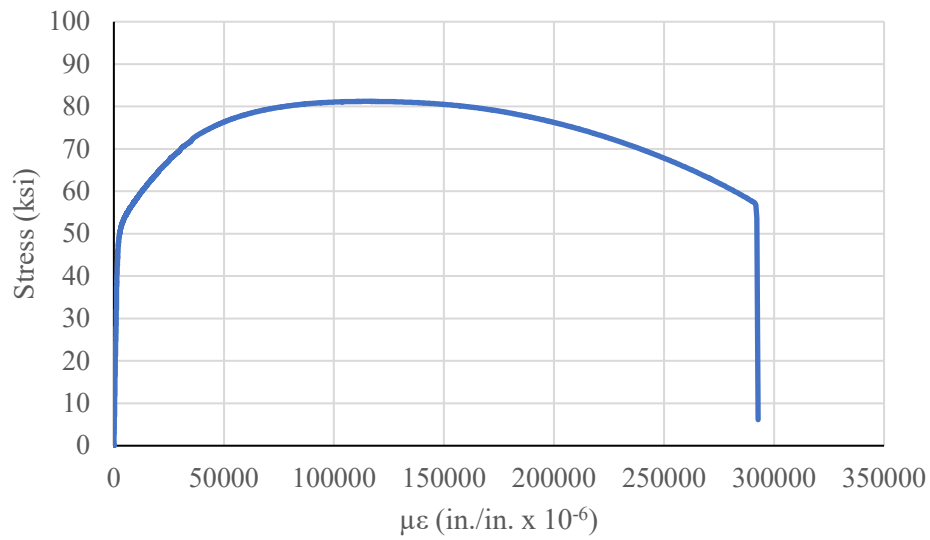


Figure D.18. Stress-strain curve for specimen 2A2.

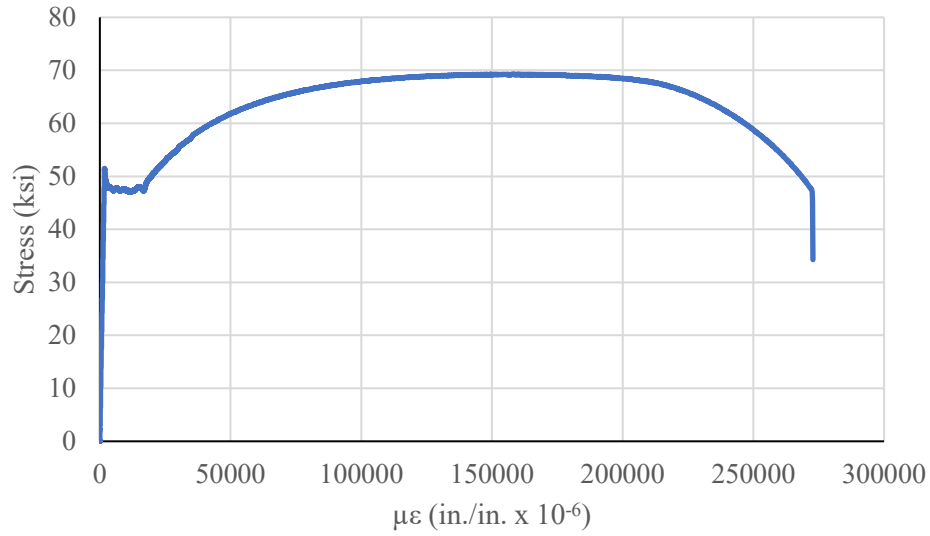


Figure D.19. Stress-strain curve for specimen 2B1.

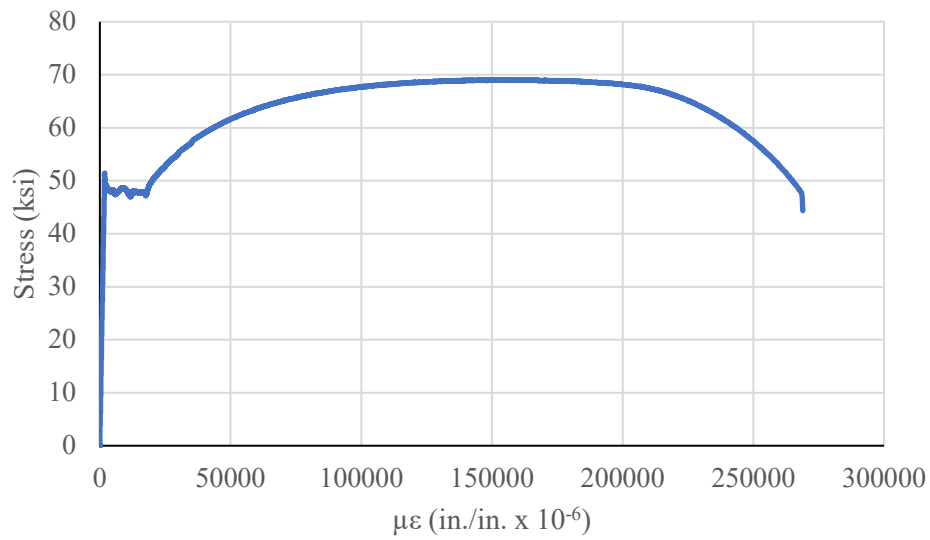


Figure D.20. Stress-strain curve for specimen 2B2.

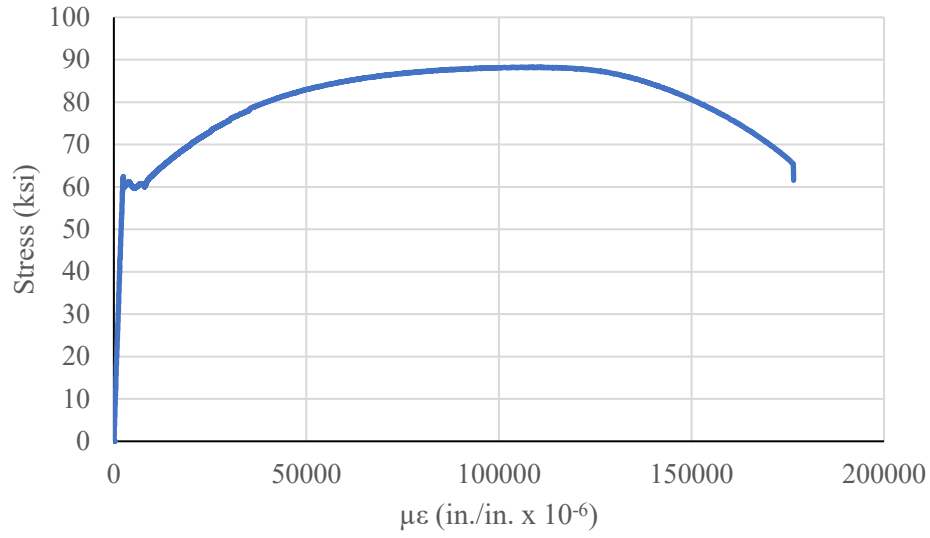


Figure D.21. Stress-strain curve for specimen 2Q1.

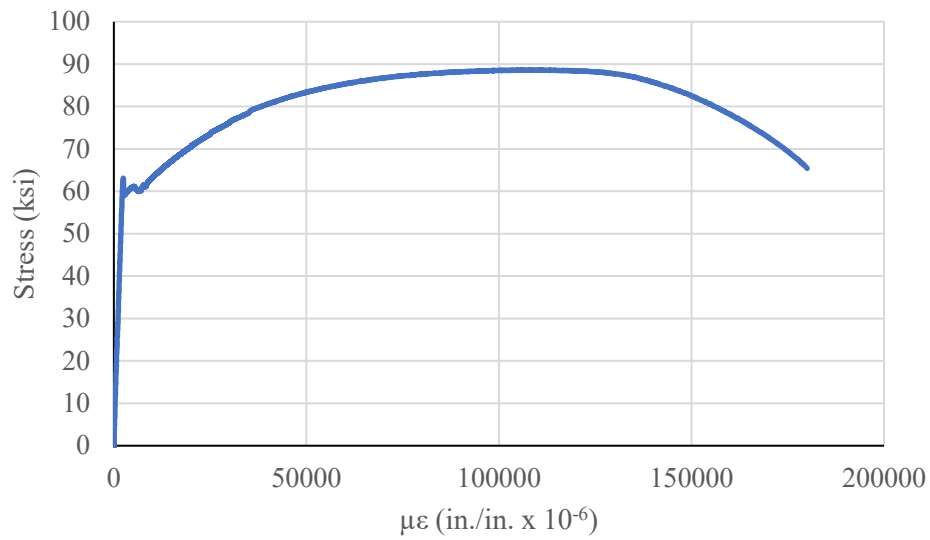


Figure D.22. Stress-strain curve for specimen 2Q2.

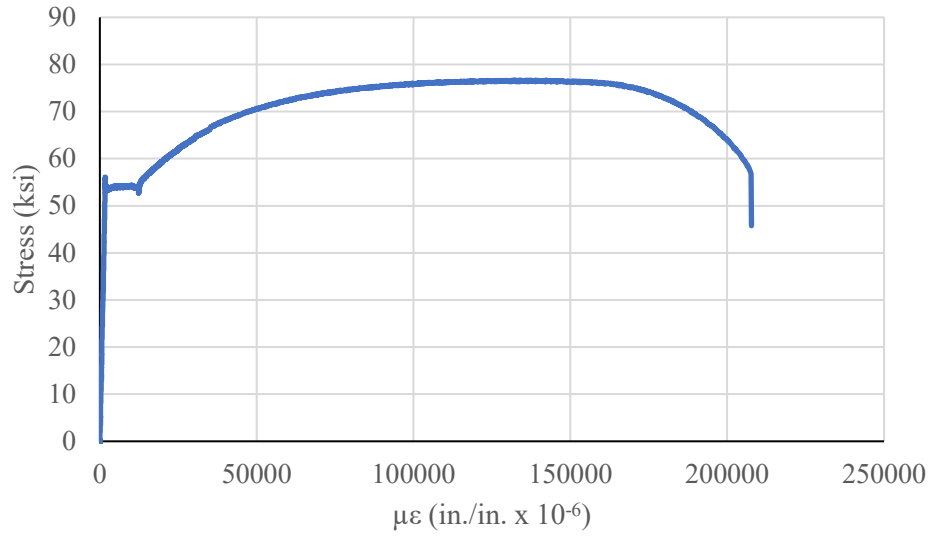


Figure D.23. Stress-strain curve for specimen 2T1.

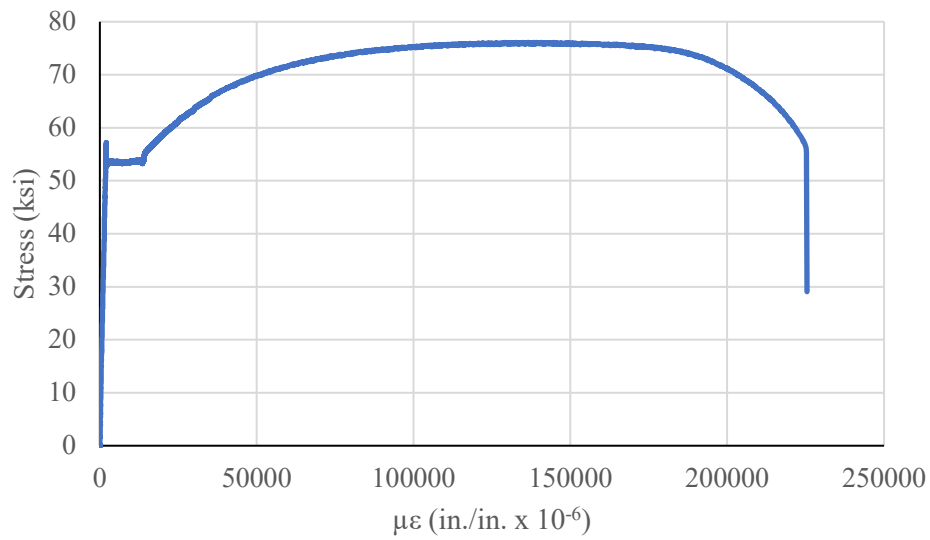


Figure D.24. Stress-strain curve for specimen 2T2.

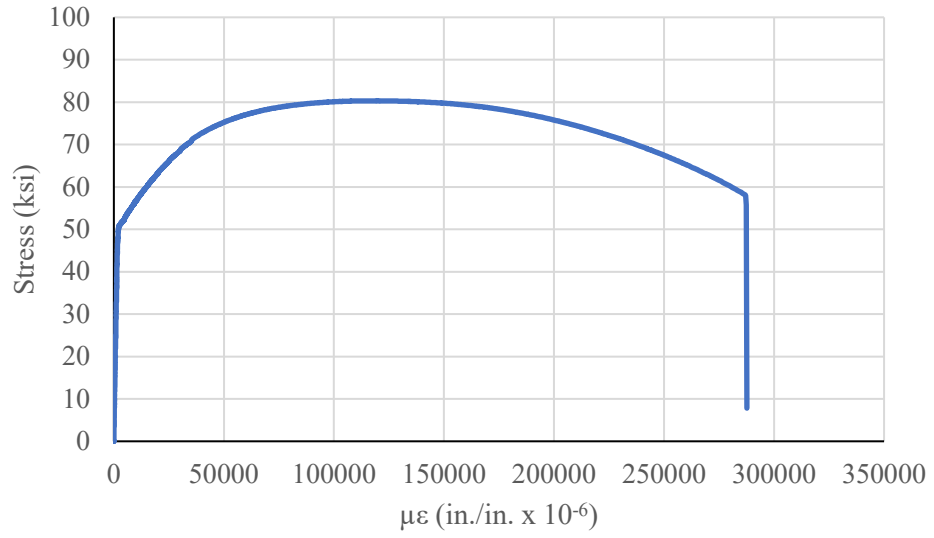


Figure D.25. Stress-strain curve for specimen 3A1.

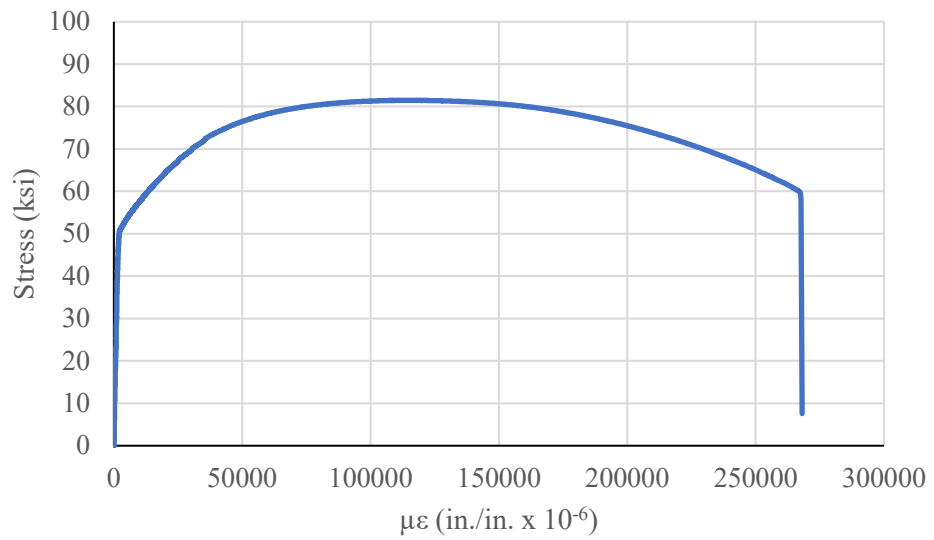


Figure D.26. Stress-strain curve for specimen 3A2.

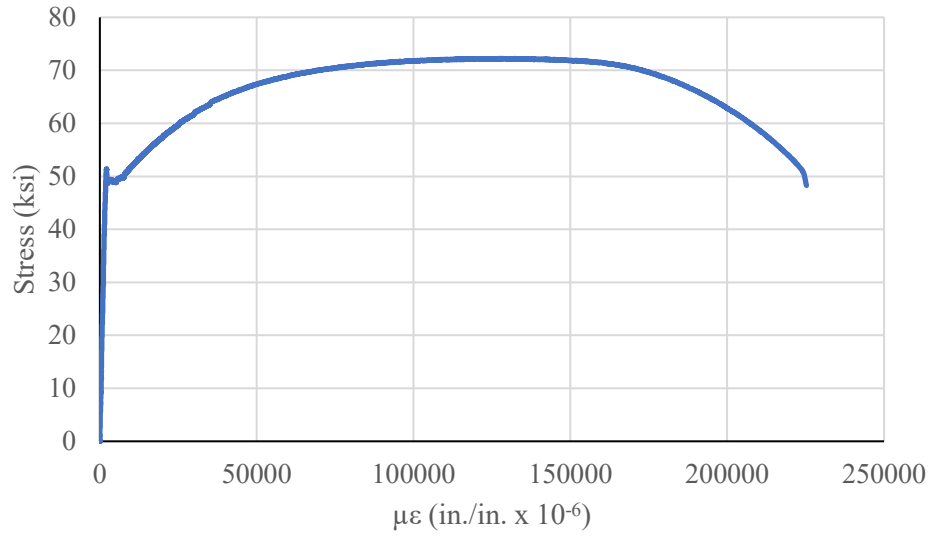


Figure D.27. Stress-strain curve for specimen 3B1.

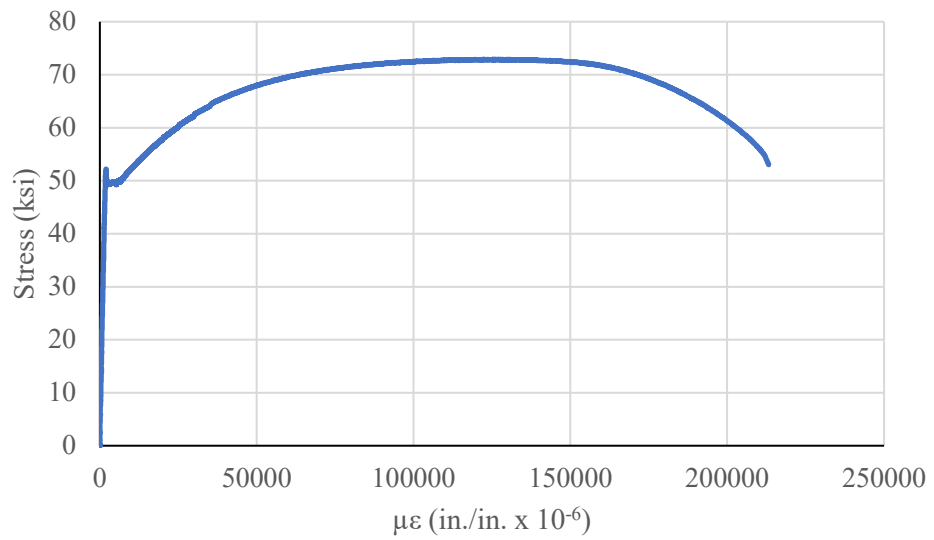


Figure D.28. Stress-strain curve for specimen 3B2.

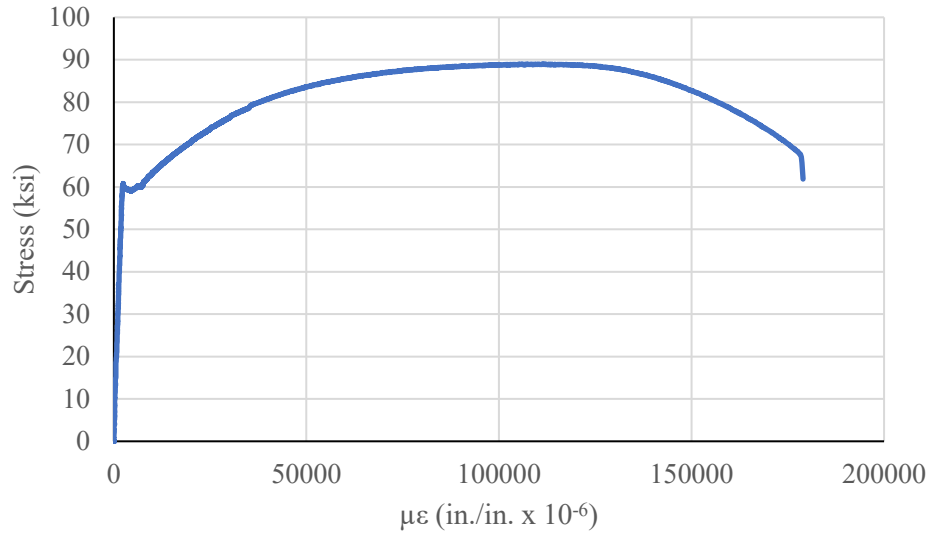


Figure D.29. Stress-strain curve for specimen 3Q1.

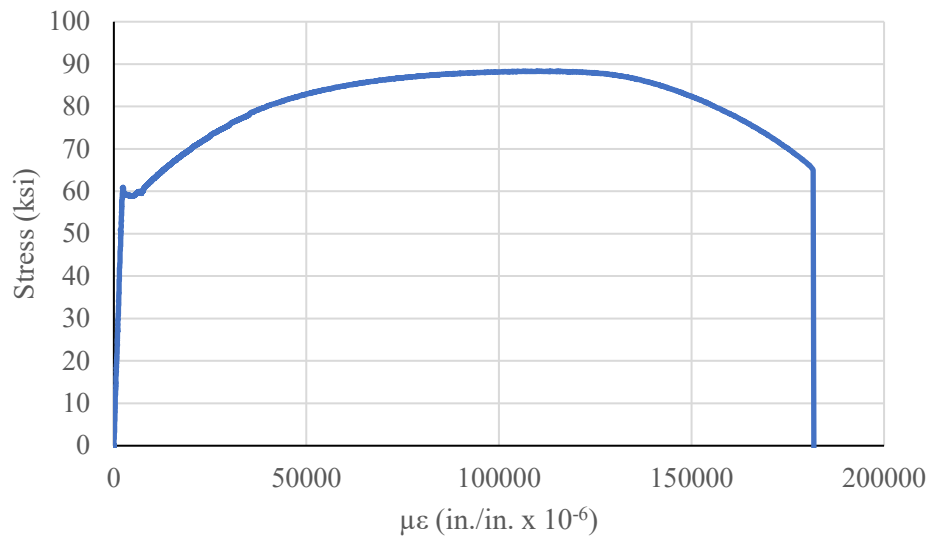


Figure D.30. Stress-strain curve for specimen 3Q2.

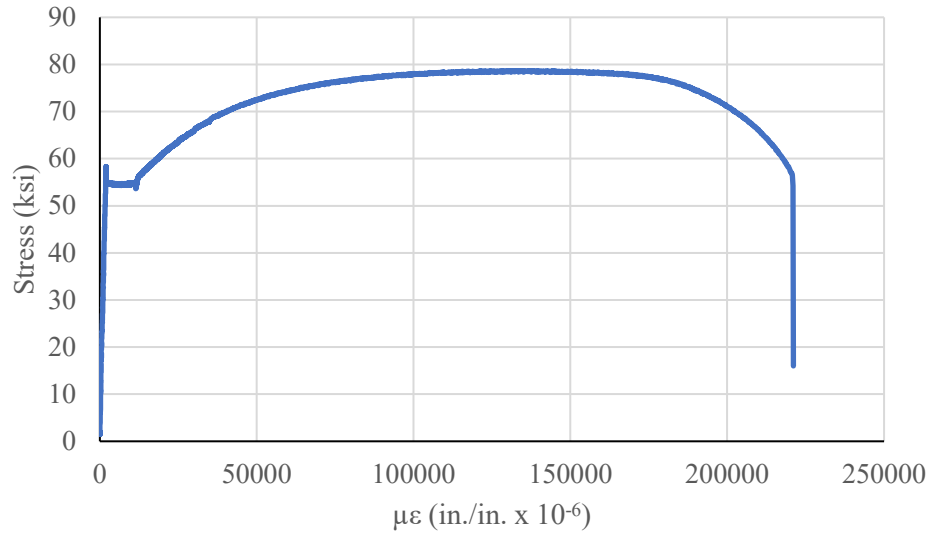


Figure D.31. Stress-strain curve for specimen 3T1.

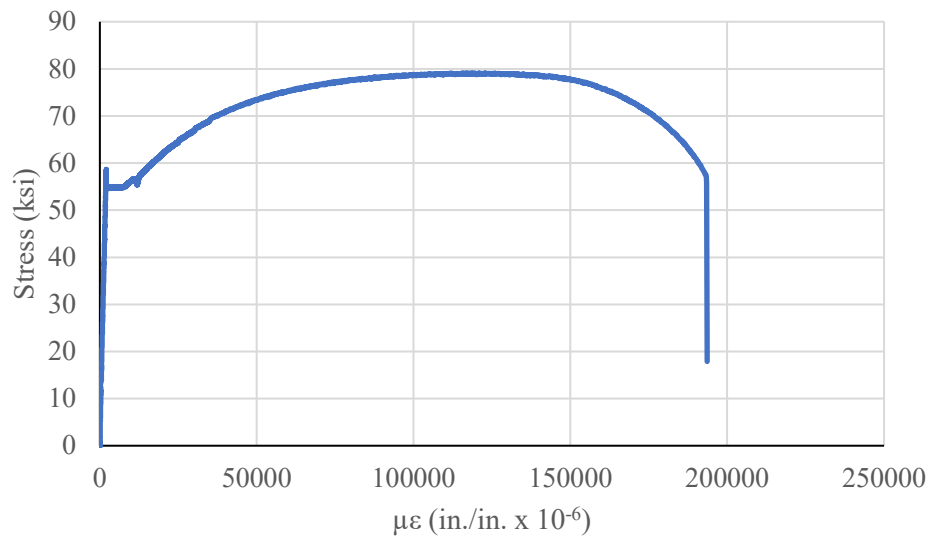


Figure D.32. Stress-strain curve for specimen 3T2.

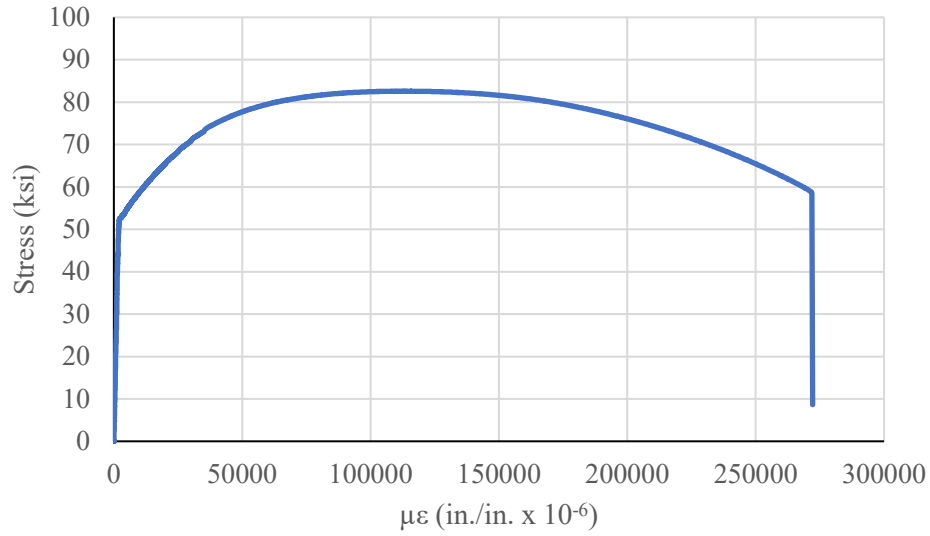


Figure D.33. Stress-strain curve for specimen 4A1.

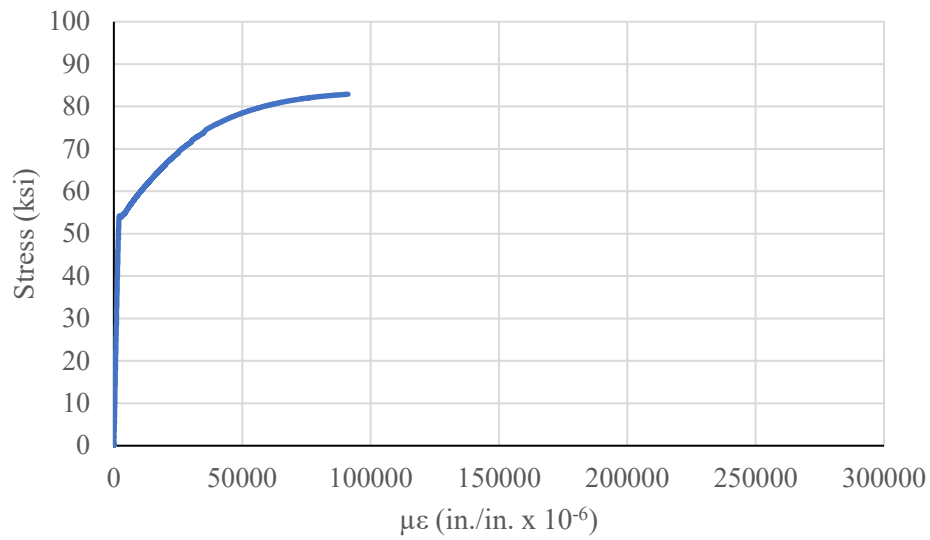


Figure D.34. Stress-strain curve for specimen 4A2, where the DIC camera unexpectedly shutoff.

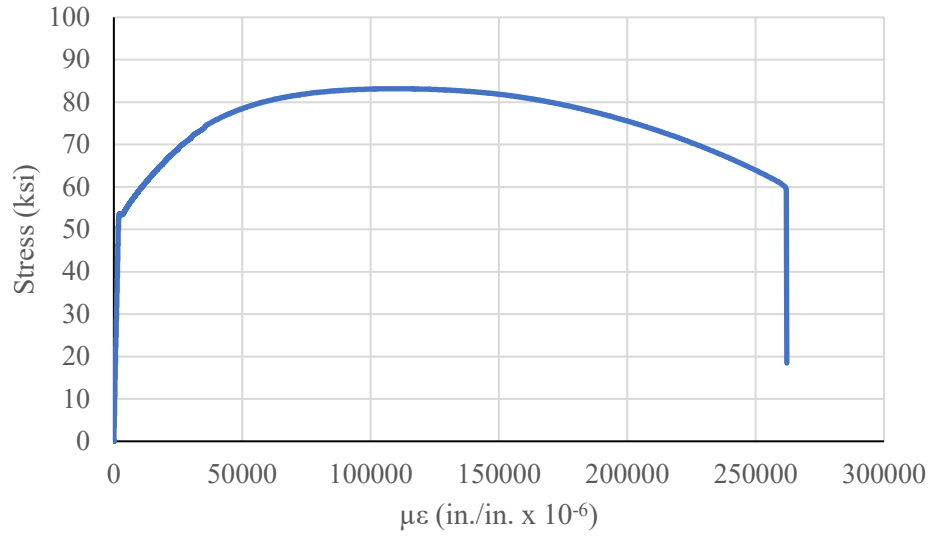


Figure D.35. Stress-strain curve for specimen 4A2 duplicate (machined from 4A3).

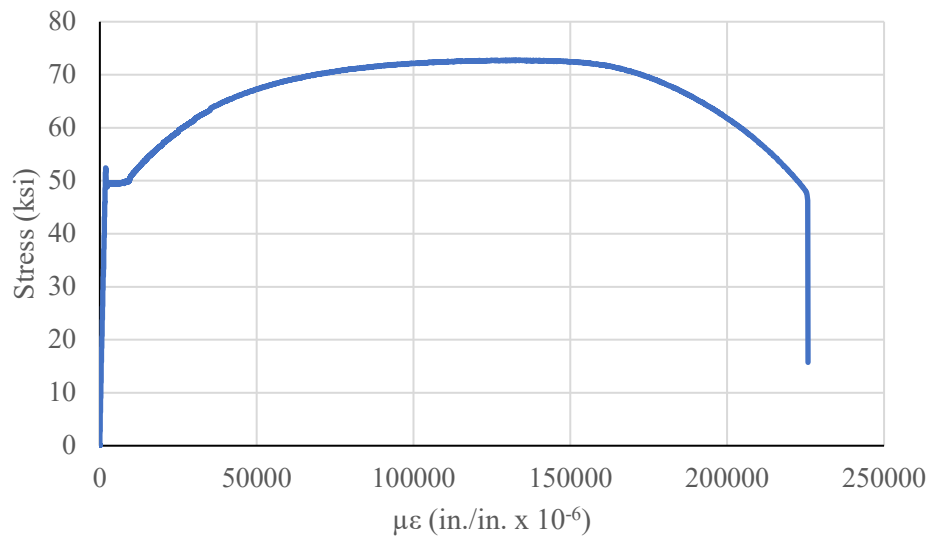


Figure D.36. Stress-strain curve for specimen 4B1.

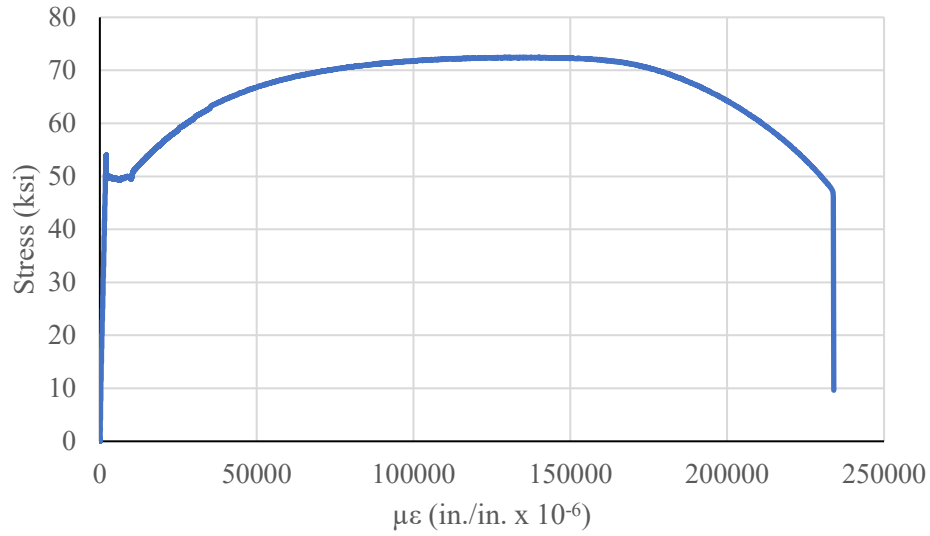


Figure D.37. Stress-strain curve for specimen 4B2.

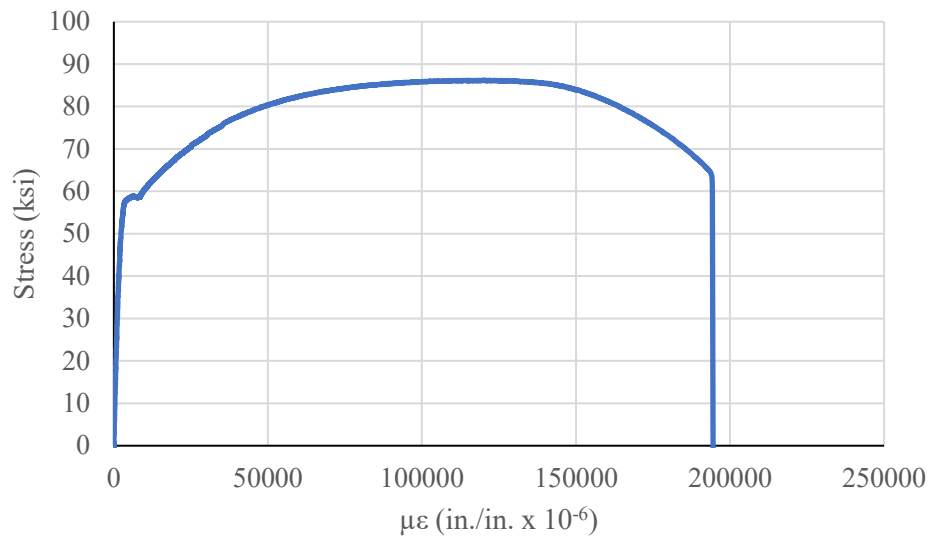


Figure D.38. Stress-strain curve for specimen 4Q1.

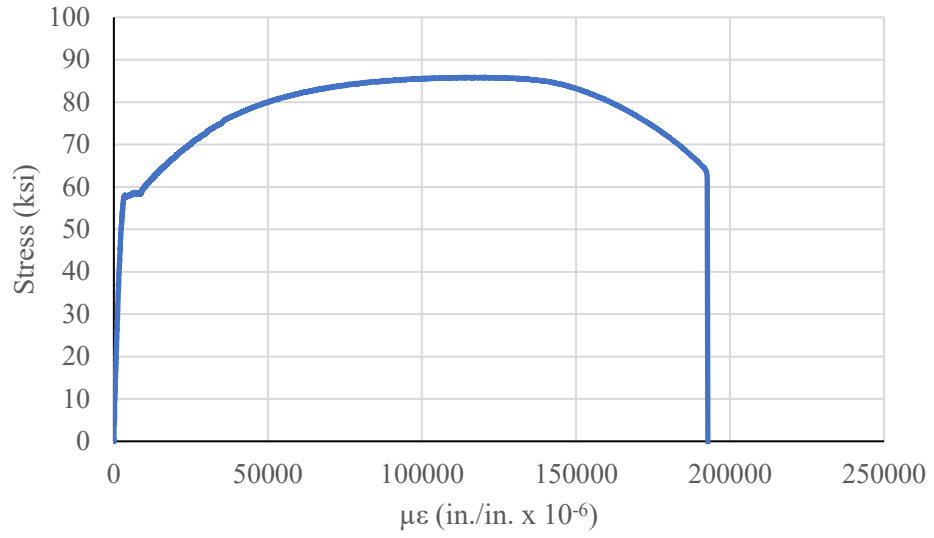


Figure D.39. Stress-strain curve for specimen 4Q2.

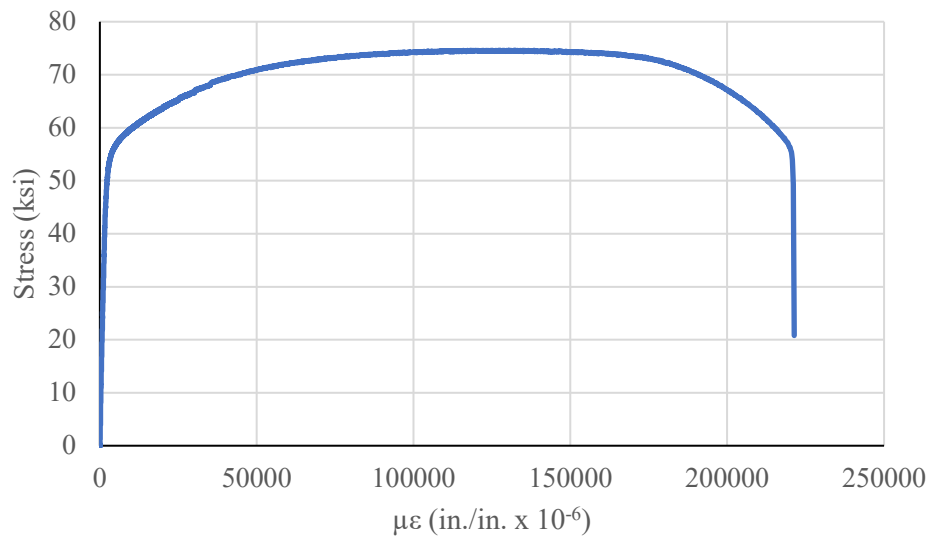


Figure D.40. Stress-strain curve for specimen 4R1.

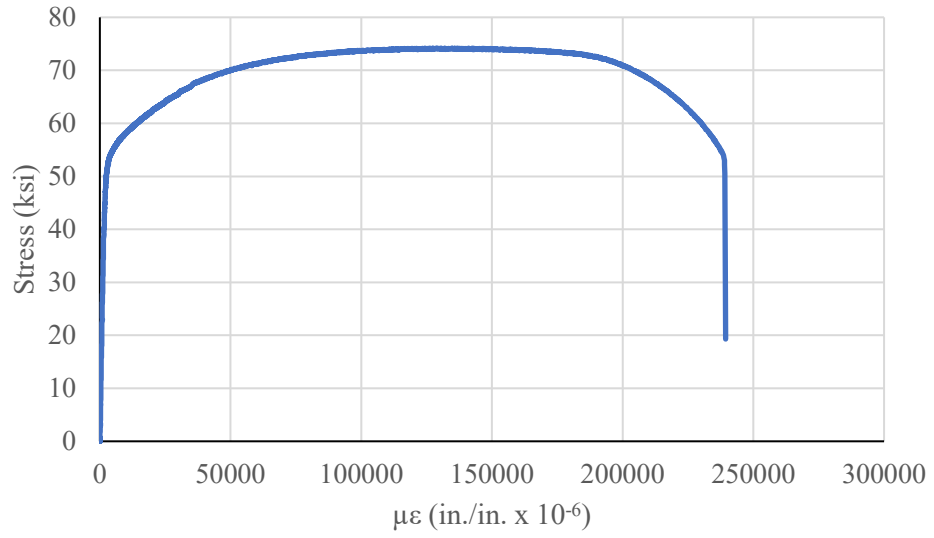


Figure D.41. Stress-strain curve for specimen 4R2.

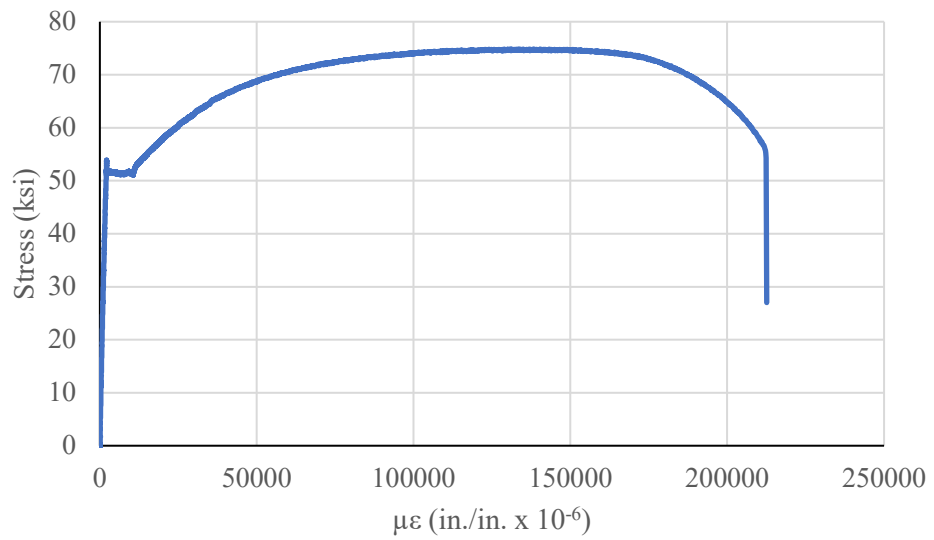


Figure D.42. Stress-strain curve for specimen 4T1.

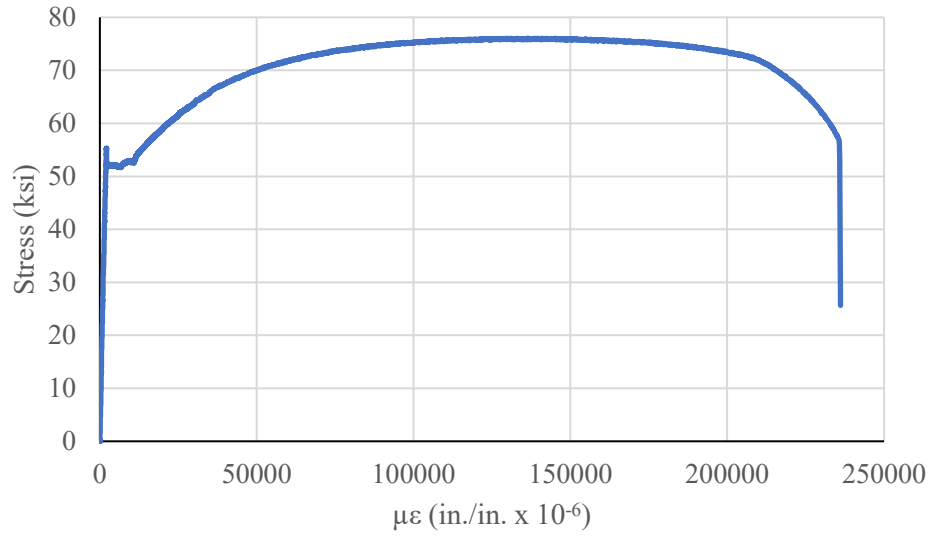


Figure D.43. Stress-strain curve for specimen 4T2.

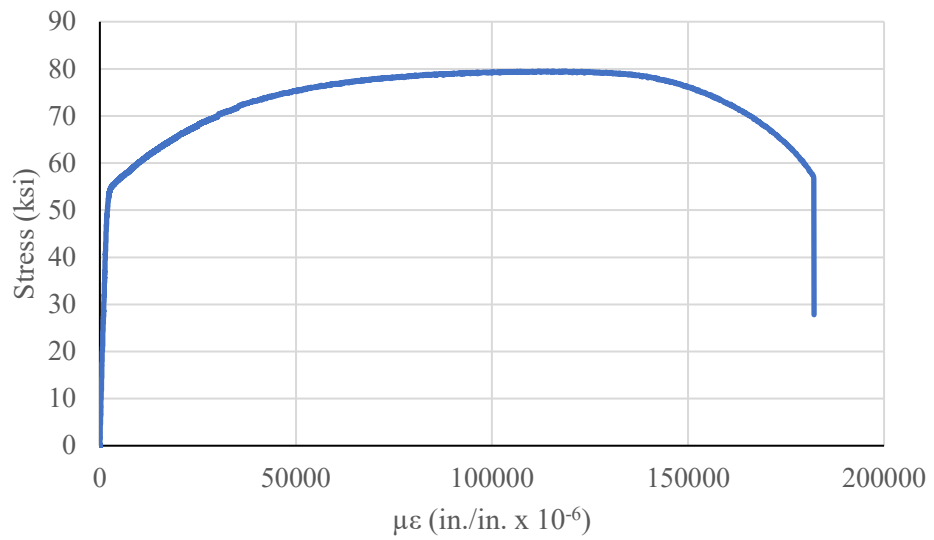


Figure D.44. Stress-strain curve for specimen 1U1.

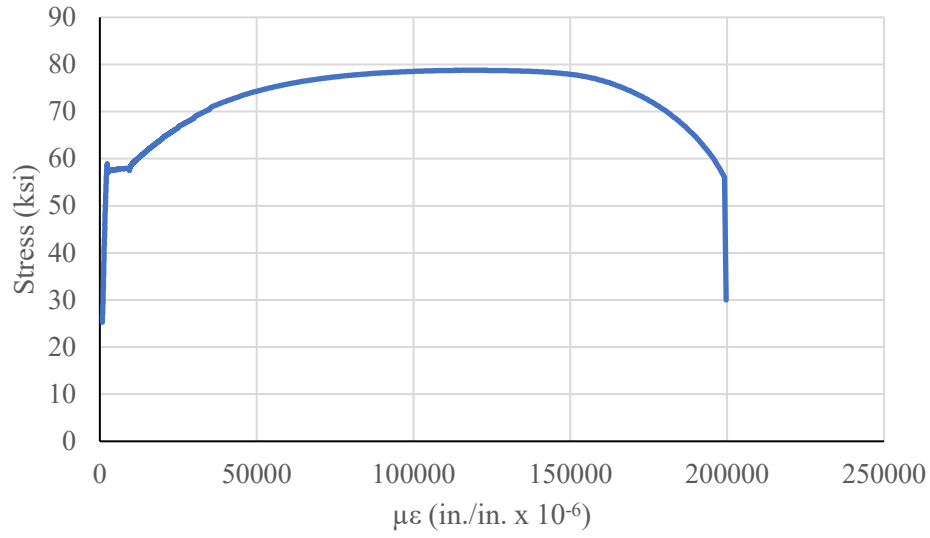


Figure D.45. Stress-strain curve for specimen 2U1.

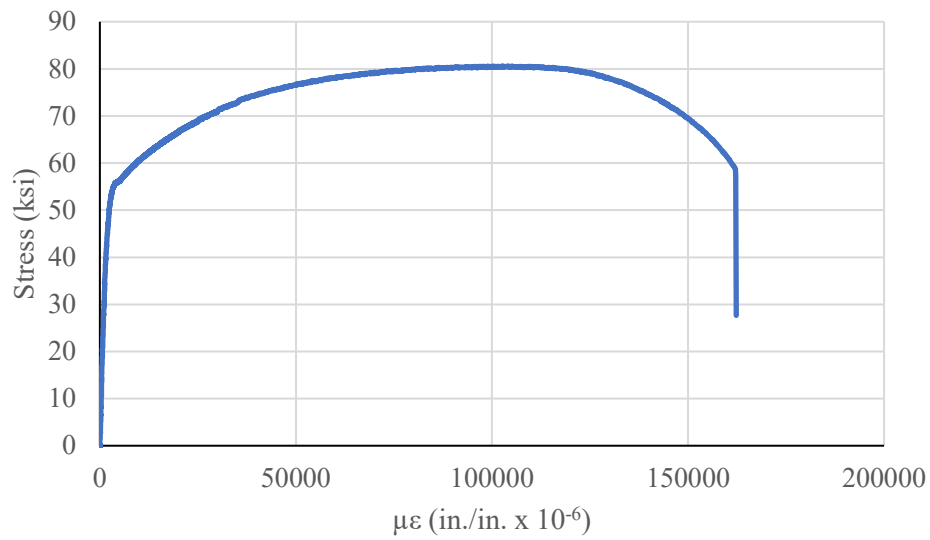


Figure D.46. Stress-strain curve for specimen 3U1.

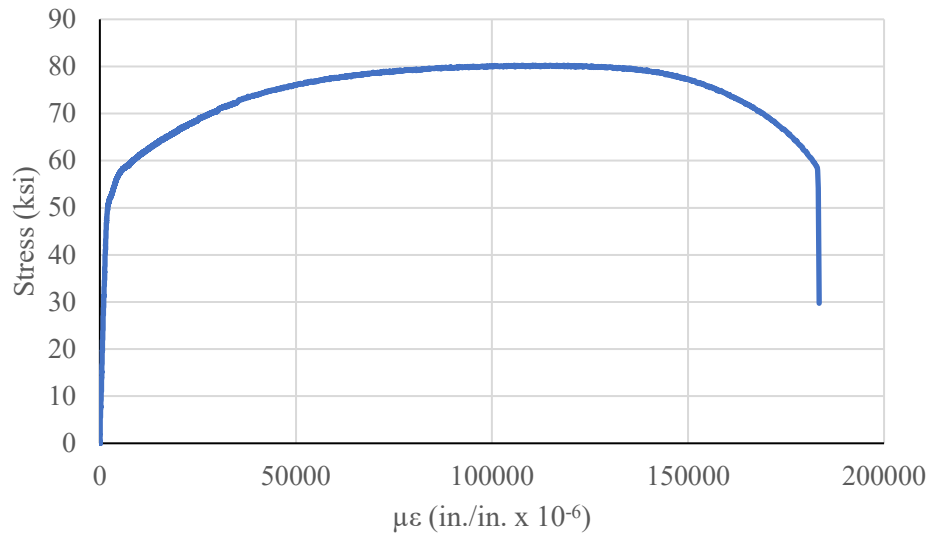


Figure D.47. Stress-strain curve for specimen 4U1.

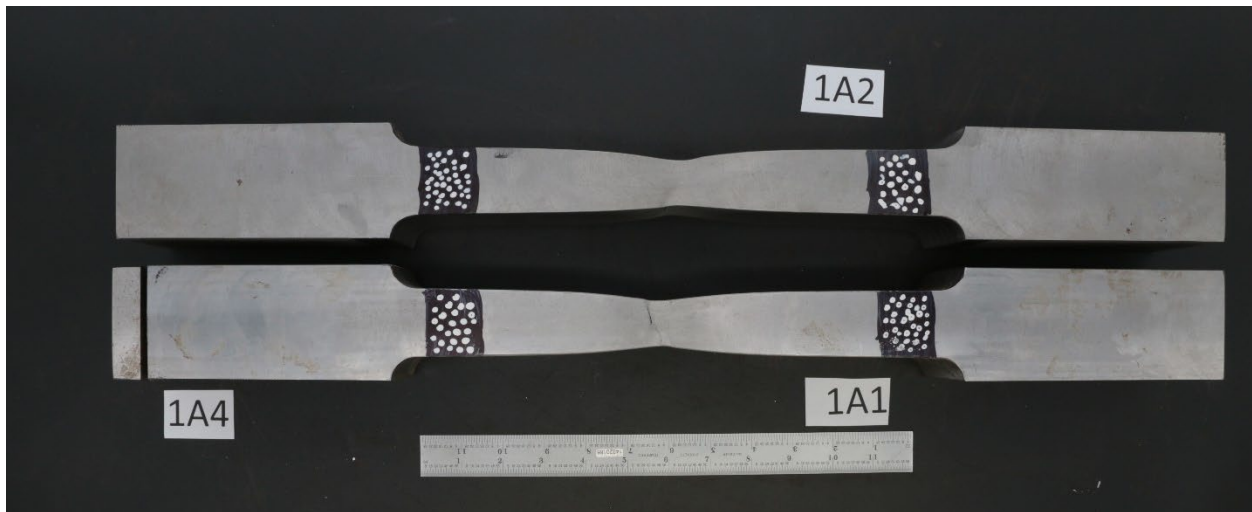


Figure D.48. Completed tensile and chemical specimens for plate 1A (1A1, 1A2, 1A4).



Figure D.49. Completed tensile and chemical specimens for plate 1B (1B1, 1B2, 1B4).



Figure D.50. Completed tensile and chemical specimens for plate 1C (1C1, 1C2, 1C4).



Figure D.51. Completed tensile and chemical specimens for plate 1H (1H1, 1H2, 1H4).



Figure D.52. Completed tensile and chemical specimens for plate 1N (1N1, 1N2, 1N4).



Figure D.53. Completed tensile and chemical specimens for plate 1Q (1Q1, 1Q2, 1Q4).

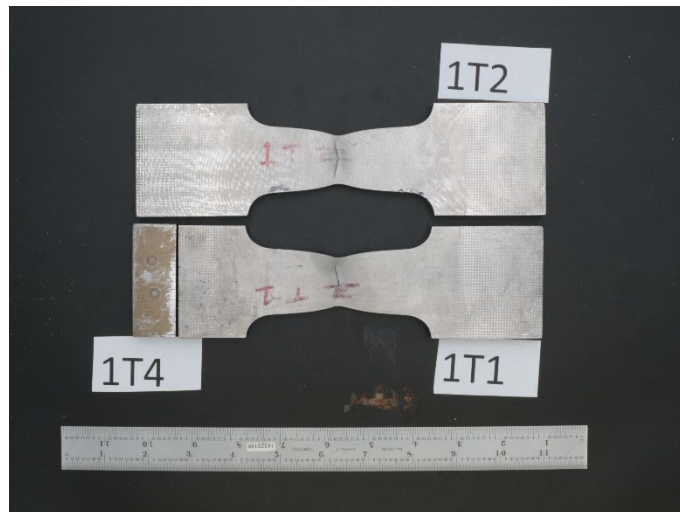


Figure D.54. Completed tensile and chemical specimens for plate 1T (1T1, 1T2, 1T4).

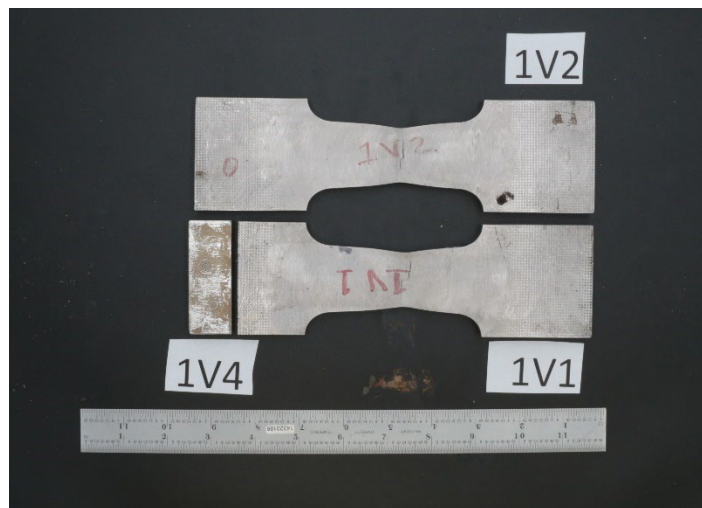


Figure D.55. Completed tensile and chemical specimens for plate 1V (1V1, 1V2, 1V4).



Figure D.56. Completed tensile and chemical specimens for plate 2A (2A1, 2A2, 2A4).



Figure D.57. Completed tensile and chemical specimens for plate 2B (2B1, 2B2, 2B4).



Figure D.58. Completed tensile and chemical specimens for plate 2Q (2Q1, 2Q2, 2Q4).



Figure D.59. Completed tensile and chemical specimens for plate 2T (2T1, 2T2, 2T4).

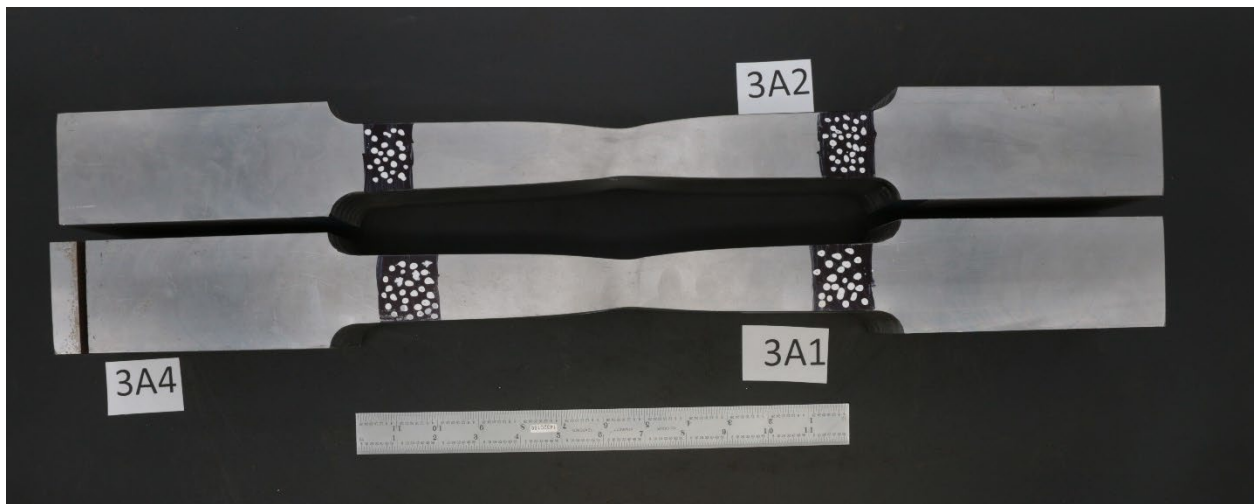


Figure D.60. Completed tensile and chemical specimens for plate 3A (3A1, 3A2, 3A4).



Figure D.61. Completed tensile and chemical specimens for plate 3B (3B1, 3B2, 3B4).



Figure D.62. Completed tensile and chemical specimens for plate 3Q (3Q1, 3Q2, 3Q4).



Figure D.63. Completed tensile and chemical specimens for plate 3T (3T1, 3T2, 3T4).



Figure D.64. Completed tensile and chemical specimens for plate 4A (4A1, 4A2, 4A3 (4A2 duplicate), 4A4).



Figure D.65. Completed tensile and chemical specimens for plate 4B (4B1, 4B2, 4B4).



Figure D.66. Completed tensile and chemical specimens for plate 4Q (4Q1, 4Q2, 4Q4).



Figure D.67. Completed tensile and chemical specimens for plate 4R (4R1, 4R2, 4R4).



Figure D.68. Completed tensile and chemical specimens for plate 4T (4T1, 4T2, 4T4).

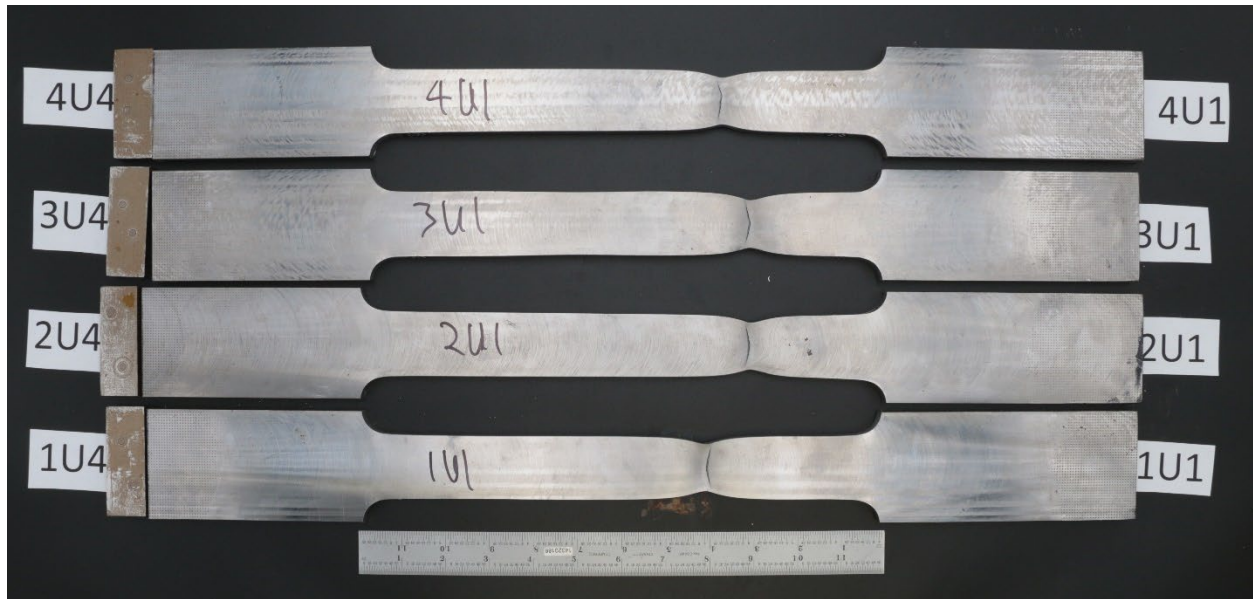


Figure D.69. Completed tensile and chemical specimens for longitudinal stiffener plate (1U1, 2U1, 3U1, 4U1, 1U4, 2U4, 3U4, 4U4).

Table D-1: Tensile test results for all specimens.

Specimen	Temperature (°F)	Gauge Length (in)	Measured Area (in ²) ^a	Yield (ksi)	Tensile (ksi)	Elongation at Fracture (%)	Reduction in Area (%)	Reduced Area (in ²)
1A1	64.5	7.573	4.502	53.2	81.2	25.5	57.3	1.921
1A2	64.6	7.575	4.500	53.7	81.5	27.8	56.0	1.981
1B1	70.1	8.212	1.017	53.5	77.5	22.3	55.8	0.449
1B2	70.1	8.250	1.014	54.1	77.9	22.4	55.2	0.455
1C1	64.8	7.511	4.505	52.2	76.7	28.2	57.0	1.937
1C2	64.0	7.323	4.503	53.3	77.8	26.8	56.8	1.943
1H1	64.7	7.719	3.612	65.6	95.5	21.0	50.2	1.798
1H2	64.9	7.678	3.603	66.2	96.3	20.2	48.0	1.875
1N1	64.2	7.793	3.192	54.6	79.4	27.1	63.4	1.167
1N2	68.2	8.150	3.194	55.6	80.0	27.1	62.4	1.201
1Q1	69.1	8.027	1.097	59.4	86.9	20.1	51.8	0.529
1Q2	69.0	8.102	1.103	58.3	86.6	20.5	53.3	0.515
1T1	71.8	2.151	0.607	51.8	77.3	34.3	47.8	0.317
1T2	71.6	2.129	0.622	52.3	78.0	34.9	48.5	0.320
1U1	71.1	7.928	0.609	56.7	79.5	18.0	48.0	0.317
1V1	71.9	2.065	0.665	55.4	79.7	24.8	33.1	0.445
1V2	71.8	1.990	0.659	56.6	81.8	24.9	34.5	0.431
2A1	65.0	7.039	4.502	56.1	84.2	24.9	52.6	2.135
2A2	64.8	7.091	4.503	53.9	81.2	26.0	55.6	1.998
2B1	70.2	8.058	1.125	47.4	69.3	27.5	59.5	0.456
2B2	70.9	8.259	1.131	48.3	69.1	27.7	59.8	0.455

Table D-1 (cont.): Tensile test results for all specimens.

Specimen	Temperature (°F)	Gauge Length (in)	Measured Area (in ²) ^a	Yield (ksi)	Tensile (ksi)	Elongation at Fracture (%)	Reduction in Area (%)	Reduced Area (in ²)
2Q1	69.2	8.120	1.128	59.8	88.3	17.9	52.6	0.535
2Q2	69.3	8.087	1.121	61.0	88.7	18.2	52.2	0.536
2T1	66.4	7.959	0.591	54.0	76.7	20.7	48.5	0.304
2T2	71.8	7.947	0.591	53.3	76.1	22.4	49.1	0.301
2U1	70.8	7.970	0.588	57.7	78.8	19.8	50.4	0.292
3A1	64.2	7.233	4.514	52.7	80.3	26.0	54.8	2.040
3A2	63.7	7.846	4.511	53.6	81.5	26.3	51.8	2.174
3B1	70.9	8.113	1.130	49.0	72.2	22.8	59.5	0.458
3B2	70.8	7.984	1.122	49.6	72.9	21.3	55.0	0.504
3Q1	67.1	7.907	1.119	59.4	89.0	17.7	51.7	0.540
3Q2	67.1	7.899	1.121	58.9	88.4	17.9	52.7	0.530
3T1	70.6	7.966	0.602	54.6	78.7	22.0	49.1	0.306
3T2	72.0	7.981	0.602	54.6	79.1	19.3	47.7	0.314
3U1	71.6	8.027	0.606	56.2	80.6	16.3	47.6	0.317
4A1	64.5	7.720	4.523	54.7	82.6	26.2	55.2	2.028
4A2	65.0	7.946	4.512	55.6	82.9	9.1	52.9	2.125
4A2 (duplicate)	69.8	7.762	4.505	55.1	83.2	25.4	51.3	2.193
4B1	71.0	8.117	1.164	49.5	72.8	22.9	60.7	0.457
4B2	71.0	8.043	1.167	49.7	72.5	23.5	60.3	0.464
4Q1	67.3	7.990	1.095	58.4	86.2	19.4	49.8	0.550
4Q2	68.9	7.990	1.098	58.0	85.9	19.2	50.4	0.545
4R1	72.4	7.954	0.795	56.7	74.6	22.0	50.5	0.393
4R2	72.4	7.906	0.795	55.0	74.2	23.6	52.3	0.379
4T1	72.0	7.944	0.611	51.4	74.9	21.1	49.8	0.307
4T2	72.4	8.040	0.606	52.0	76.1	23.7	49.3	0.307
4U1	71.4	8.004	0.563	57.4	80.3	18.3	47.2	0.297

^aPer A370-21 Section 9.5.1, the CNC machined center width was within 0.001 in. for both the 8 in. and 2 in. gauge length specimens and was therefore not included in Table D-1; the nominal machined center width is 1.500 in. Thickness measurements represent an average of three caliper measurement, reported to the nearest 0.001 in.

Appendix E: CVN Test Results

Table E-1: CVN impact results in the L-T direction.

Specimen	Temperature (°F)	Energy (ft-lbf)	Specimen	Temperature (°F)	Energy (ft-lbf)
1AX	40.6	71.0	3BX	39.6	139.0
1AY	39.5	48.0	3BY	39.5	251.0
1AZ	39.5	44.0	3BZ	39.5	142.0
1BX	39.5	26.0	3QX	39.6	15.0
1BY	39.5	41.0	3QY	39.6	23.0
1BZ	40.2	40.0	3QZ	39.6	27.0
1CX	39.6	93.0	3TX	39.6	73.0
1CY	39.6	101.0	3TY	39.6	73.5
1CZ	39.5	96.0	3TZ	39.6	48.5
1HX	39.3	24.0	4AX	40	51.0
1HY	39.2	17.5	4AY	39.5	41.0
1HZ	39.3	32.5	4AZ	39.5	36.0
1NX	39.2	120.0	4BX	39.4	60.5
1NY	39.2	138.0	4BY	39.3	117.5
1NZ	39.2	138.0	4BZ	39.4	125.0
1QX	39.5	24.0	4QX	39.4	65.5
1QY	39.5	26.5	4QY	39.4	69.0
1QZ	39.5	25.0	4QZ	39.4	62.5
1TX	39.1	73.5	4RX	39.4	95.0
1TY	39.1	56.0	4RY	39.5	86.0
1TZ	39	46.0	4RZ	39.5	89.0
1VX	40.1	20.5	4TX	39.4	88.0
1VY	39.1	15.0	4TY	39.5	73.0
1VZ	39.7	32.0	4TZ	39.5	66.0
2AX	40.6	28.5			
2AY	39.7	42.0			
2AZ	39.5	34.0			
2BX	39.5	102.5			
2BY	39.5	102.0			
2BZ	39.5	96.0			
2QX	39.5	29.0			
2QY	39.5	38.0			
2QZ	39.5	20.5			
2TX	39.5	78.0			
2TY	39.5	94.5			
2TZ	39.5	85.5			
3AX	39.5	40.0			
3AY	39.5	33.5			
3AZ	39.5	47.0			



Figure E.1. Shear fracture surfaces for plate 1A.

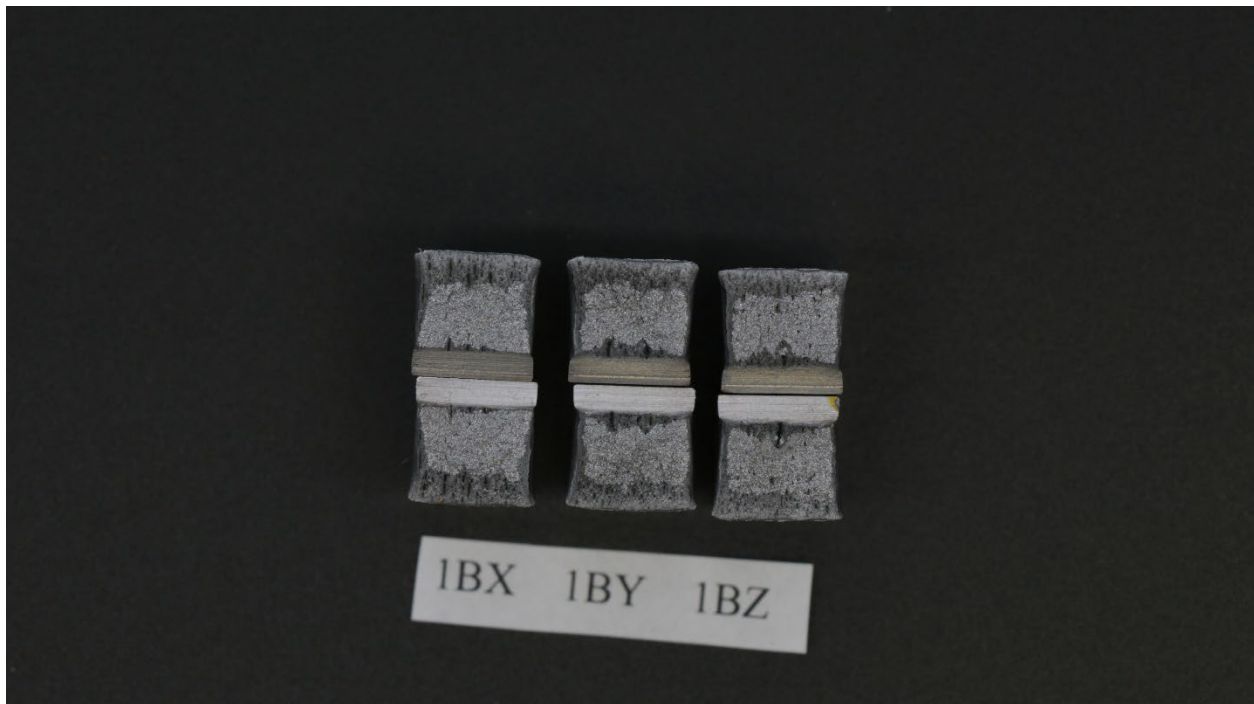


Figure E.2. Shear fracture surfaces for plate 1B.



Figure E.3. Shear fracture surfaces for plate 1C.

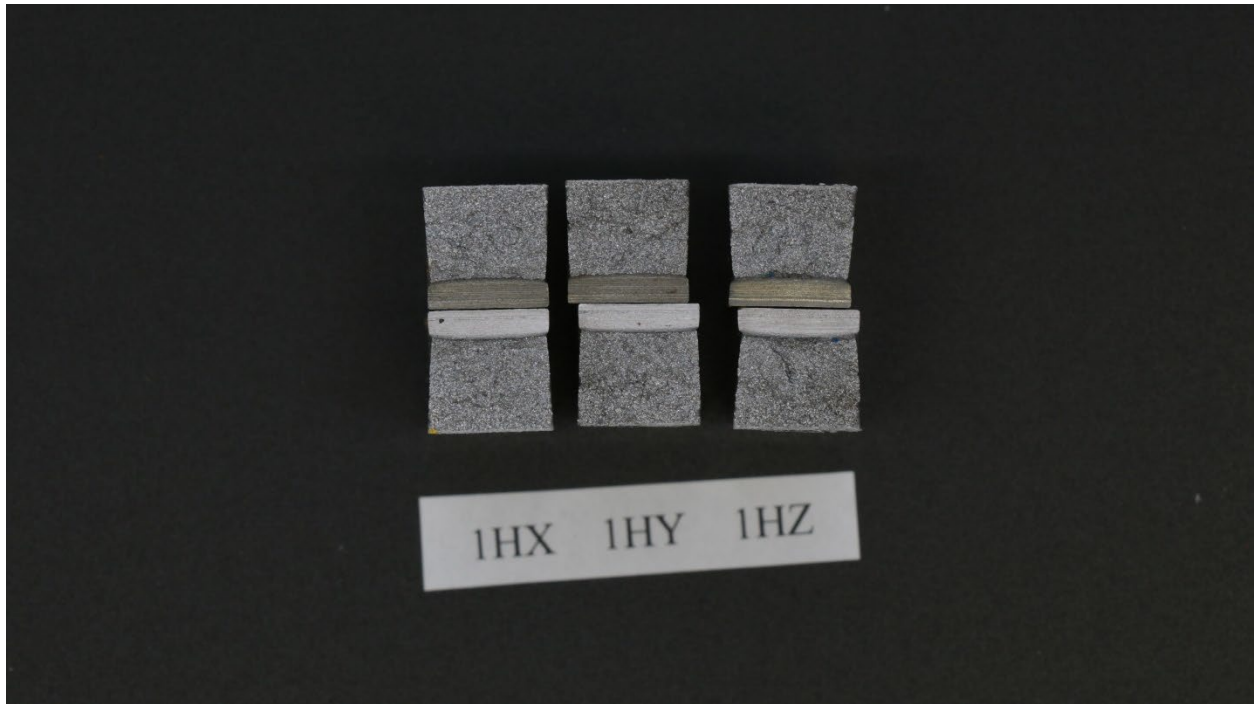


Figure E.4. Shear fracture surfaces for plate 1H.



Figure E.5. Shear fracture surfaces for plate 1N.

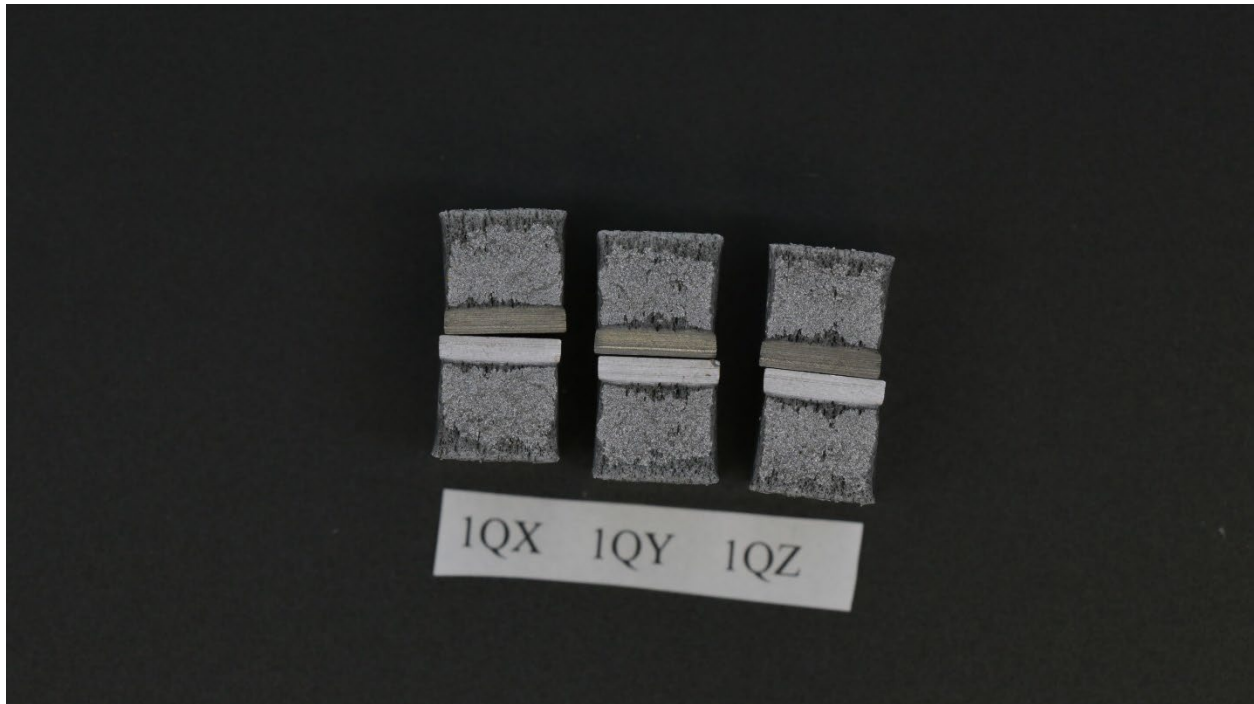


Figure E.6. Shear fracture surfaces for plate 1Q.

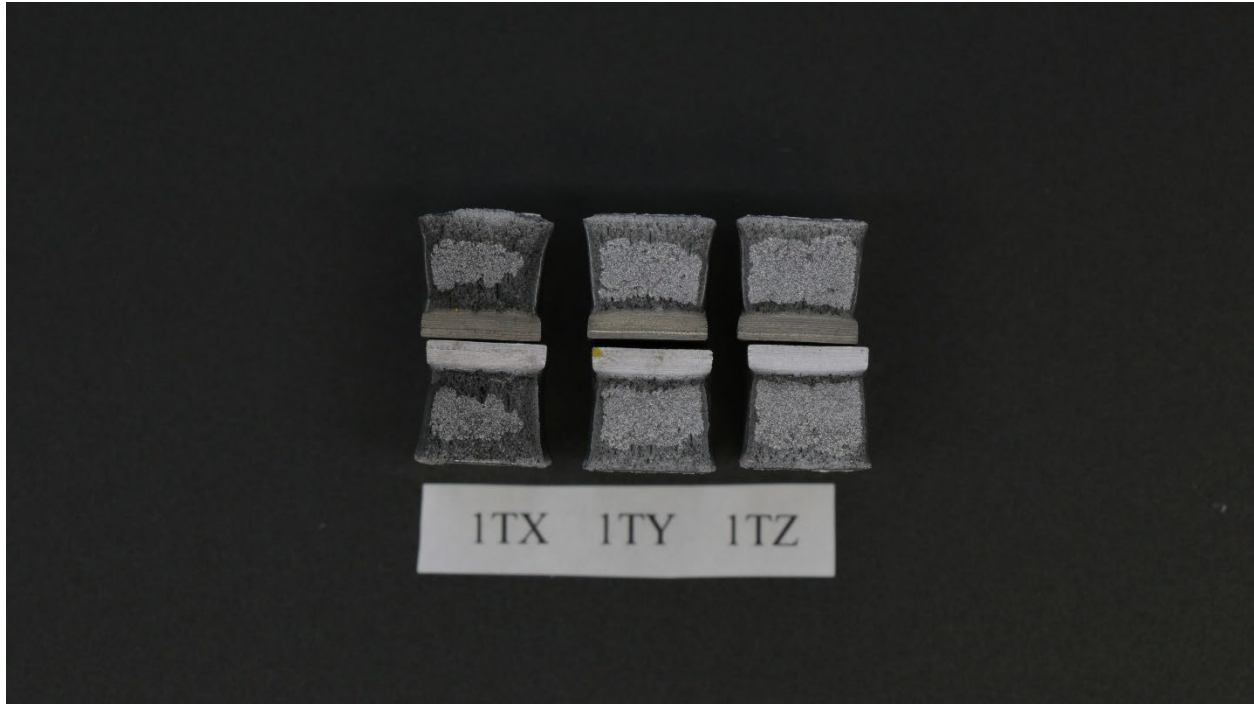


Figure E.7. Shear fracture surfaces for plate 1T.

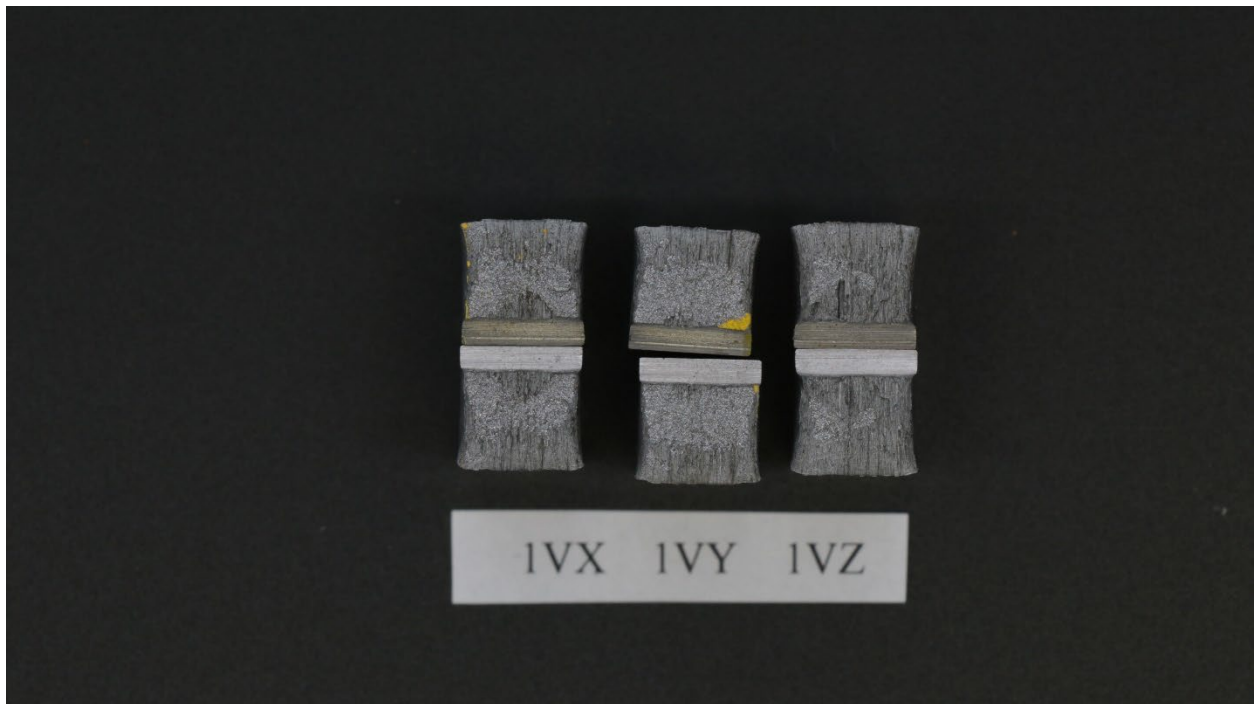


Figure E.8. Shear fracture surfaces for plate 1V.



Figure E.9. Shear fracture surfaces for plate 2A.



Figure E.10. Shear fracture surfaces for plate 2B.

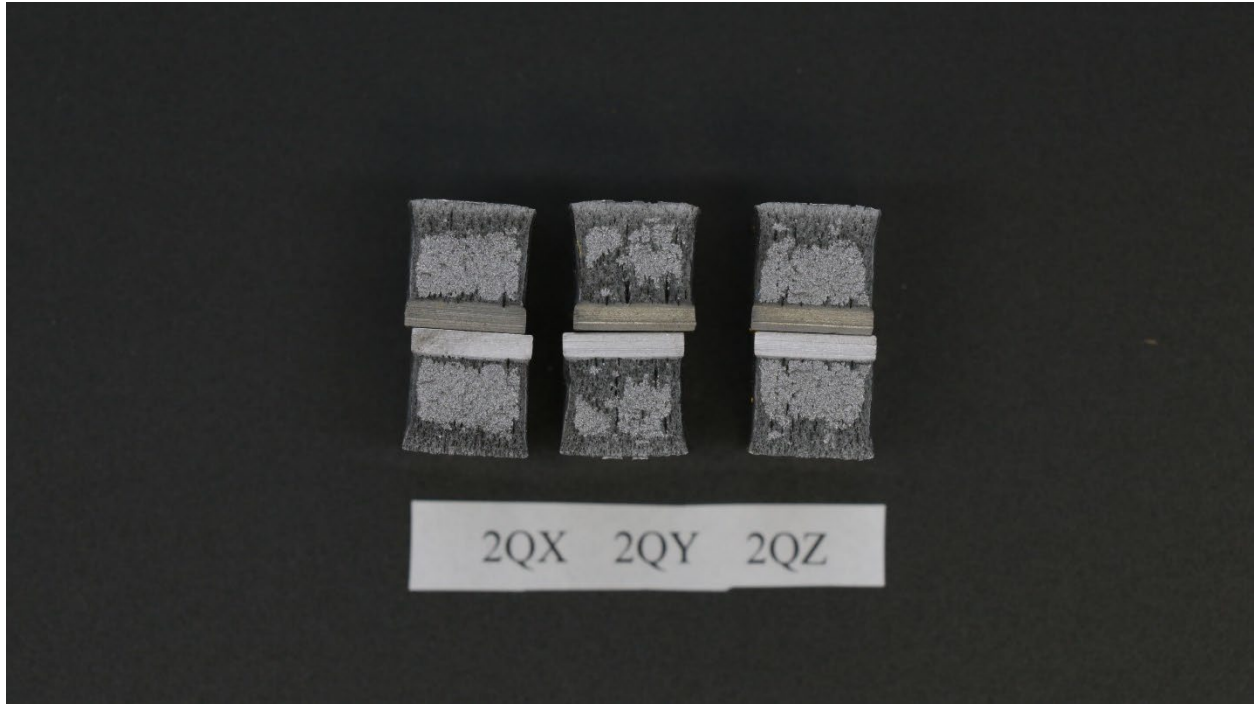


Figure E.11. Shear fracture surfaces for plate 2Q.



Figure E.12. Shear fracture surfaces for plate 2T.



Figure E.13. Shear fracture surfaces for plate 3A.



Figure E.14. Shear fracture surfaces for plate 3B.



Figure E.15. Shear fracture surfaces for plate 3Q.



Figure E.16. Shear fracture surfaces for plate 3T.



Figure E.17. Shear fracture surfaces for plate 4A.



Figure E.18. Shear fracture surfaces for plate 4B.

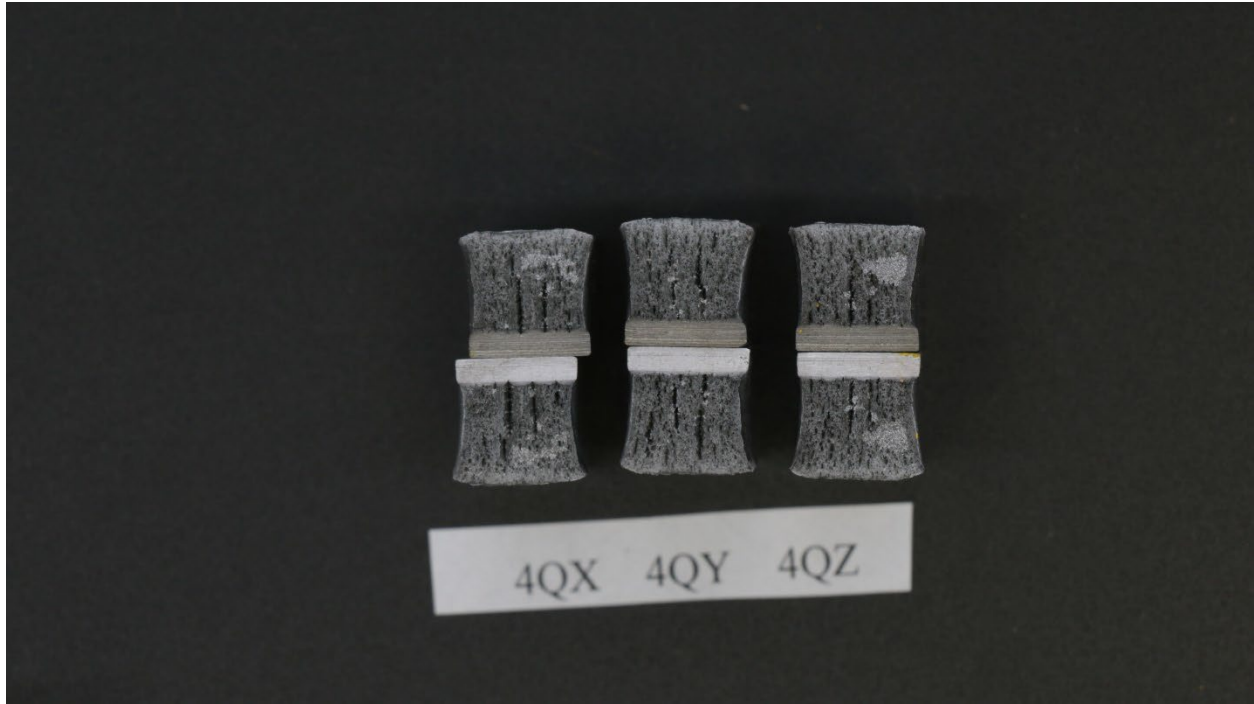


Figure E.19. Shear fracture surfaces for plate 4Q.

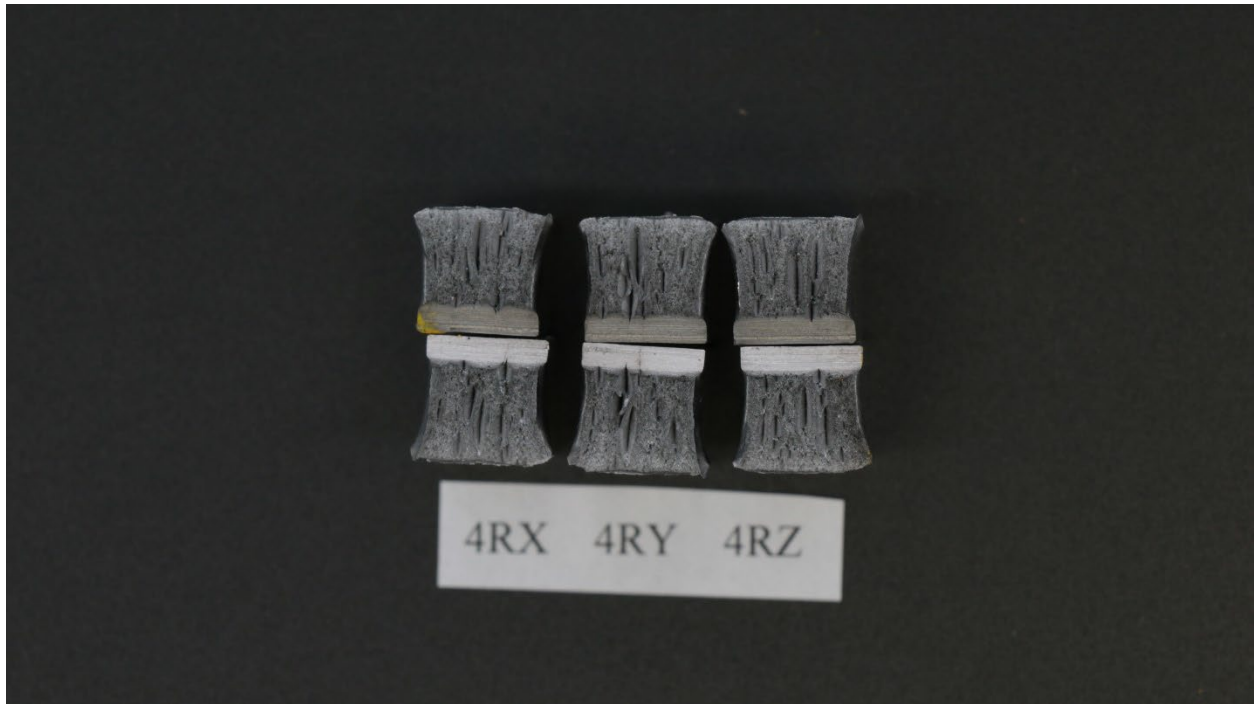


Figure E.20. Shear fracture surfaces for plate 4R.

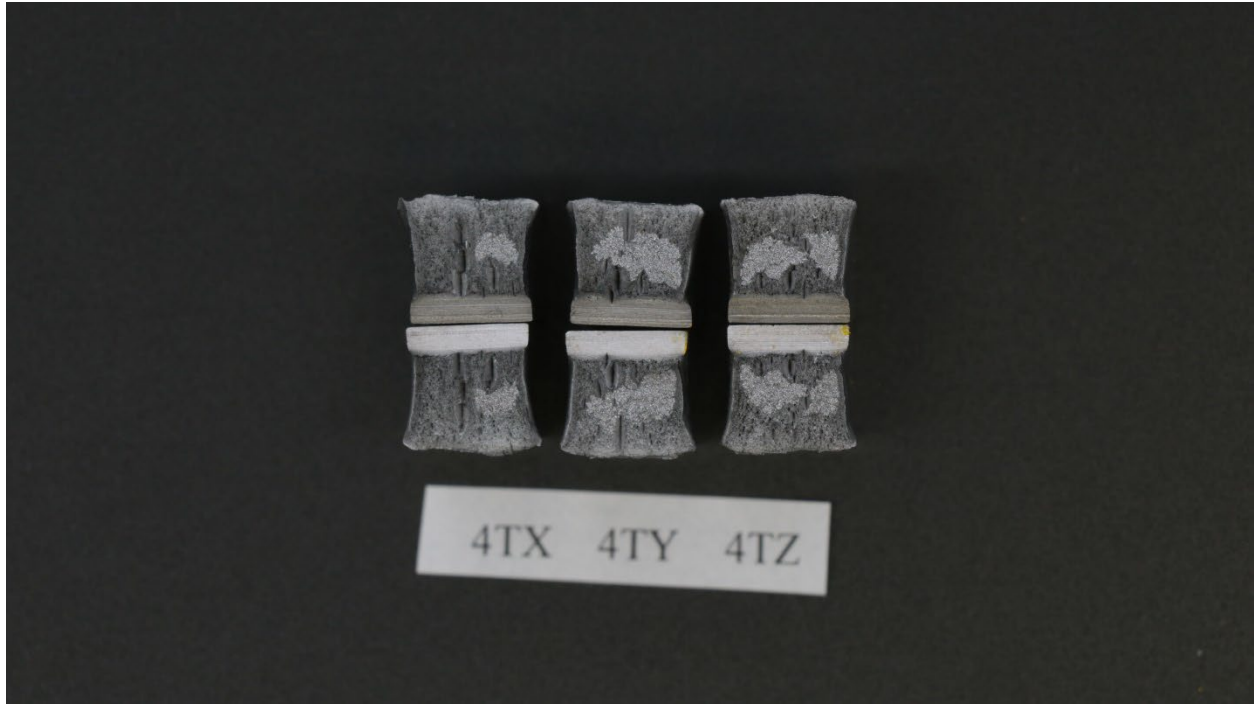


Figure E.21. Shear fracture surfaces for plate 4T.

Table E-2: Percent shear fracture areas of CVN specimens.

Sample ID	% Shear Fracture Area (Mask Area Method)	% Shear Fracture Area (Pixel Intensity Method)	Sample ID	% Shear Fracture Area (Mask Area Method)	% Shear Fracture Area (Pixel Intensity Method)
1AX	25	30	3BX	95	15
1AY	20	15	3BY	-	-
1AZ	15	25	3BZ	100	35
1BX	40	30	3QX	35	15
1BY	45	40	3QY	55	20
1BZ	40	30	3QZ	40	25
1CX	25	25	3TX	85	45
1CY	30	30	3TY	80	40
1CZ	25	25	3TZ	40	25
1HX	10	5	4AX	10	5
1HY	10	10	4AY	5	5
1HZ	15	20	4AZ	5	5
1NX	40	25	4BX	25	10
1NY	40	40	4BY	50	15
1NZ	45	30	4BZ	55	15
1QX	25	25	4QX	90	50
1QY	30	25	4QY	100	50
1QZ	25	25	4QZ	90	50
1TX	70	65	4RX	100	30
1TY	50	30	4RY	100	40
1TZ	40	25	4RZ	100	40
1VX	55	15	4TX	90	35
1VY	50	10	4TY	70	30
1VZ	85	20	4TZ	75	35
2AX	5	15			
2AY	10	15			
2AZ	10	15			
2BX	100	45			
2BY	100	45			
2BZ	95	40			
2QX	45	30			
2QY	70	40			
2QZ	50	25			
2TX	80	35			
2TY	100	45			
2TZ	95	50			
3AX	5	5			
3AY	5	5			
3AZ	10	5			

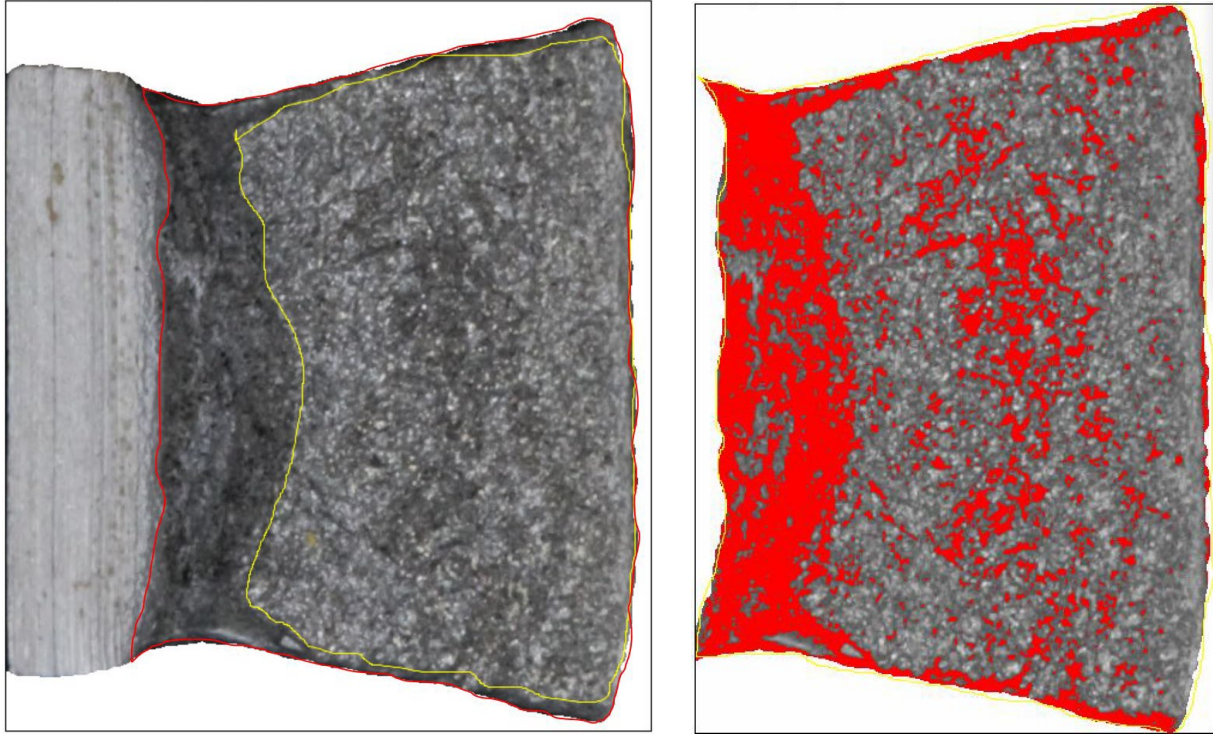


Figure E.22. Shear fracture areas for specimen 1AX using a Mask Area Method (left) and a Pixel Intensity Method (right).

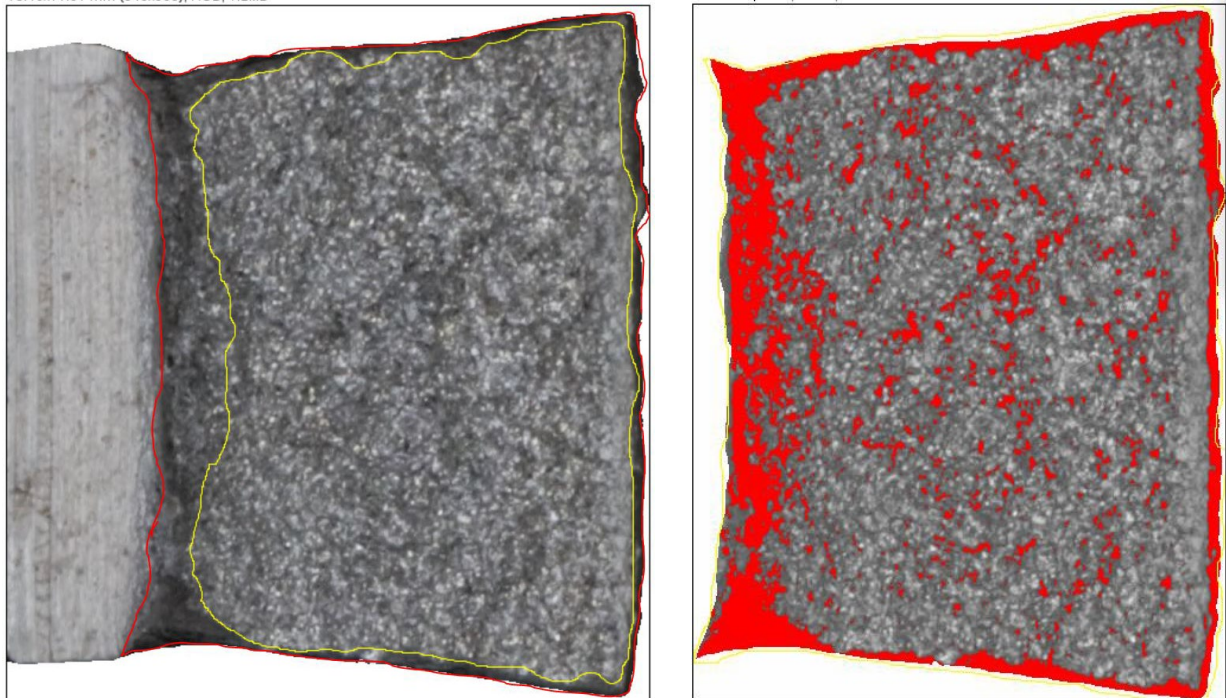


Figure E.23. Shear fracture areas for specimen 1AY using a Mask Area Method (left) and a Pixel Intensity Method (right).

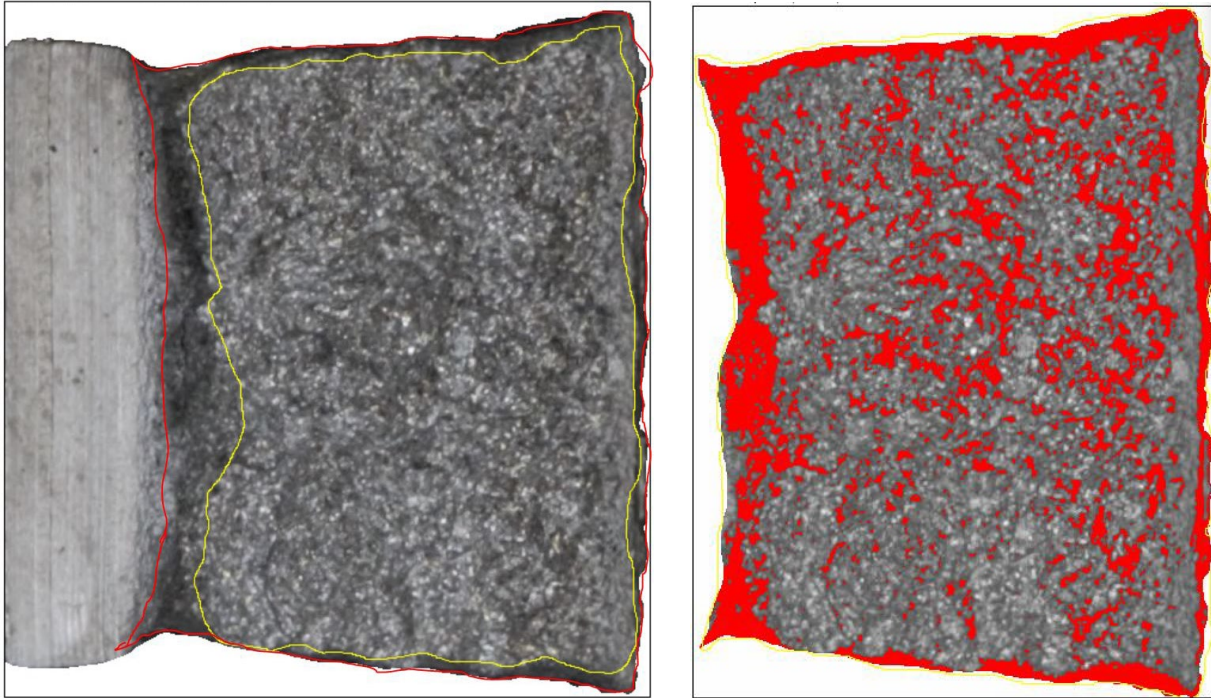


Figure E.24. Shear fracture areas for specimen 1AZ using a Mask Area Method (left) and a Pixel Intensity Method (right).

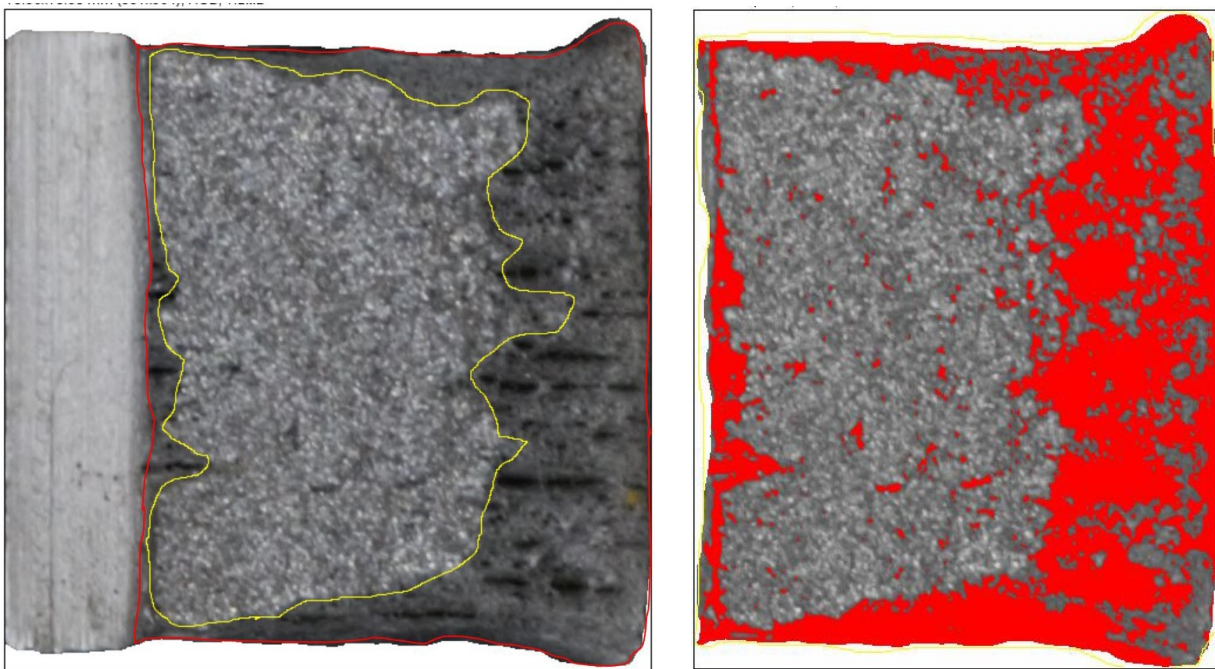


Figure E.25. Shear fracture areas for specimen 1BX using a Mask Area Method (left) and a Pixel Intensity Method (right).

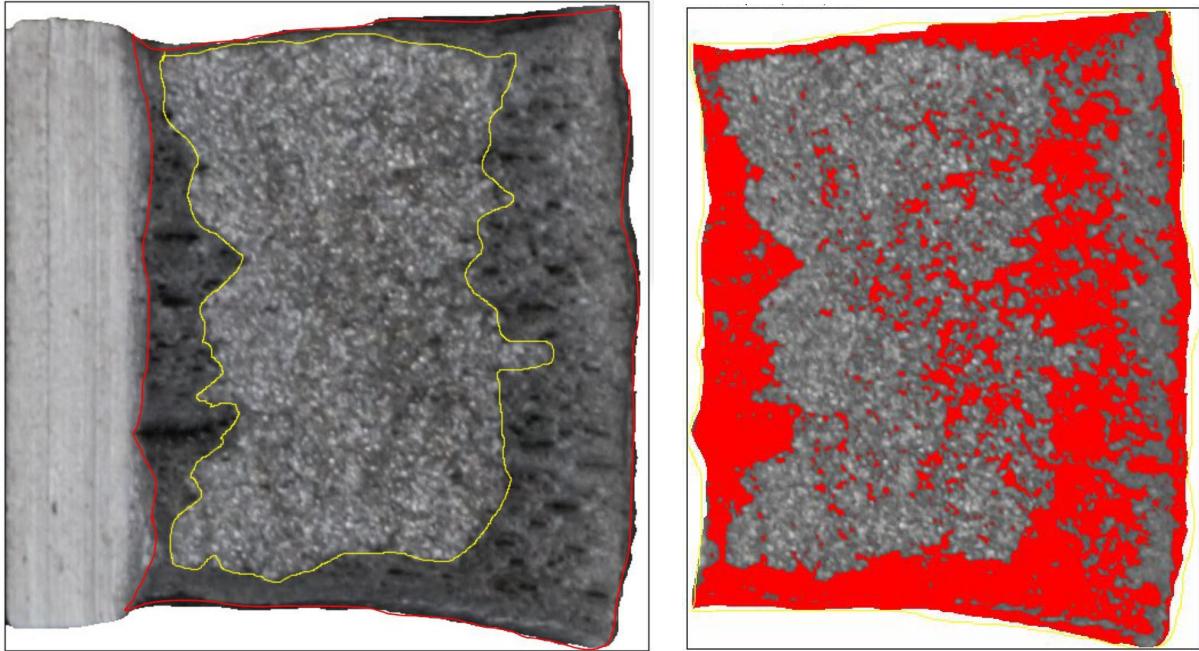


Figure E.26. Shear fracture areas for specimen 1BY using a Mask Area Method (left) and a Pixel Intensity Method (right).

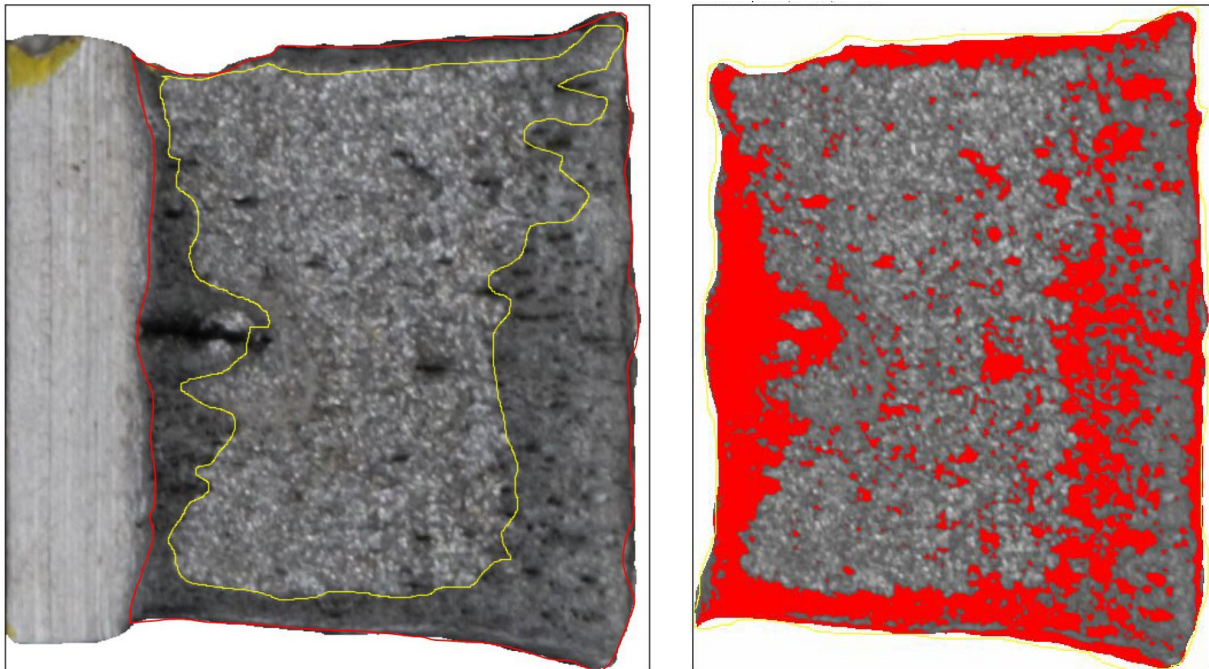


Figure E.27. Shear fracture areas for specimen 1BZ using a Mask Area Method (left) and a Pixel Intensity Method (right).

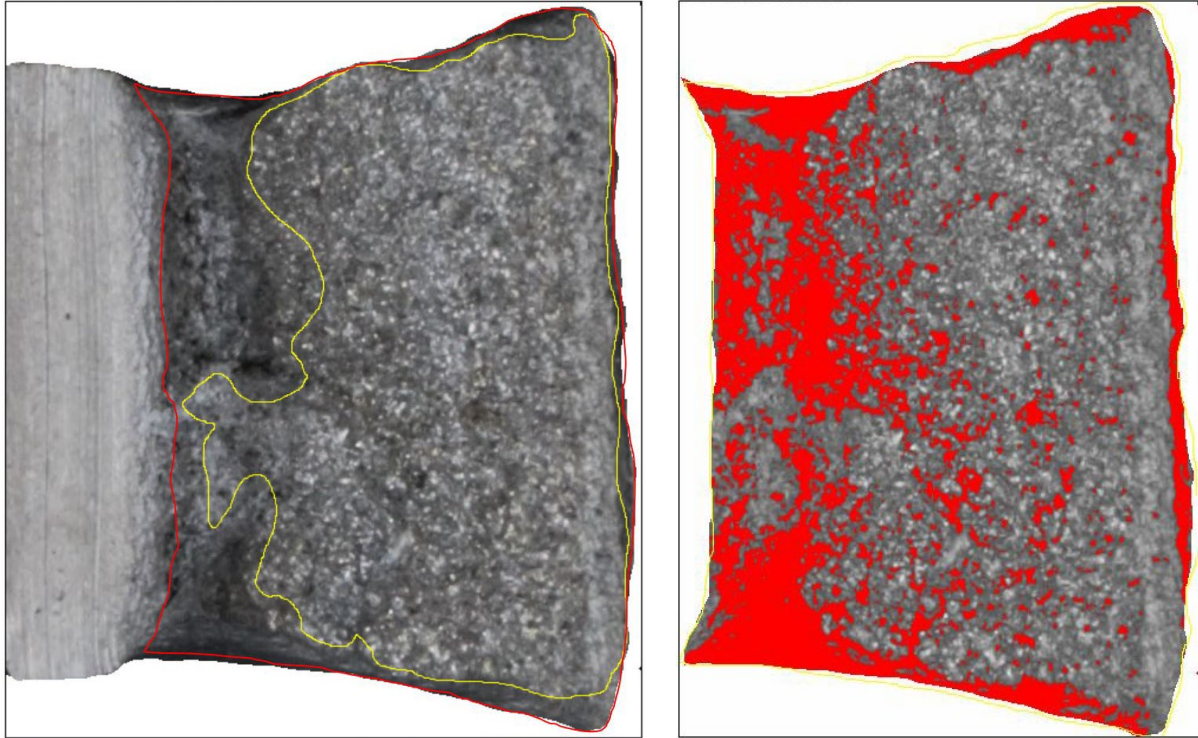


Figure E.28. Shear fracture areas for specimen 1CX using a Mask Area Method (left) and a Pixel Intensity Method (right).

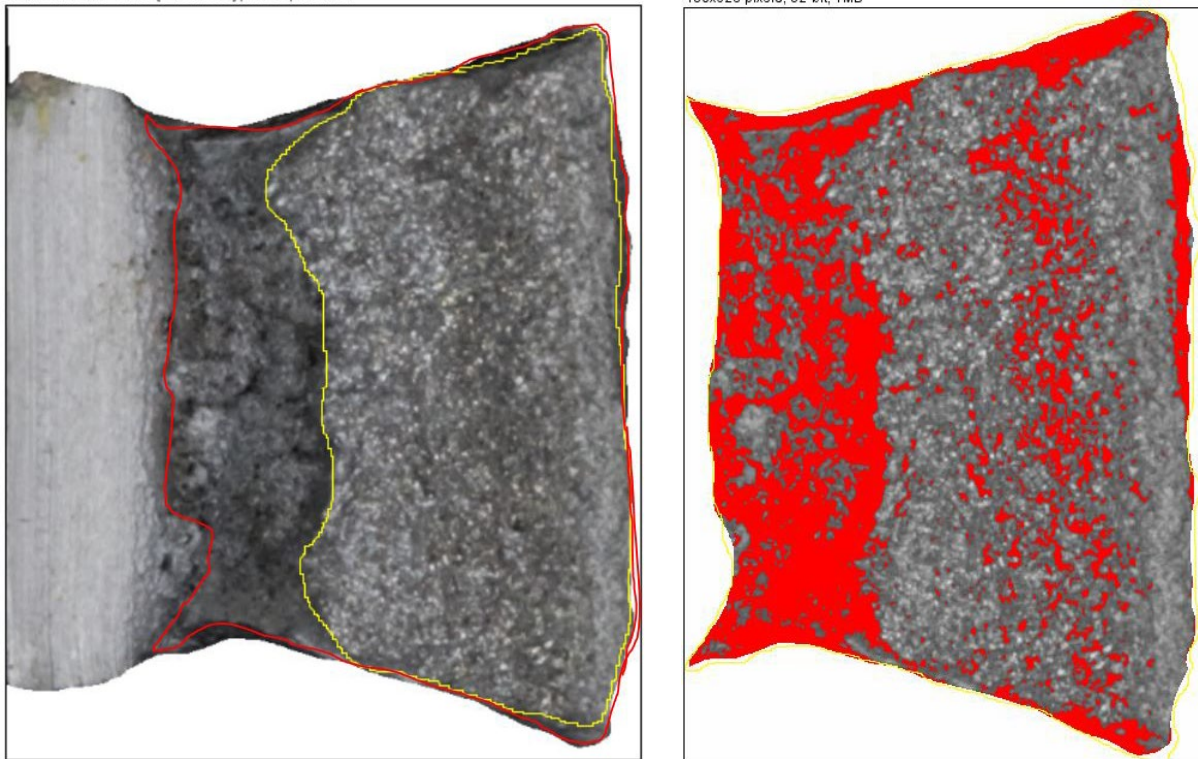


Figure E.29. Shear fracture areas for specimen 1CY using a Mask Area Method (left) and a Pixel Intensity Method (right).

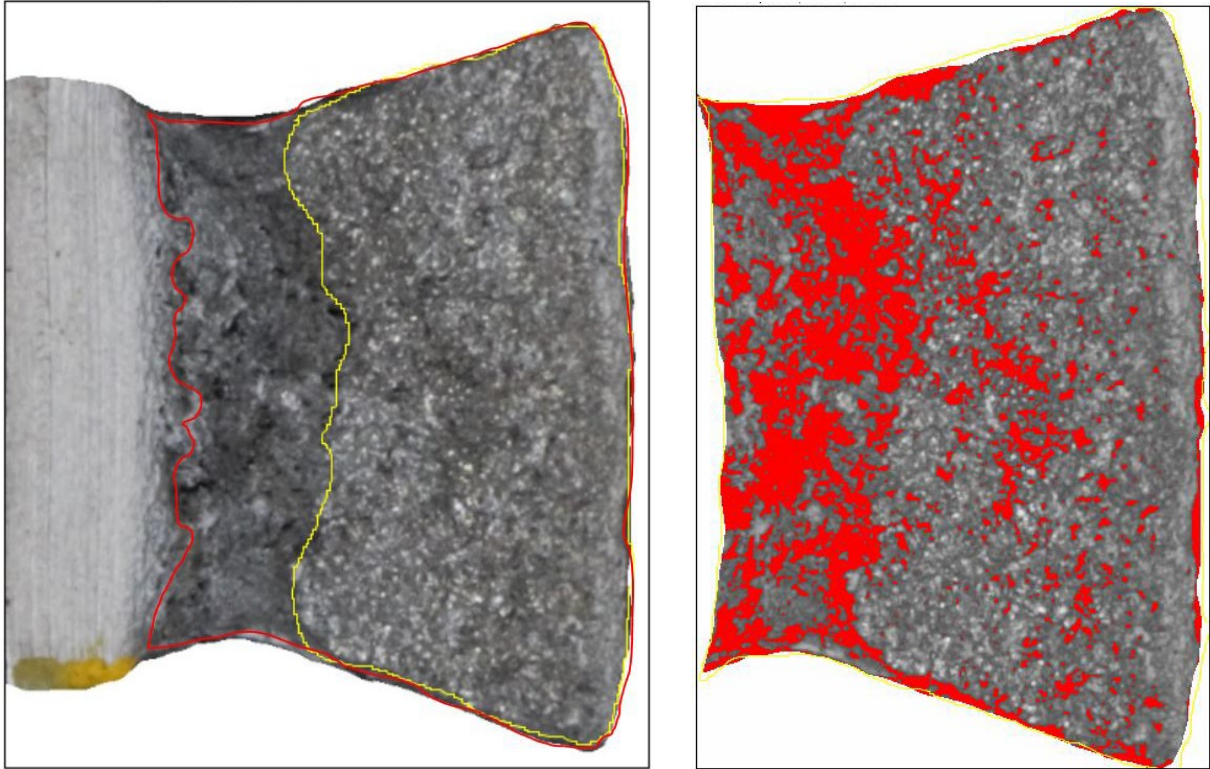


Figure E.30. Shear fracture areas for specimen 1CZ using a Mask Area Method (left) and a Pixel Intensity Method (right).

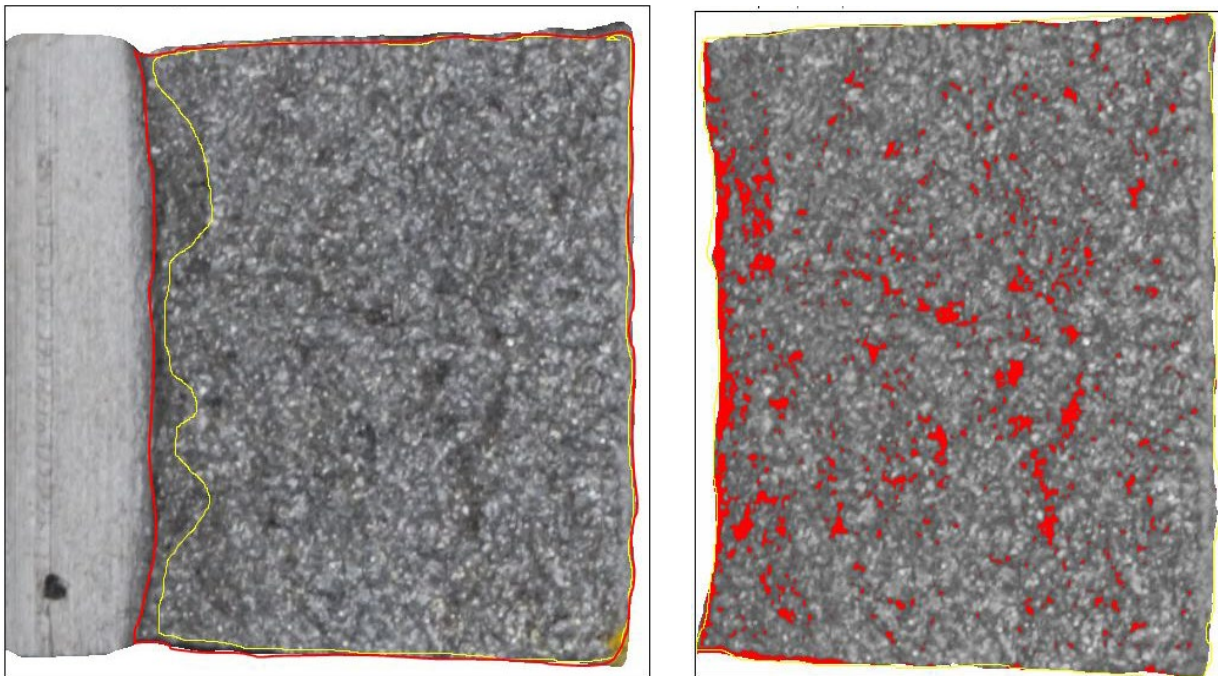


Figure E.31. Shear fracture areas for specimen 1HX using a Mask Area Method (left) and a Pixel Intensity Method (right).

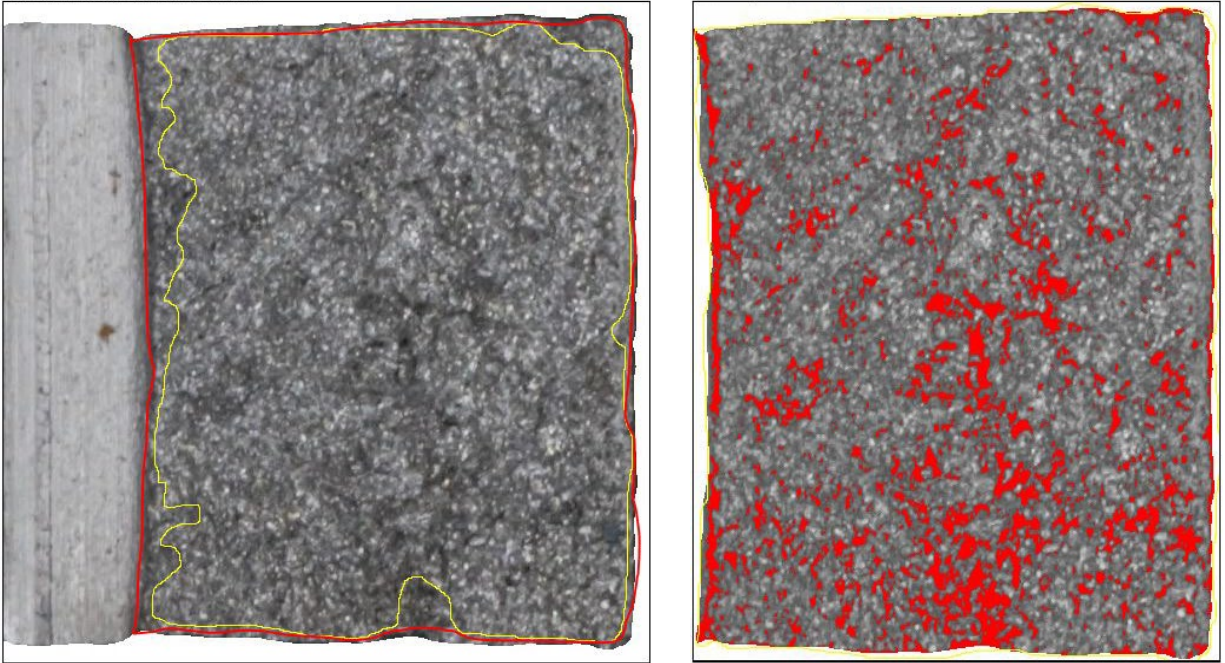


Figure E.32. Shear fracture areas for specimen 1HY using a Mask Area Method (left) and a Pixel Intensity Method (right).

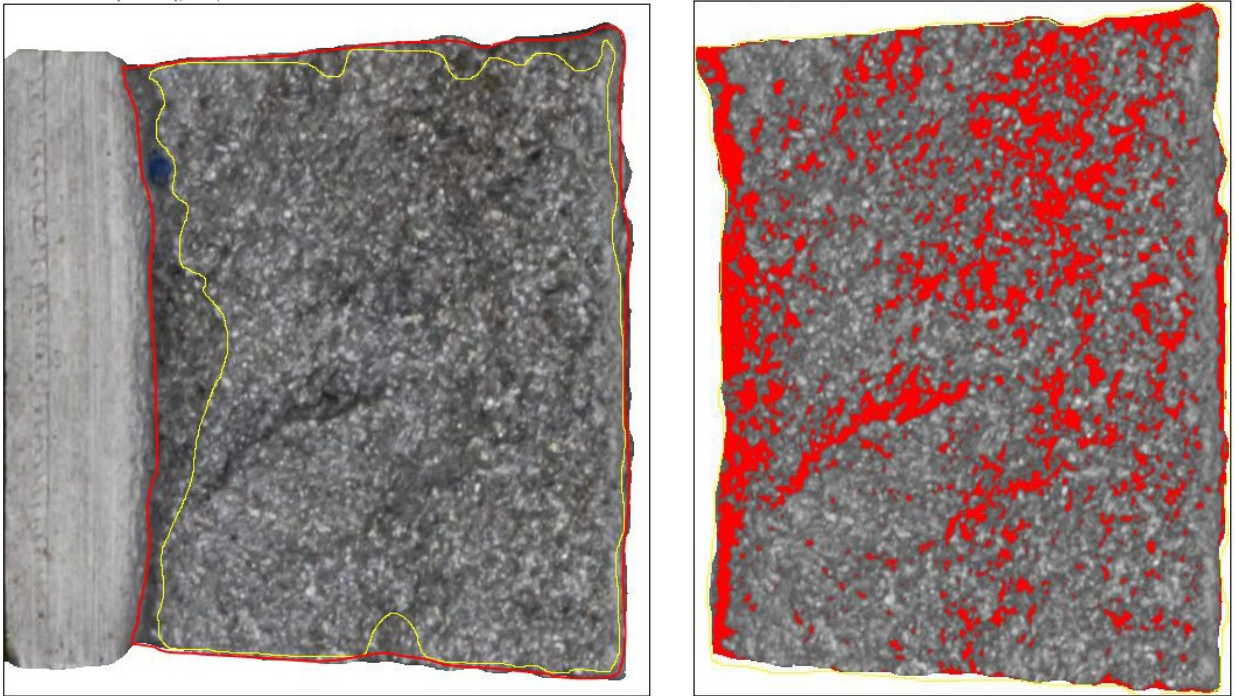


Figure E.33. Shear fracture areas for specimen 1HZ using a Mask Area Method (left) and a Pixel Intensity Method (right).

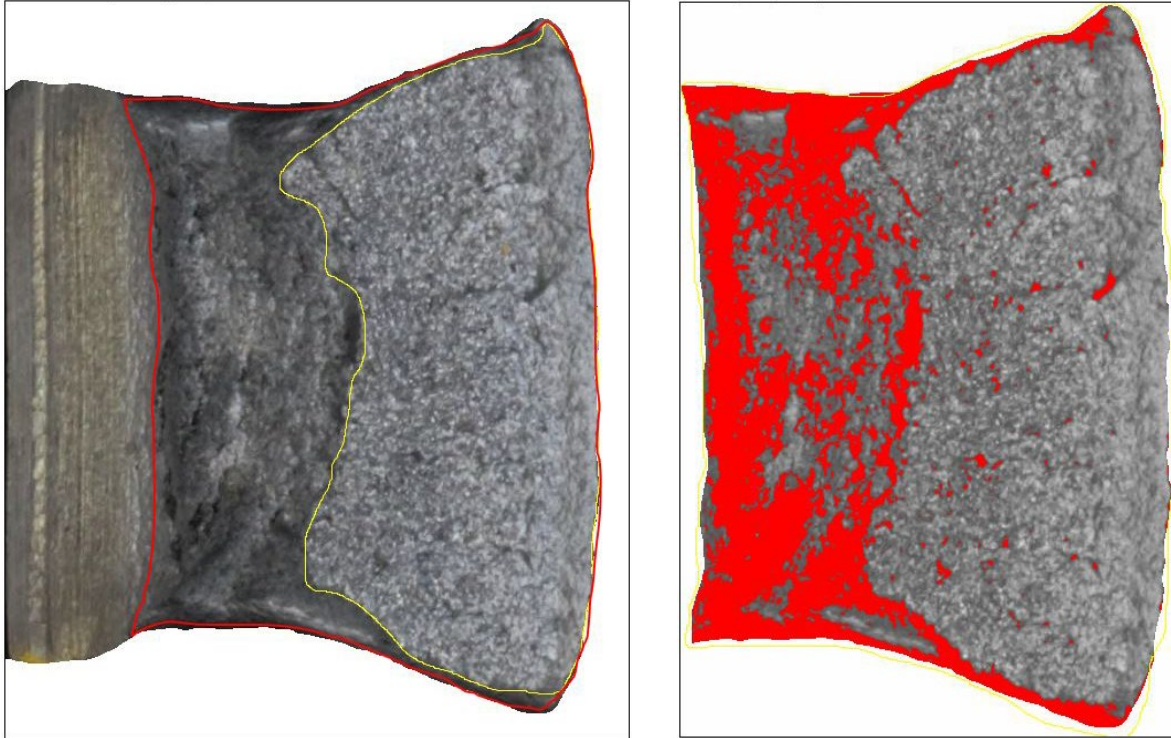


Figure E.34. Shear fracture areas for specimen 1NX using a Mask Area Method (left) and a Pixel Intensity Method (right).

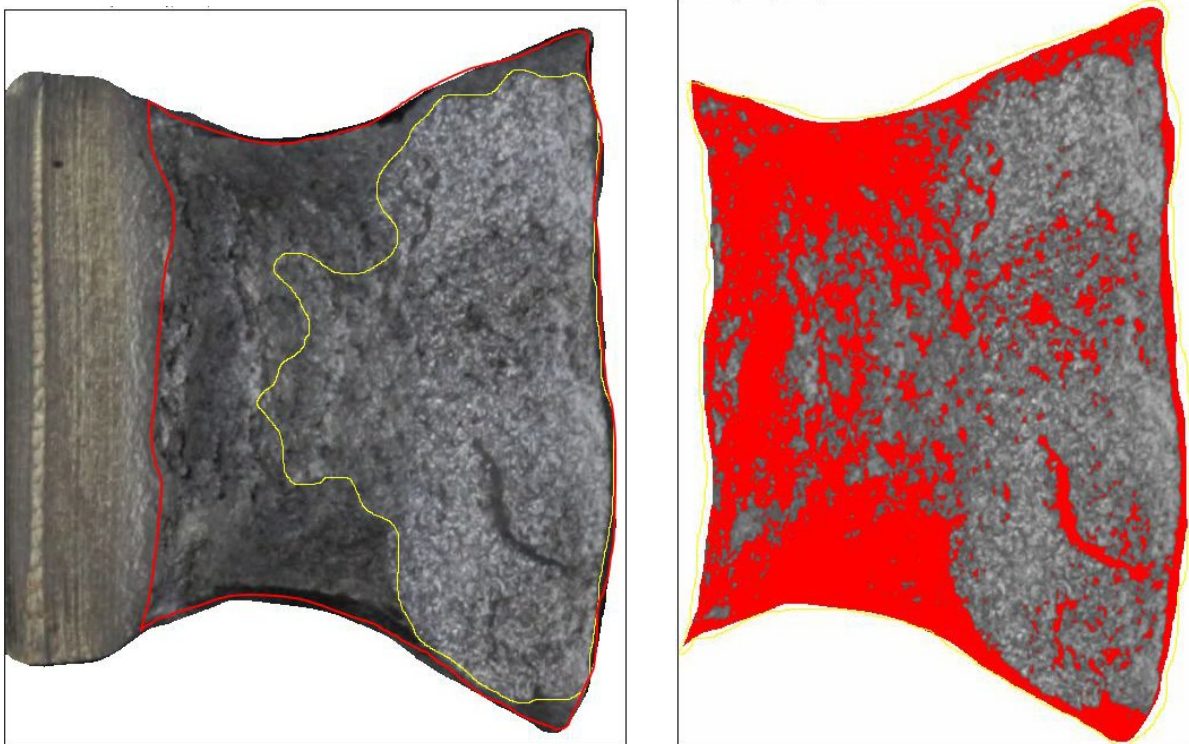


Figure E.35. Shear fracture areas for specimen 1NY using a Mask Area Method (left) and a Pixel Intensity Method (right).

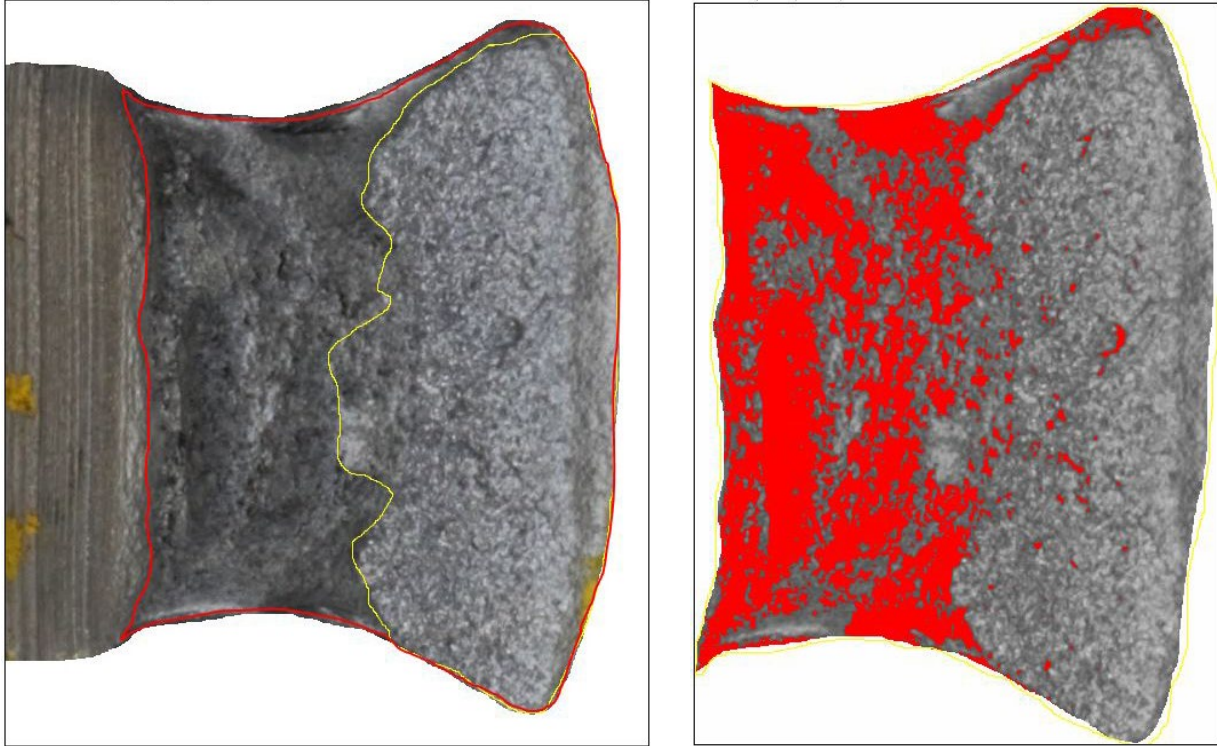


Figure E.36. Shear fracture areas for specimen 1NZ using a Mask Area Method (left) and a Pixel Intensity Method (right).

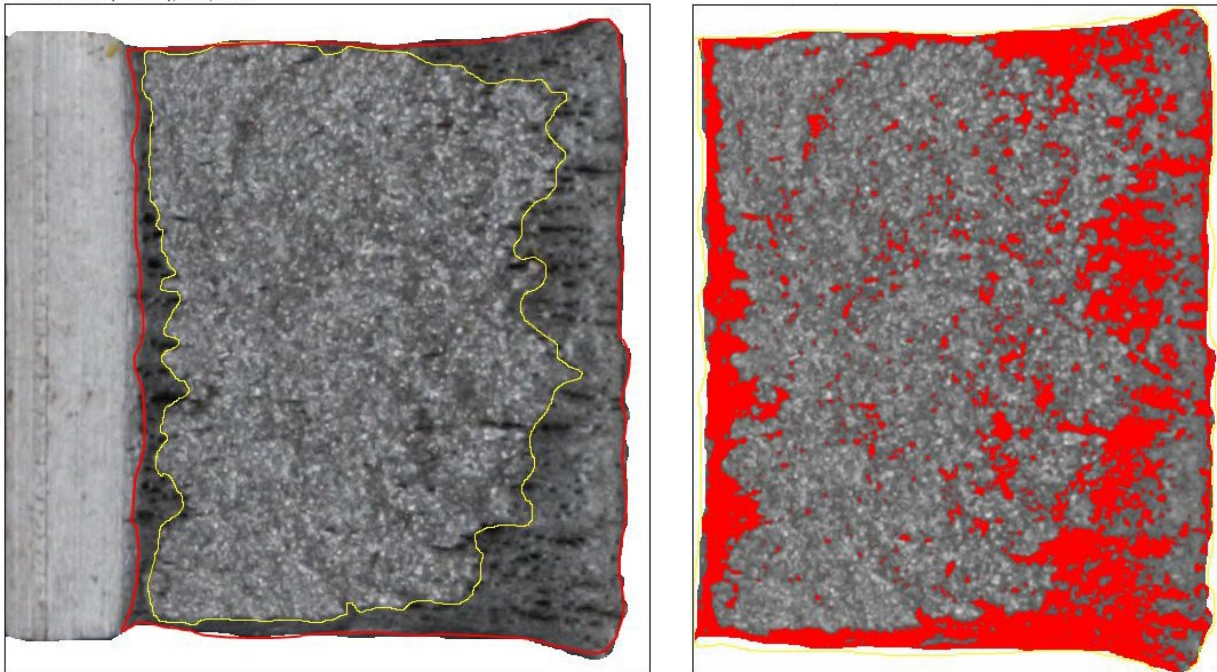


Figure E.37. Shear fracture areas for specimen 1QX using a Mask Area Method (left) and a Pixel Intensity Method (right).

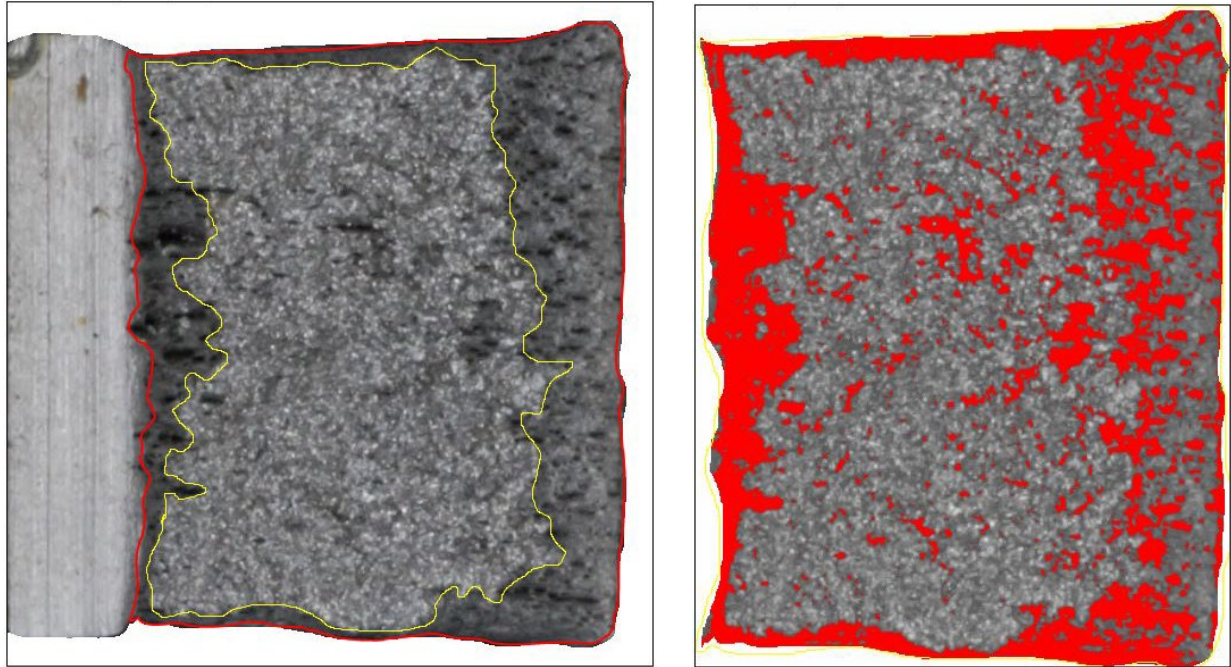


Figure E.38. Shear fracture areas for specimen 1QY using a Mask Area Method (left) and a Pixel Intensity Method (right).

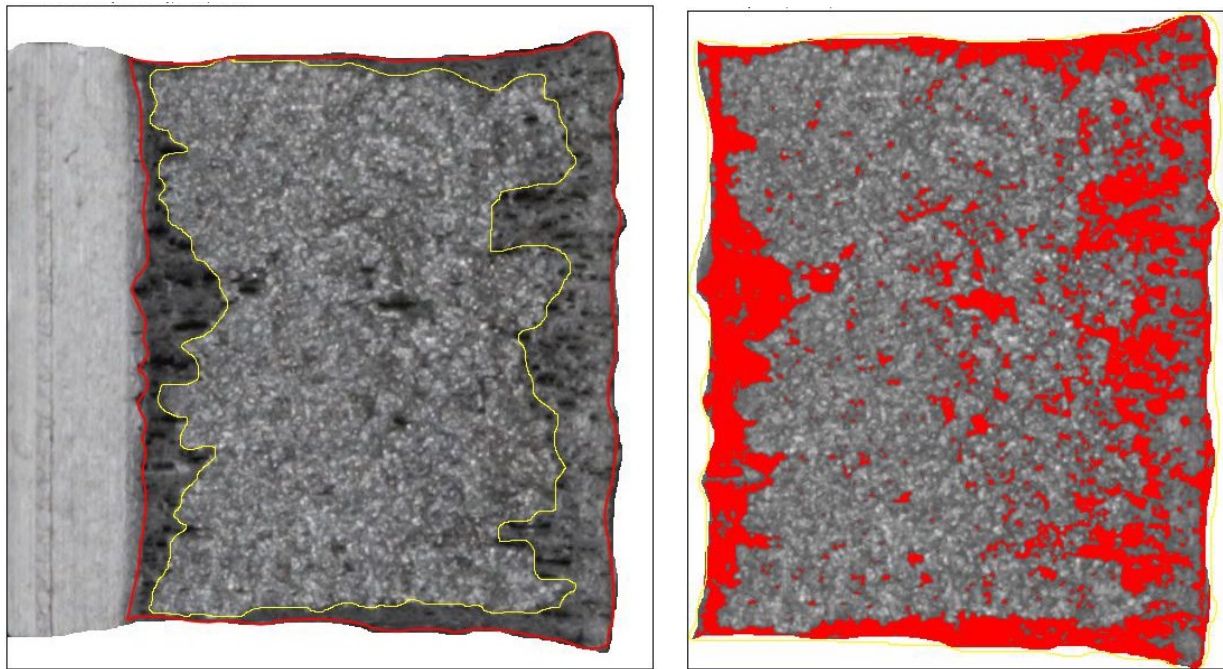


Figure E.39. Shear fracture areas for specimen 1QZ using a Mask Area Method (left) and a Pixel Intensity Method (right).

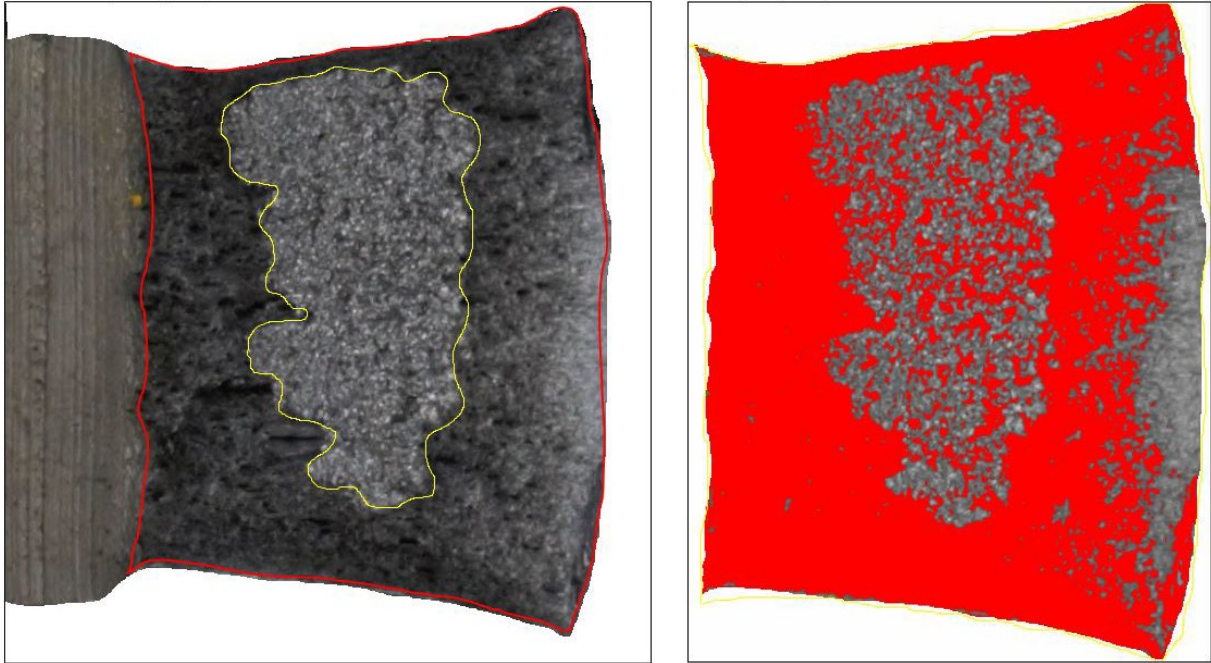


Figure E.40. Shear fracture areas for specimen 1TX using a Mask Area Method (left) and a Pixel Intensity Method (right).

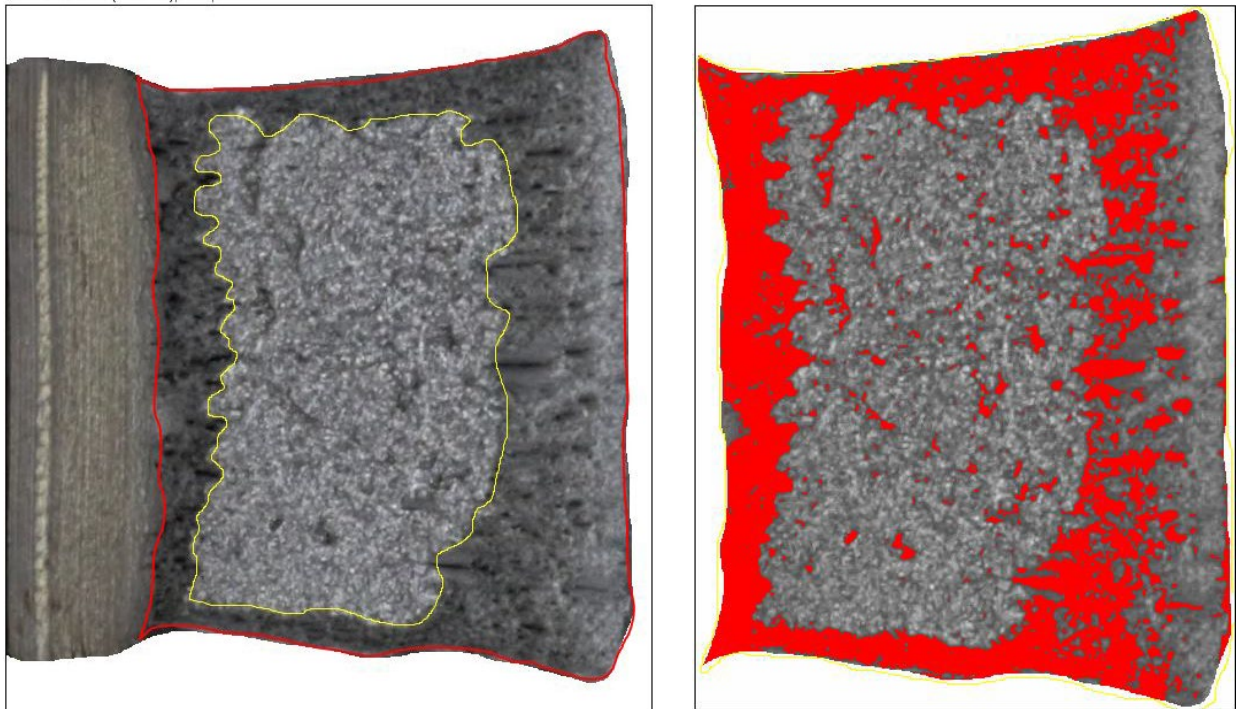


Figure E.41. Shear fracture areas for specimen 1TY using a Mask Area Method (left) and a Pixel Intensity Method (right).

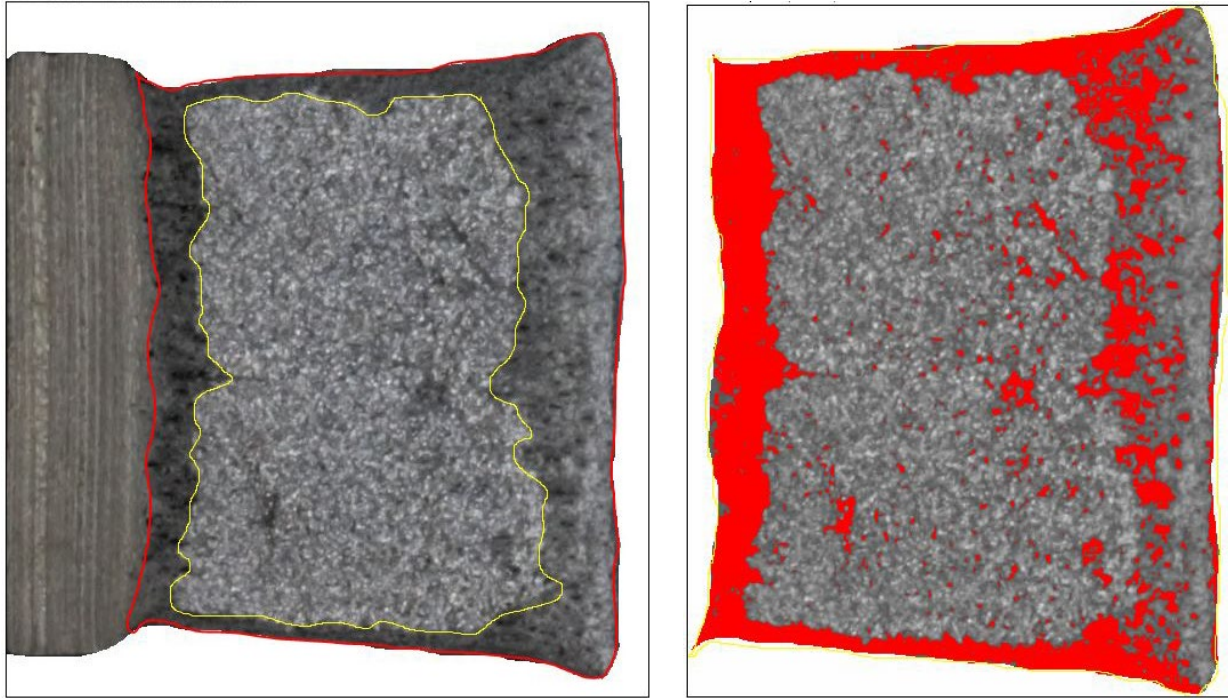


Figure E.42. Shear fracture areas for specimen 1TZ using a Mask Area Method (left) and a Pixel Intensity Method (right).

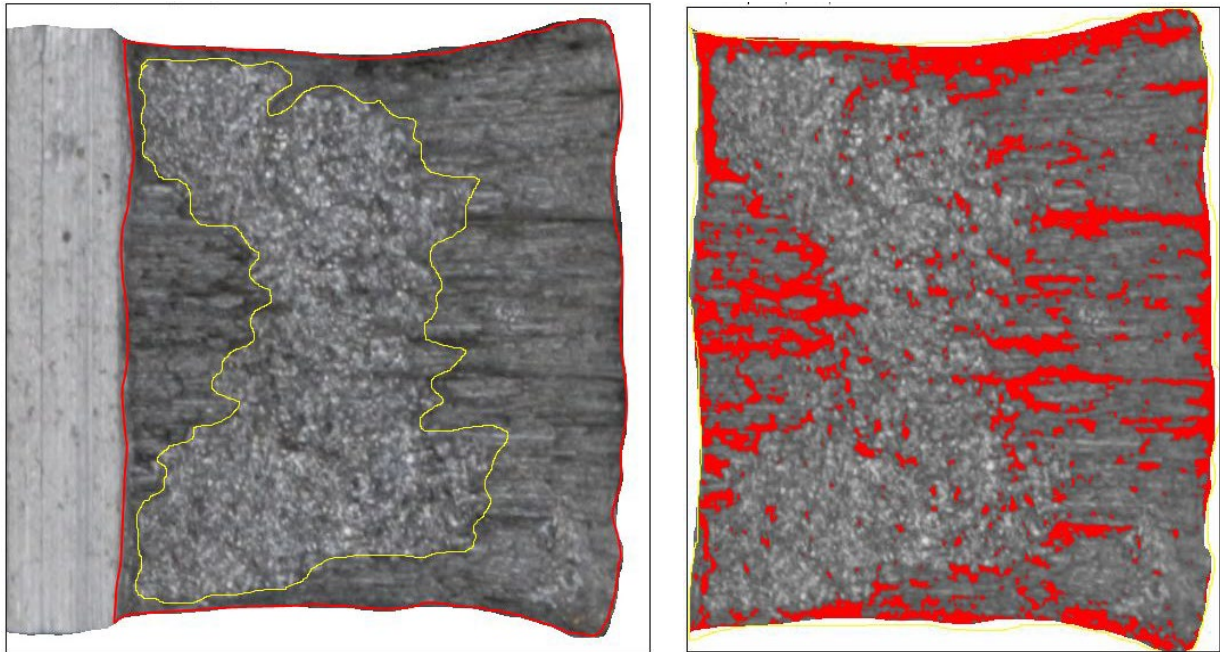


Figure E.43. Shear fracture areas for specimen 1VX using a Mask Area Method (left) and a Pixel Intensity Method (right).

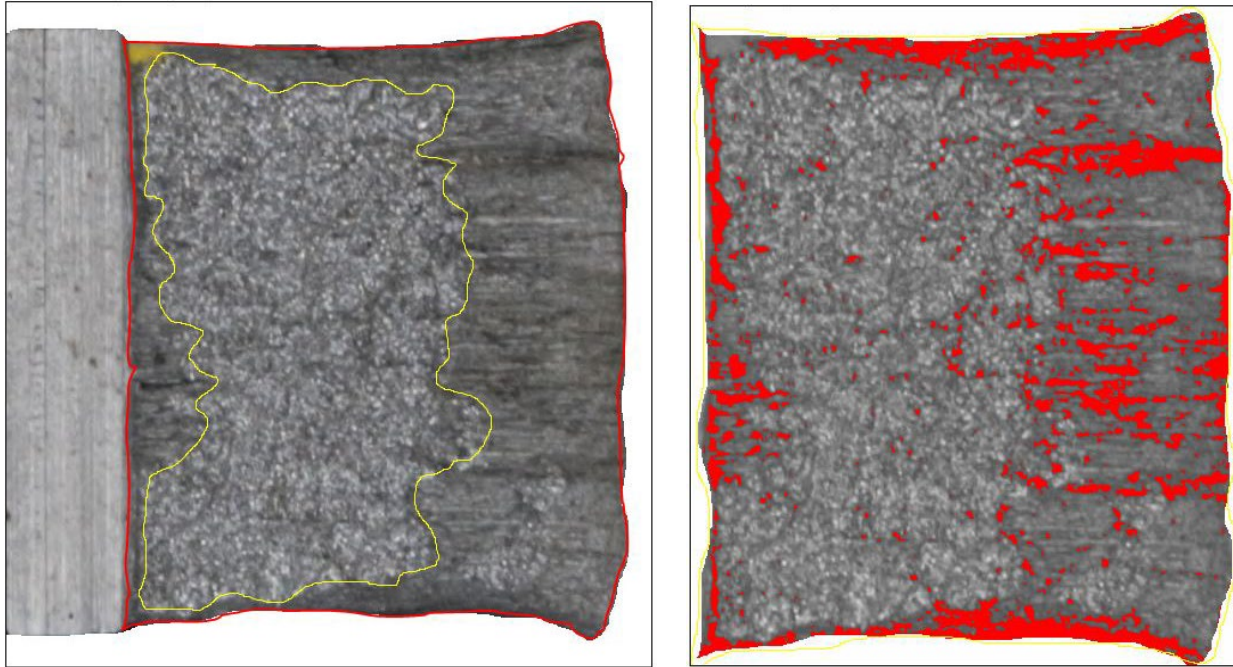


Figure E.44. Shear fracture areas for specimen 1VY using a Mask Area Method (left) and a Pixel Intensity Method (right).

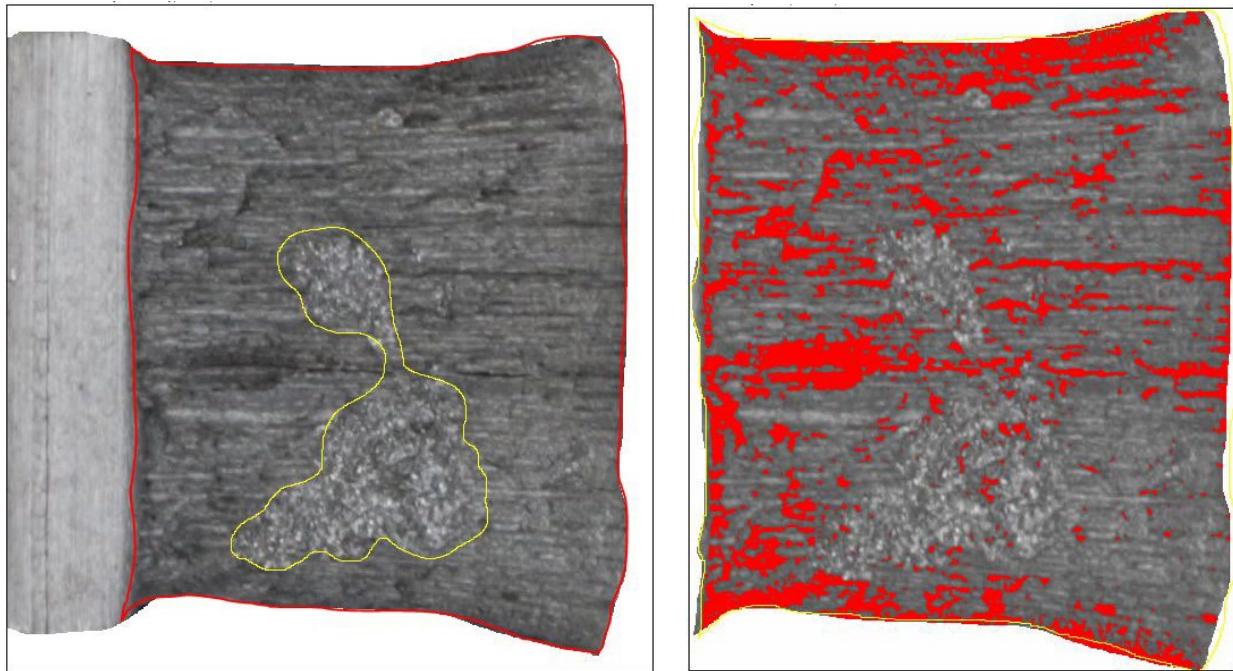


Figure E.45. Shear fracture areas for specimen 1VZ using a Mask Area Method (left) and a Pixel Intensity Method (right).

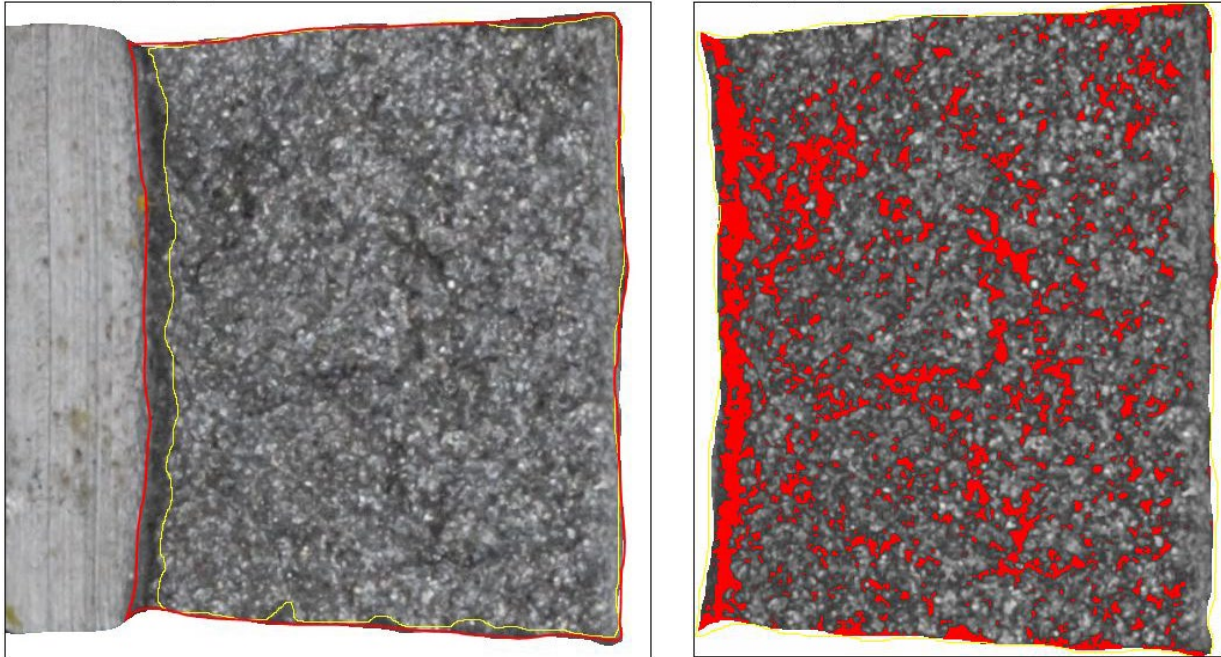


Figure E.46. Shear fracture areas for specimen 2AX using a Mask Area Method (left) and a Pixel Intensity Method (right).

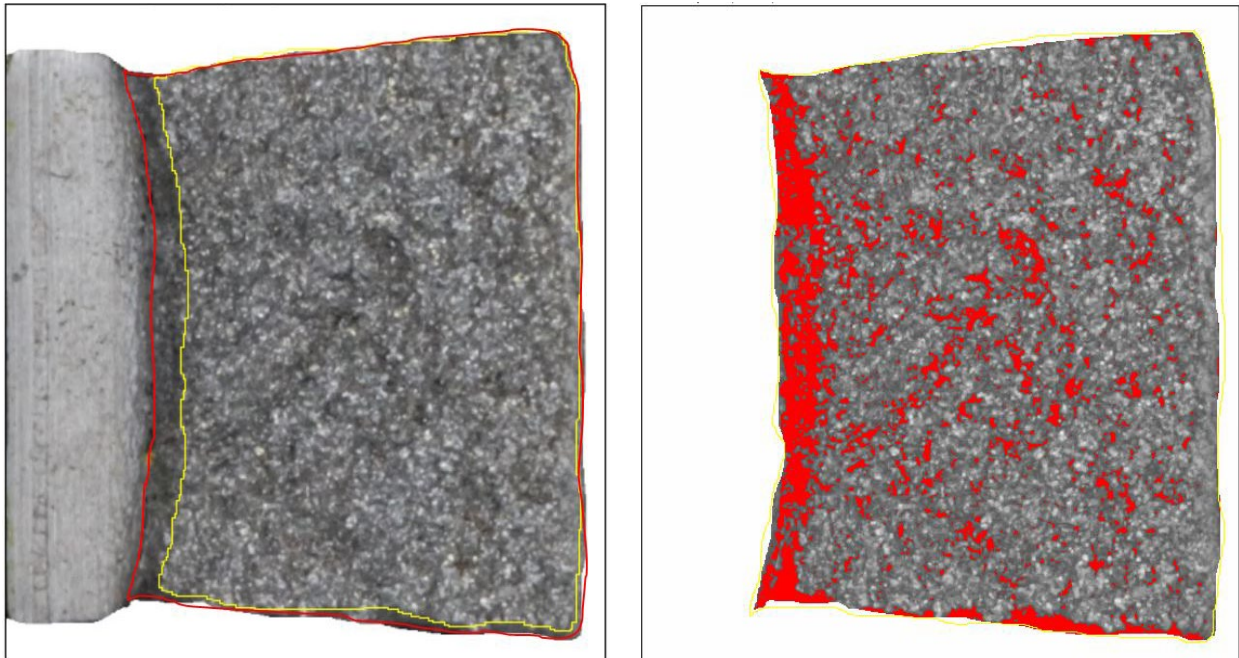


Figure E.47. Shear fracture areas for specimen 2AY using a Mask Area Method (left) and a Pixel Intensity Method (right).

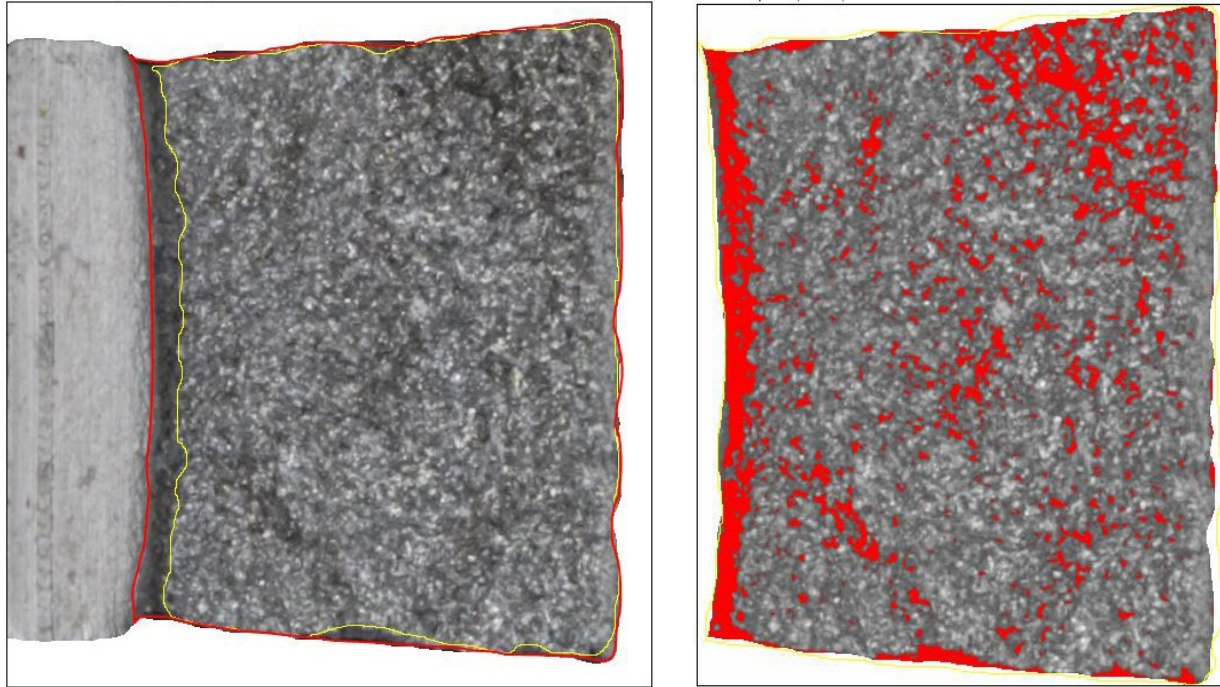


Figure E.48. Shear fracture areas for specimen 2AZ using a Mask Area Method (left) and a Pixel Intensity Method (right).

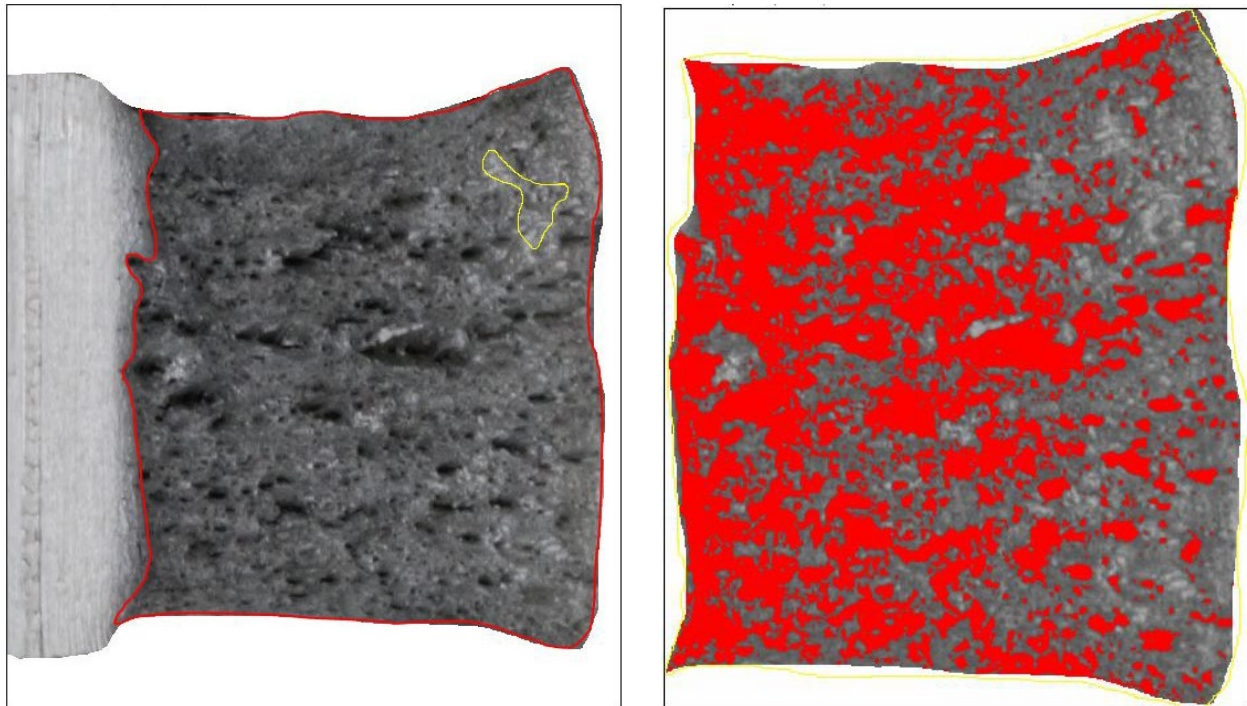


Figure E.49. Shear fracture areas for specimen 2BX using a Mask Area Method (left) and a Pixel Intensity Method (right).

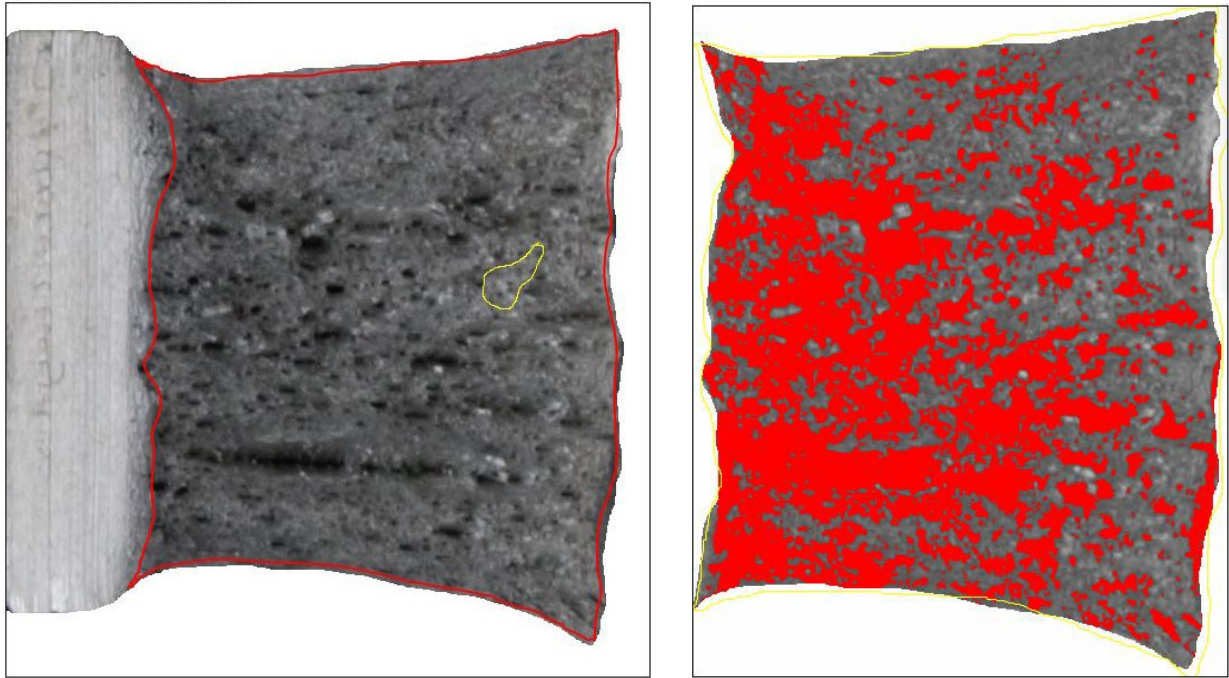


Figure E.50. Shear fracture areas for specimen 2BY using a Mask Area Method (left) and a Pixel Intensity Method (right).

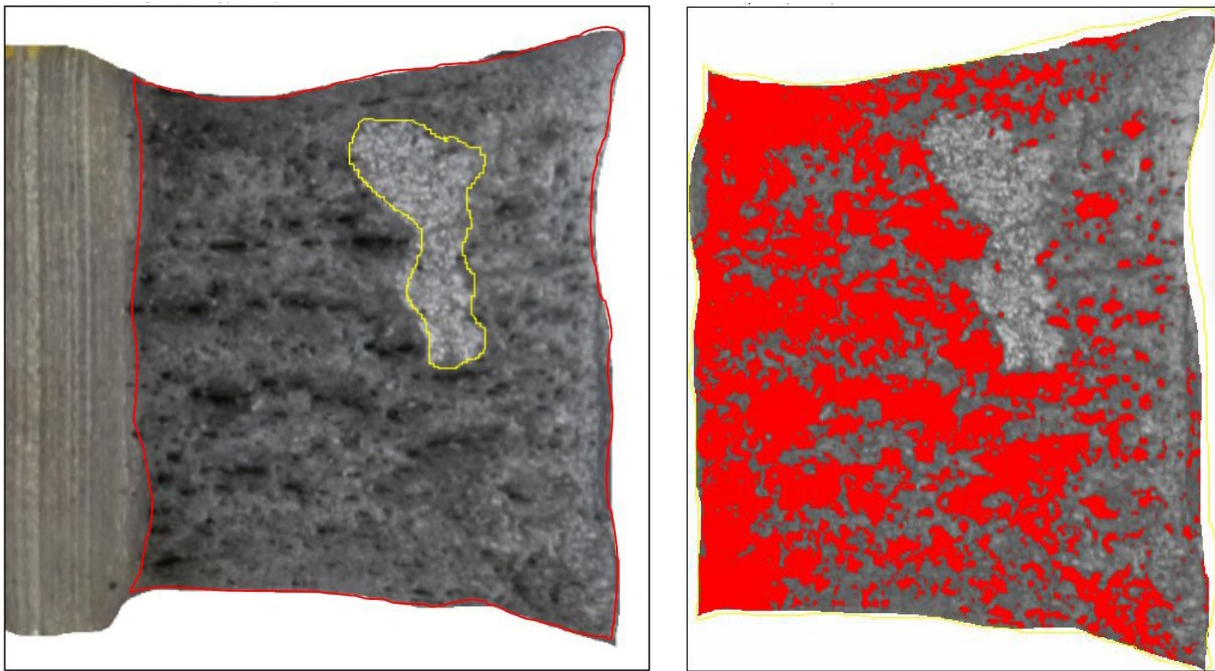


Figure E.51. Shear fracture areas for specimen 2BZ using a Mask Area Method (left) and a Pixel Intensity Method (right).

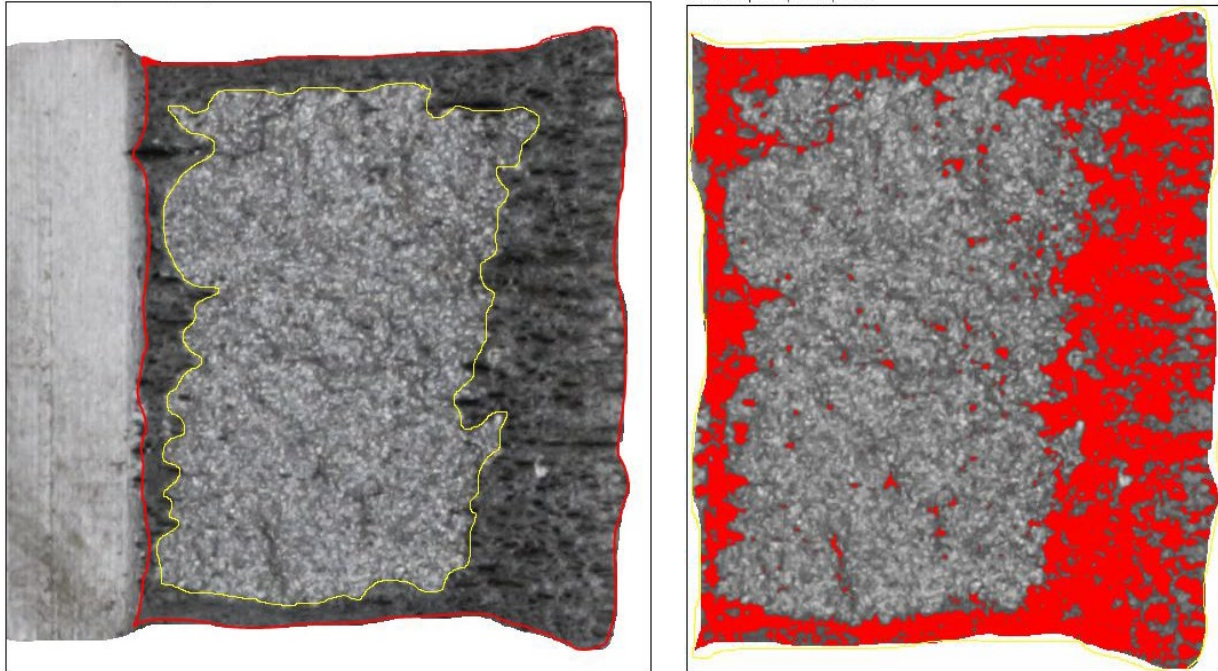


Figure E.52. Shear fracture areas for specimen 2QX using a Mask Area Method (left) and a Pixel Intensity Method (right).

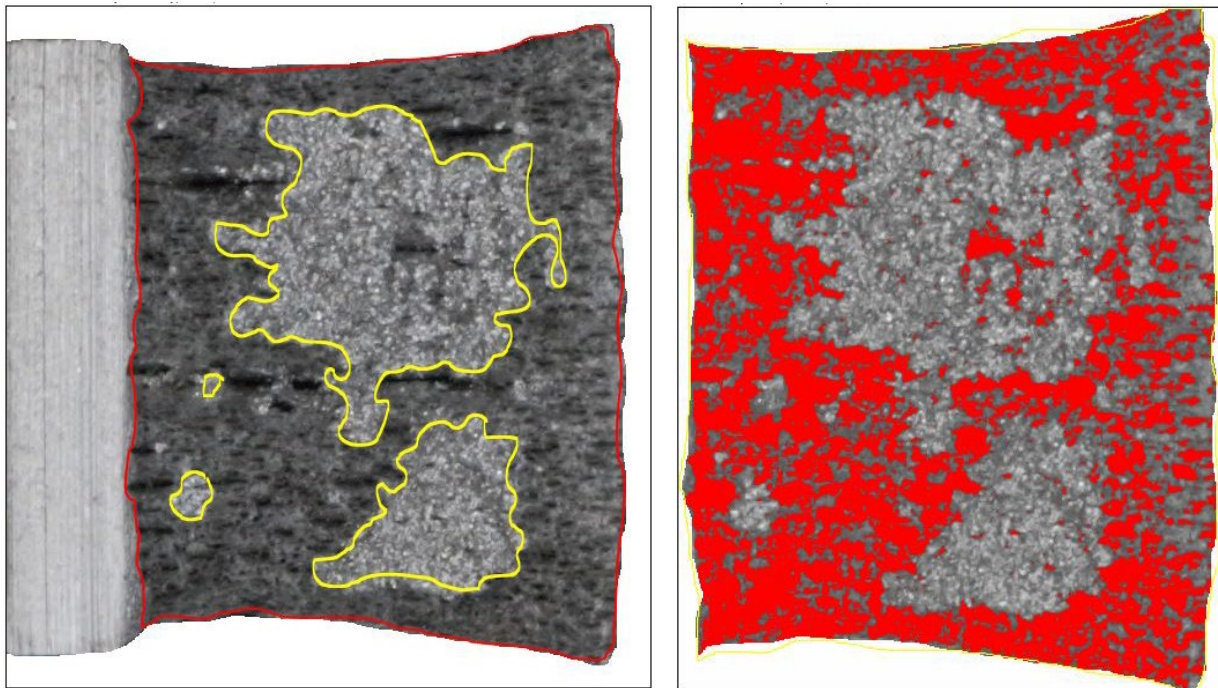


Figure E.53. Shear fracture areas for specimen 2QY using a Mask Area Method (left) and a Pixel Intensity Method (right).

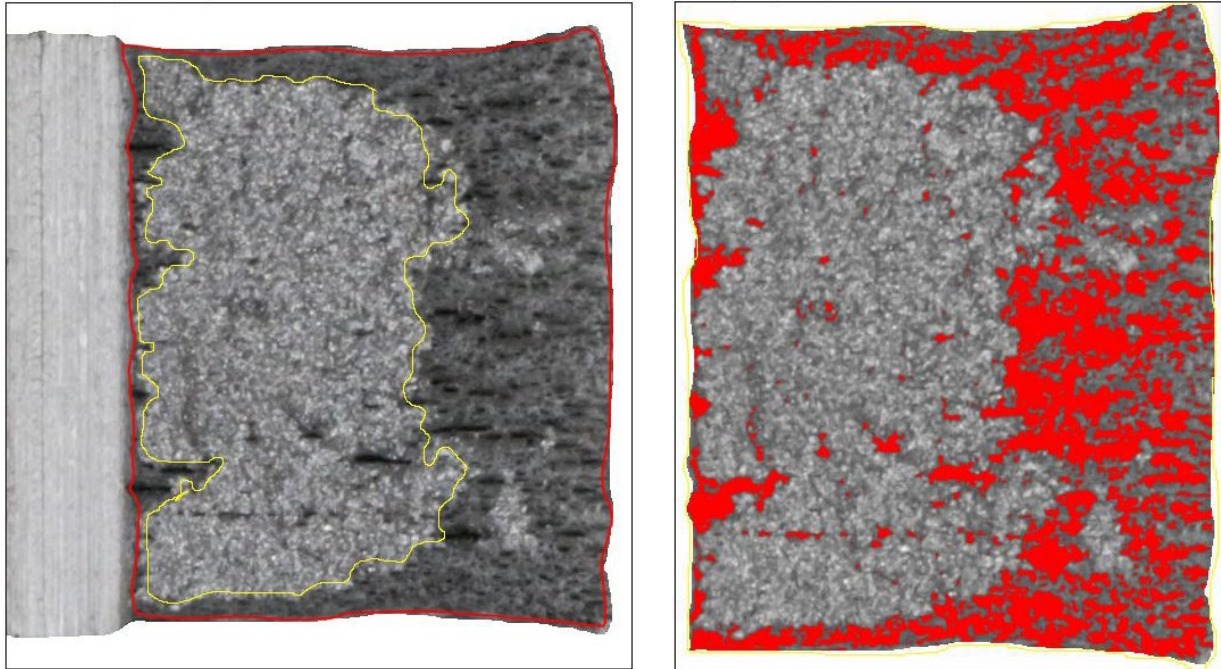


Figure E.54. Shear fracture areas for specimen 2QZ using a Mask Area Method (left) and a Pixel Intensity Method (right).

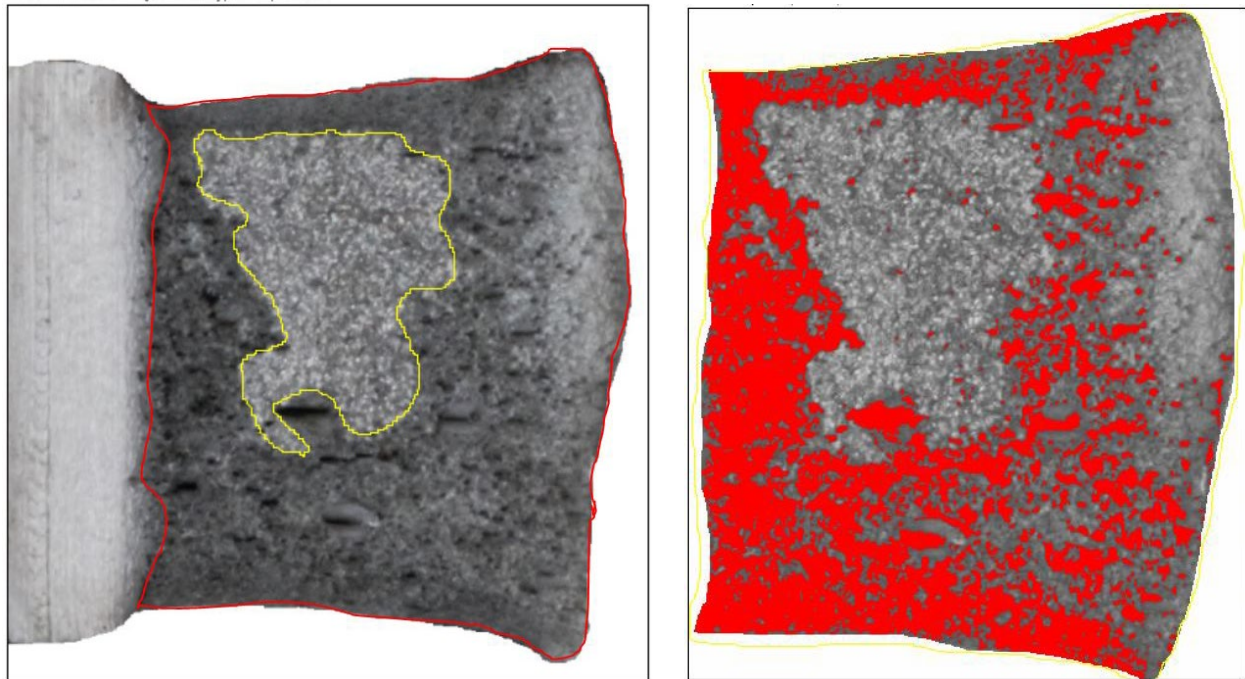


Figure E.55. Shear fracture areas for specimen 2TX using a Mask Area Method (left) and a Pixel Intensity Method (right).

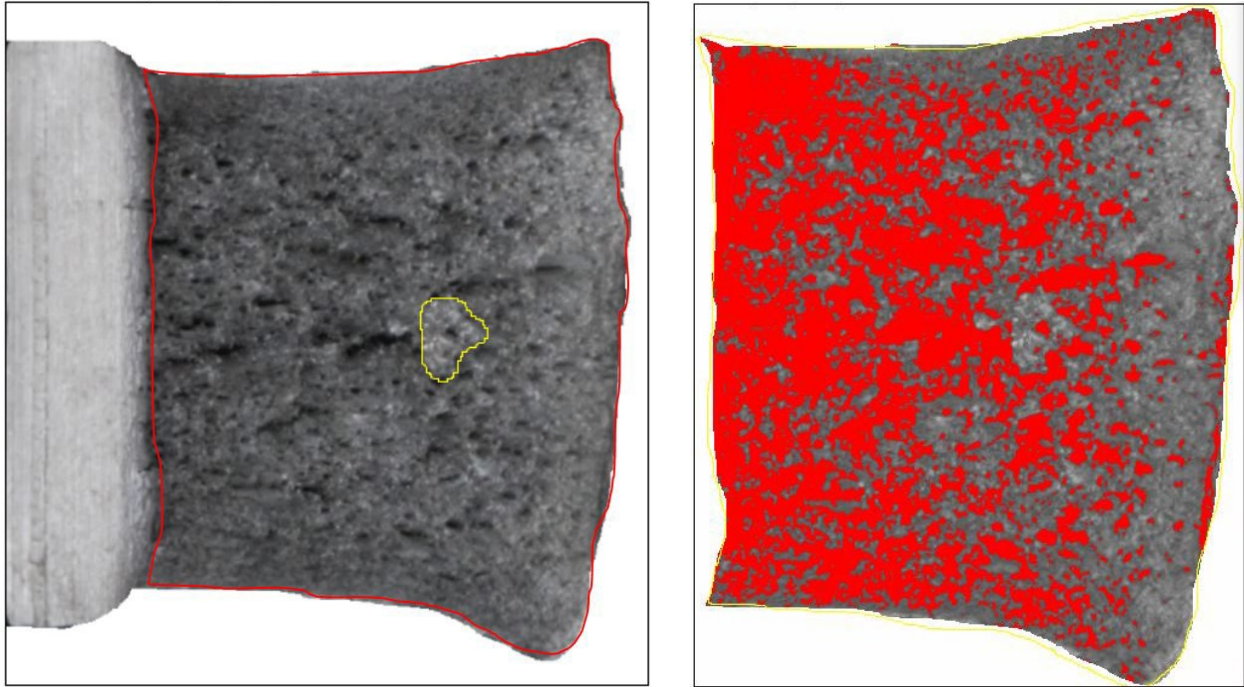


Figure E.56. Shear fracture areas for specimen 2TY using a Mask Area Method (left) and a Pixel Intensity Method (right).

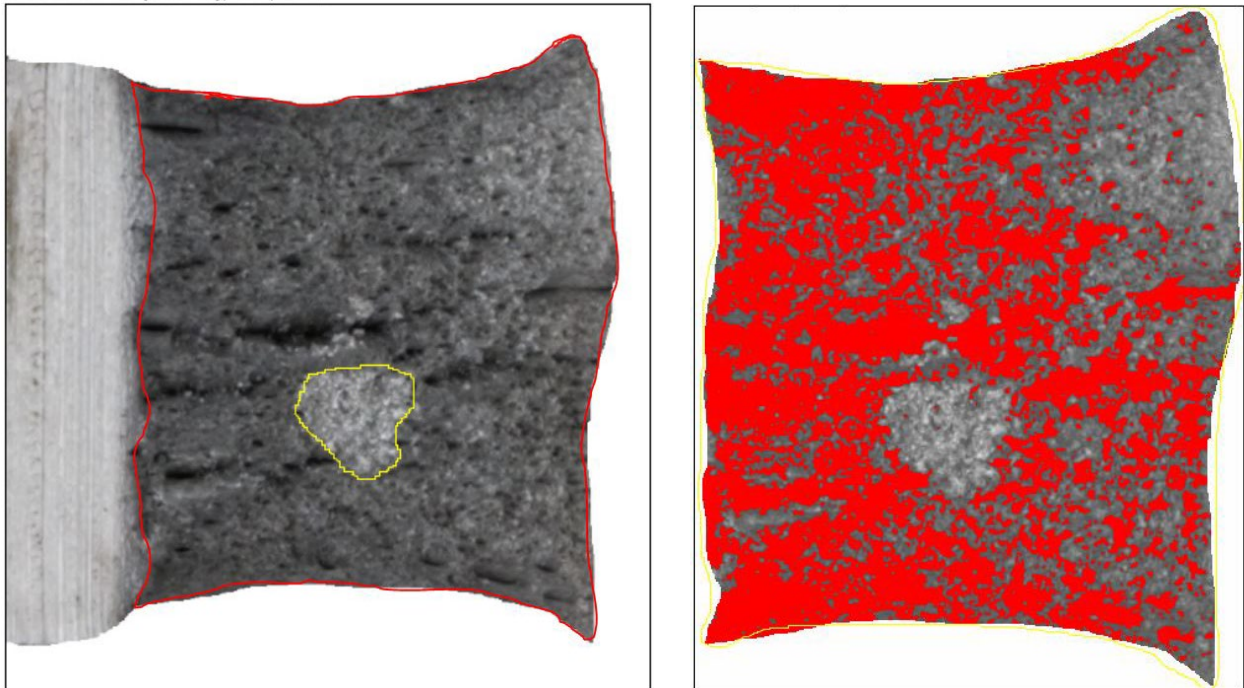


Figure E.57. Shear fracture areas for specimen 2TZ using a Mask Area Method (left) and a Pixel Intensity Method (right).

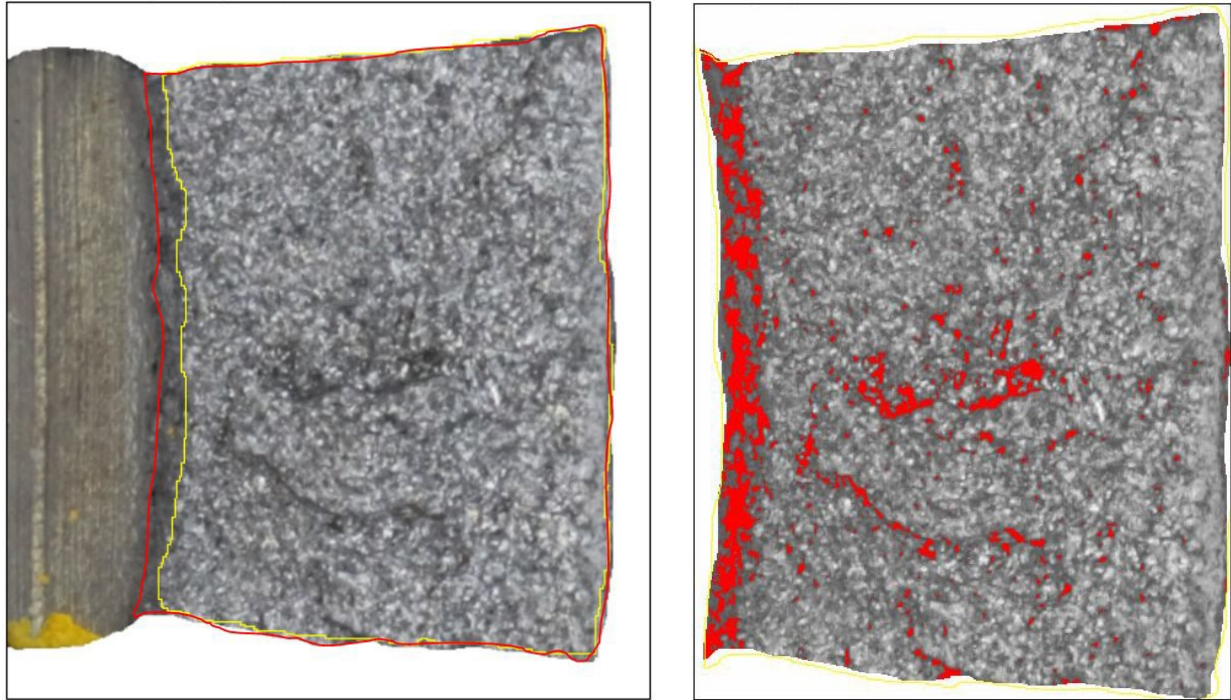


Figure E.58. Shear fracture areas for specimen 3AX using a Mask Area Method (left) and a Pixel Intensity Method (right).

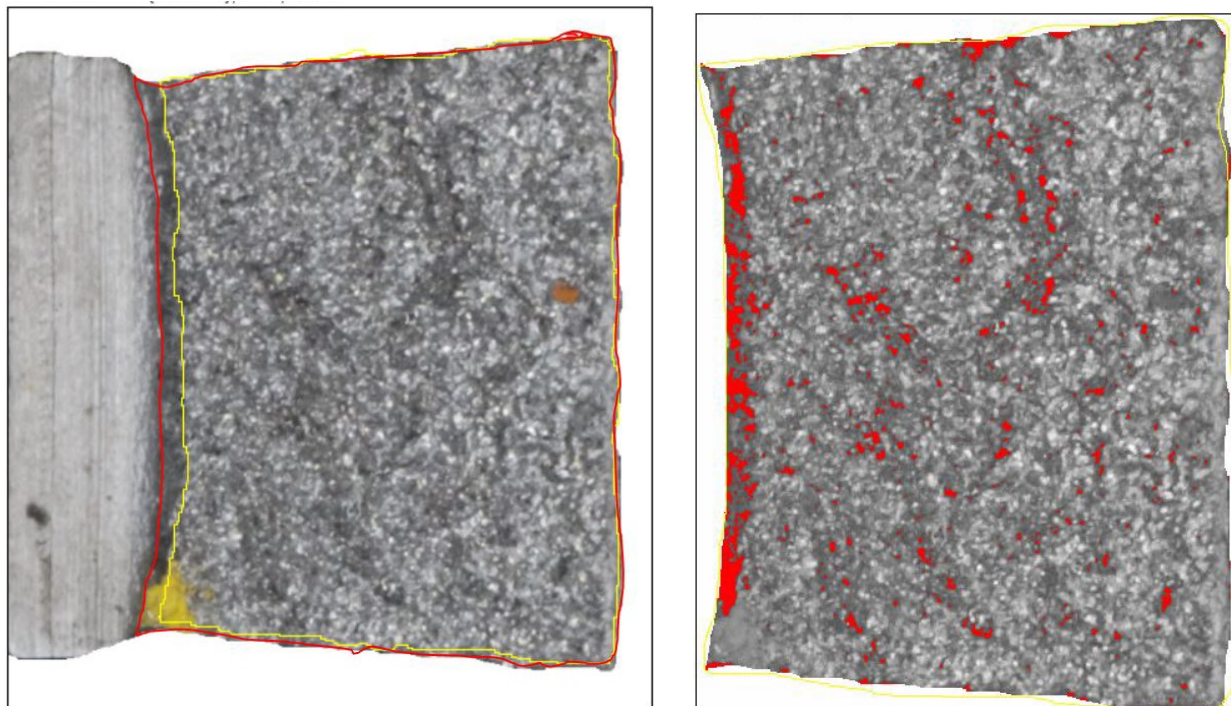


Figure E.59. Shear fracture areas for specimen 3AY using a Mask Area Method (left) and a Pixel Intensity Method (right).

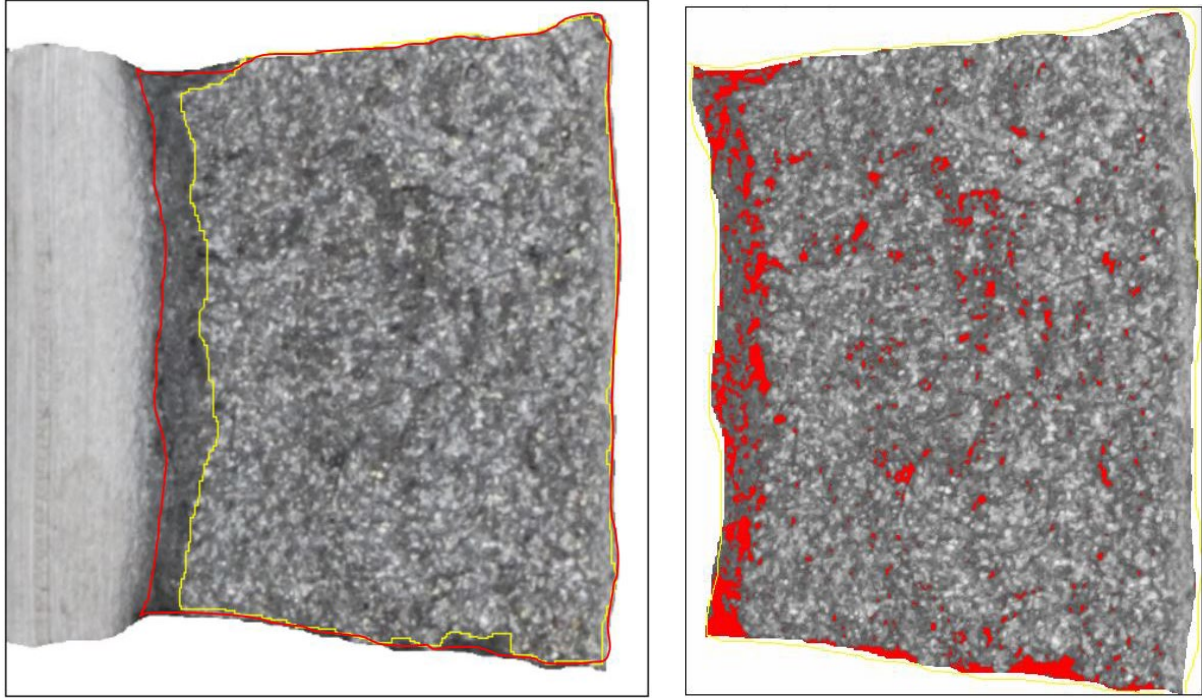


Figure E.60. Shear fracture areas for specimen 3AZ using a Mask Area Method (left) and a Pixel Intensity Method (right).

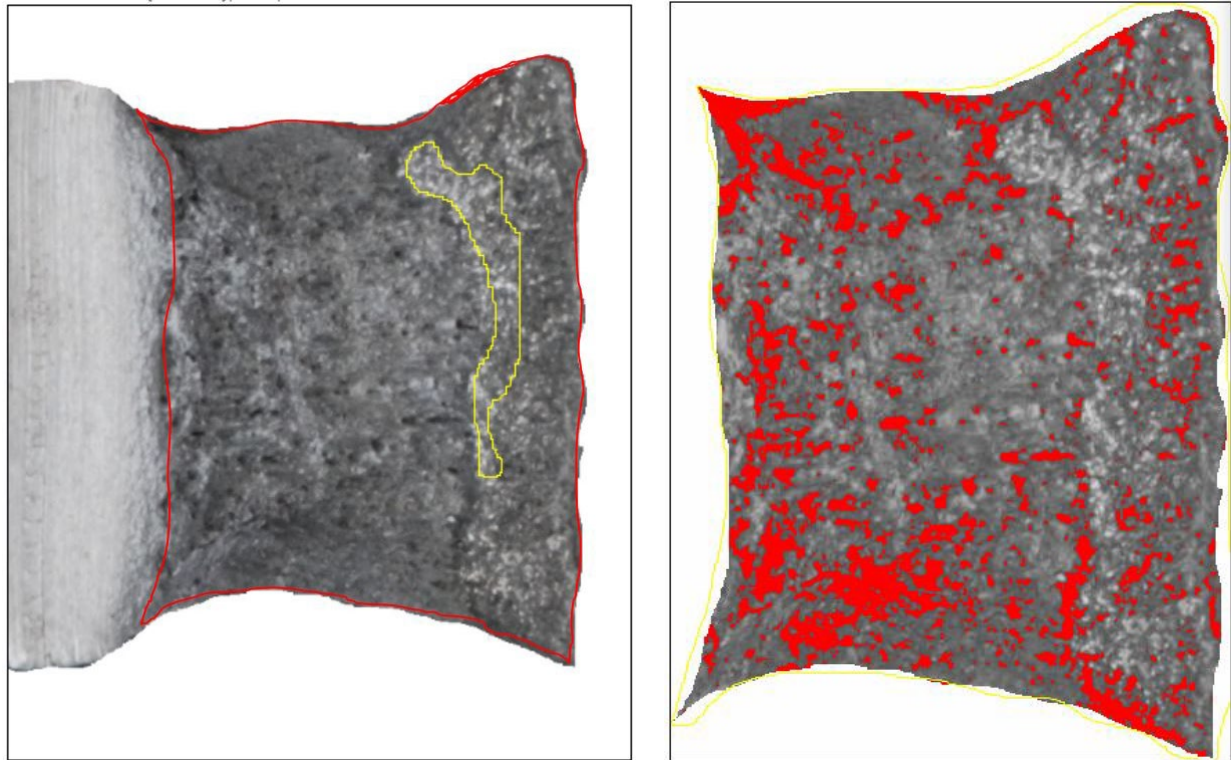


Figure E.61. Shear fracture areas for specimen 3BX using a Mask Area Method (left) and a Pixel Intensity Method (right).

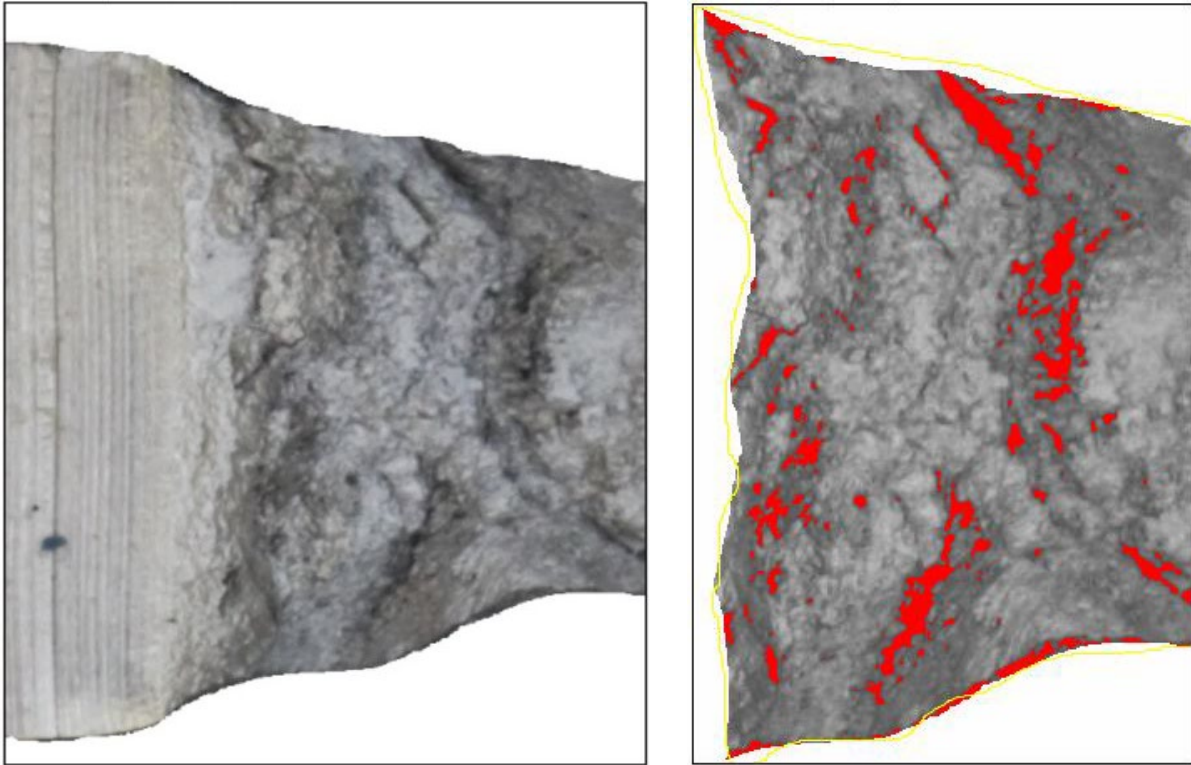


Figure E.62. Shear fracture areas for specimen 3BY using a Mask Area Method (left) and a Pixel Intensity Method (right). Note this specimen did not separate in two pieces.

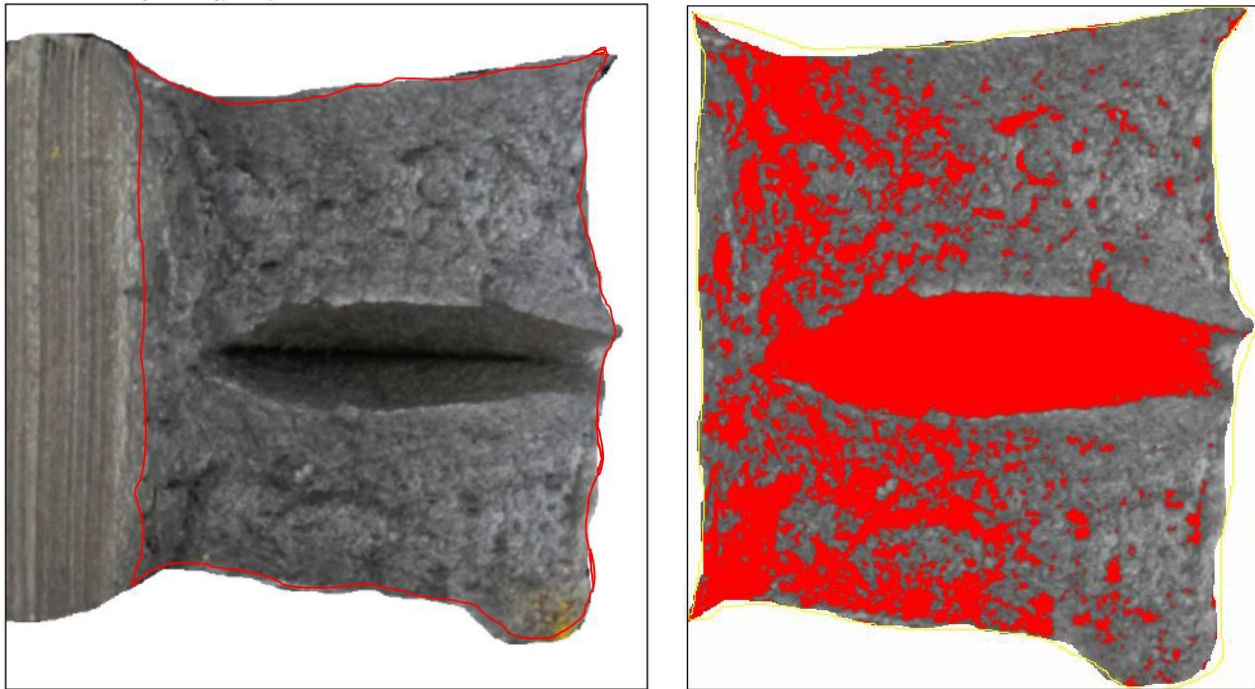


Figure E.63. Shear fracture areas for specimen 3BZ using a Mask Area Method (left) and a Pixel Intensity Method (right).

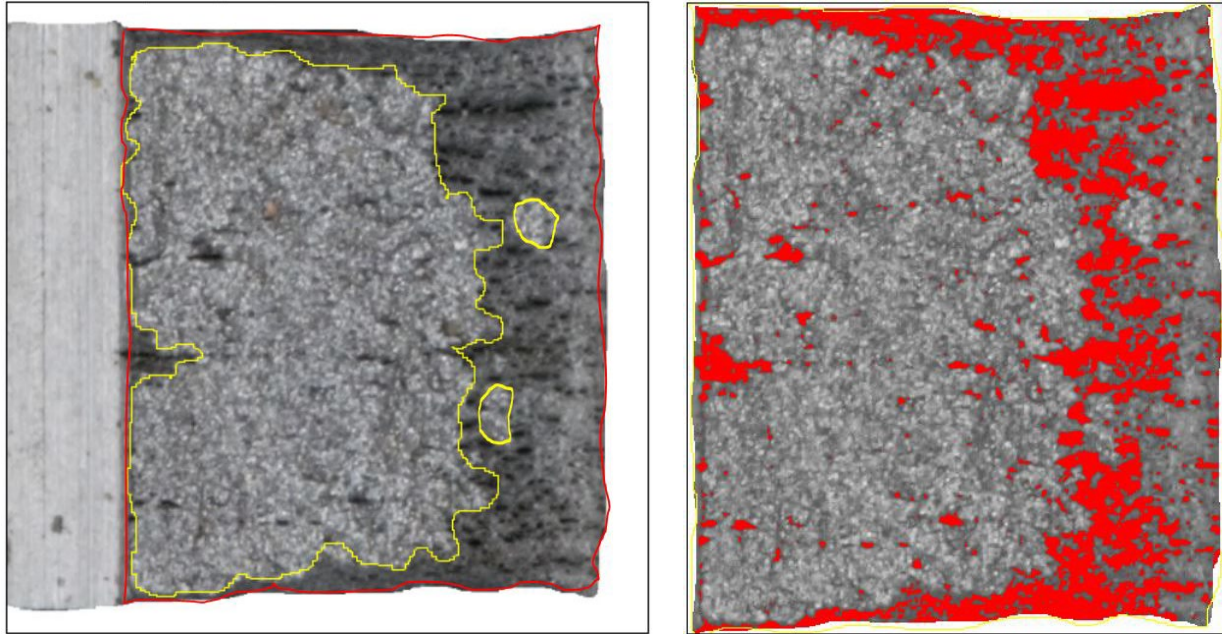


Figure E.64. Shear fracture areas for specimen 3QX using a Mask Area Method (left) and a Pixel Intensity Method (right).

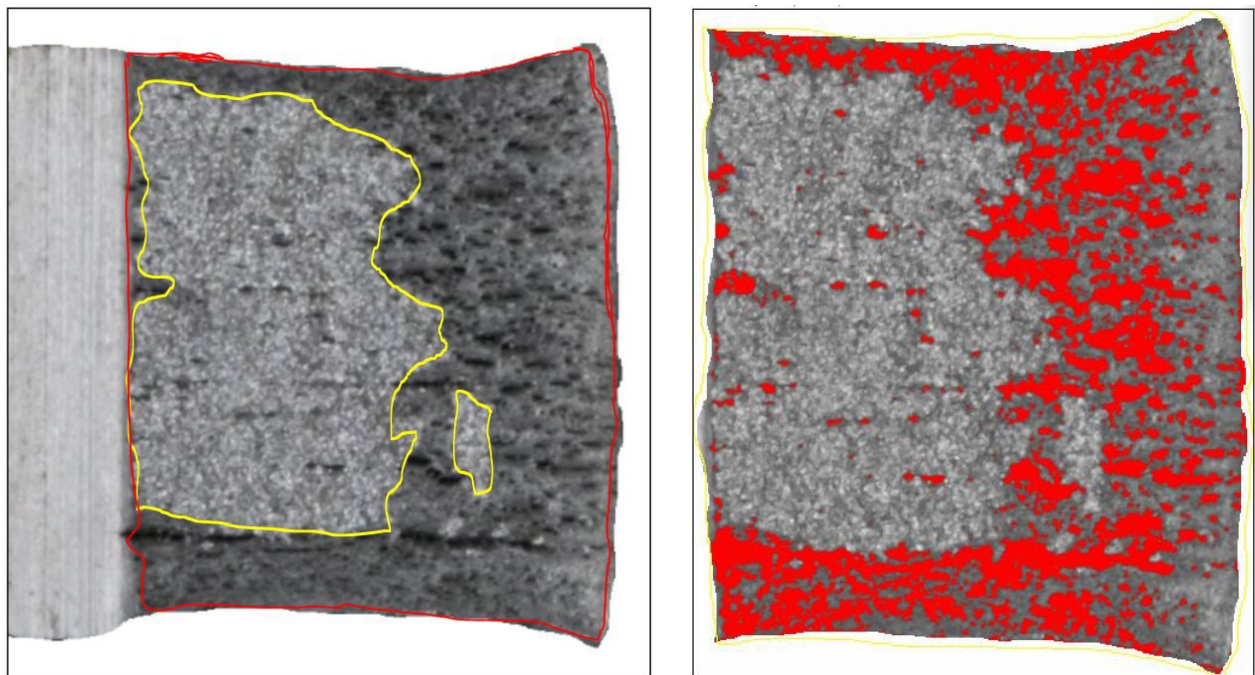


Figure E.65. Shear fracture areas for specimen 3QY using a Mask Area Method (left) and a Pixel Intensity Method (right).

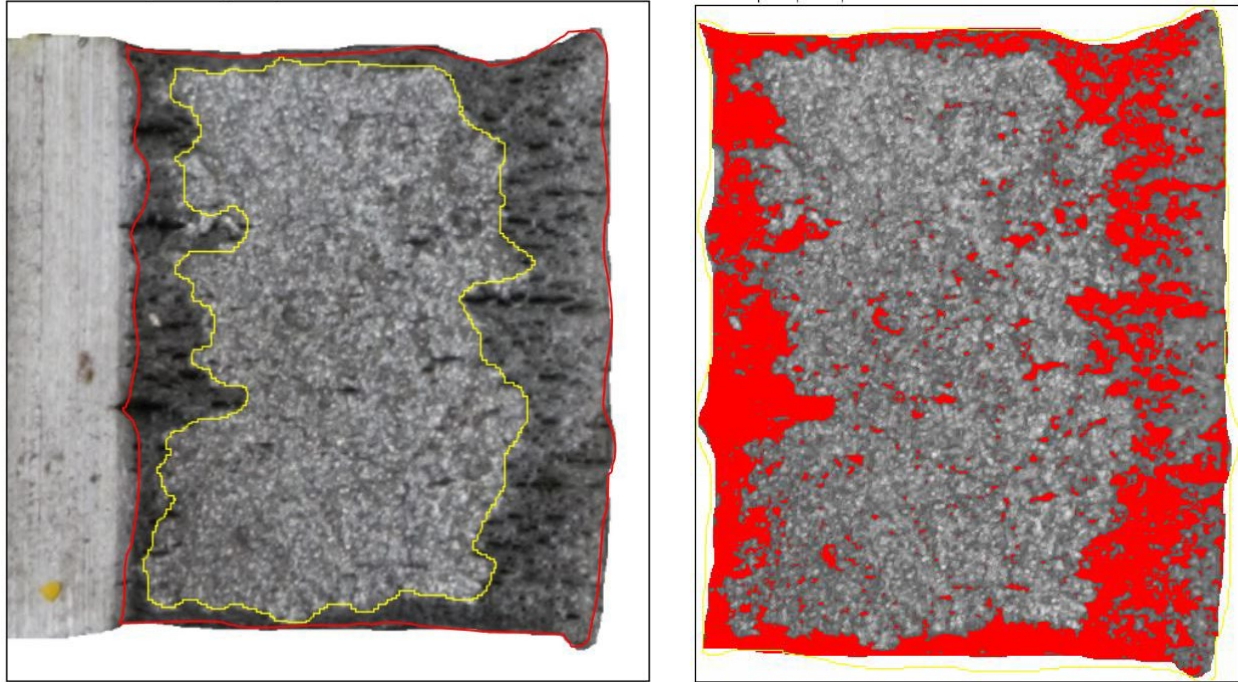


Figure E.66. Shear fracture areas for specimen 3QZ using a Mask Area Method (left) and a Pixel Intensity Method (right).

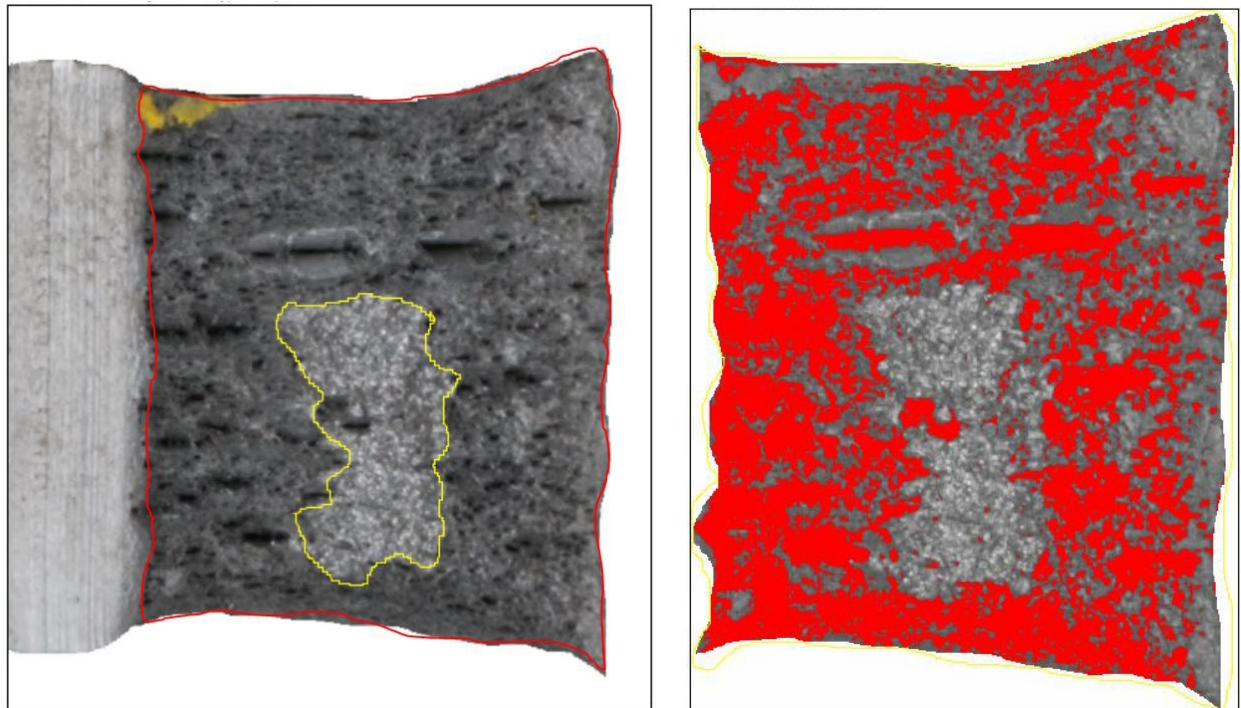


Figure E.67. Shear fracture areas for specimen 3TX using a Mask Area Method (left) and a Pixel Intensity Method (right).

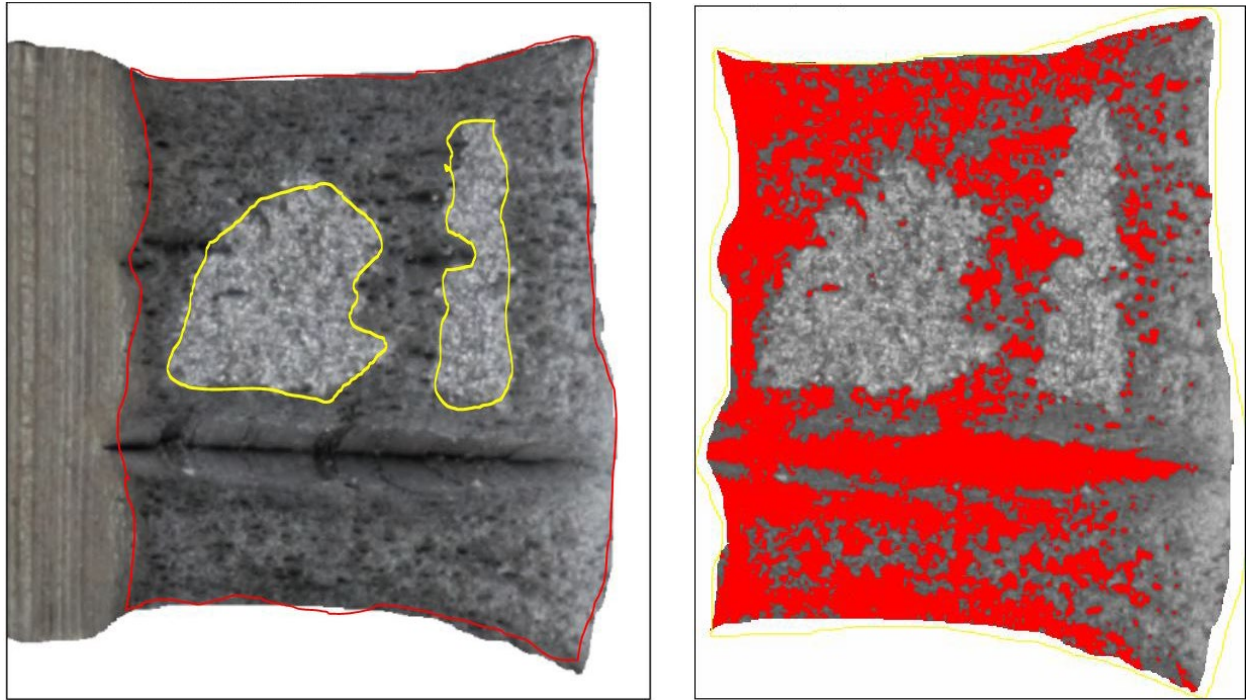


Figure E.68. Shear fracture areas for specimen 3TY using a Mask Area Method (left) and a Pixel Intensity Method (right).

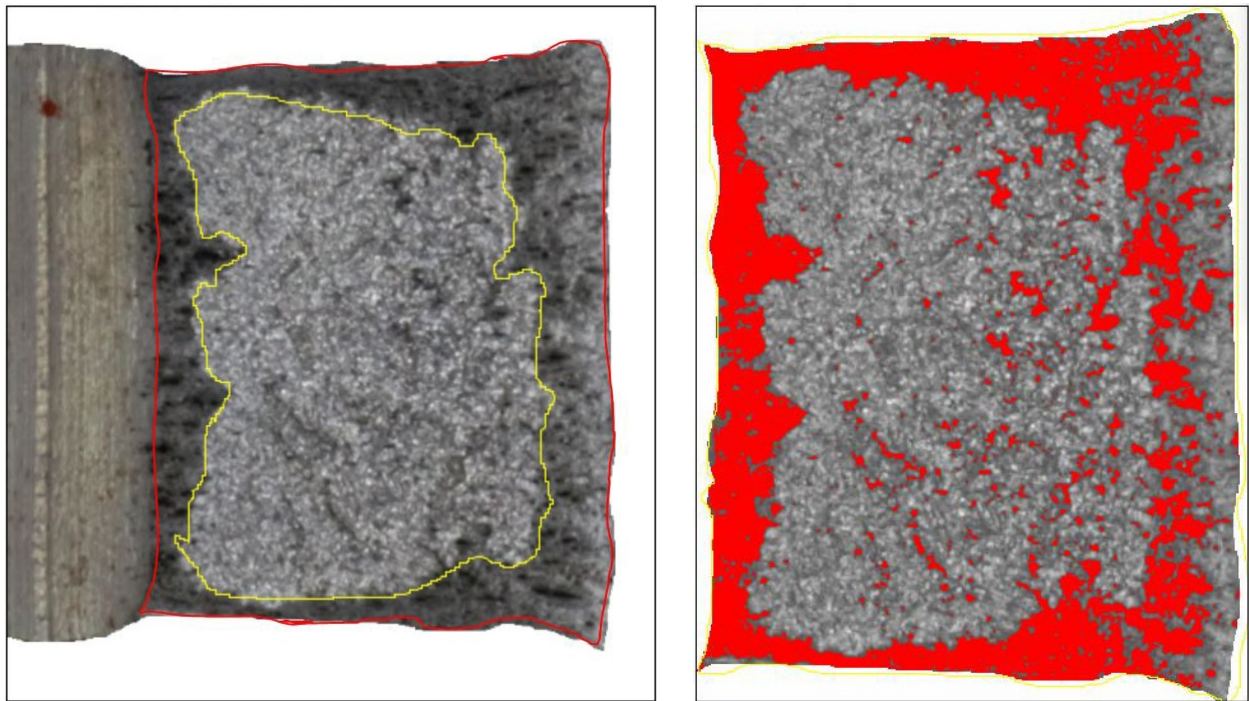


Figure E.69. Shear fracture areas for specimen 3TZ using a Mask Area Method (left) and a Pixel Intensity Method (right).

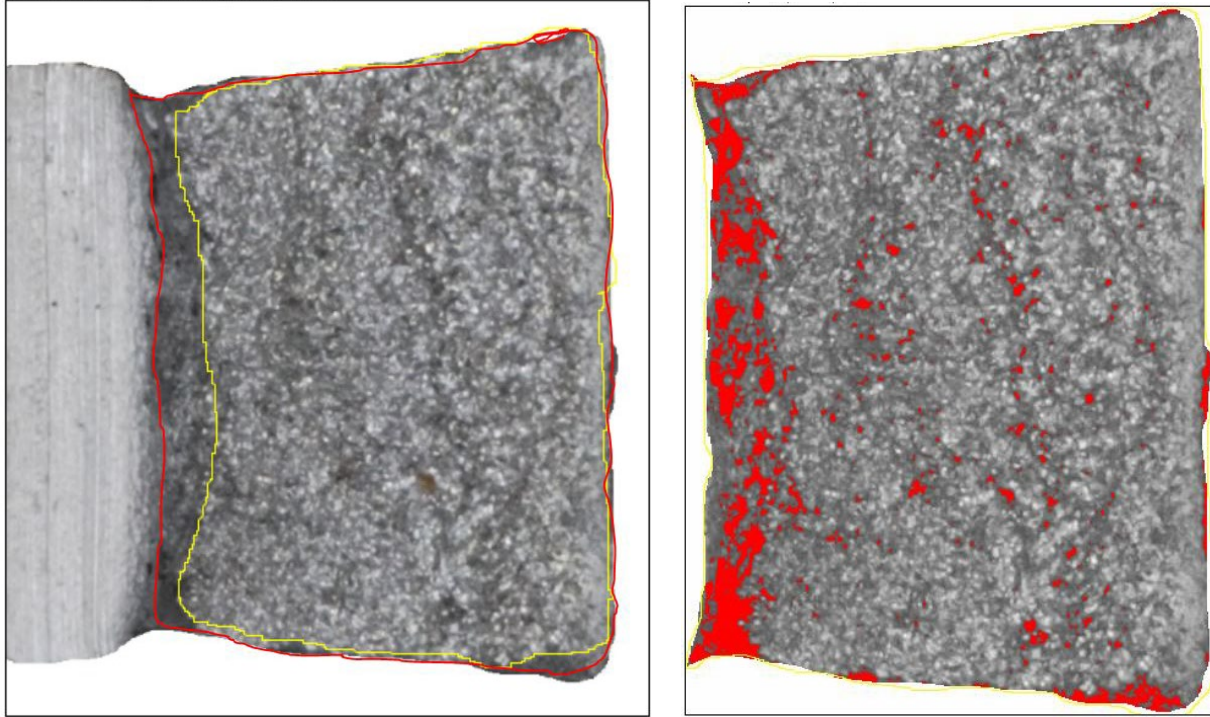


Figure E.70. Shear fracture areas for specimen 4AX using a Mask Area Method (left) and a Pixel Intensity Method (right).

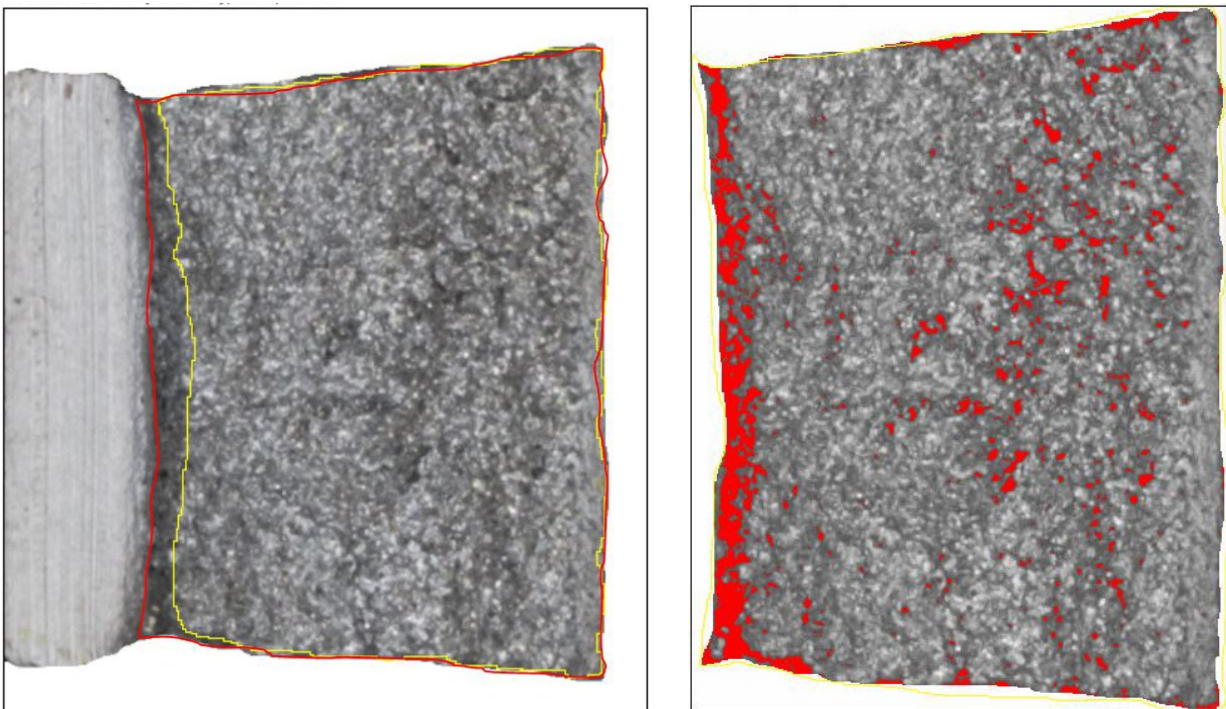


Figure E.71. Shear fracture areas for specimen 4AY using a Mask Area Method (left) and a Pixel Intensity Method (right).

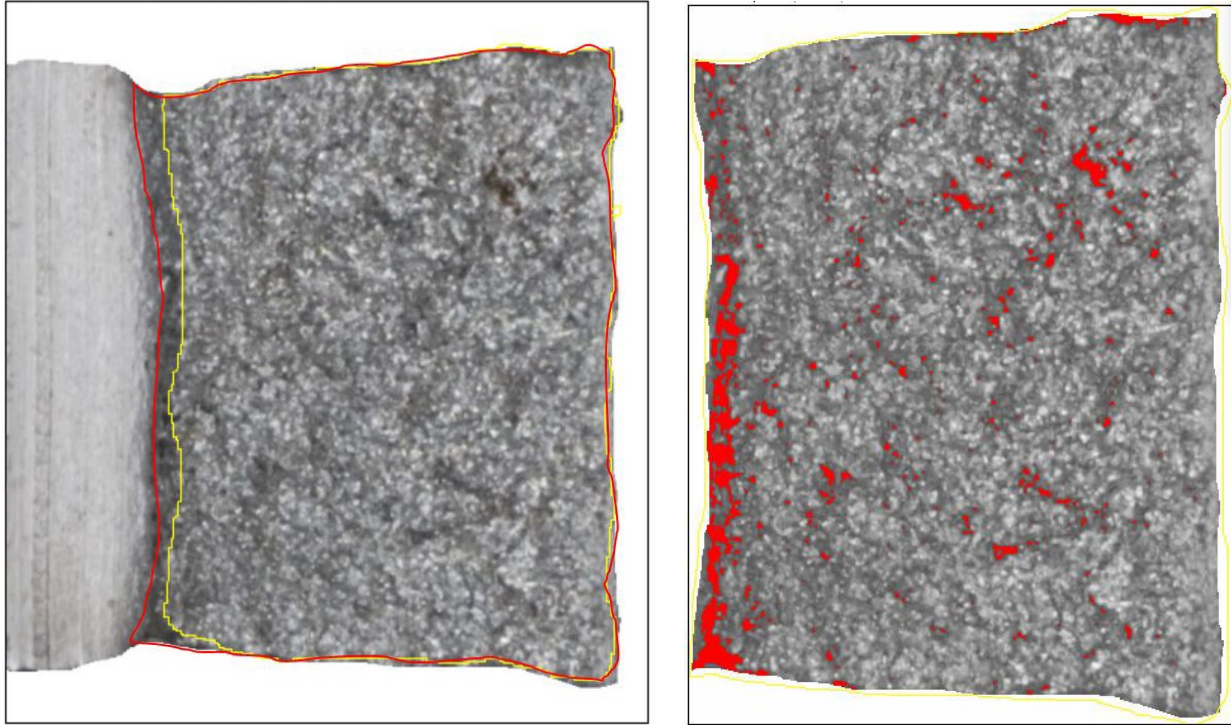


Figure E.72. Shear fracture areas for specimen 4AZ using a Mask Area Method (left) and a Pixel Intensity Method (right).

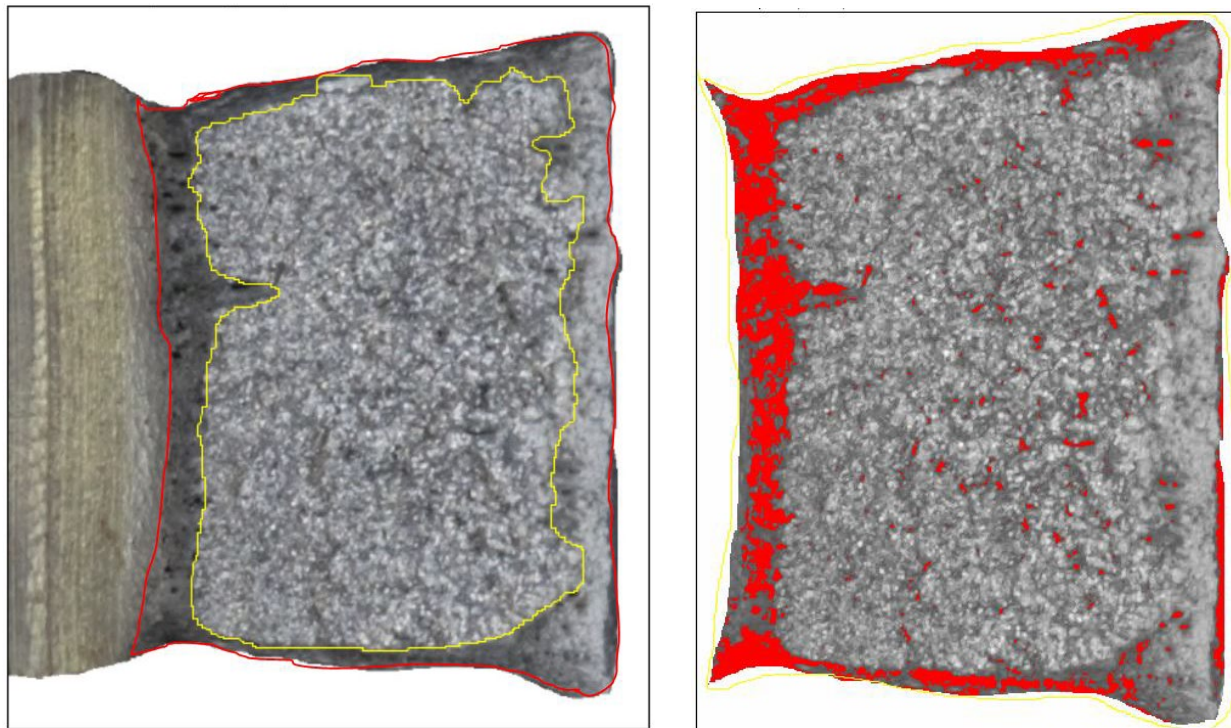


Figure E.73. Shear fracture areas for specimen 4BX using a Mask Area Method (left) and a Pixel Intensity Method (right).

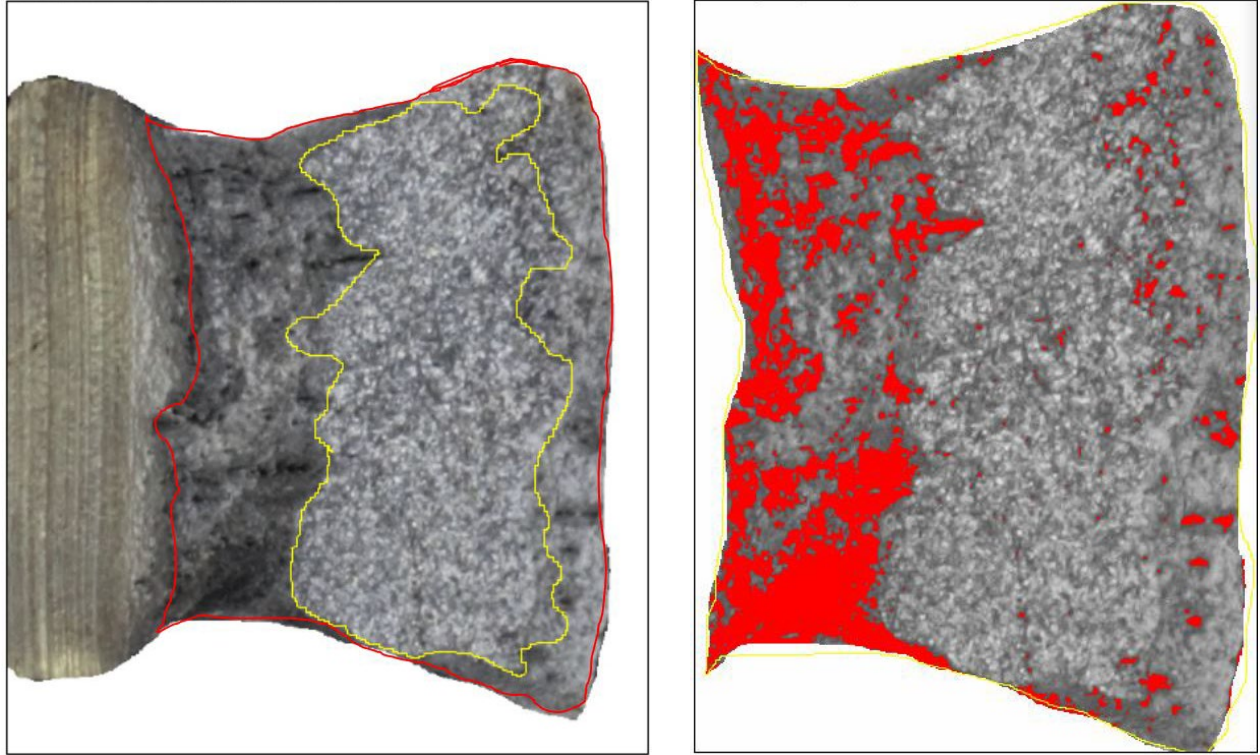


Figure E.74. Shear fracture areas for specimen 4BY using a Mask Area Method (left) and a Pixel Intensity Method (right).

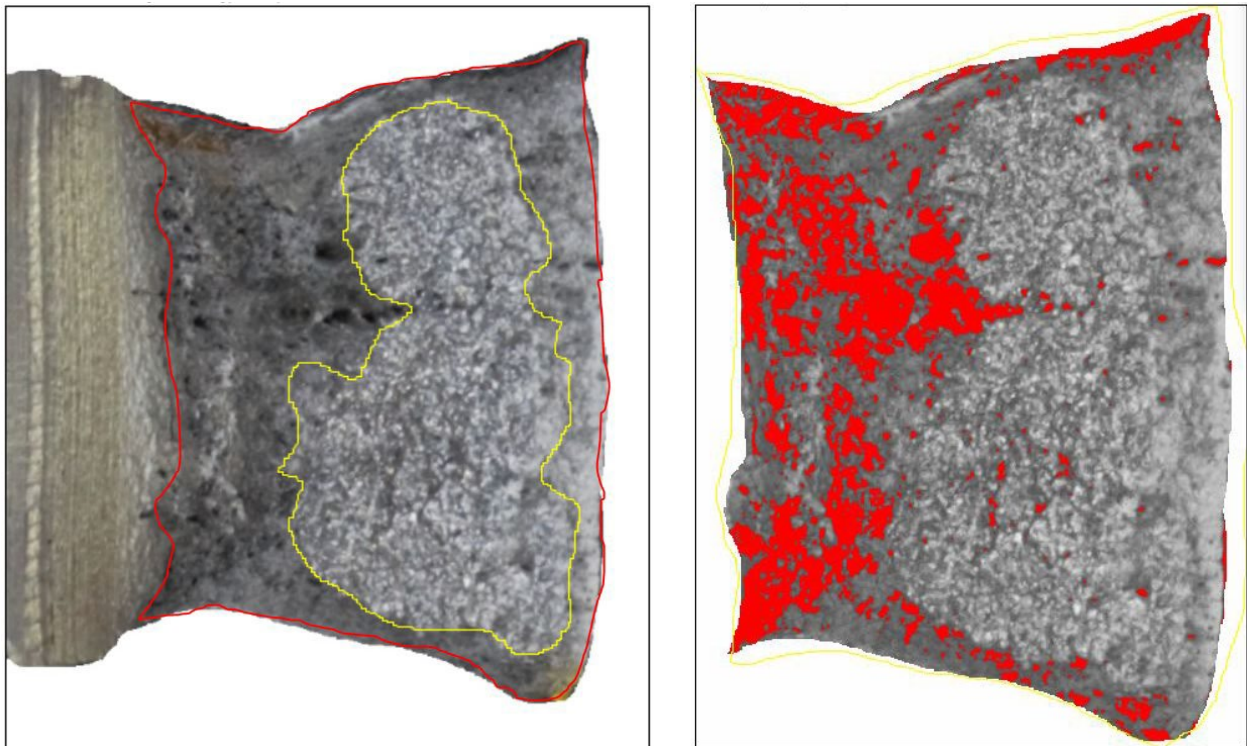


Figure E.75. Shear fracture areas for specimen 4BZ using a Mask Area Method (left) and a Pixel Intensity Method (right).

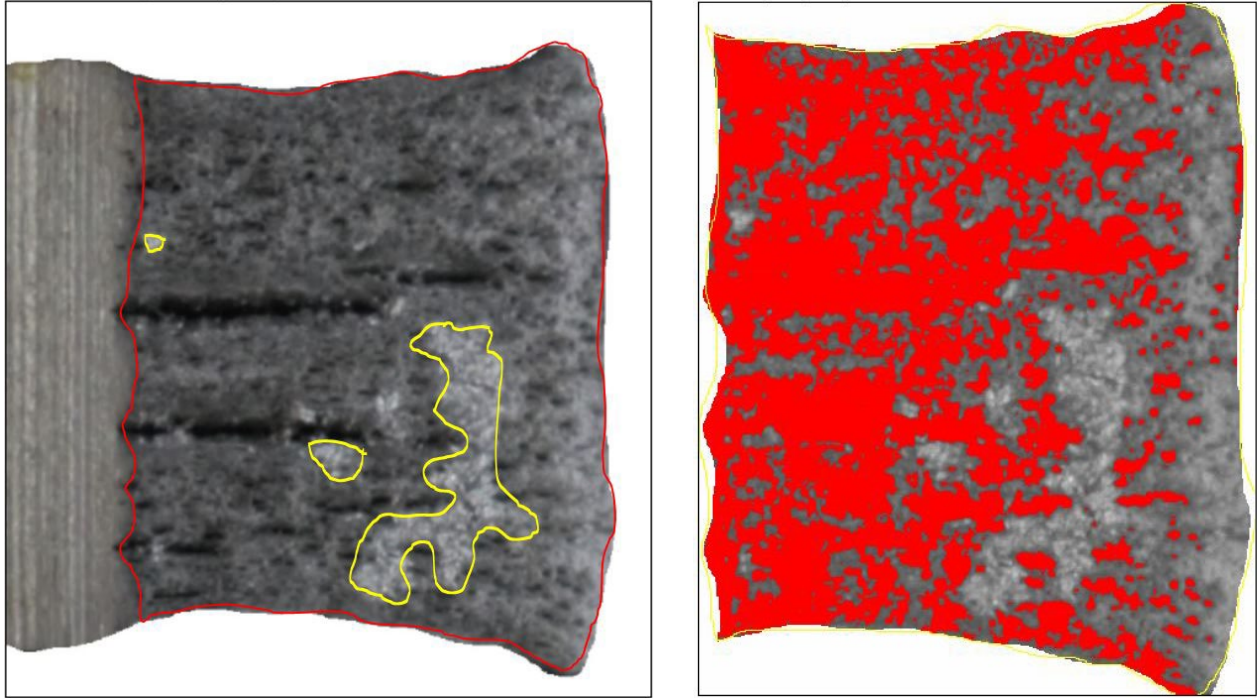


Figure E.76. Shear fracture areas for specimen 4QX using a Mask Area Method (left) and a Pixel Intensity Method (right).

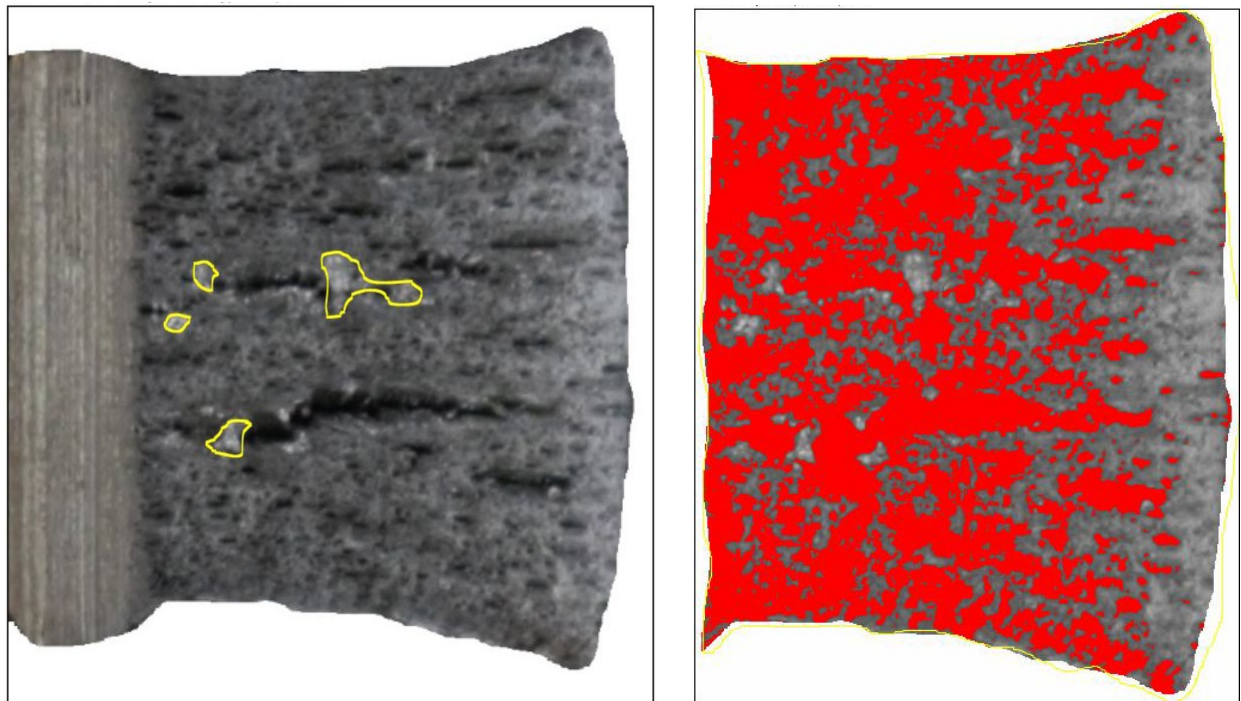


Figure E.77. Shear fracture areas for specimen 4QY using a Mask Area Method (left) and a Pixel Intensity Method (right).

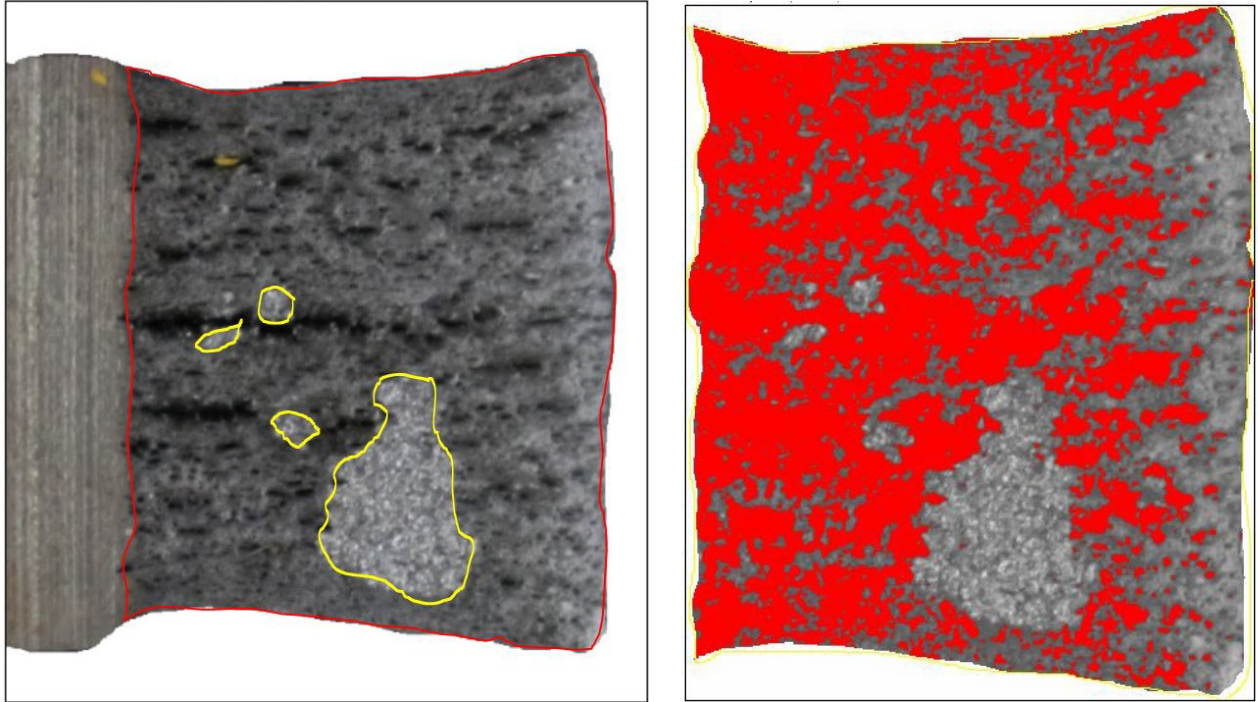


Figure E.78. Shear fracture areas for specimen 4QZ using a Mask Area Method (left) and a Pixel Intensity Method (right).



Figure E.79. Shear fracture areas for specimen 4RX using a Mask Area Method (left) and a Pixel Intensity Method (right).

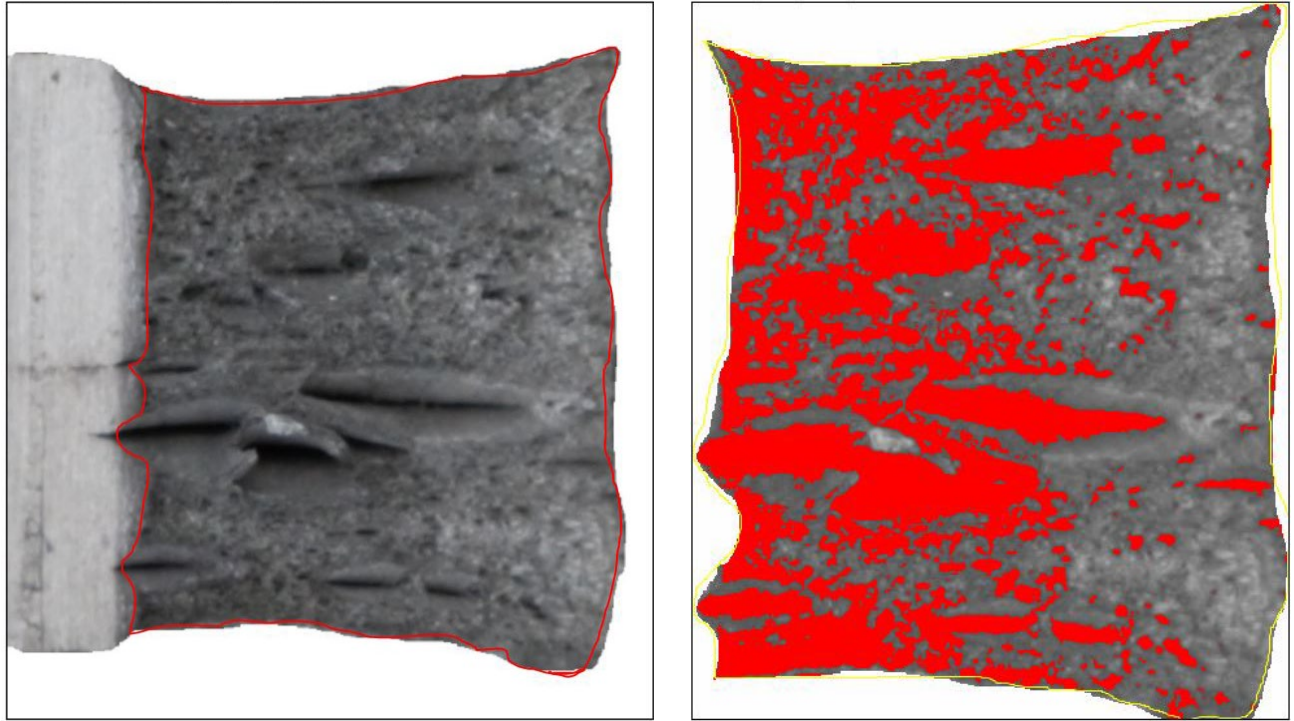


Figure E.80. Shear fracture areas for specimen 4RY using a Mask Area Method (left) and a Pixel Intensity Method (right).

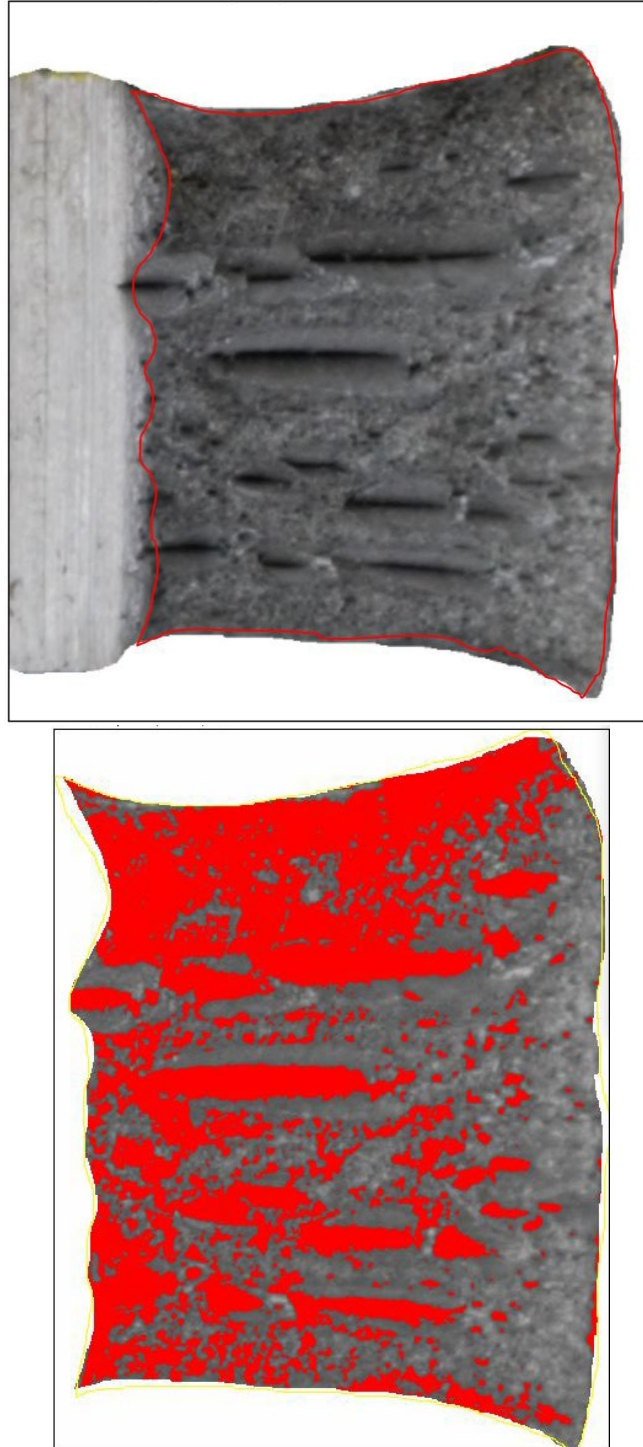


Figure E.81. Shear fracture areas for specimen 4RZ using a Mask Area Method (left) and a Pixel Intensity Method (right).

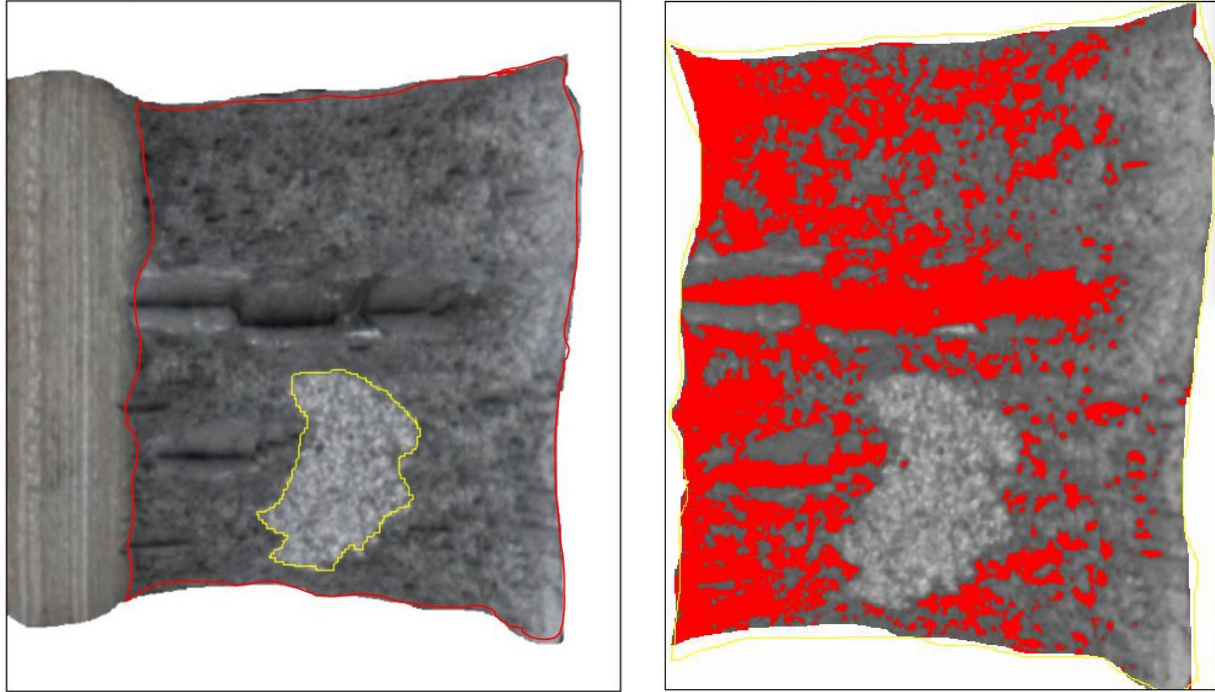


Figure E.82. Shear fracture areas for specimen 4TX using a Mask Area Method (left) and a Pixel Intensity Method (right).

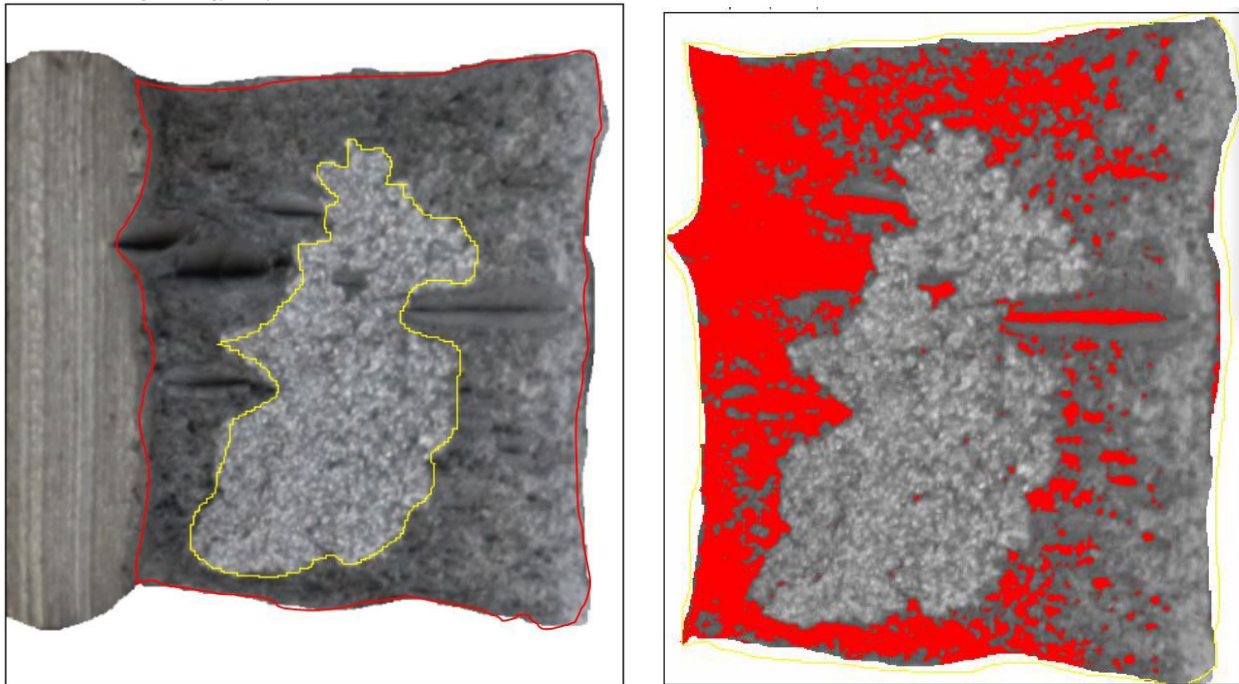


Figure E.83. Shear fracture areas for specimen 4TY using a Mask Area Method (left) and a Pixel Intensity Method (right).

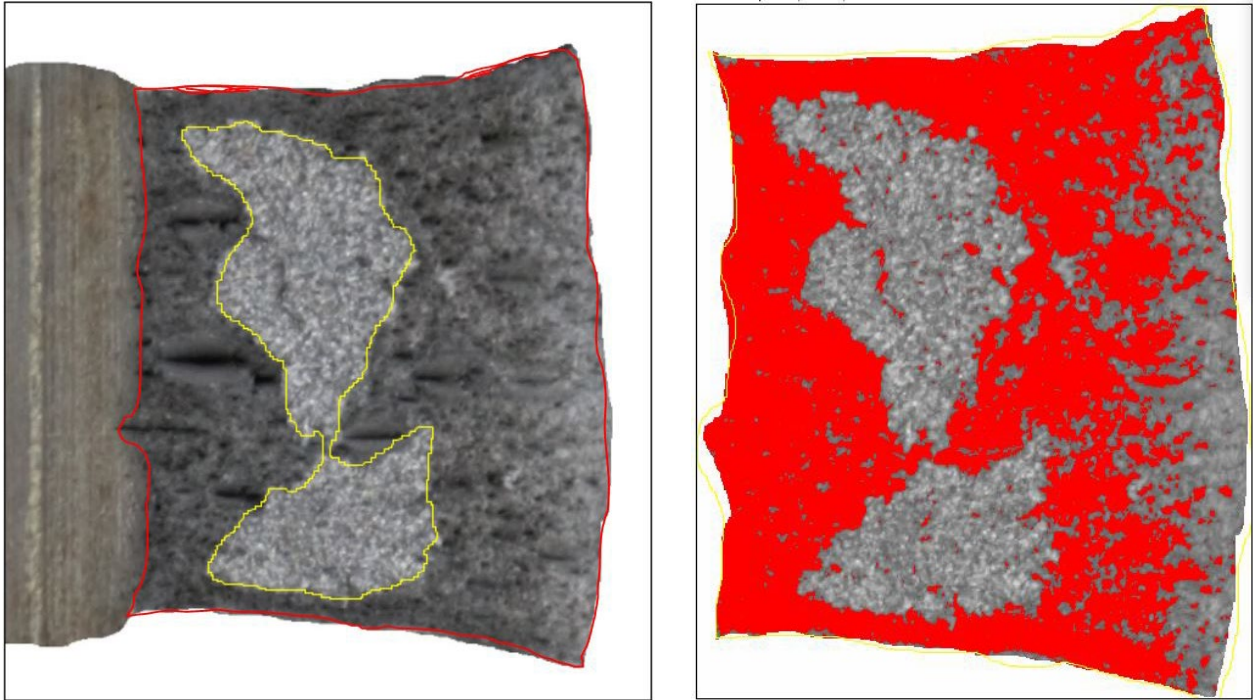


Figure E.84. Shear fracture areas for specimen 4TZ using a Mask Area Method (left) and a Pixel Intensity Method (right).

Table E-3: Lateral expansion of CVN specimens.

Specimen	Lateral Expansion ¹ (in.)	A1 (in.)	A2 (in.)	A3 (in.)	A4 (in.)
1AX	0.080	0.066	0.066	0.066	0.063
1AY	0.069	0.060	0.060	0.061	0.060
1AZ	0.062	0.057	0.057	0.057	0.057
1BX	0.049	0.050	0.050	0.051	0.048
1BY	0.063	0.056	0.058	0.055	0.057
1BZ	0.060	0.056	0.056	0.056	0.055
1CX	0.103	0.077	0.073	0.075	0.078
1CY	0.105	0.080	0.074	0.077	0.077
1CZ	0.105	0.075	0.076	0.081	0.079
1HX	0.042	0.047	0.046	0.047	0.047
1HY	0.036	0.044	0.043	0.042	0.044
1HZ	0.048	0.048	0.049	0.051	0.050
1NX	0.115	0.084	0.077	0.083	0.078
1NY	0.109	0.076	0.073	0.082	0.085
1NZ	0.122	0.087	0.077	0.087	0.077
1QX	0.045	0.048	0.049	0.048	0.047
1QY	0.041	0.048	0.048	0.045	0.044
1QZ	0.040	0.046	0.046	0.045	0.046
1TX	0.076	0.062	0.060	0.066	0.064
1TY	0.063	0.059	0.056	0.056	0.056
1TZ	0.058	0.055	0.053	0.053	0.055
1VX	0.037	0.044	0.044	0.044	0.045
1VY	0.032	0.041	0.041	0.041	0.043
1VZ	0.045	0.047	0.047	0.050	0.049
2AX	0.037	0.045	0.045	0.044	0.043
2AY	0.050	0.048	0.052	0.050	0.050
2AZ	0.039	0.046	0.046	0.045	0.044
2BX	0.081	0.065	0.064	0.068	0.066
2BY	0.080	0.064	0.064	0.068	0.054
2BZ	0.083	0.056	0.066	0.055	0.069
2QX	0.032	0.041	0.039	0.043	0.039
2QY	0.037	0.041	0.047	0.040	0.042
2QZ	0.024	0.039	0.035	0.037	0.036
2TX	0.064	0.054	0.058	0.056	0.058
2TY	0.073	0.054	0.062	0.063	0.053
2TZ	0.064	0.059	0.052	0.057	0.054
3AX	0.034	0.042	0.043	0.043	0.043
3AY	0.029	0.040	0.038	0.040	0.041
3AZ	0.041	0.047	0.047	0.046	0.046

Table E-3 (cont.): Lateral expansion of CVN specimens.

Specimen	Lateral Expansion ¹ (in.)	A1 (in.)	A2 (in.)	A3 (in.)	A4 (in.)
3BX	0.094	0.074	0.064	0.072	0.067
3BY	-	-	-	-	-
3BZ	0.077	0.060	0.062	0.067	0.046
3QX	0.013	0.031	0.031	0.034	0.033
3QY	0.021	0.037	0.037	0.033	0.036
3QZ	0.024	0.038	0.039	0.037	0.036
3TX	0.061	0.055	0.052	0.058	0.056
3TY	0.056	0.050	0.055	0.052	0.053
3TZ	0.042	0.048	0.045	0.046	0.045
4AX	0.053	0.048	0.046	0.045	0.057
4AY	0.031	0.040	0.041	0.041	0.042
4AZ	0.029	0.040	0.040	0.039	0.041
4BX	0.049	0.049	0.050	0.051	0.050
4BY	0.083	0.067	0.067	0.068	0.063
4BZ	0.076	0.064	0.063	0.064	0.063
4QX	0.051	0.049	0.054	0.049	0.048
4QY	0.052	0.050	0.051	0.053	0.049
4QZ	0.051	0.049	0.052	0.047	0.051
4RX	0.069	0.062	0.056	0.058	0.059
4RY	0.068	0.059	0.058	0.061	0.054
4RZ	0.070	0.059	0.061	0.052	0.061
4TX	0.068	0.057	0.059	0.061	0.054
4TY	0.057	0.051	0.056	0.053	0.052
4TZ	0.052	0.051	0.052	0.051	0.052

¹The lateral expansion is calculated by summing the maximum of (A1, A2) and (A3, A4), and subtracting out a dial indicator zero for both values. In this case the dial indicator zero is 0.026 in. A dial indicator zero greater than zero was used to ensure the ability to capture negative expansion (contraction), which did not occur in this data set.

Appendix F: GDS Results

Table F-1: Raw GDS measurements.

Specimen	Analysis Date	C	Mn	Si	P	S	Ni	Cr	Mo	Cu	V	Ti	Nb	Zr	Fe
1B4 Burn 1	12/16/2022 10:17	0.139	1.027	0.207	0.005	0.010	0.343	0.462	0.004	0.237	0.035	0.000	0.005	0.003	97.20
1B4 Burn 2	12/16/2022 10:22	0.137	1.031	0.212	0.005	0.010	0.342	0.464	0.005	0.238	0.035	0.000	0.005	0.003	97.19
1Q4 Burn 1	12/16/2022 10:26	0.163	1.151	0.218	0.015	0.012	0.081	0.561	0.012	0.282	0.037	0.000	0.002	0.004	97.21
1Q4 Burn 2	12/16/2022 10:30	0.179	1.219	0.225	0.017	0.033	0.084	0.581	0.013	0.293	0.040	0.001	0.003	0.004	97.10
1T4 Burn 1	12/16/2022 10:35	0.163	1.176	0.217	0.015	0.028	0.081	0.569	0.012	0.284	0.037	0.001	0.003	0.005	97.22
1T4 Burn 2	12/16/2022 10:38	0.173	1.190	0.223	0.016	0.024	0.084	0.571	0.013	0.288	0.038	0.001	0.002	0.004	97.18
1V4 Burn 1	12/16/2022 10:42	0.133	1.025	0.207	0.005	0.013	0.341	0.460	0.004	0.237	0.034	0.000	0.004	0.003	97.27
1V4 Burn 2	12/16/2022 10:46	0.147	1.058	0.218	0.005	0.022	0.349	0.470	0.004	0.249	0.035	0.000	0.004	0.004	97.25
2B4 Burn 1	12/16/2022 10:54	0.110	0.898	0.214	0.005	0.008	0.306	0.474	0.005	0.235	0.032	0.001	0.003	0.007	97.55
2B4 Burn 2	12/16/2022 11:00	0.120	0.913	0.218	0.006	0.010	0.311	0.481	0.006	0.241	0.033	0.001	0.003	0.004	97.51
2T4 Burn 1	12/16/2022 11:05	0.132	1.116	0.214	0.013	0.017	0.078	0.557	0.012	0.270	0.036	0.001	0.002	0.005	97.35
2T4 Burn 2	12/16/2022 11:09	0.135	1.096	0.210	0.012	0.014	0.077	0.553	0.012	0.268	0.036	0.000	0.002	0.004	97.43
2Q4 Burn 1	12/16/2022 11:14	0.180	1.187	0.216	0.015	0.018	0.084	0.582	0.015	0.274	0.038	0.001	0.003	0.000	97.18
2Q4 Burn 2	12/16/2022 11:18	0.173	1.193	0.221	0.016	0.021	0.084	0.584	0.014	0.275	0.038	0.000	0.002	0.000	97.17
2A4 Burn 1	12/16/2022 11:23	0.156	1.161	0.273	0.014	0.024	0.352	0.557	0.007	0.265	0.030	0.001	0.004	0.000	96.79
2A4 Burn 2	12/16/2022 11:26	0.155	1.153	0.281	0.014	0.022	0.351	0.553	0.007	0.265	0.030	0.001	0.004	0.000	96.75
3B4 Burn 1	12/16/2022 11:30	0.122	1.085	0.251	0.007	0.023	0.350	0.498	0.007	0.264	0.038	0.000	0.002	0.000	97.25
3B4 Burn 2	12/16/2022 11:33	0.122	1.054	0.256	0.008	0.019	0.350	0.503	0.007	0.267	0.038	0.000	0.002	0.000	97.21
3U4 Burn 1	12/16/2022 11:35	0.095	1.116	0.257	0.007	0.011	0.309	0.578	0.011	0.230	0.053	0.000	0.002	0.000	97.28
3U4 Burn 2	12/16/2022 11:37	0.090	1.125	0.264	0.007	0.008	0.314	0.580	0.011	0.231	0.055	0.000	0.002	0.000	97.17
3Q4 Burn 1	12/16/2022 11:40	0.173	1.313	0.235	0.017	0.024	0.085	0.588	0.016	0.270	0.038	0.000	0.002	0.000	97.13
3Q4 Burn 2	12/16/2022 11:42	0.174	1.290	0.229	0.016	0.018	0.084	0.584	0.015	0.267	0.038	0.000	0.002	0.000	97.12
3T4 Burn 1	12/16/2022 11:45	0.161	1.342	0.245	0.025	0.033	0.090	0.612	0.016	0.289	0.040	0.001	0.002	0.000	97.00
3T4 Burn 2	12/16/2022 11:47	0.152	1.276	0.232	0.018	0.028	0.085	0.592	0.015	0.273	0.038	0.001	0.003	0.000	97.17
3A4 Burn 1	12/16/2022 11:49	0.148	1.183	0.246	0.019	0.025	0.345	0.548	0.009	0.265	0.030	0.001	0.003	0.000	96.93
3A4 Burn 2	12/16/2022 11:51	0.145	1.186	0.245	0.019	0.023	0.344	0.549	0.008	0.265	0.030	0.001	0.002	0.000	96.91
4U4 Burn 1	12/16/2022 11:56	0.094	1.119	0.253	0.008	0.022	0.322	0.582	0.011	0.239	0.054	0.000	0.003	0.000	97.11
4U4 Burn 2	12/16/2022 11:58	0.088	1.102	0.255	0.007	0.017	0.318	0.578	0.011	0.235	0.053	0.000	0.004	0.000	97.10
4B4 Burn 1	12/16/2022 12:00	0.126	1.064	0.210	0.007	0.014	0.307	0.549	0.008	0.240	0.026	0.001	0.004	0.000	97.14
4B4 Burn 2	12/16/2022 12:02	0.122	1.070	0.209	0.008	0.014	0.308	0.551	0.009	0.240	0.026	0.001	0.004	0.000	97.19
4Q4 Burn 1	12/16/2022 12:05	0.171	1.197	0.219	0.014	0.024	0.085	0.585	0.015	0.273	0.039	0.000	0.002	0.000	97.12
4Q4 Burn 2	12/16/2022 12:07	0.169	1.201	0.221	0.016	0.030	0.085	0.588	0.016	0.273	0.039	0.000	0.003	0.000	97.10

Table F-1 (cont.): Raw GDS measurements.

Specimen	Analysis Date	C	Mn	Si	P	S	Ni	Cr	Mo	Cu	V	Ti	Nb	Zr	Fe
4A4 Burn 1	12/16/2022 12:09	0.147	1.136	0.275	0.013	0.020	0.351	0.554	0.008	0.260	0.031	0.001	0.002	0.000	96.84
4A4 Burn 2	12/16/2022 12:12	0.148	1.127	0.274	0.012	0.022	0.349	0.552	0.008	0.257	0.030	0.001	0.004	0.000	96.85
4R4 Burn 1	12/16/2022 12:15	0.167	1.192	0.217	0.014	0.031	0.084	0.582	0.015	0.268	0.038	0.000	0.003	0.000	97.10
4R4 Burn 2	12/16/2022 12:17	0.158	1.134	0.213	0.013	0.021	0.082	0.571	0.015	0.261	0.037	0.000	0.003	0.000	97.17
4T4 Burn 1	12/16/2022 12:19	0.142	1.131	0.209	0.012	0.014	0.082	0.571	0.015	0.260	0.037	0.000	0.003	0.000	97.19
4T4 Burn 2	12/16/2022 12:22	0.155	1.166	0.217	0.014	0.016	0.084	0.580	0.016	0.267	0.037	0.000	0.003	0.000	97.17
1U4 Burn 1	12/16/2022 12:24	0.090	1.105	0.255	0.007	0.016	0.320	0.584	0.012	0.240	0.055	0.000	0.003	0.000	97.02
1U4 Burn 2	12/16/2022 12:26	0.089	1.104	0.252	0.007	0.016	0.319	0.582	0.011	0.239	0.055	0.000	0.004	0.000	97.00
1N4 Burn 1	12/16/2022 12:29	0.077	1.276	0.487	0.021	0.026	0.068	0.119	0.011	0.103	0.024	0.010	0.003	0.000	97.81
1N4 Burn 2	12/16/2022 12:31	0.067	1.423	0.624	0.023	0.027	0.066	0.109	0.011	0.095	0.024	0.015	0.006	0.000	97.56
1H4 Burn 1	12/16/2022 12:35	0.183	1.205	0.217	0.015	0.015	0.161	0.641	0.015	0.334	0.062	0.001	0.003	0.000	96.93
1H4 Burn 2	12/16/2022 12:38	0.185	1.207	0.215	0.015	0.016	0.161	0.640	0.016	0.331	0.063	0.001	0.004	0.000	96.84
1A4 Burn 1	12/16/2022 12:45	0.158	1.187	0.240	0.018	0.024	0.341	0.551	0.009	0.265	0.030	0.001	0.002	0.000	96.91
1A4 Burn 2	12/16/2022 12:48	0.148	1.242	0.258	0.018	0.025	0.341	0.551	0.008	0.266	0.030	0.001	0.003	0.000	96.93
2U4 Burn 1	12/16/2022 12:50	0.097	1.152	0.256	0.007	0.014	0.318	0.591	0.011	0.238	0.055	0.000	0.002	0.000	97.16
2U4 Burn 2	12/16/2022 12:52	0.094	1.085	0.245	0.006	0.017	0.314	0.577	0.012	0.231	0.054	0.000	0.003	0.000	97.21
1C4 Burn 1	12/16/2022 12:55	0.092	1.228	0.266	0.009	0.018	0.337	0.599	0.013	0.325	0.075	0.000	0.003	0.000	96.91
1C4 Burn 2	12/16/2022 12:57	0.097	1.239	0.268	0.009	0.018	0.339	0.599	0.012	0.326	0.075	0.000	0.002	0.000	96.84

Table F-2: Averaged GDS measurements per specimen.

Specimen	C	Mn	Si	P	S	Ni	Cr	Mo	Cu	V	Ti	Nb	Zr	Fe
1B4	0.138	1.029	0.210	0.005	0.010	0.343	0.463	0.005	0.238	0.035	0.000	0.005	0.003	97.20
1Q4	0.171	1.185	0.222	0.016	0.023	0.083	0.571	0.013	0.288	0.039	0.001	0.003	0.004	97.16
1T4	0.168	1.183	0.220	0.016	0.026	0.083	0.570	0.013	0.286	0.038	0.001	0.003	0.005	97.20
1V4	0.140	1.042	0.213	0.005	0.018	0.345	0.465	0.004	0.243	0.035	0.000	0.004	0.004	97.26
2B4	0.115	0.906	0.216	0.006	0.009	0.309	0.478	0.006	0.238	0.033	0.001	0.003	0.006	97.53
2T4	0.134	1.106	0.212	0.013	0.016	0.078	0.555	0.012	0.269	0.036	0.001	0.002	0.005	97.39
2Q4	0.177	1.190	0.219	0.016	0.020	0.084	0.583	0.015	0.275	0.038	0.001	0.003	0.000	97.18
2A4	0.156	1.157	0.277	0.014	0.023	0.352	0.555	0.007	0.265	0.030	0.001	0.004	0.000	96.77
3B4	0.122	1.070	0.254	0.008	0.021	0.350	0.501	0.007	0.266	0.038	0.000	0.002	0.000	97.23
3U4	0.093	1.121	0.261	0.007	0.010	0.312	0.579	0.011	0.231	0.054	0.000	0.002	0.000	97.23
3Q4	0.174	1.302	0.232	0.017	0.021	0.085	0.586	0.016	0.269	0.038	0.000	0.002	0.000	97.13
3T4	0.157	1.309	0.239	0.022	0.031	0.088	0.602	0.016	0.281	0.039	0.001	0.003	0.000	97.09
3A4	0.147	1.185	0.246	0.019	0.024	0.345	0.549	0.009	0.265	0.030	0.001	0.003	0.000	96.92
4U4	0.091	1.111	0.254	0.008	0.020	0.320	0.580	0.011	0.237	0.054	0.000	0.004	0.000	97.11
4B4	0.124	1.067	0.210	0.008	0.014	0.308	0.550	0.009	0.240	0.026	0.001	0.004	0.000	97.17
4Q4	0.170	1.199	0.220	0.015	0.027	0.085	0.587	0.016	0.273	0.039	0.000	0.003	0.000	97.11
4A4	0.148	1.132	0.275	0.013	0.021	0.350	0.553	0.008	0.259	0.031	0.001	0.003	0.000	96.85
4R4	0.163	1.163	0.215	0.014	0.026	0.083	0.577	0.015	0.265	0.038	0.000	0.003	0.000	97.14
4T4	0.149	1.149	0.213	0.013	0.015	0.083	0.576	0.016	0.264	0.037	0.000	0.003	0.000	97.18
1U4	0.090	1.105	0.254	0.007	0.016	0.320	0.583	0.012	0.240	0.055	0.000	0.004	0.000	97.01
1N4	0.072	1.350	0.556	0.022	0.027	0.067	0.114	0.011	0.099	0.024	0.013	0.005	0.000	97.69
1H4	0.184	1.206	0.216	0.015	0.016	0.161	0.641	0.016	0.333	0.063	0.001	0.004	0.000	96.89
1A4	0.153	1.215	0.249	0.018	0.025	0.341	0.551	0.009	0.266	0.030	0.001	0.003	0.000	96.92
2U4	0.096	1.119	0.251	0.007	0.016	0.316	0.584	0.012	0.235	0.055	0.000	0.003	0.000	97.19
1C4	0.095	1.234	0.267	0.009	0.018	0.338	0.599	0.013	0.326	0.075	0.000	0.003	0.000	96.88

Table F-3: NIST SRM 1269 checks.

Name	Analysis Date	C	Mn	Si	P	S	Ni	Cr	Mo	Cu	V	Ti	Nb	Zr	Fe
Initial Check	12/16/2022 10:01	0.300	1.376	0.190	0.010	0.003	0.104	0.190	0.034	0.090	0.011	0.008	0.001	0.006	97.49
Intermediate Check	12/16/2022 10:50	0.293	1.373	0.190	0.011	0.004	0.104	0.192	0.034	0.091	0.011	0.007	0.002	0.005	97.61
Intermediate Check	12/16/2022 11:53	0.300	1.401	0.184	0.011	0.003	0.106	0.200	0.038	0.085	0.011	0.007	0.000	0.000	97.47
Final Check	12/16/2022 12:59	0.300	1.389	0.182	0.011	0.002	0.107	0.198	0.039	0.084	0.011	0.007	0.000	0.000	97.43

Table F-4: Drift check with condition block.

Conditioning Sample	Analysis Date	C	Mn	Si	P	S	Ni	Cr	Mo	Cu	V	Ti	Nb	Zr	Fe
1	12/16/2022 7:34	0.088	1.356	0.392	0.015	0.001	0.294	0.545	0.054	0.320	0.063	0.009	0.006	0.000	96.87
2	12/16/2022 8:43	0.097	1.367	0.389	0.015	0.000	0.300	0.539	0.053	0.324	0.061	0.002	0.004	0.005	96.90
3	12/16/2022 8:50	0.099	1.333	0.389	0.015	0.001	0.300	0.529	0.052	0.321	0.062	0.001	0.004	0.004	96.86
4	12/16/2022 8:59	0.090	1.274	0.387	0.016	0.002	0.300	0.533	0.052	0.323	0.062	0.001	0.006	0.003	96.83
5	12/16/2022 9:30	0.250	0.530	0.056	0.009	0.035	0.028	0.026	0.005	0.063	0.007	0.000	0.005	0.003	98.76
6	12/16/2022 9:37	0.251	0.528	0.056	0.008	0.036	0.028	0.026	0.005	0.063	0.008	0.000	0.005	0.003	98.82
7	12/16/2022 9:44	0.244	0.533	0.056	0.009	0.037	0.029	0.026	0.005	0.063	0.008	0.000	0.005	0.004	98.88
8	12/16/2022 9:52	0.250	0.532	0.056	0.008	0.039	0.028	0.026	0.005	0.063	0.007	0.000	0.006	0.003	98.81

Appendix G: Macroetches



Figure G.1. Macroetch of 1D5 with planar reference scales.

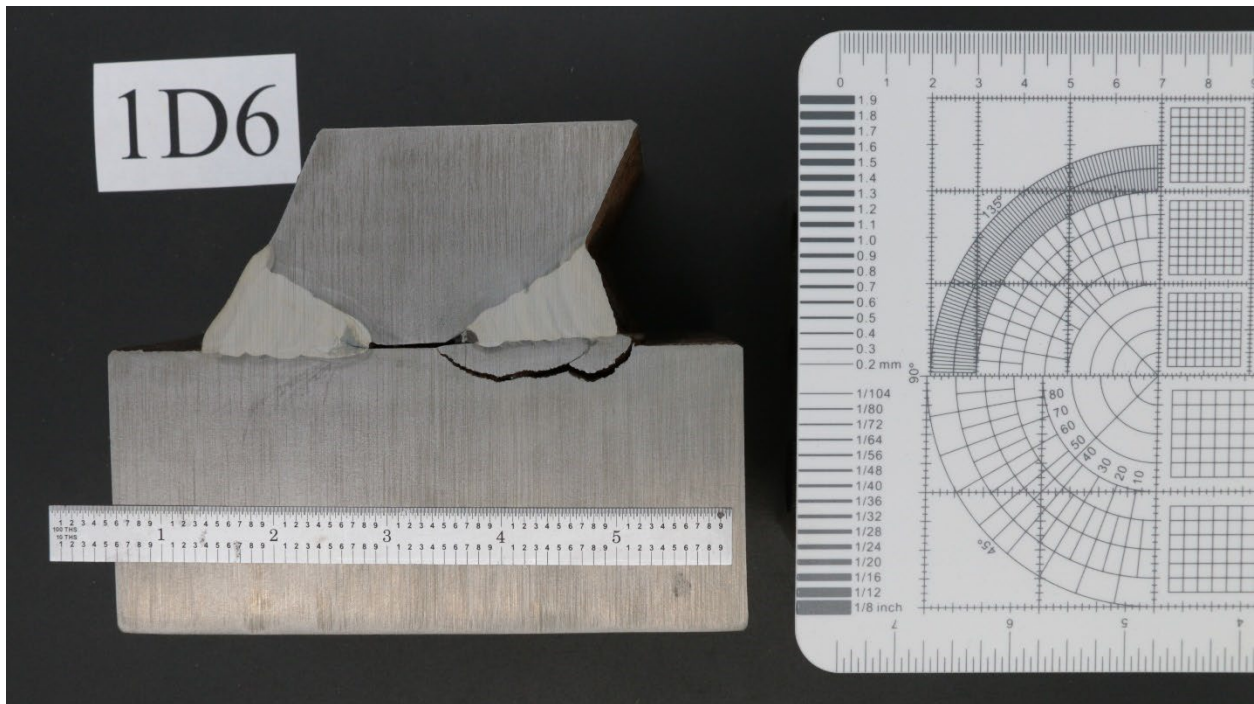


Figure G.2. Macroetch of 1D6 with planar reference scales.

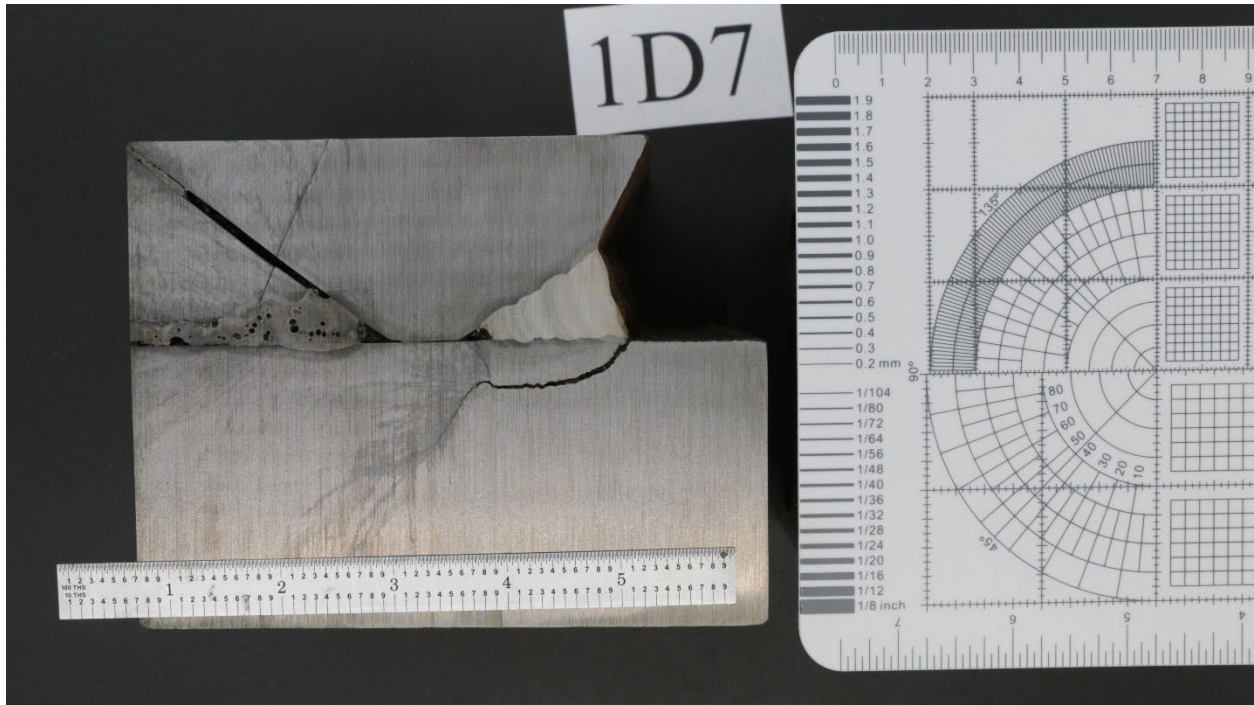


Figure G.3. Macroetch of 1D7 with planar reference scales.

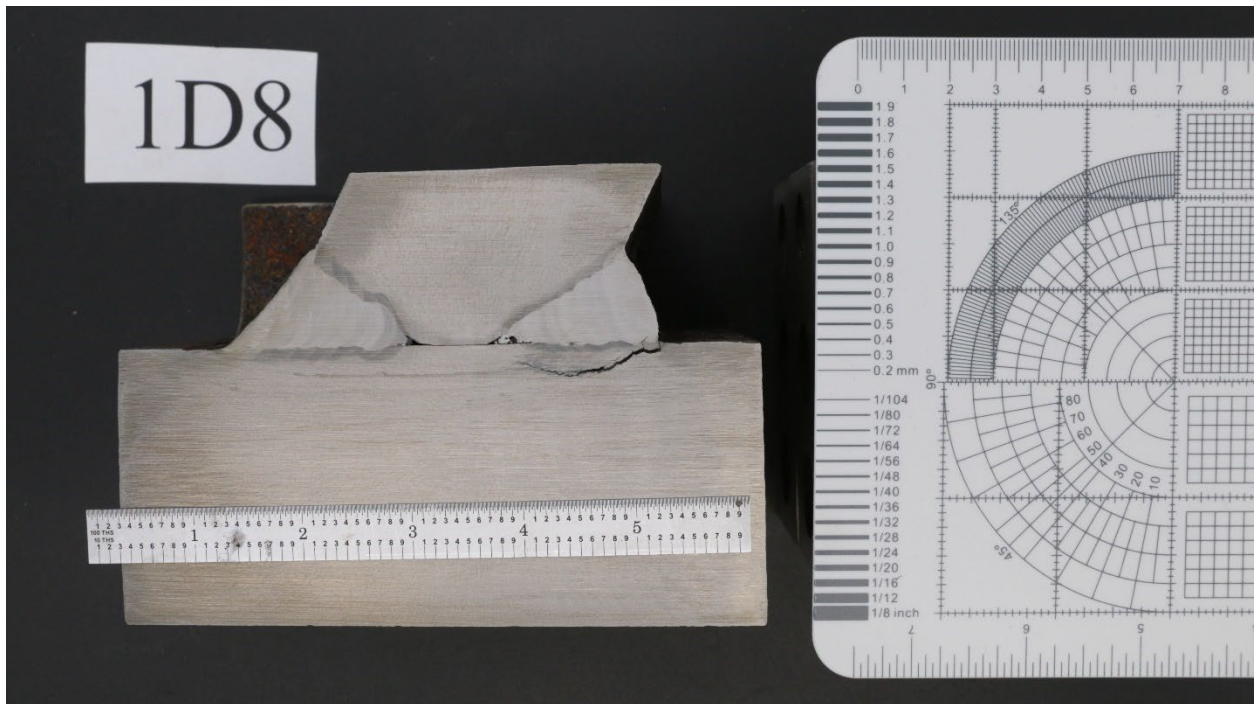


Figure G.4. Macroetch of 1D8 with planar reference scales.

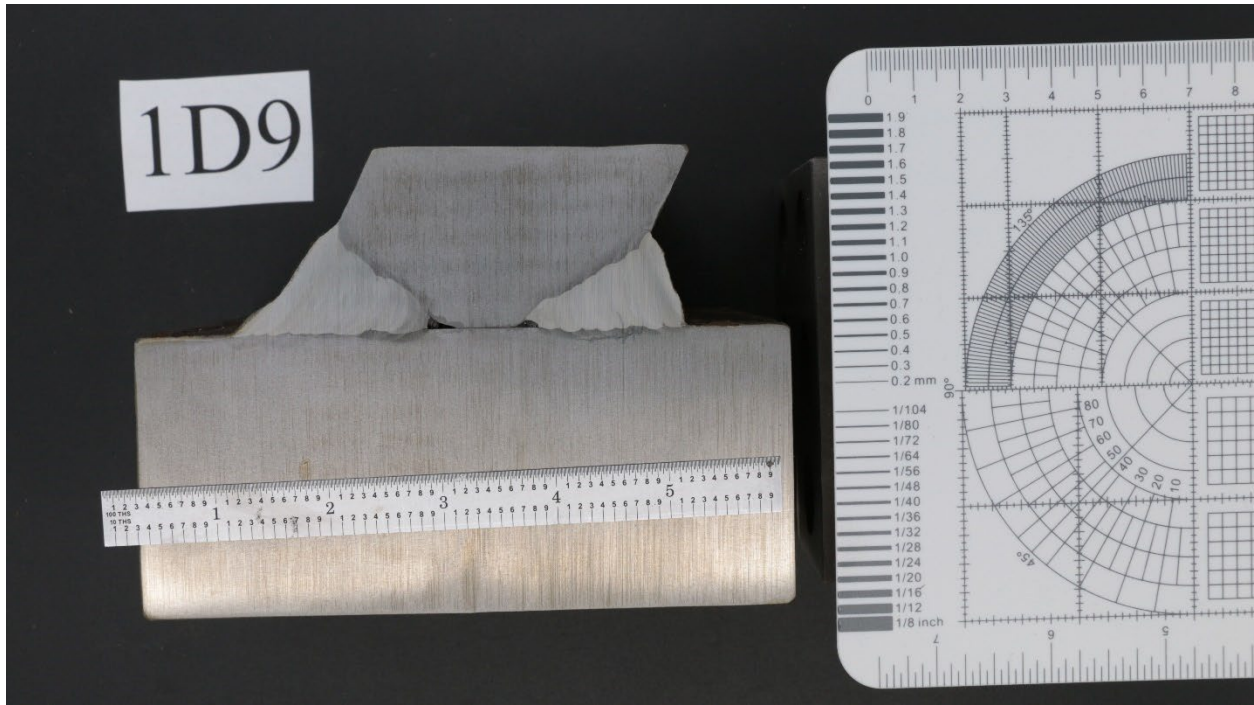


Figure G.5. Macroetch of 1D9 with planar reference scales.

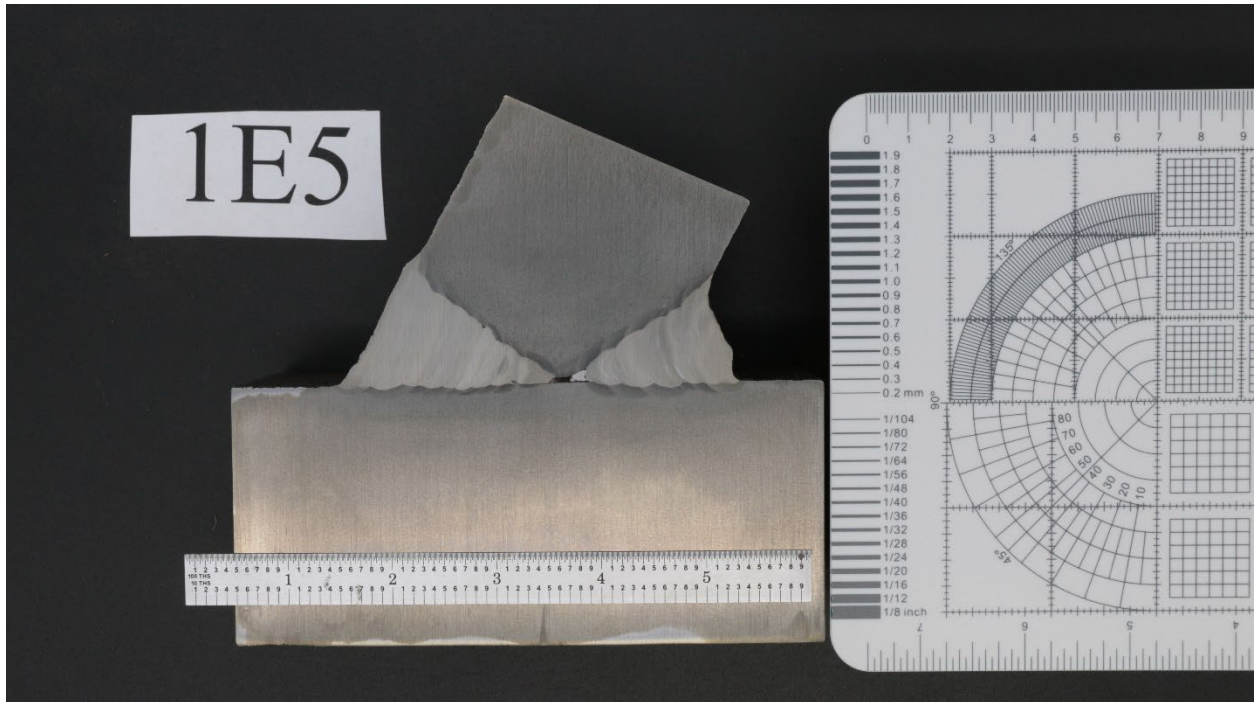


Figure G.6. Macroetch of 1E5 with planar reference scales.

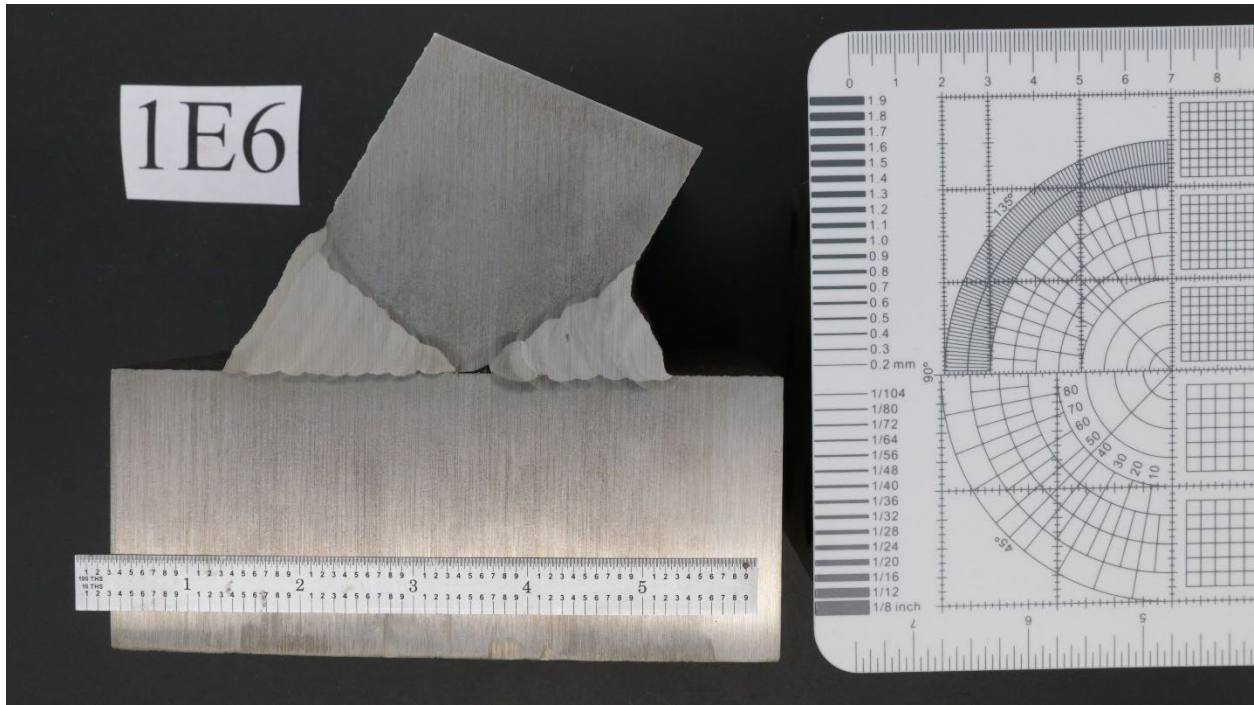


Figure G.7. Macroetch of 1E6 with planar reference scales.

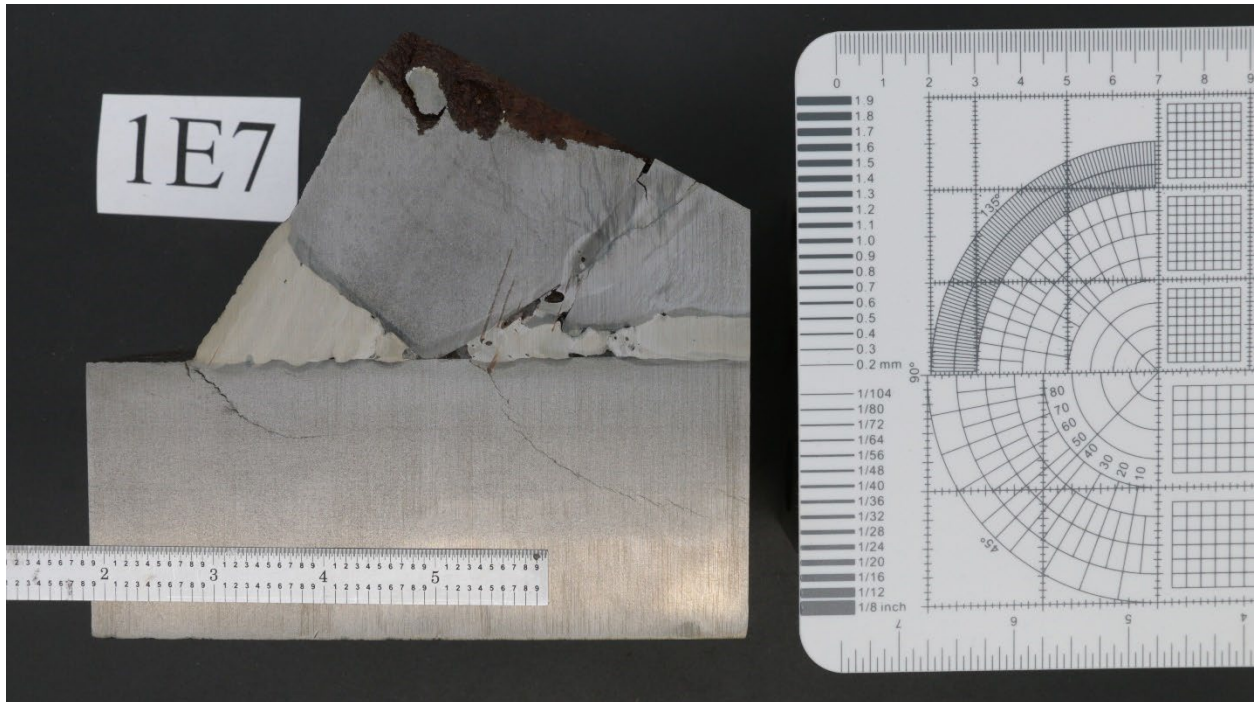


Figure G.8. Macroetch of 1E7 with planar reference scales.

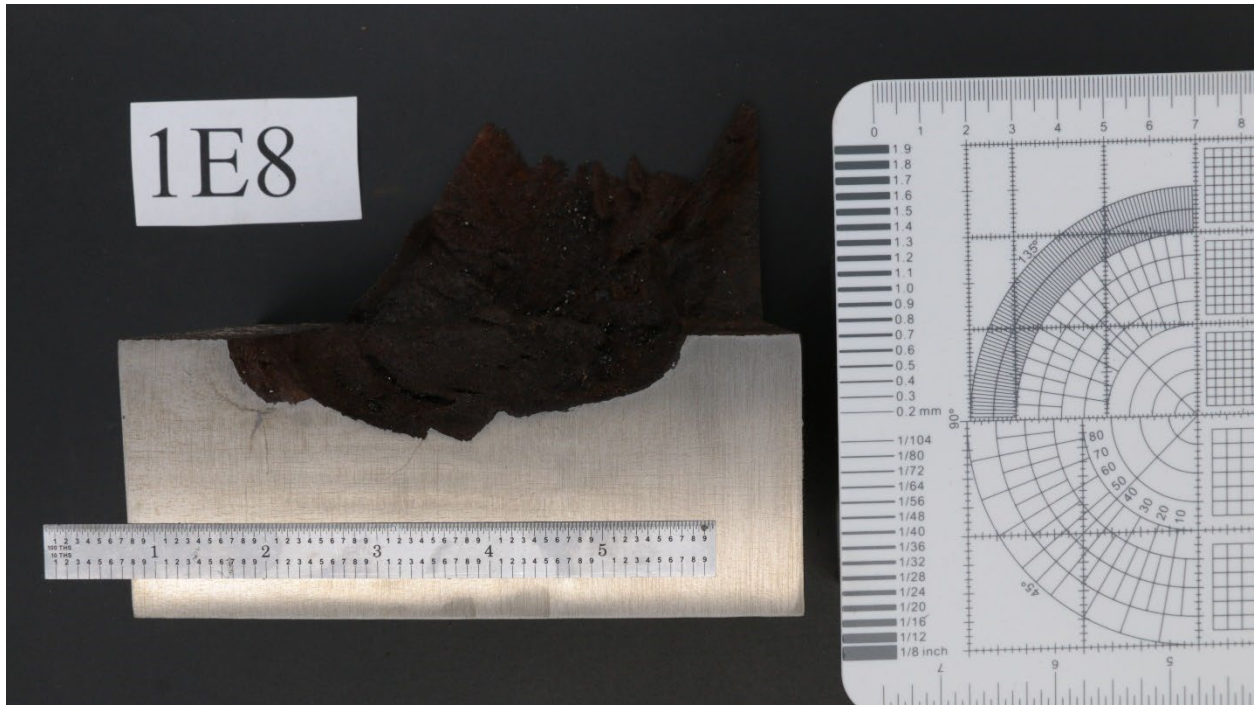


Figure G.9. Macroetch of 1E8 with planar reference scales.



Figure G.10. Macroetch of 1E9 with planar reference scales.



Figure G.11. Macroetch of 2D5 with planar reference scales.

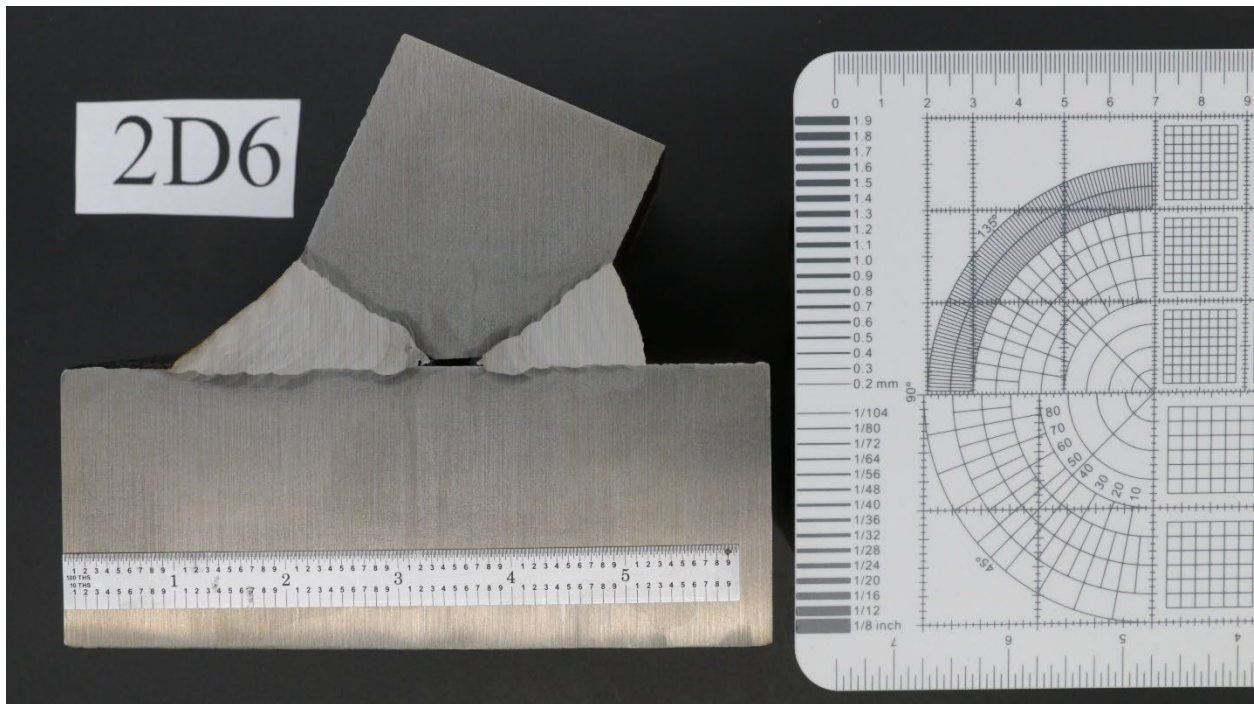


Figure G.12. Macroetch of 2D6 with planar reference scales.

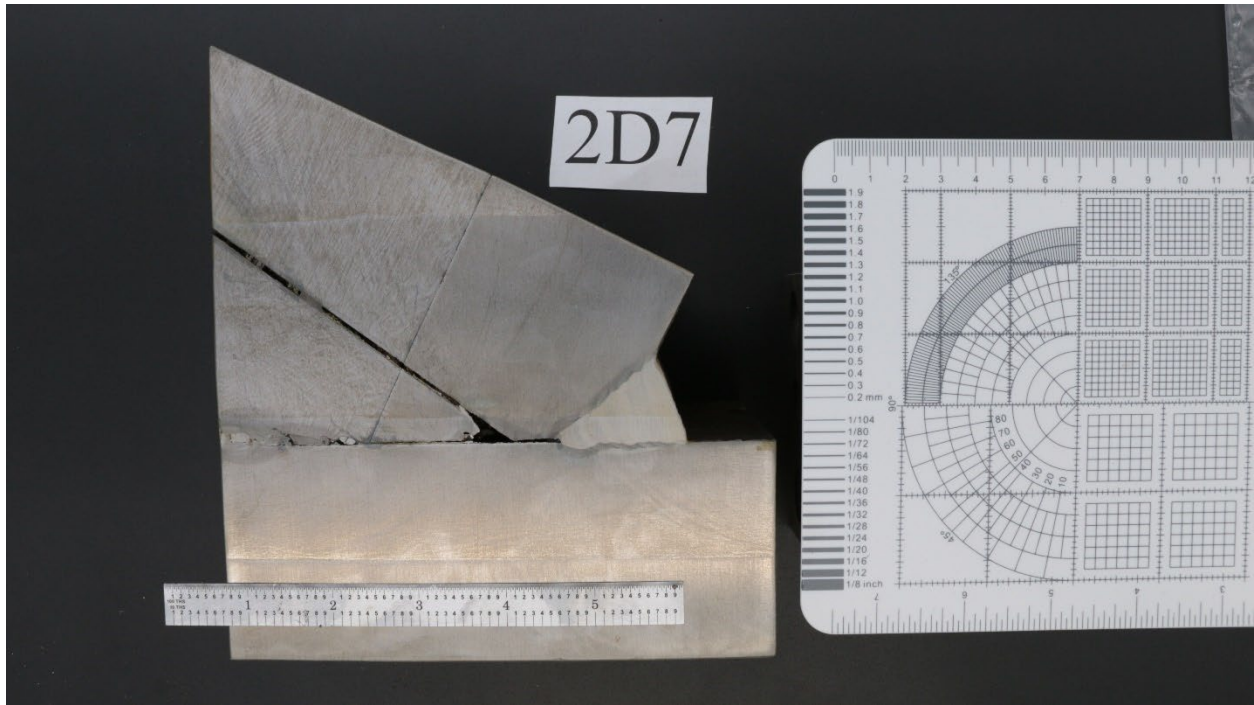


Figure G.13. Macroetch of 2D7 with planar reference scales.

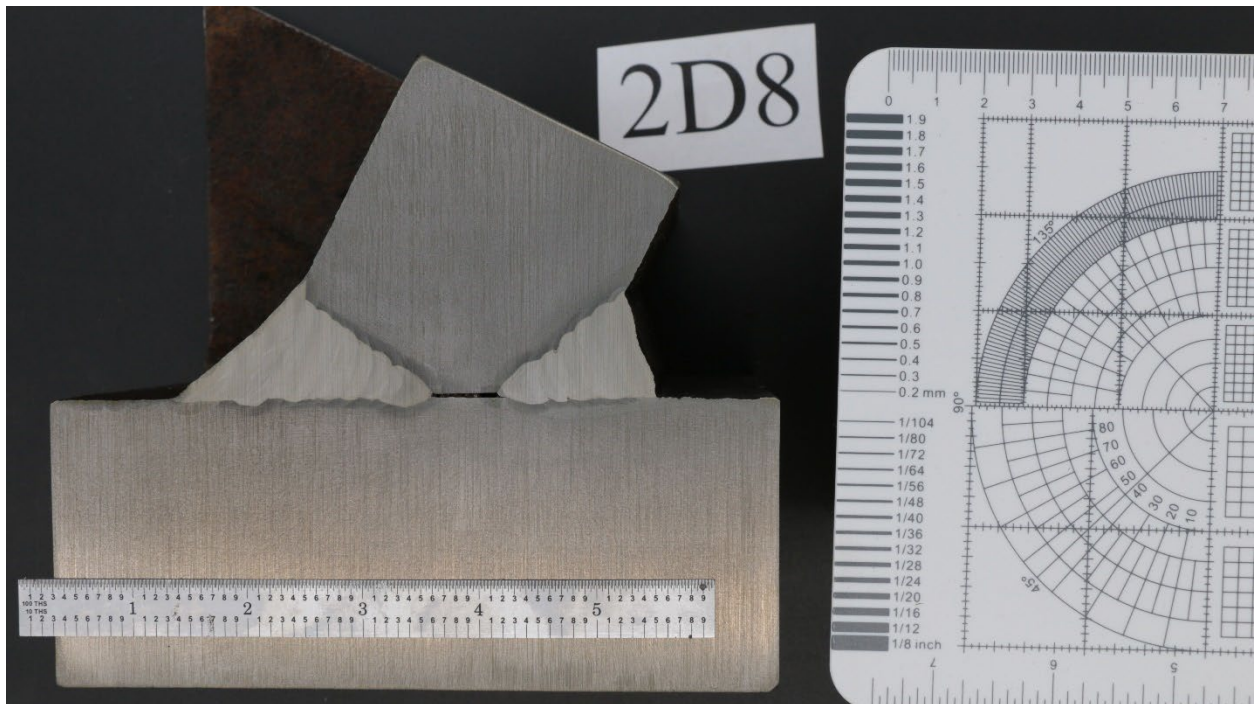


Figure G.14. Macroetch of 2D8 with planar reference scales.

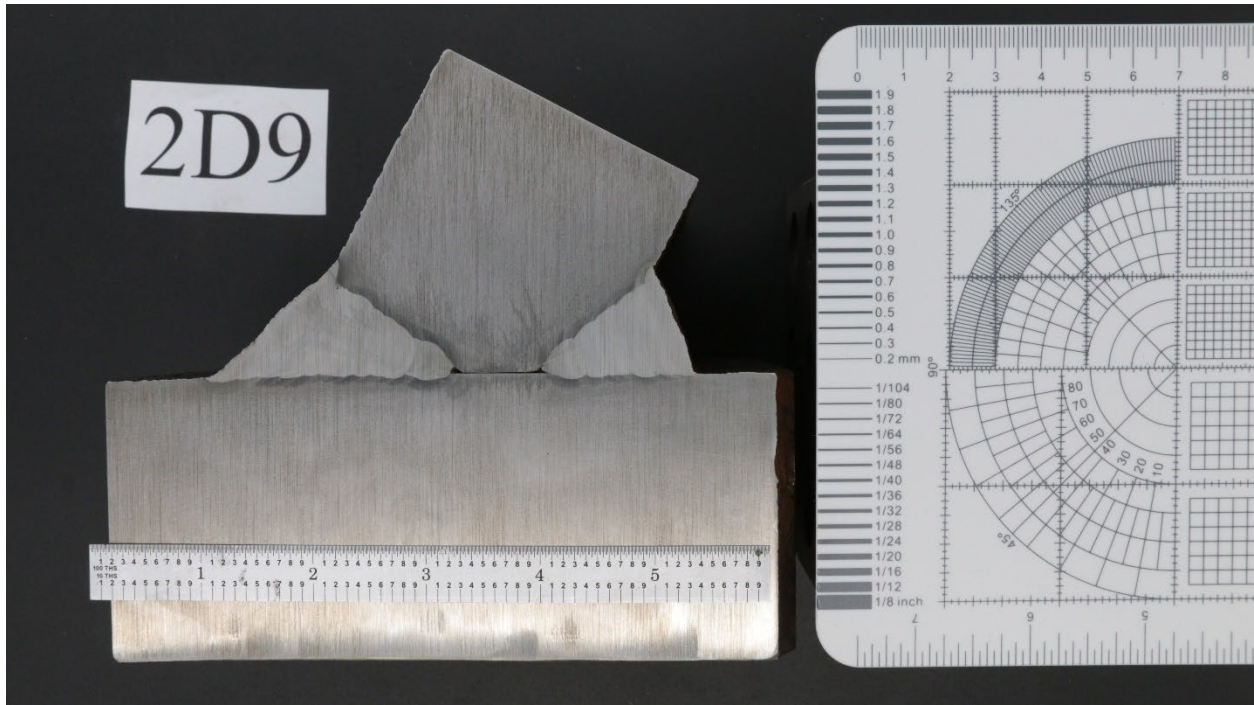


Figure G.15. Macroetch of 2D9 with planar reference scales.

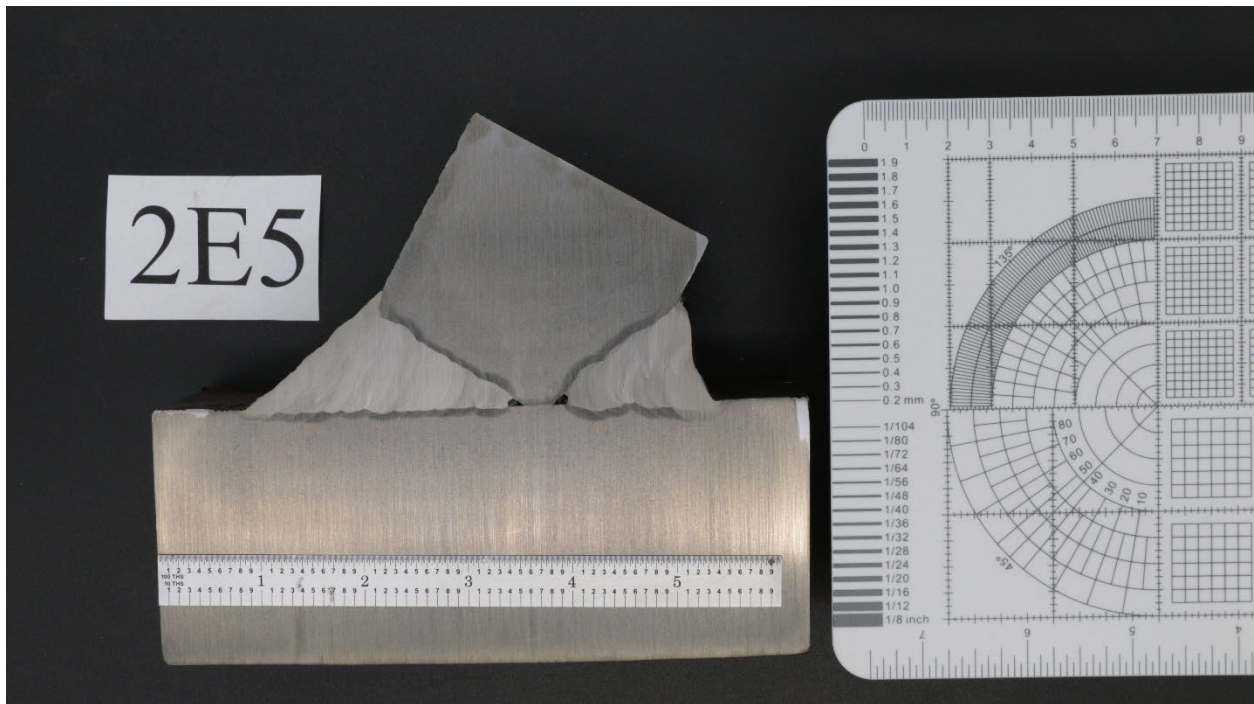


Figure G.16. Macroetch of 2E5 with planar reference scales.

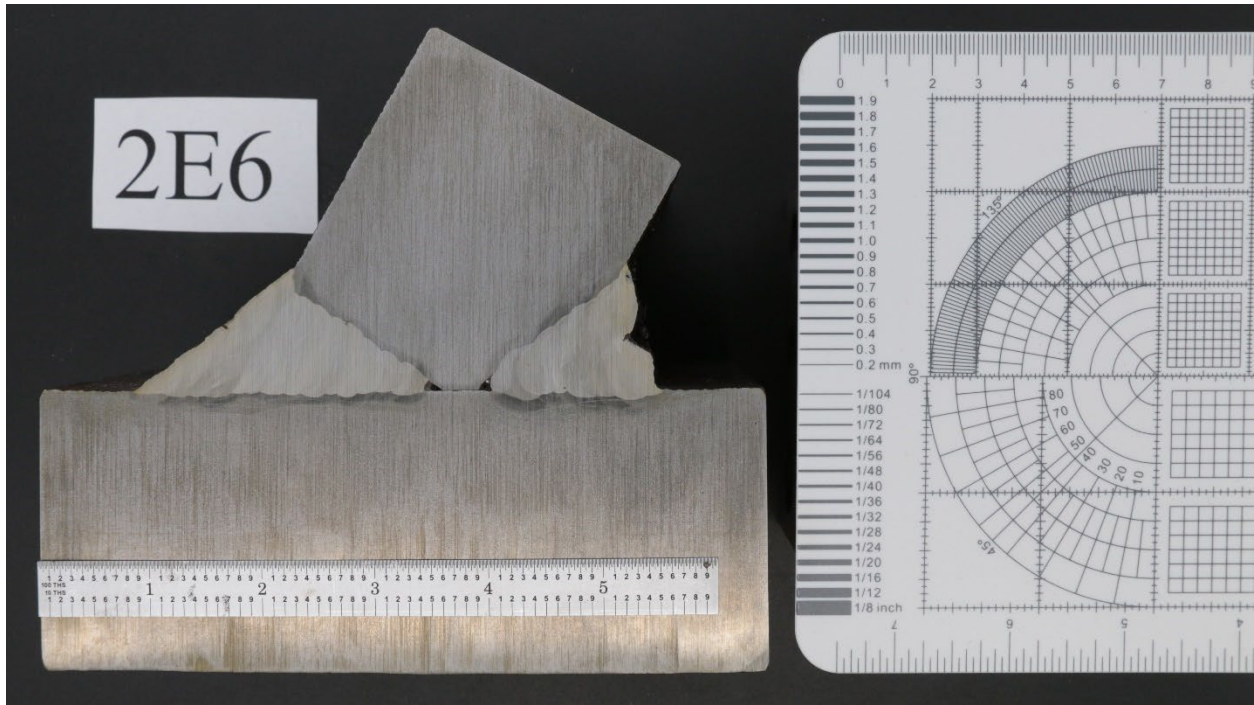


Figure G.17. Macroetch of 2E6 with planar reference scales.

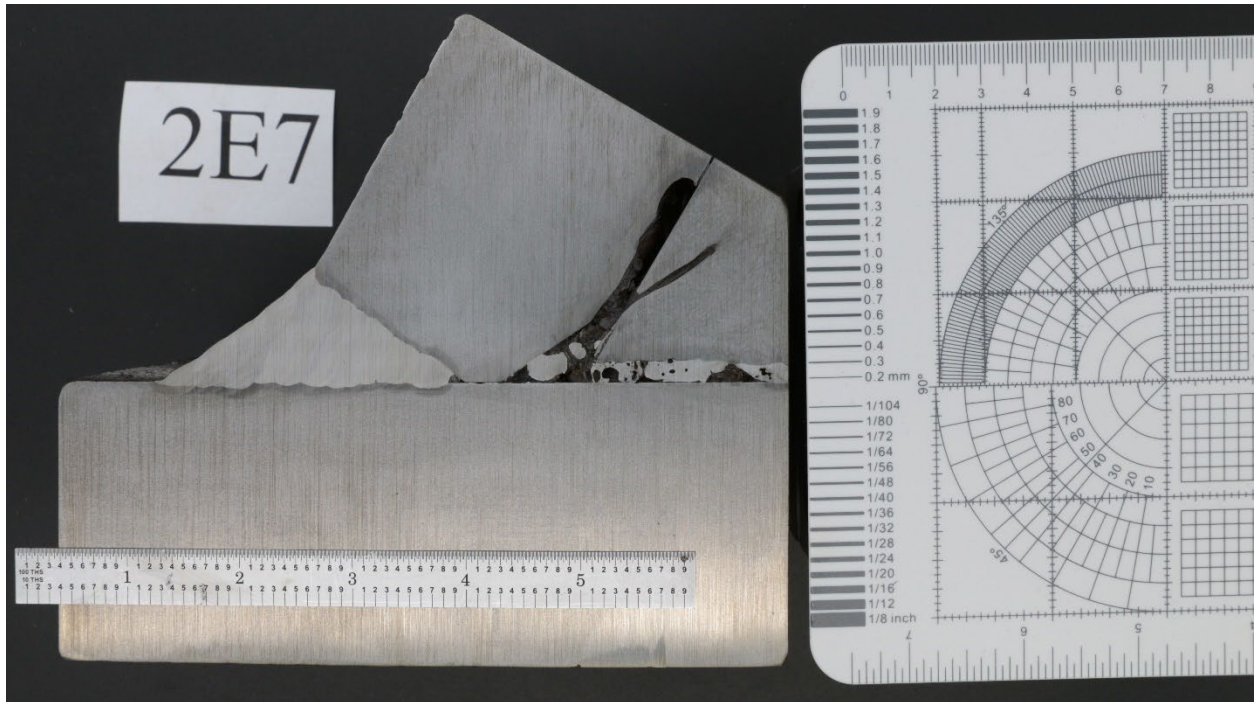


Figure G.18. Macroetch of 2E7 with planar reference scales.

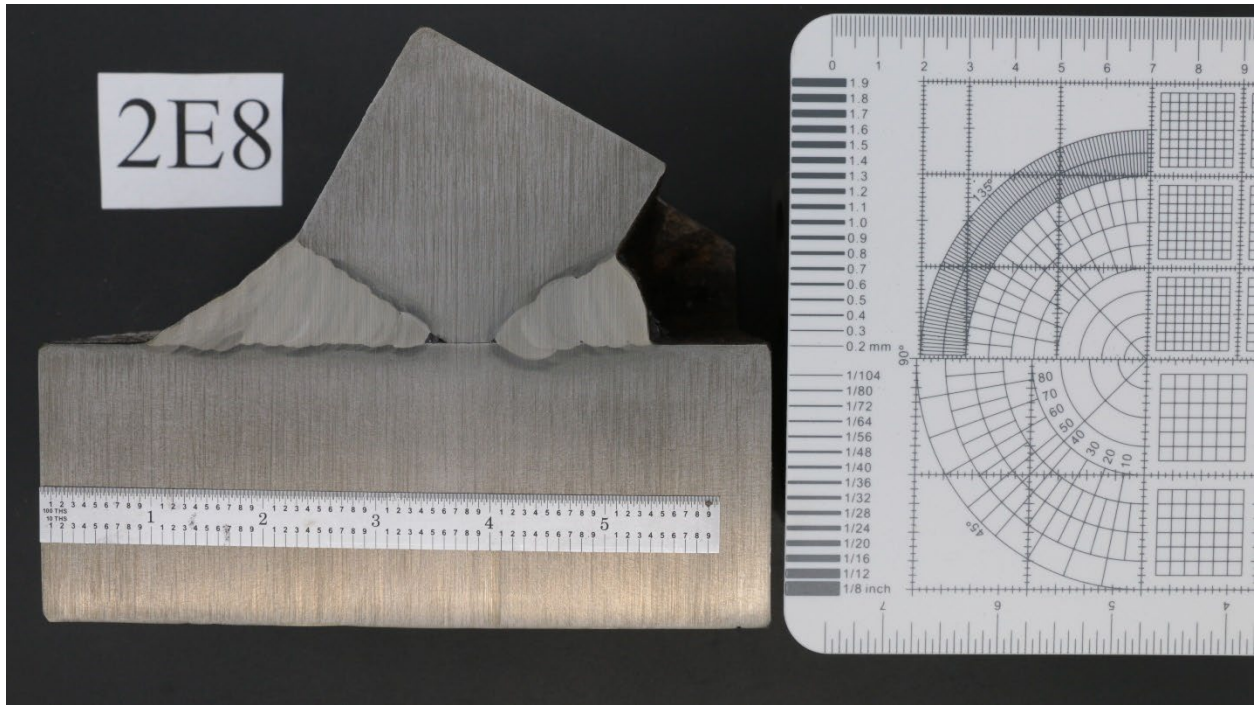


Figure G.19. Macroetch of 2E8 with planar reference scales.

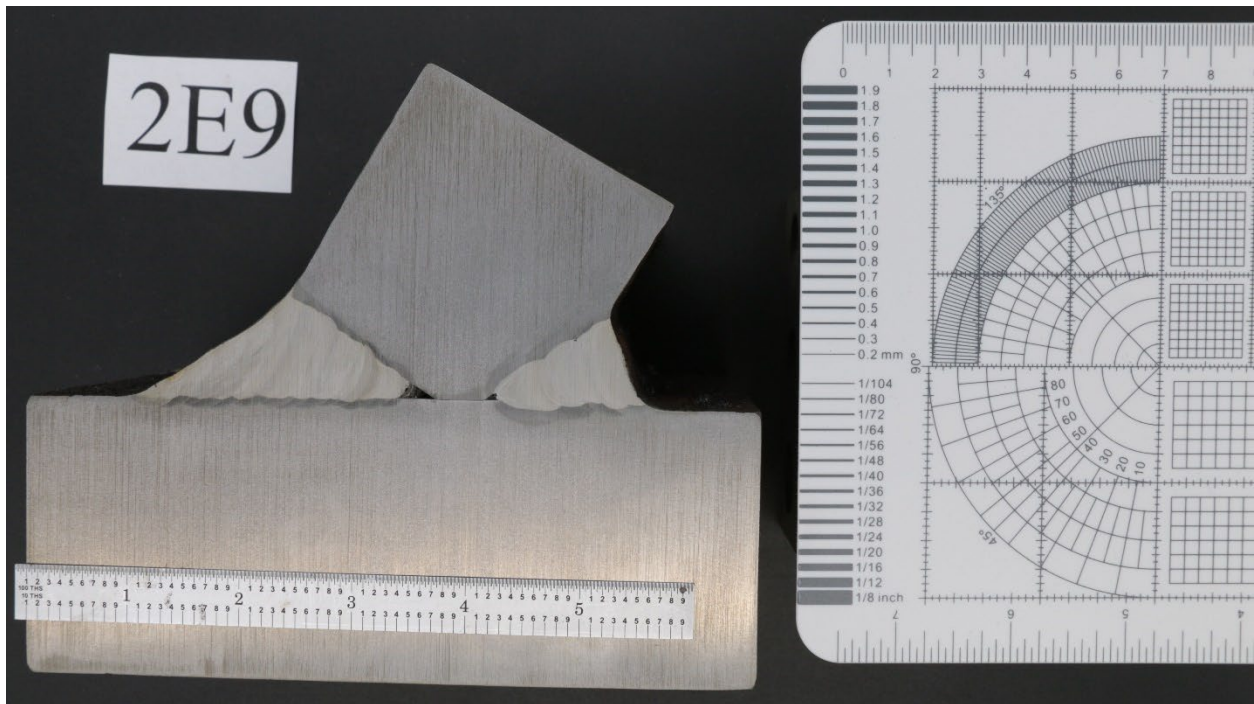


Figure G.20. Macroetch of 2E9 with planar reference scales.

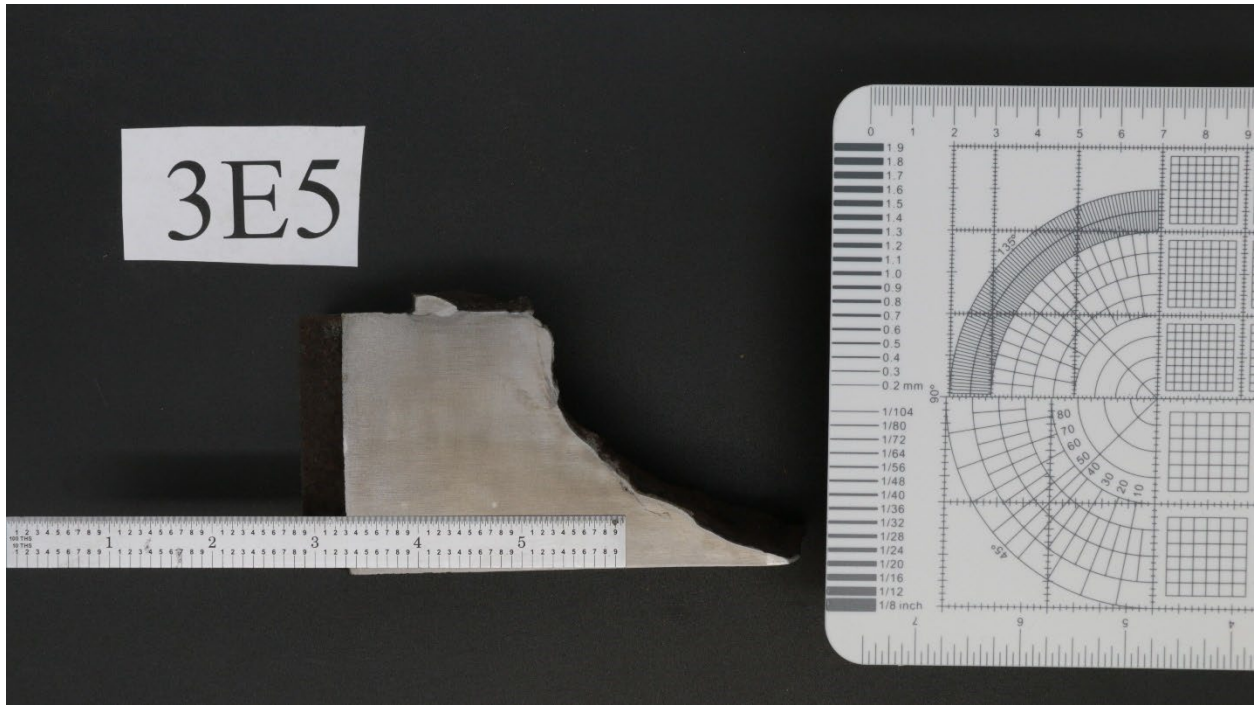


Figure G.31. Macroetch of 3E5 with planar reference scales.

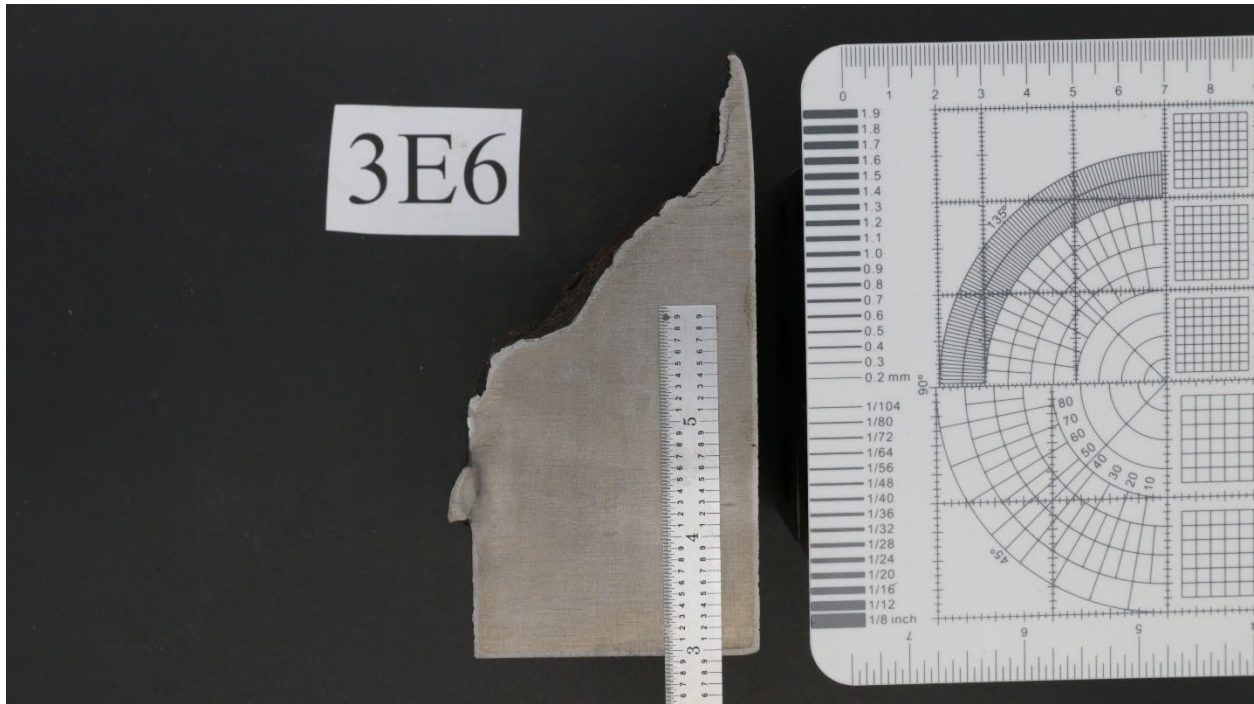


Figure G.32. Macroetch of 3E6 with planar reference scales, taken in the vertical position (90-degree planar rotation) for improved camera focus.

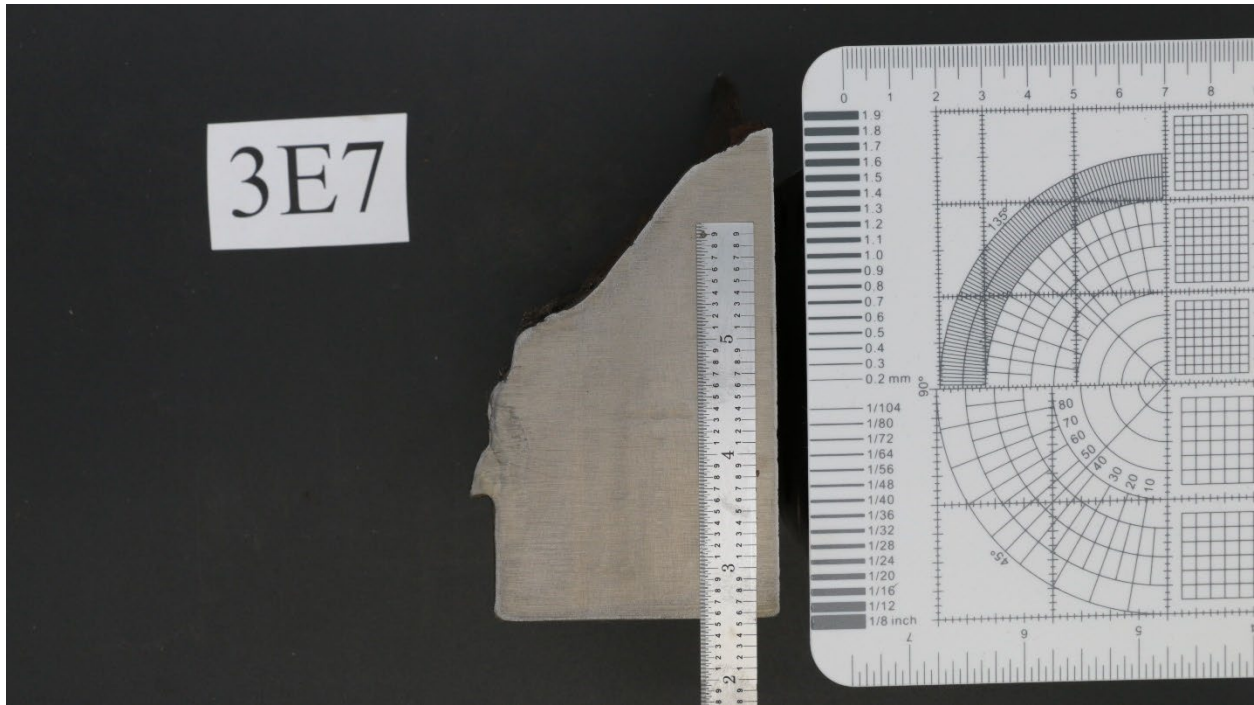


Figure G.33. Macroetch of 3E7 with planar reference scales, taken in the vertical position (90-degree planar rotation) for improved camera focus.



Figure G.34. Macroetch of 3E8 with planar reference scales. The right half of the specimen separated during preparation and is supported by a machined 1-2-3 block.



Figure G.35. Macroetch of 3E9 with planar reference scales.

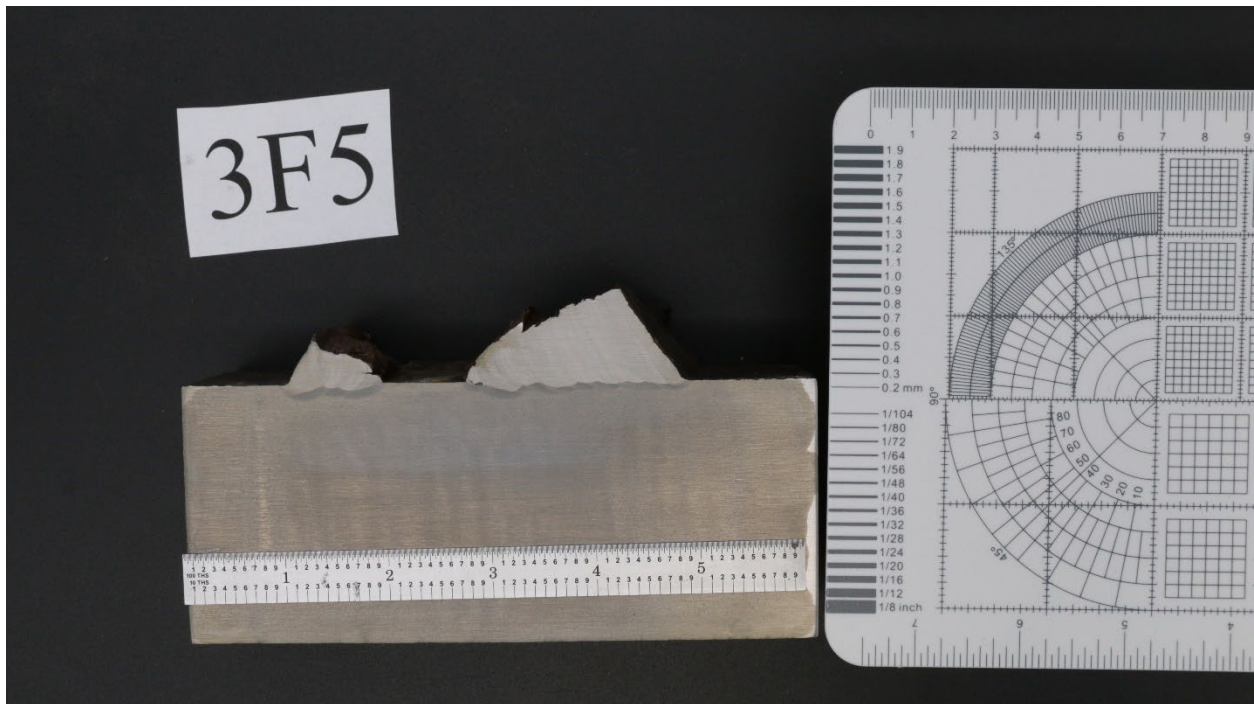


Figure G.36. Macroetch of 3F5 with planar reference scales.

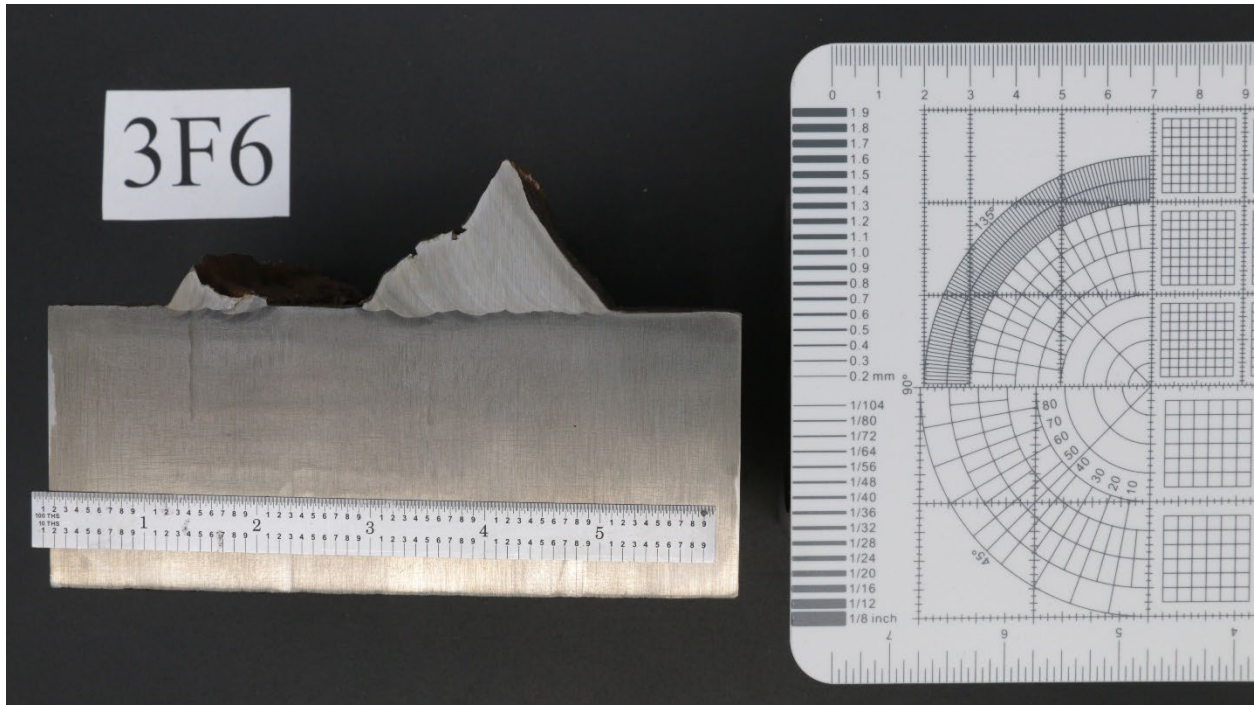


Figure G.37. Macroetch of 3F6 with planar reference scales.

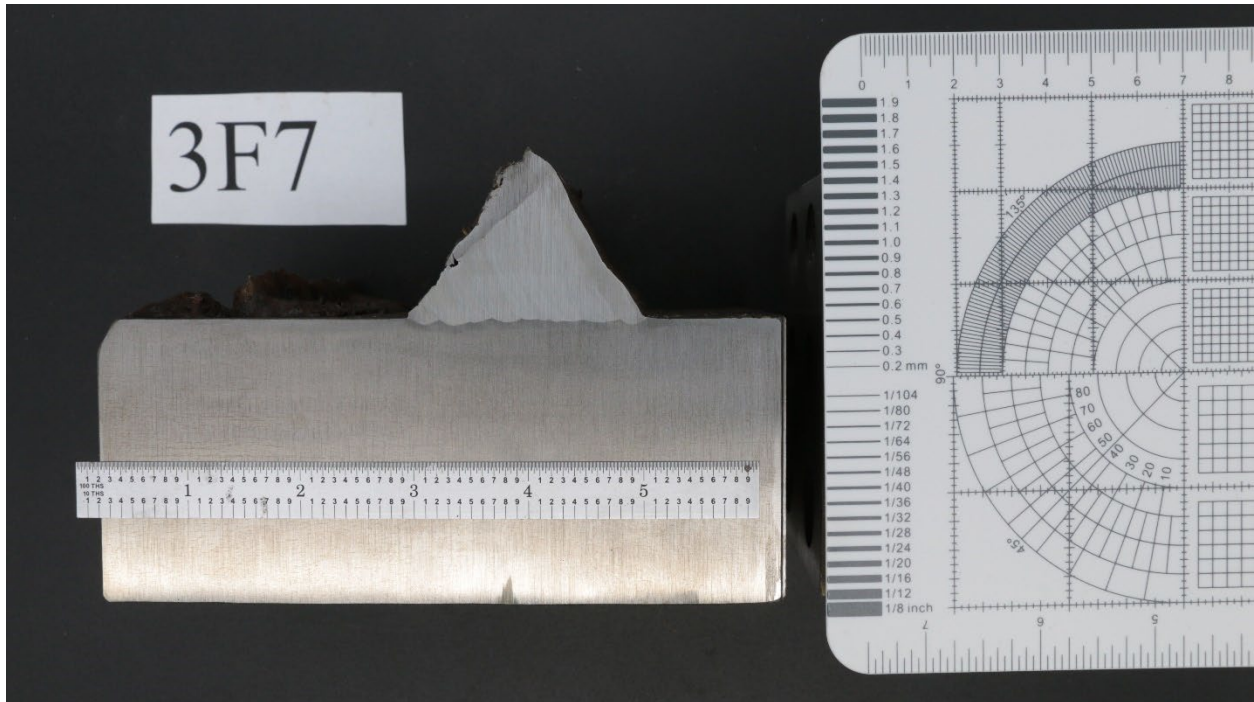


Figure G.38. Macroetch of 3F7 with planar reference scales.



Figure G.39. Macroetch of 3F8 with planar reference scales.

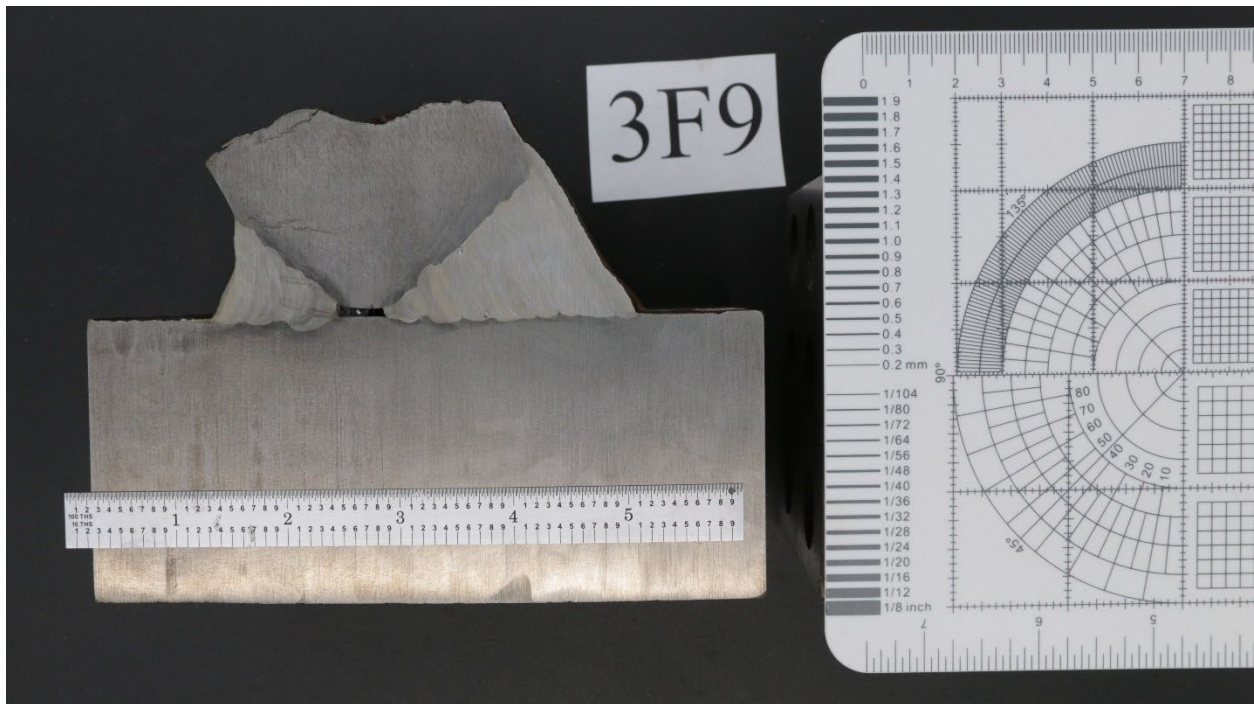


Figure G.40. Macroetch of 3F9 with planar reference scales.



Figure G.41. Macroetch of 4E5 with planar reference scales.

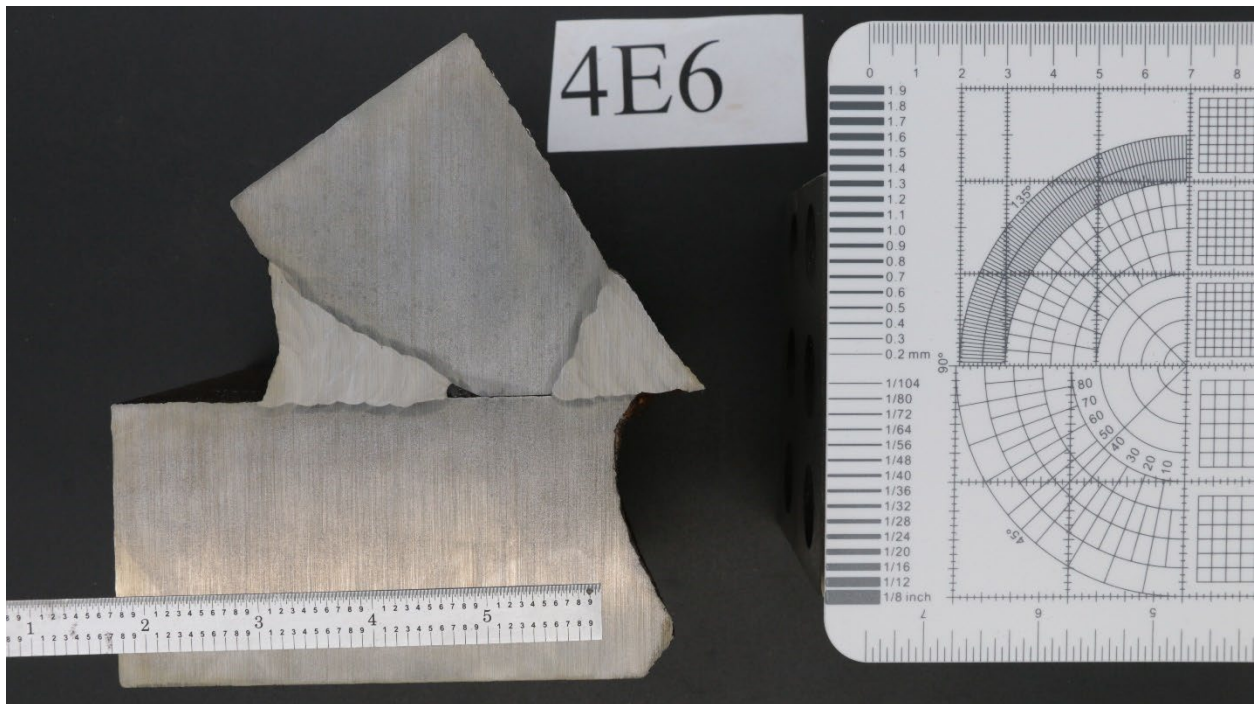


Figure G.42. Macroetch of 4E6 with planar reference scales.

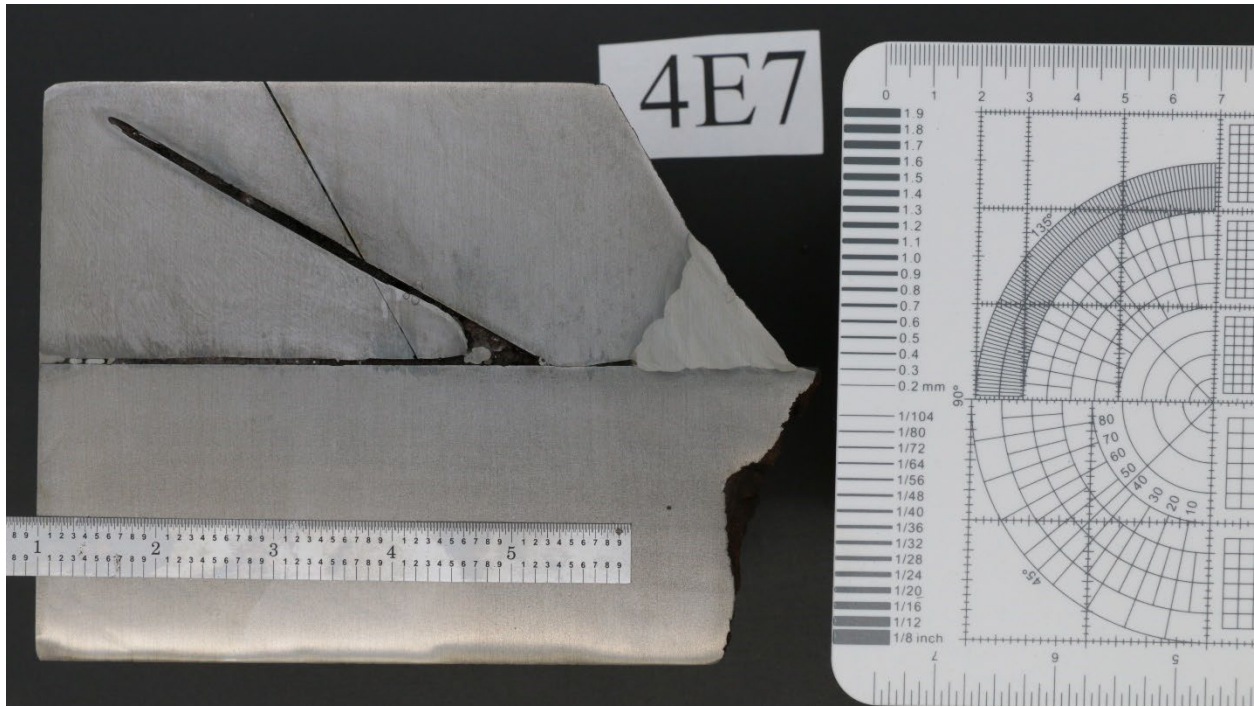


Figure G.43. Macroetch of 4E7 with planar reference scales.



Figure G.44. Macroetch of 4E8 with planar reference scales.

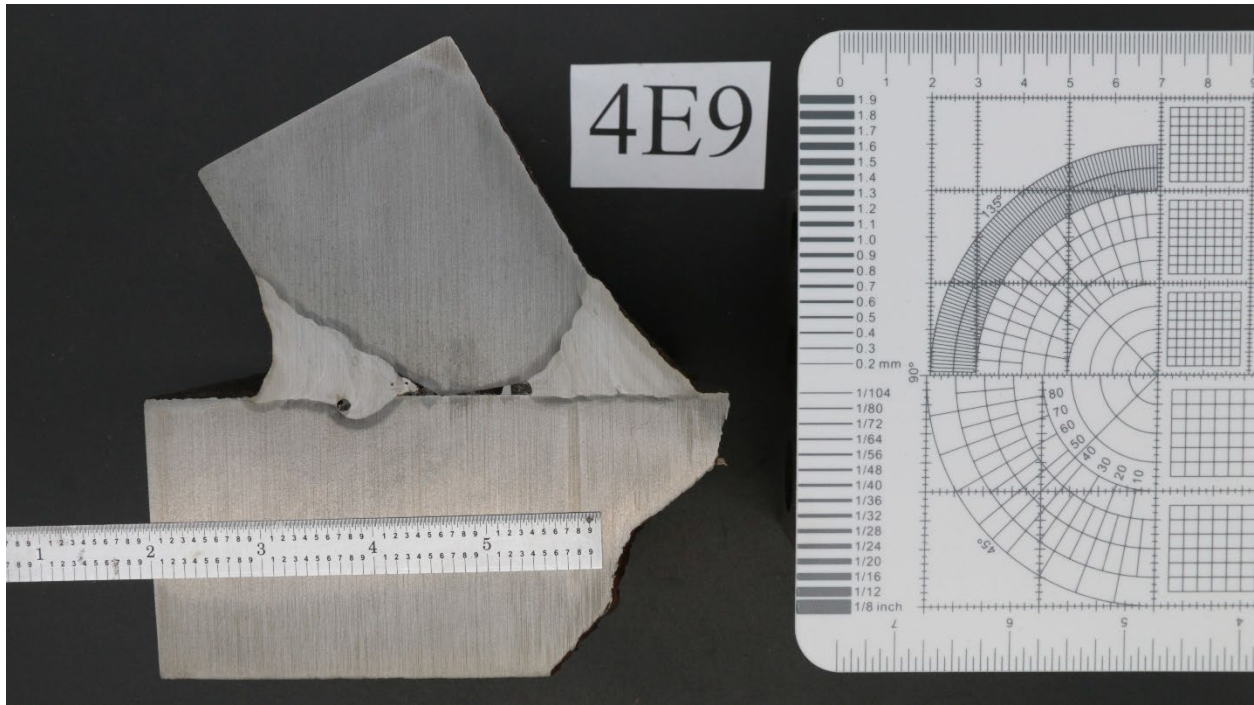


Figure G.45. Macroetch of 4E9 with planar reference scales.

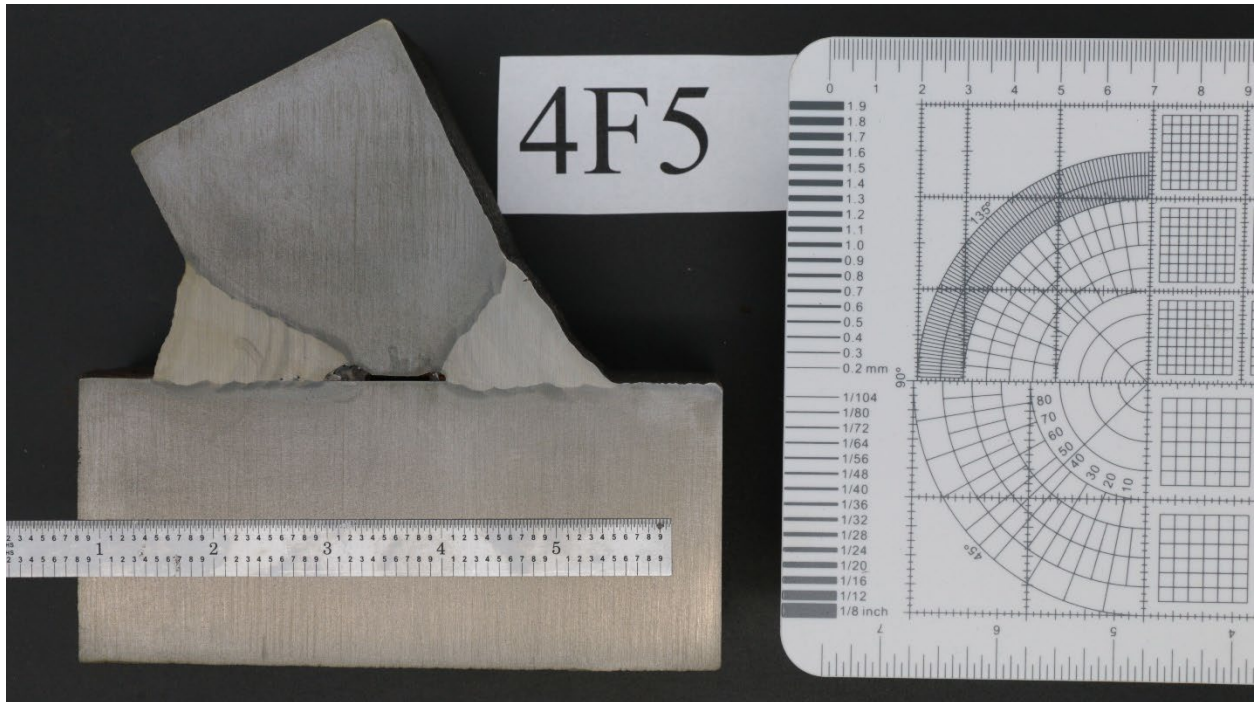


Figure G.46. Macroetch of 4F5 with planar reference scales.

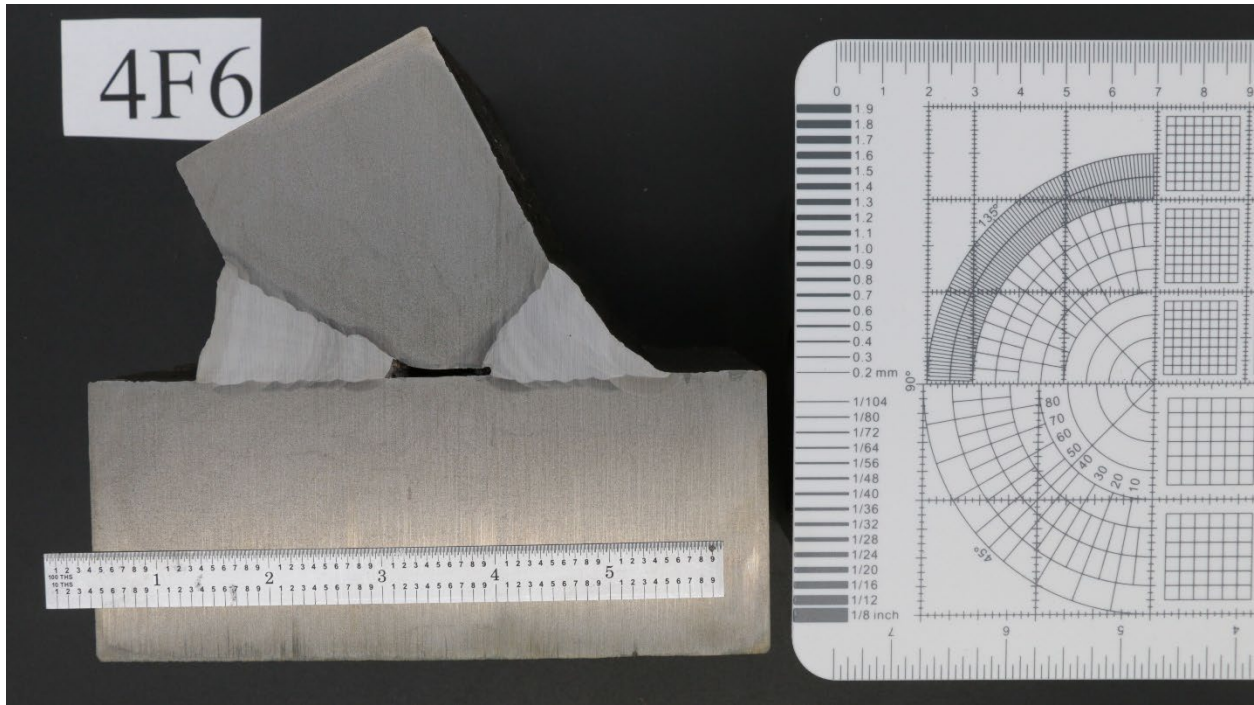


Figure G.47. Macroetch of 4F6 with planar reference scales.

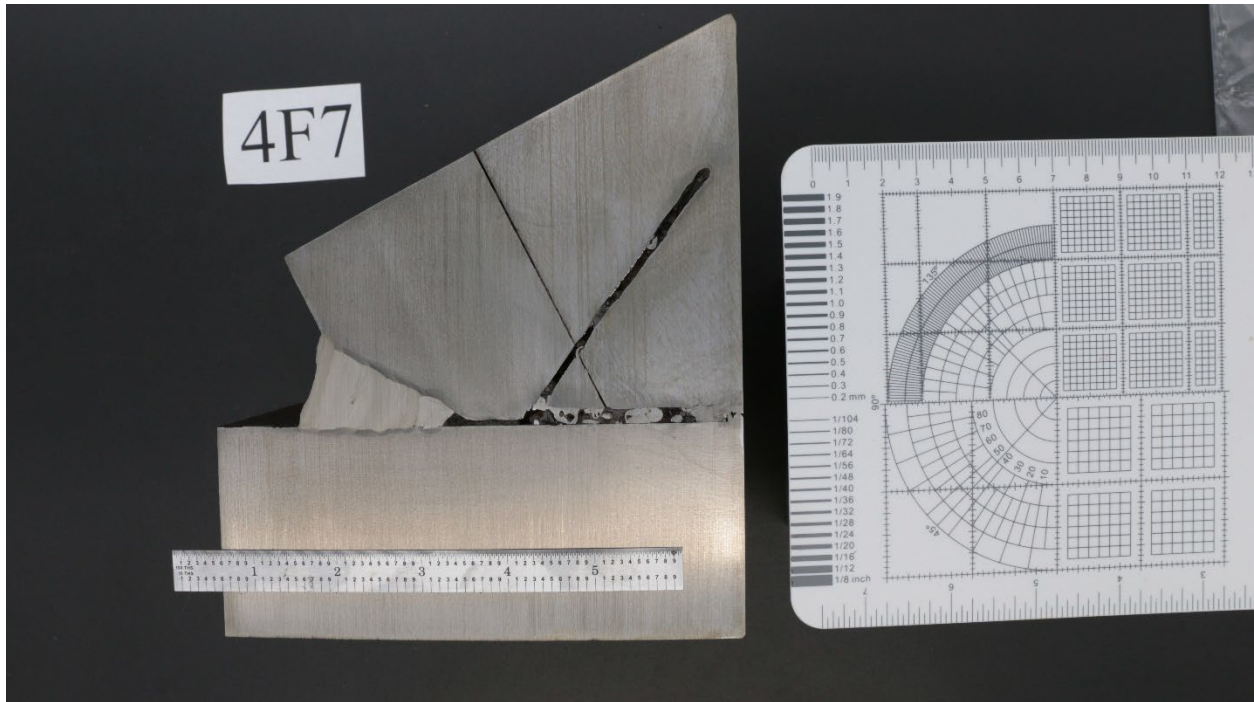


Figure G.48. Macroetch of 4F7 with planar reference scales.

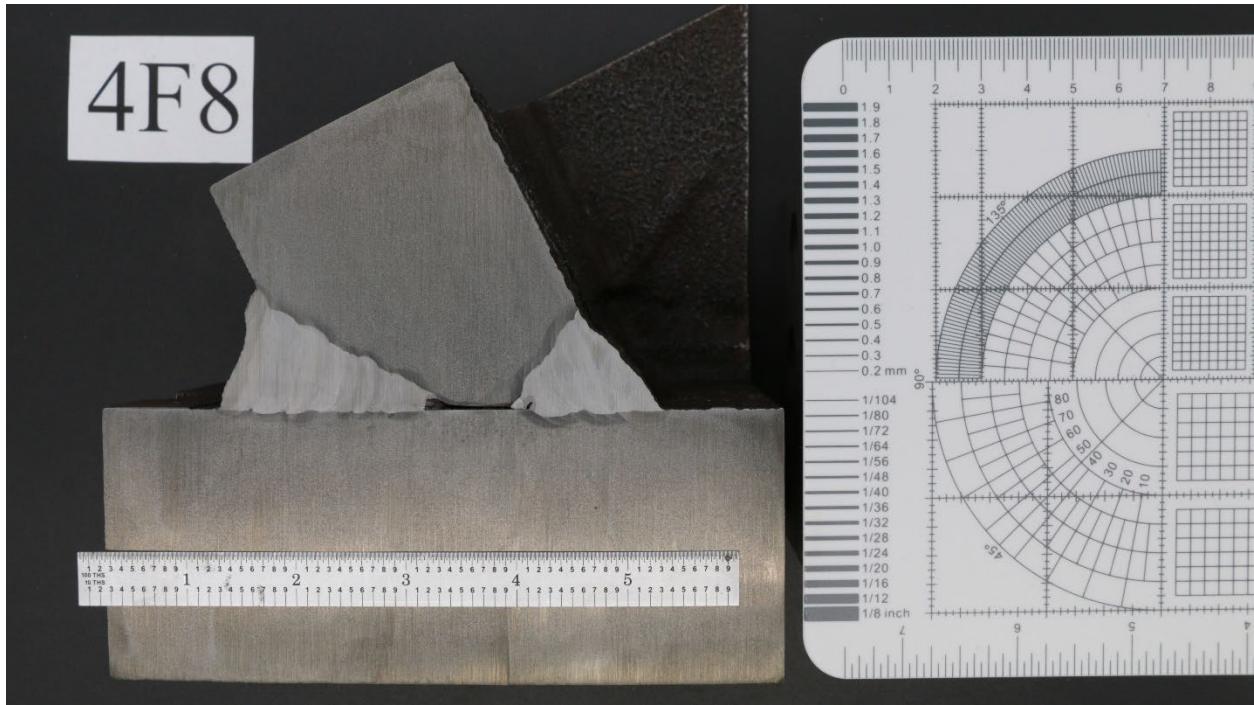


Figure G.49. Macroetch of 4F8 with planar reference scales.

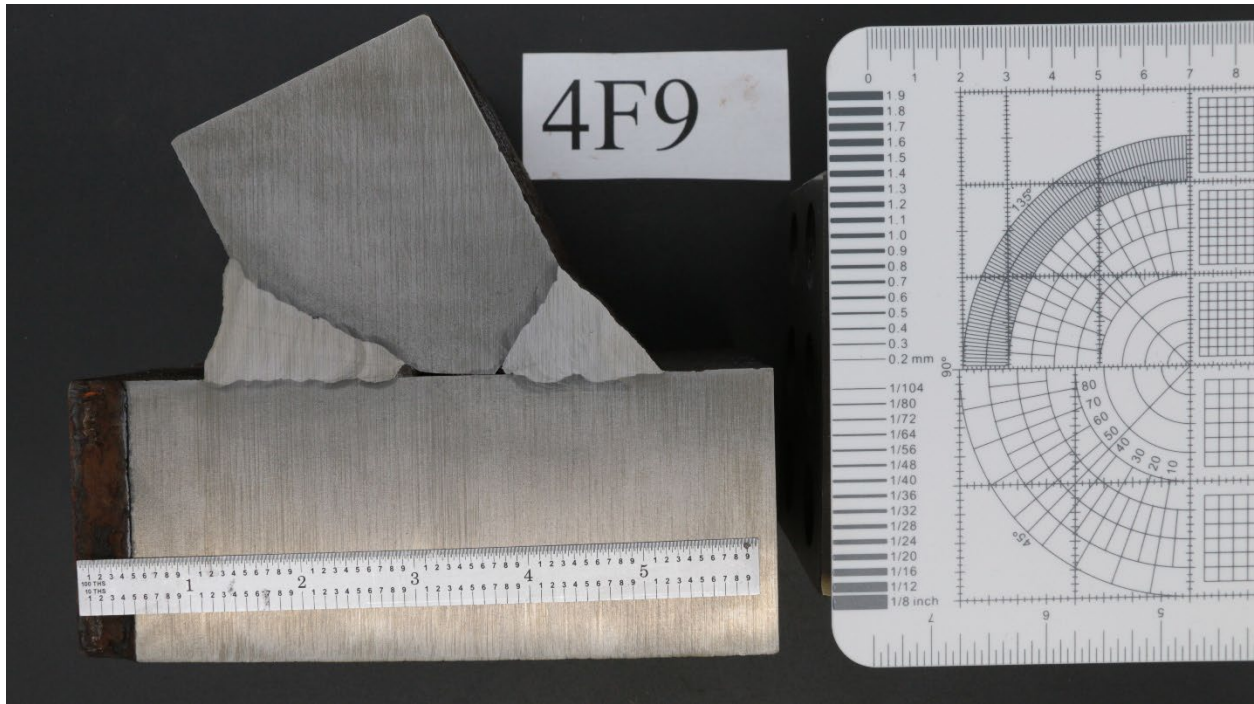


Figure G.50. Macroetch of 4F9 with planar reference scales.

Appendix H: Supporting Calibration, Service, and SRM Documentation



MTS Field Service



Customer Address:
6300 Georgetown Pike
McLean, VA 22101
US

MTS Systems Corporation
14000 Technology Drive
Eden Prairie, MN 55344-2290

Certificate of Calibration

Page: 1 of 3

Customer

Name: Federal Highway Administration
System ID: 222 MTS System No: US1_39341
Machine ID: 222 Location: Structures Lab

Certificate Number: 11210-319
Site: 505729
Country: US

Equipment

Device Type: Length Model: 244.51 Serial No.: 1029526
Device ID: LVDT Manufacturer: MTS Manufacture Date: None
Conditioner Model: 494.16 AC S2-J3A Serial No.: 2054484
Readout Device Model: 494.06 Serial No.: 2070160 Channel: Displacement

MTS Field Service is accredited by the American Association for Laboratory Accreditation (A2LA Cert. No. 1145.01). The basis for this accreditation is the international standard for calibration laboratories, ISO/IEC 17025 "General Requirements for the Competence of Testing and Calibration Laboratories". Defined and documented measurement assurance techniques or uncertainty analyses are used to verify the adequacy of the measurement processes.

Calibrations are performed with standards whose values and measurements are traceable to the International System of Units (SI) through a National Metrology Institute (NMI).

The results of this calibration relate only to the items calibrated. When parameter(s) are reported to be within specified tolerance(s), the measured value(s) shall fall within the appropriate specification limit and the uncertainty of the measured value(s) shall be stated.

CALIBRATION INFORMATION

As Found: In Tolerance Calibration Date: 09-Aug-2022
As Left: In Tolerance Calibration Due: 09-Aug-2023
Class: B
Calibration Procedure: FS-CA 2124 Rev. G ASTM E2309/E2309M-20
Full Scale Ranges: 3 in
Note: Return to zero errors are not included in the Classification Criteria.

STANDARDS USED FOR CALIBRATION

<u>MTS Asset Number</u>	<u>Manufacturer</u>	<u>Model Number</u>	<u>Description</u>	<u>Cal. Date</u>	<u>Cal. Due</u>
26928	Rotronic	HL-20D	Temp & Hum Meter	10-Aug-21	10-Aug-22
22355	MTS	MTS 1800	Displacement Calibrator	7-Jul-21	24-Aug-22

Performed by: [Redacted] Issued on: 9-Aug-22

ACS Version: 12.1

ACSRepRevBL



Calibration Report



Customer Name: Federal Highway Administration
System ID: 222 MTS System No: US1_39341
Machine ID: 222 Location: Structures Lab

Equipment

Device Type: Length Model: 244.51 Serial No.: 1029526
Device ID: LVDT Manufacturer: MTS Manufacture Date: None
Conditioner Model: 494.16 AC S2-J3A Serial No.: 2054484
Readout Device Model: 494.06 Serial No.: 2070160 Channel: Displacement

Procedure

MTS Procedure: FS-CA 2124 Rev. G ACS Version: 12.1
Calibration has been performed in accordance with: ASTM E2309/E2309M-20
Method of Verification: Follow-the-Displacement Method

Calibration Equipment Asset No.

Dead Weight Set: N/A Standard Asset No.: 22355
DW Compensation: N/A DMM: N/A Digital Indicator: N/A Lower Limit: N/A
Temperature Readout: 26928 Additional Equipment: N/A Standardizer: N/A

Conditions

Initial Temperature: 75 F Final Temperature: 75 F Bidirectional: N/A Cable Length: 30 Feet
Initial Humidity: 60 % Final Humidity: 60 % Polarity(+): Retraction

In Tolerance

X

As Found:

X

ASTM E2309 Classification: B

Out of Tolerance

As Adjusted:

As Found System Condition: Good

Conditioner Parameters

Total Gain: 1.21059 Fine zero: 0.0
Polarity: Normal Pre-amp gain: 0.9025
Excitation: 10.0 Volts Post-amp gain: 1.34137 Phase: 42.0 deg

Calibration Data

Range: 1
Extension Resolution: 0.00005 Full Scale: 3
Report Units: in

Applied Percent of Full Scale Length	Series 1		Series 1 Errors				Series 2		Series 2 Errors				Repeatability Percent Error	
	Indicated Reading Ascending	Indicated Reading Descending	Indicated Error Asc	Percent Error Asc	Units Error Desc	Percent Error Desc	Indicated Reading Ascending	Indicated Reading Descending	Units Error Asc	Percent Error Asc	Units Error Desc	Percent Error Desc	Asc	Desc
0	0.00005	0.00050	0.00005	0.00	-	-	0.00003	0.00012	0.00003	0.00	-	-	-	-
-2	-0.05927	-	-0.00074	-1.23	-	-	-0.05924	-	-0.00076	-1.26	-	-	0.03	-
-4	-0.11888	-	-0.00112	-0.93	-	-	-0.11896	-	-0.00104	-0.87	-	-	0.07	-
-6	-0.17853	-	-0.00147	-0.82	-	-	-0.17882	-	-0.00118	-0.66	-	-	0.16	-
-8	-0.23837	-	-0.00163	-0.68	-	-	-0.23857	-	-0.00143	-0.60	-	-	0.08	-
-10	-0.29831	-	-0.00169	-0.56	-	-	-0.29852	-	-0.00148	-0.49	-	-	0.07	-
-20	-0.59742	-	-0.00258	-0.43	-	-	-0.59778	-	-0.00222	-0.37	-	-	0.06	-
-40	-1.19760	-	-0.00240	-0.20	-	-	-1.19790	-	-0.00210	-0.17	-	-	0.03	-
-70	-2.08850	-	-0.01150	-0.55	-	-	-2.08880	-	-0.01120	-0.53	-	-	0.01	-
-100	-2.99380	-	-0.00620	-0.21	-	-	-2.99040	-	-0.00960	-0.32	-	-	0.11	-
-	-	-	-	-	-	-	-	-	-	-	-	-	-	-

Range: 1

Crosshead Start Position: N/A

Retraction

Applied Percent of Full Scale Length	Series 1		Series 1 Errors				Series 2		Series 2 Errors				Repeatability Percent Error	
	Indicated Reading Ascending	Indicated Reading Descending	Units Error Asc	Percent Error Asc	Units Error Desc	Percent Error Desc	Indicated Reading Ascending	Indicated Reading Descending	Units Error Asc	Percent Error Asc	Units Error Desc	Percent Error Desc	Asc	Desc
0	0.00002	-0.00002	0.00002	0.00	-	-	0.00007	0.00002	0.00007	0.00	-	-	-	-
2	0.05960	-	-0.00040	-0.67	-	-	0.05955	-	-0.00045	-0.76	-	-	0.08	-
4	0.11913	-	-0.00087	-0.72	-	-	0.11919	-	-0.00081	-0.68	-	-	0.05	-
6	0.17861	-	-0.00139	-0.77	-	-	0.17859	-	-0.00141	-0.78	-	-	0.01	-
8	0.23818	-	-0.00182	-0.76	-	-	0.23827	-	-0.00173	-0.72	-	-	0.04	-
10	0.29795	-	-0.00205	-0.68	-	-	0.29799	-	-0.00201	-0.67	-	-	0.01	-
20	0.59663	-	-0.00337	-0.56	-	-	0.59667	-	-0.00333	-0.56	-	-	0.01	-
40	1.19470	-	-0.00530	-0.44	-	-	1.19480	-	-0.00520	-0.43	-	-	0.01	-
70	2.09590	-	-0.00410	-0.20	-	-	2.09590	-	-0.00410	-0.20	-	-	0.00	-
100	2.99410	-	-0.00590	-0.20	-	-	2.99400	-	-0.00600	-0.20	-	-	0.00	-
-	-	-	-	-	-	-	-	-	-	-	-	-	-	-

Errors at Zero are computed in % of Range.

Table entries with a (-) are left intentionally blank.

Uncertainty of the calibration data supplied is equal to or less than the greater of, ±0.25% of reading or ±50µ inches, for a coverage factor of k=2 and an approximate confidence level of 95%.

This report shall not be reproduced except in full, without the written approval of the laboratory.

Out of Tolerance in % column

American Association of Laboratory Accreditation Certificate Number: 1145.01

Nothing to note at this time.

Performed By: [Redacted] Field Service Engineer

Date: 9-Aug-22

Signature: [Redacted]

Next Customer Agreed Upon Calibration Date: 9-Aug-23

ACSRepRevBL



MTS Field Service



Customer Address:
6300 Georgetown Pike
McLean, VA 22101
US

MTS Systems Corporation
14000 Technology Drive
Eden Prairie, MN 55344-2290

Certificate of Calibration

Page: 1 of 3

Customer

Name: Federal Highway Administration
System ID: 222 MTS System No: US1_39341
Machine ID: 222 Location: Structures Lab

Certificate Number: 11210-320
Site: 505729
Country: US

Equipment

Device Type: Force Model: 661.31E-01 Serial No.: 10295782
Device ID: Load Cell Manufacturer: MTS Manufacture Date: None
Conditioner Model: 494-26 DC S2-J4A Serial No.: 2124926
Readout Device Model: 494.06 Serial No.: 2070160 Channel: Force

MTS Field Service is accredited by the American Association for Laboratory Accreditation (A2LA Cert. No. 1145.01). The basis for this accreditation is the international standard for calibration laboratories, ISO/IEC 17025 "General Requirements for the Competence of Testing and Calibration Laboratories". Defined and documented measurement assurance techniques or uncertainty analyses are used to verify the adequacy of the measurement processes.

Calibrations are performed with standards whose values and measurements are traceable to the International System of Units (SI) through a National Metrology Institute (NMI). MTS Reference Force Transducers are calibrated in compliance with ASTM E74. The results of this calibration relate only to the items calibrated. When parameter(s) are reported to be within specified tolerance(s), the measured value(s) shall fall within the appropriate specification limit and the uncertainty of the measured value(s) shall be stated.

CALIBRATION INFORMATION

As Found: In Tolerance Calibration Date: 09-Aug-2022
As Left: In Tolerance Calibration Due: 09-Aug-2023
Tolerance: +/-1.0% of Applied Force
Calibration Procedure: FS-CA 2122 Rev. F ASTM E4-20
Full Scale Ranges: 200 kip
Note:

STANDARDS USED FOR CALIBRATION

<u>MTS Asset Number</u>	<u>Manufacturer</u>	<u>Model Number</u>	<u>Description</u>	<u>Cal. Date</u>	<u>Cal. Due</u>
26546	Interface	9840	mV/V Indicator	10-Aug-21	10-Aug-22
26928	Rotronic	HL-20D	Temp & Hum Meter	10-Aug-21	10-Aug-22
26545	Interface	CX-0220-1	Bridge Simulator	11-Aug-21	11-Aug-22
26585	Interface	2160EEA-220K	Load Cell	28-Feb-22	28-Feb-23

Performed by: [Redacted]

Issued on: 9-Aug-22

ACS Version: 12.1

ACSRepRevBL



Calibration Report



Customer Name: Federal Highway Administration
System ID: 222 MTS System No: US1_39341
Machine ID: 222 Location: Structures Lab

Equipment

Device Type: Force Model: 661.31E-01 Serial No.: 10295782
Device ID: Load Cell Manufacturer: MTS Manufacture Date: None
Conditioner Model: 494-26 DC S2-J4A Serial No.: 2124926
Readout Device Model: 494.06 Serial No.: 2070160 Channel: Force

Procedure

MTS Procedure: FS-CA 2122 Rev. F ACS Version: 12.1
Calibration has been performed in accordance with: ASTM E4-20
Method of Verification: Follow-the-Force Method using Elastic Calibration Devices

Calibration Equipment Asset No.

Dead Weight Set: N/A Standard Asset No.: 26585
DW Compensation: N/A DMM: N/A Digital Indicator: 26546 Lower Limit: 4 kip
Temperature Readout: 26928 Additional Equipment: N/A Standardizer: 26545

Conditions

Initial Temperature: 75 F Final Temperature: 75 F Bidirectional: N/A Cable Length: 30 Feet
Initial Humidity: 61 % Final Humidity: 60 % Polarity(+): Tension

In Tolerance **As Found:** **Maximum Relative Error:** -0.64 %
Out of Tolerance **As Adjusted:** **Tolerance: +/-1.0% of Applied Force**
As Found System Condition: Good

Conditioner Parameters

Total Gain: 465.2121 Fine zero: -0.094
Polarity: Normal Pre-amp gain: 285.98
Excitation: 9.171 Volts Post-amp gain: 1.62673

Calibration Data

Range: 1
Compression Resolution: 0.014 Full Scale: 200
Report Units: kip

Applied Percent of Full Scale Force	Series 1		Series 1 Errors				Series 2		Series 2 Errors				Repeatability Percent Error	
	Indicated Reading Ascending	Indicated Reading Descending	Indicated Error Asc	Percent Error Asc	Units Error Desc	Percent Error Desc	Indicated Reading Ascending	Indicated Reading Descending	Units Error Asc	Percent Error Asc	Units Error Desc	Percent Error Desc	Asc	Desc
0	-0.003	0.001	-0.003	0.00	-	-	0.000	0.001	0.000	0.00	-	-	-	-
-2	-3.979	-	-0.021	-0.52	-	-	-3.974	-	-0.026	-0.64	-	-	0.12	-
-4	-7.958	-	-0.042	-0.52	-	-	-7.957	-	-0.043	-0.53	-	-	0.01	-
-6	-11.940	-	-0.060	-0.50	-	-	-11.938	-	-0.062	-0.52	-	-	0.02	-
-8	-15.924	-	-0.076	-0.48	-	-	-15.926	-	-0.074	-0.46	-	-	0.01	-
-10	-19.901	-	-0.099	-0.50	-	-	-19.902	-	-0.098	-0.49	-	-	0.01	-
-20	-39.807	-	-0.193	-0.48	-	-	-39.814	-	-0.186	-0.47	-	-	0.02	-
-40	-79.651	-	-0.349	-0.44	-	-	-79.654	-	-0.346	-0.43	-	-	0.00	-
-70	-139.330	-	-0.670	-0.48	-	-	-139.330	-	-0.670	-0.48	-	-	0.00	-
-100	-198.910	-	-1.090	-0.54	-	-	-198.910	-	-1.090	-0.54	-	-	0.00	-
-	-	-	-	-	-	-	-	-	-	-	-	-	-	-

Range: 1

Tension

Applied Percent of Full Scale Force	Series 1		Series 1 Errors				Series 2		Series 2 Errors				Repeatability Percent Error	
	Indicated Reading Ascending	Indicated Reading Descending	Units Error Asc	Percent Error Asc	Units Error Desc	Percent Error Desc	Indicated Reading Ascending	Indicated Reading Descending	Units Error Asc	Percent Error Asc	Units Error Desc	Percent Error Desc	Asc	Desc
0	0.000	0.001	0.000	0.00	-	-	0.000	-0.001	0.000	0.00	-	-	-	-
2	3.983	-	-0.017	-0.42	-	-	3.984	-	-0.016	-0.40	-	-	0.03	-
4	7.972	-	-0.028	-0.35	-	-	7.964	-	-0.036	-0.45	-	-	0.10	-
6	11.957	-	-0.043	-0.36	-	-	11.950	-	-0.050	-0.42	-	-	0.06	-
8	15.943	-	-0.057	-0.36	-	-	15.939	-	-0.061	-0.38	-	-	0.02	-
10	19.926	-	-0.074	-0.37	-	-	19.933	-	-0.067	-0.33	-	-	0.03	-
20	39.998	-	-0.002	0.00	-	-	39.995	-	-0.005	-0.01	-	-	0.01	-
40	80.066	-	0.066	0.08	-	-	80.061	-	0.061	0.08	-	-	0.01	-
70	140.260	-	0.260	0.19	-	-	140.260	-	0.260	0.19	-	-	0.00	-
100	200.460	-	0.460	0.23	-	-	200.460	-	0.460	0.23	-	-	0.00	-
-	-	-	-	-	-	-	-	-	-	-	-	-	-	-

Errors at Zero are computed in % of Range.

Table entries with a (-) are left intentionally blank.

Uncertainty of the data supplied is equal to or less than ±0.25% of reading for a coverage factor of k=2 and an approximate confidence level of 95%.

This report shall not be reproduced except in full, without the written approval of the laboratory.

 Out of Tolerance in % column

MTS Reference Force Transducers are temperature compensated over the range of use.

American Association of Laboratory Accreditation Certificate Number: 1145.01

Nothing to note at this time.

Performed By: XXXXXXXXXX Field Service Engineer

Date: 9-Aug-22

Signature: XXXXXXXXXX

Next Customer Agreed Upon Calibration Date: 9-Aug-23

ACSRepRevBL



MTS Field Service



Customer Address:
6300 Georgetown Pike
McLean, VA 22101
US

MTS Systems Corporation
14000 Technology Drive
Eden Prairie, MN 55344-2290

Certificate of Calibration

Page: 1 of 3

Customer

Name: Federal Highway Administration
System ID: 100279394 MTS System No: 311.41_550Kip
Machine ID: 10441081 Location: Federal Highway

Certificate Number: 11210-366
Site: 505729
Country: US

Equipment

Device Type: Length Model: 311.41 Serial No.: 10438863
Device ID: LVDT Manufacturer: MTS Manufacture Date: None
Conditioner Model: 494.16 AC S2-J1A Serial No.: 9022586
Readout Device Model: 494.06 Serial No.: 9025058 Channel: Displacement

MTS Field Service is accredited by the American Association for Laboratory Accreditation (A2LA Cert. No. 1145.01). The basis for this accreditation is the international standard for calibration laboratories, ISO/IEC 17025 "General Requirements for the Competence of Testing and Calibration Laboratories". Defined and documented measurement assurance techniques or uncertainty analyses are used to verify the adequacy of the measurement processes.

Calibrations are performed with standards whose values and measurements are traceable to the International System of Units (SI) through a National Metrology Institute (NMI).

The results of this calibration relate only to the items calibrated. When parameter(s) are reported to be within specified tolerance(s), the measured value(s) shall fall within the appropriate specification limit and the uncertainty of the measured value(s) shall be stated.

CALIBRATION INFORMATION

As Found: In Tolerance Calibration Date: 28-Oct-2022
As Left: In Tolerance Calibration Due: 28-Oct-2023
Class: C
Calibration Procedure: FS-CA 2124 Rev. G ASTM E2309/E2309M-20
Full Scale Ranges: 6 in
Note: Return to zero errors are not included in the Classification Criteria.

STANDARDS USED FOR CALIBRATION

<u>MTS Asset Number</u>	<u>Manufacturer</u>	<u>Model Number</u>	<u>Description</u>	<u>Cal. Date</u>	<u>Cal. Due</u>
26928	Rotronic	HL-20D	Temp & Hum Meter	23-Aug-22	23-Aug-23
23112	MTS	MTS 1800	Displacement Calibrator	22-Aug-22	22-Dec-23

Performed by: ██████████ Issued on: 28-Oct-22

ACS Version: 12.1



Calibration Report



Customer Name: Federal Highway Administration
System ID: 100279394 MTS System No: 311.41_550Kip
Machine ID: 10441081 Location: Federal Highway

Equipment

Device Type: Length Model: 311.41 Serial No.: 10438863
Device ID: LVDT Manufacturer: MTS Manufacture Date: None
Conditioner Model: 494.16 AC S2-J1A Serial No.: 9022586
Readout Device Model: 494.06 Serial No.: 9025058 Channel: Displacement

Procedure

MTS Procedure: FS-CA 2124 Rev. G ACS Version: 12.1
Calibration has been performed in accordance with: ASTM E2309/E2309M-20
Method of Verification: Follow-the-Displacement Method

Calibration Equipment Asset No.

Dead Weight Set: N/A Standard Asset No.: 23112
DW Compensation: N/A DMM: N/A Digital Indicator: N/A Lower Limit: N/A
Temperature Readout: 26928 Additional Equipment: N/A Standardizer: N/A

Conditions

Initial Temperature: 62 F Final Temperature: 65 F Bidirectional: N/A Cable Length: 15 Feet
Initial Humidity: 42 % Final Humidity: 40 % Polarity(+): Retraction

In Tolerance

X

As Found:

X

ASTM E2309 Classification: C

Out of Tolerance

As Adjusted:

As Found System Condition: Good

Conditioner Parameters

Total Gain: 2.37968 Fine zero: 0.0
Polarity: Normal Pre-amp gain: 0.9025
Excitation: 10.0 Volts Post-amp gain: 2.63677 Phase: 67.0 deg

Calibration Data

Range: 1
Extension Resolution: 0.00012 Full Scale: 6
Report Units: In

Applied Percent of Full Scale Length	Series 1		Series 1 Errors				Series 2		Series 2 Errors				Repeatability Percent Error	
	Indicated Reading Ascending	Indicated Reading Descending	Indicated Error Asc	Percent Error Asc	Units Error Desc	Percent Error Desc	Indicated Reading Ascending	Indicated Reading Descending	Units Error Asc	Percent Error Asc	Units Error Desc	Percent Error Desc	Asc	Desc
0	-0.00010	0.00179	-0.00010	0.00	-	-	-0.00002	0.00041	-0.00002	0.00	-	-	-	-
-2	-0.12041	-	0.00041	0.34	-	-	-0.12066	-	0.00066	0.55	-	-	0.21	-
-4	-0.24132	-	0.00132	0.55	-	-	-0.24156	-	0.00156	0.65	-	-	0.10	-
-6	-0.36334	-	0.00334	0.93	-	-	-0.36356	-	0.00356	0.99	-	-	0.06	-
-8	-0.48557	-	0.00557	1.16	-	-	-0.48579	-	0.00579	1.21	-	-	0.05	-
-10	-0.60616	-	0.00616	1.03	-	-	-0.60639	-	0.00639	1.06	-	-	0.04	-
-20	-1.20770	-	0.00770	0.64	-	-	-1.20750	-	0.00750	0.62	-	-	0.02	-
-40	-2.40860	-	0.00860	0.36	-	-	-2.40840	-	0.00840	0.35	-	-	0.01	-
-70	-4.20430	-	0.00430	0.10	-	-	-4.20430	-	0.00430	0.10	-	-	0.00	-
-100	-6.00420	-	0.00420	0.07	-	-	-6.00440	-	0.00440	0.07	-	-	0.00	-
-	-	-	-	-	-	-	-	-	-	-	-	-	-	-

Range: 1

Crosshead Start Position: N/A

Retraction

Applied Percent of Full Scale Length	Series 1		Series 1 Errors				Series 2		Series 2 Errors				Repeatability Percent Error	
	Indicated Reading Ascending	Indicated Reading Descending	Units Error Asc	Percent Error Asc	Units Error Desc	Percent Error Desc	Indicated Reading Ascending	Indicated Reading Descending	Units Error Asc	Percent Error Asc	Units Error Desc	Percent Error Desc	Asc	Desc
0	0.00034	-0.00213	0.00034	0.01	-	-	0.00002	-0.00107	0.00002	0.00	-	-	-	-
2	0.12116	-	0.00116	0.97	-	-	0.12103	-	0.00103	0.86	-	-	0.11	-
4	0.24198	-	0.00198	0.83	-	-	0.24200	-	0.00200	0.83	-	-	0.01	-
6	0.36304	-	0.00304	0.84	-	-	0.36325	-	0.00325	0.90	-	-	0.06	-
8	0.48361	-	0.00361	0.75	-	-	0.48370	-	0.00370	0.77	-	-	0.02	-
10	0.60299	-	0.00299	0.50	-	-	0.60297	-	0.00297	0.50	-	-	0.00	-
20	1.20750	-	0.00750	0.62	-	-	1.20760	-	0.00760	0.63	-	-	0.01	-
40	2.40950	-	0.00950	0.40	-	-	2.40910	-	0.00910	0.38	-	-	0.02	-
70	4.20890	-	0.00890	0.21	-	-	4.20890	-	0.00890	0.21	-	-	0.00	-
100	6.01340	-	0.01340	0.22	-	-	6.01380	-	0.01380	0.23	-	-	0.01	-
-	-	-	-	-	-	-	-	-	-	-	-	-	-	-

Errors at Zero are computed in % of Range.

Table entries with a (-) are left intentionally blank.

Uncertainty of the calibration data supplied is equal to or less than the greater of, ±0.25% of reading or ±50µ inches, for a coverage factor of k=2 and an approximate confidence level of 95%.

This report shall not be reproduced except in full, without the written approval of the laboratory.

Out of Tolerance in % column

American Association of Laboratory Accreditation Certificate Number: 1145.01

Nothing to note at this time.

Performed By: [Redacted]

Field Service Engineer

Date: 28-Oct-22

Signature: [Redacted]

Next Customer Agreed Upon Calibration Date: 28-Oct-23

ACSRepRevBL



MTS Field Service



Customer Address:
6300 Georgetown Pike
McLean, VA 22101
US

MTS Systems Corporation
14000 Technology Drive
Eden Prairie, MN 55344-2290

Certificate of Calibration

Page: 1 of 3

Customer

Name: Federal Highway Administration
System ID: 100279394 MTS System No: 311.41_550Kip
Machine ID: 10441081 Location: Federal Highway

Certificate Number: 11210-367
Site: 505729
Country: US

Equipment

Device Type: Force Model: 661.36D-03 Serial No.: 10436789
Device ID: Load Cell Manufacturer: MTS Manufacture Date: None
Conditioner Model: 494.26 DC S2-J2A Serial No.: 9033379
Readout Device Model: 494.06 Serial No.: 9025058 Channel: Force

MTS Field Service is accredited by the American Association for Laboratory Accreditation (A2LA Cert. No. 1145.01). The basis for this accreditation is the international standard for calibration laboratories, ISO/IEC 17025 "General Requirements for the Competence of Testing and Calibration Laboratories". Defined and documented measurement assurance techniques or uncertainty analyses are used to verify the adequacy of the measurement processes.

Calibrations are performed with standards whose values and measurements are traceable to the International System of Units (SI) through a National Metrology Institute (NMI). MTS Reference Force Transducers are calibrated in compliance with ASTM E74. The results of this calibration relate only to the items calibrated. When parameter(s) are reported to be within specified tolerance(s), the measured value(s) shall fall within the appropriate specification limit and the uncertainty of the measured value(s) shall be stated.

CALIBRATION INFORMATION

As Found: In Tolerance Calibration Date: 28-Oct-2022
As Left: In Tolerance Calibration Due: 28-Oct-2023
Tolerance: +/-1.0% of Applied Force
Calibration Procedure: FS-CA 2122 Rev. G ASTM E4-20
Full Scale Ranges: 500 kip
Note:

STANDARDS USED FOR CALIBRATION

<u>MTS Asset Number</u>	<u>Manufacturer</u>	<u>Model Number</u>	<u>Description</u>	<u>Cal. Date</u>	<u>Cal. Due</u>
26546	Interface	9840	mV/V Indicator	22-Aug-22	22-Aug-23
26928	Rotronic	HL-20D	Temp & Hum Meter	23-Aug-22	23-Aug-23
26545	Interface	CX-0220-1	Bridge Simulator	22-Aug-22	22-Aug-23
18329	StrainSense	SST105U	Load Cell	9-Feb-21	9-Dec-22

Performed by: [REDACTED]

Issued on: 28-Oct-22

ACS Version: 12.1



Calibration Report



Customer Name: Federal Highway Administration
System ID: 100279394 MTS System No: 311.41_550Kip
Machine ID: 10441081 Location: Federal Highway

Equipment

Device Type: Force Model: 661.36D-03 Serial No.: 10436789
Device ID: Load Cell Manufacturer: MTS Manufacture Date: None
Conditioner Model: 494.26 DC S2-J2A Serial No.: 9033379
Readout Device Model: 494.06 Serial No.: 9025058 Channel: Force

Procedure

MTS Procedure: FS-CA 2122 Rev. G ACS Version: 12.1
Calibration has been performed in accordance with: ASTM E4-20
Method of Verification: Follow-the-Force Method using Elastic Calibration Devices

Calibration Equipment Asset No.

Dead Weight Set: N/A Standard Asset No.: 18329
DW Compensation: N/A DMM: N/A Digital Indicator: 26546 Lower Limit: 20 kip
Temperature Readout: 26928 Additional Equipment: N/A Standardizer: 26545

Conditions

Initial Temperature: 67 F Final Temperature: 68 F Bidirectional: N/A Cable Length: 15 Feet
Initial Humidity: 40 % Final Humidity: 41 % Polarity(+): Tension

In Tolerance **As Found:** **Maximum Relative Error:** 0.45 %
Out of Tolerance **As Adjusted:** **Tolerance: +/-1.0% of Applied Force**
As Found System Condition: Good

Conditioner Parameters

Total Gain: 436.85962 Fine zero: 0.064 Shunt Cal (+): 426.4661 Kip
Polarity: Normal Pre-amp gain: 285.98
Excitation: 10.0 Volts Post-amp gain: 1.52759

Calibration Data

Range: 1
Compression Resolution: 0.012 Full Scale: 500
Report Units: kip

Applied Percent of Full Scale Force	Series 1		Series 1 Errors				Series 2		Series 2 Errors				Repeatability Percent Error	
	Indicated Reading Ascending	Indicated Reading Descending	Indicated Error Asc	Percent Error Asc	Units Error Desc	Percent Error Desc	Indicated Reading Ascending	Indicated Reading Descending	Units Error Asc	Percent Error Asc	Units Error Desc	Percent Error Desc	Asc	Desc
0	-0.017	0.000	-0.017	0.00	-	-	-0.023	0.001	-0.023	0.00	-	-	-	-
-4	-20.089	-	0.089	0.45	-	-	-20.079	-	0.079	0.40	-	-	0.05	-
-6	-30.098	-	0.098	0.33	-	-	-30.098	-	0.098	0.33	-	-	0.00	-
-8	-40.122	-	0.122	0.31	-	-	-40.077	-	0.077	0.19	-	-	0.11	-
-10	-50.110	-	0.110	0.22	-	-	-50.111	-	0.111	0.22	-	-	0.00	-
-20	-100.170	-	0.170	0.17	-	-	-100.140	-	0.140	0.14	-	-	0.03	-
-40	-200.080	-	0.080	0.04	-	-	-200.090	-	0.090	0.04	-	-	0.00	-
-70	-349.680	-	-0.320	-0.09	-	-	-349.670	-	-0.330	-0.09	-	-	0.00	-
-100	-498.940	-	-1.060	-0.21	-	-	-498.900	-	-1.100	-0.22	-	-	0.01	-
-	-	-	-	-	-	-	-	-	-	-	-	-	-	-
-	-	-	-	-	-	-	-	-	-	-	-	-	-	-

Range: 1

Tension

Applied Percent of Full Scale Force	Series 1		Series 1 Errors				Series 2		Series 2 Errors				Repeatability Percent Error	
	Indicated Reading Ascending	Indicated Reading Descending	Units Error Asc	Percent Error Asc	Units Error Desc	Percent Error Desc	Indicated Reading Ascending	Indicated Reading Descending	Units Error Asc	Percent Error Asc	Units Error Desc	Percent Error Desc	Asc	Desc
0	0.007	0.002	0.007	0.00	-	-	0.012	-0.002	0.012	0.00	-	-	-	-
4	20.062	-	0.062	0.31	-	-	20.053	-	0.053	0.26	-	-	0.05	-
6	30.107	-	0.107	0.36	-	-	30.065	-	0.065	0.22	-	-	0.14	-
8	40.151	-	0.151	0.38	-	-	40.127	-	0.127	0.32	-	-	0.06	-
10	50.175	-	0.175	0.35	-	-	50.154	-	0.154	0.31	-	-	0.04	-
20	100.290	-	0.290	0.29	-	-	100.290	-	0.290	0.29	-	-	0.00	-
40	200.620	-	0.620	0.31	-	-	200.570	-	0.570	0.29	-	-	0.02	-
70	351.250	-	1.250	0.36	-	-	351.180	-	1.180	0.34	-	-	0.02	-
100	502.060	-	2.060	0.41	-	-	501.980	-	1.980	0.40	-	-	0.02	-
-	-	-	-	-	-	-	-	-	-	-	-	-	-	-
-	-	-	-	-	-	-	-	-	-	-	-	-	-	-

Errors at Zero are computed in % of Range.

Table entries with a (-) are left intentionally blank.

Uncertainty of the data supplied is equal to or less than ±0.25% of reading for a coverage factor of k=2 and an approximate confidence level of 95%.

This report shall not be reproduced except in full, without the written approval of the laboratory.

 Out of Tolerance in % column

MTS Reference Force Transducers are temperature compensated over the range of use.

American Association of Laboratory Accreditation Certificate Number: 1145.01

Nothing to note at this time.

Performed By: XXXXXXXXXX

Field Service Engineer

Date: 28-Oct-22

Signature: XXXXXXXXXX

Next Customer Agreed Upon Calibration Date: 28-Oct-23

ACSRepRevBL



UNITED STATES DEPARTMENT OF COMMERCE
National Institute of Standards and Technology
325 Broadway
Boulder, CO 80305-3337

August 31, 2022

██████████
Genex Systems / Turner Fairbank Highway Research Center
6300 Georgetown Pike, Structures Laboratory TO-130
McLean, Virginia 22101
USA

Dear ██████████:

Charpy verification specimens tested on the 406.7 J (300.0 ft-lbf) capacity Tinius Olsen Machine, Serial No. 195892, have been received for evaluation along with the completed questionnaire. We have analyzed the results (see attached table) and find that the average values fall within the acceptable ranges at all the energy levels tested, in accordance with the current ASTM E23 standard. The following paragraphs describe further analysis of the questionnaire, the test results, and the fractured specimens.

This machine satisfies the indirect verification requirements of the current ASTM E23 standard from an absorbed energy level of 8.5 J (6.3 ft-lbf) to 80 % of the maximum capacity of the machine.

Enclosed is a Charpy Verification Sticker to attach to your machine.

If the machine is moved or undergoes any major repairs or adjustments, this verification becomes invalid and the machine must be rechecked (see ASTM E23). If a specimen stops the pendulum during a test, the machine should be checked to assure that the pendulum is straight, the anvils and striker have not been damaged, and that all bolts are still tight.

If you have any questions concerning the verification of your machine, you may contact me by phone at +1-303-497-3351, by fax at +1-303-497-5939, or by email at charpy@boulder.nist.gov.

Sincerely,

██████████
██████████

Applied Chemicals & Materials Division

3 Enclosures

National Institute of Standards and Technology
 Applied Chemicals & Materials Division
 325 Broadway, Boulder, CO 80305-3328

Facility: Genex Systems / Turner Fairbank Highway Research Center, 6300 Georgetown Pike, Structures Laboratory TO-130
 Mclean, Virginia 22101 USA

Machine Manufacturer: Tinius Olsen Serial Number: 195892

Test Date: 8/31/2022

Reference Standard: ASTM E23

SERIES NUMBER	PT* Code	CLIENT VALUES					UNITS	AVERAGE (J)		DIFFERENCE	RESULT
		1	2	3	4	5		CLIENT	NIST		
Low LL-187	100315	17.0	16.3	12.9	16.3	15.6	J	15.6	15.2	0.4 J	Pass
High HH-180	100316	84.7	84.1	86.1	81.4	85.4	J	84.3	80.6	4.6%	Pass
Super-High SH-60H	100317	211.5	208.8	207.4	202.0	210.2	J	208.0	204.2	1.9%	Pass

Allowable difference is 1.4 J or 5 %, whichever is greater.

* Proficiency Test (PT) results for your data are available online. To access the PT data, you need to go to the [PT website](#) and enter the Series Number and PT Code for each energy level of interest.

Additional Information

The information contained in Table 1 can be used to compute the uncertainty for a new material tested in your laboratory using the procedure outlined in NIST SP 960-18 [1].

See also: <https://www.nist.gov/programs-projects/nist-impact-verification-program>.

Table 1. Summary statistics for SRM materials and customer's verification test result.

Series Number	Client Statistics					NIST SRM Statistics			
	Client Average \bar{V} (J)	Standard Deviation S_V (J)	Number of Tests n_V	$S_V / \sqrt{n_V}$ (J)	Degrees Of Freedom df_V	Certified Reference Value R (J)	Combined Uncertainty $u(R)$ (J)	Degrees Of Freedom df_R	Expanded Uncertainty U (J)
LL-187	15.6	1.59	5	0.71	4	15.2	0.119	68	0.238
HH-180	84.3	1.83	5	0.82	4	80.6	0.217	72	0.432
SH-60H	208.0	3.66	5	1.64	4	204.2	0.535	104	1.06

The fifth column, labeled $S_V / \sqrt{n_V}$, is the uncertainty of the verification test mean, \bar{V} , if there are no additional sources of systematic error that need to be included. It is the customer's responsibility to determine the final uncertainty of \bar{V} .

The expanded uncertainty of the NIST reference value (U), corresponding to a 95 % uncertainty interval, is based on a coverage factor from the Student's t distribution with df_R degrees of freedom. The expanded uncertainties include sources of error in the measurement and testing process at NIST, and are not the expanded uncertainties of the individual verification specimens or the uncertainties of tests performed in your laboratory.

Reference

- [1] Splett, J. D., McCowan, C. N., Iyer, H. K., Wang, C.-M., "NIST Recommended Practice Guide: Computing Uncertainty for Charpy Impact Machine Test Results," NIST Special Publication 960-18, September, 2007 (available at: https://www.nist.gov/sites/default/files/documents/mml/acmd/structural_materials/SP9602-18Final-2.pdf).

NIST Charpy Verification Sticker

This machine meets the indirect verification requirements of the current ASTM Standard E23

Machine Serial Number: 195892

Verification Date: August 31, 2022

Range of Verification: *From 8.5 J (6.3 ft-lbf) to 80% of the machine capacity*

Signature:



, Charpy Program Coordinator
National Institute of Standards and Technology



UNITED STATES DEPARTMENT OF COMMERCE
National Institute of Standards and Technology
325 Broadway
Boulder, CO 80305-3337

August 31, 2022

██████████
Genex Systems / Turner Fairbank Highway Research Center
6300 Georgetown Pike, Structures Laboratory TO-130
McLean, Virginia 22101
USA

Dear ██████████:

Charpy verification specimens tested on the 406.7 J (300.0 ft-lbf) capacity Tinius Olsen Machine, Serial No. 195892, have been received for evaluation along with the completed questionnaire. We have analyzed the results (see attached table) and find that they satisfy the requirements of the current ISO 148-2 standard. The following paragraphs describe further analysis of the questionnaire, the test results, and the fractured specimens.

This machine satisfies the indirect verification requirements of the current ISO 148-2 Standard at the energy levels tested.

Enclosed is a Charpy Verification Sticker to attach to your machine.

If the machine is moved or undergoes any major repairs or adjustments, this verification becomes invalid and the machine must be rechecked (ISO 148-2). If a specimen stops the pendulum during a test, the machine should be checked to assure that the pendulum is straight, the anvils and striker have not been damaged, and that all bolts are still tight.

If you have any questions concerning the verification of your machine, you may contact me by phone at +1-303-497-3351, by fax at +1-303-497-5939, or by email at charpy@boulder.nist.gov.

Sincerely,

██████████
██████████
██████████

Applied Chemicals & Materials Division

3 Enclosures

National Institute of Standards and Technology
 Applied Chemicals & Materials Division
 325 Broadway, Boulder, CO 80305-3328

Facility: Genex Systems / Turner Fairbank Highway Research Center, 6300 Georgetown Pike, Structures Laboratory TO-130
 Mclean, Virginia 22101 USA

Machine Manufacturer: Tinius Olsen Serial Number: 195892

Test Date: 8/31/2022

Reference Standard: ISO 148-2

SERIES NUMBER	CLIENT VALUES					UNITS	AVERAGE (J)		BIAS	REPEATABILITY	RESULT
	1	2	3	4	5		CLIENT	NIST			
Low LL-187	17.0	16.3	12.9	16.3	15.6	J	15.6	15.2	0.4 J	4.1	Pass
High HH-180	84.7	84.1	86.1	81.4	85.4	J	84.3	80.6	4.6%	5.88%	Pass
Super High SH-60H	211.5	208.8	207.4	202.0	210.2	J	208.0	204.2	1.9%	4.65%	Pass

Allowable bias is 4 J or 10 %, whichever is greater; allowable repeatability is 6 J or 15 %, whichever is greater (ISO Standard 148-2).

Additional Information

The information contained in Table 1 can be used to compute the uncertainty for a new material tested in your laboratory using the procedure outlined in NIST SP 960-18 [1].

See also: <https://www.nist.gov/programs-projects/nist-impact-verification-program>.

Table 1. Summary statistics for SRM materials and customer's verification test result.

Series Number	Client Statistics					NIST SRM Statistics			
	Client Average \bar{V} (J)	Standard Deviation S_V (J)	Number of Tests n_V	$S_V / \sqrt{n_V}$ (J)	Degrees Of Freedom df_V	Certified Reference Value R (J)	Combined Uncertainty $u(R)$ (J)	Degrees Of Freedom df_R	Expanded Uncertainty U (J)
LL-187	15.6	1.59	5	0.71	4	15.2	0.119	68	0.238
HH-180	84.3	1.83	5	0.82	4	80.6	0.217	72	0.432
SH-60H	208.0	3.66	5	1.64	4	204.2	0.535	104	1.06

The fifth column, labeled $S_V / \sqrt{n_V}$, is the uncertainty of the verification test mean, \bar{V} , if there are no additional sources of systematic error that need to be included. It is the customer's responsibility to determine the final uncertainty of \bar{V} .

The expanded uncertainty of the NIST reference value (U), corresponding to a 95 % uncertainty interval, is based on a coverage factor from the Student's t distribution with df_R degrees of freedom. The expanded uncertainties include sources of error in the measurement and testing process at NIST, and are not the expanded uncertainties of the individual verification specimens or the uncertainties of tests performed in your laboratory.

Reference

- [1] Splett, J. D., McCowan, C. N., Iyer, H. K., Wang, C.-M., "NIST Recommended Practice Guide: Computing Uncertainty for Charpy Impact Machine Test Results," NIST Special Publication 960-18, September, 2007 (available at: https://www.nist.gov/sites/default/files/documents/mml/acmd/structural_materials/SP9602-18Final-2.pdf).

NIST Charpy Verification Sticker

This machine meets the indirect verification requirements of the current ISO Standard 148-2

Machine Serial Number: 195892

Verification Date: August 31, 2022

Signature: 

, Charpy Program Coordinator
National Institute of Standards and Technology

1. GDS500A Maintenance Checklist

Customer Number	[REDACTED]
Service Call Number	8789
Assignment Number	3508
Customer / Company Name	FEDERAL HIGHWAY ADMINISTRATION
Customer/Company Address	6300 Georgetown pike
Primary Contact	[REDACTED]
Telephone	[REDACTED]
E-mail	[REDACTED]
Secondary Contact	
Telephone	
E-mail	
Instrument	Gds500a
Serial Number	14406
Client Asset ID Number	110084
Software Version	1.81

2. Major Components

Table name		
Description / Model No.	S/N	Software Version
Gds500a	14406	1.81
Computer Brand & Model	Hp440	
PC Serial Number	14214	
Operating System	WIN7	
Specify if other OS is selected		
Application	Metal testing	



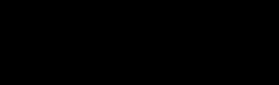

3. Procedure

Take a screen capture of the ambient monitor & system counters	<input checked="" type="checkbox"/> Yes	<input type="checkbox"/> No
Corrective Action / Comments		
Analyze Drift standards and take a screen capture of the calculated results	<input checked="" type="checkbox"/> Yes	<input type="checkbox"/> No
Corrective Action / Comments		
Remove all .bak files under the GDS500A database	<input checked="" type="checkbox"/> Yes	<input type="checkbox"/> No
Corrective Action / Comments		
Backup all methods & copy the GDS500A folder. Return backups & copy of GDS500A folder to LECO	<input checked="" type="checkbox"/> Yes	<input type="checkbox"/> No
Corrective Action / Comments		
Change the vacuum pump oil	<input checked="" type="checkbox"/> Yes	<input type="checkbox"/> No

Corrective Action / Comments	
Clean the cone filter on the rough pump inlet	<input checked="" type="checkbox"/> Yes <input type="checkbox"/> No
Corrective Action / Comments	
Inspect the odor/mist filter (replace every 12 months)	<input checked="" type="checkbox"/> Yes <input type="checkbox"/> No
Corrective Action / Comments	Replaced
Check and record the resistance of the water before replacing it. Be sure to disconnect the HV BNC cable from the lamp. With the water pump running, place red lead on the HV connection. (<20MΩ = change water). Replace the 607-437 Tubing if necessary.	Replaced water
MΩ before	
MΩ after	
Corrective Action / Comments	
Leak check the argon tank, inlet lines, pneumatic pistons and solenoids	Pass
Corrective Action / Comments	
Check and record the anode depth (should be 0.12 to 0.17mm)	0.13
Corrective Action / Comments	
Check reamer bit, pulley and motor operation and clean where needed	<input checked="" type="checkbox"/> Yes <input type="checkbox"/> No
Corrective Action / Comments	
Remove the GD lamp and clean the outer lens (clean the inner lens as needed)	Cleaned outer lens
Corrective Action / Comments	
Clean the GD lamp. Rebuild the lamp & anneal the anode if necessary	Cleaned
Corrective Action / Comments	
Inspect and clean the poppet valve (vacuum enable valve), replace it if necessary.	Cleaned
Corrective Action / Comments	
Inspect and clean the 611-351-263 poppet valve (vacuum enable valve) solenoid, replace it if necessary.	Cleaned
Corrective Action / Comments	
Perform a lamp vacuum test (0.03 Torr or less)	Pass
Corrective Action / Comments	
Check the function of the dead man switch	Pass
Corrective Action / Comments	
Check the alignment of the analysis door and align it if necessary	Pass
Corrective Action / Comments	
Check the alignment of the safety interlock magnets	Pass
Corrective Action / Comments	

Clean the air inlet dust filters on the front of the instrument	<input checked="" type="checkbox"/> Yes <input type="checkbox"/> No
Corrective Action / Comments	
Clean the tower air inlet dust filters	<input checked="" type="checkbox"/> Yes <input type="checkbox"/> No
Corrective Action / Comments	
Check the function of the three cooling fans	Pass
Corrective Action / Comments	
Check and record the AC line voltage	<input checked="" type="checkbox"/> Yes <input type="checkbox"/> No
Voltage in VAC	217
Corrective Action / Comments	
Reset all the counters that had maintenance performed on them	<input checked="" type="checkbox"/> Yes <input type="checkbox"/> No
Corrective Action / Comments	
Verify the GDL vacuum solenoid counter is set for the same burns as the anode (5000 to 7000)	<input checked="" type="checkbox"/> Yes <input type="checkbox"/> No
Corrective Action / Comments	
Clean and vacuum the printer and change the ribbon if necessary	N/A
Corrective Action / Comments	
Perform a detector alignment - take a screen capture of the results	<input checked="" type="checkbox"/> Yes <input type="checkbox"/> No
Corrective Action / Comments	
Analyze Drift standards and take a screen capture of the calculated results	<input checked="" type="checkbox"/> Yes <input type="checkbox"/> No
Corrective Action / Comments	
Analyze Check standards for the method that was just drifted - take screen captures of the results	<input checked="" type="checkbox"/> Yes <input type="checkbox"/> No
Corrective Action / Comments	
Check and record the anode depth (should be 0.12 to 0.17mm)	0.13
Corrective Action / Comments	
Review Checklist with Customer	<input checked="" type="checkbox"/> Yes <input type="checkbox"/> No
Corrective Action / Comments	

4. Signatures

Customer Approval	 
Date	2022-03-23
LECO Representative	 
Date	2022-03-23

National Bureau of Standards

Certificate of Analysis

Standard Reference Material 1269

Low Alloy Steel (AISI 1526, Mod.)

"Line Pipe Steel"

In cooperation with
American Society for Testing and Materials
and
Steel Founders' Society of America

This SRM is in the form of disks 32 mm (1 1/4 in) in diameter and 19 mm (3/4 in) thick, intended for use in optical emission and x-ray spectrometric methods of analysis.

Element	Certified Value, ¹ % by wt.	Estimated Uncertainty ²
Carbon	0.298	0.004
Manganese	1.35	.02
Phosphorus	0.012	.002
Sulfur	.0061	.0004
Silicon	.189	.008
Copper	.095	.005
Nickel	.108	.005
Chromium	.201	.009
Vanadium	.004	.001
Molybdenum	.036	.003
Lead	.005	.001
Aluminum	.016	.003

1. The certified value listed for a constituent is the *present best estimate* of the "true" value based on the results of the cooperative program for certification.
2. The estimated uncertainty listed for a constituent is based on judgment and represents an evaluation of the combined effects of method imprecision, possible systematic errors among methods, and material variability. (No attempt was made to derive exact statistical measures of imprecision because several methods were involved in the determination of most constituents.)

METALLURGICAL CONDITION: The structure of the specimens is that resulting from hot working, followed by annealing.

The overall coordination of the technical measurements leading to certification was performed under the direction of J. I. Shultz, Research Associate, ASTM-NBS Research Associate Program.

The technical and support aspects involved in the preparation, certification, and issuance of this Standard Reference Material were coordinated through the Office of Standard Reference Materials by R. E. Michaelis.

Washington, D.C. 20234
June 11, 1981

George A. Uriano, Chief
Office of Standard Reference Materials

(over)

PLANNING, PREPARATION, TESTING, ANALYSIS:

The composition of this SRM was chosen for the "line-pipe" steel industry, especially with respect to low sulfur. In addition, this SRM is expected to serve as Supplement No. 2 to the "1200 Series" of irons and steels. The material for this SRM was melted and cast at Esco Corporation, Portland, Ore., (L. E. Finch), under an NBS contract with the Steel Founders' Society of America. A single ingot was fabricated at the Puget Sound Naval Shipyard, Bremerton, Washington, where it was forged and swaged to rods (oversize 32 mm in diameter). The rods were given a sub-critical anneal and then centerless ground to the final size of 32 mm in diameter. Homogeneity testing was performed at NBS by optical emission spectrometric analysis, J. A. Norris; by x-ray fluorescence analysis, P. A. Pella; and chemical analysis by B. I. Diamondstone and by R. K. Bell, Assistant Research Associate, ASTM/NBS Research Associate Program.

Composite samples for chemical analysis were prepared in the form of millings cut from representative specimens of the rods.

Cooperative analyses for certification were performed in the following laboratories:

Bethlehem Steel Corporation, Homer Research Laboratories, Bethlehem, Pa., D. A. Flinchbaugh and J. L. Fernandez.

Ledoux & Company, Teaneck, N.J., S. Kallmann, E. Komarkova, and C. L. Maul.

National Bureau of Standards, Inorganic Analytical Research Division, B. I. Diamondstone, E. R. Deardorff, E. J. Maienthal, S. Hanamura, T. C. Rains, and R. K. Bell, ASTM/NBS Assistant Research Associate.

Republic Steel Corporation, Chicago District, Chicago, Ill., P. P. Blaszak.

Sharon Steel Corporation, Sharon, Pa., N. J. Williams.

Elements other than those certified may be present in this material as indicated below. These are *not certified*, but are given as additional information on the composition.

<u>Element</u>	<u>Concentration</u> <u>% by weight</u>
Antimony	(0.0014)
Arsenic	(.006)
Barium	(.0003)
Bismuth	(.0002)
Boron	(<.0001)
Calcium	(.0004)
Cerium	(.004)
Cobalt	(.014)
Gold	(.0002)
Hafnium	(.002)
Magnesium	(.0001)
Niobium	(.0002)
Nitrogen	(.009)
Oxygen	(.006)
Selenium	(.0004)
Silver	(.0002)
Strontium	(<.0001)
Tantalum	(.008)
Tellurium	(.0003)
Thallium	(.0002)
Tin	(.039)
Titanium	(.009)
Tungsten	(.001)
Zinc	-----
Zirconium	(.003)

()Determined

----- Not added nor determined



UNITED STATES DEPARTMENT OF COMMERCE
National Institute of Standards and Technology
Gaithersburg, Maryland 20899-0001

DATE: 07 April 2014

Product Identifier

SRM Number: 1269

SRM Name: Low Alloy Steel (AISI 1526, Mod.) "Line Pipe Steel"

Under the U.S. Department of Labor, Occupational Safety and Health Administration (OSHA) 29 CFR 1910.1200, this Standard Reference Material (SRM) is NOT classified as a physical hazard or a health hazard, a simple asphyxiant, combustible dust, pyrophoric gas, or hazard not otherwise classified. There are no hazard pictograms, hazard statements or signal word associated with it. Safety Data Sheet information is not required. This document may be used in conjunction with your hazard communication program.

Exemption: 1910.1200 (c). This SRM is an Article, as the word is defined by OSHA, where *Article* means a manufactured item other than a fluid or particle: (i) which is formed to a specific shape or design during manufacture; (ii) which has end use function(s) dependent in whole or in part upon its shape or design during end use; and (iii) which under normal conditions of use does not release more than very small quantities, e.g., minute or trace amounts of a hazardous chemical (as determined under paragraph (d) of 1910.1200), and does not pose a physical hazard or health risk to employees.

Description: This SRM is intended for applications in optical and X-ray spectrometric methods of analysis. A unit of SRM 1269 is provided in the form of an annealed, solid disk, 3.2 cm in diameter and 1.9 cm thick.

Disposal: SRM 1269 should be disposed of in accordance with local, state, and federal regulations.

Transport Information: This material is not regulated by the U.S. Department of Transportation (DOT) and/or International Air Transportation Association (IATA).

Disclaimer: This document was prepared carefully, using current references. Users of this SRM should ensure that this document and the corresponding Certificate of Analysis in their possession are current. This can be accomplished by contacting the SRM Program: telephone (301) 975-2200; fax (301) 948-3730; e-mail srmmsds@nist.gov; or via the Internet at <http://www.nist.gov/srm>.



Safety Note

****These procedures involve use of mechanically powered machinery which may produce hazardous dusts or vapors. The user's responsibility is to establish appropriate safety and health practices and to determine the applicability of regulatory limitations prior to application. These are minimum surface requirements. A better finish can always be used.***

The following procedures have been employed in the preparation of samples for LECO® GDS analysis:

- Grooves on the surface created by the grinding operation should always go in the same direction. Avoid crisscross patterns.
- Avoid overheating the sample which may form a glazed surface.
- New abrasive materials will provide a sharp cutting surface.
- Softer materials require less pressure than harder materials. Excessive pressure on softer samples may cause smearing of the elements.
- When using the wet disks, flood the disk heavily with water.
- A LECO® BG-31 belt grinder is used with ZrO2 belts.
- A LECO® VP-50 disk polisher is used with SiC disks.

****A suggested minimum final grinding of specimens is detailed below:***

FINAL SAMPLE PREPARATION				
Material	120 Grit ZrO2 Dry/Wet 120 SiC Wet	180 Grit SiC Wet	320 Grit SiC Wet	600 Grit SiC Wet
Aluminum			X	
Cemented WC			1 25jt diamond	
Brass			X	
Bronze			X	
Copper			X	
Cobalt	X			
Iron-As Cast				X
Iron - Chilled	X			
Lead			X	
Magnesium			X	
Nickel	X			
Ni-Resist	X			
Nitrogen in Stainless			X	
Powder Metal			X (dry)	
Silver			X	
Solder			X	
Stainless	X			
Steel	X			
Titanium	X			
Zinc			X	

GDS500A Caveat for Acceptance Criteria of FAT

Spectrochemical analysis is a comparative technique. The reference material uncertainty is one part of the total uncertainty budget. The other parts of the measurement system shall include the instrument and operator error. The sum of the errors must be taken into account (error propagation law).

The certified values in solid CRM's and RM's have been established using primary methods and the Certified Value (CV) assigned is related to mass or mole. They have, for the most part (exceptions: unusual metallurgical history, specimens exhibiting inordinately large granularity, peculiar composition), been proven to be fit for purpose; i.e. suitable for spectrochemical analysis.

If the CV falls within a confidence interval, Equation 1, the FAT is considered statistically rigorous and should be used and accepted for general practice.

$$\text{Test Result} = \text{Certified Value} \pm (s*t) \text{ -----Equation 1}$$

Where:

s = standard deviation or uncertainty of CV

t = Student t value 3.18 for ($n = 3$)

n = number of analyses

Results shall be judged to be statistically sound for the average of 3 replications ($n = 3$), using a fully expanded uncertainty, by factoring the Student's t probability (95% confidence interval, two tails) to the uncertainty of the CV, for elements in solid solution > 0.1%.

As an option, and in due course, the laboratory may obtain an estimate of s from a control chart maintained as a part of their quality control program. When the control chart contains a large number of measurements, t may be set as low as 2 at the 95% confidence level. At its discretion, the laboratory may choose to set a smaller range for the acceptable test result.

**APPENDIX B - "Forbes Avenue Over Fern Hollow Bridge Collapse Investigation:
Weld Microstructure Factual Report", prepared by Federal Highway
Administration (FHWA)**

Forbes Avenue Over Fern Hollow Bridge Collapse Investigation: Weld Microstructure Factual Report

Prepared For:
National Transportation Safety Board
NTSB Accident ID: HWY22MH003

Prepared by:

Ryan Slein, Ph.D.
Federal Highway Administration
Turner-Fairbank Highway Research Center
6300 Georgetown Pike, McLean, VA 22101

Justin Ocel, Ph.D., P.E.
Federal Highway Administration
Resource Center Structures Team
31 Hopkins Plaza, Suite 840
Baltimore, MD 21201

Benjamin Graybeal, Ph.D., P.E.
Federal Highway Administration
Turner-Fairbank Highway Research Center
6300 Georgetown Pike, McLean, VA 22101

June 20, 2023

Table of Contents

List of Figures ii

List of Tables vi

List of Abbreviations vii

1. Introduction..... 1

 1.1. Weld quality indicators 1

 1.2. Report scope..... 2

2. Testing plan..... 3

 2.1. Vickers hardness 4

 2.2. Microstructure..... 4

3. Test results 5

 3.1. Summary of Vickers hardness measurements..... 13

 3.2. Microstructures of 1D7 13

 3.2.1. Gradient line 1D7-1 14

 3.2.2. Gradient line 1D7-2 20

 3.2.3. Gradient line 1D7-3 26

 3.3. Microstructures of 1E7 32

 3.3.1. Gradient line 1E7-1 32

 3.3.2. Gradient line 1E7-2..... 38

 3.3.3. Gradient line 1E7-3..... 44

Acknowledgements..... 50

References..... 50

Appendix A: Hardness Verification and SRM Documentation..... 51

List of Figures

Figure 1. Macroetch of 1D7 with planar reference scales. (Figure G.3 of the FHWA Factual Report).	3
Figure 2. Macroetch of 1E7 with planar reference scales. (Figure G.8 of the FHWA Factual Report).	4
Figure 3. Macroetch of 1D7 with approximate sectioned area and gradient line path.....	5
Figure 4. Mounted sectioned area and measurement locations for gradient line 1D7-1.....	6
Figure 5. Mounted sectioned area and measurement locations for gradient line 1D7-2.....	7
Figure 6. Mounted sectioned area and measurement locations for gradient line 1D7-3.....	8
Figure 7. Macroetch of 1E7 with approximate sectioned area and gradient line path.....	9
Figure 8. Mounted sectioned area and measurement locations for gradient line 1E7-1.	10
Figure 9. Mounted sectioned area and measurement locations for gradient line 1E7-2.	11
Figure 10. Mounted sectioned area and measurement locations for gradient line 1E7-3.	12
Figure 11. 1D7-1 Sample ID B1 microstructure prior to indentation (left) and with the Vickers microindentation (right). 5% Nital etch. 40x magnification. Ferrite/pearlite dominant.	14
Figure 12. 1D7-1 Sample ID B2 microstructure prior to indentation (left) and with the Vickers microindentation (right). 5% Nital etch. 40x magnification. Ferrite/pearlite dominant.	14
Figure 13. 1D7-1 Sample ID B3 microstructure prior to indentation (left) and with the Vickers microindentation (right). 5% Nital etch. 40x magnification. Ferrite/pearlite dominant.	15
Figure 14. 1D7-1 Sample ID B4 microstructure prior to indentation (left) and with the Vickers microindentation (right). 5% Nital etch. 40x magnification. Ferrite/pearlite dominant.	15
Figure 15. 1D7-1 Sample ID H1 microstructure prior to indentation (left) and with the Vickers microindentation (right). 5% Nital etch. 40x magnification. Refined ferrite/pearlite from the heat cycle.	16
Figure 16. 1D7-1 Sample ID H2 microstructure prior to indentation (left) and with the Vickers microindentation (right). 5% Nital etch. 40x magnification. Martensite dominant.....	16
Figure 17. 1D7-1 Sample ID H3 microstructure prior to indentation (left) and with the Vickers microindentation (right). 5% Nital etch. 40x magnification. Martensite dominant.....	17
Figure 18. 1D7-1 Sample ID H4 microstructure prior to indentation (left) and with the Vickers microindentation (right). 5% Nital etch. 40x magnification. Martensite dominant.....	17
Figure 19. 1D7-1 Sample ID W1 microstructure prior to indentation (left) and with the Vickers microindentation (right). 5% Nital etch. 40x magnification. Acicular ferrite dominant with some proeutectoid ferrite.....	18
Figure 20. 1D7-1 Sample ID W2 microstructure prior to indentation (left) and with the Vickers microindentation (right). 5% Nital etch. 40x magnification. Acicular ferrite dominant with some proeutectoid ferrite and Widmanstätten ferrite.....	18
Figure 21. 1D7-1 Sample ID W3 microstructure prior to indentation (left) and with the Vickers microindentation (right). 5% Nital etch. 40x magnification. Acicular ferrite dominant with some proeutectoid ferrite and Widmanstätten ferrite.....	19
Figure 22. 1D7-1 Sample ID W4 microstructure prior to indentation (left) and with the Vickers microindentation (right). 5% Nital etch. 40x magnification. Acicular ferrite dominant with some proeutectoid ferrite and Widmanstätten ferrite.....	19
Figure 23. 1D7-2 Sample ID B1 microstructure prior to indentation (left) and with the Vickers microindentation (right). 5% Nital etch. 40x magnification. Ferrite/pearlite dominant.	20
Figure 24. 1D7-2 Sample ID B2 microstructure prior to indentation (left) and with the Vickers microindentation (right). 5% Nital etch. 40x magnification. Ferrite/pearlite dominant.	20
Figure 25. 1D7-2 Sample ID B3 microstructure prior to indentation (left) and with the Vickers microindentation (right). 5% Nital etch. 40x magnification. Ferrite/pearlite dominant.	21

Figure 26. 1D7-2 Sample ID B4 microstructure prior to indentation (left) and with the Vickers microindentation (right). 5% Nital etch. 40x magnification. Ferrite/pearlite dominant.	21
Figure 27. 1D7-2 Sample ID H1 microstructure prior to indentation (left) and with the Vickers microindentation (right). 5% Nital etch. 40x magnification. Refined ferrite/pearlite from the heat cycle.	22
Figure 28. 1D7-2 Sample ID H2 microstructure prior to indentation (left) and with the Vickers microindentation (right). 5% Nital etch. 40x magnification. Refined ferrite/pearlite dominant with some martensite.....	22
Figure 29. 1D7-2 Sample ID H3 microstructure prior to indentation (left) and with the Vickers microindentation (right). 5% Nital etch. 40x magnification. Martensite dominant.	23
Figure 30. 1D7-2 Sample ID H4 microstructure prior to indentation (left) and with the Vickers microindentation (right). 5% Nital etch. 40x magnification. Martensite dominant.	23
Figure 31. 1D7-2 Sample ID W1 microstructure prior to indentation (left) and with the Vickers microindentation (right). 5% Nital etch. 40x magnification. Note that the upper left corner blotch is marker. Acicular ferrite dominant with some proeutectoid ferrite and Widmanstätten ferrite.	24
Figure 32. 1D7-2 Sample ID W2 microstructure prior to indentation (left) and with the Vickers microindentation (right). 5% Nital etch. 40x magnification. Note that the blotch about the left edge is marker. Acicular ferrite dominant with some proeutectoid ferrite and Widmanstätten ferrite.	24
Figure 33. 1D7-2 Sample ID W3 microstructure prior to indentation (left) and with the Vickers microindentation (right). 5% Nital etch. 40x magnification. Acicular ferrite dominant with some proeutectoid ferrite and Widmanstätten ferrite.	25
Figure 34. 1D7-2 Sample ID W4 microstructure prior to indentation (left) and with the Vickers microindentation (right). 5% Nital etch. 40x magnification. Acicular ferrite dominant.....	25
Figure 35. 1D7-3 Sample ID B1 microstructure prior to indentation (left) and with the Vickers microindentation (right). 5% Nital etch. 40x magnification. Ferrite/pearlite dominant.	26
Figure 36. 1D7-3 Sample ID B2 microstructure prior to indentation (left) and with the Vickers microindentation (right). 5% Nital etch. 40x magnification. Ferrite/pearlite dominant.	26
Figure 37. 1D7-3 Sample ID B3 microstructure prior to indentation (left) and with the Vickers microindentation (right). 5% Nital etch. 40x magnification. Ferrite/pearlite dominant.	27
Figure 38. 1D7-3 Sample ID B4 microstructure prior to indentation (left) and with the Vickers microindentation (right). 5% Nital etch. 40x magnification. Ferrite/pearlite dominant.	27
Figure 39. 1D7-3 Sample ID H1 microstructure prior to indentation (left) and with the Vickers microindentation (right). 5% Nital etch. 40x magnification. Refined ferrite/pearlite from the heat cycle.	28
Figure 40. 1D7-3 Sample ID H2 microstructure prior to indentation (left) and with the Vickers microindentation (right). 5% Nital etch. 40x magnification. Martensite dominant.	28
Figure 41. 1D7-3 Sample ID H3 microstructure prior to indentation (left) and with the Vickers microindentation (right). 5% Nital etch. 40x magnification. Martensite dominant.	29
Figure 42. 1D7-3 Sample ID H4 microstructure prior to indentation (left) and with the Vickers microindentation (right). 5% Nital etch. 40x magnification. Martensite dominant.	29
Figure 43. 1D7-3 Sample ID W1 microstructure prior to indentation (left) and with the Vickers microindentation (right). 5% Nital etch. 40x magnification. Acicular ferrite with proeutectoid ferrite and Widmanstätten ferrite.....	30
Figure 44. 1D7-3 Sample ID W2 microstructure prior to indentation (left) and with the Vickers microindentation (right). 5% Nital etch. 40x magnification. Acicular ferrite.....	30
Figure 45. 1D7-3 Sample ID W3 microstructure prior to indentation (left) and with the Vickers microindentation (right). 5% Nital etch. 40x magnification. Acicular ferrite and martensite with some proeutectoid ferrite and Widmanstätten ferrite.	31

Figure 46. 1D7-3 Sample ID W4 microstructure prior to indentation (left) and with the Vickers microindentation (right). 5% Nital etch. 40x magnification. Acicular ferrite and martensite with some proeutectoid ferrite and Widmanstätten ferrite. 31

Figure 47. 1E7-1 Sample ID B1 microstructure prior to indentation (left) and with the Vickers microindentation (right). 5% Nital etch. 40x magnification. Ferrite/pearlite dominant. 32

Figure 48. 1E7-1 Sample ID B2 microstructure prior to indentation (left) and with the Vickers microindentation (right). 5% Nital etch. 40x magnification. Ferrite/pearlite dominant. 33

Figure 49. 1E7-1 Sample ID B3 microstructure prior to indentation (left) and with the Vickers microindentation (right). 5% Nital etch. 40x magnification. Ferrite/pearlite dominant. 33

Figure 50. 1E7-1 Sample ID B4 microstructure prior to indentation (left) and with the Vickers microindentation (right). 5% Nital etch. 40x magnification. Ferrite/pearlite dominant. 34

Figure 51. 1E7-1 Sample ID H1 microstructure prior to indentation (left) and with the Vickers microindentation (right). 5% Nital etch. 40x magnification. Refined ferrite/pearlite from the heat cycle. 34

Figure 52. 1E7-1 Sample ID H2 microstructure prior to indentation (left) and with the Vickers microindentation (right). 5% Nital etch. 40x magnification. Refined ferrite/pearlite from the heat cycle. 35

Figure 53. 1E7-1 Sample ID H3 microstructure prior to indentation (left) and with the Vickers microindentation (right). 5% Nital etch. 40x magnification. Ferrite and martensite. 35

Figure 54. 1E7-1 Sample ID H4 microstructure prior to indentation (left) and with the Vickers microindentation (right). 5% Nital etch. 40x magnification. Ferrite and martensite. 36

Figure 55. 1E7-1 Sample ID W1 microstructure prior to indentation (left) and with the Vickers microindentation (right). 5% Nital etch. 40x magnification. Proeutectoid and acicular ferrite. 36

Figure 56. 1E7-1 Sample ID W2 microstructure prior to indentation (left) and with the Vickers microindentation (right). 5% Nital etch. 40x magnification. Refined ferrite dominant. 37

Figure 57. 1E7-1 Sample ID W3 microstructure prior to indentation (left) and with the Vickers microindentation (right). 5% Nital etch. 40x magnification. Refined ferrite dominant. 37

Figure 58. 1E7-1 Sample ID W4 microstructure prior to indentation (left) and with the Vickers microindentation (right). 5% Nital etch. 40x magnification. Refined ferrite dominant. 38

Figure 59. 1E7-2 Sample ID B1 microstructure prior to indentation (left) and with the Vickers microindentation (right). 5% Nital etch. 40x magnification. Ferrite/pearlite dominant. 38

Figure 60. 1E7-2 Sample ID B2 microstructure prior to indentation (left) and with the Vickers microindentation (right). 5% Nital etch. 40x magnification. Ferrite/pearlite dominant. 39

Figure 61. 1E7-2 Sample ID B3 microstructure prior to indentation (left) and with the Vickers microindentation (right). 5% Nital etch. 40x magnification. Ferrite/pearlite dominant. 39

Figure 62. 1E7-2 Sample ID B4 microstructure prior to indentation (left) and with the Vickers microindentation (right). 5% Nital etch. 40x magnification. Ferrite/pearlite dominant. 40

Figure 63. 1E7-2 Sample ID H1 microstructure prior to indentation (left) and with the Vickers microindentation (right). 5% Nital etch. 40x magnification. Refined ferrite/pearlite from the heat cycle. 40

Figure 64. 1E7-2 Sample ID H2 microstructure prior to indentation (left) and with the Vickers microindentation (right). 5% Nital etch. 40x magnification. Martensite dominant. 41

Figure 65. 1E7-2 Sample ID H3 microstructure prior to indentation (left) and with the Vickers microindentation (right). 5% Nital etch. 40x magnification. Martensite dominant. 41

Figure 66. 1E7-2 Sample ID H4 microstructure prior to indentation (left) and with the Vickers microindentation (right). 5% Nital etch. 40x magnification. Martensite dominant. 42

Figure 67. 1E7-2 Sample ID W1 microstructure prior to indentation (left) and with the Vickers microindentation (right). 5% Nital etch. 40x magnification. Acicular ferrite with proeutectoid ferrite and Widmanstätten ferrite. 42

Figure 68. 1E7-2 Sample ID W2 microstructure prior to indentation (left) and with the Vickers microindentation (right). 5% Nital etch. 40x magnification. Acicular ferrite with proeutectoid ferrite and Widmanstätten ferrite.....	43
Figure 69. 1E7-2 Sample ID W3 microstructure prior to indentation (left) and with the Vickers microindentation (right). 5% Nital etch. 40x magnification. Acicular ferrite with proeutectoid ferrite and Widmanstätten ferrite.....	43
Figure 70. 1E7-2 Sample ID W4 microstructure prior to indentation (left) and with the Vickers microindentation (right). 5% Nital etch. 40x magnification. Acicular ferrite with proeutectoid ferrite and Widmanstätten ferrite.....	44
Figure 71. 1E7-3 Sample ID B1 microstructure prior to indentation (left) and with the Vickers microindentation (right). 5% Nital etch. 40x magnification. Ferrite/pearlite dominant.	44
Figure 72. 1E7-3 Sample ID B2 microstructure prior to indentation (left) and with the Vickers microindentation (right). 5% Nital etch. 40x magnification. Ferrite/pearlite dominant.	45
Figure 73. 1E7-3 Sample ID B3 microstructure prior to indentation (left) and with the Vickers microindentation (right). 5% Nital etch. 40x magnification. Ferrite/pearlite dominant.	45
Figure 74. 1E7-3 Sample ID B4 microstructure prior to indentation (left) and with the Vickers microindentation (right). 5% Nital etch. 40x magnification. Ferrite/pearlite dominant.	46
Figure 75. 1E7-3 Sample ID H1 microstructure prior to indentation (left) and with the Vickers microindentation (right). 5% Nital etch. 40x magnification. Refined ferrite/pearlite from the heat cycle.	46
Figure 76. 1E7-3 Sample ID H2 microstructure prior to indentation (left) and with the Vickers microindentation (right). 5% Nital etch. 40x magnification. Ferrite/pearlite and martensite.	47
Figure 77. 1E7-3 Sample ID H3 microstructure prior to indentation (left) and with the Vickers microindentation (right). 5% Nital etch. 40x magnification. Ferrite/pearlite and martensite.	47
Figure 78. 1E7-3 Sample ID H4 microstructure prior to indentation (left) and with the Vickers microindentation (right). 5% Nital etch. 40x magnification. Ferrite/pearlite and martensite.	48
Figure 79. 1E7-3 Sample ID W1 microstructure prior to indentation (left) and with the Vickers microindentation (right). 5% Nital etch. 40x magnification. Acicular ferrite dominant with some proeutectoid ferrite and Widmanstätten ferrite.	48
Figure 80. 1E7-3 Sample ID W2 microstructure prior to indentation (left) and with the Vickers microindentation (right). 5% Nital etch. 40x magnification. Martensite with some acicular ferrite proeutectoid ferrite.....	49
Figure 81. 1E7-3 Sample ID W3 microstructure prior to indentation (left) and with the Vickers microindentation (right). 5% Nital etch. 40x magnification. Acicular ferrite dominant with some proeutectoid ferrite and Widmanstätten ferrite.	49
Figure 82. 1E7-3 Sample ID W4 microstructure prior to indentation (left) and with the Vickers microindentation (right). 5% Nital etch. 40x magnification. Acicular ferrite dominant with some proeutectoid ferrite and Widmanstätten ferrite.	50

List of Tables

Table 1: Vickers microindentation hardness values for a 500 gf indent with a 13 second dwell. 13
Table A-1: Indirect verification of Vickers microhardness using three SRM blocks. 57

List of Abbreviations

ASM	American Society for Metals
ASTM	American Society for Testing and Materials
FHWA	Federal Highway Administration
NTSB	National Transportation Safety Board
TFHRC	Turner-Fairbank Highway Research Center
<i>CE</i>	carbon equivalency
HAZ	heat-affected zone
MP	mega-pixel
SRM	standard reference material
STR	structural (a component of the evidence identifier to signify mechanical/material testing)
gf	gram force

1. INTRODUCTION

The Fern Hollow Bridge carried Forbes Avenue over Fern Hollow and 9 Mile Run through Frick Park within the City of Pittsburgh, Pennsylvania. The bridge used a rigid, K-frame superstructure type built-up with ASTM A 588 uncoated weathering steel. On January 28th, 2022, the bridge collapsed. Investigators from the National Transportation Safety Board (NTSB) were dispatched to the scene. Engineers from the Federal Highway Administration (FHWA) were also dispatched to the scene to assist NTSB with the investigation. During the on-site investigation, evidence was collected which was to be later used to assist in determining the cause of the bridge failure. The extracted evidence was transported to the FHWA's Turner-Fairbank Highway Research Center (TFHRC) in McLean, Virginia for testing and assessment.

Testing methodologies and results are presented in FHWA's *Forbes Avenue Over Fern Hollow Bridge Collapse Investigation: Steel Mechanical and Materials Testing Factual Report* (Slein et al. 2023), hereafter referred to as the FHWA Factual Report. The work conducted to develop the content of this report uncovered several indicators that raised concern with the quality of some welds. Primarily that proper preheating may have not been followed as; 1) steel chemical compositions having calculated carbon equivalencies (*CE*) greater than 0.50, and 2) damage to bandsaw blades during sectioning of the macroetches (i.e., indication of a harder than expected heat-affected zones (HAZ)). Additionally, there was observed poor base metal fusion and weld quality (e.g., porosity, unmelted flux) indicating lack of attention and poor workmanship during fabrication.

Due to the aforementioned concerns, an exploratory hardness and microstructural testing regimen was conducted to assess the leg flange-to-endplate welds. Testing consisted of taking discrete Vickers hardness measurements along a vector that spanned the base metal-to-HAZ-to-weld metal. Four measurements were taken in each respective zone to monitor the hardness gradient. A threshold of 350 HV 0.5 (i.e., Vickers hardness under a 500 gf microindentation) was determined to be a reasonable probabilistic indicator of a microstructural phase change. A corresponding image of the steel microstructure was captured at each hardness testing location with optical microscopy. The images of the microstructure reinforced hardness findings through direct observation of martensite, upper bainite, and/or lower bainite. Note that though it may be possible to differentiate between these three phases with the use of various etchants, no attempt is made to do so in this report. Further, no attempt to differentiate acicular versus bainitic ferrite is made.

1.1. Weld quality indicators

As described in Section 5.3 of the FHWA Factual Report, the calculated carbon equivalency provides a metric for the hardenability of the steel resulting from activities like welding. Low *CE* values (<0.28) indicate that the steel should be easily weldable, tolerant of little to no preheat, and is insensitive to low hydrogen practice. High *CE* values (>0.50) indicate steel which requires more care using a combination of low hydrogen practice, preheat, and perhaps post-heat treatment. Table 20 from the Factual Report shows that the majority of the measured specimens have *CE* values greater than 0.50 which, if proper welding procedures were not used, could have created embrittled heat-affected zones in the base metal from welding. This is primarily due to the thickness of the elements being joined effectively quenching the weld with high cooling rates leading to the development of brittle microphases.

The original set of design plans contained the only set of drawings discovered during the investigation, no shop drawings completed by the bridge fabricator were found. The design plans for the bridge specified the leg flange-to-endplate weld as a single-sided U-groove with a far side reinforcing fillet. There was no information in the weld symbol tail indicating that the weld was required to be a complete joint penetration weld. However, the construction plans listed in Steelwork General Notes that "All welding shall be

performed in accordance with AWS D2.0-69...” In review of AWS D2.0-69, welding symbols “...shall be those shown in the latest edition of Standard Welding Symbols AWS A2.0-68.” Review of AWS A2.0-68 found a statement that “the size of groove welds with no specified root penetration shall...extend completely through the member or members being joined.” Thus, the original design intent of these welds is that they should have been complete joint penetration. As demonstrated in Section 5.4 and Appendix G of the FHWA Factual Report, each macroetch shows the leg flange-to-endplate welds only achieved partial joint penetration using a double-bevel groove geometry.

Based on macroetches taken over the leg webs (Figures G.3, G.8, G.13, G.18, G.43, and G.48 of the FHWA Factual Report), it appears that the leg I-shape (leg flanges and leg web) was welded first, then the leg end was cut to the correct angle to mate against the endplate, then the endplate was welded. This sequence is evidenced through the leg flange welds which were not continuous through the leg web. Note that the bevel preparation for the flange to the inside of the I-shape appears to have been cut with a drop bandsaw. The bandsaw cut through the flange, but also into the leg web for some distance that varied with each leg. The sawcut in the leg web was welded over to seal the cut. The bevel preparation on the flange was not consistent between the four legs. Preparation was similar for the two Bent 1 legs, and also similar for the two Bent 2 legs, indicating each pair of bent legs was likely fabricated at different points in time.

None of the welds seemed to achieve significant fusion to either sidewall of the weld preparation. Sometimes there appeared to be no fusion. This indicated either poor access with the small bevel angles, particularly in the two Bent 1 legs, or inadequate welding procedure with either low heat input and/or poor angle of the electrode while welding. Further, porosity and unmelted flux was apparent in the macros at the leg flange-to-endplate-to-leg web weld junction, again indicating inadequate welding procedure and technique. This was further evidenced during the sectioning of the welds, where damage occurred to multiple bandsaw blades when cutting through the centerline of the web plate, particularly in leg B1R and B2R.

All these welding quality indicators, combined with the high *CE* values, led to the exploratory study covered in this report. From the FHWA Factual Report, all 2 1/2 in. flange plate at the top of each leg came from a single heat. As such, mechanical and chemical assessment was taken on leg B1R (i.e., plate 1H) which had a measured *CE* of 0.60. Therefore, in conjunction with the observations in the macroetch and damaging of blades during sectioning, the exploratory study focuses on the weld quality of the flange-endplate weld and the flange-web-endplate weld for leg B1R for both the acute and obtuse side. Corresponding to section 1D7 for the Span 1 (acute) end plate weld extracted from evidence NTSB-STR-004 and section 1E7 for the Span 2 (obtuse) end plate weld extracted from evidence NSTB-STR-003.

1.2. Report scope

This factual report documents Vickers microhardness measurements and microstructure analysis at multiple discrete points across the leg-to-endplate welds in leg B1R. These measurements are exploratory in nature, intended to assess whether there is clear evidence of elevated hardness values and/or martensitic/bainite phases present in the microstructure, as such measured values are not necessarily representative of all welds in the bridge.

This report frequently refers to the FHWA *Forbes Avenue Over Fern Hollow Bridge Collapse Investigation: Steel Mechanical and Materials Testing Factual Report* for description of the evidence received by TFHRC and describes the assessments and testing completed on the evidence. Limited information is repeated in this report for brevity.

2. TESTING PLAN

Photographic documentation of all macroetches of the sectioned leg flange-to-endplate welds are provided in Appendix G of the FHWA Factual Report. Each image includes two planar scales to measure weld size and crack properties. The first planar scale is a graded ruler placed directly on top of the specimen. The second scale is a protractor, with various additional calibration references, elevated to be at a plane common with the macroetch. Figures 1 and 2 show the macroetches for 1D7 and 1E7, respectively.

For each macroetch, three prescribed vectors (see Sections 3 of this report) define lines perpendicular to the base metal-HAZ interface where twelve hardness measurements are taken over a 0.75 in. length. Measurements are nonuniformly spaced along a gradation of thirty 0.025 in. increments such that four points fall within base metal, HAZ, and weld metal, each. Vectors are spaced in higher concentration around the web-to-flange and web-to-endplate welds for 1D7 and 1E7 where it was expected that the largest hardness values existed due to observed poor weld quality. However, the intent was to collectively capture at least one vector along areas of high porosity and/or unmelted flux, along a nominal flange-to-end plate weld with some fusion into the base metal, and along the web-to-flange weld (even though the weld nugget is generally not visible). For each hardness location measurement, a corresponding image of the steel microstructure was captured with optical microscopy to look for potential changes in metallographic phase.

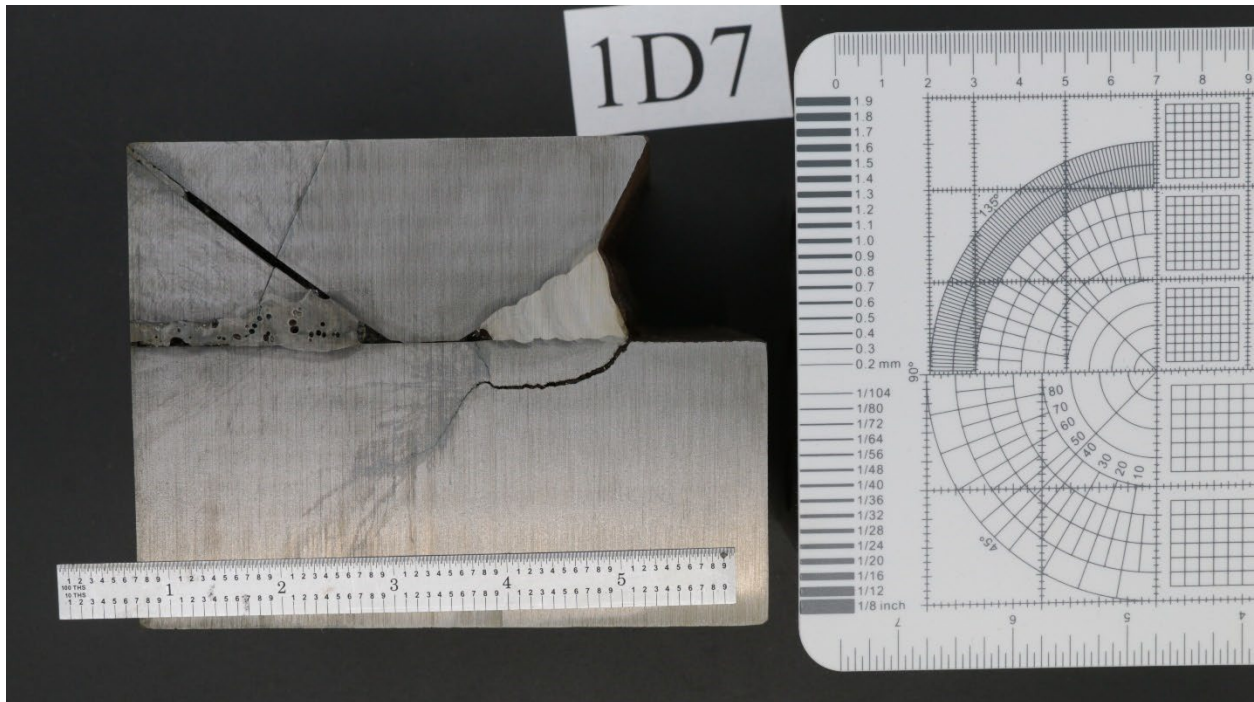


Figure 1. Macroetch of 1D7 with planar reference scales. (Figure G.3 of the FHWA Factual Report).

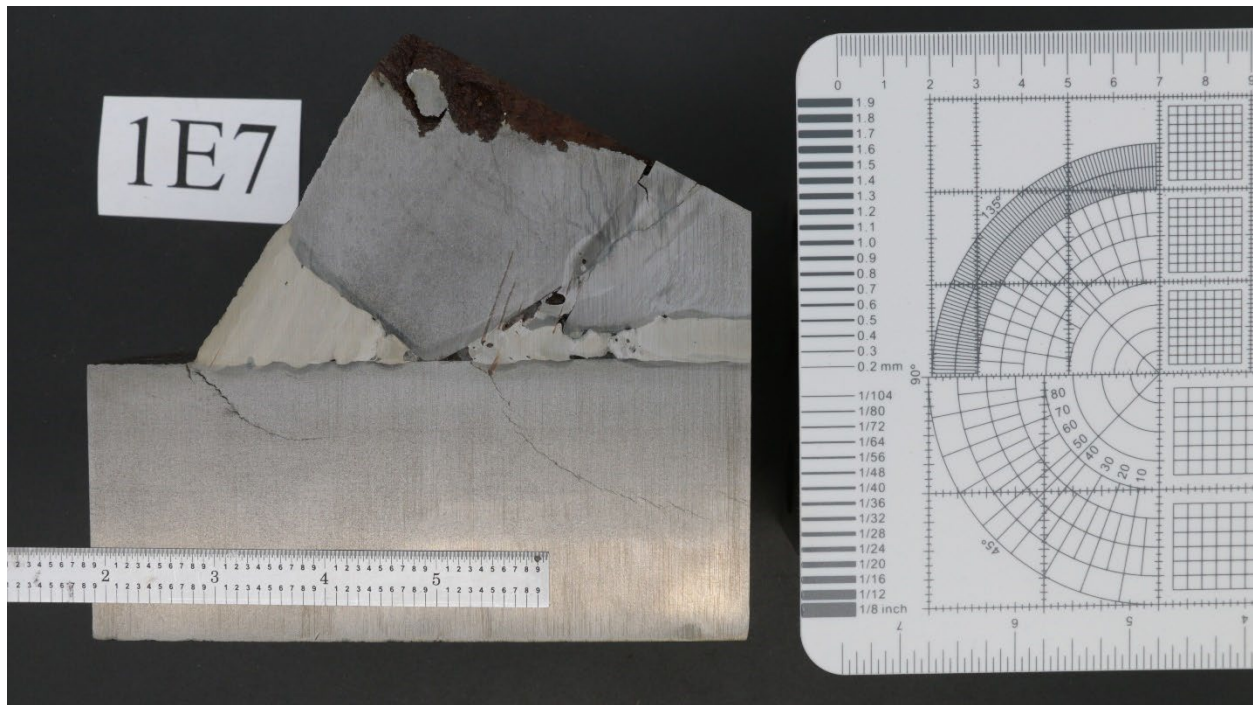


Figure 2. Macroetch of 1E7 with planar reference scales. (Figure G.8 of the FHWA Factual Report).

2.1. Vickers hardness

All hardness values in this report are 500 gf Vickers microhardness indentation measurements, performed at room temperature on a LECO LM-110AT following ASTM E92-17. Vickers microhardness employs a standard square-based pyramidal diamond indenter that imprints the test specimen at a prescribed force and dwell time. The corresponding projected base length of the pyramidal diagonal imprints are used to calculate a hardness.

All samples were mounted, ground, polished, and etched with a 5-percent solution of nitric acid in ethyl alcohol (Nital) prior to indentation to expose the crystal structure. In the event that an indentation crossed grain boundaries, the base of the impressed pyramid may not be perfectly square due differing stiffnesses of the crystalline phases. Per ASTM E92-17 Section 7.10.1, the lengths of the diagonals were checked to ensure a quality measurement and the indentation measurement was retaken if needed.

Measurement verification following ASTM E92-17 Sections A1.3 and A1.4 (direct and indirect verification) and SRM certificates are provided in Appendix A of this report.

2.2. Microstructure

The microstructure of the metal was observed at each hardness measurement location with optical microscopy. Images were captured directly on the LECO LM-110AT hardness indenter machine at a 40x zoom, both just prior to and subsequent to the indent.

Note that no differentiation is made within the HAZ to distinguish between grain-coarsened zones due to reheating in multipass welds, as there is insufficient measurement fidelity.

3. TEST RESULTS

This section of the report provides a hardness measurement and microstructural image at 72 discrete locations along the base metal, HAZ, and weld metal for 1D7 and 1E7. Figures 3 and 7 show three prescribed vectors that define lines approximately perpendicular to the base metal-HAZ interface where twelve hardness measurements are taken over a 0.75 in. length. Figures 4-6 and 8-10 show the mounted specimens that were further sectioned from 1D7 and 1E7. The figures also show the measurement discretization where the measurements are nonuniformly spaced along a gradation of thirty 0.025 in. increments such that four points fall within base metal, HAZ, and weld metal, respectively.

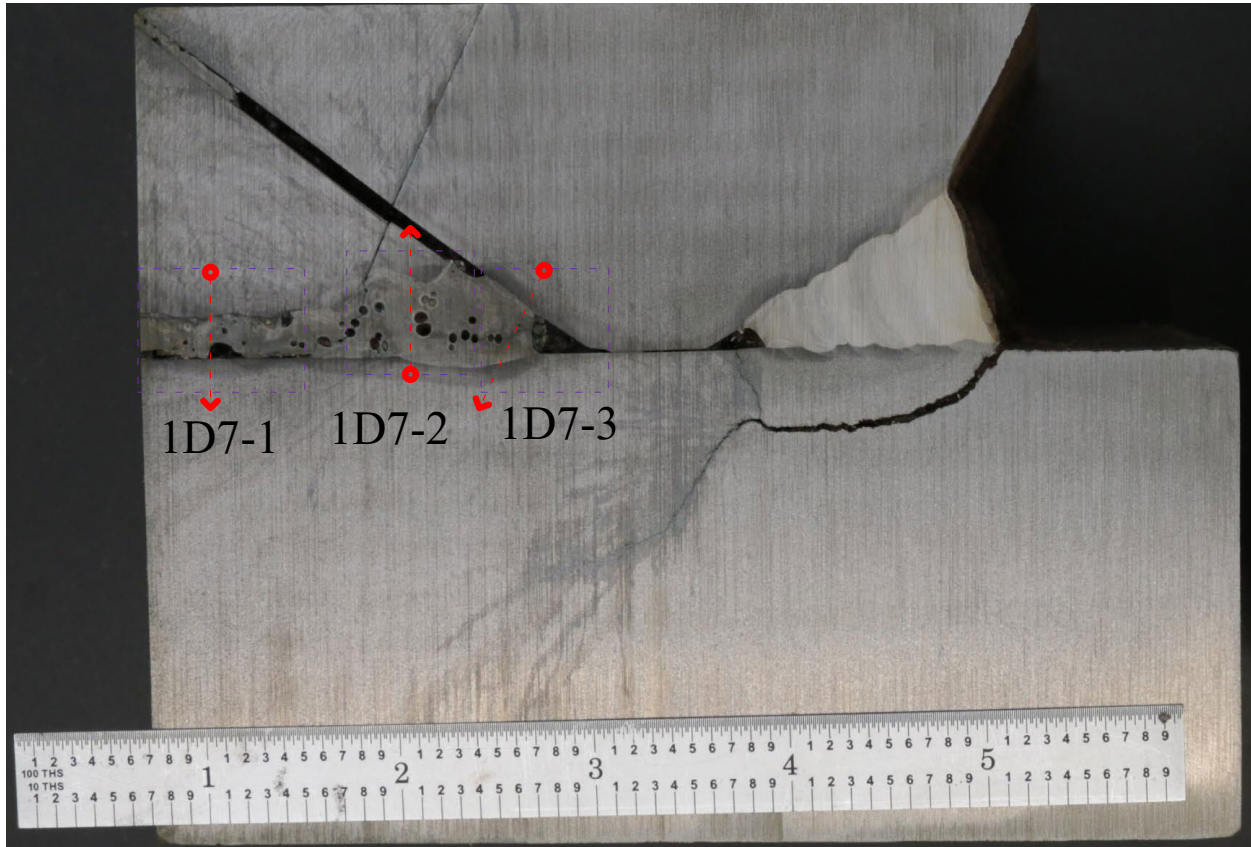


Figure 3. Macroetch of 1D7 with approximate sectioned area and gradient line path.

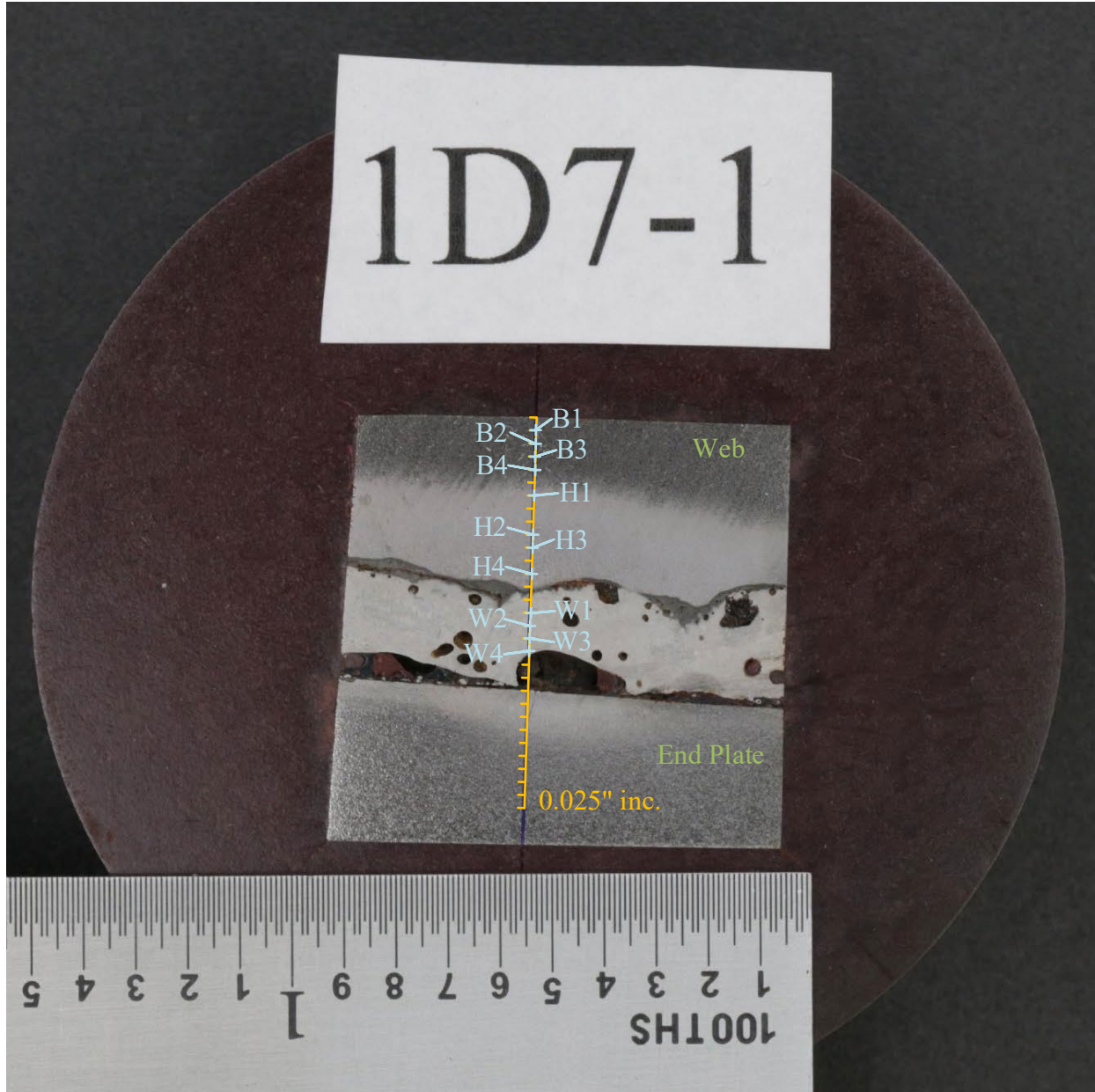


Figure 4. Mounted sectioned area and measurement locations for gradient line 1D7-1.

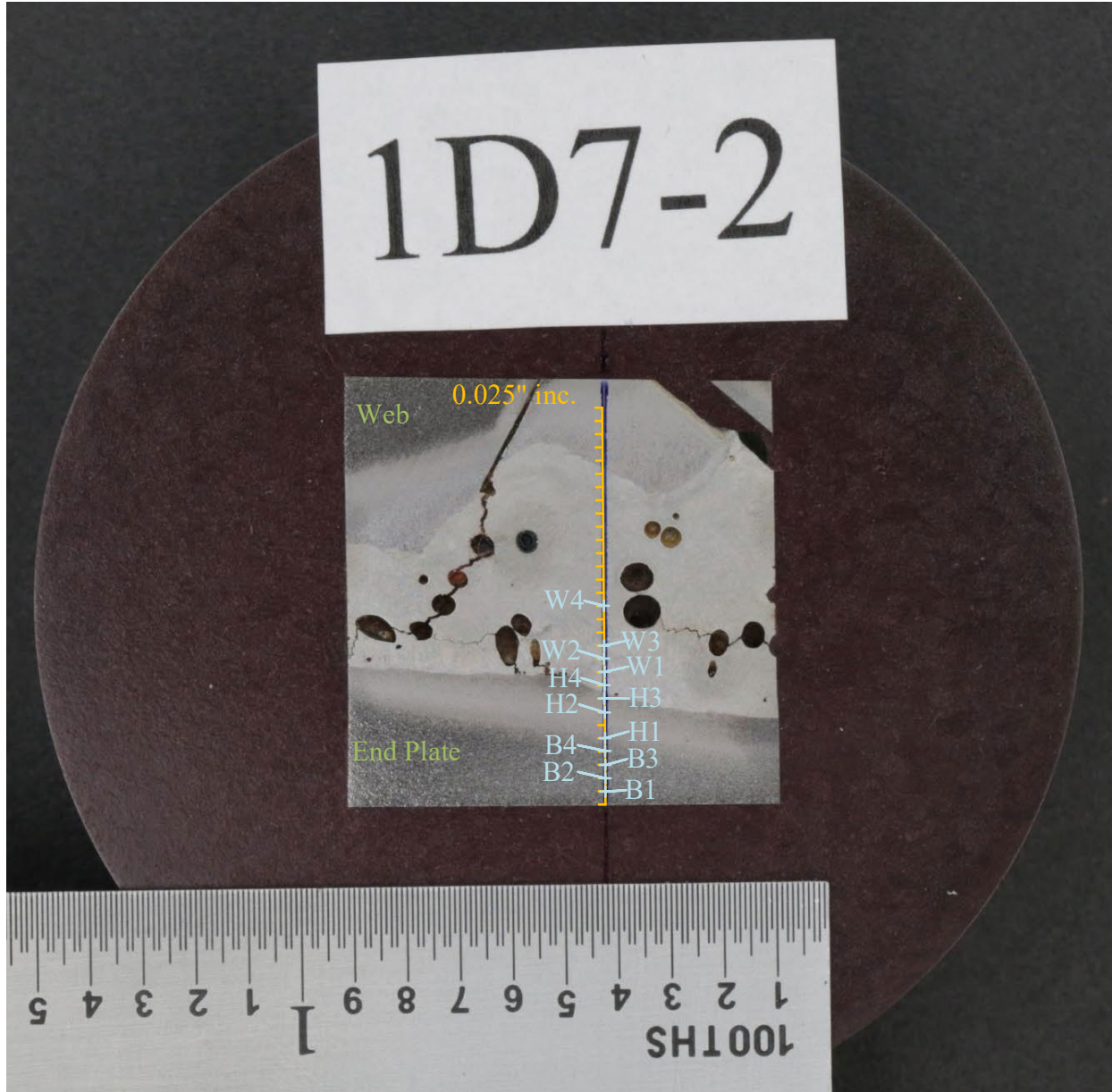


Figure 5. Mounted sectioned area and measurement locations for gradient line 1D7-2.

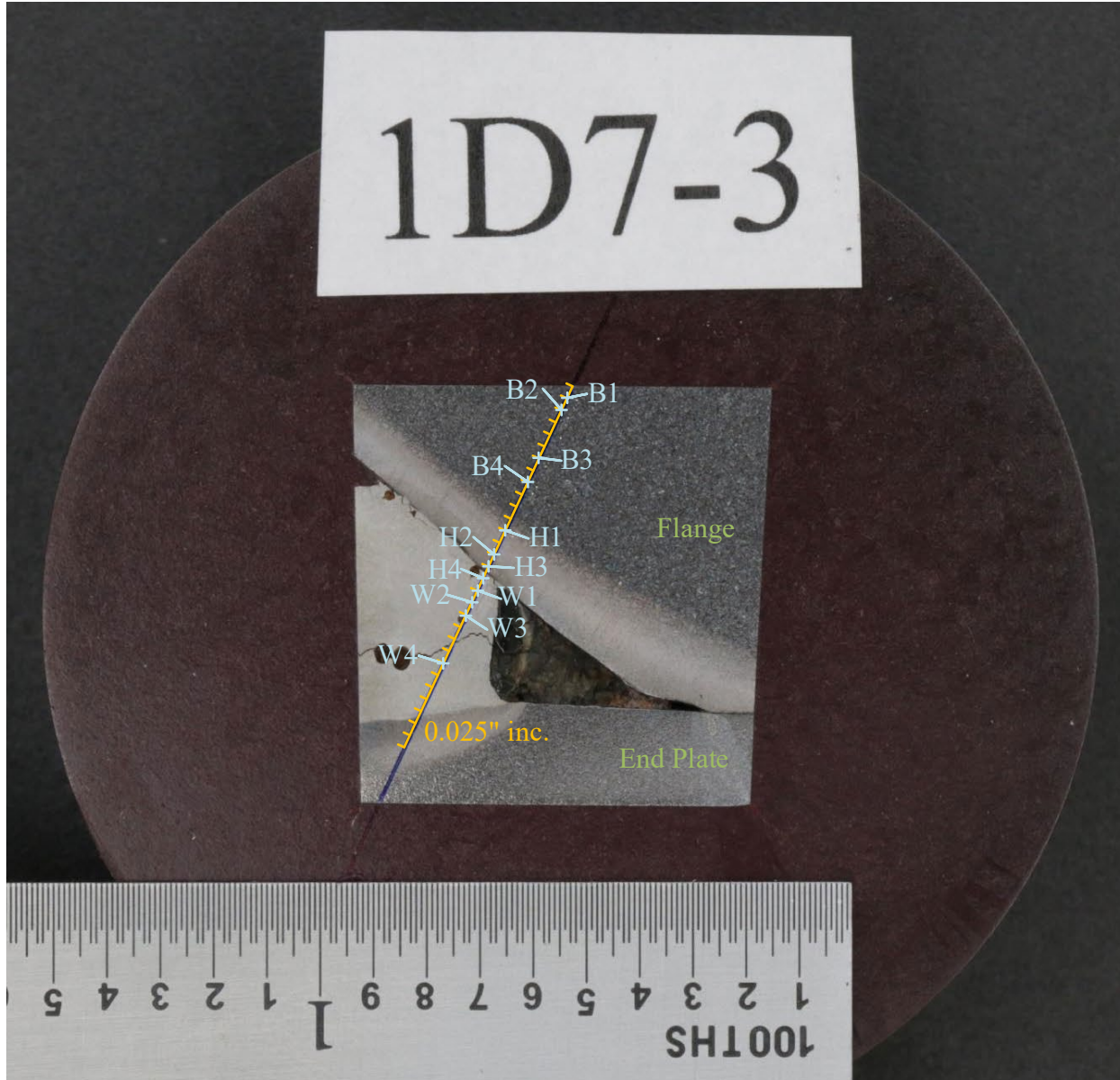


Figure 6. Mounted sectioned area and measurement locations for gradient line 1D7-3.

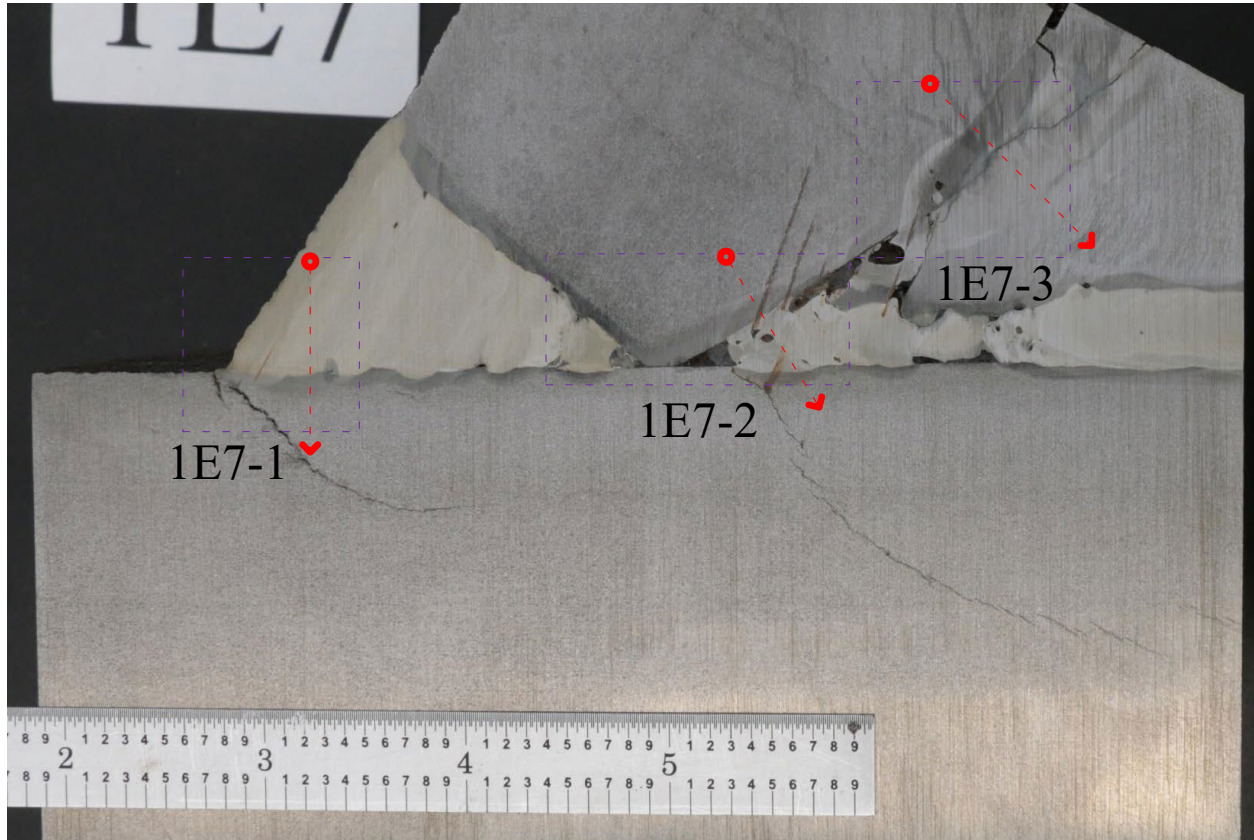


Figure 7. Macroetch of 1E7 with approximate sectioned area and gradient line path.

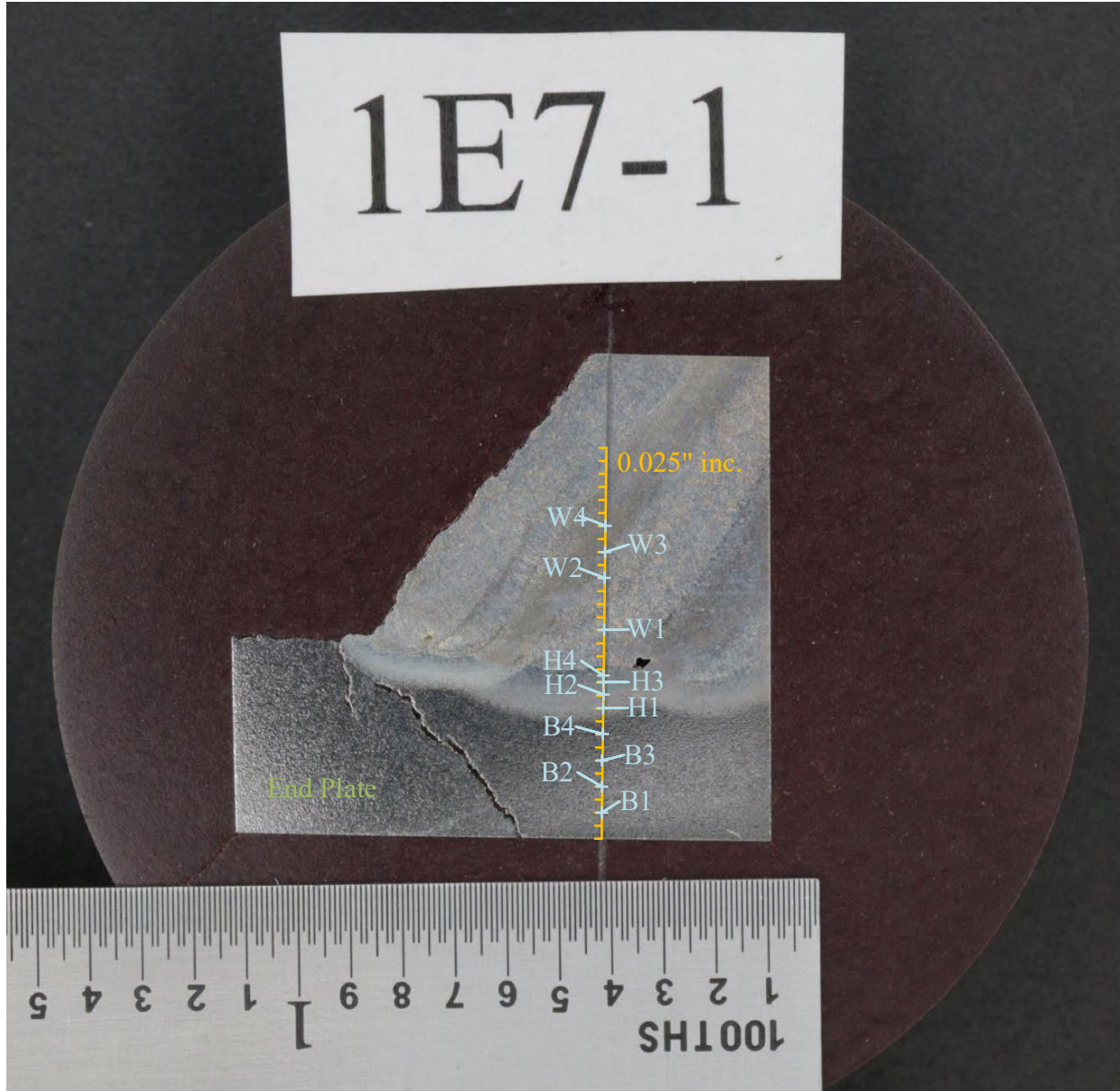


Figure 8. Mounted sectioned area and measurement locations for gradient line 1E7-1.

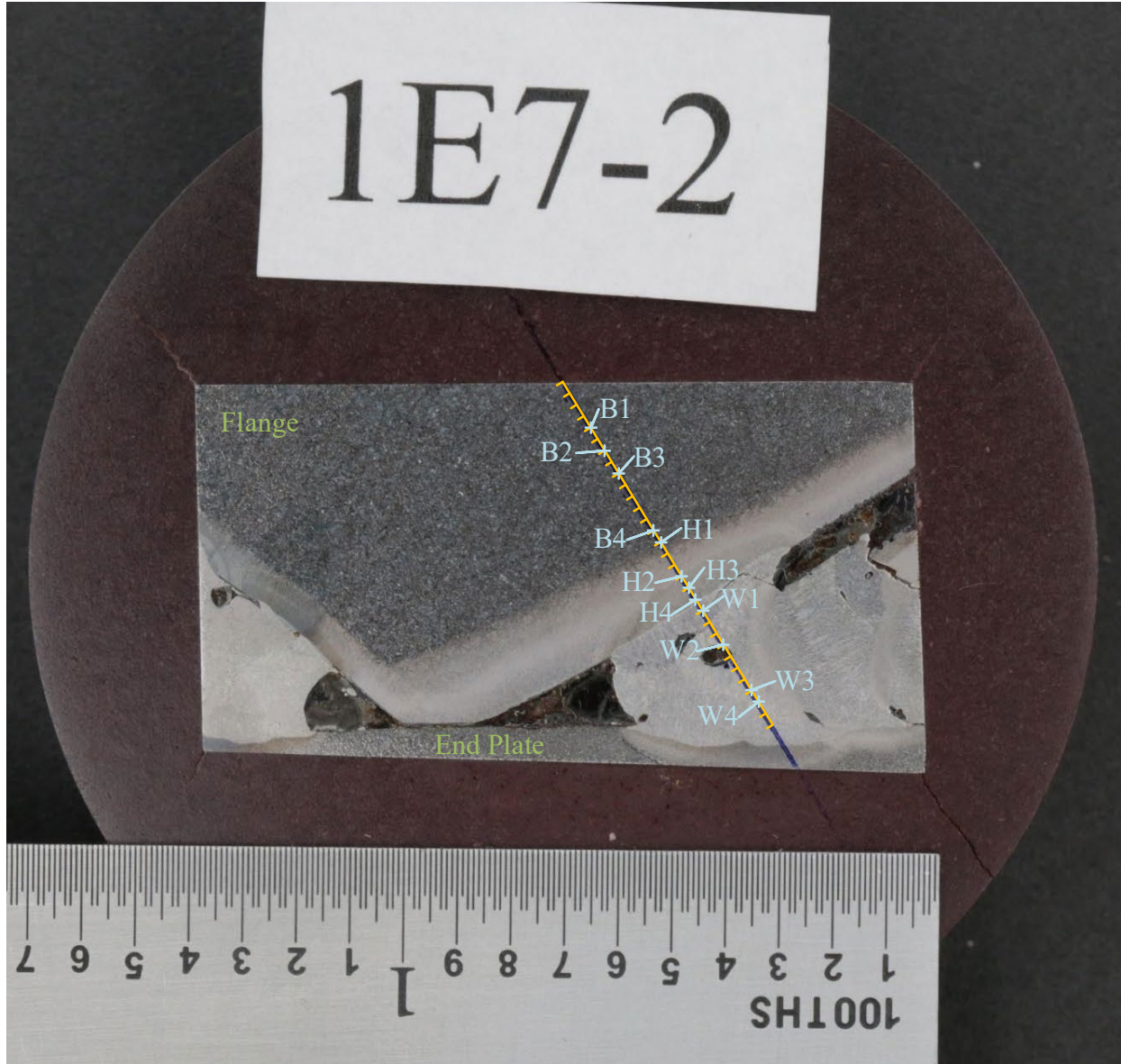


Figure 9. Mounted sectioned area and measurement locations for gradient line 1E7-2.

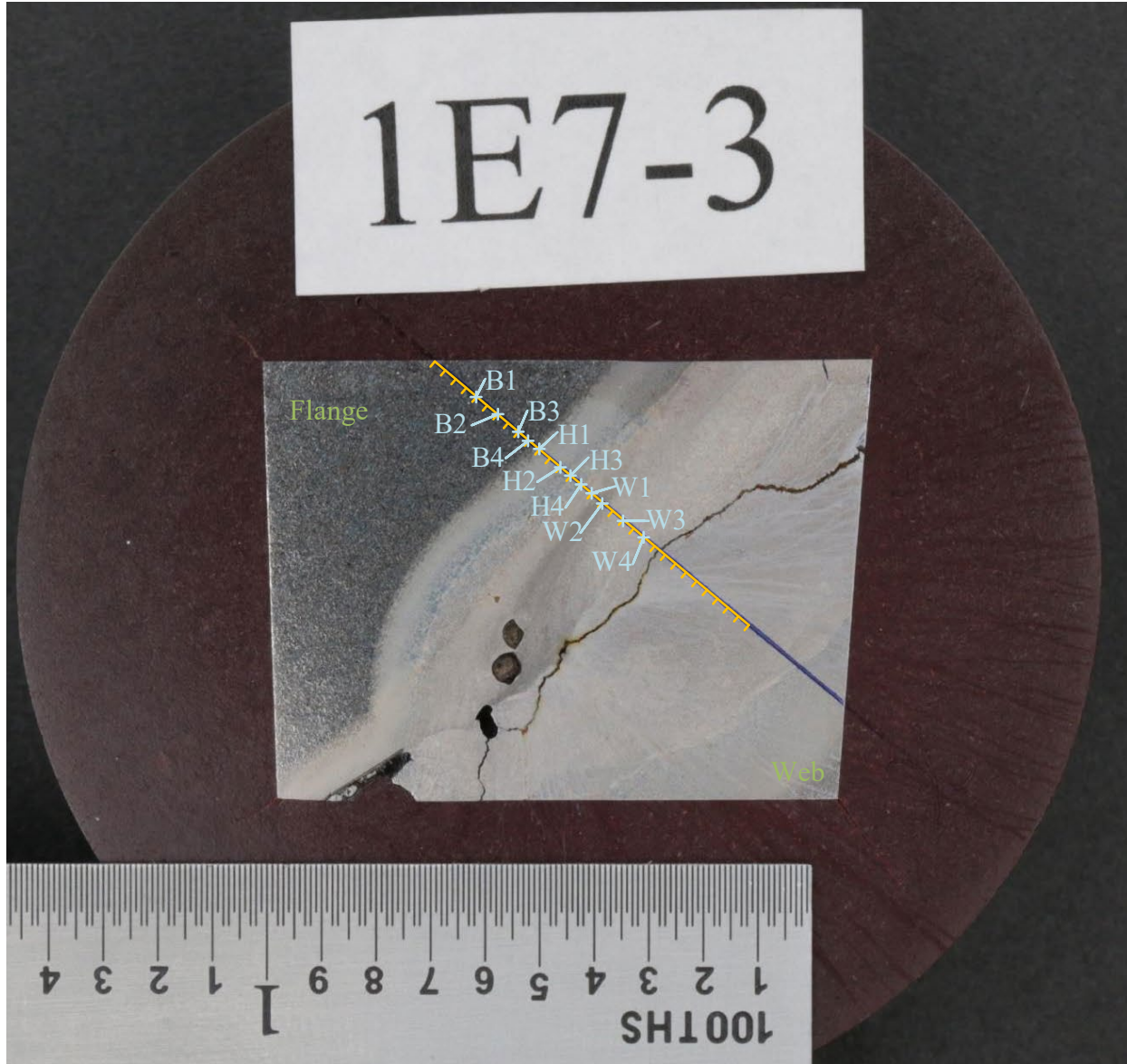


Figure 10. Mounted sectioned area and measurement locations for gradient line 1E7-3.

Images were captured in a light box using a 20.2 MP camera with a dynamic optical lens set to roughly 20 mm at a 16 in. standoff for the macroetches, and 120 mm at a 12 in. standoff for the mounted sections.

Section 3.1 summarizes the measured Vickers hardness values, following ASTM E92-17, at each defined measurement point. Sections 3.2 and 3.3 show the corresponding microstructures.

Observation and inference of microstructural phase was made through visual comparison to reference images in the American Society for Metals (ASM) *Handbook on Metallography and Microstructures* (ASM 2004). Further verification of specific microstructural phases could be accomplished through an incremental addition of various etchant solutions; however, the primary objective was to identify the presence of dark needlelike crystals typical in martensite.

3.1. Summary of Vickers hardness measurements

The measured Vickers microindentation hardness values for the 72 testing locations are summarized in Table 1. The reported Vickers hardness number is rounded to three significant digits in accordance with ASTM E29-22.

The hardness values aligned with expectations: values in the base metal were the lowest, followed by a rapid spike in hardness in the HAZ, then a return to hardness values slightly above that of the base metal within the weld metal. Within the HAZ, there were six measured hardness values that surpassed the prescribed 350 HV 0.5 probabilistic indicator threshold for a microstructural phase change. These are denoted in Table 1 with shaded cells.

Minor localized variation of hardness within the gradient line was likely due to the HAZ being from a multipass weldment and due to the discrete-nonuniform spacing of measurements.

Table 1: Vickers microindentation hardness values for a 500 gf indent with a 13 second dwell.

Location	Vickers Hardness (HV 0.5)											
	Base Metal				HAZ				Weld Metal			
Sample ID	B1	B2	B3	B4	H1	H2	H3	H4	W1	W2	W3	W4
1D7-1	194	209	194	210	240	280	283	288	249	249	261	256
1D7-2	214	243	221	232	311	326	346	339	268	257	296	278
1D7-3	218	236	229	265	257	412	433	427 ^a	267	309	315	302
1E7-1	230	236	226	239	239	265	274	283	200	195	187	184
1E7-2	240	224	245	230	251	382	395	415	252	261	277	269
1E7-3	223	226	238	222	272	290	305	310	233	334	298	259

Note: Shaded cells indicate that the measured Vickers hardness value is greater than 350 HV 0.5.

^aMeasurement 1D7-3 Sample ID H4 fell inside the weld material, just outside of the HAZ

3.2. Microstructures of 1D7

This section shows the microstructures along gradient lines 1D7-1, 1D7-2, and 1D7-3. The caption for each microstructure contains what the authors believe to be the dominant crystalline phases. The typical observed structures along the gradient are as follows,

- The base metal showed a relatively consistent, and expected, distribution and size of pearlite (dark coloration) to ferrite (light coloration) crystals.
- The HAZ had intermediate decomposition into smaller pearlite and ferrite crystals towards the base metal, followed by martensitic (dark coloration) needlelike crystals further into the HAZ towards the weld.
- The weld metal was generally acicular ferrite dominant with proeutectoid ferrite forming along prior austenite grain boundaries. The weld metal also often contained Widmanstätten ferrite, a needlelike structure coming off the grain boundaries, and occasionally contained martensite.

Table 1 shows that Specimen 1D7-3 had hardness values greater than 350 HV 0.5 at H2, H3, and H4. The corresponding microstructures appear to be martensitic.

3.2.1. Gradient line 1D7-1

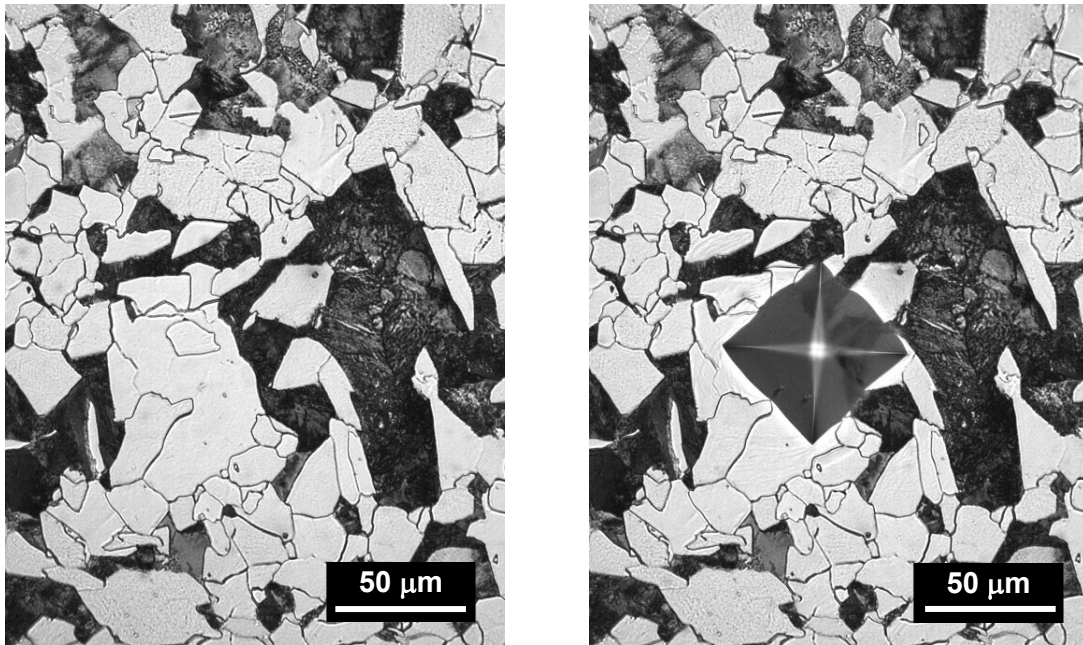


Figure 11. 1D7-1 Sample ID B1 microstructure prior to indentation (left) and with the Vickers microindentation (right). 5% Nital etch. 40x magnification. Ferrite/pearlite dominant.

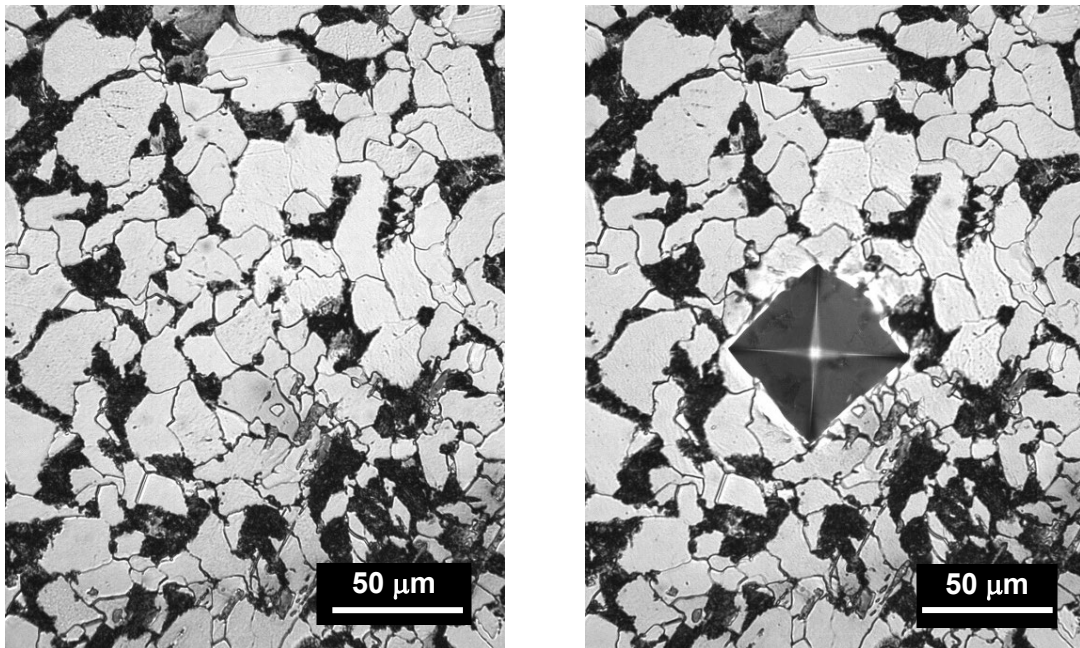


Figure 12. 1D7-1 Sample ID B2 microstructure prior to indentation (left) and with the Vickers microindentation (right). 5% Nital etch. 40x magnification. Ferrite/pearlite dominant.

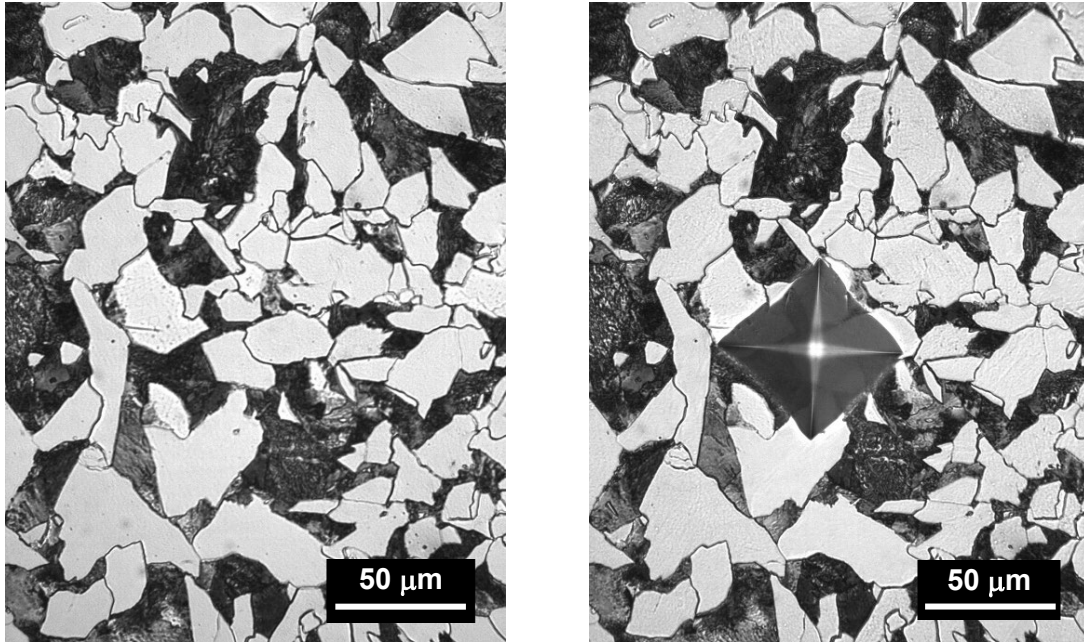


Figure 13. 1D7-1 Sample ID B3 microstructure prior to indentation (left) and with the Vickers microindentation (right). 5% Nital etch. 40x magnification. Ferrite/pearlite dominant.

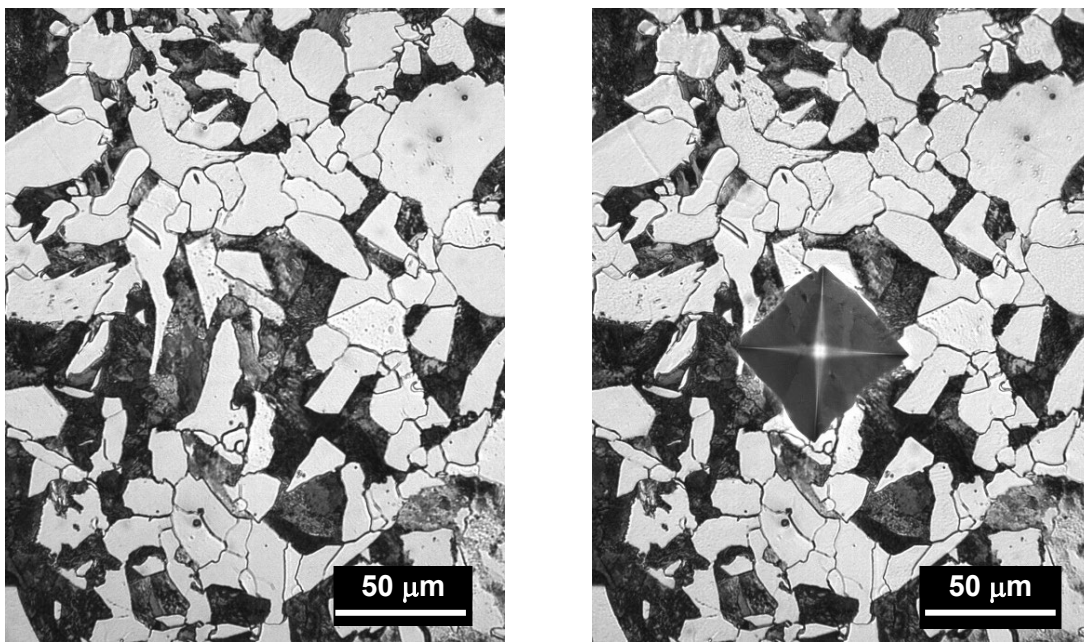


Figure 14. 1D7-1 Sample ID B4 microstructure prior to indentation (left) and with the Vickers microindentation (right). 5% Nital etch. 40x magnification. Ferrite/pearlite dominant.

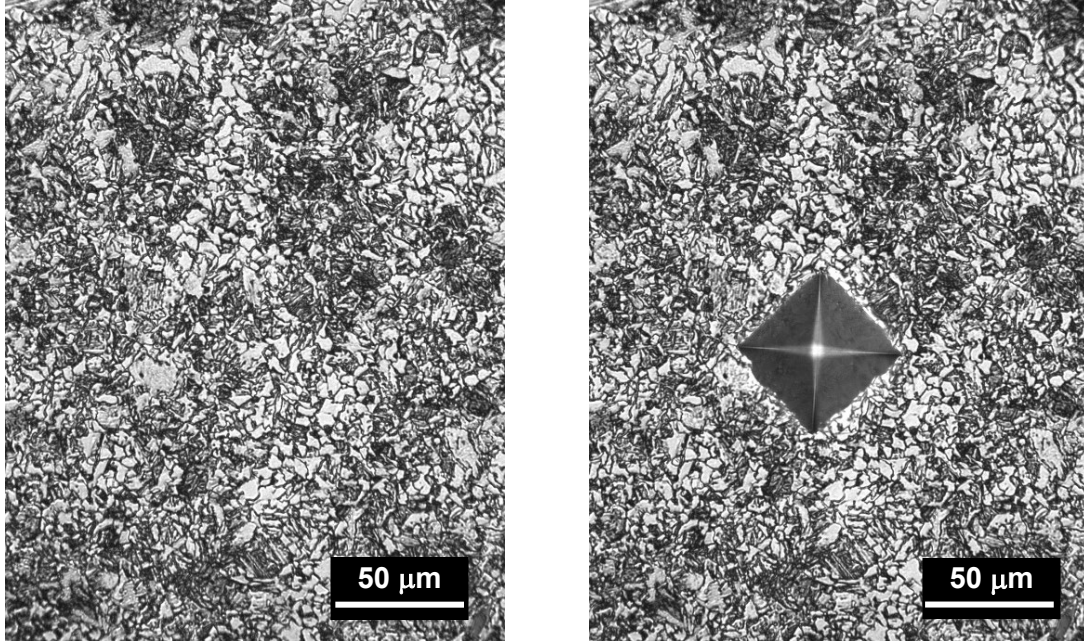


Figure 15. 1D7-1 Sample ID H1 microstructure prior to indentation (left) and with the Vickers microindentation (right). 5% Nital etch. 40x magnification. Refined ferrite/pearlite from the heat cycle.

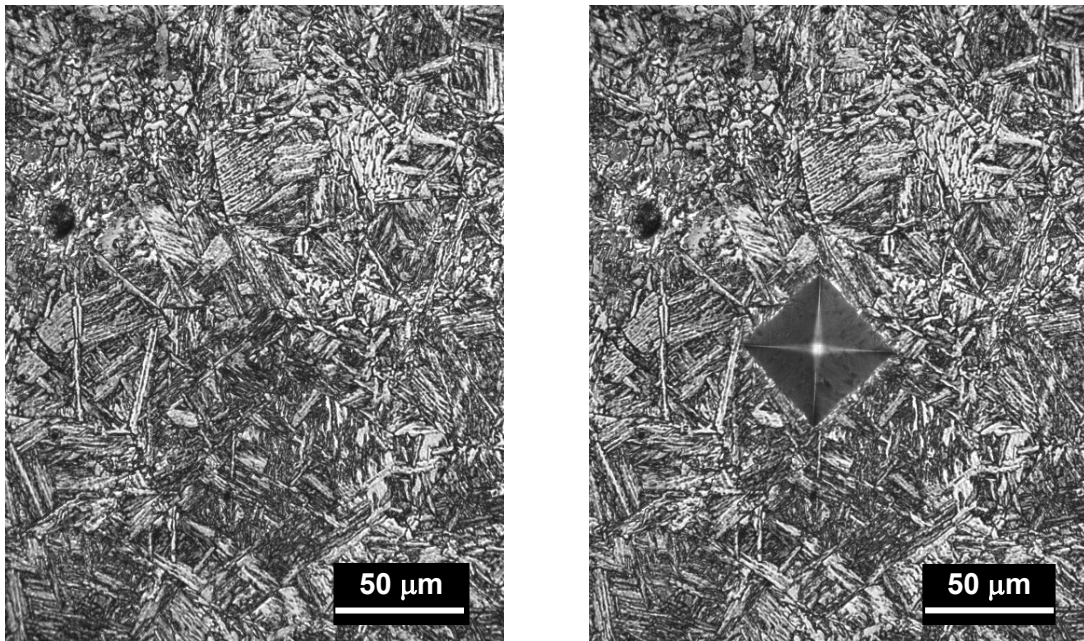


Figure 16. 1D7-1 Sample ID H2 microstructure prior to indentation (left) and with the Vickers microindentation (right). 5% Nital etch. 40x magnification. Martensite dominant.

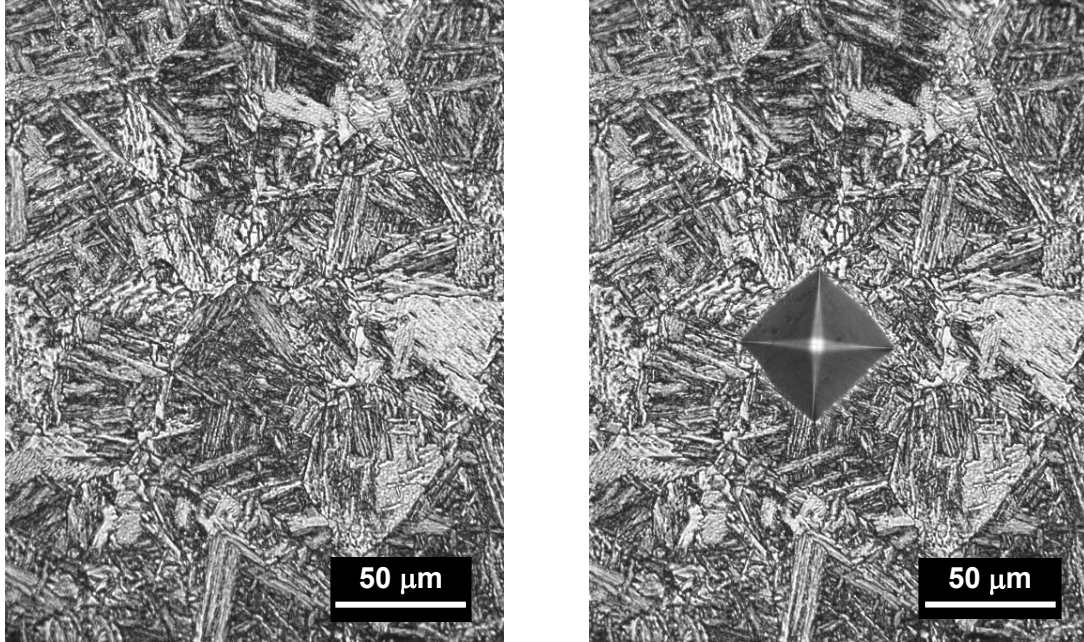


Figure 17. 1D7-1 Sample ID H3 microstructure prior to indentation (left) and with the Vickers microindentation (right). 5% Nital etch. 40x magnification. Martensite dominant.

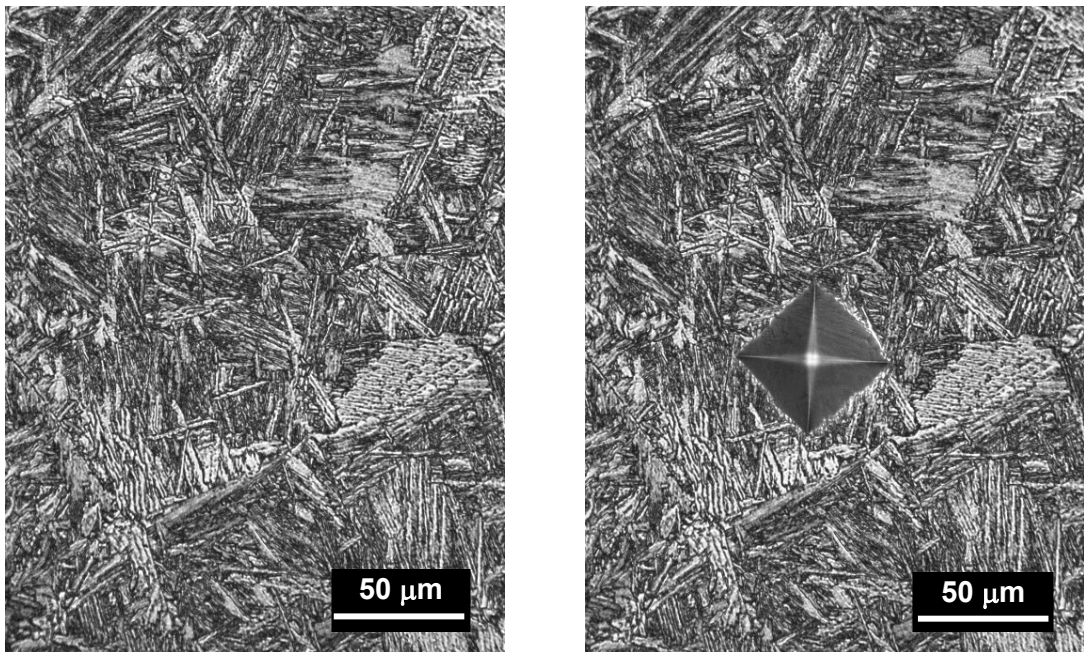


Figure 18. 1D7-1 Sample ID H4 microstructure prior to indentation (left) and with the Vickers microindentation (right). 5% Nital etch. 40x magnification. Martensite dominant.

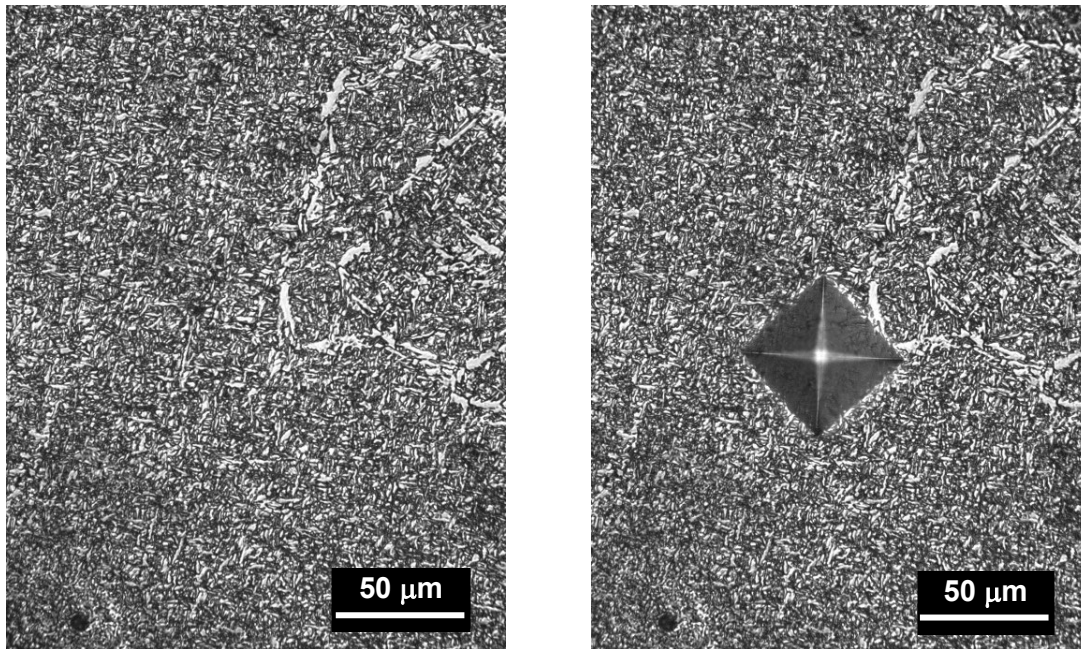


Figure 19. 1D7-1 Sample ID W1 microstructure prior to indentation (left) and with the Vickers microindentation (right). 5% Nital etch. 40x magnification. Acicular ferrite dominant with some proeutectoid ferrite.

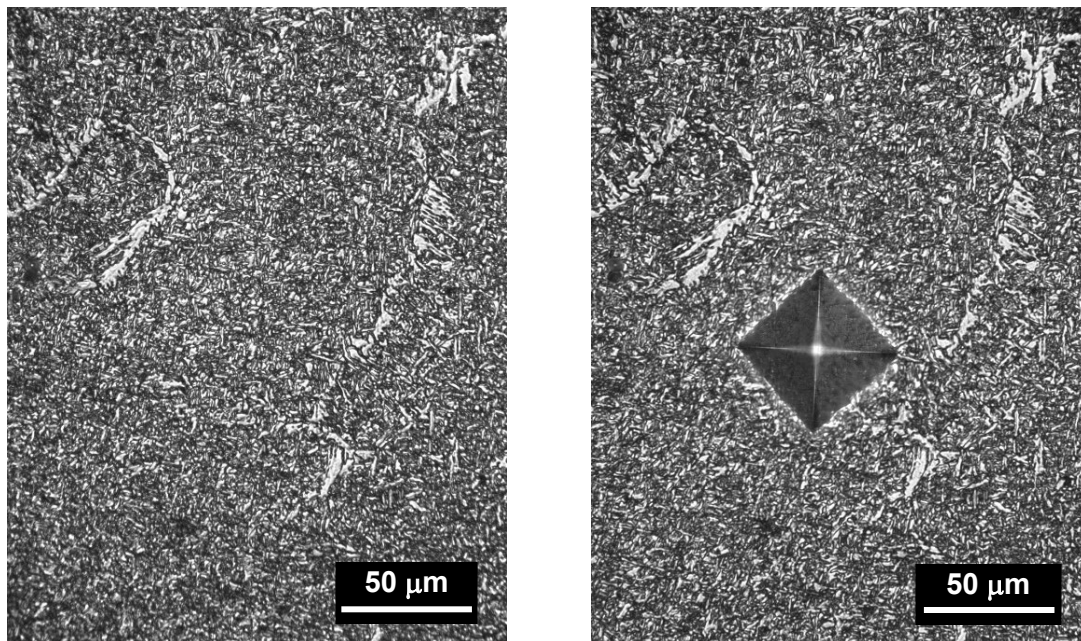


Figure 20. 1D7-1 Sample ID W2 microstructure prior to indentation (left) and with the Vickers microindentation (right). 5% Nital etch. 40x magnification. Acicular ferrite dominant with some proeutectoid ferrite and Widmanstätten ferrite.

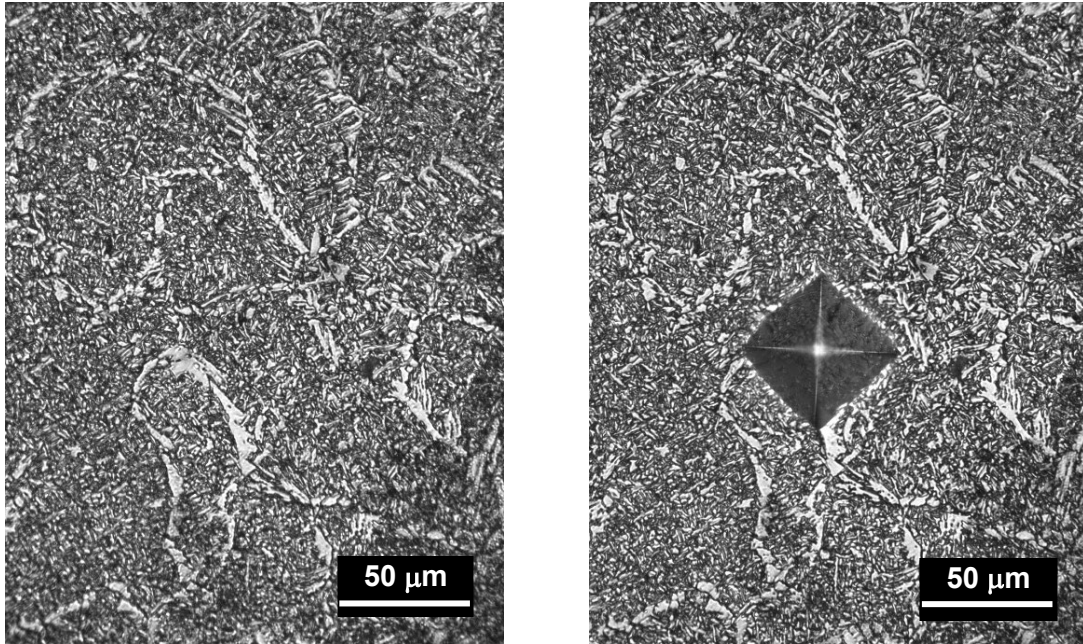


Figure 21. 1D7-1 Sample ID W3 microstructure prior to indentation (left) and with the Vickers microindentation (right). 5% Nital etch. 40x magnification. Acicular ferrite dominant with some proeutectoid ferrite and Widmanstätten ferrite.

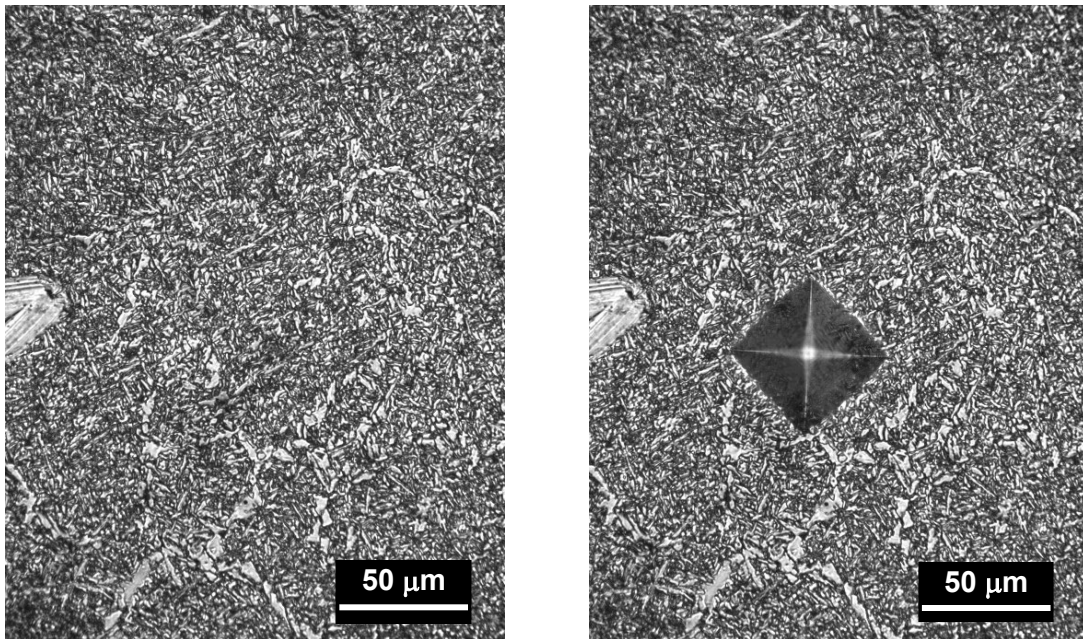


Figure 22. 1D7-1 Sample ID W4 microstructure prior to indentation (left) and with the Vickers microindentation (right). 5% Nital etch. 40x magnification. Acicular ferrite dominant with some proeutectoid ferrite and Widmanstätten ferrite.

3.2.2. Gradient line 1D7-2

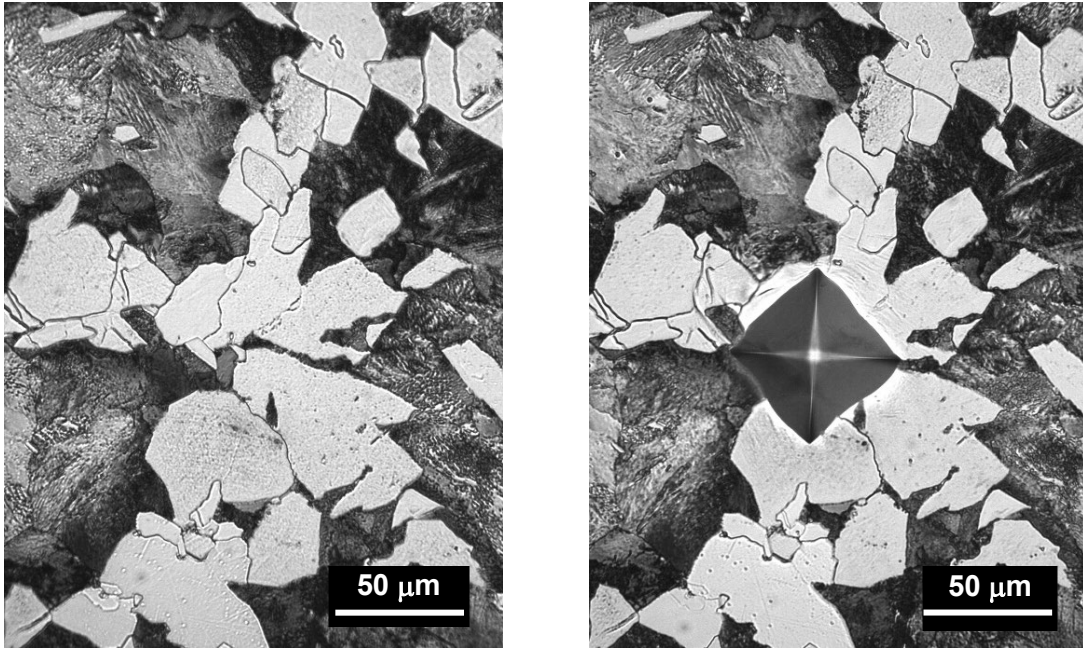


Figure 23. 1D7-2 Sample ID B1 microstructure prior to indentation (left) and with the Vickers microindentation (right). 5% Nital etch. 40x magnification. Ferrite/pearlite dominant.

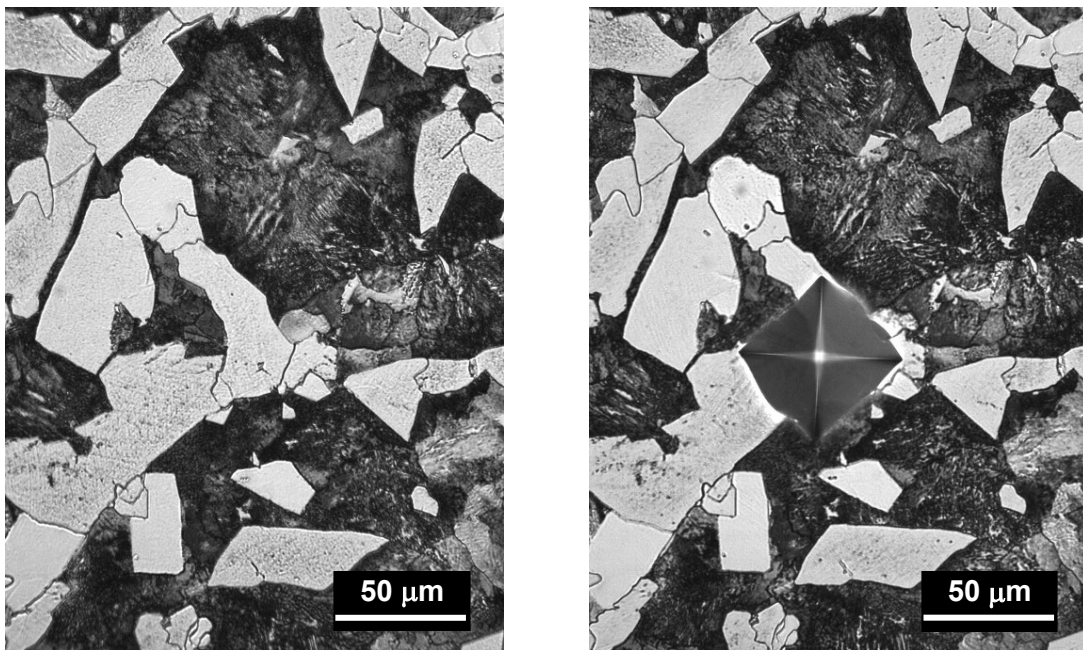


Figure 24. 1D7-2 Sample ID B2 microstructure prior to indentation (left) and with the Vickers microindentation (right). 5% Nital etch. 40x magnification. Ferrite/pearlite dominant.

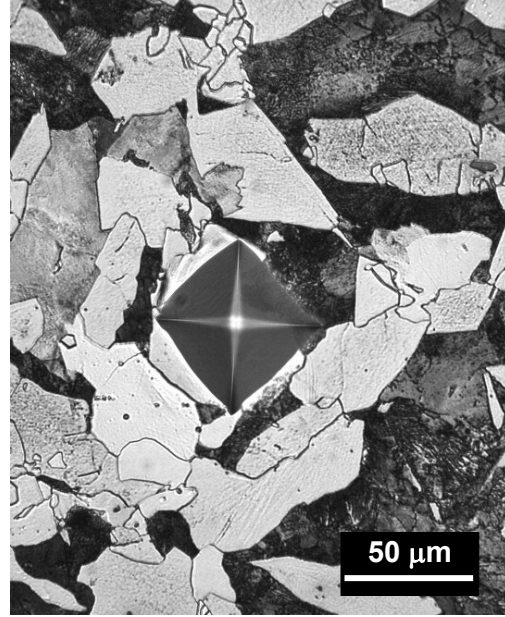
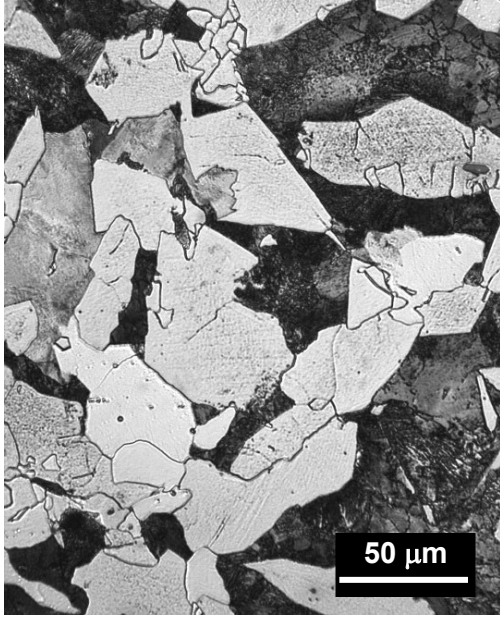


Figure 25. 1D7-2 Sample ID B3 microstructure prior to indentation (left) and with the Vickers microindentation (right). 5% Nital etch. 40x magnification. Ferrite/pearlite dominant.

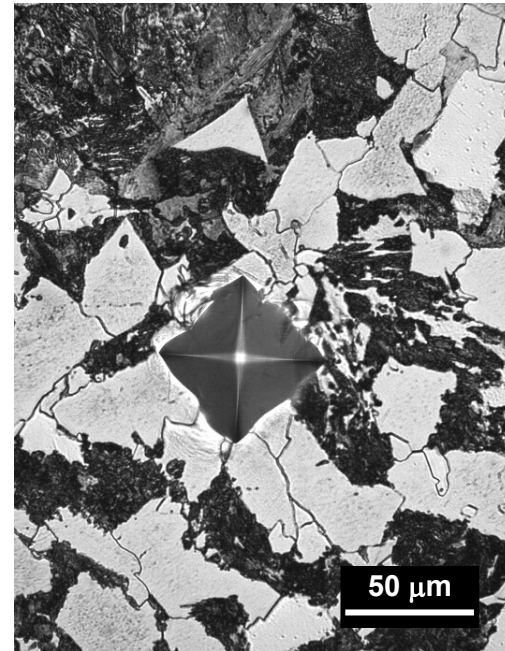
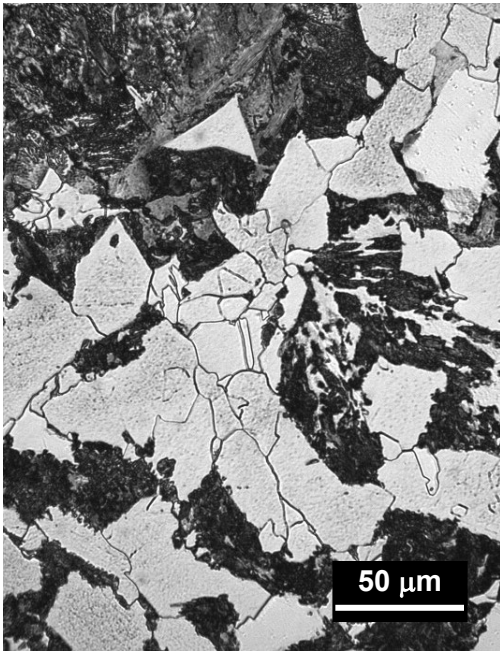


Figure 26. 1D7-2 Sample ID B4 microstructure prior to indentation (left) and with the Vickers microindentation (right). 5% Nital etch. 40x magnification. Ferrite/pearlite dominant.

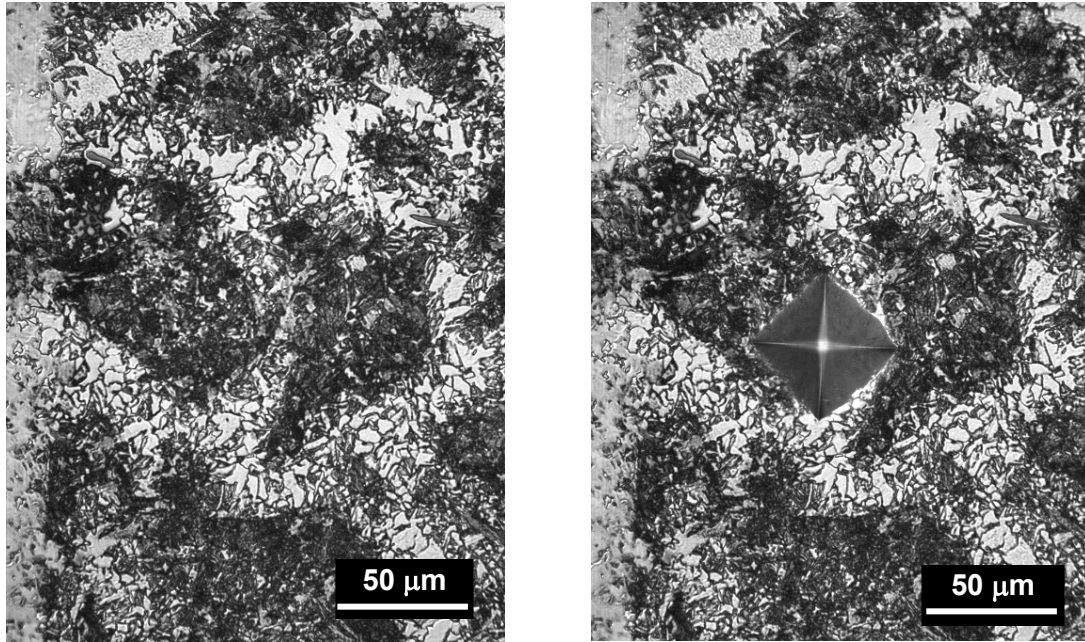


Figure 27. 1D7-2 Sample ID H1 microstructure prior to indentation (left) and with the Vickers microindentation (right). 5% Nital etch. 40x magnification. Refined ferrite/pearlite from the heat cycle.

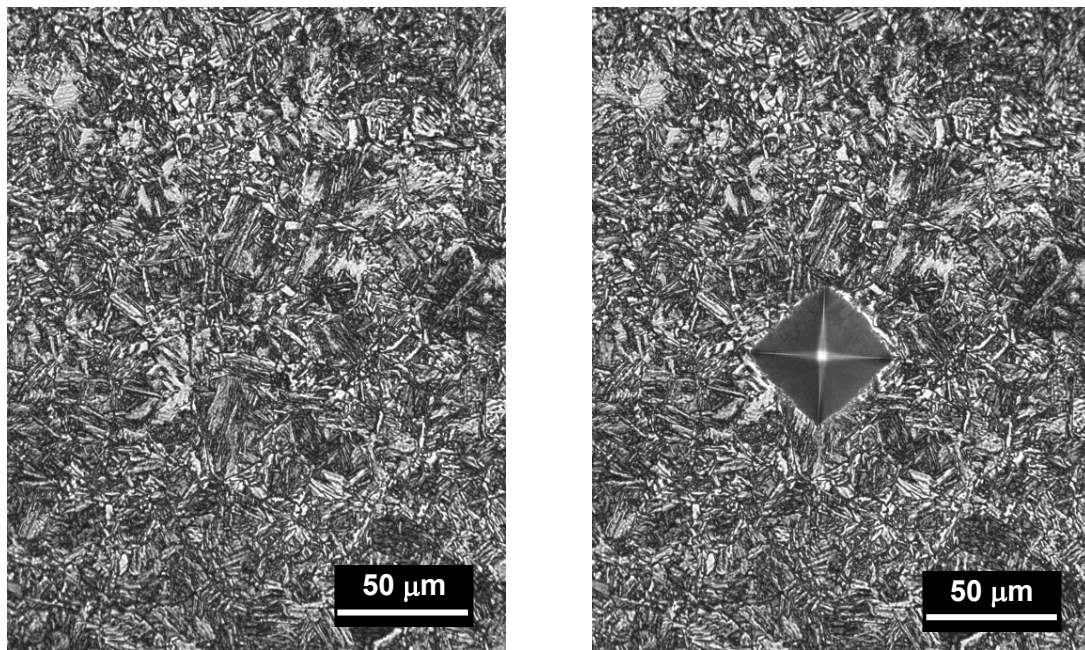


Figure 28. 1D7-2 Sample ID H2 microstructure prior to indentation (left) and with the Vickers microindentation (right). 5% Nital etch. 40x magnification. Refined ferrite/pearlite dominant with some martensite.

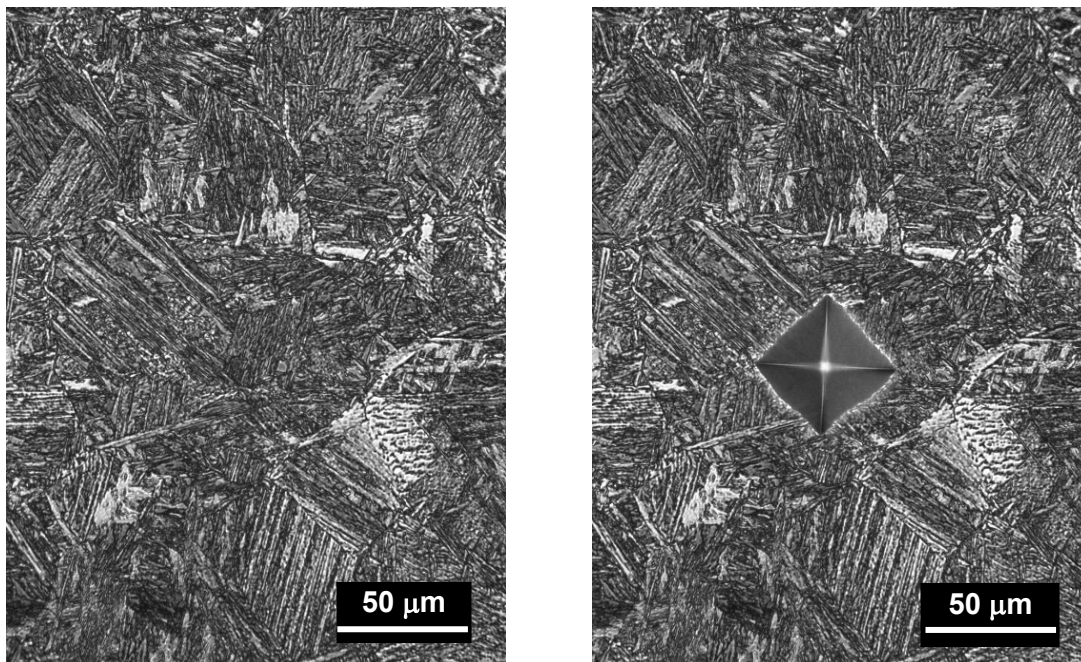


Figure 29. 1D7-2 Sample ID H3 microstructure prior to indentation (left) and with the Vickers microindentation (right). 5% Nital etch. 40x magnification. Martensite dominant.

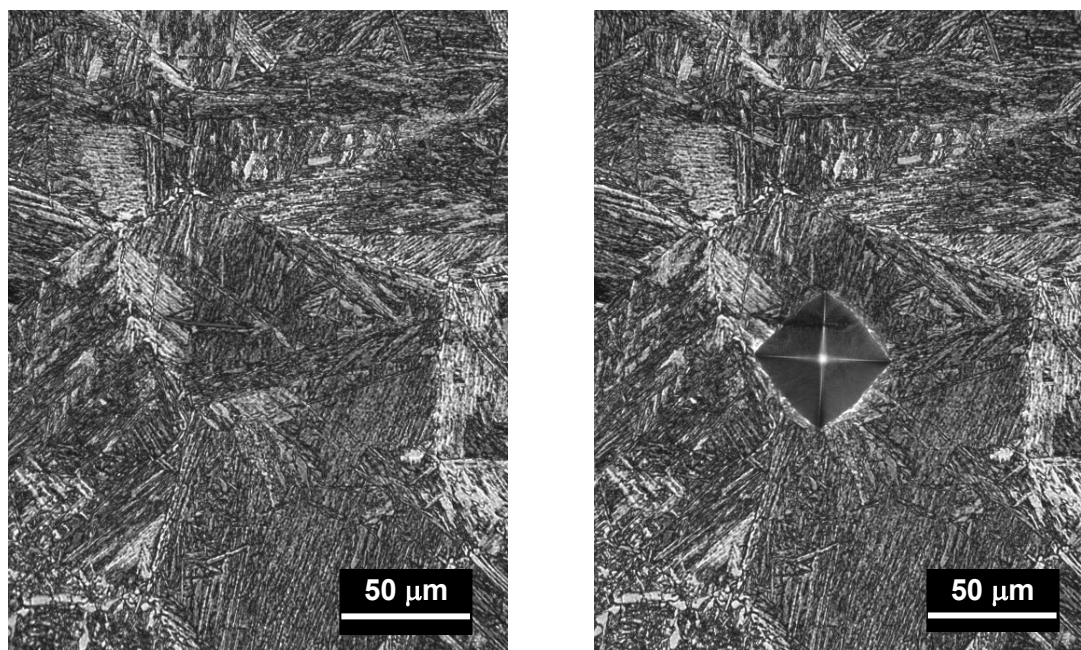


Figure 30. 1D7-2 Sample ID H4 microstructure prior to indentation (left) and with the Vickers microindentation (right). 5% Nital etch. 40x magnification. Martensite dominant.

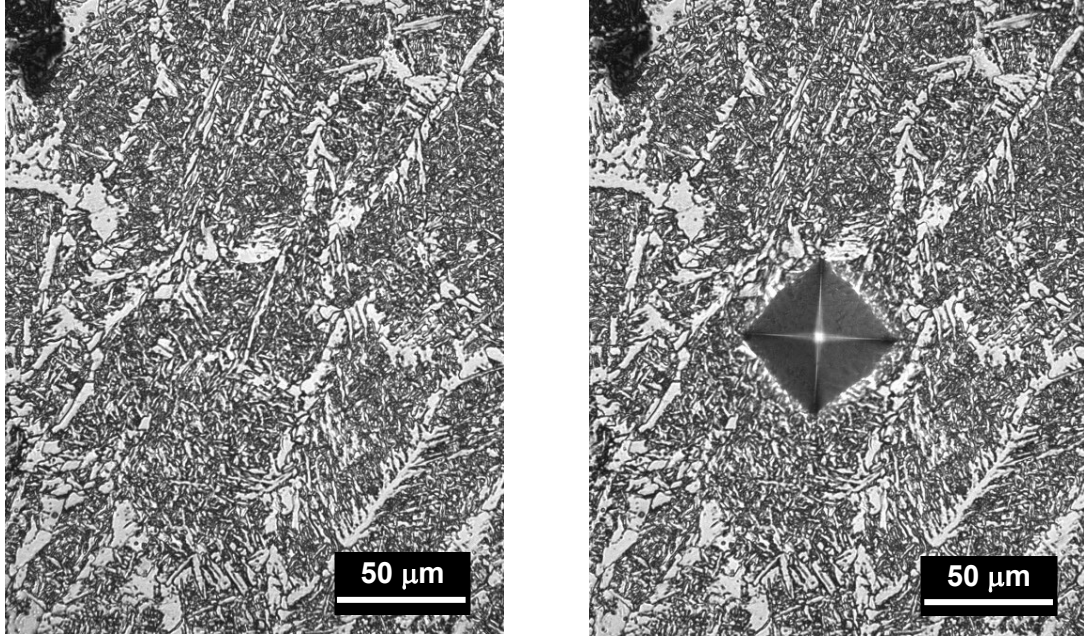


Figure 31. 1D7-2 Sample ID W1 microstructure prior to indentation (left) and with the Vickers microindentation (right). 5% Nital etch. 40x magnification. Note that the upper left corner blotch is marker. Acicular ferrite dominant with some proeutectoid ferrite and Widmanstätten ferrite.

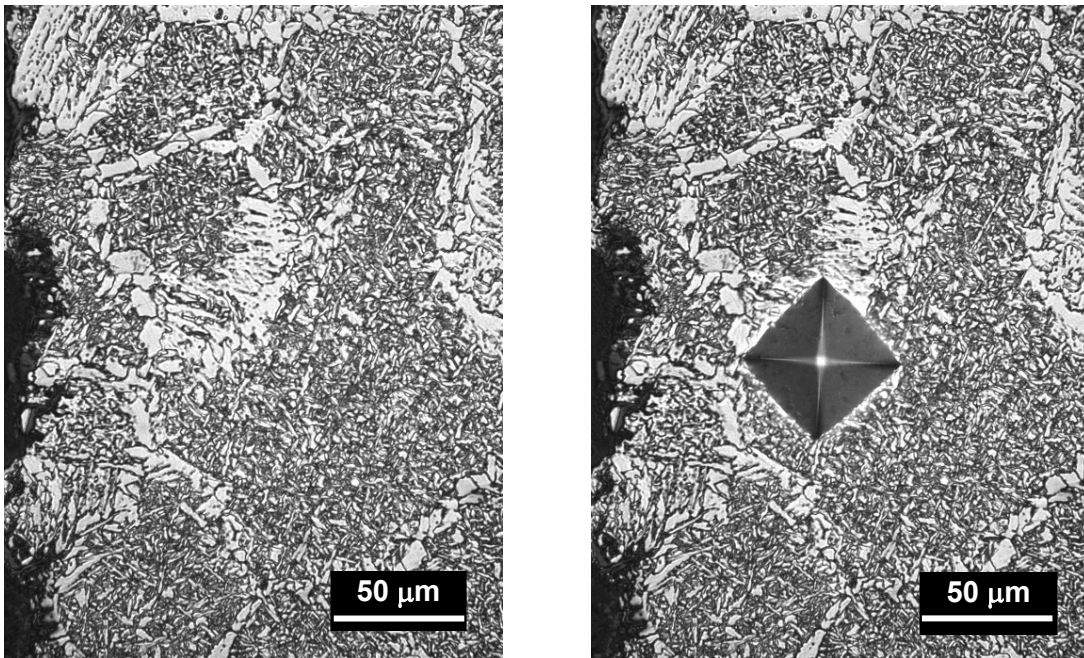


Figure 32. 1D7-2 Sample ID W2 microstructure prior to indentation (left) and with the Vickers microindentation (right). 5% Nital etch. 40x magnification. Note that the blotch about the left edge is marker. Acicular ferrite dominant with some proeutectoid ferrite and Widmanstätten ferrite.

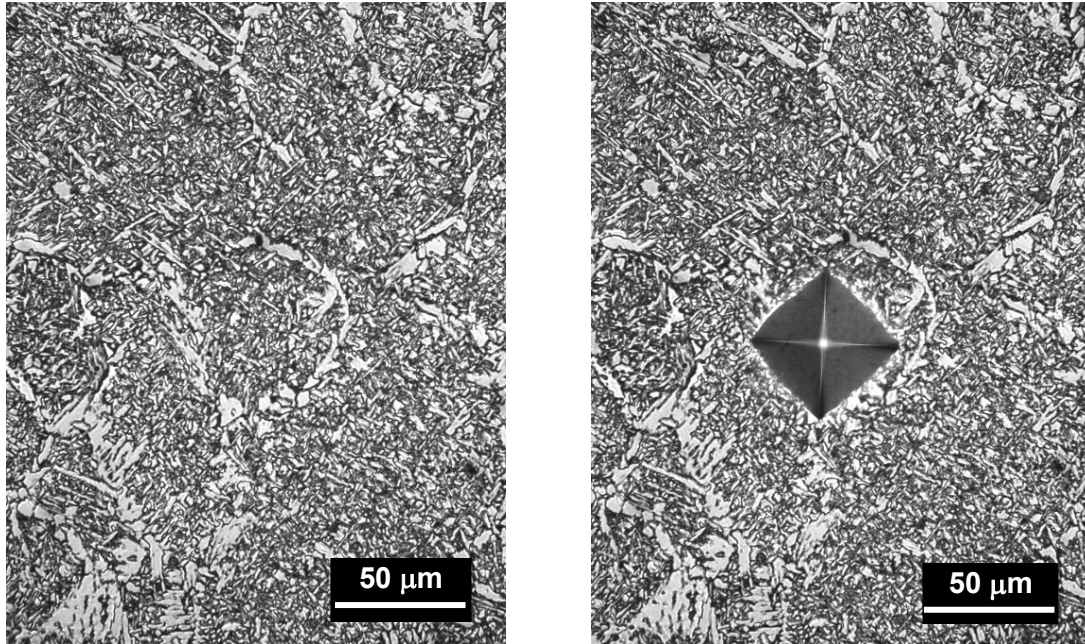


Figure 33. 1D7-2 Sample ID W3 microstructure prior to indentation (left) and with the Vickers microindentation (right). 5% Nital etch. 40x magnification. Acicular ferrite dominant with some proeutectoid ferrite and Widmanstätten ferrite.

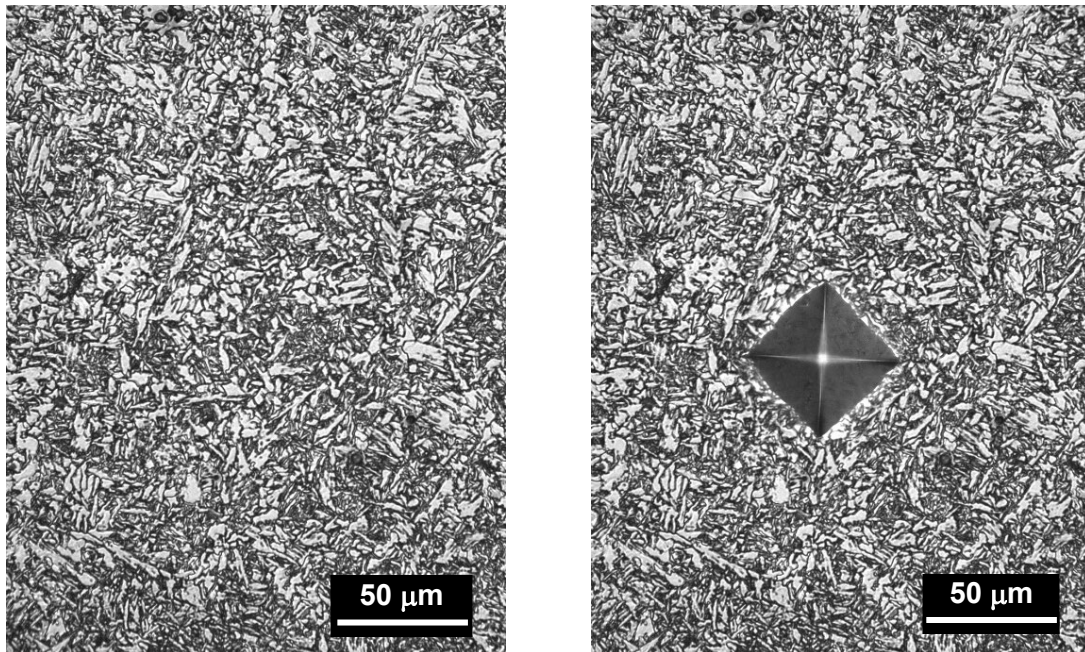


Figure 34. 1D7-2 Sample ID W4 microstructure prior to indentation (left) and with the Vickers microindentation (right). 5% Nital etch. 40x magnification. Acicular ferrite dominant.

3.2.3. Gradient line 1D7-3

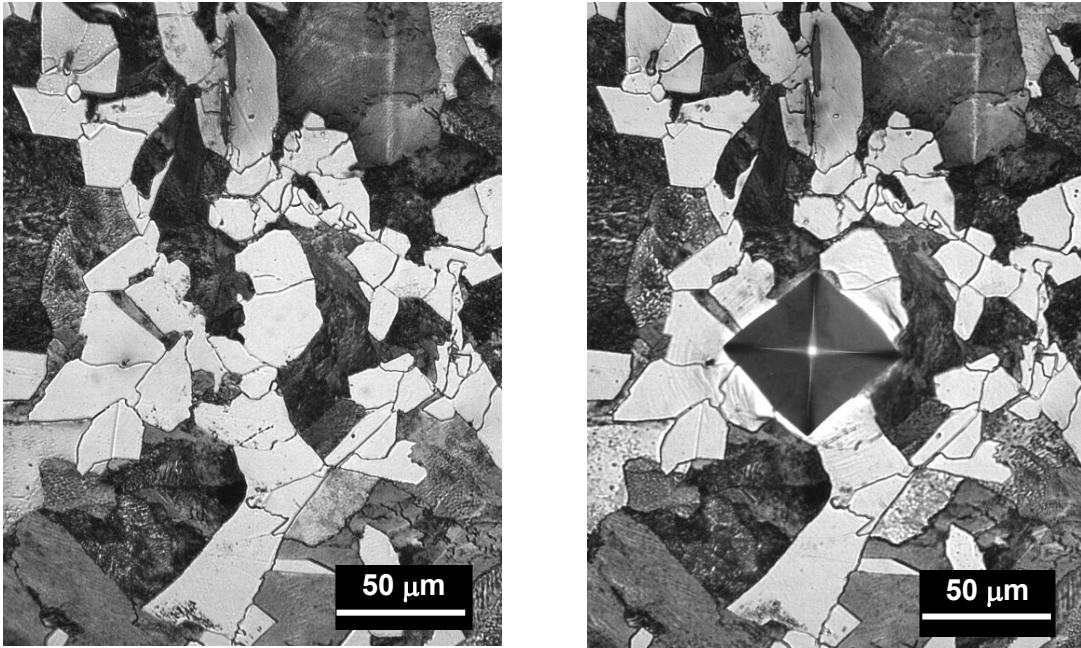


Figure 35. 1D7-3 Sample ID B1 microstructure prior to indentation (left) and with the Vickers microindentation (right). 5% Nital etch. 40x magnification. Ferrite/pearlite dominant.

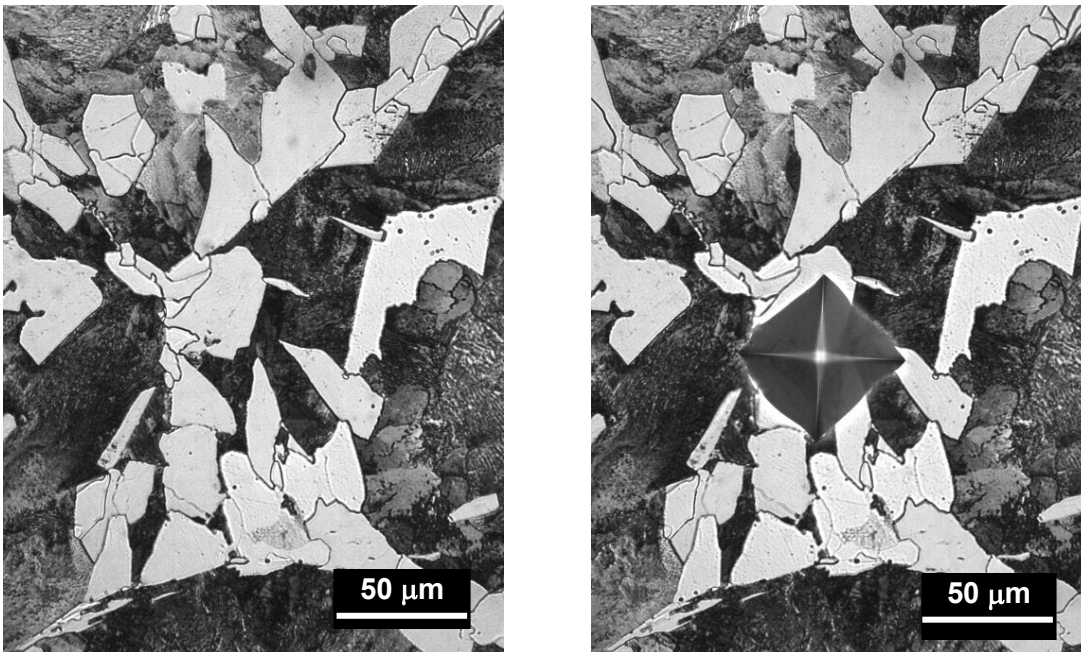


Figure 36. 1D7-3 Sample ID B2 microstructure prior to indentation (left) and with the Vickers microindentation (right). 5% Nital etch. 40x magnification. Ferrite/pearlite dominant.

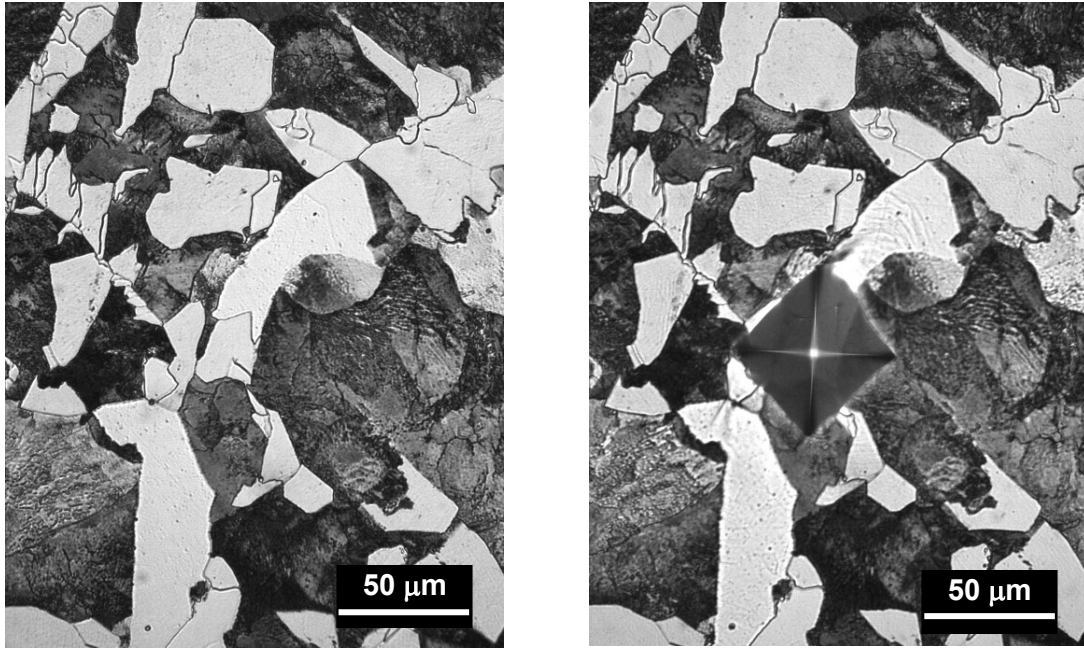


Figure 37. 1D7-3 Sample ID B3 microstructure prior to indentation (left) and with the Vickers microindentation (right). 5% Nital etch. 40x magnification. Ferrite/pearlite dominant.

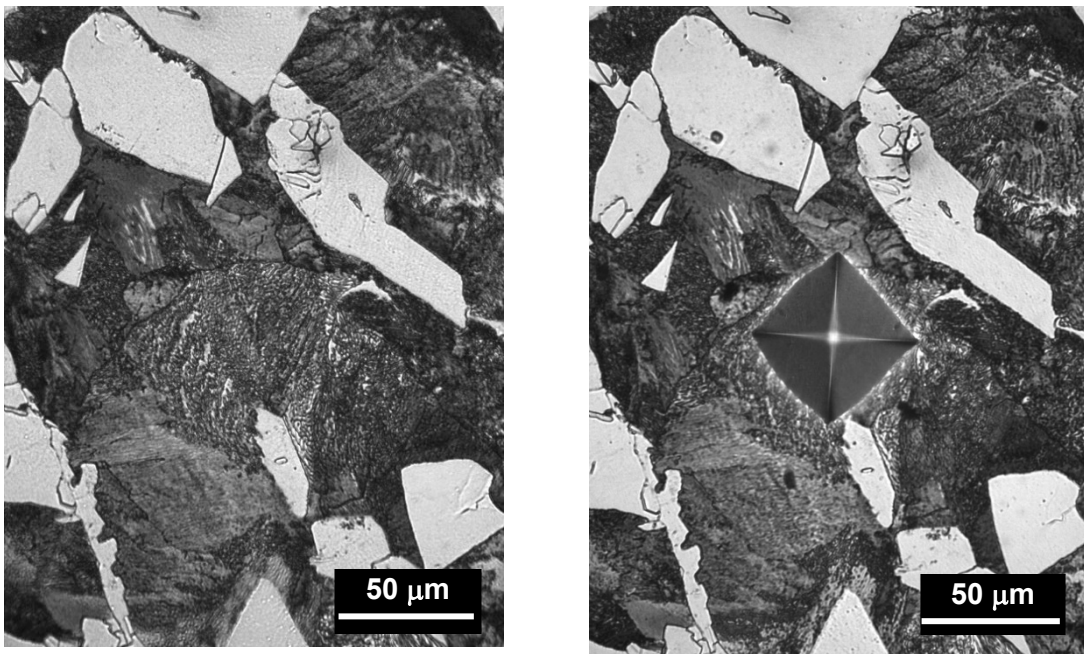


Figure 38. 1D7-3 Sample ID B4 microstructure prior to indentation (left) and with the Vickers microindentation (right). 5% Nital etch. 40x magnification. Ferrite/pearlite dominant.

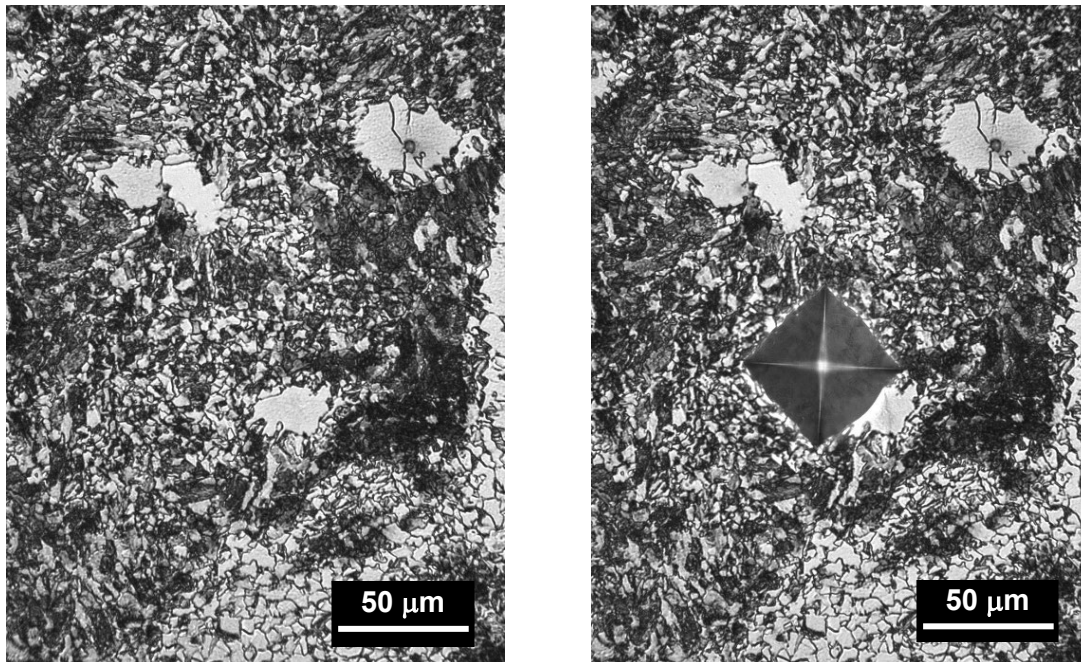


Figure 39. 1D7-3 Sample ID H1 microstructure prior to indentation (left) and with the Vickers microindentation (right). 5% Nital etch. 40x magnification. Refined ferrite/pearlite from the heat cycle.

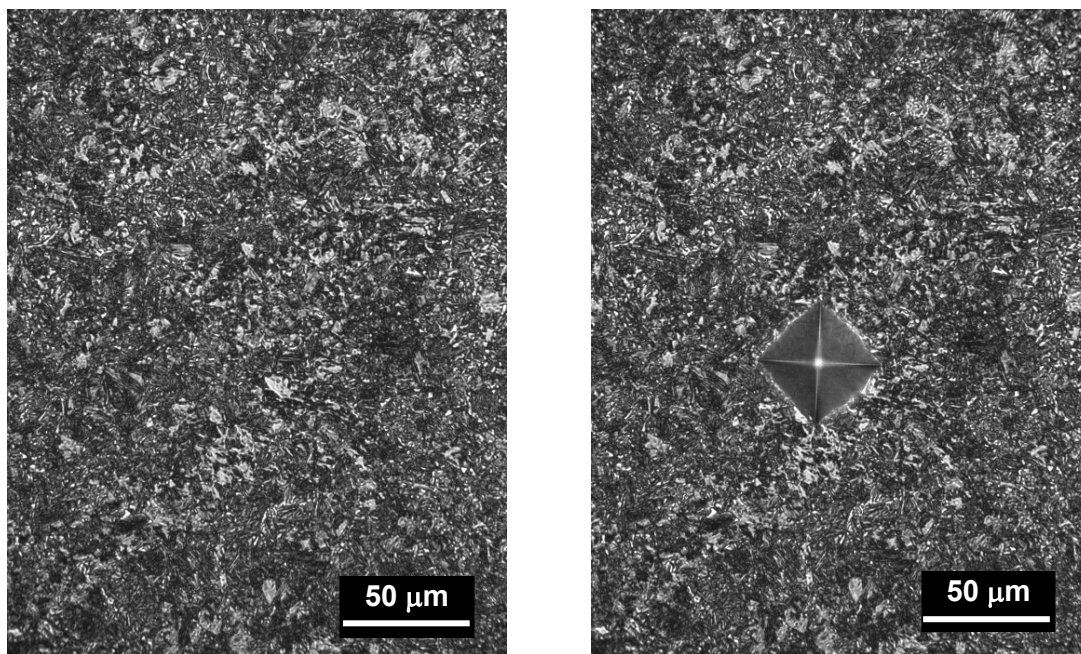


Figure 40. 1D7-3 Sample ID H2 microstructure prior to indentation (left) and with the Vickers microindentation (right). 5% Nital etch. 40x magnification. Martensite dominant.

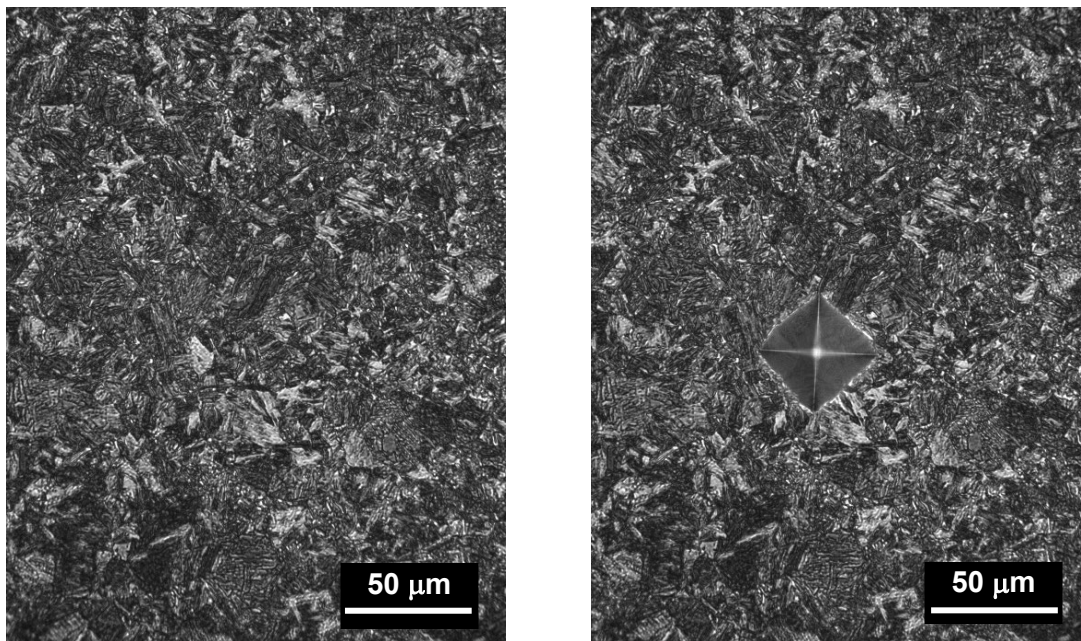


Figure 41. 1D7-3 Sample ID H3 microstructure prior to indentation (left) and with the Vickers microindentation (right). 5% Nital etch. 40x magnification. Martensite dominant.

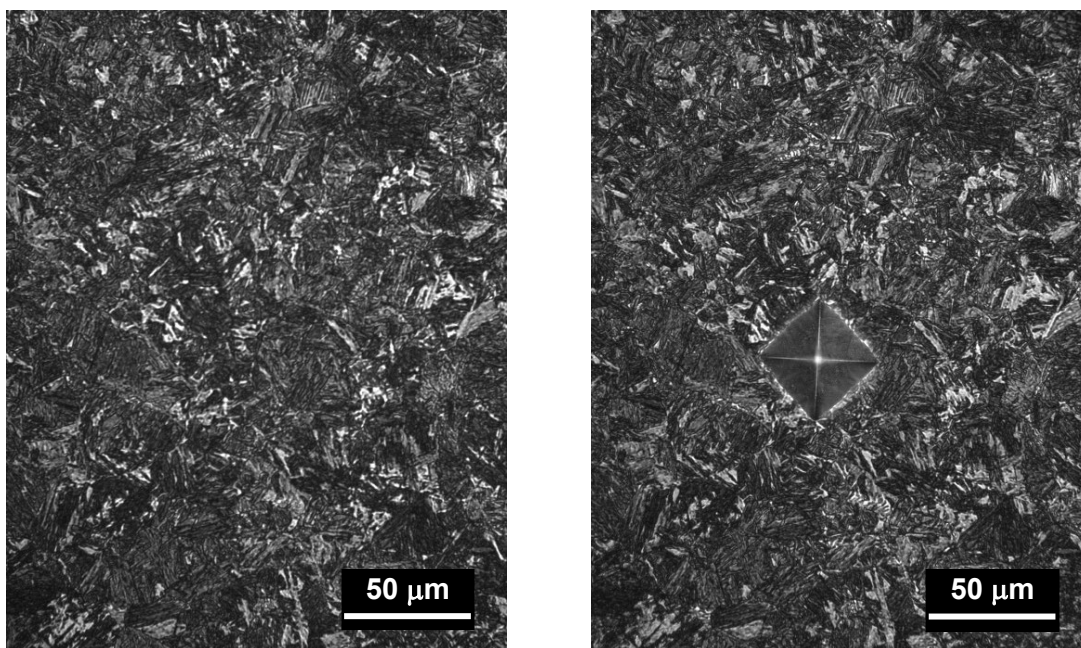


Figure 42. 1D7-3 Sample ID H4 microstructure prior to indentation (left) and with the Vickers microindentation (right). 5% Nital etch. 40x magnification. Martensite dominant.

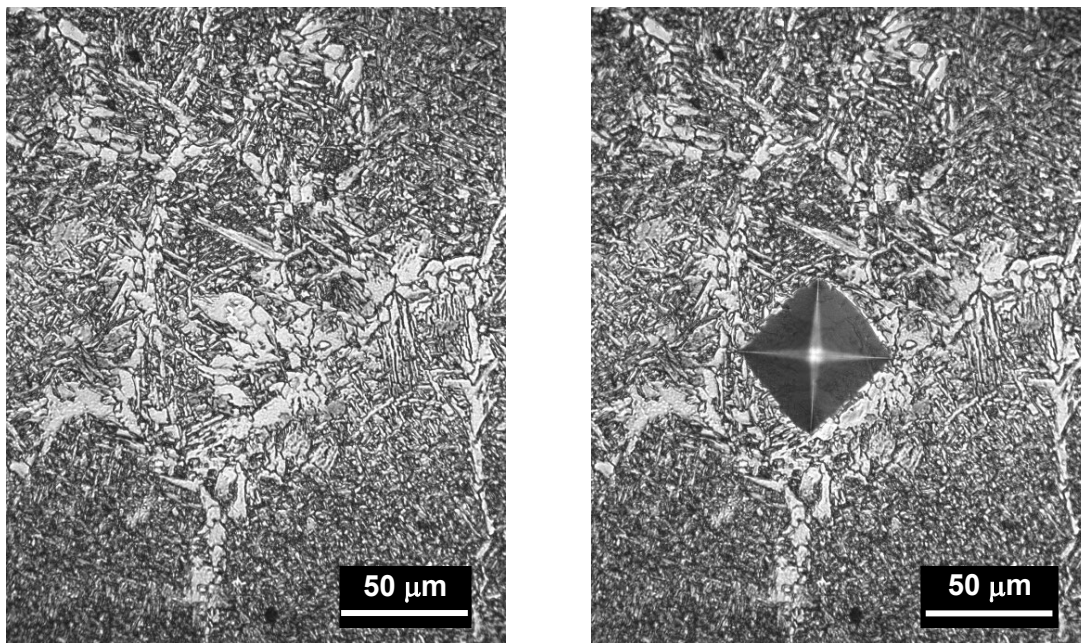


Figure 43. 1D7-3 Sample ID W1 microstructure prior to indentation (left) and with the Vickers microindentation (right). 5% Nital etch. 40x magnification. Acicular ferrite with proeutectoid ferrite and Widmanstätten ferrite.

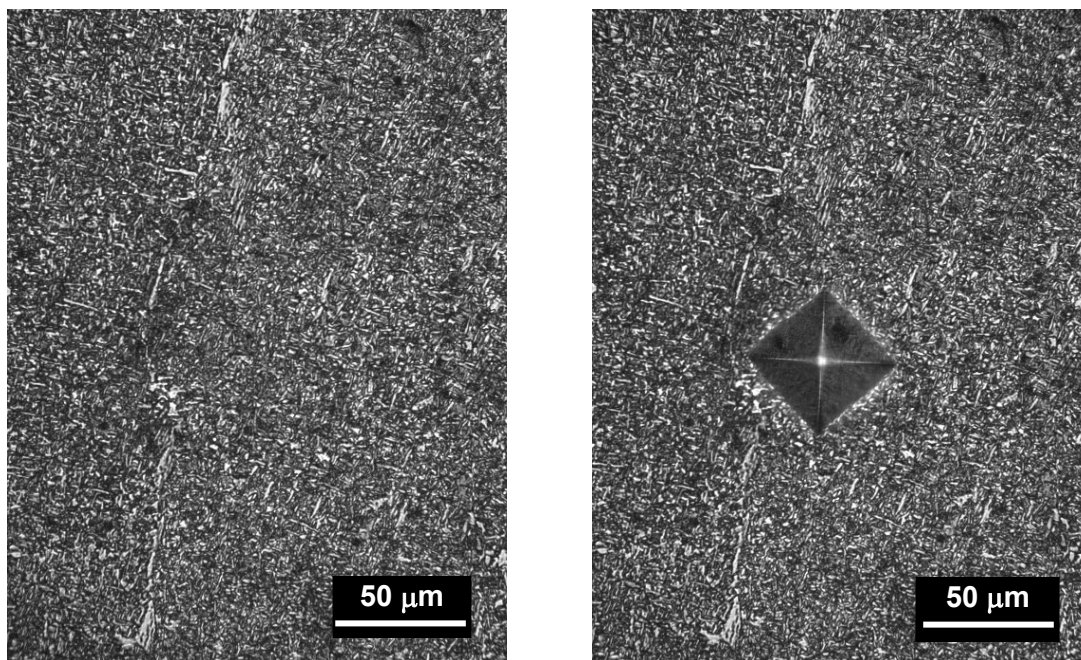


Figure 44. 1D7-3 Sample ID W2 microstructure prior to indentation (left) and with the Vickers microindentation (right). 5% Nital etch. 40x magnification. Acicular ferrite.

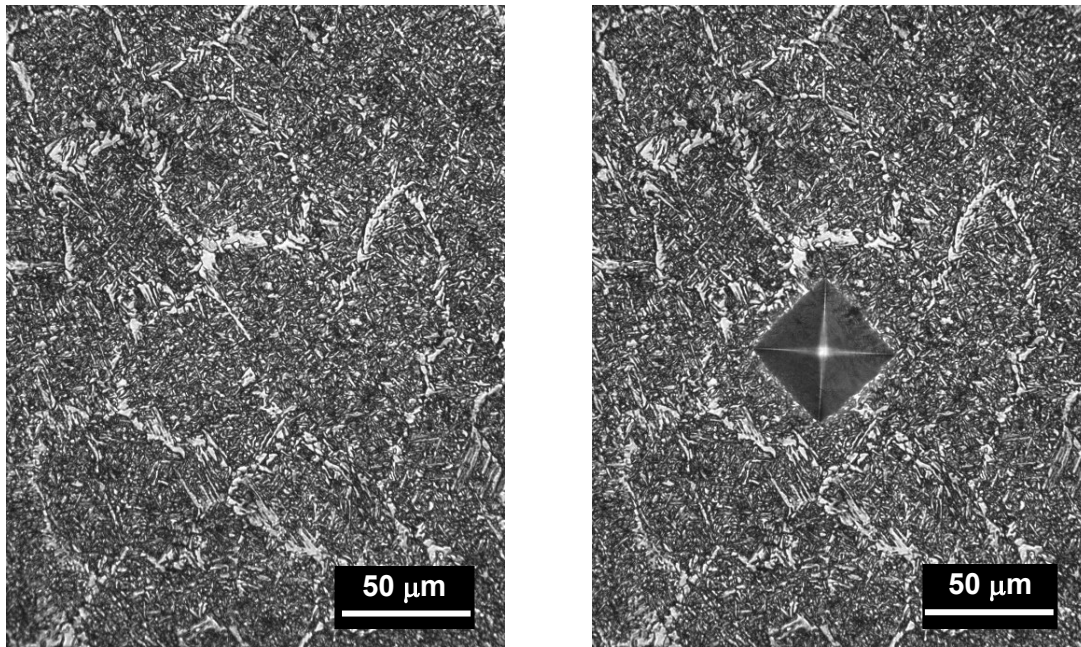


Figure 45. 1D7-3 Sample ID W3 microstructure prior to indentation (left) and with the Vickers microindentation (right). 5% Nital etch. 40x magnification. Acicular ferrite and martensite with some proeutectoid ferrite and Widmanstätten ferrite.

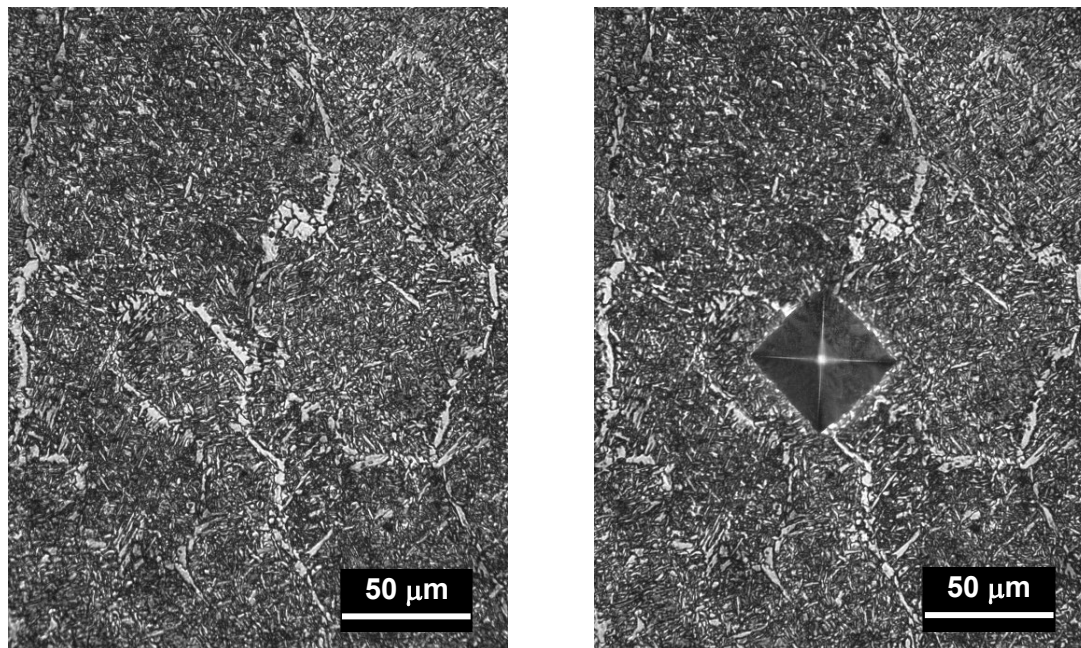


Figure 46. 1D7-3 Sample ID W4 microstructure prior to indentation (left) and with the Vickers microindentation (right). 5% Nital etch. 40x magnification. Acicular ferrite and martensite with some proeutectoid ferrite and Widmanstätten ferrite.

3.3. Microstructures of 1E7

This section shows the microstructures along gradient lines 1E7-1, 1E7-2, and 1E7-3. The caption for each microstructure contains what the authors believe to be the dominant crystalline phases. The microstructures for 1E7 largely followed similar trends to 1D7. The typical observed structures along the gradient are as follows,

- The base metal showed a relatively consistent distribution and size of pearlite (dark coloration) to ferrite (light coloration) crystals. The size of the ferrite grains and pearlite areas were slightly larger than expected but this may be a product of ingot casting.
- The HAZ had intermediate decomposition into smaller pearlite and ferrite crystals towards the base metal, followed by martensitic (dark coloration) needlelike crystals further into the HAZ towards the weld.
- The weld metal structure was more variable than what was observed in 1D7. Many of the microstructures were acicular ferrite dominant with proeutectoid and Widmanstätten ferrite forming along prior austenite grain boundaries, occasionally containing or being primarily martensite. Other microstructures were observed to be simply refined ferrite dominant.

Table 1 shows that Specimen 1E7-2 had hardness values greater than 350 HV 0.5 at H2, H3, and H4. The corresponding microstructures appear to be martensitic.

3.3.1. Gradient line 1E7-1

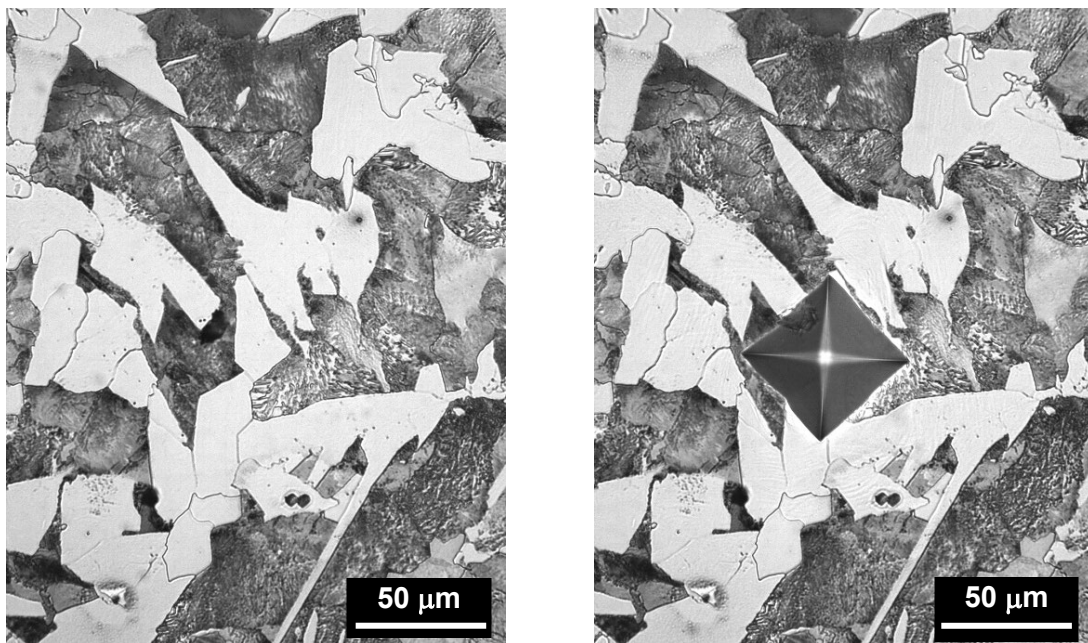


Figure 47. 1E7-1 Sample ID B1 microstructure prior to indentation (left) and with the Vickers microindentation (right). 5% Nital etch. 40x magnification. Ferrite/pearlite dominant.

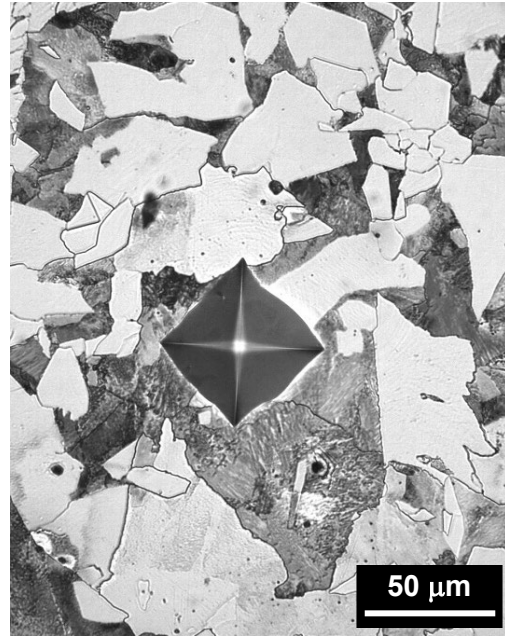


Figure 48. 1E7-1 Sample ID B2 microstructure prior to indentation (left) and with the Vickers microindentation (right). 5% Nital etch. 40x magnification. Ferrite/pearlite dominant.



Figure 49. 1E7-1 Sample ID B3 microstructure prior to indentation (left) and with the Vickers microindentation (right). 5% Nital etch. 40x magnification. Ferrite/pearlite dominant.

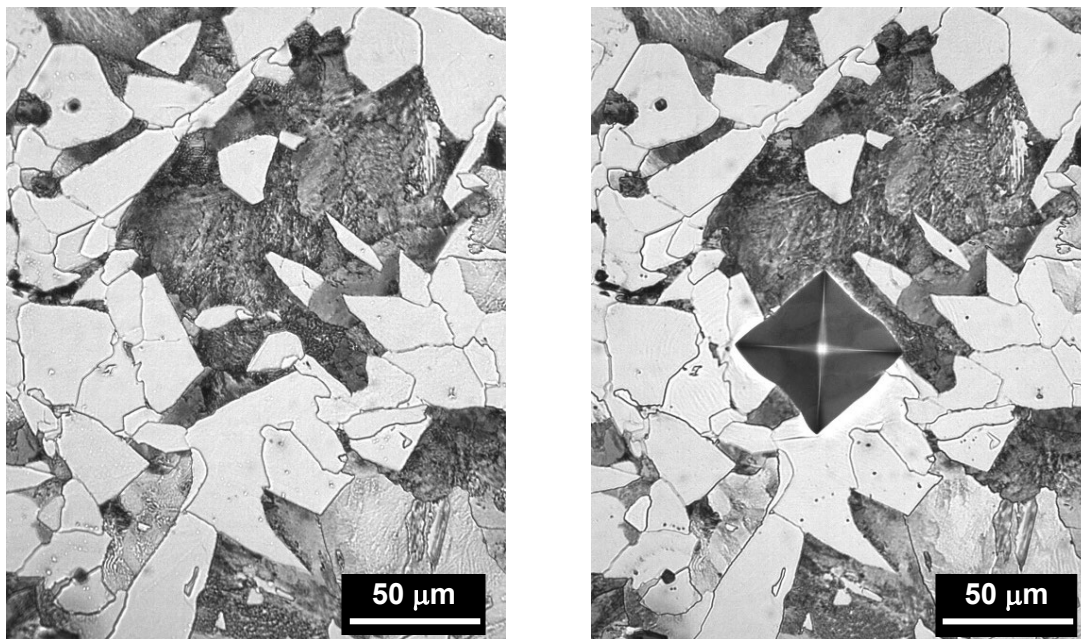


Figure 50. 1E7-1 Sample ID B4 microstructure prior to indentation (left) and with the Vickers microindentation (right). 5% Nital etch. 40x magnification. Ferrite/pearlite dominant.

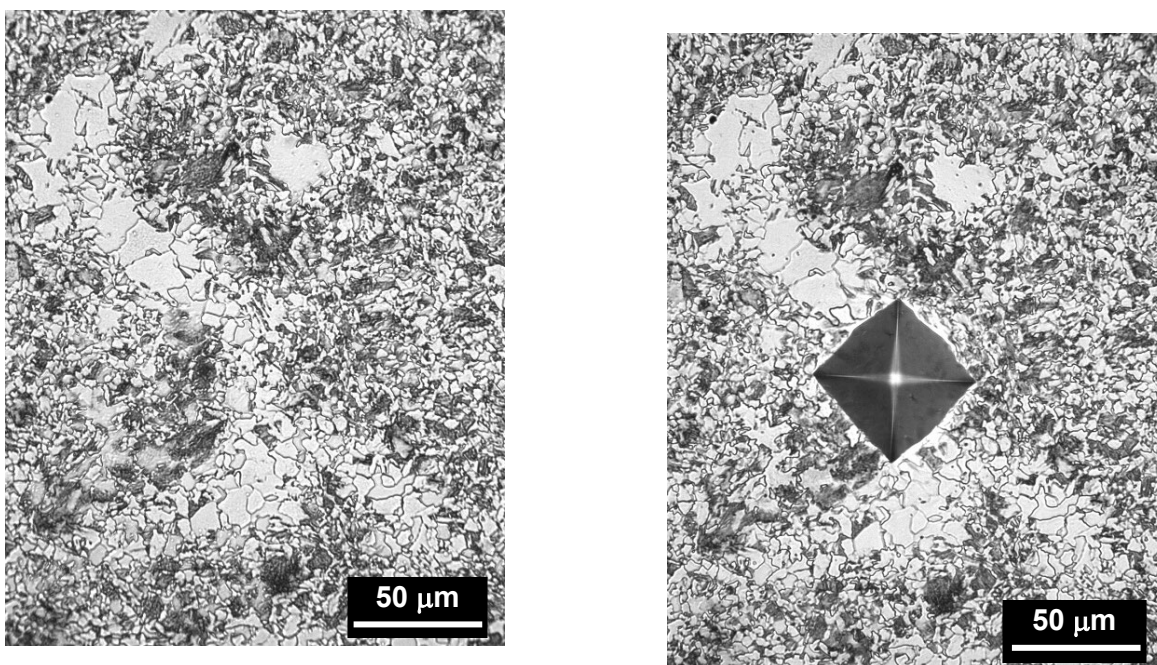


Figure 51. 1E7-1 Sample ID H1 microstructure prior to indentation (left) and with the Vickers microindentation (right). 5% Nital etch. 40x magnification. Refined ferrite/pearlite from the heat cycle.

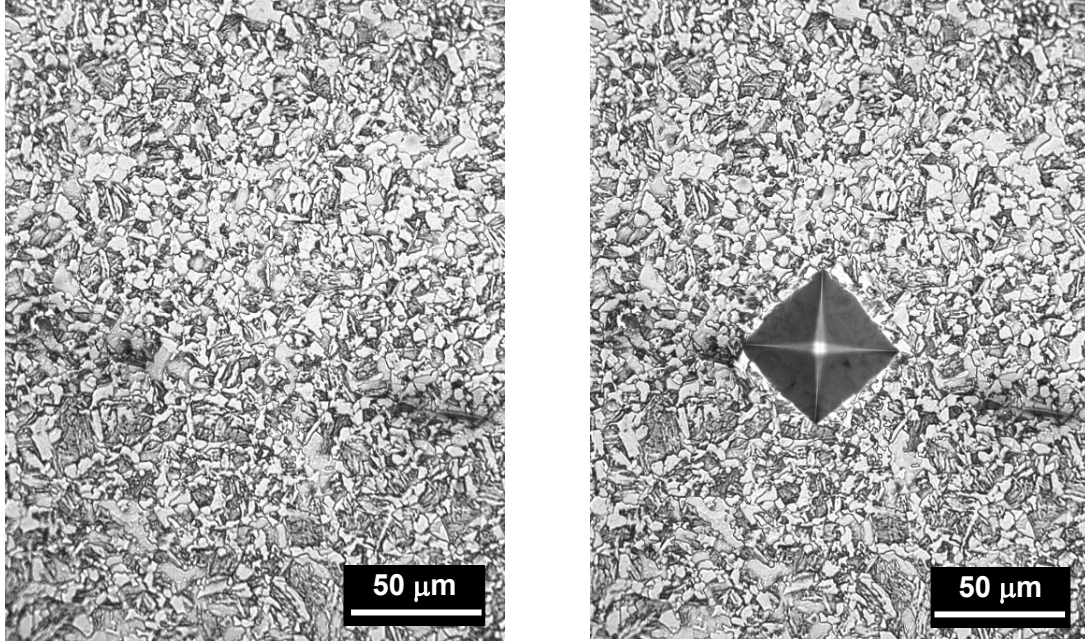


Figure 52. 1E7-1 Sample ID H2 microstructure prior to indentation (left) and with the Vickers microindentation (right). 5% Nital etch. 40x magnification. Refined ferrite/pearlite from the heat cycle.

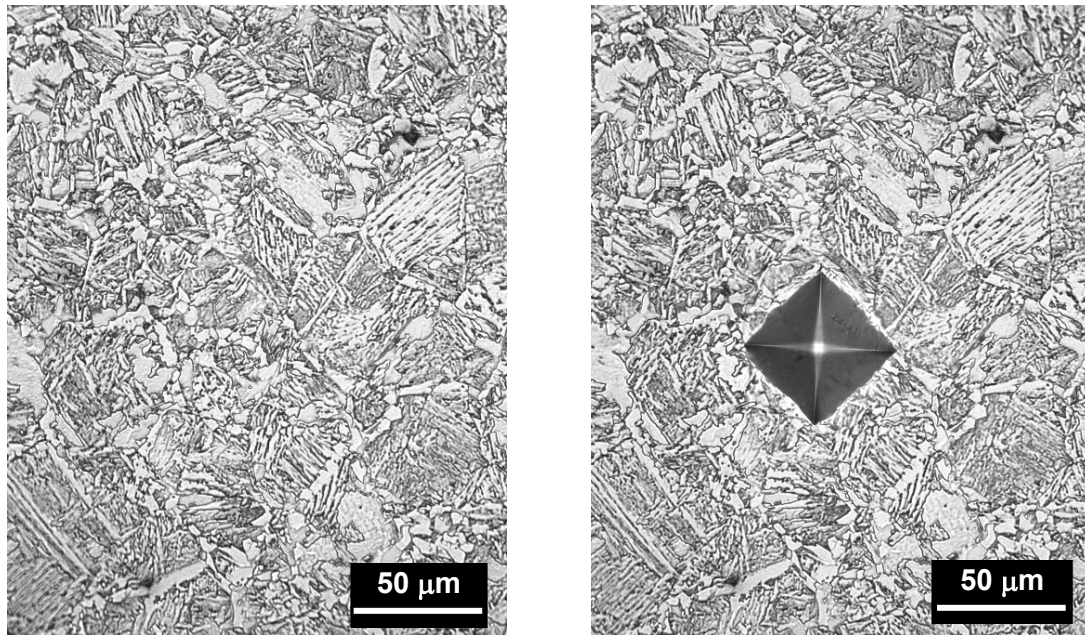


Figure 53. 1E7-1 Sample ID H3 microstructure prior to indentation (left) and with the Vickers microindentation (right). 5% Nital etch. 40x magnification. Ferrite and martensite.

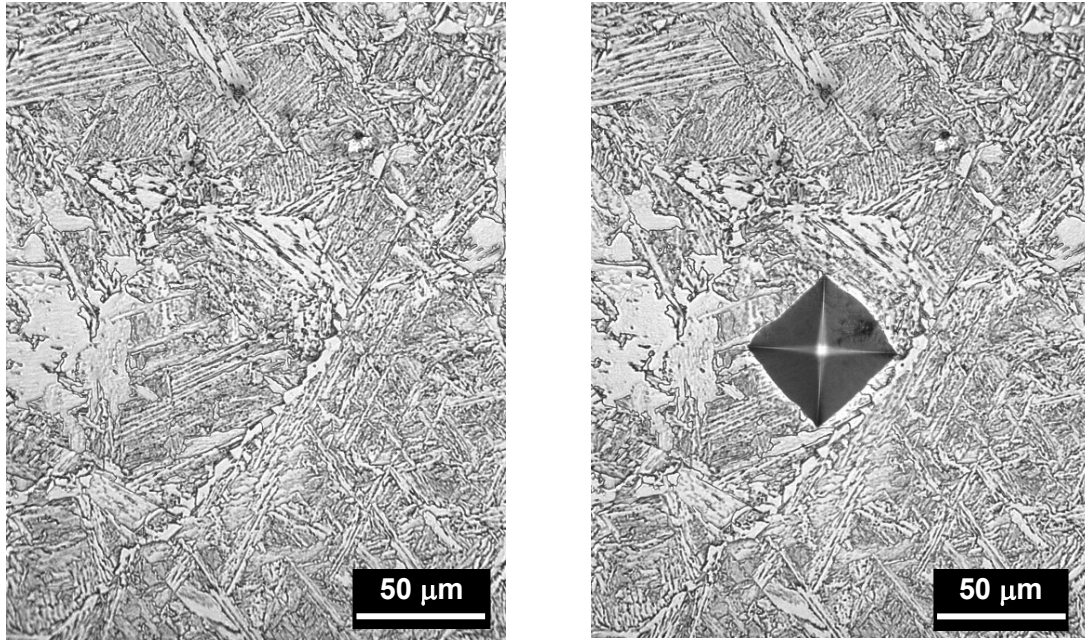


Figure 54. 1E7-1 Sample ID H4 microstructure prior to indentation (left) and with the Vickers microindentation (right). 5% Nital etch. 40x magnification. Ferrite and martensite.

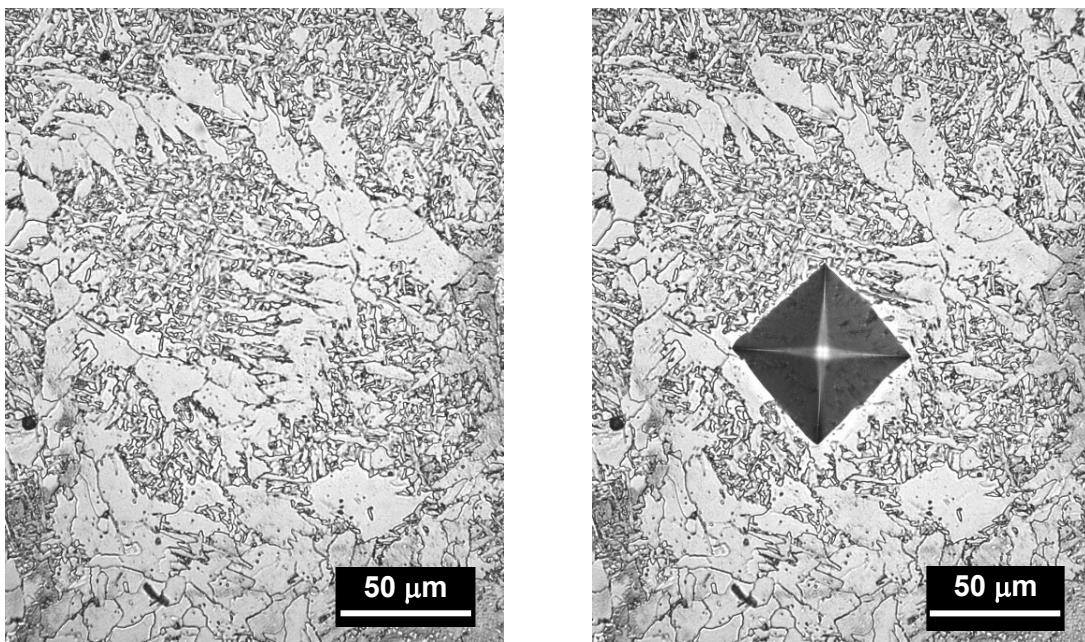


Figure 55. 1E7-1 Sample ID W1 microstructure prior to indentation (left) and with the Vickers microindentation (right). 5% Nital etch. 40x magnification. Proeutectoid and acicular ferrite.

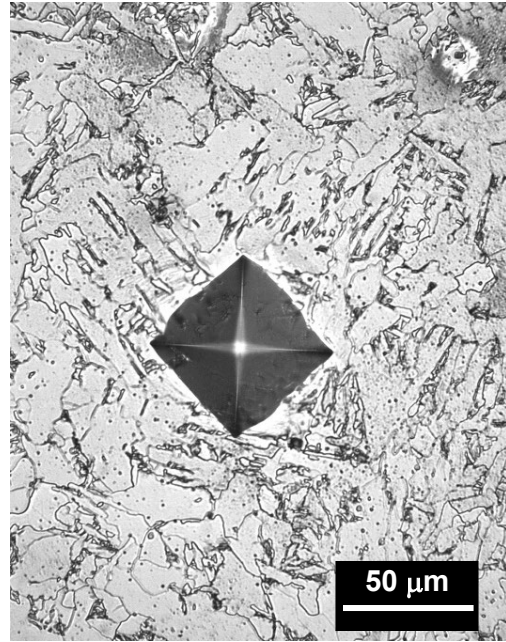
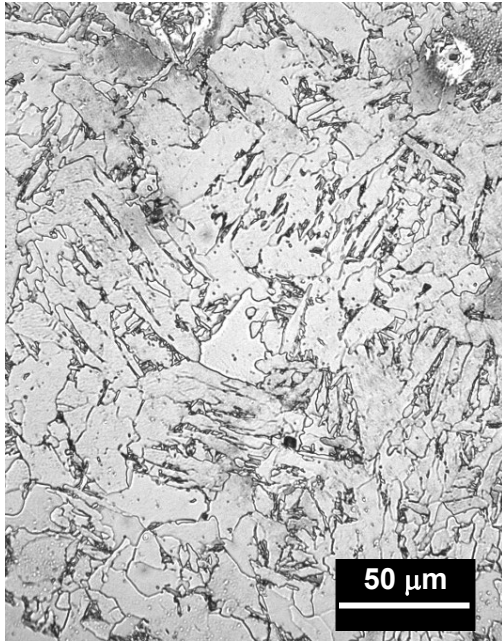


Figure 56. 1E7-1 Sample ID W2 microstructure prior to indentation (left) and with the Vickers microindentation (right). 5% Nital etch. 40x magnification. Refined ferrite dominant.

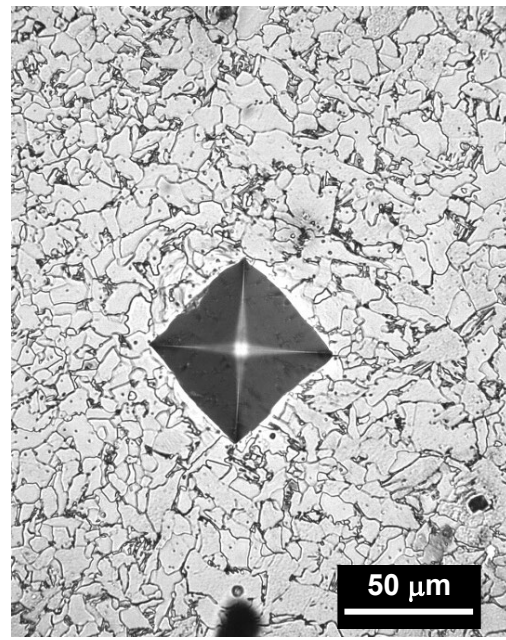


Figure 57. 1E7-1 Sample ID W3 microstructure prior to indentation (left) and with the Vickers microindentation (right). 5% Nital etch. 40x magnification. Refined ferrite dominant.

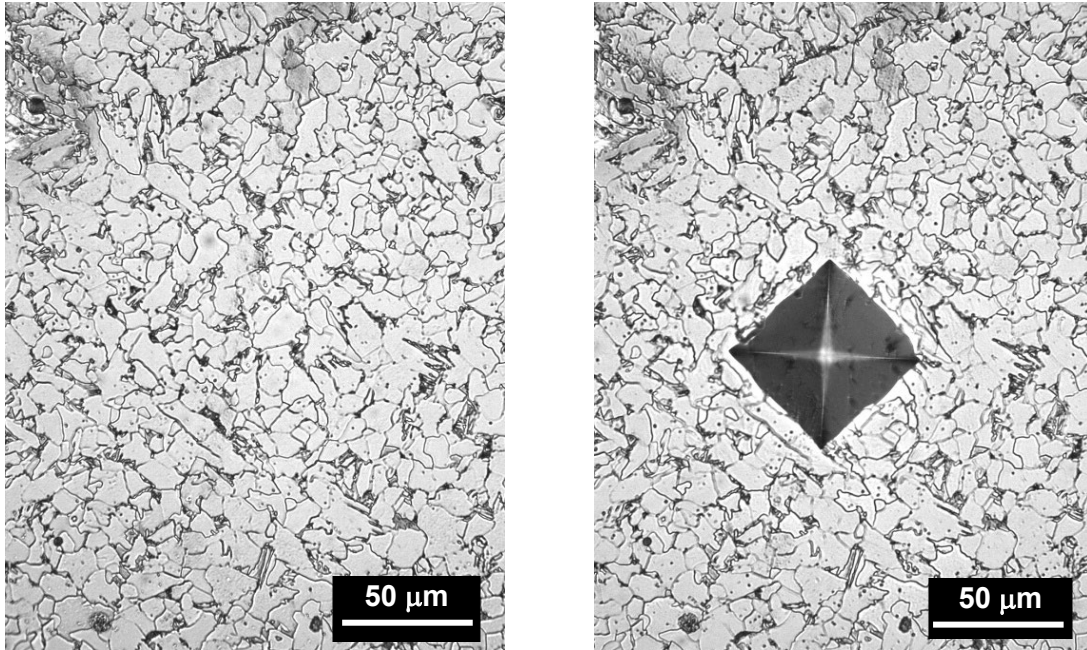


Figure 58. 1E7-1 Sample ID W4 microstructure prior to indentation (left) and with the Vickers microindentation (right). 5% Nital etch. 40x magnification. Refined ferrite dominant.

3.3.2. Gradient line 1E7-2

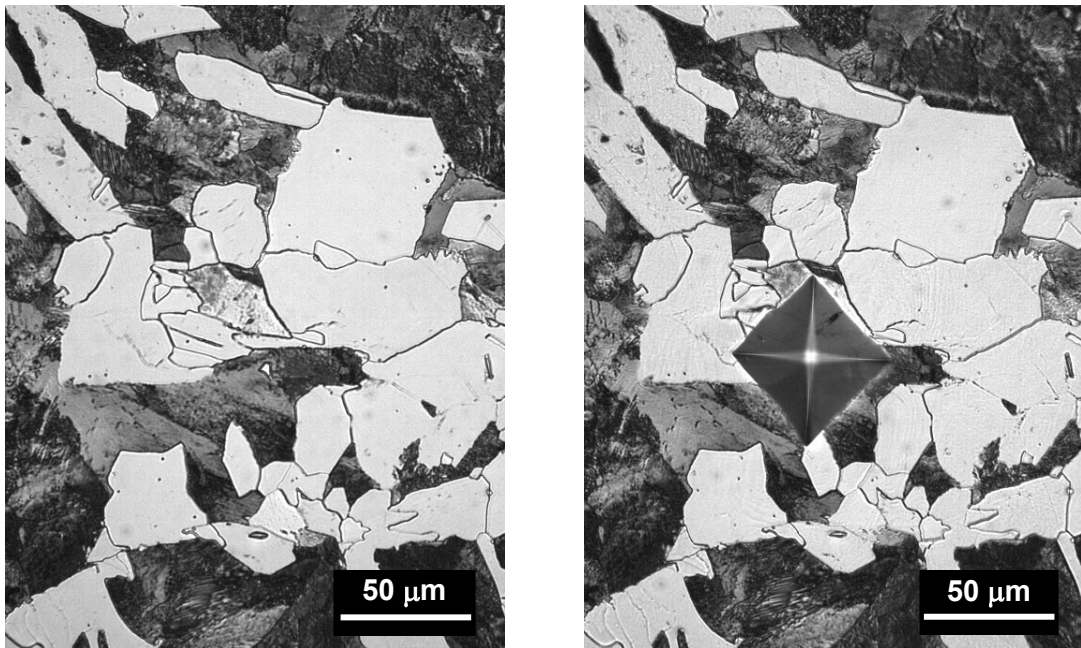


Figure 59. 1E7-2 Sample ID B1 microstructure prior to indentation (left) and with the Vickers microindentation (right). 5% Nital etch. 40x magnification. Ferrite/pearlite dominant.

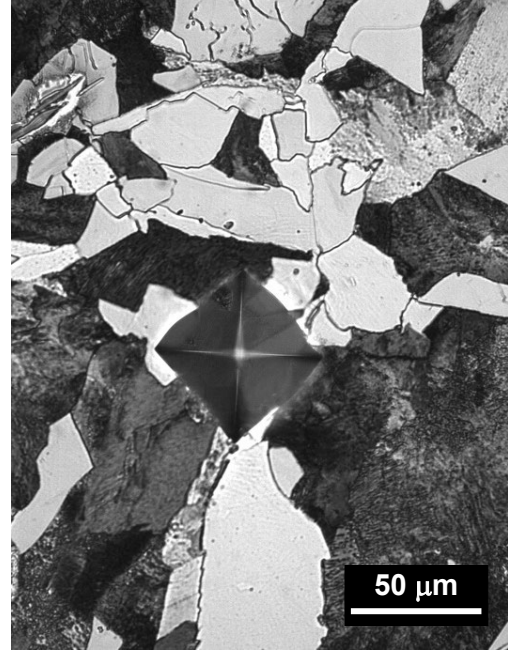


Figure 60. 1E7-2 Sample ID B2 microstructure prior to indentation (left) and with the Vickers microindentation (right). 5% Nital etch. 40x magnification. Ferrite/pearlite dominant.



Figure 61. 1E7-2 Sample ID B3 microstructure prior to indentation (left) and with the Vickers microindentation (right). 5% Nital etch. 40x magnification. Ferrite/pearlite dominant.

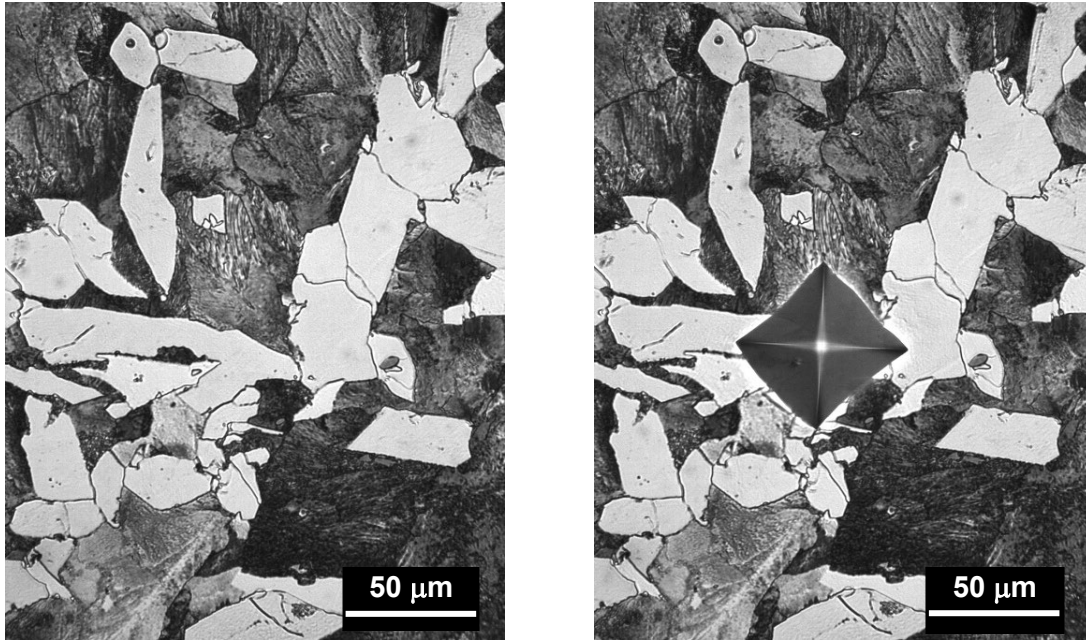


Figure 62. 1E7-2 Sample ID B4 microstructure prior to indentation (left) and with the Vickers microindentation (right). 5% Nital etch. 40x magnification. Ferrite/pearlite dominant.

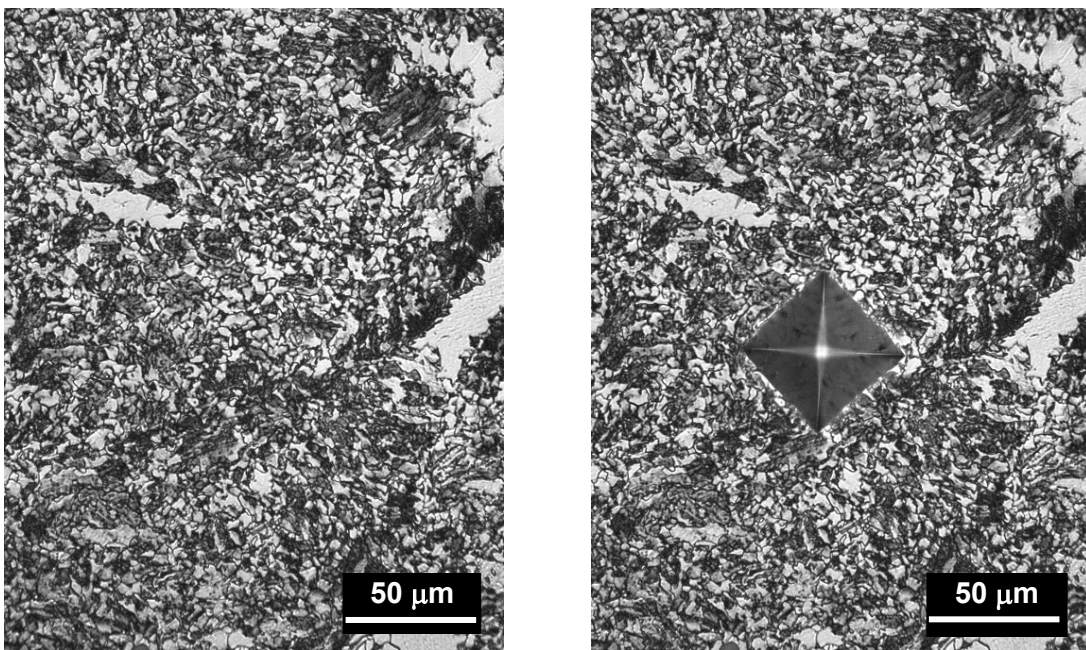


Figure 63. 1E7-2 Sample ID H1 microstructure prior to indentation (left) and with the Vickers microindentation (right). 5% Nital etch. 40x magnification. Refined ferrite/pearlite from the heat cycle.

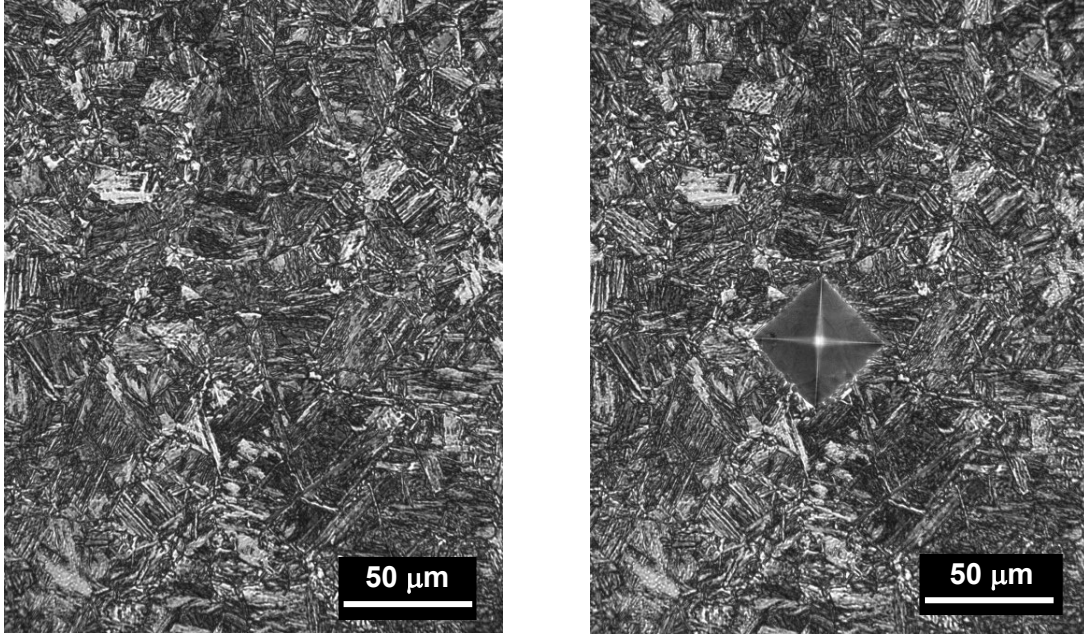


Figure 64. 1E7-2 Sample ID H2 microstructure prior to indentation (left) and with the Vickers microindentation (right). 5% Nital etch. 40x magnification. Martensite dominant.

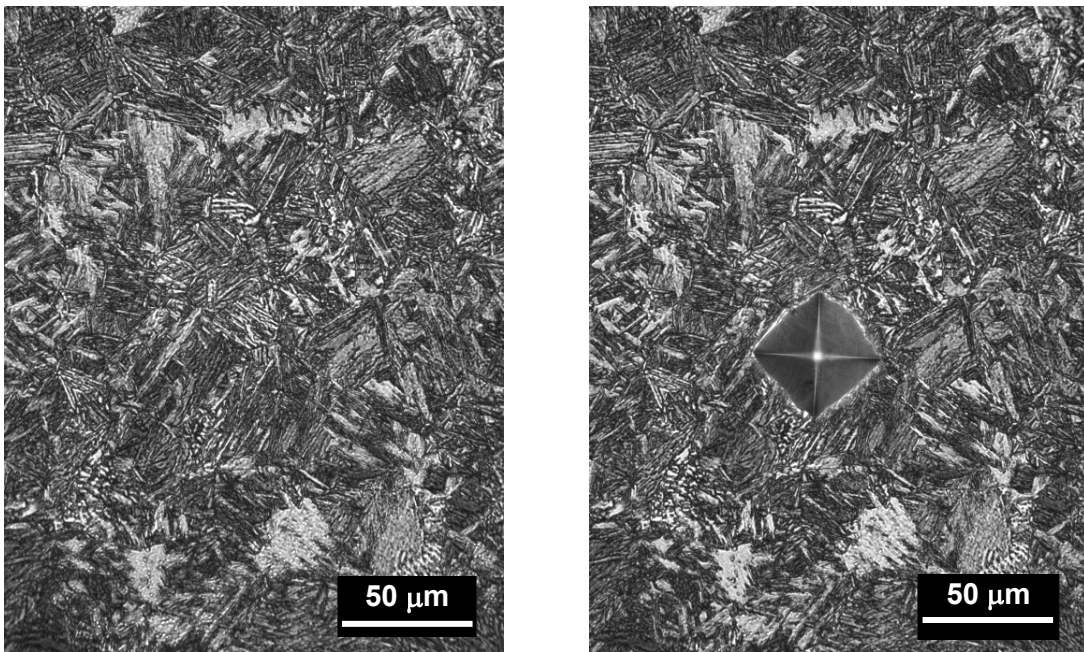


Figure 65. 1E7-2 Sample ID H3 microstructure prior to indentation (left) and with the Vickers microindentation (right). 5% Nital etch. 40x magnification. Martensite dominant.

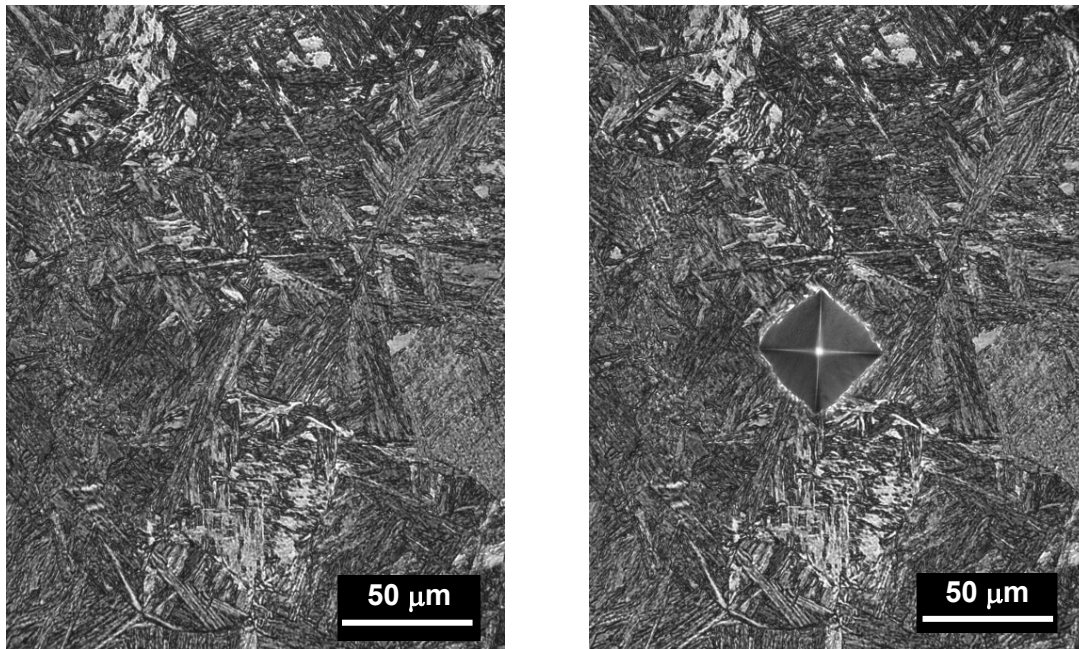


Figure 66. 1E7-2 Sample ID H4 microstructure prior to indentation (left) and with the Vickers microindentation (right). 5% Nital etch. 40x magnification. Martensite dominant.

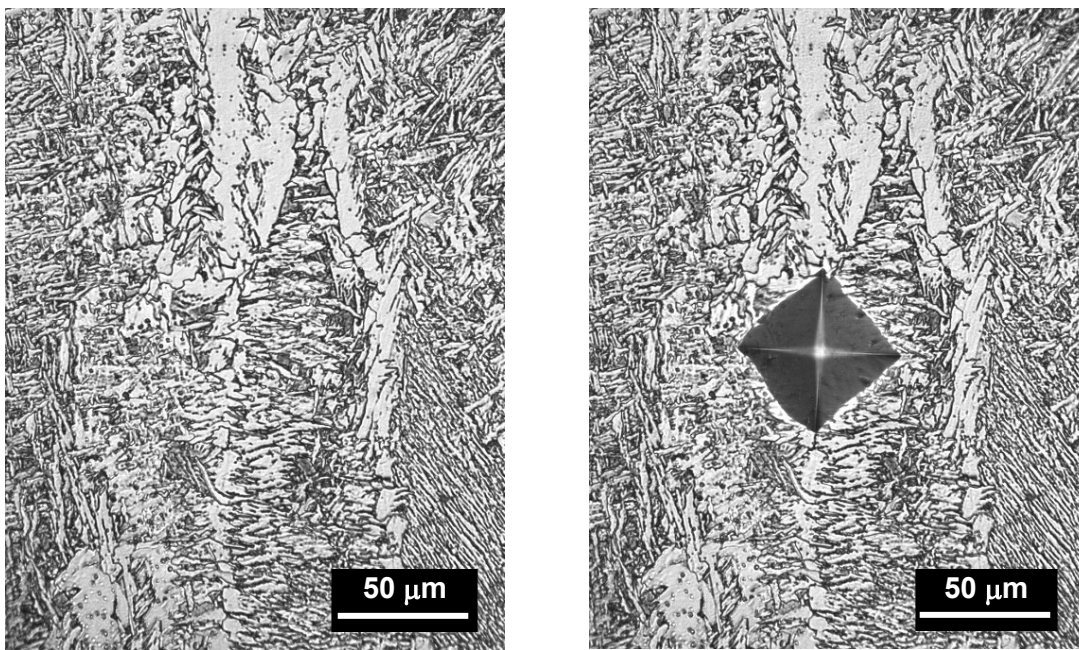


Figure 67. 1E7-2 Sample ID W1 microstructure prior to indentation (left) and with the Vickers microindentation (right). 5% Nital etch. 40x magnification. Acicular ferrite with proeutectoid ferrite and Widmanstätten ferrite.

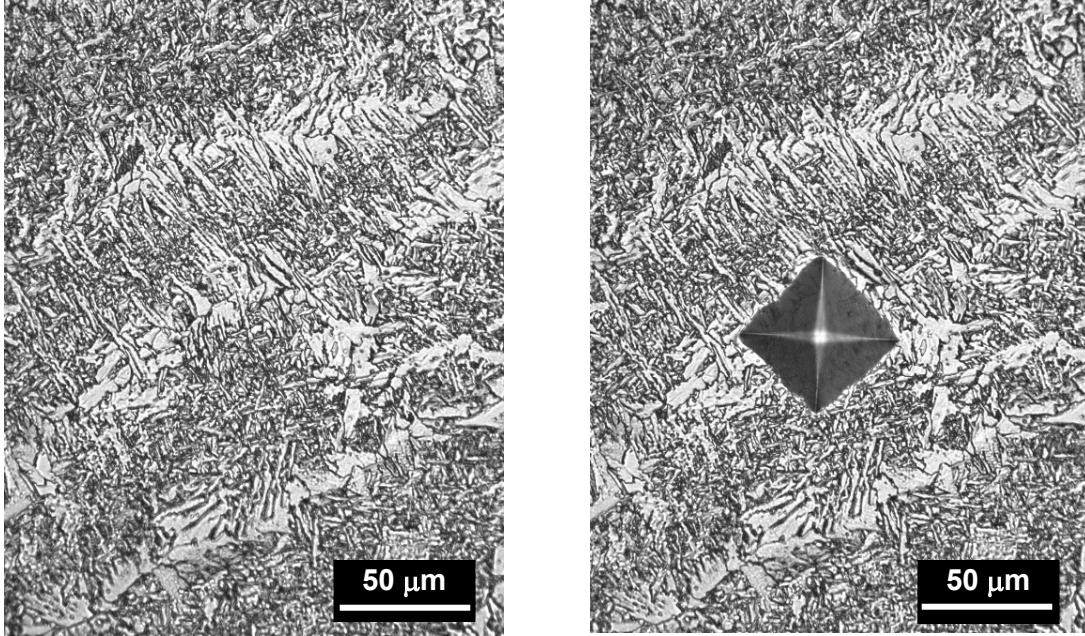


Figure 68. 1E7-2 Sample ID W2 microstructure prior to indentation (left) and with the Vickers microindentation (right). 5% Nital etch. 40x magnification. Acicular ferrite with proeutectoid ferrite and Widmanstätten ferrite.

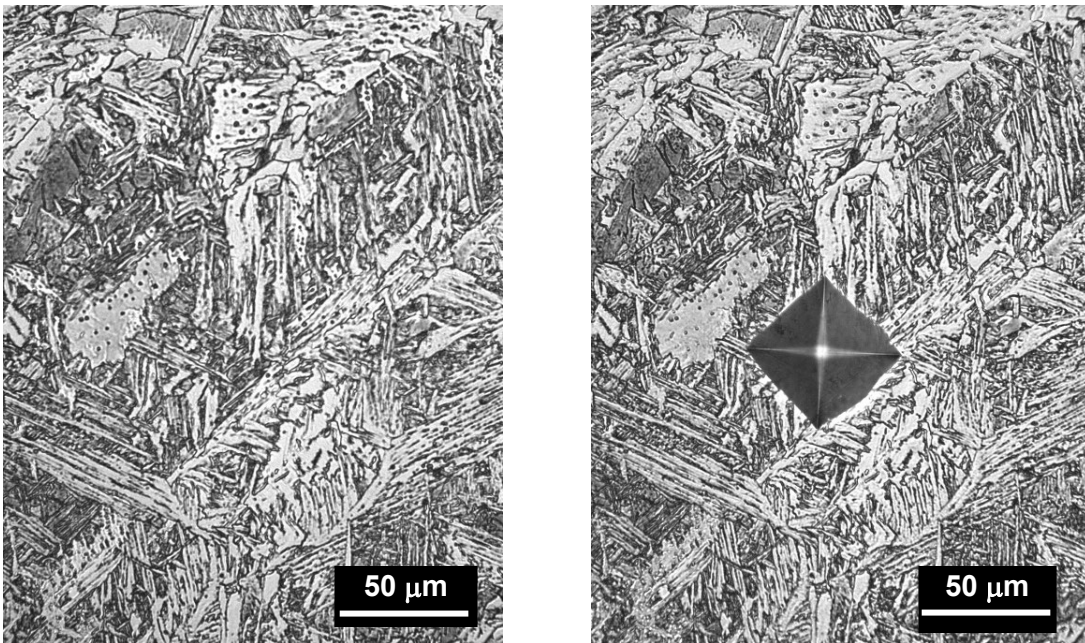


Figure 69. 1E7-2 Sample ID W3 microstructure prior to indentation (left) and with the Vickers microindentation (right). 5% Nital etch. 40x magnification. Acicular ferrite with proeutectoid ferrite and Widmanstätten ferrite.

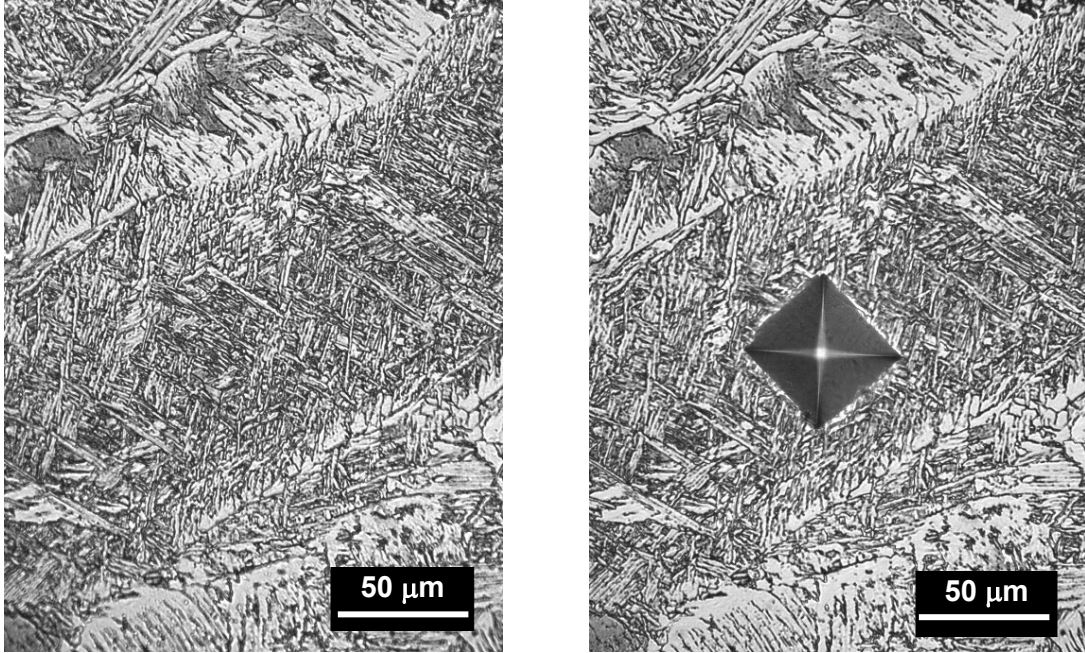


Figure 70. 1E7-2 Sample ID W4 microstructure prior to indentation (left) and with the Vickers microindentation (right). 5% Nital etch. 40x magnification. Acicular ferrite with proeutectoid ferrite and Widmanstätten ferrite.

3.3.3. Gradient line 1E7-3

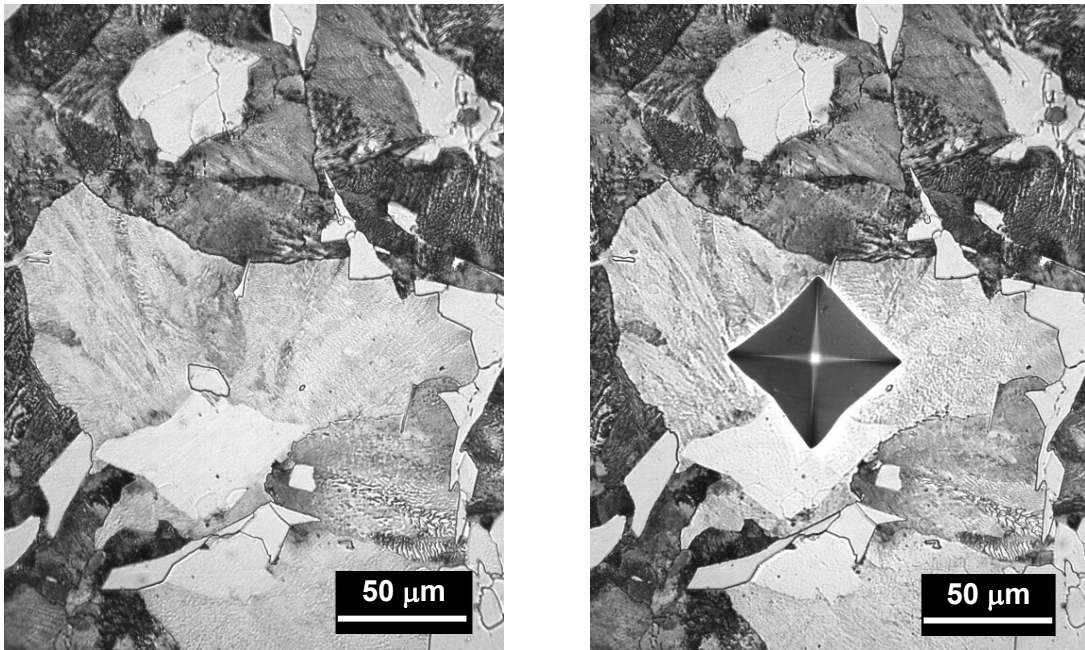


Figure 71. 1E7-3 Sample ID B1 microstructure prior to indentation (left) and with the Vickers microindentation (right). 5% Nital etch. 40x magnification. Ferrite/pearlite dominant.

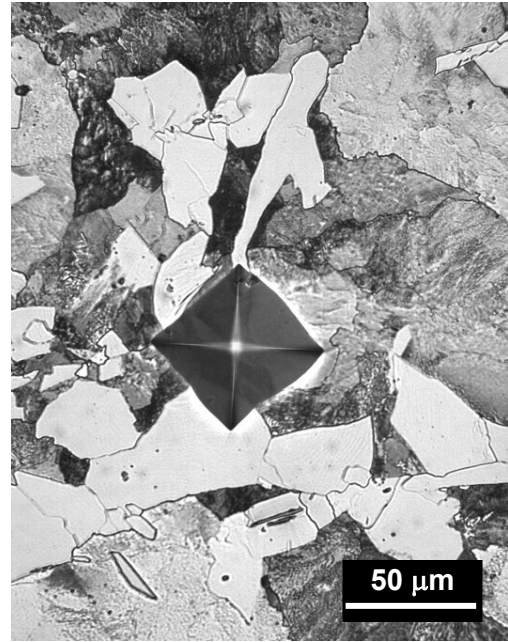


Figure 72. 1E7-3 Sample ID B2 microstructure prior to indentation (left) and with the Vickers microindentation (right). 5% Nital etch. 40x magnification. Ferrite/pearlite dominant.



Figure 73. 1E7-3 Sample ID B3 microstructure prior to indentation (left) and with the Vickers microindentation (right). 5% Nital etch. 40x magnification. Ferrite/pearlite dominant.

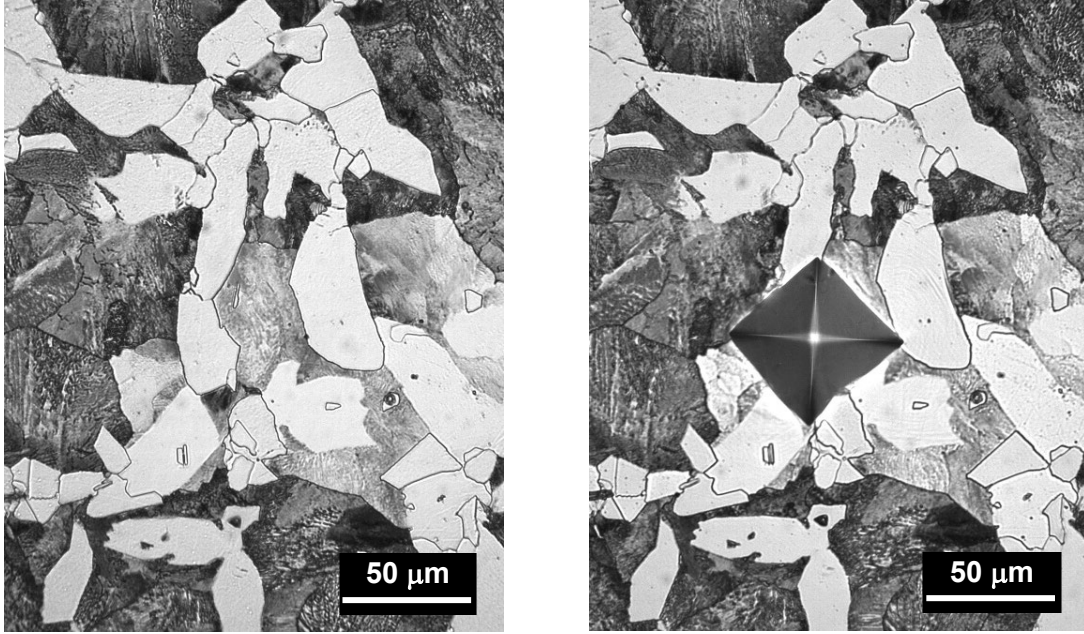


Figure 74. 1E7-3 Sample ID B4 microstructure prior to indentation (left) and with the Vickers microindentation (right). 5% Nital etch. 40x magnification. Ferrite/pearlite dominant.

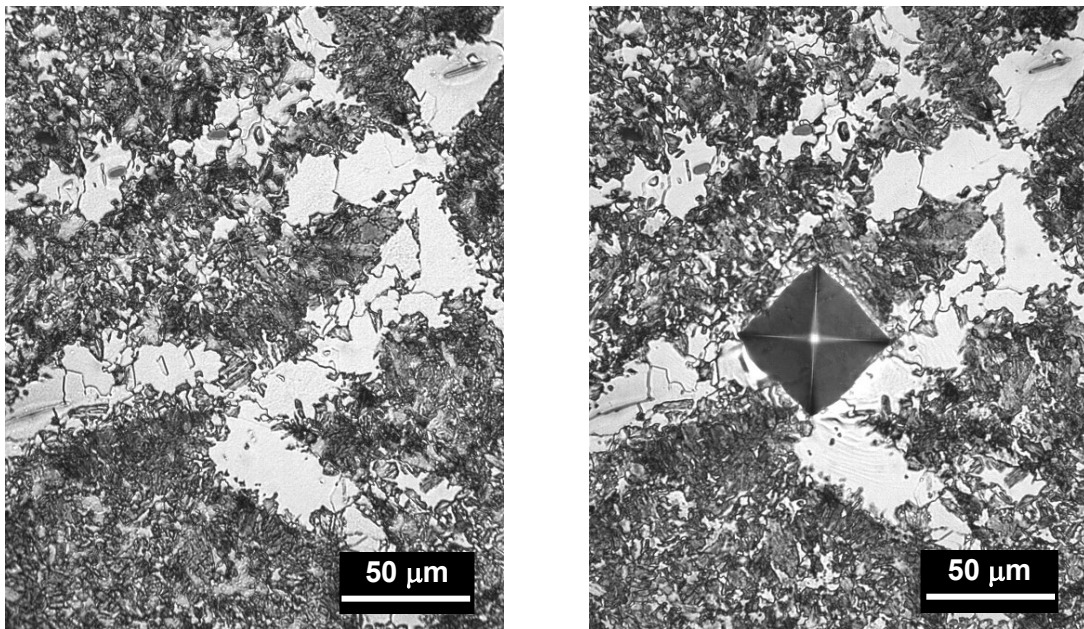


Figure 75. 1E7-3 Sample ID H1 microstructure prior to indentation (left) and with the Vickers microindentation (right). 5% Nital etch. 40x magnification. Refined ferrite/pearlite from the heat cycle.

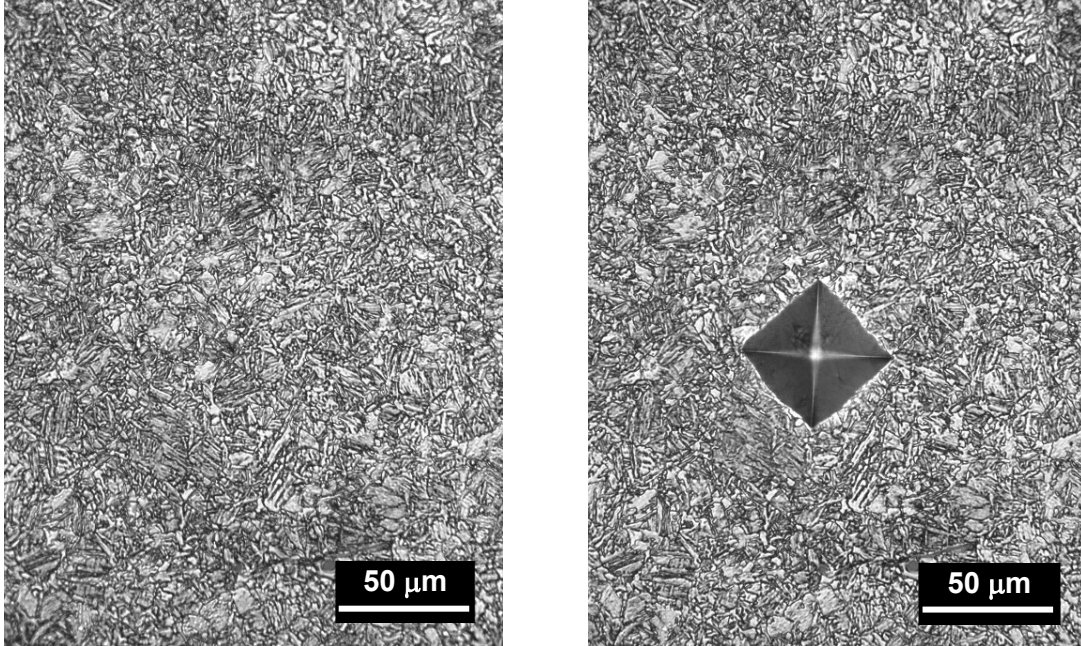


Figure 76. 1E7-3 Sample ID H2 microstructure prior to indentation (left) and with the Vickers microindentation (right). 5% Nital etch. 40x magnification. Ferrite/pearlite and martensite.

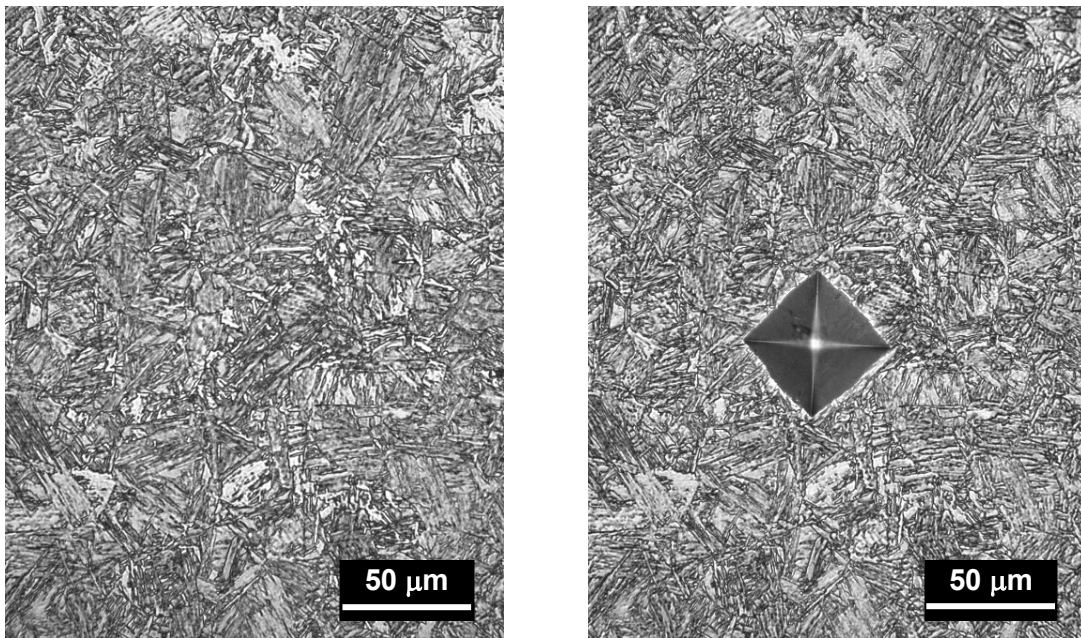


Figure 77. 1E7-3 Sample ID H3 microstructure prior to indentation (left) and with the Vickers microindentation (right). 5% Nital etch. 40x magnification. Ferrite/pearlite and martensite.

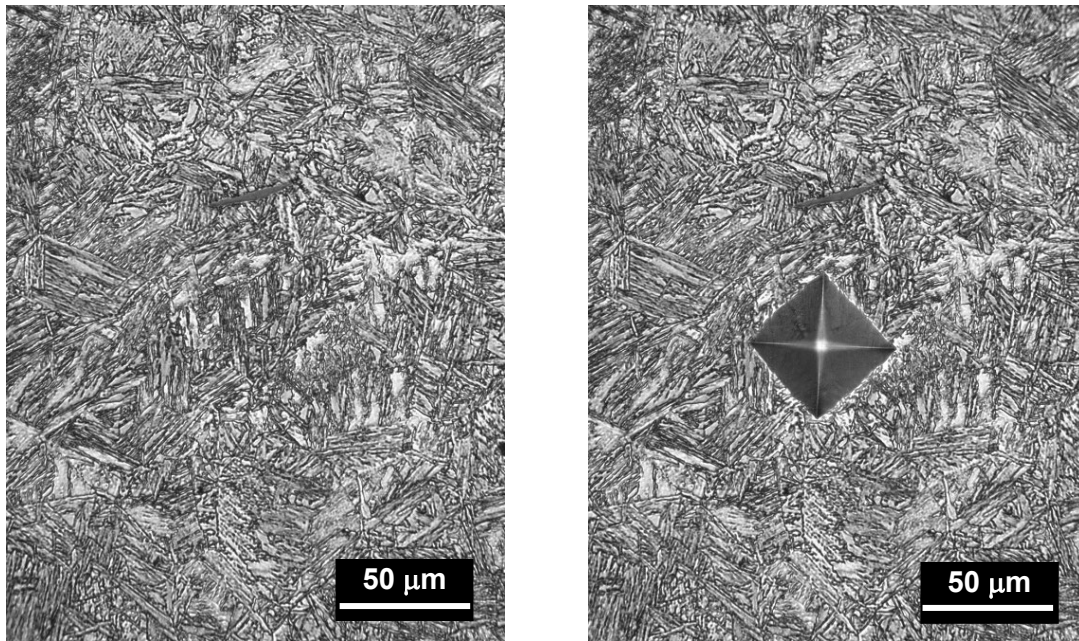


Figure 78. 1E7-3 Sample ID H4 microstructure prior to indentation (left) and with the Vickers microindentation (right). 5% Nital etch. 40x magnification. Ferrite/pearlite and martensite.

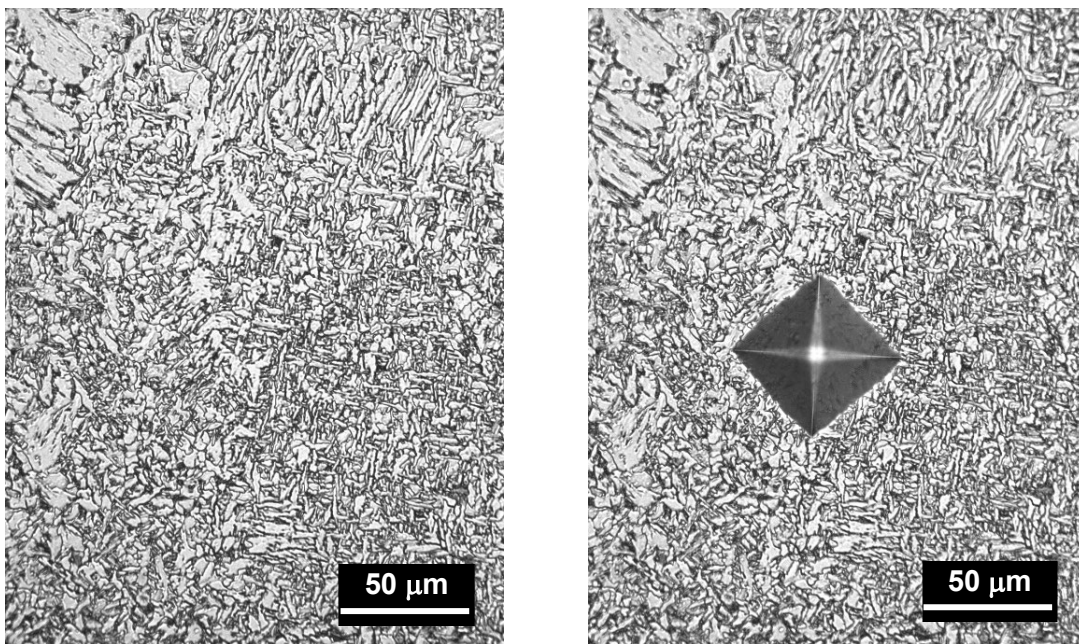


Figure 79. 1E7-3 Sample ID W1 microstructure prior to indentation (left) and with the Vickers microindentation (right). 5% Nital etch. 40x magnification. Acicular ferrite dominant with some proeutectoid ferrite and Widmanstätten ferrite.

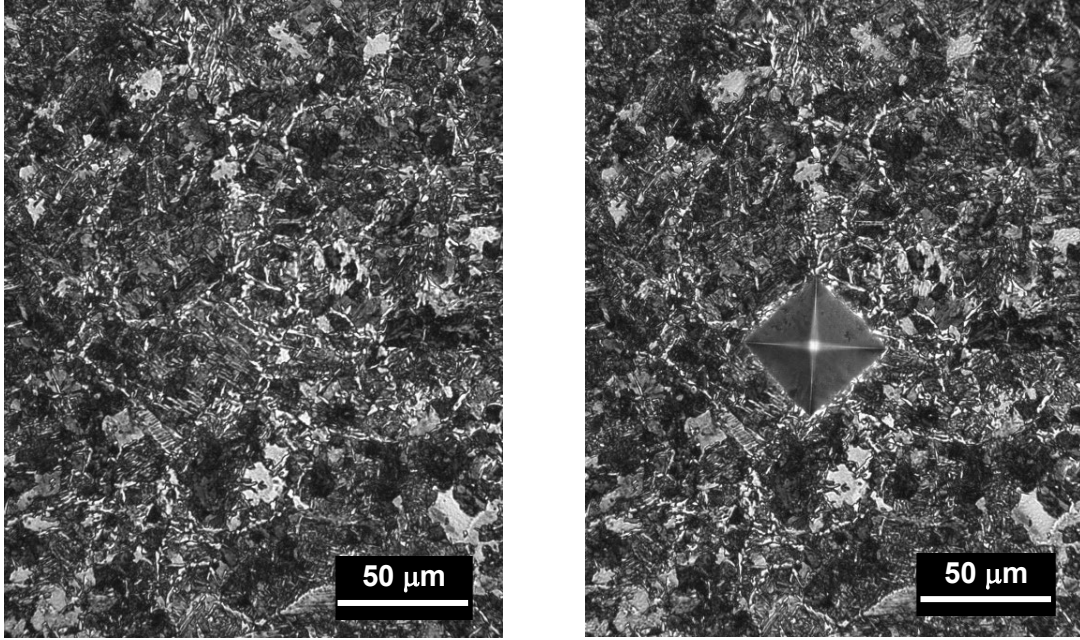


Figure 80. 1E7-3 Sample ID W2 microstructure prior to indentation (left) and with the Vickers microindentation (right). 5% Nital etch. 40x magnification. Martensite with some acicular ferrite proeutectoid ferrite.

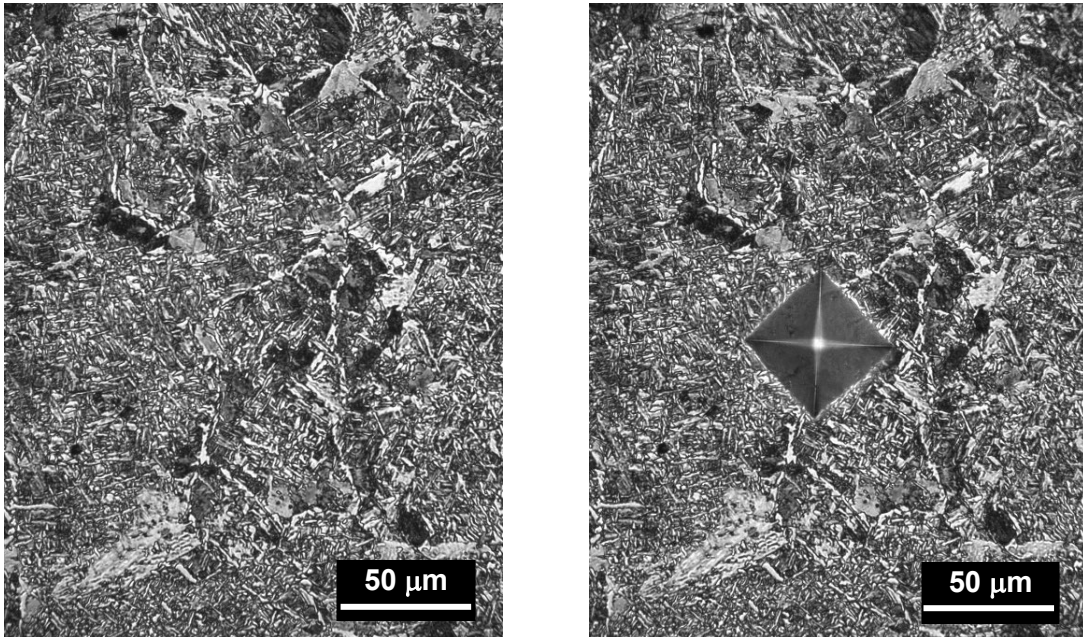


Figure 81. 1E7-3 Sample ID W3 microstructure prior to indentation (left) and with the Vickers microindentation (right). 5% Nital etch. 40x magnification. Acicular ferrite dominant with some proeutectoid ferrite and Widmanstätten ferrite.

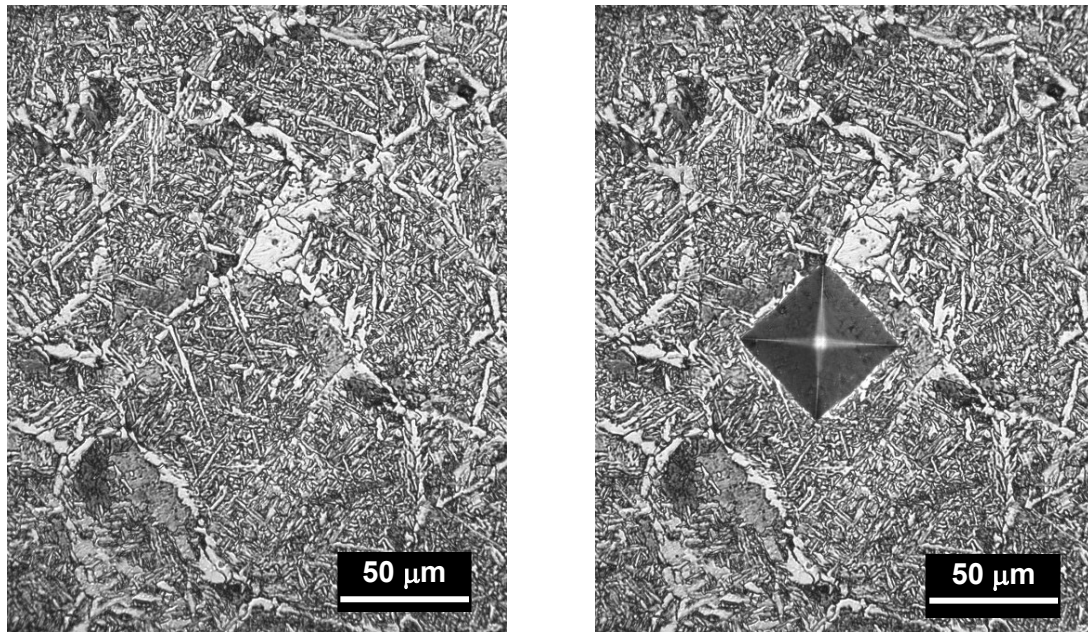


Figure 82. 1E7-3 Sample ID W4 microstructure prior to indentation (left) and with the Vickers microindentation (right). 5% Nital etch. 40x magnification. Acicular ferrite dominant with some proeutectoid ferrite and Widmanstätten ferrite.

ACKNOWLEDGEMENTS

The authors would like to thank Federal and Contractor personnel from the TFHRC Structures Laboratory for their many contributions from assisting in specimen extraction and testing to providing technical guidance. The authors would also like to acknowledge and thank personnel across FHWA’s Headquarters and Resource Center for providing technical guidance related to the investigation.

REFERENCES

- ASM (2004). “Metallography and Microstructures.” ASM Handbook, Vol. 9. ASM International. Materials Park, OH.
- ASTM E29 (2022). “Standard Practice for Using Significant Digits in Test Data to Determine Conformance with Specifications.” ASTM Annual Book of Standards. ASTM International. West Conshohocken, PA.
- ASTM E92 (2017). “Standard Test Methods for Vickers Hardness and Knoop Hardness of Metallic Materials.” ASTM Annual Book of Standards. ASTM International. West Conshohocken, PA.
- AWS A2.0. (1968). “Standard Welding Symbols.” 3rd Edition, American Welding Society. Miami, FL.
- AWS D2.0. (1969). “Specifications for Welded Highway and Railway Bridges.” 8th Edition, American Welding Society. Miami, FL.
- Slein, R., Ocel, J., and Graybeal, B (2023). *Forbes Avenue Over Fern Hollow Bridge Collapse Investigation: Steel Mechanical and Materials Testing Factual Report*. Federal Highway Administration Report Prepared on Behalf of the National Transportation Board Investigation HWY22MH003.

Appendix A: Hardness Verification and SRM Documentation



Certification Number: 117244v

Vickers Diamond Indenter CERTIFICATE OF CALIBRATION

This Vickers Diamond Indenter has been manufactured, standardized, and complies with ASTM E92-17, ISO/IEC 17025 and ANSI/NCSL Z540-1. This Indenter's geometry is directly measured on a Calibrated High Accuracy Dimensional system traceable to NIST. This indenter meets all of the geometric requirements for the type and class reported. No deviations from these methods occurred.

Indenter Serial Number: 117244v
 Class: **B** Type: Vickers
 Indenter Force \geq 1gf: X
 Indenter Force \geq 1 kgf: _____
 Note: 7mm

Requirements

	Nominal	Measured	Tolerance	Uncertainty
Edge Angle	148° 06' 36"	147° 57' 31"	$\pm 45'$	0.05°
Edge Angle equally inclined to the axis of indenter	74°	73° 59' 46"	$\pm 30'$	0.05°
Four faces equally inclined to the axis of indenter	90°	0° 07' 38"	$\pm 30'$	0.05°
Offset	Load \geq 1 gf $\leq 0.5 \mu\text{m}$.44 μm	$\leq 0.5 \mu\text{m}$	0.25 μm
	Load $>$ 1 kgf $\leq 1 \mu\text{m}$		$\leq 1 \mu\text{m}$	0.25 μm

The expanded uncertainty in the measurements were calculated in accordance with the guide to the Expression of Uncertainty in Measurement (GUM). Expanded uncertainties associated with the measurement of this indenter are based on a standard uncertainty multiplied by a coverage factor K=2, providing a level of confidence of approximately 95%.

Standardizing Laboratory

Environment: 22°C, Humidity 33%
 Date: December 16, 2021

Calibrated By: #6

Authorized By: _____



CALIBRATION CERT #1934.01

This report shall not be reproduced except in full without written permission from STC 46590 Ryan Court, Novi, MI 48377.

Made in USA
End of Certification

Page 1 of 1

LECO Corporation | 3000 Lakeview Avenue | St. Joseph, MI 49085
 Main 269.983.5531 | Sales 269.985.5496 | info@leco.com | www.leco.com

LVIC

11-01 REV. 13

LECO CORPORATION
 3000 Lakeview Ave. • St. Joseph, MI 49085-2396 • U.S.A.
 Phone: 800-292-6141 • 269-985-5496 • Fax: 269-982-8977
 info@leco.com • www.leco.com
LECO is a registered trademark of LECO Corporation.

Certificate of Direct Verification for Knoop and Vickers Hardness Testers
 Per ASTM E 92

Model: LM-110AT
Serial Number: FMS1192

Force Verification

Load (Grams Force)	1	3	5	10	25	50
Tolerance (Percent)	1.50%	1.50%	1.50%	1.50%	1.50%	1.50%
Run #1	N/A	N/A	N/A	10.00	25.01	50.01
Run #2	N/A	N/A	N/A	9.99	25.00	50.01
Run #3	N/A	N/A	N/A	9.99	25.00	50.01
Average				9.99	25.00	50.01
Load (Grams Force)	100	200	300	500	1000	2000
Tolerance (Percent)	1.50%	1.00%	1.00%	1.00%	1.00%	1.00%
Run #1	100.11	200.31	300.55	501.36	1003.43	N/A
Run #2	100.10	200.31	300.53	501.34	1003.44	N/A
Run #3	100.10	200.33	300.53	501.32	1003.43	N/A
Average	100.10	200.32	300.54	501.34	1003.43	

Forces are measured with: Precision Balance
 Serial Number: 15429814
 Calibrated with Weight set Serial number: FT-002-MK-001
 Calibrated via Calibration Certificate: 138-71812
 By: Japan Quality Assurance Organization

Measuring System Verification 40X Obj

Distance Verified (µm):	0	50	100	150	200
Tolerance:			The greater of 0.4 µm or 0.5%		
Measured Value:	0.0	50.0	99.9	149.9	200.0

Measuring system is verified with 0-1 mm stage Micrometer

Serial Number: FT-002-ML-086
 Calibrated via Calibration Certificate: 160-96953
 By: Japan Quality Assurance Organization

Test Cycle Verification

Contact Speed Range =	15 to 70	µm/second
Measured Contact Speed =	57	µm/second
Time from Initial Contact to Full Force =	< 10	seconds
Measured Initial Contact to Full Force Time =	4.5	seconds
Full Test Force Application Time =	10	seconds
Measured Full Force Application Time =	10	seconds

Test Cycle is verified with: Quartz Stopwatch
 Serial Number: 590351
 Calibrated via Calibration Certificate: 135-93094
 By: Japan Quality Assurance Organization

Values reported are based on the average results of 10 testers. LM-100 & LV-100 testers are verified individually.

Manufactured and certified by Future Tech Corporation
 Talkpier Kawasaki BLDG. No5-1-3-Chome, Fujisaki, Kawasaki-ku, Kawasaki, Kanagawa, 210-0804 Japan

Certified by:



Date of Certification: 14.03.2022

End of Report

1 of 4
 www.leco.com
 269-982-2385 | info@leco.com
 St. Joseph, MI 49085
 3000 Lakeview Avenue
 LECO Corporation

Vickers Hardness and Knoop
 Hardness Certificate of Calibration



Sun-Tec Corp. manufactures and certifies that the calibration results recorded on this certificate are true and correct and that this Hardness Standard has been manufactured and standardized in accordance with ASTM E92-17 and ISO 17025, utilizing NIST SRM where available.

This certificate may not be reproduced except in full without the approval of SUN-TEC Corporation.
 46590 Ryan Court, Novi, MI 48377
 Made in USA



CALIBRATION CERT #1934.01

4 of 4

Test Block Information

Serial No. 22900036
 Load (gf) 500
 Mean Hardness 182 HV0.5
 Mean Diagonal (µm) 71.38
 (based on 5 indentations)
 Uncertainty * .57 µm / 2.9 HV0.5
 Lab Temp 21° C Lab Humidity 27 %
 Magnification 500x
 Date Calibrated 01/18/23
 Inspector 3

* This uncertainty is an estimate of the Uncertainty of the Mean Diagonal for the Scale and Hardness range indicated with respect to Knoop and Vickers Hardness Standards maintained at NIST or Sun-Tec Corporation. This Uncertainty includes a coverage factor of 2, resulting in a confidence level of approximately 95%.

2 of 4

Calibration Readings

<u>Indent 1</u>	<u>Indent 2</u>	<u>Indent 3</u>	<u>Indent 4</u>	<u>Indent 5</u>
70.76 / 185 HV0.5	71.31 / 182 HV0.5	72.11 / 178 HV0.5	70.68 / 186 HV0.5	72.07 / 179 HV0.5

All measurements are in Micrometers (µm). Indent locations are marked on block surface.

How to Use a Standard

When using this standard for Verification of a Knoop and Vickers Hardness tester, make a series of five randomly spaced indentations on the calibrated surface. The average Diagonal of the five indentations must be within *2% or 0.5µm, whichever is greater of the Certified Diagonal. (*3% if HV/HK is <100).

The Hardness values and tolerances indicated are valid ONLY FOR THE LOAD SPECIFIED. Different loads will produce different hardness values. You should use a Hardness Standard calibrated for the load and approximate hardness that you use in production.

An average outside the range may indicate a problem with the tester. This should be investigated and corrected prior to using the tester for production purposes.

This standard should be used daily.

3 of 4



Vickers Hardness and Knoop
Hardness Certificate of Calibration

Sun-Tec Corp. manufactures and certifies that the calibration results recorded on this certificate are true and correct and that this Hardness Standard has been manufactured and standardized in accordance with ASTM E92-17 and ISO 17025, utilizing NIST SRM where available.

This certificate may not be reproduced except in full without the approval of SUN-TEC Corporation.
46590 Ryan Court, Novi, MI 48377
Made in USA



CALIBRATION CERT #1934.01

4 of 4

Test Block Information

Serial No.	21500221	
Load (gf)	500	
Mean Hardness	490 HV0.5	
Mean Diagonal (µm) (based on 5 indentations)	43.48	
Uncertainty *	.35 µm / 7.8 HV0.5	
Lab Temp	21° C	Lab Humidity 40 %
Magnification	500x	
Date Calibrated	11/02/21	
Inspector	3	

* This uncertainty is an estimate of the Uncertainty of the Mean Diagonal for the Scale and Hardness range indicated with respect to Knoop and Vickers Hardness Standards maintained at NIST or Sun-Tec Corporation. This Uncertainty includes a coverage factor of 2, resulting in a confidence level of approximately 95%.

2 of 4

Calibration Readings

Indent 1	Indent 2	Indent 3	Indent 4	Indent 5
43.46 / 491 HV0.5	43.69 / 486 HV0.5	43.43 / 492 HV0.5	43.32 / 494 HV0.5	43.51 / 490 HV0.5

All measurements are in Micrometers (µm). Indent locations are marked on block surface.

How to Use a Standard

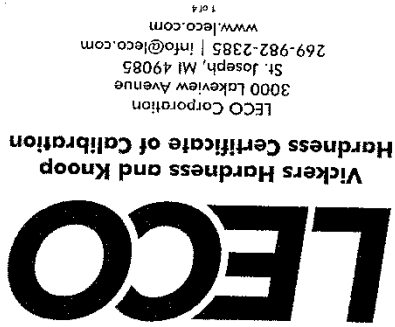
When using this standard for Verification of a Knoop and Vickers Hardness tester, make a series of five randomly spaced indentations on the calibrated surface. The average Diagonal of the five indentations must be within ±2% or 0.5µm, whichever is greater of the Certified Diagonal. (*3% if HV/HK is <100).

The Hardness values and tolerances indicated are valid ONLY FOR THE LOAD SPECIFIED. Different loads will produce different hardness values. You should use a Hardness Standard calibrated for the load and approximate hardness that you use in production.

An average outside the range may indicate a problem with the tester. This should be investigated and corrected prior to using the tester for production purposes.

This standard should be used daily.

3 of 4



Test Block Information

Serial No.	<u>22540019</u>	
Load (gf)	<u>500</u>	
Mean Hardness	<u>637 HV0.5</u>	
Mean Diagonal (µm) (based on 5 indentations)	<u>38.16</u>	
Uncertainty *	<u>.31 µm / 10 HV0.5</u>	
Lab Temp	<u>21° C</u>	Lab Humidity <u>27 %</u>
Magnification	<u>500x</u>	
Date Calibrated	<u>01/18/23</u>	
Inspector	<u>3</u>	

Sun-Tec Corp. manufactures and certifies that the calibration results recorded on this certificate are true and correct and that this Hardness Standard has been manufactured and standardized in accordance with ASTM E92-17 and ISO 17025, utilizing NIST SRM where available.

*This certificate may not be reproduced except in full without the approval of SUN-TEC Corporation.
 46590 Ryan Court, Novi, MI 48377
 Made in USA*



CALIBRATION CERT #1934.01

4 of 4

2 of 4

* This uncertainty is an estimate of the Uncertainty of the Mean Diagonal for the Scale and Hardness range indicated with respect to Knoop and Vickers Hardness Standards maintained at NIST or Sun-Tec Corporation. This Uncertainty includes a coverage factor of 2, resulting in a confidence level of approximately 95%.

Calibration Readings

<u>Indent 1</u>	<u>Indent 2</u>	<u>Indent 3</u>	<u>Indent 4</u>	<u>Indent 5</u>
38.17 / 636 HV0.5	38.28 / 633 HV0.5	38.33 / 631 HV0.5	38.16 / 637 HV0.5	37.85 / 647 HV0.5

All measurements are in Micrometers (µm). Indent locations are marked on block surface.

How to Use a Standard

When using this standard for Verification of a Knoop and Vickers Hardness tester, make a series of five randomly spaced indentations on the calibrated surface. The average Diagonal of the five indentations must be within *2% or 0.5µm, whichever is greater of the Certified Diagonal. (*3% if HV/HK is <100).

The Hardness values and tolerances indicated are valid ONLY FOR THE LOAD SPECIFIED. Different loads will produce different hardness values. You should use a Hardness Standard calibrated for the load and approximate hardness that you use in production.

An average outside the range may indicate a problem with the tester. This should be investigated and corrected prior to using the tester for production purposes.

This standard should be used daily.

3 of 4

Table A-1: Indirect verification of Vickers microhardness using three SRM blocks.

Verification Indent	Mean Length		Mean Length		Mean Length	
	HV 0.5	(μm)	HV 0.5	(μm)	HV 0.5	(μm)
1	179	71.9	493	43.3	640	38.0
2	178	72.1	487	43.6	643	38.0
3	181	71.4	489	43.5	640	38.1
4	184	70.9	496	43.2	646	37.9
5	184	70.9	489	43.5	633	38.2
SRM	182	71.4	490	43.5	637	38.2
R (%)	1.68		0.92		0.79	
E (%)	0.08		0.14		0.31	

Note: Repeatability and error measurements are within tolerance of ASTM E92-17 Table A1.3 for all three SRM blocks.